Durham University

Durham E-Theses

The petrology and geochemistry of volcanic rocks and associated sulphide deposits of the S.E. Anatolian Ophiolite belt, near Malatya, Turkey.

Mustafa Ozcelik

How to cite:

Ozcelik, Mustafa (1982) The petrology and geochemistry of volcanic rocks and associated sulphide deposits of the S.E. Anatolian Ophiolite belt, near Malatya, Turkey. Doctoral thesis, Durham University.

Use policy

The full-text may be used and/or reproduced, and given to third parties in any format or medium, without prior permission or charge, for personal research or study, educational, or not-for-profit purposes provided that:

- a full bibliographic reference is made to the original source
- a https://etheses.durham.ac.uk/id/eprint/7782/ is made to the metadata record in Durham E-Theses
- the full-text is not changed in any way

The full-text must not be sold in any format or medium without the formal permission of the copyright holders.

Please consult the full Durham E-Theses policy for further details.

Academic Support Office, The Palatine Centre, Durham University, Stockton Road, Durham, DH1 3LE
e-mail: e-theses.admin@durham.ac.uk Tel: +44 0191 334 6107
https://etheses.durham.ac.uk

THE PETROLOGY AND GEOCHEMISTRY OF VOLCANIC ROCKS AND ASSOCIATED SULPHIDE DEPOSITS OF THE S.E. ANATOLIAN OPHIOLITE BELT, NEAR MALATYA, TURKEY.

MUSTAFA ÖZÇELİK

B.Sc., A.R.S.M.

A thesis submitted for the degree of

Doctor of Philosophy

at the University of Durham.

July 1982

The copyright of this thesis rests with the author. No quotation from it should be published without his prior written consent and information derived from it should be acknowledged.

DURHAM UNIVERSITY
23 SEP 1982
SCIENCE LIBRARY

Ablama ve Babama

(to my parents)

ABSTRACT

The Fe-Cu-Zn sulphide mineralisation of the Polusagi and Canakci areas are two of many cupriferous deposits which occur along the S.E. Anatolian ophiolite belt. The Polusagi stratiform mineralisation is within the lavas of an Upper Cretaceous-Eocene submarine volcanogenic sequence which is thrust over the crystalline Palaeozoic basement rocks. The Canakci mineralisation occurs within the volcanogenic sediments of probable Upper Cretaceous-Eocene age.

The host and associated rocks of the mineralisation at Polusagi are studied in detail. Extensive submarine alteration has changed the igneous mineralogy and rock chemistry. Element mobility during the alteration is determined and a chemical classification scheme is proposed on the basis of the immobile elements Zr, Y, Nb, La, Ce and Ti. The igneous rocks belong to a tholeiitic suite and were formed during the early stages of an island-arc development on a Tethyan marginal basin floor.

The Polusagi magma originated from a high degree partial melting of an upper mantle source rock and the various rock types were produced by a process of fractional crystallisation involving olivine, clinopyroxene, magnetite, plagioclase and apatite.

Mineralogy and mineral chemistry of the Polusagi rocks are studied in detail. The rocks were metamorphosed to prehnite-pumpellyite facies at higher stratigraphic levels and to greenschist facies at lower, under pressures < 3kb and probably around 2kb. Metamorphism was basically a result of sea-water-rock interaction i.e. "ocean-floor hydrothermal metamorphism".

Ore mineral chemistry and mineralisation at both areas are examined in detail. The Polusagi massive sulphides are fine grained and composed mainly of pyrite, chalcopyrite and sphalerite with minor fahlore, galena, bornite and covellite and traces of magnetite, hematite and idaite. They show strong mineralogical banding and exhibit features ascribable to precipitation

from solutions in an unrestricted environment. The massive sulphides are underlain by pyritic stockwork mineralisation and are overlain by and associated with Fe-Mn-oxide rich siliceous sedimentary horizons. The mineralisation at Canakci is in two forms : massive and disseminated. In many aspects, the former is similar to the massive banded ore and the latter to the stockwork mineralisation of the Polusagi deposit. The Canakci massive sulphide is composed mainly of pyrite, bornite, fahlore, sphalerite and galena with minor chalcopyrite, digenite, idaite, covellite and traces of mawsonite, hexastannite, colusite and native gold.

A model is presented to account for the genesis of both deposits. In the submarine geothermal system set up following the volcanism, the sea-water percolated through the volcanic pile, became heated and reacted with and leached metals from the rocks. The hydrothermal metal bearing solutions were then discharged onto the sea-floor through channels now represented by the stockwork mineralisation. Upon reaching the sea-water-rock interface with temperatures up to 400°C, the solutions mixed with the sea-water and precipitated massive sulphides as a result of a sudden drop in temperature and increases in pH and oxygen fugacity. With further dilution, Fe-Mn oxide rich siliceous sediments precipitated from cool and now oxidised solutions.

ACKNOWLEDGEMENTS

It is gratefully acknowledged that this research was financially supported by the Mineral Research and Exploration Institute of Turkey (M.T.A. Enstitusu), including trips to the fields in 1978 and 1979. Research facilities were provided by Prof. G.M. Brown, former Head of Department of Geological Sciences and Prof. M.H.P. Bott, present Head.

I am grateful to my supervisor, Mr. R. Phillips, for his advice and help throughout the course of this research and for reading of the manuscript. Dr. D.M. Hirst is thanked for critically reading Chapter five of this thesis and making constructive suggestions.

I would like to thank Dr. A. Peckett and Dr. B. Beddoe-Stephens for instructions in the use of the electron microprobe and Mr. R.G. Hardy and Dr. J.G. Holland for instructions in XRF analyses techniques. Mr. R. Lambert gave instructions in the methods of analysing for H_2O and FeO. Polished ore mounts and polished thin sections were prepared by Mr. G. Randall and thin sections by Mr. L. MacGregor. Help in the production of various photographic plates was received from Mr. G. Dresser and of figures from Mr. R.O. Smart.

I wish to take this opportunity to thank all past and present academic and technical staff of the Department for their generous help and advice, in particular : Dr. C.H. Emeleus, Mrs. C.L. Mines, Mr. D. Asbery and Mr. A. Carr. This research has benefitted from useful discussions and suggestions by my contemporaries: Dr's. A.P. Jones, R.M. Forster, R. Dogan, R.S. Taylor and Mr. J.W. Faithfull.

I extend my thanks to Misses G. Sladdin, S.F.G. Gregory, C.M.A. Burge and C.M. Quirk for translations from French and to Mr. J.H.K. MacRae for assistance with computing. My special thanks go to Miss F.M. Davies for her help and encouragement during the final stages of this research.

Finally, I thank Mrs. J. Scott and Mrs. B.K. Dain for patiently and efficiently typing this thesis.

CONTENTS Page

Abstract I

Acknowledgements III

Contents IV

List of Figures XII

List of Tables XVII

List of Plates XIX

CHAPTER ONE : INTRODUCTION

1.1 - Introduction 1

1.2 - A brief review of regional structure and ophiolites in Turkey 1

1.3 - Sulphide mineralisation along the SE Anatolian ophiolite belt 6

1.4 - Location of the Polusagi and Canakci areas 9

CHAPTER TWO : ROCK UNITS AND FIELD RELATIONS

2.1 - The Polusagi area 11

2.1.1 - Introduction 11

2.1.2 - Stratigraphy and the rock units 14

2.1.2.1 - Crystalline basement rocks 14

2.1.2.2 - Limestone 15

2.1.2.3 - Calc-schists 16

2.1.2.4 - Red-schists 16

2.1.2.5 - Agglomerates 18

2.1.2.6 - Volcanics 18

2.1.2.7 - Hypabyssal rocks 21

2.1.2.8 - Fe-Mn rich siliceous sediments 21

2.1.2.9 - Sulphide mineralisation 22

2.1.3 - Structural geology 24

2.1.4 - Summary and conclusions 26

2.2 - The Canakci area 28

2.2.1 - Introduction 28

2.2.2 - Stratigraphy 28

2.2.2.1 - Metamorphic rocks of Palaeozoic basement 31

2.2.2.2 - Breccia - Conglomerate 31

		Page
2.2.2.3	- Limestone	31
2.2.2.4	- Calc-schists and red-schists	33
2.2.2.5	- Agglomerates	33
2.2.2.6	- Serpentinite	33
2.2.2.7	- Sulphide mineralisation	34
2.2.3	- Structural geology	34
2.2.4	- Summary and conclusions	35
CHAPTER THREE	: ELEMENT MOBILITY IN THE POLUSAGI ROCKS	
3.1	- Introduction	36
3.2	- Element mobility under alteration processes	37
3.3	- Element mobility in the Polusagi rocks	43
3.3.1	- Introduction	43
3.3.2	- Inter-element correlations and element mobility in the volcanics	46
3.3.2.1	- Introduction	46
3.3.2.2	- Correlation coefficients	48
3.3.2.3	- Direction of element mobility	62
3.3.3	- Element mobility in the hypabyssal rocks	66
3.4	- Summary and conclusions	66
CHAPTER FOUR	: CLASSIFICATION AND TECTONIC SETTING	
4.1	- Introduction	70
4.2	- Classification of the Polusagi rocks	70
4.2.1	- Introduction	70
4.2.2	- Subdivision of the Polusagi rock suite	72
4.2.2.1	- Subdivision of the volcanic rocks	73
4.2.2.2	- Comparison with other chemical schemes of subdivision	75
4.2.2.3	- Subdivision of the hypabyssal rocks	78
4.2.2.4	- Further considerations of the subdivided rocks	80
4.2.3	- The Polusagi magma type - sub-alkaline or alkaline?	85
4.2.4	- The Polusagi subalkaline rock series: tholeiitic or calc-alkaline?	90
4.3	- Tectonic setting of the Polusagi tholeiitic rock suite	97

		Page
4.3.1	- Introduction	97
4.3.2	- Tectonic Setting	98
4.3.3	- A discussion	105
4.3.4	- Further considerations of the tectonic setting	106
4.3.5	- Chemical comparison with rocks from known tectonic settings and from ophiolites	111
4.3.5.1	- Introduction	111
4.3.5.2	- Chemical comparison of the basalts with those from known tectonic settings	112
4.3.5.3	- Chemical comparison of the basalts with ophiolitic basalts	117
4.3.5.4	- Chemical comparison of the Polusagi andesites and dacites	122
4.3.5.5	- Conclusion	123
CHAPTER FIVE	: ORIGIN AND PETROGENESIS OF THE POLUSAGI MAGMA	
5.1	- Introduction	124
5.2	- Origin of the Polusagi magma	129
5.3	- Fractional crystallisation vs. progressive partial melting	130
5.4	- Partial melting of upper mantle in Polusagi	135
5.4.1	- Partial melt composition	135
5.4.2	- Degree of partial melting	136
5.5	- Fractional crystallisation of the Polusagi magma	
5.5.1	- Introduction	140
5.5.2	- Chemical variations in major oxides	140
5.5.3	- Chemical variations in trace elements	153
5.5.4	- Major and trace element variations in the hypabyssal rock	161
5.6	- Summary and conclusions	161
CHAPTER SIX	: PETROGRAPHY AND MINERALOGY	
6.1	- Introduction	163
6.2	- Clinopyroxene	164
6.2.1	- Mode of occurrence	164
6.2.2	- Chemistry	166

		Page
6.2.2.1	- Nomenclature	166
6.2.2.2	- Chemical variation	168
6.2.2.3	- Crystal chemistry	173
6.2.3	- Factors controlling the chemical variations	176
6.2.4	- Petrogenetic implications of clinopyroxene chemistry	178
6.2.4.1	- Introduction	178
6.2.4.2	- The Polusagi magma type as indicated by cpx chemistry	180
6.3	- Amphibole	183
6.3.1	- Mode of occurrence	183
6.3.2	- Chemistry	184
6.3.2.1	- Introduction	184
6.3.2.2	- Nomenclature	187
6.3.2.3	- Chemical variation	191
6.3.2.4	- Crystal chemistry	195
6.3.3	- Factors controlling the chemical variations	200
6.3.3.1	- Chemical factors	200
6.3.3.2	- Physical factors	200
6.4	- Chlorite	205
6.4.1	- Mode of occurrence	205
6.4.2	- Chemistry	208
6.4.2.1	- Introduction	208
6.4.2.2	- Nomenclature	209
6.4.2.3	- Crystal chemistry	209
6.4.2.4	- Chemical variation	212
6.4.3	- Factors controlling the chemical variation	216
6.4.3.1	- Chemical factors	216
6.4.3.2	- Physical factors or grade of metamorphism	218
6.5	- Plagioclase	220
6.5.1	- Mode of occurrence	220
6.5.2	- Chemistry	222
6.5.3	- Factors controlling the chemistry	222
6.6	- Epidote	225
6.6.1	- Mode of occurrence	225
6.6.2	- Chemistry	225
6.6.2.1	- Nomenclature	226

		Page
6.6.2.2	- Chemical variation and crystal chemistry	226
6.6.3	- Factors controlling the chemistry	227
6.6.3.1	- Chemical factors	227
6.6.3.2	- Physical factors	229
6.7	- Prehnite	230
6.7.1	- Mode of occurrence	230
6.7.2	- Chemistry	230
6.7.2.1	- Chemical variation and crystal chemistry	231
6.7.3	- Factors controlling the chemistry	231
6.8	- Pumpellyite	233
6.8.1	- Mode of occurrence	233
6.8.2	- Chemistry	233
6.8.2.1	- Introduction	233
6.8.2.2	- Nomenclature	235
6.8.2.3	- Chemical variation and crystal chemistry	235
6.8.3	- Factors controlling the chemistry	237
6.9	- Other mineral phases	240
6.9.1	- Calcite	240
6.9.2	- Quartz	241
6.9.3	- The opaque oxides, sphene and leucoxene	241
6.10	- General features and textural relations in the metamorphic zones	242
6.10.1	- Introduction	242
6.10.2	- General features of metamorphic zones	242
6.10.3	- Mineral relations and abundances across the zones	244
6.10.4	- General order of crystallisation in gas vesicles	246
6.11	- Evaluation of metamorphic conditions	248
6.11.1	- Introduction	248
6.11.2	- Zone A	248
6.11.3	- Zone B	249
6.12	- Nature of metamorphism	251
6.12.1	- Introduction	251
6.12.2	- The Polusagi metamorphism	253

Page

CHAPTER SEVEN : ORE MINERALOGY

7.1 - Introduction 256

7.2 - Ore mineralisation in Polusagi 257

7.2.1 - Sulphide mineralisation 257

7.2.1.1 - Introduction 257

7.2.1.2 - Zonation 258

7.2.1.3 - Factors controlling the zonation 260

7.2.1.4 - Banding in the massive sulphide mineralisation 263

7.2.1.4.1 - Introduction 263

7.2.1.4.2 - Pyrite-rich bands 264

7.2.1.4.3 - Chalcopyrite-rich bands 264

7.2.1.4.4 - Sphalerite-rich bands 266

7.2.1.4.5 - Siliceous-hematitic bands 266

7.2.1.5 - Factors leading to banding in the massive sulphide ore 270

7.2.1.6 - Sulphide mineral textures 272

7.2.1.6.1 - Pyrite forms 272

7.2.1.6.2 - Inclusions in pyrite crystals or aggregates 278

7.2.1.6.3 - Interrelations of pyrite, chalcopyrite and sphalerite 283

7.2.2 - Fe-Mn oxide mineralisation 286

7.2.2.1 - Introduction

7.2.2.2 - Factors controlling the formation and distribution of minerals 286

7.3 - Sulphide mineralisation in Canakci 291

7.3.1 - Introduction 291

7.3.2 - Ore and gangue mineral contents 291

7.3.2.1 - Massive sulphides 291

7.3.2.2 - Disseminated pyrite mineralisation 292

7.3.3 - Banding in the massive sulphides 292

7.3.4 - Mineral textures 293

7.3.4.1 - Pyrite forms 293

7.3.4.2 - Inclusions in pyrite 294

7.3.4.3 - Inter-relations of ore minerals in the massive sulphides 294

	Page
7.3.5 - A discussion of the origin of mineralisation	296
7.4 - Ore minerals	299
7.4.1 - Introduction	299
7.4.2 - Primary ore minerals	299
7.4.2.1 - Sulphides	299
7.4.2.1.1 - Pyrite	299
7.4.2.1.2 - Chalcopyrite	301
7.4.2.1.3 - Sphalerite	303
7.4.2.1.4. - Galena	304
7.4.2.1.5 - Bornite	307
7.4.2.1.6 - Mawsonite or 'orange bornite' and hexastannite or 'stannite jaune'	307
7.4.2.1.6.1 - Introduction	307
7.4.2.1.6.2 - Chemistry	308
7.4.2.1.7 - Colusite	309
7.4.2.1.7.1 - Introduction	309
7.4.2.1.7.2 - Chemistry	312
7.4.2.2 - Sulphosalts	315
7.4.2.2.1 - Fahlore group minerals	315
7.4.2.2.1.1 - Introduction	315
7.4.2.2.1.2 - Chemistry	316
7.4.2.3 - Oxides	322
7.4.2.3.1 - Magnetite	322
7.4.2.3.2 - Hematite and Mn-oxides	323
7.4.2.3.3 - Chromite	323
7.4.2.4 - Native metals	324
7.4.2.4.1 - Gold	324
7.4.3 - Secondary ore minerals	325
7.4.3.1 - Sulphides	325
7.4.3.1.1 - Idaite	325
7.4.3.1.1.1 - Introduction	325
7.4.3.1.1.2 - Chemistry	326
7.4.3.1.2 - Covellite	329
7.4.3.1.3 - Digenite	329
7.4.3.2 - Miscellaneous minerals	330
7.4.3.2.1 - Hematite and goethite	330
7.4.3.2.2 - Cuprite, native copper and malachite	330

Page

7.4 - Some further considerations of the ore mineralisation 330

7.5 - Summary of the model for sulphide mineralisation 332

References 334

Appendix I - Sample collection and nomenclature 360

Appendix II - H_2O and FeO determination 361

Appendix III - X-ray fluorescence analyses 363

III.1 - Sample preparation and operating conditions 363

III.2 - Results 365

Appendix IV - Electron probe analyses 390

IV.1 - Operating conditions 390

IV.2 - Silicate analyses 392

IV.3 - Ore mineral analyses 392

LIST OF FIGURES

			Page
Figure	1.1	Tectonic units and distribution of ophiolites in Turkey	3
	1.2	Plate tectonics model for the geological evolution of East Anatolia	7
	1.3	Geological map of SE Turkey and the cupriferous sulphide occurrences along the SE Anatolian ophiolite belt	8
	1.4	Location map of the two studied areas	10
	2.1	Geological map of the Polusagi area	12
	2.2	Idealised stratigraphic section and the sulphide mineralisation at Polusagi	27
	2.3	Geological map of the Canakci area	29
	2.4	Stratigraphic section at the Canakci area	32
	3.1	Scatter plots of the elements having non-linear variation with the immobile elements	55-67
	3.2	Variations of MgO, CaO and Sr with Fe_2O_3/FeO ratio	64
	4.1	Variation of CaO + MgO with SiO_2 and the subdivision of the rocks (Group A)	74
	4.2	Zr/TiO_2-Nb/Y discriminant diagram showing the Polusagi rocks and the fields delimited by Winchester and Floyd (1977)	76
	4.3	Cr/TiO_2 - Ce diagram showing the Polusagi rocks and the fields defined by Winchester and Floyd (1977)	77
	4.4	Normative colour index vs. normative plagioclase composition	79
	4.5	Triangular diagram of normative contents of Ab, An and Or for the Polusagi plagiogranites and the oceanic plagiogranites	81
	4.6	Total alkali vs. SiO_2 diagram for the Polusagi rock suite	87

			Page
Figure	4.7	Discriminant diagrams for the magma types	88-89
	4.8	AFM diagram showing the degree of iron-enrichment in the Polusagi rock suite as compared with the trends of some Alpine tholeiitic rocks	91
	4.9	The Polusagi rocks plotted on discriminant diagrams of Miyashiro	93-94
	4.10	Al_2O_3 wt% vs. normative plagioclase composition diagram for the basic rocks	96
	4.11	$MgO-Al_2O_3-(Fe_2O_3 + TiO_2)$ triangular diagram showing Fe-Ti enrichment in the Polusagi rock suite	96
	4.12	Polusagi basalts and gabbros plotted in the Zr/Y-Ti/Y diagram separating plate margin basalts and within plate basalts	99
	4.13	Ti-Zr-Y triangular discriminant diagram separating basic rocks from various tectonic settings	99
	4.14	Polusagi basalts and gabbros plotted in Ti-Zr diagram of Pearce and Cann (1973)	101
	4.15	Group A and B basalts and gabbros plotted in Ti-Cr diagram of Pearce (1975)	103
	4.16	Ni vs. Ti/Cr for the group A and B basalts and gabbros	104
	4.17	La vs. Nb	104
	4.18	Comparison of proportions of volcanic rock types	108
	4.19a	K_2O vs. SiO_2 contents of the Polusagi rock suite	110
	4.19b	Rb vs. SiO_2 for the Polusagi rocks	110
	4.20	Geochemical patterns of some present day marginal basin and back arc basin basalts as compared with the Polusagi "more primitive" basalts	114
	4.21	Geochemical patterns of some present day island arc tholeiites as compared with the "more differentiated" basalts	116
	4.22	Geochemical patterns of Western Mediterranean ophiolitic basalts, compared with the "more primitive" basalts	120

			Page
Figure	4.23	Geochemical patterns of basaltic rocks from Eastern Mediterranean ophiolites as compared with the "more differentiated" basalts	121
	5.1	Two possible mechanisms of back-arc opening	125
	5.2	Variations in the partial melt composition and enrichment factors of incompatible elements as a result of melting of a garnet lherzolite source	131
	5.3	Zr vs. total Fe/Mg ratio for the Polusagi rocks	133
	5.4a	CaO/TiO_2 vs. TiO_2	138
	5.4b	Al_2O_3/TiO_2 vs. TiO_2	138
	5.5	Element variation trends with increasing Zr concentrations in the Polusagi rock suite	143-152
	5.6	Ce vs. Ce/Y ratio in the Polusagi rock suite	159
	5.7	Zr vs. Cr/Ni ratio for the basic rocks	159
	5.8	Fractionation trends of the Polusagi rocks	160
	6.1a	Classification and chemical variation of clinopyroxenes from basalts and andesites in the system Diopside-Hedenbergite-Ferrosilite-Enstatite	167
	6.1b	Same as above for clinopyroxenes from the "more primitive" gabbros and "more differentiated" gabbros	167
	6.2	Chemical variation in clinopyroxenes from volcanics and gabbros with Mg-number	169-170
	6.3	Si vs. Al in clinopyroxenes from volcanics and gabbros	174
	6.4	Tetrahedrally co-ordinated Al vs. octahedrally co-ordinated Al in clinopyroxenes from volcanics	175
	6.5	Ti vs. Na in clinopyroxenes	175
	6.6	Na vs. octahedrally co-ordinated Al in clinopyroxenes from volcanics and gabbros	177
	6.7	Whole-rock Mg-number vs. clinopyroxene Mg-numbers	177

			Page
Figure	6.8	Clinopyroxene analyses plotted in the ternary diagram of Le Bas (1962)	181
	6.9	SiO_2 vs. Al_2O_3 for clinopyroxenes from volcanics and gabbros	181
	6.10	Clinopyroxene analyses plotted in Al_z vs. TiO_2 diagram of Le Bas (1962)	182
	6.11	Al^{iv} vs. (Al^{vi} + Fe^{3+} + Ti) classification diagram for amphiboles	188
	6.12	Al vs. (Na + K) classification diagram for amphiboles	188
	6.13	Mg-number vs. Si classification diagram of Leake (1978) for Ca-amphiboles	190
	6.14	Mg-number vs. Si classification diagram of Leake (1978) for Ca-amphiboles	190
	6.15	Chemical variation in amphiboles with Mg-number	192-194
	6.16	Al^{iv} vs. (Al^{iv} + Fe^{3+} + 2Ti) in amphiboles	196
	6.17	Na_{M4} vs. (Al^{vi} + Fe^{3+}) in amphiboles	196
	6.18	Na_{M4} vs. A site occupancy in brown hornblendes	198
	6.19	A site occupancy vs. Ti in brown hornblendes and green amphiboles	198
	6.20	Diagram showing the charge balancing as a result of coupled substitution reactions in amphiboles	199
	6.21	Whole-rock Mg-number vs. amphibole Mg-number	201
	6.22	Al^{iv} vs. Al^{vi} in amphiboles	201
	6.23	Actinolites plotted in Crossite content (Na_{M4}) vs. Al^{iv} diagram of Brown (1977)	204
	6.24	Diagram for the nomenclature of unoxidised chlorites	210
	6.25	Al^{iv} vs. Al^{vi} in chlorites	211
	6.26	Al^{vi} vs. (Fe^{2+} + Mg + Mn) in chlorites	211
	6.27	Fe^{2+} - Mg variation in chlorites	213

			Page
Figure	6.28	Variation of Al^{iv} with Mg-number in chlorites	214
	6.29	Variation of total Al with Mg-number in chlorites	214
	6.30	Whole-rock Mg-number vs. chlorite Mg-number	217
	6.31a	Al^{iv} vs. Mg-number in chlorites	219
	6.31b	Total Al vs. Mg-number in chlorites	219
	6.32	Plagioclase analyses plotted in ternary feldspar diagram	223
	6.33	Fe^{3+} vs. Al in epidotes	228
	6.34	Total Fe (as $Fe^{3+} + Fe^{2+}$) vs. Al in epidotes	228
	6.35	$(Fe^{3+} + Fe^{2+})$ vs. Al in prehnites	232
	6.36	Mg-Al-Fe^{total} triangular diagram showing the compositional variation in pumpellyites	238
	6.37	$(Fe^{3+} + Fe^{2+})$ vs. (Al + Mg) in pumpellyites	239
	6.38	Metamorphic zones in the Polusagi area	243
	6.39	Mineral abundances in the metamorphic zones	247
	7.1	As vs. Sb (+ Te + Bi for Canakci) diagram for the fahlore group	319
	7.2	Fe-Zn variation diagram for the fahlore group	319
	7.3	Classification diagram for tetrahedrite-tennantite series on the basis of relative proportions of Fe and Zn in the "B" site	321
	7.4	Tennantite analyses from Polusagi and Canakci plotted in the classification diagram	321

LIST OF TABLES

			Page
Table	3.1	Mobility of elements as inflicted by main alteration processes	42
	3.2A	Correlation matrix for Group A volcanics	50
	3.2B	Correlation matrix for Group B volcanics	51
	3.2C	Correlation matrix for Group C volcanics	52
	3.3	Element mobility directions	65
	3.4	Correlation matrix for the hypabyssal rocks	67
	3.5	Mobility of elements in the Polusagi rocks	68
	4.1	Group A rock compositions	83
	4.2	Average compositions of subdivided basalts, andesites and gabbros	84
	4.3	Comparative chemical data from known tectonic settings and ophiolites	112-113
	5.1	Mineral/liquid distribution coefficients	157
	6.1	Chemical analyses of zoned cpx grains	172
	6.2	Chemical formula calculations in amphiboles	186
	6.3	Chemical formula calculations for the pumpellyites	236
	7.1	Chemical composition of Fe-Mn rich cherts	290
	7.2	Range and average element concentrations in pyrite, chalcopyrite and sphalerites	302
	7.3	Range and average element concentrations in galenas and bornite	306
	7.4	Comparative chemical data on mawsonite and hexastannite	310
	7.5	Composition of colusite and related sulphides	314
	7.6	Range and average element concentrations in fahlores	317
	II.1	FeO and water determinations by wet chemical methods	362
	III.1	Operating conditions for PW 1400 x-ray spectometer	364
	III.2.1	Group A - whole rock analyses	366
	III.2.2	Group B - whole rock analyses	374
	III.2.3	Group C - whole rock analyses	378
	III.2.4	Fe-Mn - oxide rich cherts whole rock analyses	381
	III.3.1	Group A rocks - normative tables	382

			Page
Table	IV.1	Optimum analysing conditions and standards used for electron microprobe analyses	391
	IV.2.1	Clinopyroxene analyses	393
	IV.2.2	Amphibole analyses	401
	IV.2.3	Chlorite analyses	407
	IV.2.4	Plagioclase analyses	415
	IV.2.5	Epidote analyses	424
	IV.2.6	Prehnite analyses	428
	IV.2.7	Pumpellyite analyses	430
	IV.3.1	Pyrite analyses from Polusagi	431
	IV.3.2	Chalcopyrite analyses from Polusagi	434
	IV.3.3A	Sphalerite analyses from Polusagi	435
	IV.3.3B	Sphalerite analyses from Canakci	437
	IV.3.4A	Galena analyses from Polusagi	438
	IV.3.4B	Galena analyses from Canakci	439
	IV.3.5	Bornite analyses from Canakci	440
	IV.3.6	Mawsonite analyses from Canakci	441
	IV.3.7	Hexastannite analyses from Canakci	442
	IV.3.8	Colusite analyses from Canakci	443
	IV.3.9A	Fahlore analyses from Polusagi	445
	IV.3.9B	Fahlore analyses from Canakci	449
	IV.3.10	Magnetite analyses from Polusagi	451
	IV.3.11	Chromite analyses from Canakci	452
	IV.3.12	Gold analyses from Canakci	453
	IV.3.13A	Idaite-chalcopyrite intergrowth analyses from Polusagi	454
	IV.3.13B	Idaite-chalcopyrite intergrowth analyses from Canakci	454

LIST OF PLATES

			Page
Plate	2.1	A general view of the Polusagi area	13
	2.2	Calc-schist-red-schist transition with fragments and angular blocks of calc-schist within the overlying red-schist	17
	2.3	Large pillow lavas at Hasenak Deresi	20
	2.4	Pillow lavas at Hasenak Deresi, located above the banded massive sulphides with muddy and cherty brown-red sediments filling the interstices	20
	2.5	Coarse mineralogical banding in the Polusagi massive sulphides	25
	2.6	Same as Plate 2.5	25
	2.7	A general view of the Canakci area	30
	6.1	Clinopyroxene being replaced by brown amphibole	165
	6.2	Fibrous amphibole replacing euhedral clinopyroxene	165
	6.3	Large euhedral brown amphibole being replaced by chlorite around the margins	165
	6.4	Brown amphibole being gradually taken over by green amphibole	165
	6.5	Albitised plagioclase laths and chlorite groundmass	207
	6.6	Gas vesicle filled with precipitation of chlorite followed by epidote	207
	6.7	Phenocrystic plagioclase, albitised then replaced by chlorite, sericate and prehnite	207
	6.8	Typical amygdoidal prehnite	207
	6.9	Gas vesicle filled with pumpellyite showing radial extinction	234
	6.10	Calcite with opaque inclusions	234
	6.11	Round quartz grains within chlorite	234
	6.12	Ti-rich magnetite being replaced by fibrous amphibole	234
	7.1	Fe-Mn rich sedimentary band and framboidal pyrite band boundary	265
	7.2	Microbands of chalcopyrite (+ pyrite) and gangue in sphalerite rich matrix	265
	7.3	Sharp boundary between the coarse sphalerite (+ chalcopyrite) rich band and chalcopyrite (+ pyrite) rich band	267

			Page
Plate	7.4	Aligned chalcopyrite exsolution in sphalerite rich matrix	267
	7.5	"Strings" of fine grained pyrite in chalcopyrite matrix	268
	7.6	Alternating, fine pyrite and sphalerite rich micro-stratifications	268
	7.7	Warping of fine grained delicate pyrite and gangue rich bands in chalcopyrite matrix by large and competent pyrite grains	269
	7.8	Warping of fine grained pyrite and gangue rich microbands in sphalerite matrix by a large fragment of gangue material	269
	7.9	Large aggregates of porous pyrite composed of fine pyrite crystals and gangue material	273
	7.10	Fine porous pyrite, chalcopyrite and gangue grading into coarser pyrite in a dominantly chalcopyrite matrix	273
	7.11	Crystalline euhedral pyrite in a gangue rich matrix containing numerous chalcopyrite inclusions	273
	7.12	Euhedral pyrite with chalcopyrite, sphalerite and gangue inclusions along growth zones	273
	7.13	Framboidal pyrite starting to recrystallise with chalcopyrite filling the interstices	274
	7.14	'Rosettes' or 'spheroids' of pyrite with hematite, galena and chalcopyrite cores	274
	7.15	Porous and colloform fine grained pyrite in chalcopyrite and gangue rich matrix, showing concentric and radial growth surfaces	275
	7.16	Porous and colloform pyrite in sphalerite and chalcopyrite rich matrix	275
	7.17	A general view of massive sulphides at Polusagi	281
	7.18	Fractured euhedral pyrite grains with inclusions along cubic growth zones, embedded in chalcopyrite which fills the cracks without apparent replacement	282
	7.19	Large euhedral pyrite with sphalerite, chalcopyrite and gangue inclusions concentrated along grain boundaries of pyrite	282

			Page
Plate	7.20	Etched euhedral pyrite with framboidal pyrite remains	282
	7.21	Porous pyrite transforming into better crystalline coarser pyrite within the "soft" chalcopyrite matrix	282
	7.22	Porous pyrite becoming progressively coarser towards the chalcopyrite rich matrix	285
	7.23	Oriented chalcopyrite exsolution in sphalerite	285
	7.24	Hematite, euhedral magnetite and chalcopyrite inclusions in sphalerite matrix	285
	7.25	Hematite laths in chalcopyrite	285
	7.26	'Honeycomb' textured colloform growth of silica in Fe-Mn rich siliceous sediments	287
	7.27	Extremely fine grained silica spheroids in the siliceous matrix	287
	7.28	Extremely fine hematite micro-crystals aligned in bands in the siliceous matrix of Fe-Mn rich sediments	288
	7.29	A typical view of the Canakci massive sulphides	288
	7.30	Large euhedral pyrite with inclusions of galena, sphalerite, bornite and some chalcopyrite, concentrating in the centre	295
	7.31	Pyrite grain with concentric "shrinkage" cracks now filled with bornite which is partially replaced by digenite	295
	7.32	Cataclastic texture of pyrite with a preferred orientation of shattering	295
	7.33	Mawsonite in bornite	295
	7.34	Colusite associated with bornite and pyrite	311
	7.35	Gold streak in tennantite	311
	7.36	Extremely fine intergrowth of chalcopyrite and idaite	311
	7.37	Bornite being replaced by digenite along numerous veins with a "mosaic" texture	311

CHAPTER ONE

INTRODUCTION

1.1 Introduction

The subject of this thesis, the geology and geochemistry of certain sulphide deposits in the province of Malatya, central SE Turkey, was suggested by the Mineral Research and Exploration Institute of Turkey (MTA), a state-owned establishment. The writer visited a number of reported ore mineral occurrences and subsequently detailed mapping and sample collecting work was carried out in the areas around the villages of Gevenis and Canakci during summer 1978, and Polusagi during summer 1979, all within 40 km (aerially) east-southeast of the provincial capital, Malatya.

The main purpose of this work is to gain an insight into the setting, geology and genesis of the mineralisations in the studied areas. However, the mineralisation in the Gevenis area proved to be unimportant and is mainly a scattered and minor fracture filling pyritic mineralisation associated with a complex mixture of volcanics, volcanogenic sediments and acid intrusions. On the other hand, the mineralisation at the other areas include massive, poly-metallic (mainly Fe-Cu-Zn) sulphide mineralisation as well as 'stockwork' type disseminated ore occurrences. Therefore, the work carried out around the village of Gevenis is not included in this study and the thesis is concerned with the relatively important sulphide mineralisations and associated rocks in the Polusagi area and to a lesser extent the Canakci area.

1.2 A brief review of regional structure and ophiolites in Turkey

There have been many attempts at dividing Turkey into tectonic units and today the most commonly accepted division is based on Ketin (1966). He broadly divides the country into four major units : The Pontids, the

DURHAM UNIVERSITY
23 SEP 1982
SCIENCE LIBRARY

Anatolids, the Tauridsand the Border Folds (Iranids) which are roughly parallel to each other in an east-west direction. See Fig.1.1.

a) The Pontids or the Northern Anatolian Folds (Ilhan, 1971): This unit mainly contains unmetamorphosed fossiliferous marine formations from the Silurian to the Pliocene. Some of the oldest mountains, the Caledonian and Hercynian massifs,occur in this zone in addition to the early Alpine orogenic movements. At the beginning of Mesozoic, the area was locally raised above sea-level as islands, while the rest of Anatolia was still under water.

b) The Anatolids: This unit comprises the intermediate folds and the middle and western Anatolian crystalline massifs and some ophiolites developed at the end of the Cretaceous. It is relatively free from pre-Alpine movements.

c) The Taurids or the Southern Anatolian Folds: This belt is the westward extension of the southern Alps, the Apennines and the fold zones of Yugoslavia, Albania and southern Greece,which then passes to the east into the Zagros Crush Zone in Iran. It mainly consists of marine sediments from the Ordivician up to the Miocene. Two major crystalline massifs, the Puturge Massif, SE of Malatya,and the Bitlis Massif further towards the east occur in the zone lying parallel to the general trend. The alpine movement reached its peak at the end of the Cretaceous and the Taurus mountain range, which gives its name to the unit, assumed its main form after the Miocene.

d) The Border Folds: This region appears to have formed by continued sedimentation from the Pre-cambrian to late Pliocene. Shallow water sediments generally did not suffer metamorphism or magmatic activity. This unit is the NW extension of the Middle East foredeep belts and in the north, it is separated from the orogenic belt by a significant thrust zone.

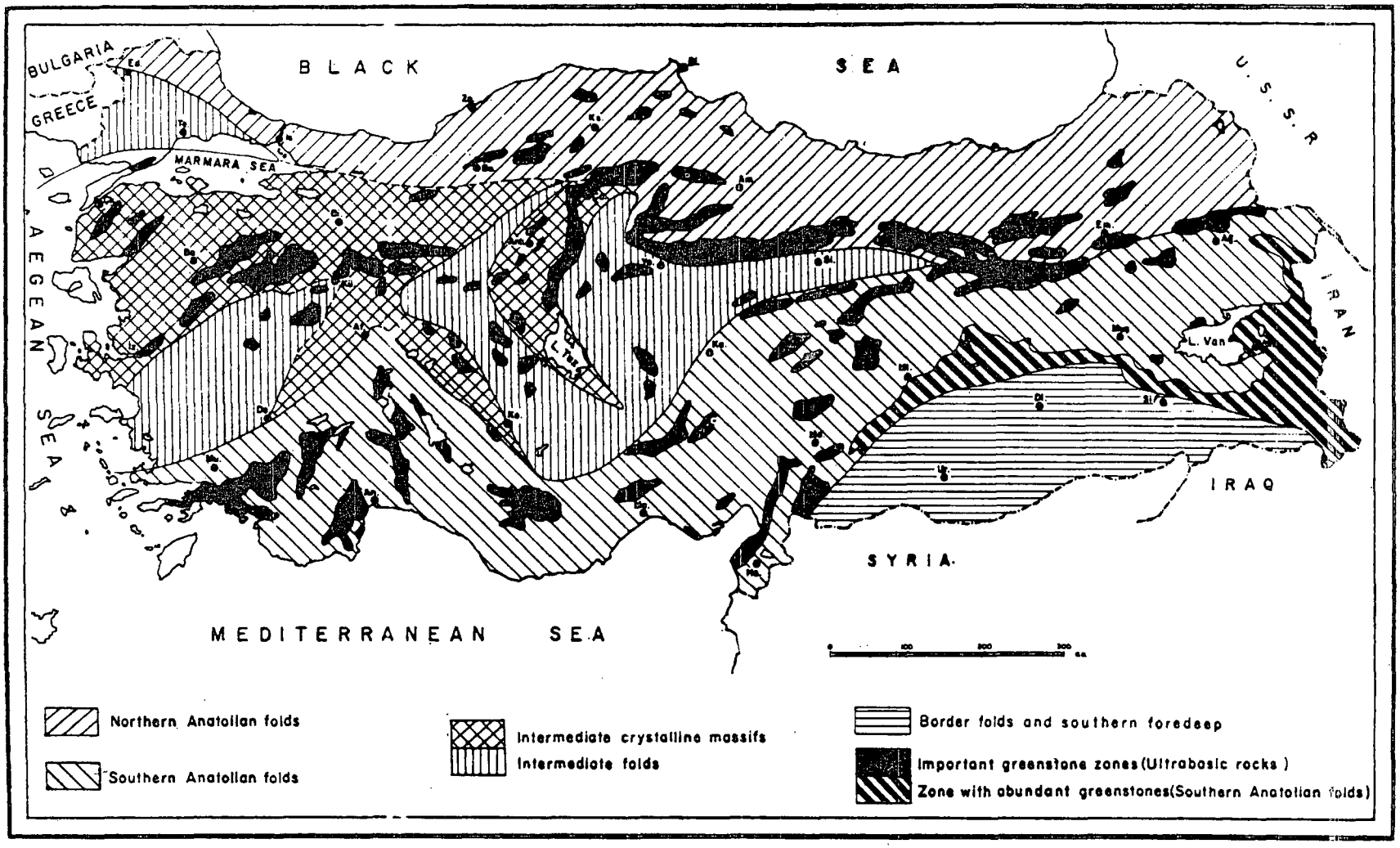


Fig.1.1 Tectonic units and distribution of ophiolites in Turkey (after Ilhan, 1971)

According to Ketin (1966) the tectonic-orogenic evolution of Anatolia proceeded gradually from the north to the south i.e. the first stronger and effective movements began in the Northern ranges and passed towards central Anatolia, then to the Taurids and the southern Border Folds.

The Northern and the Southern Anatolian Folds form the major fold patterns in Turkey. The areas between the major branches of these folds are occupied by less intensively folded areas which are predominantly metamorphic and plutonic rocks forming stable areas such as the Menderes and Central Anatolian Massifs. The minor folds in these areas extend in directions different from those in the Pontids and the Taurids.

The above outlined orogenic belts in Turkey also show strong affiliations with ophiolites and melange zones (Fig. 1.1). The ophiolitic series follow the tectonic boundaries and show striking parallelism to the main earthquake zones. The major ophiolitic zones are briefly described below:

a) The Northern Anatolian ophiolites follow the internal zone of the North Anatolian Folds (the Pontids) and in the east they join the ophiolites occurring within the internal sectors of the Southern Anatolian Folds (the Taurids).

b) The Central Anatolian ophiolites mainly consist of ultrabasic occurrences scattered over the border sections of the folds and the Central Anatolian Massifs.

c) SE Anatolian ophiolite zone: This belt occurs in the Southern Anatolian Folds as an eastward extension of the Troodos ophiolite in Cyprus and continues south-eastward into Iraq and the Zagros Mountains Crush Zone in Iran, passing into Oman and finally to the Himalayas. This ophiolitic zone separates the Taurids from the Border Folds. In general the ophiolites show upward sequences very similar to the typical

succession assumed for the oceanic crust i.e. ultramafics, gabbros sheeted dolerite dykes, pillow lavas and at the top, submarine sediments (Ileri et al, 1976). The ultramafic and basic rocks (dunites, harzburgites, gabbros, dolerites etc) are serpentinised, sericitised or schistose. They are associated with radiolarites, dark and green coloured flysch-like sediments, thin bedded limestones and exotic blocks of plutonic, metamorphic and sedimentary rocks. Large scale Alpine type structures such as thrusts, tectonic slides and nappes are extensive. For instance, crystalline rocks of the Bitlis Massif are thrust southward over the ophiolitic rocks and the Upper Cretaceous and Paleocene rocks of the Border Folds by at least 15-20 km (Stoneley, 1974).

The ophiolites of the inner sectors of the tectonic units are generally considered to be of early Mesozoic age, and the SE Anatolian ophiolites of Upper Cretaceous and Paleocene age (Baykal and Erentoz, 1966; Ilhan, 1971; Brinkman , 1972).

Ophiolitic rocks are generally considered to be obducted slices of past oceanic crust and the upper mantle (e.g. Dewey and Bird, 1970, 71; Gannser, 1974; Coleman, 1977). Studies over the SE Anatolian ophiolites and their westward and eastward extensions lead various workers to consider them as the suture line of the former Tethys Ocean (e.g. Stocklin, 1974; Dixon and Pereira, 1974). Such considerations of the ophiolites suggest that the stable Massifs of Anatolia are micro-plates between the major plates of Laurasia and Gondwanaland. Andesites, dacites and rhyolites of the eastern Pontids have been shown to have formed by island arc volcanism (Egin et al, 1979). The SE Anatolian ophiolites can, similarly, be interpreted as representative of the Tethyan ocean floor or island arcs or a complex combination of such tectonic settings. The Tethys Ocean started closing up in early Mesozoic times and probably continued until Oligo-Miocene times when the collision of the Anotolian

Massifs with the Arabian block occurred as a result of continuous movement of the Arabian Shield (then part of Gondwanaland) towards the Russian Platform (Laurasia). The oceanic floor of Tethys must have been consumed under the Anatolian micro-plate or plates when the Arabian block was moving northward, leading to the obduction of the oceanic rocks as ophiolites and melange deposits, and to orogenic belts and large scale Alpine type structures. The collision of the Arabian block with the Anatolian Massifs took place in Oligocene and Miocene times but the northward movement did not stop. The Anatolian Massifs then started moving northward with the Arabian block, forming another subduction zone beneath the eastern Pontid islands during the Pliocene; later the oceanic floor of the Black Sea was underthrust beneath the eastern Pontid Island Arc, producing yet another subduction zone. This plate tectonics model for the development of Eastern Turkey (Ataman et al, 1975) is summarised in Fig. 1.2.

1.3 Sulphide mineralisation along the SE Anatolian ophiolite belt

This belt, marking the boundary between the collided blocks of the Anatolian micro-plate or plates and the Arabian Shield, is also interesting and important in terms of mineral deposits and their relations and implications to the tectonics of the area. There are numerous occurrences of cupriferous mineralisation along this ophiolitic belt (Fig.1.3). The well known Ergani-Maden copper deposits (Griffitts et al, 1972; Ileri et al, 1976; Cagatay, 1977) which have been worked for around a thousand years, and the economically important pyrite-chalcopyrite-magnetite deposit of Madenkoy-Siirt (Calgin, 1976; Ozcelik, 1977) occur in this belt. Other relatively better studied sulphide deposits include the Karadere-Lice and Midyekoyu-Cungus occurrences (Cagatay, 1977). The sulphide occurrences at Polusagi and Canakci, province of Malatya, are the subject of the present study.

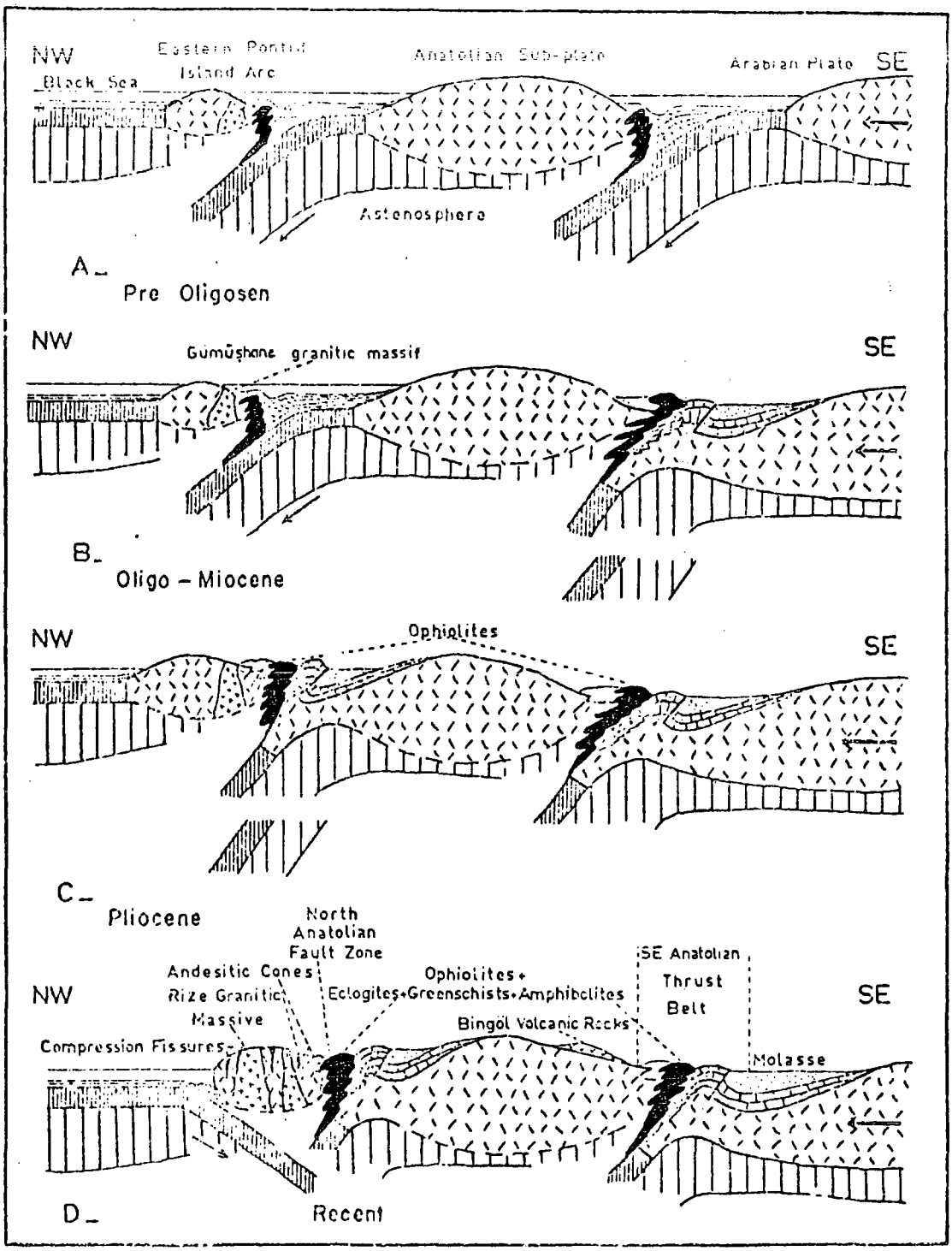


Fig.1.2 Plate tectonics model for the geological evolution of East Anatolia (after Ataman et al, 1975).

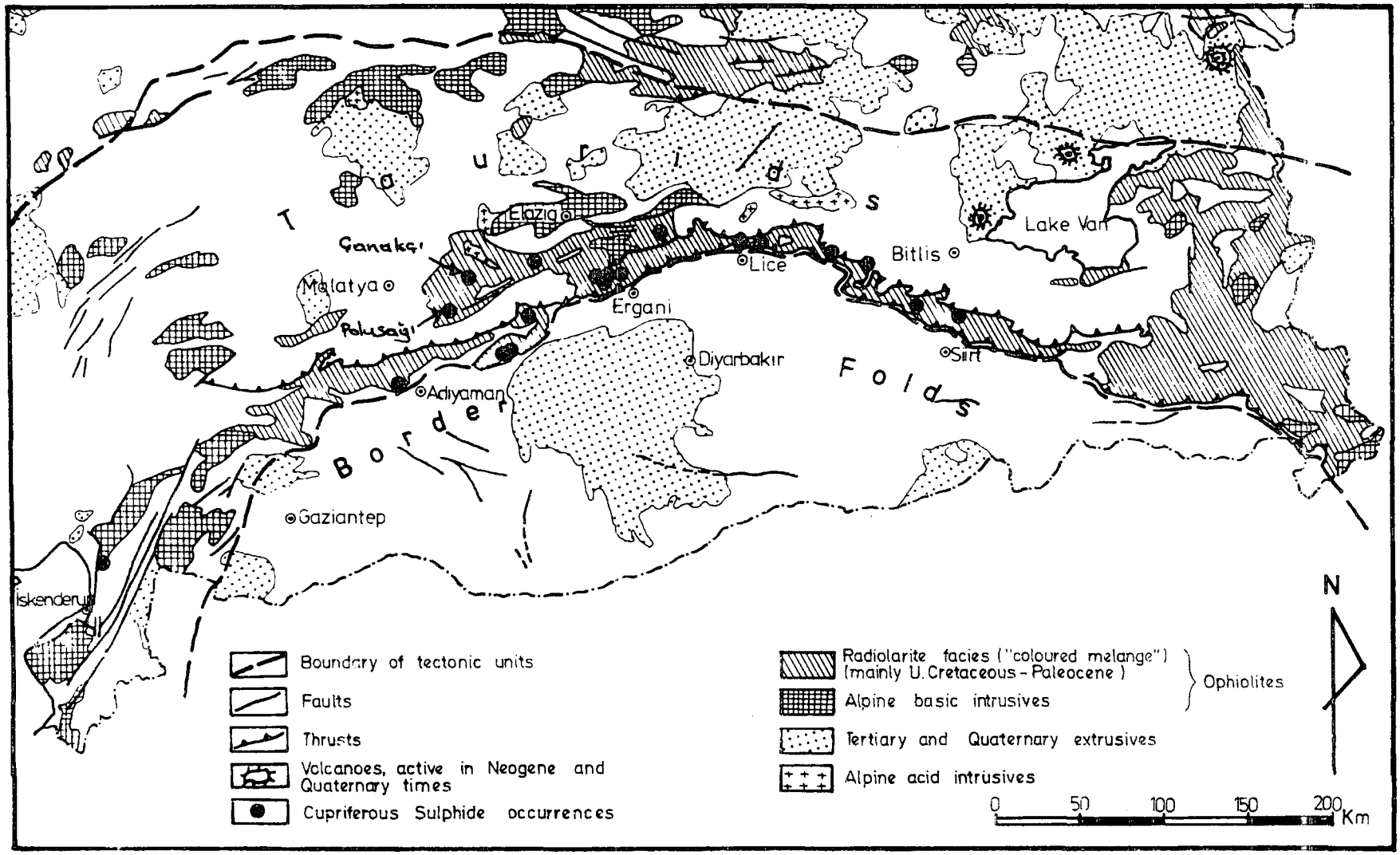


Fig.1.3. Geological map of SE Turkey and the cupriferous sulphide occurrences along the SE Anatolian ophiolite belt.

If the cupriferous deposits associated with the Troodos ophiolites are considered as occurring in a south-westward extension of the SE Anatolian ophiolite belt, it becomes clear that a chain of sulphide deposits occurs along the ophiolitic belt which shows similar characteristics. The Ergani-Maden deposits(Ileri et al, 1976) and the Madenkoy-Siirt deposit are of Cyprus type with similar ages, and are related to the volcanogenic activities of the Tethys ocean and to the tectonic evolution of the belt as a whole.

1.4 Location of the Polusagi and Canakci areas

The studied areas are on the Sivas sheet of the series of explanatory texts of the geological map of Turkey (scale 1 : 500000) and within what is described as the Upper Cretaceous ophiolitic rocks (Baykal and Erentoz, 1966) in the province of Malatya, SE Turkey. The Polusagi area is situated 30 km (aerially) to the SE and the Canakci area 40 km to the east of the provincial capital, Malatya (Fig. 1.4). Both areas are accessible through a stabilised road for roughly the first half of the distances and thereafter by non-stablised roads. Access to the areas during the winter months can be difficult.

The topography in general is ragged and the vegetation is poor. Hot and dry summer months are followed by wet, cold and snowy winters.

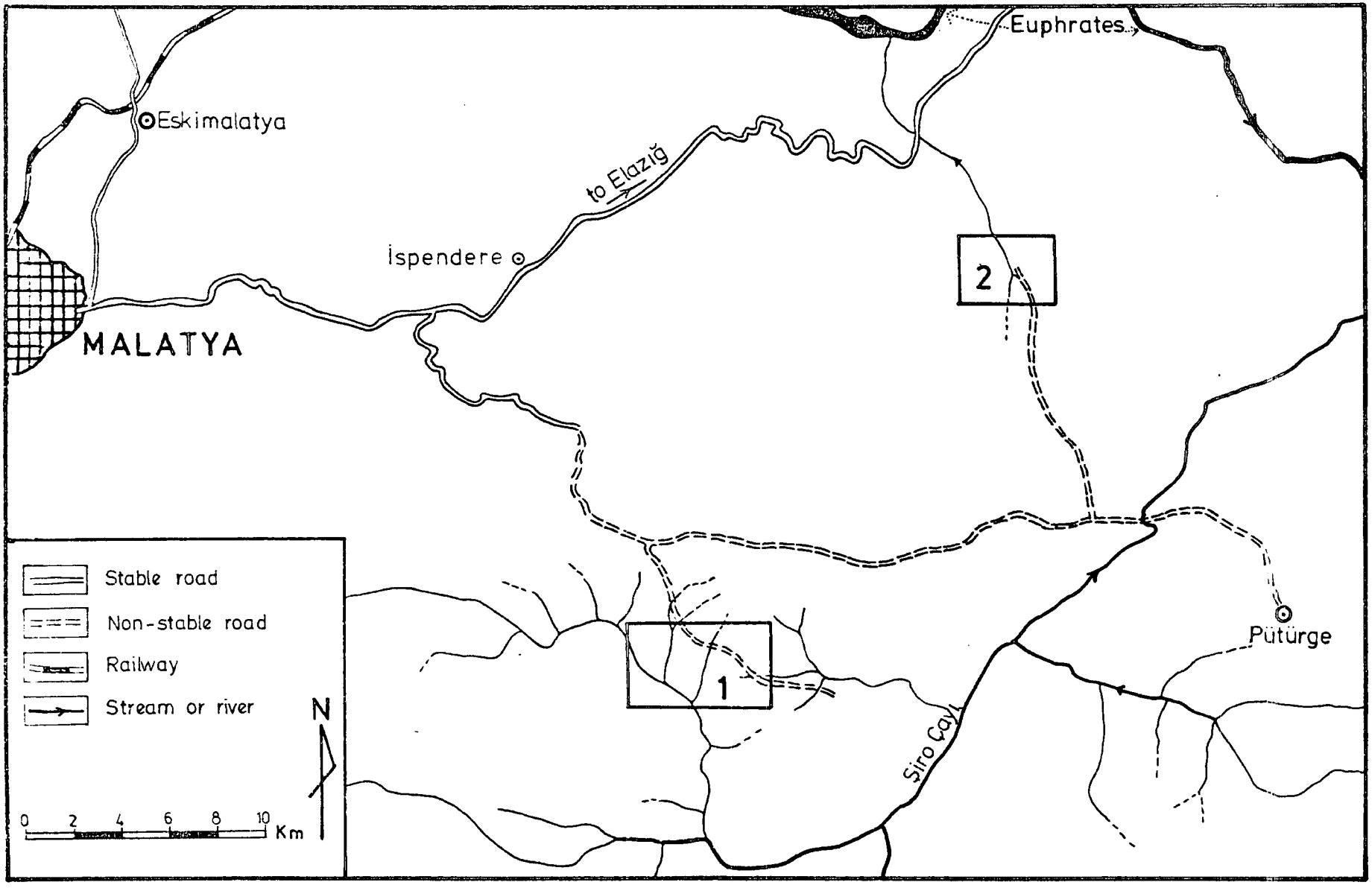


Fig. 1.4 Location map of the two studied areas : 1) Polusagi and 2) Canakci

CHAPTER TWO

ROCK UNITS AND FIELD RELATIONS

2.1 The Polusagi area

2.1.1 Introduction

The first notable geological work in the area was undertaken by Etibank (a state owned mining company) in 1968 and 1969 to explore the economic potential of the sulphide mineralisation. The work included some geophysical surveys, detailed mapping, small scale excavations and four drilling projects with a total depth of 566 m, completed in 1969. Unfortunately the drill cores were not available for inspection but an unpublished report (Buyukyanbolu, 1969) gives an account of the work carried out by Etibank. Yazgan (1969,1972) made a detailed petrographic study of the rocks around and including the area presently described. MTA started geological work on the area in 1978 and detailed mapping and small excavations over the sulphide exposures were being carried out when the writer visited the area in July-August 1979 for 5 weeks. The writer completed a map of the area,with a scale of 1:10000 and covering 21 km^2, within this period which is enclosed in the back-pocket (Map 1). See Fig.2.1.

The mapped area is rectangular in outline and the main topographic features are the Gelipolan stream with its main tributaries the Hasenak and Maden streams running roughly south, and the various peaks around the steep-sloped valleys of these streams. These streams join the Siro Cayi, the main local tributary of the Euphrates, to the south of the area. The topography is ragged and considerable landslides occur along the steep slopes of the Gelipolan and Maden streams. The altitude reaches its highest levels at Cuticalli Tepesi (1845 m) and Zer Tepesi (1840 m) and the lowest (below 1200 m) in the southern end of the Gelipolan stream. Peaks above 1700 m are common (Plate 2.1).

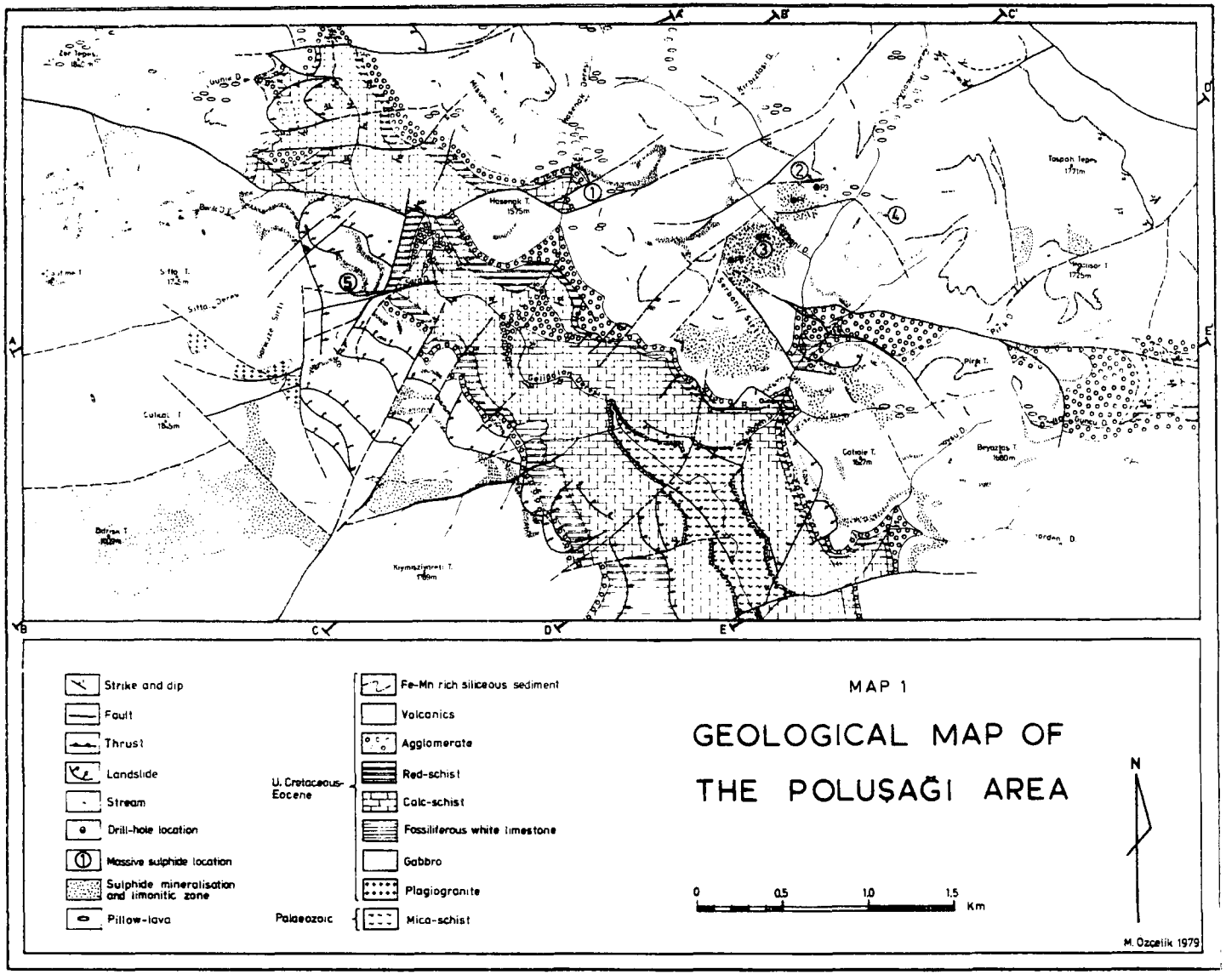


Fig.2.1. Geological map of the Polusagi area.



Plate 2.1 : A general view of the Polusagi area

2.1.2 Stratigraphy and the rock units

The rocks belong to two different age groups, the Palaeozoic basement crystalline series and the overlying Upper Cretaceous-Eocene ophiolitic series which are separated by a thrust plane (Yazgan, 1969,72). The ophiolitic volcano-sedimentary rocks are intruded by basic and acid igneous rocks. The stratification of the rocks from top to bottom is:

a) Agglomerates, to the north outside the mapped area (Yazgan, 1969,72)

b) Volcanic rocks containing Fe-Mn rich siliceous sediment levels and the sulphide mineralisation

c) Agglomerates

d) Red schists or argillites

e) Calc-schists

f) Fossiliferous limestone

T h r u s t p l a n e

g) Crystalline basement rocks

2.1.2.1 Crystalline basement rocks of Palaeozoic age

These rocks occupy a limited area and topographically the lowermost levels around the SE end of the Gelipolan valley. Yazgan (1972) considers them to be older than Permo-Carboniferous and differentiates these metamorphic rocks into 3 units. These units represent increasing grade of metamorphism from top to bottom and are briefly described below:

a) Arkosic greywakes: This is the least metamorphosed level and occurs immediately below the thrust plane. It is not a continuous horizon and may be missing. Schistosity is weakly developed. Fragments of plagioclase, K-feldspars and quartz with grain sizes around 1 mm occur in a clastic matrix with mica. Some quartz porphyryblasts may be up to 1 cm in diameter. Mylonitisation and cataclastic textures are common in the upper parts but disappear in the lower parts with better schistosity.

The other minerals found are hornblende, iron oxides, zircon and leucoxenised-sphene.

b) Upper mica-schists: This level is about 30 m thick and may occur directly below the thrust plane. It is green as opposed to the brownish underlying level, and characterised by the presence of chlorite and muscovite forming the schistose matrix for the alternating quartz and albite rich bands. The unit probably represents a metamorphosed pelitic sequence.

c) Lower mica-schists: The colour is grey-black to brownish due to the abundant biotite and white mica with well developed schistosity. This unit is widely distributed and the apparent thickness may reach 200 m around the mapped area. The upper parts of this level are characterised by porphyryblasts (around 1 mm) of albite with quartz, chlorite and iron-oxide inclusions, with occasional garnet and quartz in a matrix of biotite and white mica. In the lower parts the amounts and the sizes of garnet grains are increased (from 1 mm to 5 mm). The schistosity is pronounced. The unit is probably a metamorphosed pelitic sequence.

The presence of thin carbon-rich levels is taken by Yazgan (1972) to be evidence of a sedimentary origin for these rocks.

In the mapped area the basement rocks are mica-schists containing garnet, biotite, white mica and quartz corresponding to the Lower mica-schists described by Yazgan (1972). Due to the presence of the thrust plane, the relevance of the basement rocks to the overlying volcano-sedimentary rocks is uncertain.

2.1.2.2 Limestone

A greyish limestone, up to 10 m thick, covers the top of the crystalline basement rocks i.e. immediately above the thrust plane. At lower parts it consists of angular and unsorted fragments of the underlying metamorphic rocks bound together by a calcitic and sandy matrix.

The polycrstalline quartz grains and recrystallised nummilitic fragments around 5 mm in diameter are common. In places the limestone approaches a coarse unsorted sandstone. The cataclastic texture disappears towards the upper parts where it becomes a recrystallised normal fossiliferous limestone, relatively free from fragments of underlying rocks. According to Yazgan (1972) the nummilites are of Middle-Eocene age.

2.1.2.3 Calc-schists

These grey-green schistose rocks directly overlie the limestone with a gradational transition and may be up to 200 m thick. The poorly developed schistosity is parallel to bedding which is indicated by changes in colour, texture, grain size, and where it is interbedded with the other rock types. The calc-schists are basically made up of calcite, quartz and white mica and show detritic and clastic characteristics. They are normally very fine grained where quartz grains may be up to 200 microns in diameter, but generally less than 50 microns. Lenses of agglomerates are common which may be as thick as 50 m. Tuffaceous levels and interbedding with the overlying red-schists towards the top do occur. In places the fine bedding is disturbed and concorted, forming structures which suggest slumping. They sometimes show agglomeratic textures with no apparent fragments of volcanic material (Plate 2.2).

2.1.2.4 Red-schists

The calc-schists grade into this brownish, pinkish, reddish, purplish or sometimes greenish very fine grained schistose rock to which Yazgan (1972) gives the name "argillite". The average thickness is 50 m. These rocks contain less calcite but more fine grained quartz than the calc-schists, with a lot of iron-oxides, mainly hematite. The schistosity which has developed parallel to the bedding is mainly due to the alignment of white-micas. In places chlorite, prehnite, pumpellyite and some epidote may be the other important mineral phases. The reddish colour

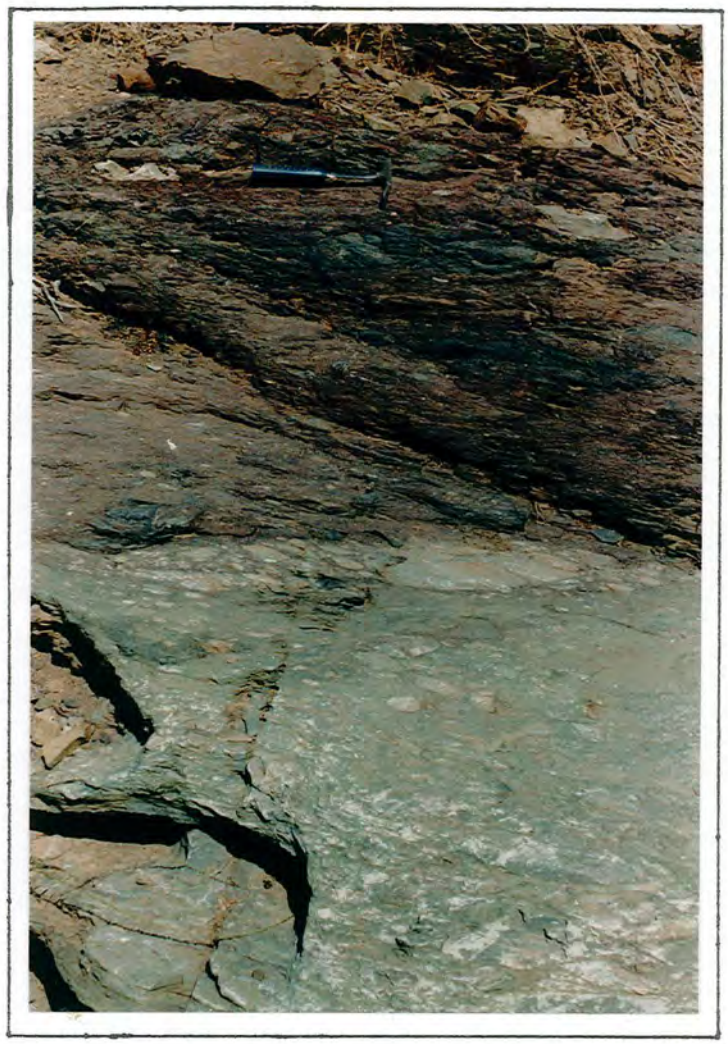


Plate 2.2 : Calc-schist-red-schist transition with fragments and angular blocks of calc-schist within the overlying red-schist.

of the rock is due to the presence of iron-oxides and the greenish colour to chlorite, so that alternating reddish colours with greenish levels may occur. Where very fine grained quartz (< 10 microns) and iron-oxides dominate, the rock resembles the Fe-Mn rich siliceous horizons occurring within the overlying volcanics.

The red-schists are banded with well sorted detritic material and the bands may be as thin as 10-15 microns. They contain thin tuffaceous lenses with occasional clinopyroxene grains. The slump structures seen in the calc-schists are also present in the red-schists.

2.1.2.5 Agglomerates

The agglomerates in the mapped area form a continuous horizon of variable thickness (20-50 m) over the red-schists. They are dominantly made up of fragments of volcanic material which are very similar to the overlying lava flows. The fragments reach sizes 30-40 cm in diameter and are cemented by a hematitic and calcitic matrix. Devitrified glassy materials, chlorite, albite and in some cases clinopyroxene and pumpellyite, are common constituents.

Immediately to the north of the field, agglomeratic levels cover large areas and Yazgan (1972) recognises three types on the basis of average grain size: a) Agglomerates, fragment size >64 mm, b) Lapilli-stone, size >2 mm and c) Tuff, where grain size is less than 2 mm.

2.1.2.6 Volcanics

These rocks are dark green coloured, fine grained and invariably aphyric lavas covering most of the mapped area. They are in two forms:

a) Pillow lavas: This form, indicating the sub-marine origin of the volcanism in the area, is common in the NE half of the mapped field. They are found on the Ger Tepesi , to the south of Pirik Tepesi and along the valleys of the streams, Hasenak Deresi, Seyhomer Deresi and around Kirbiztasi Deresi. The size of the pillows is variable and may be up to 2 m in diameter along the Hasenak Deresi. The margins are commonly

chloritised and the space between the pillows is commonly filled with red siliceous or muddy sediments (Plates 2.3 and 2.4).

b) Lava flows: This is the dominant form of the volcanics, but the recognition of individual flows is difficult. However, in many places discrete or relatively continuous thin bands or horizons of Fe-Mn rich cherty or muddy sediments occur within the lava pile, indicating a continued volcanic activity and representing the relatively quite periods during which they were deposited.

The volcanics are amygdoidal and the diameter of the amygdales rarely reaches 1 cm. They are filled with secondary minerals such as quartz, chlorite, calcite, prehnite, pumpellyite, epidote and occasionally pyrite.

In general, it is difficult to differentiate the basic, intermediate and acid volcanics into mappable units in the field. This is a result of relative scarcity of the acid extrusives and difficulty of separating basic and intermediate lavas created by secondary alteration and to some extent by extensive faulting. Therefore, no attempt was made to map the volcanics as various magmatic products, and their subdivision is discussed in Chapter four, on chemical grounds.

The volcanics are dominantly composed of plagioclase, clinopyroxene, amphibole, chlorite, quartz and calcite in varying proportions. The minor mineral phases include epidote, prehnite, pumpellyite, opaques, pyrite, sphene and small amounts of hematite. These minerals and their relations are discussed in Chapter six. Although the rocks are altered with the development of typically metamorphic minerals, it appears that clinopyroxene is an igneous relict phase and the textures exhibited by plagioclase grains, despite extensive alteration, are primary. The clinopyroxene does not occur in some lavas while it is abundant in others and the clinopyroxene poor lavas are relatively richer in albitised

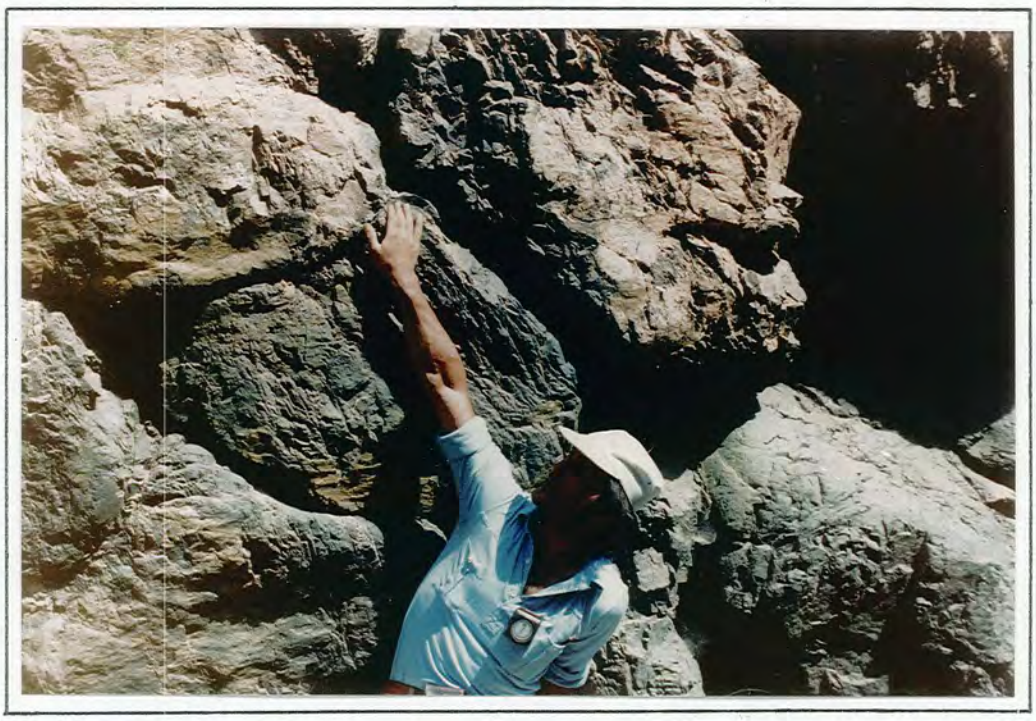


Plate 2.3 : Large pillow lavas at Hasenak Deresi. The pillow pointed at is overturned.



Plate 2.4 : Pillow lavas at Hasenak Deresi, located above the banded massive sulphides with muddy and cherty brown-red sediments filling the interstices.

plagioclases. Thus it is possible to separate the volcanics into 2 categories: a) those containing relatively abundant clinopyroxene (> 1-2%) and b) those lacking clinopyroxene but containing abundant plagioclase (crudely > 30%). This crude division corresponds to the chemical division between the basalts and andesites as discussed in Chapter four, section 4.2.2.

2.1.2.7 Hypabyssal rocks

These medium to coarse grained intrusive rocks occur within the volcanics in the west and south-west of the mapped area as scattered bodies. They show clear chilled margins against the volcanics. Yazgan (1972) considers them to be laccolithic in form. On the basis of mineralogy two types can be recognised:

a) Basic hypabyssal rocks: These are mainly composed of albitised plagioclase, clinopyroxene and amphibole and less importantly, chlorite and opaques (mainly magnetite and ilmenite). Minor phases include epidote, sphene and quartz. The grain size is generally around or less than 5 mm but occasional plagioclase grains may be up to 1 cm across. Yazgan (1972) describes them as gabbros.

b) Acid hypabyssal rocks: These rocks are dominantly made up of coarse plagioclase, up to 1 cm in diameter, with quartz. Chlorite, epidote, opaques and occasional amphibole grains are the minor phases. Yazgan (op cit) designates the term "syenites" to these rocks.

2.1.2.8 Fe-Mn rich siliceous sediments

These thin horizons are only found within the extrusives in the NE half of the mapped area and are apparently common further to the north (Yazgan, 1972). In general they form discontinuous and scattered bands less than 1 m thick; however, in the NE corner of the studied area, they are relatively continuous and may reach thickness up to 10 m. They are normally extremely fine grained, but in rare cases may be sandy. The colour varies from reddish to light-brown to dark brown or black. The

reddish colour is due to extremely fine grained hematite dust or particles spread into a silica rich matrix and the dark coloured material is rich in Mn-oxides which becomes black on weathering.

The reddish types are associated with the sulphide mineralisation or occur in the vicinity of it and may contain some disseminated or thin lenses of sulphide minerals. The dark or black coloured types occur normally away from the mineralisation and are free of sulphides. This feature may possibly be used as a guide to unexposed sulphide occurrences.

The dark coloured type is especially well banded in millimeter scale, exhibited by alternating lighter and darker shades of parallel stratification.

To the NW of the Megalisor Tepesi, there is an exposure of roughly 100 m x 200 m dimensions which is composed almost totally of a hematitic and very porous material. It contains no sulphides and possibly represents an oxidised pyritic body. However, its relevance to the Fe-Mn rich sediments or to the mineralisation is not understood and further work is necessary.

2.1.2.9 Sulphide mineralisation

The sulphide mineralisation is exclusively within the volcanic rocks and mostly occurs in the NW half of the mapped area. There are extensive limonitic zones, marked on Map 1.(Fig.2.1). The mineralisation was exploited to a limited extent, probably by the Armenians at the end of the last century. Limited amounts have also been mined by a small company in the last few decades with crude and primitive methods.

3 types of sulphide mineralisation are recognised in the field:

1) Stockwork mineralisation: This type is basically a fracture and less commonly fault filling pyritic mineralisation accompanied by silicification and to a lesser extent chloritisation. Disseminated or semi-massive forms in a siliceous matrix are typical. There is also a certain amount of replacement of the host volcanics by pyrite and quartz.

This type of mineralisation is typically seen on the Serbani Sirti and along the Serbani stream, and is responsible for the relatively extensive limonitisation there.

2) Massive sulphide mineralisation: There are 5 different localities where massive ore exposures are found in the area, see Fig.2.1. At each locality, the massive ore had been exposed by small scale excavations, however, only at localities 1 and 2 was the writer able to observe the mineralisation and collect samples in situ. At the other localities the exposures were buried by scree and debris and the samples were collected from loose fragmentary ore material.

Locality 1 (Hasenak Deresi): The massive ore overlies a weakly developed stockwork type mineralisation. The thickness varies from 0.3 to 1.5 m and, due to faulting, the lateral extent is unknown but is at least 50 m long. The mineralisation, broken and displaced by faulting in a number of places, is intimately associated, mixed and overlain by a red siliceous sedimentary horizon of similar thickness.

Locality 2: The massive ore occurs stratigraphically at the top of the stockwork mineralisation at Serbani Sirti and to the north of the Serbani stream. Similar to locality 1, it is associated with a red cherty sedimentary horizon. The thickness of the massive ore is around 1 m. It is separated from the overlying lavas by a fault.

The following features of the massive ores can be generalised:

a) The massive ore is a compact fine grain material, composed dominantly of pyrite, chalcopyrite and sphalerite. The individual grains are normally around or below 0.5 mm in diameter.

b) They are associated and overlain by the red hematitic cherty bands and occur towards and at the top of the stockwork mineralisation. The transition from the pyritic stockwork mineralisation is gradational through an increase in the sulphide/gangue ratio and Cu and Zn content.

c) In most cases they show strong mineralogical banding where pyrite- or chalcopyrite- or sphalerite-rich bands may be up to 1 cm thick (Plates 2.5 and 2.6). The bands are sometimes disturbed, concorted or churned around larger and probably more compact fragments of either cherty sediments or other gangue materials.

d) The volcanics stratigraphically above the massive ore horizons are generally not mineralised while those below i.e. where stockwork mineralisation typically occurs, are more extensively altered, silicified, kaolinised and chloritised.

3) Stratified disseminated sulphide mineralisation: This type is typically seen on the western flank of the Gelipolan stream and around Cuticalli Tepesi, where they form two horizons, up to 10 m thick, parallel to the general bedding. The mineralogy is generally one of disseminated pyrite, with grains around or less than 1 mm, which is accompanied by silicified volcanics. This type also forms thin and discontinuous lenses in various places. Around Catiole Tepesi, the levels are underlain by stockwork type mineralisation and contain small amounts of chalcopyrite and sphalerite, showing mineralogical banding. There, the mineralisation is spacially associated with discrete and thin red cherty sedimentary lenses. This type is considered to be a transitional form of the other two types.

2.1.3 Structural geology

Despite the relatively simple stratigraphy, the area possesses some structural complexity. The presence of the thrust plane between the Palaeozoic basement rocks and the overlying Upper Cretaceous-Eocene rocks is accepted by all the previous workers (Buyukyanbolu, 1969; Yazgan, 1969,72). The extent of the movement along the thrust plane is unknown.

There are numerous major and minor faults in the area generally running in E-W and NEE-SWW directions. The rocks on the steep slopes of



Plate 2.5 : Coarse mineralogical banding in the Polusagi massive sulphides. Grey-dark-grey bands are sphalerite rich, lighter bands are pyrite-chalcopyrite rich and black is gangue. Sample : P72B, field width = 37mm.



Plate 2.6 : Same as above. Sample : P211B, field width = 37mm.

the valleys of the Gelipolan and Maden streams are considerably displaced by landslides which make it difficult to take reliable dip or strike measurements. Nevertheless, the sedimentary rocks above the thrust plane, the Fe-Mn rich siliceous sediments within the volcanics and rarely the pillow lavas, do allow certain structural measurements and these are marked on Map 1 and used to construct the cross-sections included in the back-pocket (Cross-sections 1). Although the dip and strike values show some variations, the rocks are broadly tilted towards NE with dips varying in the range 20-45°. There is no apparent large scale folding.

The major structural problem concerning the area was introduced by Yazgan (1969,72) who states that the rock sequence above the thrust plane is overturned. Probably the most serious criteria he uses is the overturned position of some of the pillow lavas in the area (Plate 2.3). However, the pillow lava occurrences within the mapped area and to the north are generally disturbed, probably due to sub-marine slumping or tectonic movements so that it is possible to recognise overturned and upright positioned pillows within the same exposure. Some exposures indicate widely variable dip and strike values for the pillows. These features suggest that the structural measurements obtained from the pillow-lavas should be treated with caution, and even if some pillows are overturned they represent local disturbances. Furthermore, some rare graded bedding structures in the ophiolitic sediments imply an upright position. Therefore, it is thought that the rocks in the mapped area are the right way up. However, the detailed structural features and their implications for the full evaluation of the extent of the sulphide mineralisation in the area remain in need of further work.

2.1.4 Summary and conclusions

An idealised stratigraphic section of the rocks and mineralisation in the area is presented in Fig.2.2.

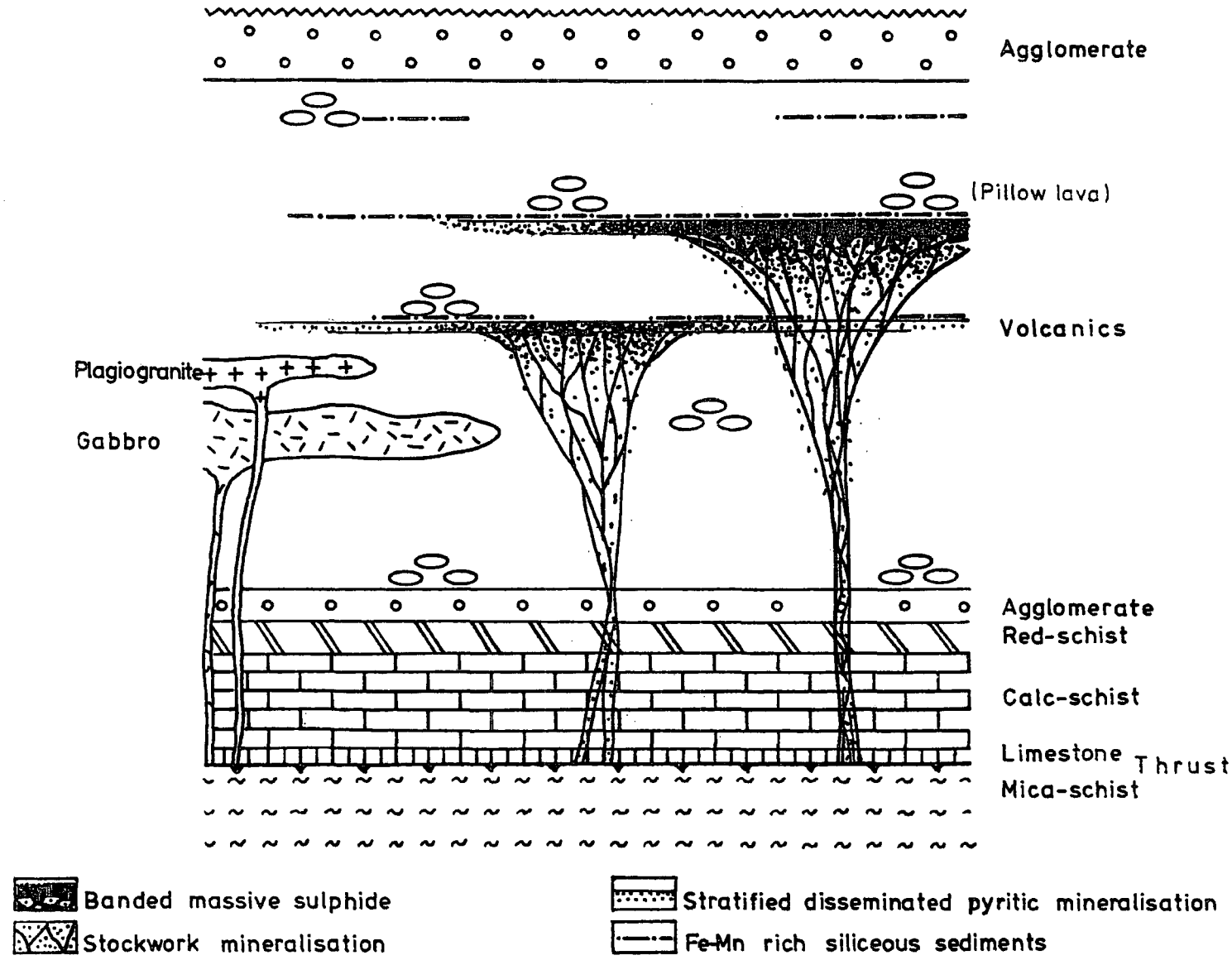


Fig.2.2 Idealised stratigraphic section and the sulphide mineralisation at Polusagi.

It is apparent from the pillow lavas and conformable and gradational features that the younger rock sequence above the thrust plane is produced as a result of sub-marine volcanism and associated sedimentation. Considering that these rocks belong to an ophiolitic sequence, the lack of sheeted dykes and the ultrabasic rocks and the presence of volcanogenic sedimentary rocks suggest that the sequence represents the uppermost levels of a fully developed ophiolitic section. If it is accepted that ophiolites represent obducted oceanic crust, then the rocks belong to the layer 1 and probably the uppermost levels of Layer 2 of a typical oceanic crust (see Chapter five, section 5.1).

2.2 The Canakci area

2.2.1 Introduction

The first notable geological work in this area was started by the MTA in 1976 and included geophysical prospecting and geological mapping. Two drilling projects were carried out, CK1 in 1977 (140 m) and CK2 in 1978 (197 m) to explore the sulphide mineralisation.

The area was visited in September 1978 for two weeks by the writer and a geological map with a 1:5000 scale and covering an area of 12 km^2 was completed (Map 2, back-pocket; Fig.2.3). The highest altitudes are in the NE corner of the area reaching heights around 2400 m and altitudes above 2000 m are common. The lowest altitude (1600 m) is to the north of the area in the Dumkasik Deresi (stream) valley. The Sey Deresi, Hutan Deresi and Marz Deresi form the tributaries of the minor stream, the Dumkasik Deresi, which joins the Euphrates 10 km to the north. Plate 2.7 shows a general view of the area.

2.2.2 Stratigraphy and the rock types

Similar to the rocks in the Polusagi area, the rocks belong to two distinct ages: the Palaeozoic crystalline basement rocks and the younger and probably Upper Cretaceous-Eocene volcanogenic sediments. Although

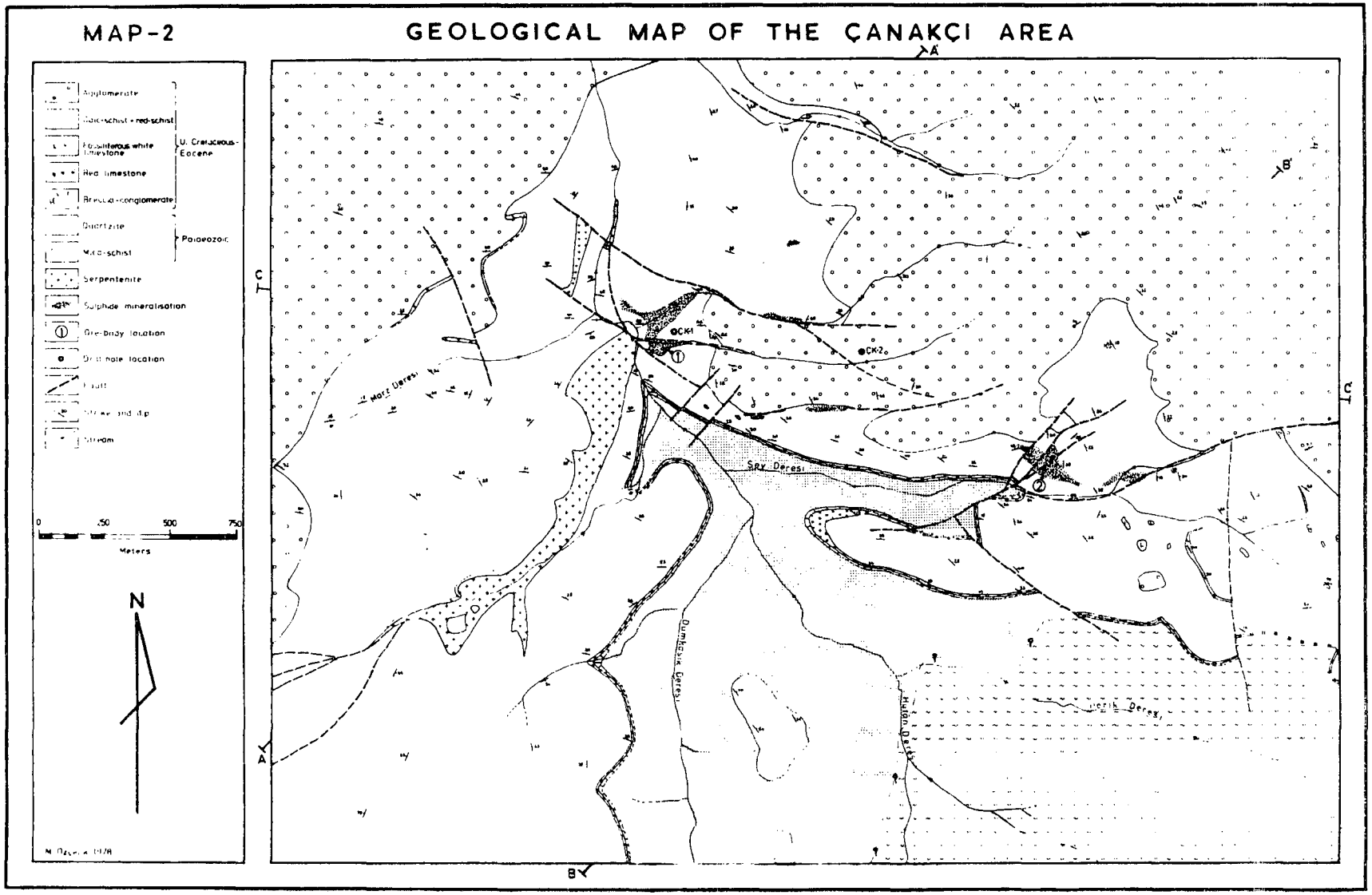


Fig.2.3. Geological map of the Canakci area.



Plate 2.7 : A general view of the Canakci area

volcanic rocks (pillow lavas) are reported to occur 4 km to the north of the area overlying the volcanogenic sediments (Karslioglu, 1976) they are not present in the mapped area. The rock types in the mapped area, from top to bottom, are as follows:

1) Agglomerates

2) Calc-schists and red-schists

3) Limestone

4) Breccia-conglomerate

5) Crystalline basement rocks

This sequence of the rocks in the area are demonstrated in Fig.2.4.

2.2.2.1 Metamorphic rocks of Palaeozoic basement

There are two different rock types in the crystalline basement: quartzites and mica-schists. The quartzites are fine to medium grained with little micaceous minerals. The mica-schists with well developed schistosity are very similar to those occurring in the Polusagi area, containing mainly quartz, plagioclase, biotite, white mica and garnet. Presence of carbonecous bands in the mica-schists, similarly indicate a sedimentary origin.

2.2.2.2 Breccia-Conglomerate

This unit unconformably overlies the basement rocks. Although well rounded pebbles in a sandy matrix locally occur (conglomerate component), it is mainly composed of angular and unsorted fragments of the underlying basement rocks cemented by a calcitic sandy matrix. Locally the matrix may be rich in iron-oxides. The thickness is normally around 2-3 m but it may be absent or very poorly developed, for instance in the SW corner of the mapped area. The occurrence of a thrust plane marked by this unit is possible.

2.2.2.3 Limestone

This is a thin, up to 10 m thick, and non-fossiliferous reddish

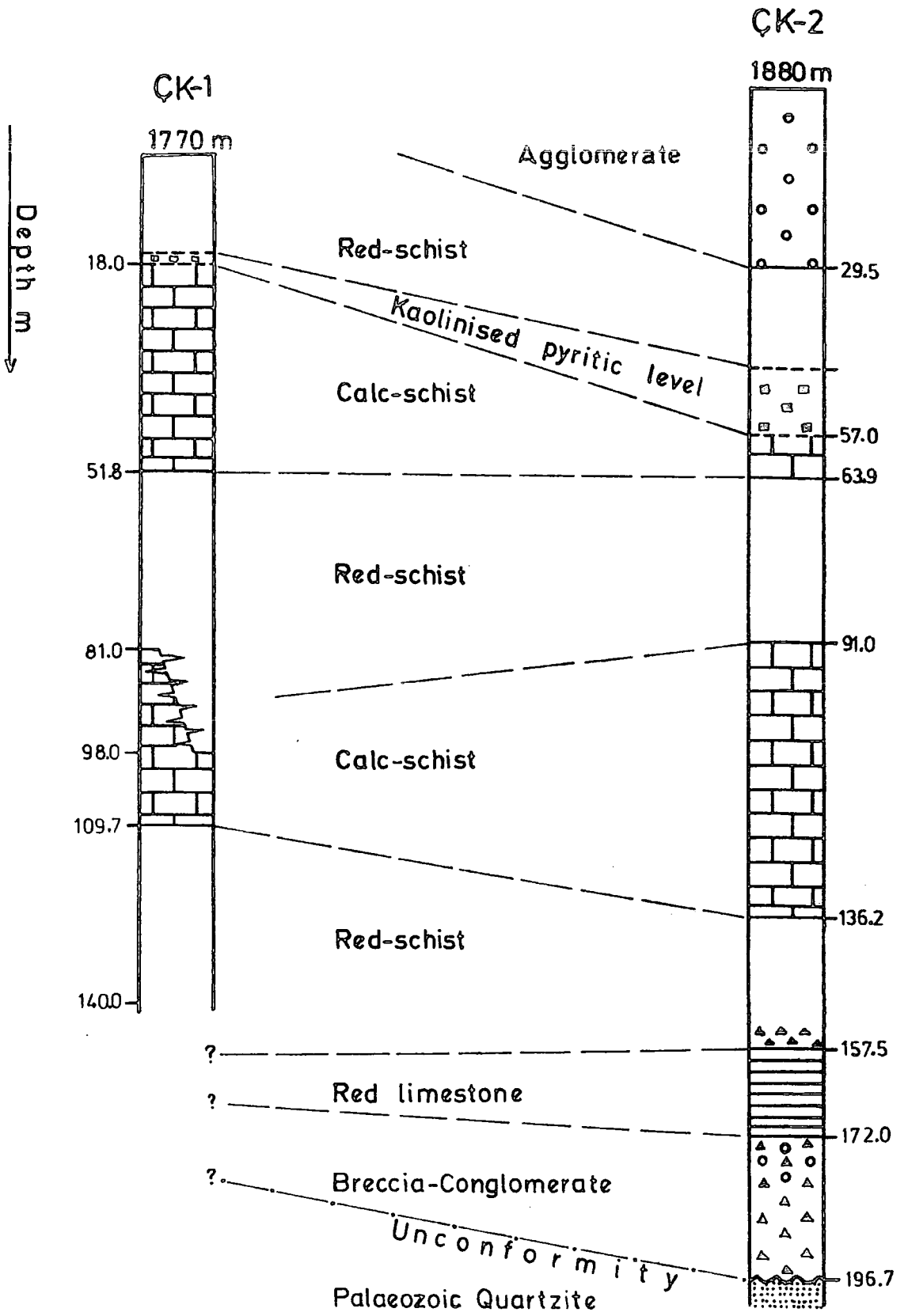


Fig.2.4. Stratigraphic section at the Canakci area as demonstrated by drill-core logs of the boreholes CK-1 and CK-2.

limestone overlying the breccia-conglomerate, or where this is missing, the basement rocks. In places, it gets sandy at the lower parts and may grade into the breccia-conglomerate.

2.2.2.4 Calc-schists and red-schists

These rock types are not separated due to frequent interbedding. As a whole the thickness is up to 150 m and in every aspect they resemble their counterparts occurring in the Polusagi area. However, in this area they contain discontinuous lenses of nummilitic whitish-grey limestones, sometimes reaching thicknesses around 3 m, and extending for 100 s of meters.

2.2.2.5 Agglomerates

These rocks occur in two forms: a) coarse grained agglomerates which are very similar to those of the Polusagi area and b) finer grained agglomerates, similar to the lappillistone of Yazgan (1972) which he reports occurs outside the mapped area in Polusagi. The "lappillistone" type agglomerate is the dominant form in the Canakci area. They are extremely variable in composition and texture and generally are non-descript, with a lot of calcite, iron oxides and sometimes with devitrified glassy grains. Some contain fragments or even thin lenses of lavas, or crystals of clinopyroxene. Certain samples may have phenocrystic plagioclases which are almost totally pseudomorphed by calcite and/or chlorite. Epidote, prehnite, pumpellyite and amphibole do occur but not commonly. The agglomerates locally contain thin red-schist lenses.

2.2.2.6 Serpentinite

A zone of shattered serpentinite, 50 to 100 m wide and over 1 km long and lying roughly NE-SW direction is found within the calc-schists. The serpentinite is fragmentary and contains occasional fragments or blocks, up to 50 cm across, of massive chromitites.

2.2.2.7 Sulphide mineralisation

The sulphide mineralisation is confined to a certain level within the calc-schists + red-schists , immediately below the agglomerates. It shows two forms:

a) Massive sulphides: These ores are found only at Locality 1 (Fig.2.3 or Map 2) where it occurs in an exposure covering roughly an area of $100m^2$. The ore is compact, fine grained and composed mainly of pyrite with some bornite, showing faint banding with the alignment of slightly coarser pyrite grains in a finer grained matrix. The ore body is well fractured and may be fault bound. The abrupt contact with the schists and the faulting suggests that the body may have been tectonically displaced.

b) Disseminated pyrite mineralisation: This type occurs along the mineralised level, which is parallel to the general bedding in the area, with much variation in the amount of pyrite. At locality 2 it takes a semi-massive form where the schists are extensively silicified. The faults related to the mineralisation suggest that it was tectonically moved up. Only occasionally is the pyritic mineralisation accompanied by chalcopyrite.

2.2.3 Structural geology

The calc-schists, red-schists and such sedimentary lenses within the agglomerates are useful for structural measurements. The general dip in the area varies mostly from 20° to 40° towards the north and the north-east. Such structural measurements do not indicate any large scale folding, despite considerable variation. The cross-sections in the back-pocket (Cross-sections 2) illustrate the general trends of the rocks.

The tectonic activity is indicated by faulting, especially where the sulphide exposures occur, and by the presence of shattered serpentinite within the schists.

2.2.4 Summary and conclusions

The rock types, lithology, stratigraphic sequence and the ages of the rock types in the Canakci area are evidently very similar to the equivalent rock types in the Polusagi area. By analogy, it is concluded that the younger volcano-sedimentary rock series in Canakci was formed in a submarine environment and probably represent the uppermost section of an ophiolitic sequence.

CHAPTER THREE

ELEMENT MOBILITY IN THE POLUSAGI ROCKS

3.1 Introduction

The classification of volcanic rocks into major magma types or various differentiation products conventionally requires an examination of the original igneous mineralogy and petrography. This is valid for those rocks which are fresh or slightly altered where the original igneous mineralogy can still be satisfactorily established. However, for those rocks where igneous mineralogy cannot be determined, rock chemistry must be the principal basis for classification. In recent years, chemical classification of common volcanic and associated rocks has gained importance partly due to the emergence of very large numbers of chemical analyses and partly to its usefulness for the altered rocks. Such chemical classification schemes employ major and trace element concentrations and their ratios as well as normative mineralogy and parameters (e.g. Thornton and Tuttle, 1960; Middlemost, 1972, 75, 80; Irvine and Baragar, 1971; Winchester and Floyd, 1977; Floyd and Winchester, 1978). But, if the rocks are altered, many elements become mobile and their concentrations deviate considerably from the original igneous values. Thus, it is of great importance to try to determine the extent and degree of element mobility in such rocks.

The Polusagi volcanics and associated hypabyssal rocks are altered to various degrees. Metamorphism and metamorphic changes are discussed in Chapter six. In summary, the rocks are metamorphosed to prehnite-pumpellyite and greenschist facies with the development of albite, chlorite, actinolite, epidote, prehnite, pumpellyite, quartz, calcite and sphene as the metamorphic minerals while igneous clinopyroxene survives as a relict and unstable phase. Some igneous textures, especially of plagioclase, are largely retained. It has been well

established that under such conditions many major and trace elements are mobilised. Therefore in this chapter the extent and degree of element mobility in the Polusagi rocks will be determined and an appropriate chemical classification will be attempted in the next chapter.

A brief review of the general problems of element mobility is presented below, before considering the particular case of the Polusagi suite.

3.2 Element mobility under alteration processes

Several types of alteration processes may operate simmultaneously and independently to cause element mobility and change in rock chemistry and it may be difficult to isolate particular stages and patterns, but three main processes are recognised by Pearce (1975, 76):

1) Sub-aerial weathering

2) Spilitisation or metamorphism

3) Sub-marine weathering

The study of chemical changes imposed upon the fresh rocks during alteration by the above major processes is generally based on one of the following procedures:

a) Comparison of fresh rocks with their metamorphosed and altered counterparts (e.g. Cann, 1969, and Vallance, 1974 a).

b) Where fresh rocks are not available, comparison between the inner and outer parts of the altered pillow-lavas or rock fragments, assuming that the alteration in the inner parts is less severe (e.g. Smith, 1968; Hart, 1969 ; Matthews, 1971; Coish, 1977; Humphris and Thompson, 1978 a, b).

c) Study of natural sub-marine geothermal systems (e.g. Reykjanes geothermal system; Tomasson and Kristmannsdottir, 1972).

d) Experimental work (e.g. Mottl and Holland, 1978, 79; Seyfried and Bischoff, 1979, 81).

Sub-aerial weathering typically involves leaching of elements such as Ca, Na, K, Mg and to a lesser extent Si; whilst total Fe, Ti and Al tend to remain fixed, taking into account the apparent increase in relative proportions due to leaching of other elements (e.g. Lisitsyana, 1968; Krauskopf, 1979, pp. 80-82).

The status and significance of "spilites" and "spilitisation" are matters of dispute. The problems are extensively discussed and reviewed by Amstutz (1967, 74) and Vallance (1960, 65, 69) and it is outside the scope of this study to go into details. Briefly, spilites are rocks of widely variable mineralogical and chemical composition. The main minerals are albite, chlorite, epidote, calcite and iron oxides, sometimes with abundant pyroxene. Actinolite, prehnite and pumpellyite are not uncommon and small granules of sphene are almost ubiquitous. They have many characteristics allying them with tholeiitic basalts and dolerites from ocean floors (Cann, 1969) and geosynclinal sequences (Smith, 1969). They are normally found as pillow-lavas in sub-marine geosynclinal environments and sometimes recognised by this association (e.g. Turner and Verhoogen, 1960; Hatch et al, 1972). Although very similar to tholeiitic basalts, spilites have higher contents of H_2O, Na, Fe^{3+} and lower K (Battey, 1974). However, major differences are not chemical but mineralogical. Like basalts, spilites are basic but the feldspar is albite and the ferro-magnesian mineral is chlorite.

It is apparent from the above referred reviews that there are two major theories for the origin of spilites:

1) Spilites are of igneous origin. The igneous textures exhibited by albite are of prime importance. The association of albite+chlorite can be formed by magmatic solutions enriched in H_2O, Na and often CO_2.

2) Spilites are perfectly ordinary basalts altered by post-magmatic processes such as low grade metamorphism and hydrothermal alteration. The peculiar chemistry and mineralogy are secondary features,

and no contemporary spilitic melts are known.

Following the studies of dredged rock samples from the ocean-floors, the second theory has now gained much acceptance (Smith, 1968, 74; Cann, 1969; Vallance, 1969, 74a, 74b; Hughes, 1972,73; Reed et al, 1971; Battey, 1974; Coombs, 1974; Shilov, 1974; Vaugnat, 1974; Floyd, 1976; Whitehead and Goodfellow, 1978; Offler et al, 1980). Cann (1969) defined the spilites as "rocks of basaltic texture in which greenschist facies mineralogy is completely or almost completely developed", while Coombs (1974) ascribed the spilites "occasionally" to zeolite facies and "more commonly" to prehnite-pumpellyite and greenschist facies metamorphism. Spilitisation may be due to burial, regional or hydrothermal metamorphic events.

Element mobility and bulk chemical changes during spilitisation of igneous rocks are now well established. The above cited literature shows that spilitisation involves take up of a large amount of water, increase in Mg and decrease in Ca. Release of Ca seems to be balanced by the gain in Mg (Mottl and Holland, 1978; Seyfried and Bischoff, 1981).

Although Si, total Fe, Na and K may become mobile during spilitisation, there does not seem to be an agreement on the direction and extent of mobility. Under such alteration conditions Si can be taken up (Cann, 1969) or lost (Wood et al, 1976; Vallance, 1974a); total Fe can increase (Cann, 1969; Vallance, 1974a; Coish, 1977) or slightly decrease (Matthews, 1971) or the change may not be significant (Wood et al, 1976). Similarly, Na and K can be enriched, depleted or changes can be unsystematic. Vallance (1974a), studying the degradation of a tholeiitic flow into spilite in a Deccan flow laid down under shallow water conditions in India, reports that the initial decrease in the alkali content was followed by an increase in alkali content downward in the section i.e. increasing grade of metamorphism. Cann (1969), comparing the fresh and spilitised rocks dredged from Carlsberg ridge, reports no significant

change in K content with spilitisation.

Al generally shows less mobility than the above discussed components. It has been shown to be stable (Smith, 1968; Wood et al, 1969; Matthews, 1971; Coish, 1977) or to decrease to some extent (Cann, 1969; Vallance, 1974a) with alteration.

Although Ti, P and Mn have been reported to change randomly during spilitisation (Smith, 1968), these three elements, particularly Ti, are usually thought to be quite immobile (Cann, 1969; Wood et al, 1976; Matthews, 1971; Vallance, 1974a; Floyd, 1976; Coish, 1977).

The picture for the mobility of trace elements under low grade metamorphism is somewhat different, since some of them appear to be extremely resistant and insensitive to alteration. Zr, Y and Nb are such immobile elements (Cann, 1970; Pearce and Cann, 1971; Hart et al, 1974; Smith and Smith, 1976; Wood et al, 1976; Coish, 1977; Humphris and Thompson, 1978 b). Although some slight variations in Ni and Cr concentrations have been reported by Floyd (1976), they are generally considered to be stable in the altered rocks (Cann, 1969; Hart et al, 1974; Coish, 1977; Humphris and Thompson, 1978 b). Finlow-Bates and Stumpfl (1981) studied the behaviour of "immobile" elements such as Zr, Ti, Y, Nb, Ce and Cr in hydrothermally altered rocks associated with volcanogenic-exhalative ore deposits. They report that under intense hydrothermal alteration and sulphidation, Y and particularly Nb and Cr may be mobile and prone to extraction. This apparently is not so for Zr and Ti and to some extent Ce which remain immobile.

The behaviour of Sr is unsystematic, but generally falls in sympathy with Ca (Cann, 1969; Vallance, 1974a). It has been shown to be fairly stable in uncarbonated rocks, below greenschist facies metamorphism (Pearce and Cann, 1973), and to decrease together with Ca during spilitisation (Floyd, 1976). Smith and Smith (1976) found that Sr concentrations varied according to the mineralogical domains in a

single basaltic flow, the Clifden outcrop: Sr increased with increasing Ca in epidotised domains when compared with Sr in albitised basalt, while it generally decreased as Ca increased in the prehnite and pumpellyite rich domains.

Ba and Rb can become mobile during spilitisation. Ba can increase (Vallance, 1974a; Hart et al, 1974), decrease (Floyd, 1976) or changes can be irregular (Hart, 1969a; Coish, 1977). Rb, although reported to have been lost during spilitisation (Floyd, 1976), generally increases with progressive alteration (Wood et al, 1969; Hart, 1969 ; Cann, 1970 ; Hart et al, 1974).

Cu and Zn are known to be mobile (Hart et al, 1974) and leached out of the spilitised rocks (Floyd, 1976).

Element mobility during sub-marine weathering is generally very similar to that of spilitisation with one major difference: the iron oxidation ratio, Fe_2O_3/FeO, is not effectively changed during spilitisation while it is substantially increased during sub-marine weathering (Floyd, 1976).

The above discussed behaviour of elements during various alteration processes is summarized in Table 3.1. It is apparent that many of the mobilised elements do not show systematic enrichment or depletion during alteration. This may be due to the nature of the process or processes involved as well as other factors, since the alteration of rocks is a complex and continuous process. Some important factors are considered below:

1) Degree of crystallinity and texture of the rocks: Chemical variations between the selvages and the cores of metamorphosed pillow-lavas are considered to be largely due to the differences in textures and crystallinity (Vallance, 1965; Coish, 1977), selvages having a larger content of glassy material and suffering greater alteration. Original difference in crystallinity and texture lead to different metamorphic

TABLE 3.1

Mobility of elements as inflicted by main alteration processes

1) Spilitisation-low grade metamorphism:

Highly mobile	=	$+H_2O$, +Mg, -Ca
Mobile	=	Si, total Fe, Na, K, Rb, Ba, Sr, Cu, Zn
Slightly mobile	=	Al
Immobile	=	Mn, P, Fe_2O_3/FeO, Cr, Ni
Highly immobile	=	Ti, Zr, Y, Nb, Ce

2) Sub-marine weathering:

Highly mobile	=	$+H_2O$, +Mg, -CaO, K, $+Fe_2O_3$/FeO
Mobile	=	Si, total Fe, Na, Mn, S
Slightly mobile	=	Al, P
Immobile	=	Ti, Zr, Y, Nb

3) Sub aerial weathering:

Highly mobile	=	$+H_2O$, -Mg, -Ca, -Na, -K
Mobile	=	-Si
Immobile	=	Ti, Al, total Fe

+ means gain

- meaus loss

mineral assemblages. Cann (1969), working on the metamorphosed (spilitised) pillow lavas from Carlsberg ridge, found that originally holocrystalline cores now consist of an albite-chlorite-augite-sphene greenschist metamorphic assemblage strongly contrasted with originally glassy and cryptocrystalline margins which now consist principally of chlorite. He attributed this to original differences in the basaltic mineralogy and texture. Experiments show that degree of crystallinity affects the rate of chemical exchange of basalts with sea-water (Seyfried and Bischoff, 1979); for example Ca is lost from the basalts much more readily if the basalt is poorly crystalline (Mottl and Holland, 1978).

2) Physical conditions of alteration: Metamorphic conditions, chiefly temperature and water/rock ratio during hydrothermal alteration, seem to affect the rate and direction of mobility of elements. Experiments suggest that at high temperatures ($\geqslant 200^{o}C$) K passes from basalt to sea-water and Mg does the opposite, while studies of ocean-floor basalt alteration indicate that the reverse is true at lower temperatures (Seyfried and Bischoff, 1979). These authors found that Na and K passed from rock to sea-water at $150^{o}C$, but went in the opposite direction at $70^{o}C$ during their experiments with a water/rock ratio of 10. Mottl and Holland (1978) report from their experimental work that, like Ca, K is removed from basalt during interaction with sea-water at $200-500^{o}C$, but unlike Ca, K shows no clear pattern due to crystallinity of basalt. Instead, the water/rock ratio of experiments exerted a strong control over the loss of K from basalt at the same temperature, the extent of K loss being proportional to the water/rock ratio.

3.3 Element mobility in the Polusagi rocks

3.3.1 Introduction

Details of the samples collected from the Polusagi area, precedure of sampling and the numbering system are given in Appendix I. H_2O and

Fe_2O_3/FeO ratios, determined for 34 samples (32 volcanics and 2 hypabyssal rocks) by wet chemical methods, are included in Appendix II. Bulk chemical analyses for 117 volcanic and 12 hypabyssal rock samples were carried out for SiO_2, Al_2O_3, total Fe (as Fe_2O_3), MgO, CaO, Na_2O, K_2O, TiO_2, MnO, S and P_2O_5 and trace elements Nb, Zr, Y, Sr, La, Ce, Rb, Ba, Zn, Cu, Ni and Cr by XRF. The analytical conditions, analyses and normative calculations are presented in Appendix III.

As there are no fresh samples amongst the Põlusagi rocks and the H_2O and CO_2 contents are unlikely to be present in original igneous abundances in altered rocks (Irvine and Baragar, 1971), an attempt to minimise the effect of alteration was made by normalising all the chemical analyses to 100% on a volatile free basis. It has also been recognised that oxidation of rocks during alteration will cause Fe_2O_3/FeO ratio to deviate considerably from original igneous values (Irvine and Baragar, 1971) and in the case of sub-marine oxidation to increase with progressive alteration (Floyd, 1976; Humphris and Thompson, 1978 a). Various procedures to approximate a reasonable Fe_2O_3/FeO ratio, which is of considerable importance in normative calculations, exist:

1) $wt\%Fe_2O_3 = wt\%TiO_2 + 1.5$ (Irvine and Baragar, 1971)

2) $Fe_2O_3/FeO^{total} < 0.4$ (Cann, 1971)

3) $wt\%Fe_2O_3 = 1.5$ if $Na_2O+K_2O < 4wt\%$ (Thompson et al, 1972)

However, since the Fe_2O_3/FeO ratios for some of the Polusagi rocks were chemically determined (Appendix II) and they have a minimum ratio around 0.3, as well as by comparison with other suites, a constant ratio of 0.3 has been assumed in the normative calculations.

The effects of sub-aerial weathering were reduced to a minimum during sample preparations as considerable efforts were made to use unweathered material or weathered patches were removed before crushing the samples for chemical analyses. Therefore, the possible chemical

variations caused by alteration in the rocks are most probably due to post-magmatic processes such as metamorphism and sub-marine weathering. Mineralogically and chemically the Polusagi volcanics and associated hypabyssal rocks can comfortably be described as 'spilites', but as apparent from the preceding section, 'spilites' are now generally taken as igneous rocks which have undergone a low-grade metamorphism especially under sub-marine conditions. As discussed in detail in Chapter six, the mineralogy of the Polusagi rocks is one of low-grade metamorphic assemblage and the relict igneous minerals are unstable under the metamorphic conditions. Therefore, in this study, a secondary i.e. metamorphic origin is advocated for the 'Polusagi spilites'and associated rocks for the observed mineralogical and chemical features. It follows that the chemical variations due to alteration must have mainly been caused by the later metamorphic events. However, since the determined Fe_2O_3/FeO ratios are high (up to 1.56), sub-marine weathering must also have contributed, to some extent, to the deviations from original igneous values. Distinction between these two alteration processes, especially under low-grade metamorphic conditions, is difficult to assess and thus 'alteration processes' in the following pages will mean both processes.

Alteration and development of metamorphic phases in the rocks are heterogenous (see Chapter six). Some samples are apparently, and when examined under the microscope, relatively fresher or more severely altered than others. Therefore, amongst the volcanic and hypabyssal rocks, 3 groups have been determined, according to the extent and degree of alteration:

1) Group A - This group consists of samples that are least affected by alteration and show relatively uniform igneous textures and less patchy development of secondary mineralogy. 56 volcanic rock samples and all the hypabyssal rocks (12 samples) belong to this group.

2) Group B - Those volcanic rocks which are relatively more altered are included in this group (35 samples). They generally contain more amygdales, filled with secondary minerals, and the igneous textures are obscured to a greater extent.

3) Group C - Comprises the samples from the vicinity of mineralisation with high concentrations of sulphides (26 samples).

Each group contains basalts, andesites and dacites, as defined chemically in the next chapter. In the absence of fresh samples the best that can be done to determine the element mobility is to inter-compare the chemical abundances of elements in these groups with the likely assumption that the groups, from A to B to C, represent progressive stages of alteration.

3.3.2 Inter-element correlations and element mobility in the volcanics

3.3.2.1 Introduction

The elements that are considered to be immobile during low-grade alteration processes, such as Zr, Nb, Y, Ce and La, are also incompatible elements with high field strengths i.e. high charge/radius ratios (Saunders et al, 1980). As a result, they are progressively enriched in the residual magmatic liquids irrespective of whether partial melting or fractional crystallisation processes are involved, so that their abundances should correlate directly with the stages of progressive magmatic differentiation (Saunders and Tarney, 1979). The concentrations of these elements, therefore, can be used and has been used (e.g. Wood et al, 1976; Winchester and Floyd, 1977) as differentiation indices. It can be assumed that any rock suite, where chemistry has not been changed by secondary alteration processes, will exhibit regular and systematic trends of changing element concentrations with progressive igneous processes. Thus, in rocks which have undergone low-grade alteration any element concentration exhibiting a regular and systematic change with the above mentioned 'immobile' elements may be

taken as essentially representative of igneous concentrations. A similar line of argument is pursued by Wood et al (1976) who studied element mobility during zeolite facies metamorphism in the Tertiary basalts of Eastern Iceland and by Coish (1977) who investigated it during the ocean floor metamorphism in Betts Cove ophiolite, Newfoundland.

It is apparent that during progressive alteration, igneous variation patterns of immobile element concentrations would be retained and those of mobile elements would be lost or in cases where some elements may be consistently and progressively enriched or depleted some new secondary patterns of element concentrations may develop. One way of studying this could be by plotting scatter diagrams of inter-element concentrations and observing the changes in the degree of correlation through progressive alteration. The process can be simplified by employing correlation coefficients rather than numerous diagrams (see Cann, 1970, 71; Narebski, 1974; Wood et al, 1976; Beddoe-Stephens, 1977). Cann (1970, 71), by comparing correlation coefficients of elements in fresh and altered basalts, showed how some elements maintained cohesion during alteration. However, correlation coefficients may only be of use where the inter-element variations are linear. For non-linear variations, they may be meaningless. Therefore, before employing such methods in the study of inter-element variations, the nature of the relationships must be established.

In this study, the element variations are displayed by plotting their concentrations against Zr which also serves as a differentiation index for igneous element abundances. The choice of Zr is made by considering the following reasons:

1) Zr is not only immobile under low-grade alteration conditions, but also one of the two elements (the other being Ti) that are truly immobile under intense alteration conditions (see section 3.2) such as hydrothermally altered rocks associated with volcanogenic submarine-

exhalative ore deposits (Finlow-Bates and Stumpfl, 1981).

2) It has commonly been used as such by other workers.

3) Zr shows the greatest variation amongst the 'immobile' elements within the Polusagi rocks (19-627 ppm).

The element variations for the least altered group of rocks i.e. group A are shown in Fig. 5.5 and discussed in detail in Chapter five. The trends exhibited by Al_2O_3, total Fe, TiO_2, P_2O_5, Cr, Ni and possibly MnO are non-linear and therefore, the mobility of these elements will be judged by comparing scatter plots, rather than simple coefficients of their correlations with the "immobile" elements.

3.3.2.2 Correlation coefficients

The degree of correlation between two variables, X and Y, can be measured by the so called "correlation coefficient", r, which is defined as:

$$r = \frac{1}{N} \sum \left(\frac{x - \bar{x}}{\sigma x} \right) \left(\frac{y - \bar{y}}{\sigma y} \right)$$

where $\bar{x}$ and $\bar{y}$ are respective means of x and y values and σx and σy are the standard deviations. The correlation coefficient cannot exceed +1 or be less than -1, these being values for perfect positive and negative correlations respectively. Value of r depends on the number of cases (N) employed in the calculation. Since each group of rocks, defined previously, contains different numbers of samples, the absolute values of coefficients cannot be used for inter-comparison. To compare the degree of correlations of any covarience from one group of rocks to another, significance levels at 5%, 1%, 0.1% and 0.01% have been used. For instance, if an element A is correlated with an immobile element such as Zr with a significance above 0.1% level in group A rocks and below or around 5% level in group B rocks, this is taken to represent mobility with alteration. At least a jump of two levels is considered significant and correlation coefficients which are well below 5% significance level are, rather arbitrarily, taken to represent "random" variations.

Correlation matrices for the groups A, B and C have been calculated and are presented in Table 3.2, together with different levels at which the coefficients may be significant. Examination of the matrices demonstrates the following points:

a) Zr, Nb, Y, La and Ce, as a group, show extremely high positive correlations, each with the other, with significances always well above 0.01% level in group A rocks. Similarly significant positive correlations are maintained in groups B and C, except that La and Ce are poorly correlated with Zr and Y in group B rocks. The poor correlations are unexpected as the same element pairs are correlated with one another highly significantly in group C rocks which were assumed to represent a later stage of alteration than group B rocks. Inspection of the likely causes of this unexpected observation reveals that out of 35 samples in group B, 4 samples (P116, P123, P168 and P185A) show consistently the highest La and Ce concentrations which are not coupled by equally high Zr and Y concentrations. The high La and Ce contents, however, are accompanied by relatively high values of Nb and P_2O_5. These high values cannot be due to extreme differentiation since 3 of the samples are clearly basic rocks. Sphene is reported to incorporate La, Ce and Nb into its structure (Deer et al, 1962) and is a common accessory mineral in the Polusagi rocks. However, microscopic examination shows that the amount of sphene present in these 4 samples is not particularly different from the other rocks. Apatite is another phase reported to incorporate La and Ce into its structure by the last mentioned authors, and although apatite is not identified in the rocks, this possibility is supported by high P concentrations.

Exclusion of these 4 samples from group B rocks pushes the significances of the positive correlations above 5% level for La and above 0.1% level for Ce against both Zr and Y.

It can now be concluded that Zr, Nb, Y, La and Ce correlate

TABLE 3.2 A

Correlation matrix for Group A volcanics. No of samples = 56. Significance levels at 0.01%=0.4964, 0.1%=0.4280, 1%=0.3415 and at 5%=0.2632.

VARIABLE	1. SIO2	2. AL203	3. FE203	4. MGO	5. CAO	6. NA20	7. K20	8. TIO2	9. MNO	10. S	11. P205	12. NB	13. ZR	14. Y	15. SR	16. LA	17. CE	18. RB	19. BA	20. ZN	21. CU	22. NI	23. CR
1.SIO2	1.0000																						
2.AL203	-.0323	1.0000																					
3.FE203	-.9039	.0868	1.0000																				
4.MGO	-.9045	.2116	.8012	1.0000																			
5.CAO	-.6300	-.6838	.4353	.3888	1.0000																		
6.NA20	.7957	-.0217	-.7179	-.8764	-.4884	1.0000																	
7.K20	-.0385	-.0890	-.1290	.0224	.2062	-.2080	1.0000																
8.TIO2	-.5687	.2308	.6491	.4658	.1077	-.3272	-.2579	1.0000															
9.MNO	-.5606	.4220	.5320	.6317	.0471	-.4854	-.0453	.2814	1.0000														
10.S	-.2647	.2816	.2792	.3755	-.0673	-.3650	.1089	.0611	.4364	1.0000													
11.P205	.0321	.5897	.1191	-.0059	-.5193	.1018	-.1836	.5293	.1738	-.0223	1.0000												
12.NB	.8911	.2782	-.7794	-.7587	-.7759	.7074	-.0136	-.4599	-.3598	-.1156	.2116	1.0000											
13.ZR	.9174	.2114	-.8105	-.7872	-.7398	.7176	-.0017	-.5329	-.3677	-.1253	.1075	.9835	1.0000										
14.Y	.8360	.3314	-.6745	-.7498	-.7967	.7137	-.0340	-.3241	-.2916	-.1370	.3723	.9444	.9291	1.0000									
15.SR	-.0643	-.1147	.1315	.0535	.0971	-.1903	.1898	-.0417	-.0513	.0460	-.0150	.0443	.0125	.0002	1.0000								
16.LA	.7828	.2873	-.6493	-.6710	-.7169	.5929	.0175	-.3773	-.2389	-.0178	.2638	.9081	.8950	.8885	.1774	1.0000							
17.CE	.8073	.3413	-.6879	-.7250	-.7555	.6784	-.0349	-.3121	-.2879	-.0398	.3620	.9154	.8983	.9304	-.0022	.9033	1.0000						
18.RB	-.2047	-.1584	-.0313	.1695	.3988	-.3404	.8704	-.2169	.0508	.0742	-.2955	-.2245	-.1909	-.2453	.1256	-.1475	-.1993	1.0000					
19.BA	-.0245	.1572	.0068	-.0339	-.0273	-.0550	.4773	.0579	-.0654	.3526	.1078	.1163	.0958	.1425	.2575	.2276	.2672	.3672	1.0000				
20.ZN	.0294	.6153	.0186	.1511	-.4737	-.0580	-.1267	.0289	.5471	.4649	.2354	.2593	.2290	.2862	-.1680	.3189	.3047	-.0966	.0804	1.0000			
21.CU	.0293	.0917	-.0047	.1006	-.1221	-.1159	-.1463	-.1742	.3639	.4173	-.0620	.0808	.0828	.0002	.1278	.1331	.0590	-.1405	-.1848	.2212	1.0000		
22.NI	-.4160	-.2949	.1466	.4116	.6072	-.4862	.4031	-.2314	.2145	.0717	-.4535	-.5504	-.5051	-.6160	.1079	-.5001	-.5475	.6364	.0238	-.1702	.0305	1.0000	
23.CR	-.4531	-.2366	.2033	.4744	.5721	-.5182	.3401	-.2258	.2605	.1369	-.4540	-.5719	-.5241	-.6445	.0989	-.5291	-.5915	.5417	-.0367	-.1372	.0826	.9667	1.0000

TABLE 3.2 B

Correlation matrix for Group B volcanics. No of samples = 35. Significance levels at 0.01%=0.6100, 0.1%=0.5322, 1%=0.4296 and at 5%=0.3338

VARIABLE	1. SIO2	2. AL203	3. FE203	4. MGO	5. CAO	6. NA2O	7. K2O	8. TIO2	9. MNO	10. S	11. P2O5	12. NB	13. ZR	14. Y	15. SR	16. LA	17. CE	18. RB	19. BA	20. ZN	21. CU	22. NI	23. CR
1.SIO2	1.0000																						
2.AL203	.0929	1.0000																					
3.FE203	-.8166	.1470	1.0000																				
4.MGO	-.5702	.3820	.4314	1.0000																			
5.CAO	-.5808	-.7993	.2516	-.1176	1.0000																		
6.NA2O	.5494	.2603	-.3836	-.3809	-.5583	1.0000																	
7.K2O	-.4328	.1126	.2460	.3032	.1492	-.3192	1.0000																
8.TIO2	-.1730	.1641	.4705	-.0336	-.1241	.0205	.0123	1.0000															
9.MNO	-.5512	.3083	.5585	.6086	-.0084	-.3342	.2336	.2529	1.0000														
10.S	-.4553	-.0292	.3909	.5591	.1507	-.3350	.0197	.0479	.4557	1.0000													
11.P2O5	.3312	.5287	-.0139	-.1081	-.6123	.3565	-.0586	.3819	.1165	-.2651	1.0000												
12.NB	.3551	.4498	-.0102	-.2570	-.5310	.4034	-.0584	.1898	.0270	-.2329	.7257	1.0000											
13.ZR	.6090	.5698	-.2966	-.2663	-.7375	.6142	-.2993	.0275	-.0744	-.4120	.5195	.6462	1.0000										
14.Y	.5625	.5852	-.1803	-.2479	-.7739	.6243	-.2766	.2843	.0516	-.2939	.6873	.7162	.9199	1.0000									
15.SR	-.0791	.3357	.1061	.2393	-.2877	.1925	.2382	.1542	.1843	-.0251	.5693	.4621	.2269	.3312	1.0000								
16.LA	-.0397	.2039	.1922	-.0965	-.1200	.1112	.1915	.0436	.0826	-.0072	.4394	.7540	.0959	.1972	.3266	1.0000							
17.CE	.1011	.2624	.0984	-.2457	-.2119	.2301	.1207	.1234	.0385	-.1354	.5266	.8460	.2880	.3804	.3107	.9486	1.0000						
18.RB	-.4912	-.0456	.2248	.3065	.2983	-.3369	.9358	-.1225	.1937	.0194	-.2054	-.2001	-.4046	-.4075	.1803	.1025	-.0073	1.0000					
19.BA	-.3295	.1263	.2953	.3308	.0120	-.2269	.7183	-.0067	.1470	.3023	.0345	.1698	-.2466	-.1851	.3478	.4097	.3244	.5858	1.0000				
20.ZN	-.1404	.3912	.2639	.4652	-.3209	-.1162	.0290	.3299	.5824	.3365	.1117	.1015	.2128	.2915	.0351	-.0666	-.0145	-.0455	-.0640	1.0000			
21.CU	-.0392	-.0293	-.1012	.1708	.0343	-.0703	-.0132	-.1035	.0172	.0331	-.0039	-.1243	-.0582	-.0824	.1140	-.0701	-.1364	.0430	.0248	-.1136	1.0000		
22.NI	-.4890	-.3068	.0685	.3770	.5357	-.5135	.4999	-.4508	.0574	.2043	-.6306	-.6037	-.6094	-.6952	-.1448	-.2304	-.3778	.6723	.2947	-.1795	.1436	1.0000	
23.CR	-.4528	-.2220	.1026	.3877	.4049	-.3586	.4637	-.3225	.0373	.1434	-.4894	-.5047	-.5144	-.5621	-.0759	-.2216	-.3597	.6139	.1932	-.0785	-.0938	.8604	1.0000

TABLE 3.2 C

Correlation matrix for Group C volcanics. No of samples = 26. Significance levels at 0.01%=0.6888, 0.1%=0.6074, 1%=0.4958 and at 5%=0.3882

VARIABLE	1. SIO2	2. AL203	3. FE203	4. MGO	5. CAO	6. NA20	7. K20	8. TIO2	9. MNO	10. S	11. P205	12. NB	13. ZR	14. Y	15. SR	16. LA	17. CE	18. RB	19. BA	20. ZN	21. CU	22. NI	23. CR
1.SIO2	1.0000																						
2.AL203	-.2682	1.0000																					
3.FE203	-.8789	-.0696	1.0000																				
4.MGO	-.8750	.1374	.7588	1.0000																			
5.CAO	-.2614	-.3001	.2504	.0762	1.0000																		
6.NA20	.3859	-.4288	-.2376	-.4940	.2337	1.0000																	
7.K20	.3782	.5775	-.3651	-.4018	-.3844	-.5098	1.0000																
8.TIO2	-.8369	.0673	.7553	.7154	.3001	-.3897	-.3343	1.0000															
9.MNO	-.6115	.0720	.7242	.3858	.0979	-.2068	-.2864	.6707	1.0000														
10.S	-.1376	.0401	.0206	.0080	-.2276	-.1886	.1660	.2291	.1027	1.0000													
11.P205	-.4996	.0617	.3458	.3829	.3268	.0034	-.2834	.4392	.2229	.1361	1.0000												
12.NB	.1108	-.2060	-.1413	-.0596	.1998	.3427	-.2944	-.1567	-.1860	-.0655	.3982	1.0000											
13.ZR	.4215	-.3615	-.3451	-.2706	.0304	.5357	-.3312	-.4364	-.3205	-.2614	.1783	.6374	1.0000										
14.Y	-.0046	-.1926	-.0146	.0566	.2830	.3653	-.4244	-.1279	-.1620	-.2169	.5412	.6778	.7987	1.0000									
15.SR	.0095	-.1416	-.0367	-.1596	.7849	.3015	-.1392	-.0651	-.1741	-.3197	-.1303	.0106	.0127	.1074	1.0000								
16.LA	.1935	-.2264	-.1544	-.1093	.0860	.0897	-.0320	-.2565	-.2736	-.0934	.3446	.6780	.6274	.6790	.0313	1.0000							
17.CE	.2524	-.2419	-.2593	-.1564	.0631	.1936	-.0692	-.3214	-.3326	.0143	.4305	.7872	.6951	.7337	-.0371	.9214	1.0000						
18.RB	.4029	.6013	-.5867	-.4572	-.3221	-.3343	.9279	-.3887	-.3337	.0120	-.3886	-.4040	-.3958	-.5205	-.0042	-.2060	-.2345	1.0000					
19.BA	.2889	.2811	-.4005	-.1621	-.3388	-.5923	.7380	-.2258	-.1808	.1581	-.1473	.0027	-.0642	-.1859	-.2912	.2355	.1772	.5017	1.0000				
20.ZN	-.4667	.1630	.5542	.2673	-.0319	-.2569	-.0665	.4733	.7963	.1244	-.0278	-.2165	-.3232	-.1347	-.0915	-.1810	-.3289	-.1495	-.0290	1.0000			
21.CU	-.3060	-.0406	.4765	.1086	.2499	-.0132	-.2388	.4243	.3769	-.1084	.0175	-.2682	-.2947	-.1578	.1033	-.3581	-.4287	-.2192	-.2701	.2457	1.0000		
22.NI	-.4955	-.0166	.5820	.4367	.2388	-.1733	-.2304	.4352	.3626	-.2508	-.0182	-.2650	-.4011	-.0929	.2561	-.1892	-.3353	-.2273	-.1784	.5589	.4571	1.0000	
23.CR	-.7233	.3100	.5994	.7428	.0245	-.6632	-.0444	.7221	.4808	.1086	.1843	-.2978	-.4920	-.1793	-.1204	-.2361	-.3286	-.1405	.0762	.3829	.3196	.4680	1.0000

positively and very strongly each with the other, through the progressive alteration in the Polusagi volcanics as a whole. This suggests that the abundances of these elements are very little affected by the alteration and thus represent original magmatic abundances. In other words, these 5 elements are immobile elements - in agreement with their strong resistance to alteration reported from other areas.

These immobile elements provide a means or a criteria through which activities of the other elements during alteration can be judged, using the correlation coefficients.

b) In group A volcanic rocks, the immobile elements show consistent and very strong correlations with each of the major oxides, SiO_2, MgO, CaO and Na_2O which are always significant above 0.01% level. Equally significant correlations also exist amongst these major oxides, each against the other. However, such highly significant correlations in group A rocks, progressively diminish through groups B and C and in group C rocks non of the mentioned major oxides is correlated to any of the 5 immobile elements with any significance. Therefore, it is concluded that although the concentrations of SiO_2, MgO, CaO and Na_2O in the least altered rocks are not affected to a great extent by the alteration processes, with progressive alteration their igneous chemical patterns change and become unacceptable for petrogenetic studies.

c) K_2O, S, Sr, Rb, Ba, Zn and Cu do not, in general, show significant correlations with the 5 immobile elements. Their correlation coefficients were also examined against other immobile elements such as Ti, P, Cr, Ni (see below) to eliminate the possibility of non-linear trends in relation to the 5 immobile elements. K_2O and Rb are significantly correlated with Cr and Ni at 1% and 0.1% levels respectively in groups A and B rocks. Zn appears to show weakly significant correlation with Nb, Y, La and Ce only in group A rocks. There are no other consistent and significant

correlations of the examined elements with any of the established immobile elements. These observations suggest that, although all of these elements have become highly mobilised during alteration K_2O, Rb and to a certain extent Zn were not highly mobile during the early stages, represented by group A rocks.

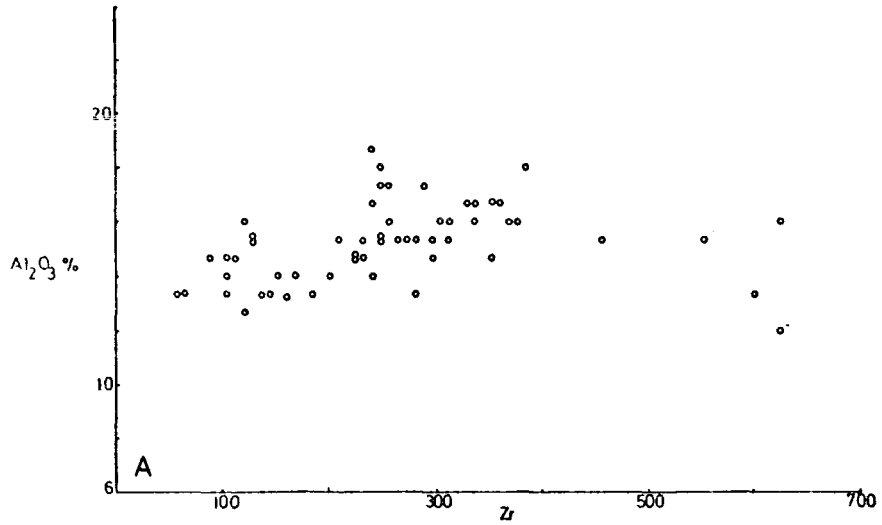
d) Inspection of the scatter plots of Al_2O_3, total Fe (as Fe_2O_3), MnO, TiO_2, P_2O_5, Cr and Ni for each group of rocks (Fig. 3.1) demonstrates that:

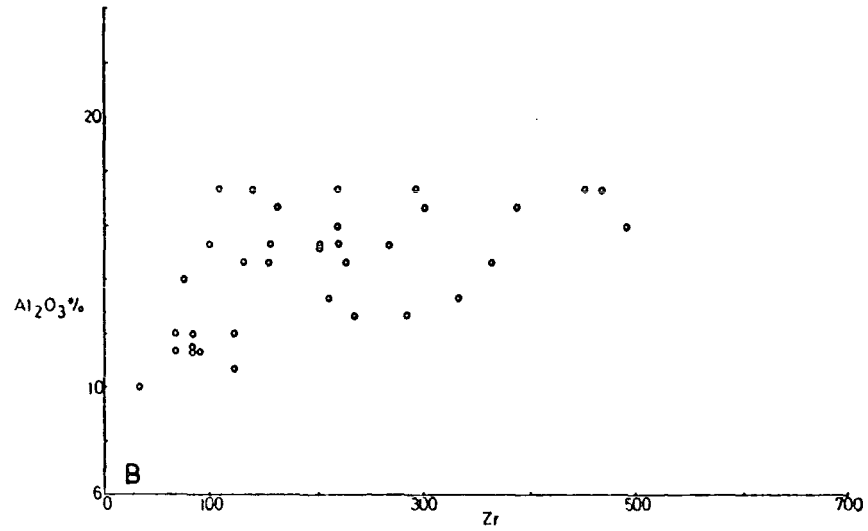
1) Scatter plot of Al is in general quite tight for group A rocks which to a lesser extent persists in group B and C rocks. This suggests that the alteration processes were not particularly affective and Al concentrations are largely of igneous quality.

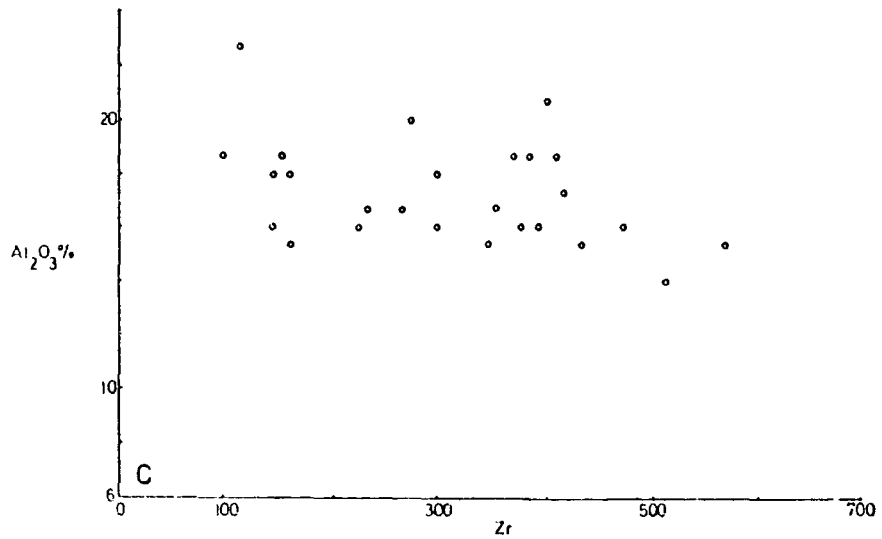
2) Variation trends of Fe_2O_3, TiO_2 and P_2O_5 are remarkably tight and go through maxima in group A volcanics. Trends of TiO_2 and P_2O_5 persist through progressive alteration, but not of Fe_2O_3, suggesting that TiO_2 and P_2O_5 should be treated as being immobile and insensitive to alteration.

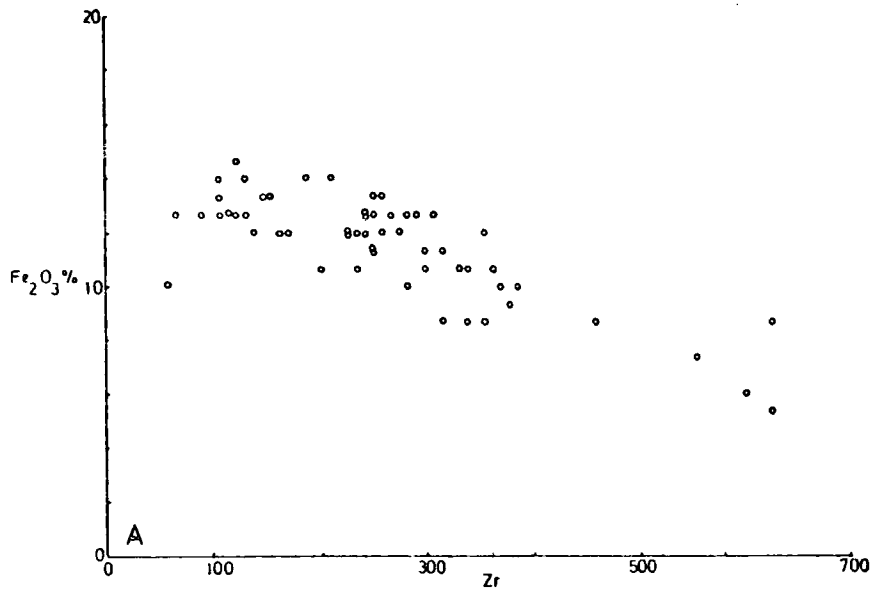
3) Scatter plots of MnO indicate loss of pattern with progressive alteration from a recognisable trend in group A rocks, where it is also significantly correlated with the 5 immobile elements (above 5% level) and particularly with Zr and Nb (at 1% level). No significant correlations exist with the 5 immobile elements in group B or C rocks. Thus, MnO is regarded as relatively immobile in group A rocks, but increasingly mobile in group B and C rocks.

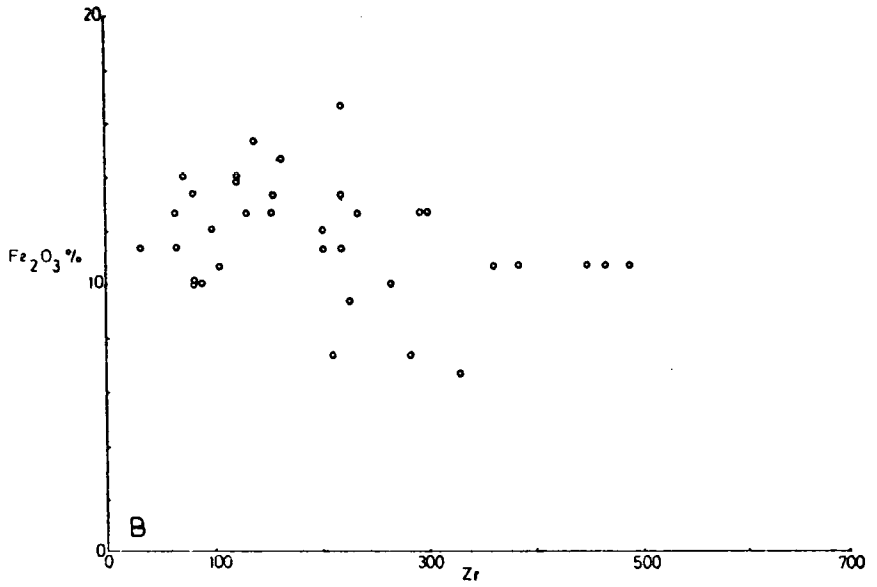
4) Similar considerations, in conjunction with correlation coefficients, show that Cr and Ni can be considered as essentially immobile in group A and B rocks, but probably

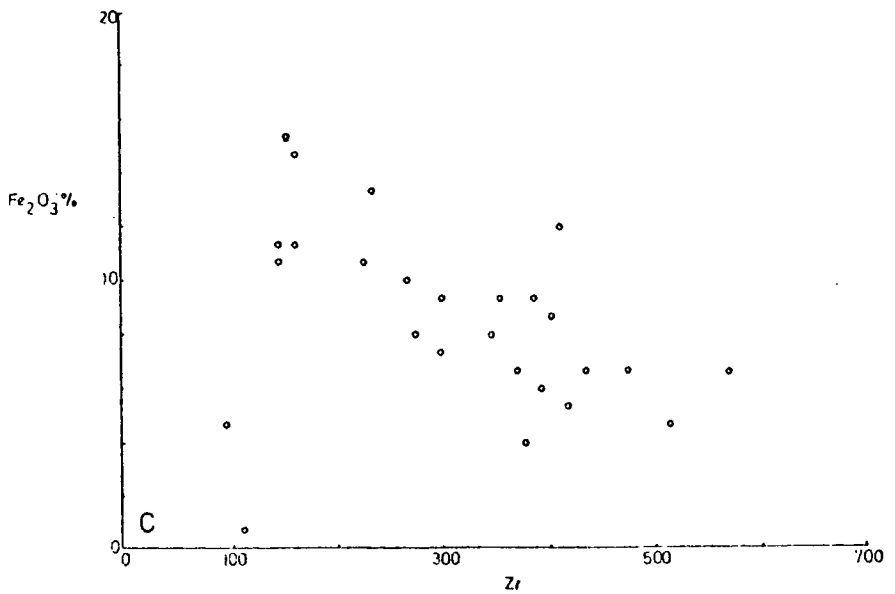

20
10
6
Al_2O_3 %
A
100
300
500
700
Zr

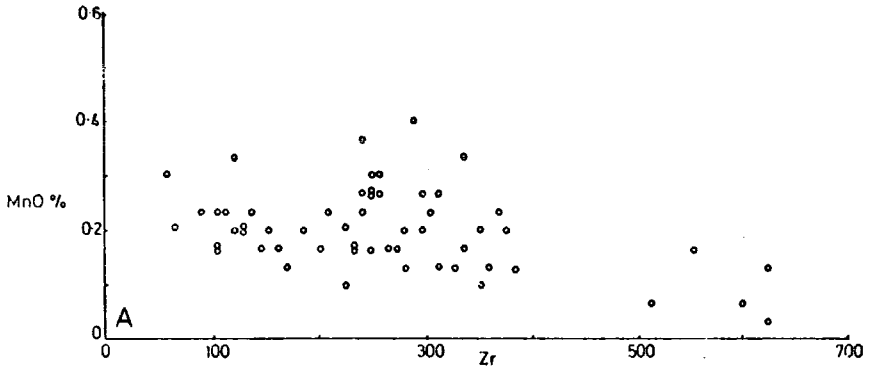

20
10
6
Al_2O_3%
B
0
100
300
500
700
Zr

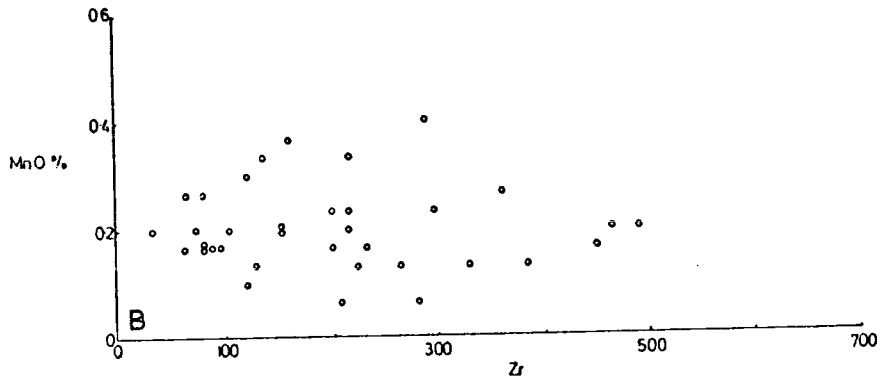

20
10
6
Al_2O_3%
C
0
100
300
500
700
Zr

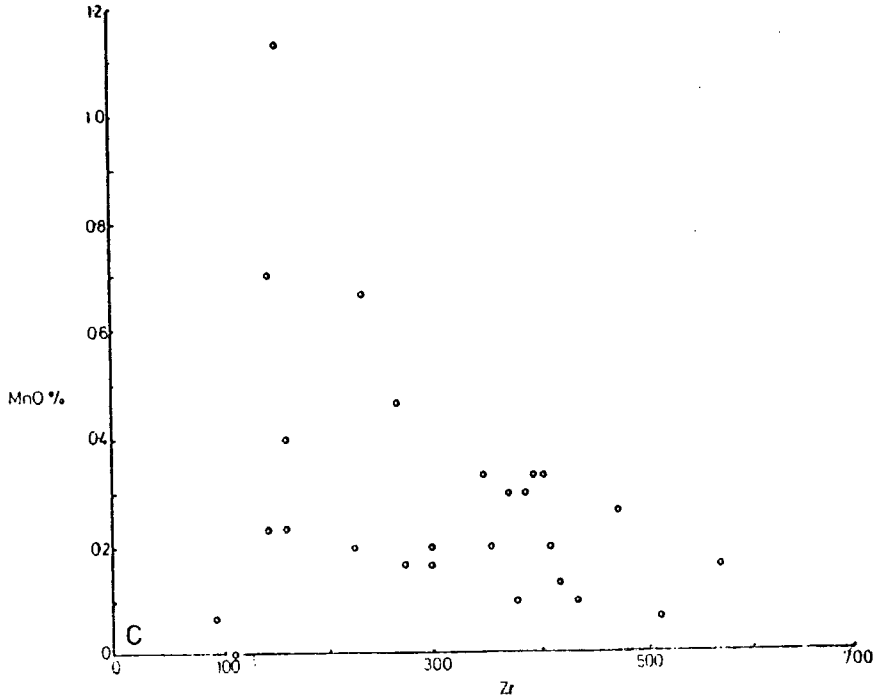

20
Fe_2O_3%
10
0
A
0
100
300
500
700
Zr

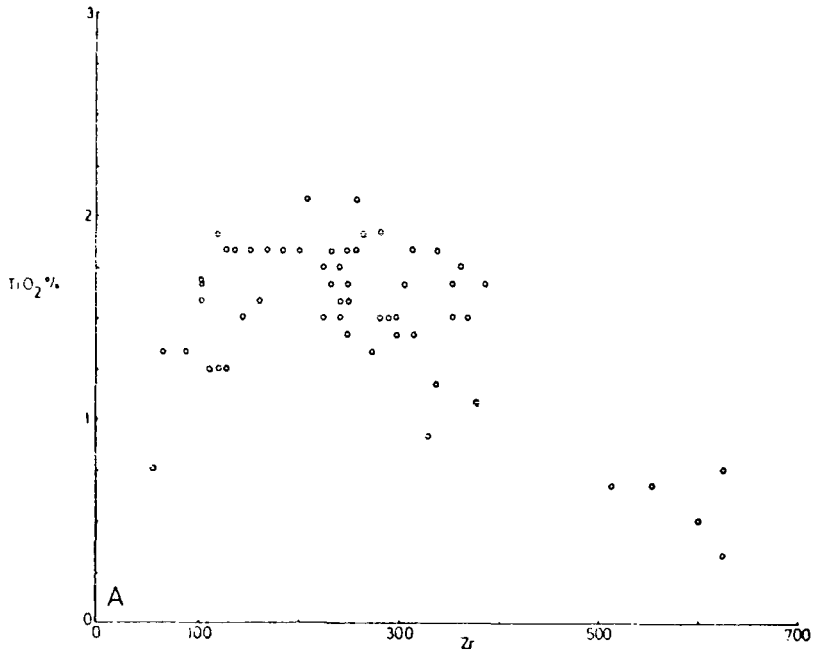

20
Fe_2O_3%
10
0
B
0
100
300
500
700
Zr

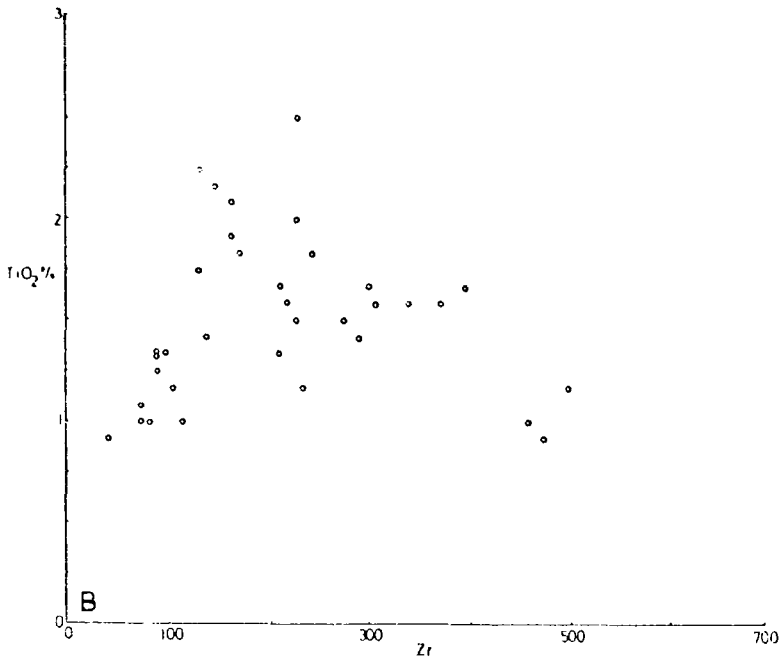

20
Fe_2O_3%
10
0
C
0
100
300
500
700
Zr

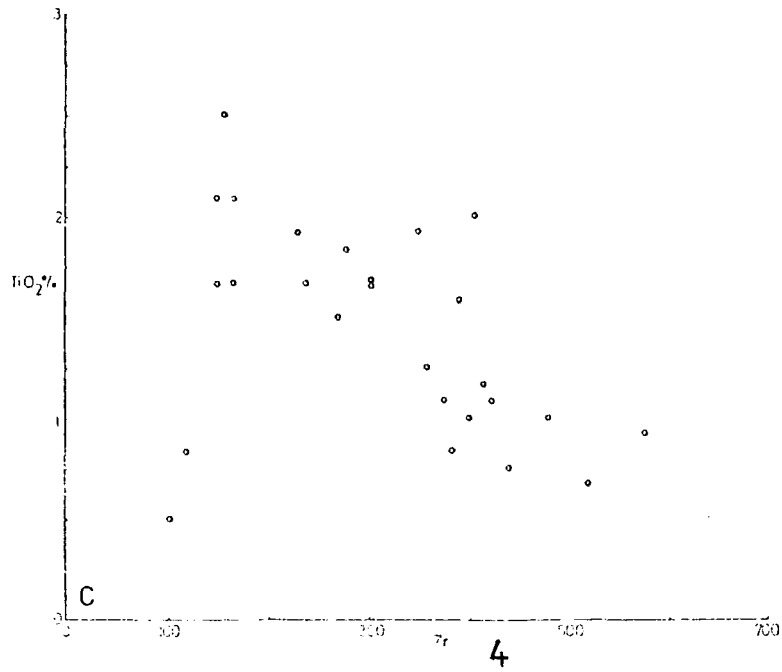

0·6
0·4
0·2
0
MnO %
A
0
100
300
500
700
Zr

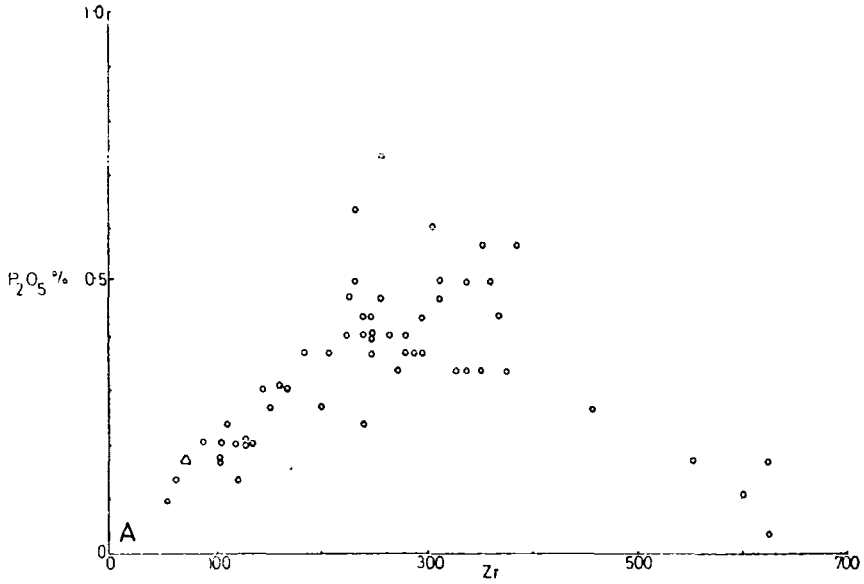

0·6
0·4
0·2
0
MnO %
B
0
100
300
500
700
Zr

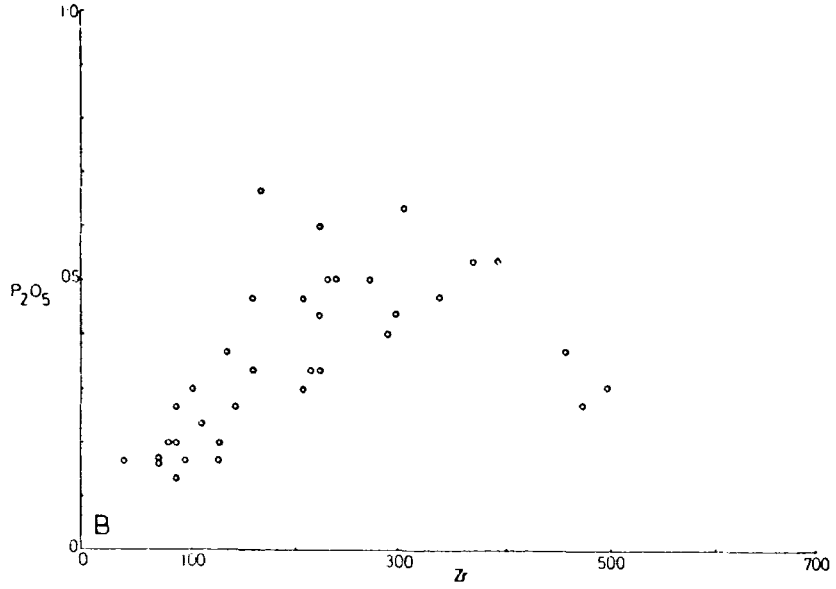

1·2
1·0
0·8
0·6
0·4
0·2
0
MnO %
C
0
100
300
500
700
Zr

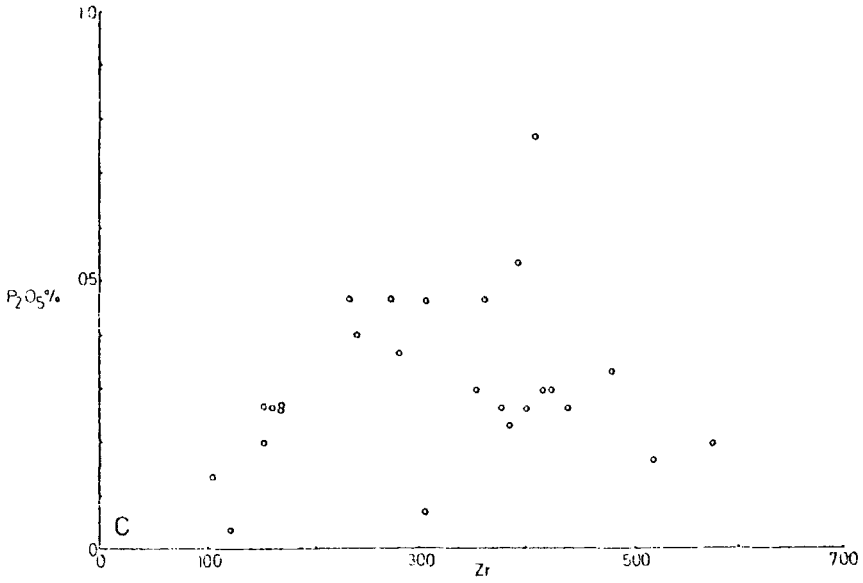

3
2
1
0
TiO_2 %
A
0
100
300
500
700
Zr

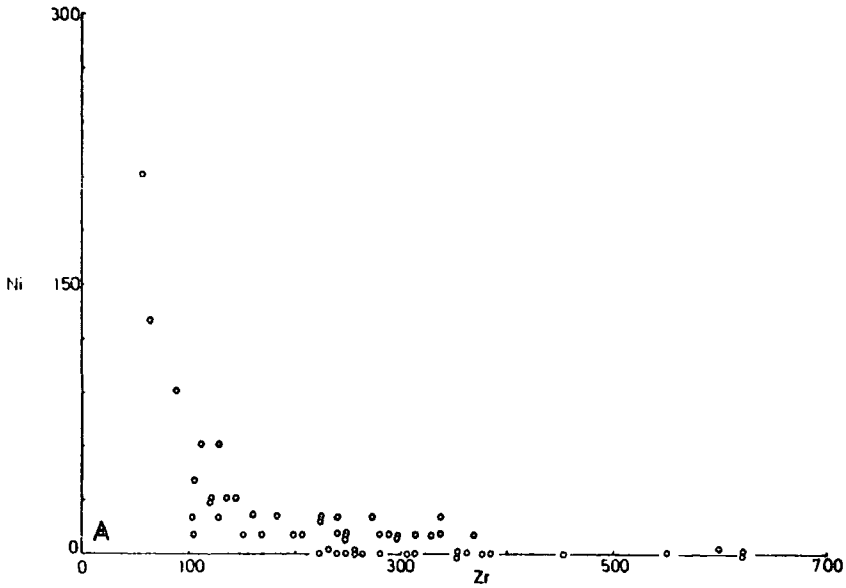

3
2
1
0
TiO_2 %
B
0
100
300
500
700
Zr

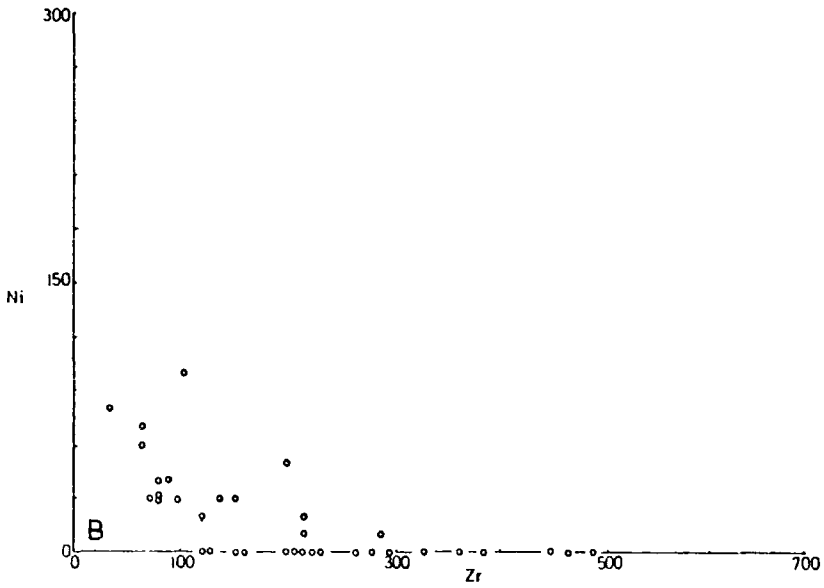

3
2
1
0
TiO_2 %
C
0
100
300
500
700
Zr

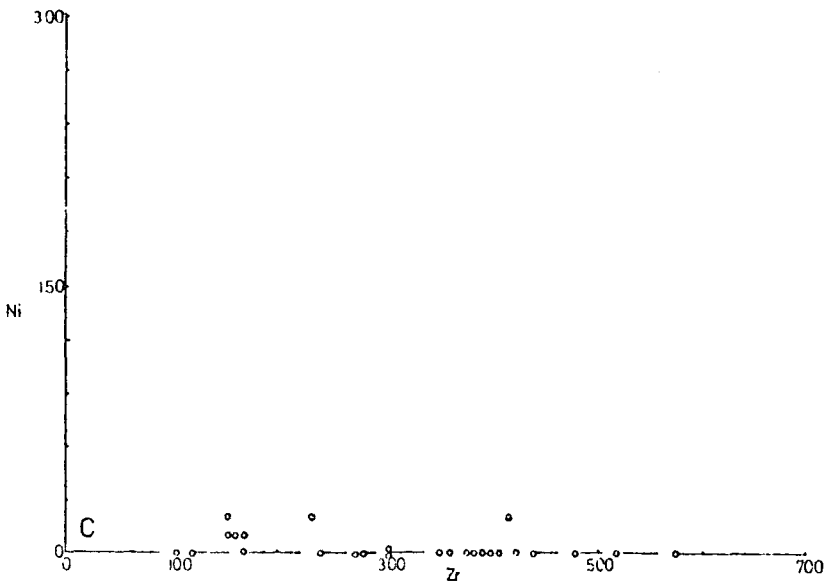

1·0
P_2O_5 % 0·5
0
A
0
100
300
500
700
Zr

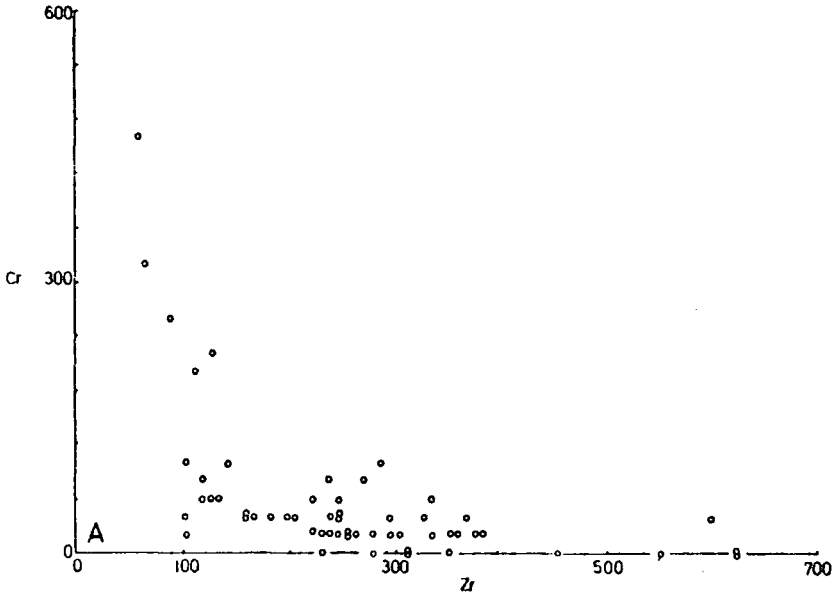

1·0
P_2O_5 0·5
0
B
0
100
300
500
700
Zr

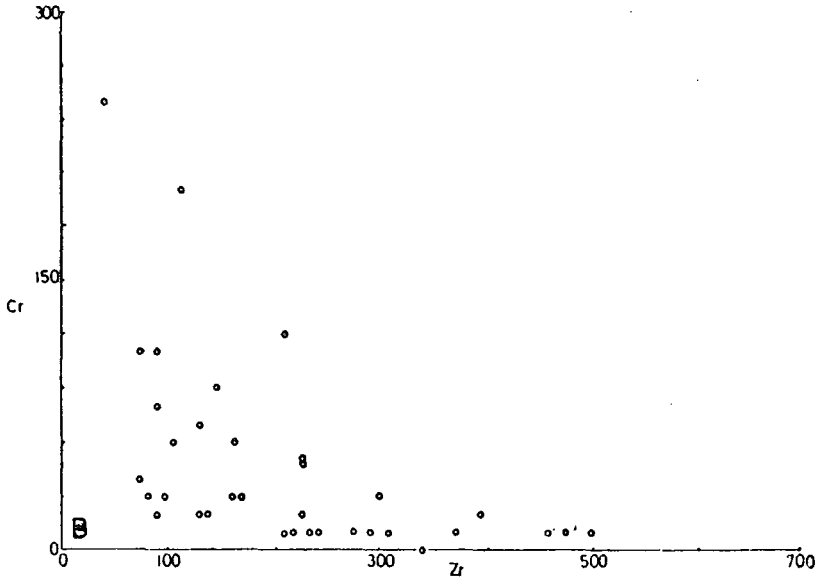

1·0
P_2O_5% 0·5
0
C
0
100
300
500
700
Zr

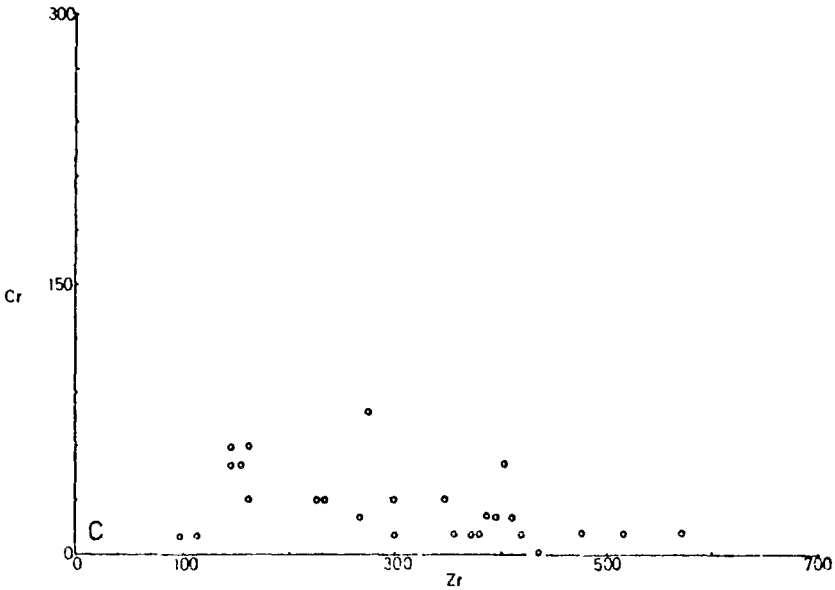

300
Ni
150
0
A
0
100
300
500
700
Zr


300
Ni
150
0
B
0
100
300
500
700
Zr


300
Ni
150
0
C
0
100
300
500
700
Zr


600
Cr
300
0
A
0
100
300
500
700
Zr


300
150
Cr
0
B
0
100
300
500
700
Zr


300
Cr
150
0
C
0
100
300
500
700
Zr

mobilised in the sulphidised rocks. This is supported by the highly significant correlations between Cr and Ni in groups A and B, but not in group C.

e) It is interesting that in group A rocks S is correlated with Zn at a significance level of 0.1% and with Cu and Ba at 1%, indicating that it is associated with Cu and Zn sulphides and barite.

f) Some of the pairs or group of elements that normally become highly mobile during alteration seem to have developed highly significant correlations amongst themselves as alteration progressed. This is certainly a consequence of the way alteration processes have operated in the area and not a magmatic effect.

Although K, Rb and Ba are highly mobile, they maintain and develop highly significant positive correlations amongst themselves, especially the pairs K-Rb and K-Ba, with progressive alteration. This indicates that alteration processes affected and distributed these elements in the same manner, in fact as will be shown, they were enriched during alteration. Thus $K/_{Rb}$ and $K/_{Ba}$ ratios tend to remain constant which may be of genetic use in the evaluation of magma types.

Ca and Sr develop a very strong positive correlation in group C rocks confirming the general and close proxy that Sr falls in with Ca through alteration. Similar highly significant positive correlations exist in the group of elements Mg-Mn-Zn in group B; but in the mineralised rocks, correlations of Mg-Mn and Mg-Zn become insignificant, Mn-Zn correlation becomes stronger and strong correlations amongst the group of elements Fe-Mn-Zn-Cu develop. These observations suggest that Fe, Cu, Zn and Mn behaved in similar fashions during inter-action with mineralising solutions.

3.3.2.3 Direction of element mobility

The question considered so far is whether some elements have been mobilised or not during the stages of alteration. The methods used are

unable to deduce if the mobilised elements were enriched or depleted with alteration.

Wood et al (1976) consider the water content and Floyd (1976) takes the Fe_2O_3/FeO ratios of the rocks as indicators of the degree of alteration i.e. further hydration and oxidation of the rocks with further alteration respectively. The water content of the Polusagi rocks shows no meaningful variation with any of the mobilised elements. However, the oxidation ratios are positively correlated with CaO and negatively with MgO and Sr in the group A rocks (Fig. 3.2) and no other convincing correlations exist. This suggests that Ca was enriched and Mg and Sr were depleted during the early stages of alteration.

Another way to estimate the direction of element mobility is to assume that Al_2O_3 remained constant during the course of alteration (Matthews, 1971; Krauskopf, 1979, pp. 82-83). This method is plausible for the Polusagi rocks, since Al_2O_3 variation is relatively small and it tends to stay immobile during alteration. In order to have a more meaningful estimation, basalts, andesites and dacites from each group are compared and the method assumes that the average Al_2O_3 contents of group A basalts, andesites and dacites are typical. Therefore the average composition of these rock types in groups B and C are recalculated to have the same Al_2O_3 contents as their counterparts in group A. The calculations were carried out as suggested by Krauskopf (op cit). A deviation of more than 20% from the average value of any oxide in the group A rock types was taken to indicate mobility. Emphasis was laid on the comparative data from basalts and andesites, since numbers of dacite samples in groups A, B and C are small and 5, 3 and 6 respectively. The results are summarised in Table 3.3. The following are the observations:

a) Further alteration from group A to group B volcanics involves marked further enrichment of Ca, marked enrichment of K, enrichment of Rb, Ba, Zn and Cu, release of Sr, some depletion in Na, probable further

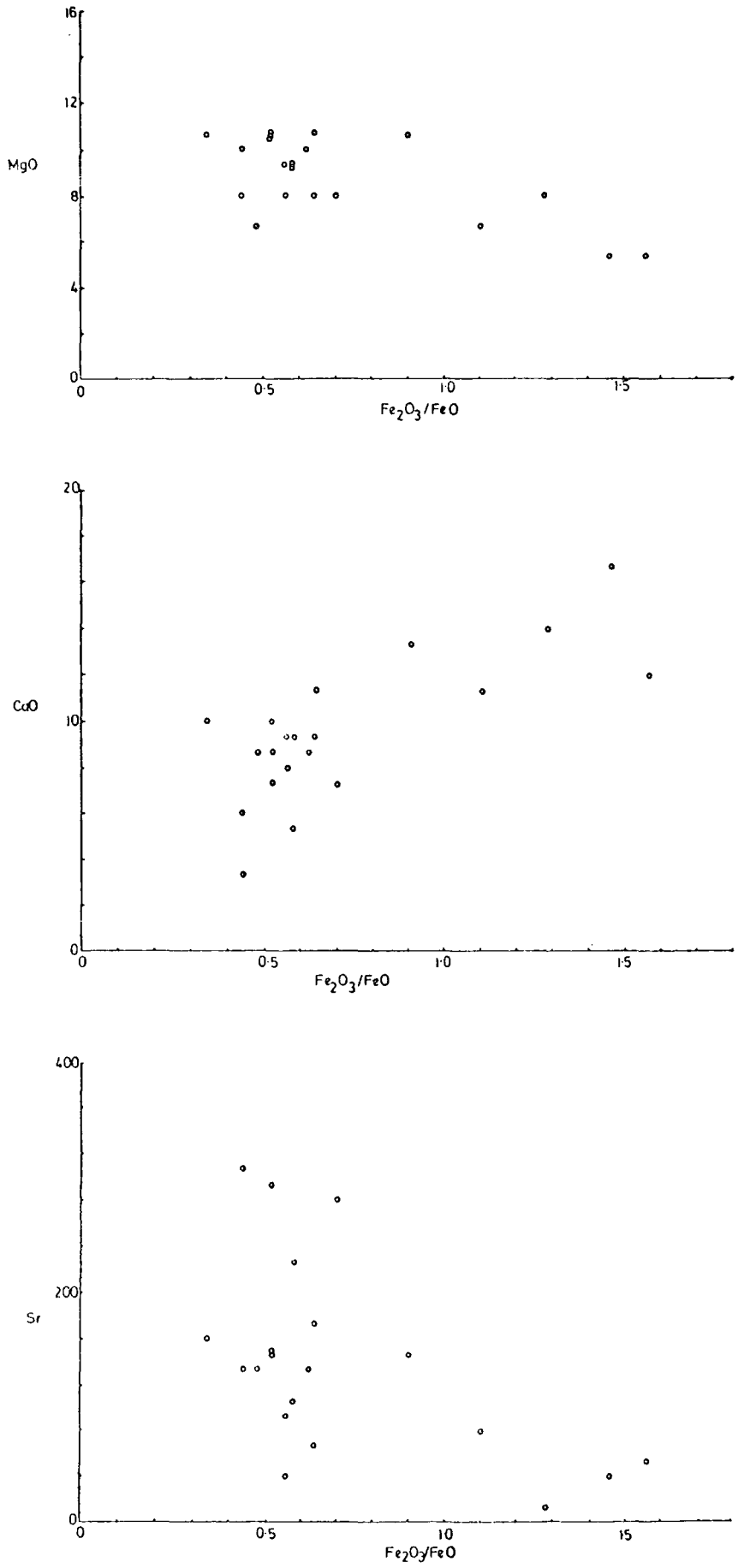


Fig.3.2. Variations of MgO, CaO and Sr with Fe_2O_3/FeO ratio.

TABLE 3.3

Element mobility directions

	GROUP B			GROUP C			GROUP A	SUMMARY FOR GROUP B	SUMMARY FOR GROUP C
	Basalt	Andesite	Dacite	Basalt	Andesite	Dacite			
SiO_2	+5	+10	-22	-11	-6	-31		NSC	depleted?
Al_2O_3	0	0	0	0	0	0		-	-
Fe_2O_3	-2	+2	+27	-40	-29	-15		NSC	depleted
MgO	-16	-18	+150	-30	+9	+219	depleted	probable depletion	probable enrichment
CaO	+31	+45	-15	-94	-60	-50	enriched	enriched	highly depleted
Na_2O	-18	-2	-24	-50	-32	-46		depleted	highly depleted
K_2O	+172	+107	-83	+483	+240	+139		highly enriched	highly enriched
MnO	+5	-10	+60	+48	+29	+130		slight enrichment?	highly enriched
Sr	-	+	-	-	-	-	depleted	depleted	depleted
Rb	+	+	(-)	+	+	+		enriched	enriched
Ba	+	+	NSC	+	+	+		enriched	enriched
Zn	+	NSC	(+)	++	++	+		some enrichment	enriched
Cu	+	+	(-)	+	+	-		enriched	enriched
Ni	NSC	NSC	NSC	-	(-)	NSC		NSC	irregular or depletion
Cr	(-)	NSC	NSC	(-)	NSC	NSC		NSC	NSC or depletion

NSC means no significant change

\+ means enrichment

\- means depletion

( ) means slight

depletion in Mg and no significant directional consistency in Si and total Fe. Although S showed large variations, it is insignificant since the differences of averages between group A and B rocks are small and a difference of 0.01wt% gives rise to 50% deviation.

b) Increased alteration into the sulphidised group C rocks involves extensive release of Ca, Na and to a lesser extent total Fe. Sr and probably some Si are released. K gets highly enriched and there are lesser enrichments of Mn, Rb, Ba, Zn and Cu and probably of Mg. Ni and Cr may have suffered leaching.

c) When these patterns of mobility directions are compared, it is apparent that the behaviours of Mg and Ca are antipathetic and there is an interesting reversal of mobility direction in group C rocks i.e. while Ca is taken up and Mg is released in groups A and B rocks, Ca is released and Mg tends to be taken up in group C rocks.

3.3.3 Element mobility in the hypabyssal rocks

A similar approach as was pursued for the volcanics reveals that these rocks are even less affected by alteration than the group A volcanic rocks. All the elements seem to have retained their original igneous abundances (see Table 3.4). For example, while K, S, Sr, Rb, Ba, Cu and Zn have been mobilised to varying degrees in group A volcanics, they are largely immobile in these group A hypabyssal rocks. The only element which does not show significant correlation with the 5 immobile elements is S and this is due to its low abundance : out of 12 samples, 7 have zero concentrations, 4 have 0.01% and only 1 has 0.10% S.

Isochemical nature of spilitisation of the hypabyssal rocks can be explained by their relatively coarser grain sizes and compactness, thus being less prone to hydrothermal solutions and sub-marine weathering.

3.4 Summary and conclusions

The behaviour of elements during alteration is summarised in Table 3.5 for each of the groups of rocks. The following conclusions are drawn:

TABLE 3.4

Correlation matrix for the hypabyssal rocks. No of samples = 12. Significance levels at 0.01%=0.8911, 0.1%=0.8233 and at 1%= 0.7079

VARIABLE	1. SIO2	2. AL2O3	3. FE2O3	4. MGO	5. CAO	6. NA2O	7. K2O	8. TIO2	9. MNO	10. S	11. P2O5	12. NB	13. ZR	14. Y	15. SR	16. LA	17. CE	18. RB	19. BA	20. ZN	21. CU	22. NI	23. CR
1.SIO2	1.0000																						
2.AL2O3	-.0088	1.0000																					
3.FE2O3	-.6941	-.2458	1.0000																				
4.MGO	-.8785	-.0873	.3724	1.0000																			
5.CAO	-.9407	-.0977	.4951	.9015	1.0000																		
6.NA2O	.9240	.0536	-.4714	-.9617	-.9408	1.0000																	
7.K2O	-.6851	.4413	.1373	.6512	.7353	-.7672	1.0000																
8.TIO2	-.4691	-.4230	.8803	.1106	.3620	-.2726	.0366	1.0000															
9.MNO	-.8942	-.0645	.6629	.6923	.8953	-.8184	.7244	.6285	1.0000														
10.S	-.2078	-.0866	.3914	.0744	.1173	-.2084	.1438	.4393	.3429	1.0000													
11.P2O5	.0534	-.0025	.5109	-.3978	-.2781	.3684	-.4435	.4864	-.0162	.3865	1.0000												
12.NB	.9138	-.0387	-.4047	-.9139	-.9583	.9468	-.8093	-.2452	-.8577	-.0215	.3987	1.0000											
13.ZR	.9535	-.0641	-.4985	-.9263	-.9522	.9730	-.8078	-.3069	-.8699	-.1977	.3007	.9701	1.0000										
14.Y	.8700	-.0044	-.3154	-.9101	-.9534	.9423	-.8152	-.1941	-.8453	-.0982	.4468	.9842	.9560	1.0000									
15.SR	-.4717	.2897	-.0405	.4279	.6035	-.4177	.5641	-.0988	.4950	-.1904	-.2754	-.5943	-.5225	-.6098	1.0000								
16.LA	.8299	.1576	-.3581	-.8344	-.9487	.8974	-.7578	-.3362	-.8633	-.1121	.4459	.9292	.9119	.9481	-.5478	1.0000							
17.CE	.8177	.0558	-.3012	-.8274	-.9283	.8778	-.7924	-.2585	-.8660	-.1502	.4305	.9337	.9159	.9628	-.6212	.9751	1.0000						
18.RB	-.7035	.4353	.1393	.6978	.7421	-.7930	.9907	-.0037	.7138	.1209	-.4570	-.8319	-.8233	-.8336	.5676	-.7432	-.7892	1.0000					
19.BA	-.7020	.3305	.2471	.6482	.7290	-.7880	.9675	.1625	.7728	.3441	-.3360	-.7783	-.8094	-.7941	.4629	-.7464	-.7762	.9605	1.0000				
20.ZN	-.8275	-.0511	.5599	.7679	.7981	-.8637	.6690	.4449	.8412	.6021	-.1157	-.7870	-.8660	-.8180	.3318	-.7650	-.7988	.6865	.7580	1.0000			
21.CU	-.5120	.1469	.0867	.5778	.5820	-.6377	.6193	-.0069	.4100	.2890	-.3146	-.5019	-.5884	-.5508	.1776	-.5915	-.5220	.5710	.6141	.4976	1.0000		
22.NI	-.6409	-.1337	.0772	.9151	.7141	-.8007	.4816	-.2078	.3876	-.1156	-.5408	-.7261	-.7159	-.7391	.3256	-.6586	-.6491	.5422	.4490	.5033	.5509	1.0000	
23.CR	-.6220	-.0722	.0372	.8788	.7120	-.7856	.5234	-.2179	.3727	-.1235	-.5505	-.7035	-.7011	-.7210	.2990	-.6729	-.6350	.5575	.4739	.4640	.7116	.9686	1.0000

TABLE 3.5

Mobility of elements in the Polusagi rocks

1) Group A volcanics:

Highly immobile	=	Zr, Ti, Y, Nb, La, Ce, P, Ni, Cr
Immobile	=	Si, Al, total Fe, Mg, Ca, Na, Mn
Mobile	=	K, Rb, Zn
Highly mobile	=	S, Sr, Ba, Cu

2) Group B volcanics:

Highly immobile	=	Zr, Ti, Y
Immobile	=	Al, Nb, La, Ce, P, Cr, Ni
Mobile	=	Si, total Fe, Mg, Ca, Na, Mn
Highly mobile	=	K, S, Sr, Rb, Ba, Cu, Zn

3) Group C volcanics:

Highly immobile	=	Zr, Ti, Y, Nb, La, Ce
Immobile	=	P
Mobile	=	Al, Cr, Ni
Highly mobile	=	Si, total Fe, Mg, Ca, Na, K, Mn, S, Sr, Rb, Ba, Zn, Cu

4) Hypabyssal rocks:

Highly immobile	=	Zr, Ti, Y, Nb, La, Ce, P, Ni, Cr
Immobile	=	Si, Al, total Fe, Mg, Ca, Na, K, Mn, Sr, Rb, Ba, Zn, Cu

1) The chemical abundances, hence, inter-element variations in the group A volcanics and hypabyssal rocks are to a large extent of original igneous values and can be employed in geochemical and petrogenetic studies. However, in such studies, the immobile elements Zr, Nb, Y, La, Ce, Ti, P, Ni and Cr should be given priority, although most of the major elements for this group can also be used. Care must be taken when dealing with K, Rb and Zn and more so with S, Sr, Ba and Cu, although their abundances are possibly not far removed from original igneous concentrations.

2) For the more altered rocks of groups B and C, major oxide concentrations have been mobilised and thus cannot be used for geochemical and petrogenetic studies. Instead, the above mentioned immobile elements, particularly Zr, Y and Ti, should be used. Caution must be exercised with Cr and Ni concentrations in the sulphidised rocks.

CHAPTER FOUR

CLASSIFICATION AND TECTONIC SETTING

4.1 Introduction

As was shown in Chapter two and will be apparent in this chapter and the next, the Polusagi rocks of igneous origin have such field relations and continuous and gradational chemical variations as to suggest that they belong to a common magmatic source. Therefore, they are considered as a suite of rocks: the Polusagi rock suite.

This chapter is composed of two different but related parts. The first part deals with the classification of the Polusagi rock suite into recognised magma types and their various magmatic products and the second part discusses the tectonic setting at which the rocks were produced.

4.2 Classification of the Polusagi rocks

4.2.1 Introduction

Although different magma types had been recognised in the 1920's (Bailey et al, 1924), it was not certain if these magma types had world-wide significance. Subsequent work by Kennedy (1933) and Tilley (1950) showed that the two types of magmas, the non-porphyritic central and plateau magma types, were of world-wide significance. They were later called tholeiitic and alkali-olivine magma types. Kennedy argued that the "olivine basalt magma type" was parental to an alkali line of descent ending with trachyte and phonolite, while the "tholeiitic magma type" led to a more siliceous association ending with rhyolite which he equated with the "calc-alkali" rock series. Tilley stressed that the tholeiitic basalt series was distinctive from the calc-alkali series in that the associated andesites were richer in iron and relatively minor, while the calc-alkali rock series, associated with orogenic belts, had the andesites as the dominant rock.

Bowen (1928) emphasised the enrichment of residual liquid in silica and alkali-feldspars; he did not consider the iron enrichment as significant and regarded the calc-alkali trend as normal fractionation trend of the tholeiitic magma. On the other hand, Fenner (1929) stressed the enrichment of residual liquid in iron rather than silica and regarded the tholeiitic trend as normal.

Following the studies of the Skaergaard intrusion, the iron-enrichment trend of residual liquid, presumably by the process of fractional crystallisation, was strikingly demonstrated (e.g. Wager and Deer, 1939). Similar trends of tholeiitic magma were recognised in many differentiated intrusive bodies, such as the Karoo dolerite sill and the Palisade dolerite sill, though the iron-enrichments found were not as strong as in the Skaergaard intrusion. The iron-enrichment during fractional crystallisation of basaltic magma was, therefore, found to be common for a certain basaltic magma type, now identified as the tholeiitic magma type.

The trends of fractional crystallisation of basaltic magmas have been investigated in detail in many volcanic suites, such as in the Japanese islands (Kuno, 1950,59,60). Kuno distinguished two different rock series on the basis of groundmass pyroxene: the "pigeonitic rock series" that contains pigeonite in the groundmass and the "hypersthenic rock series" that contains orthopyroxene in the groundmass. Kuno (1968) correlated his pigeonitic rock series with the tholeiitic rock series and the hypersthenic rock series with the calc-alkali rock series. It was demonstrated by Kuno that the volcanic rocks of calc-alkali rock series are relatively low in iron and do not exhibit iron enrichment as opposed to the tholeiitic rock series.

Kuno (1960,68) introduced a third "primary" magma type which he called "high alumina basalt", apparently distinct from the tholeiitic and calc-alkali rock series. Rocks of this series, according to Kuno, belong mostly to "pigeonitic" and partly to "hypersthenic" rock series.

Wilkinson (1968) adopted the term "sub-alkaline" to include both tholeiitic and calc-alkali rock series. This was followed in Irvine and Baragar's (1971) chemical classification of common volcanic rocks.

In the present study, the following framework for the classification of magma types has been used, which is like the one proposed by Irvine and Baragar (op cit): The main rock series are divided into a) Sub-alkaline and b) Alkaline, with the former comprising the tholeiitic and calc-alkali rock series (Wilkinson, 1968; Irvine and Baragar, 1971; Middlemost, 1972, 75,80; Winchester and Floyd, 1977; Floyd and Winchester, 1978) and the latter the alkali-olivine basalt series and the shoshonite association of Joplin (1965,68). The high-alumina basalt of Kuno (1968) is considered to be representative of basic members of the calc-alkali rock series (Wilkinson, 1968; Irvine and Baragar, 1971; Winchester and Floyd, 1977; Floyd and Winchester, 1978).

Before deciding whether the Polusagi rock suite is of alkaline or sub-alkaline nature, the rock suite will be subdivided into various magmatic products, since the chemical character of the basic members of the above mentioned rock series play an important role in the decision process.

4.2.2 Subdivision of the Polusagi rock suite

Although some discrimination amongst the volcanic and the hypabyssal rocks on mineralogical grounds were discussed in Chapter two, the rocks are best subdivided on chemical grounds due to the extensive alteration of the igneous mineralogy. Because of the problems of the element mobility, discussed in Chapter three, only the immobile elements Zr, Nb, Y, La, Ce and Ti have been used in developing a chemical classification. However, in order to be compatible with the conventional classification schemes which use major element abundances, the dividing values of the immobile element concentrations separating the basic, intermediate and

acid rock types were decided by comparison with the major element concentrations in group A rocks, where most of them have been shown to be essentially of original igneous qualities (Chapter three). Therefore, the classification based on the immobile element abundances should not only be compatible with the other schemes, but also be applicable to even the most intensely altered rocks in the studied area.

4.2.2.1 Subdivision of the volcanic rocks

In the group A volcanic rocks, SiO_2 exhibites a large variation from 44% to 74%, thus covering the basic, intermediate and acid compositional fields or more appropriately basaltic, andesitic and dacitic ranges, see sections 4.2.3 and 4.2.4. SiO_2 contents of 52% (Jakes and White, 1972; Carmichael et al, 1974; Streckeisen, 1980) and 62% (Jakes and White,1972; Middlemost, 1972,75,80; Arculus, 1973; Brown et al, 1977) are the values most commonly accepted as chemical divisions between basalt, andesite and dacite respectively, so that all three can be expected in the group A rocks. Although Mg has been used by some authors as a basis (e.g. Beddoe-Stephens,1977), because of the Ca-Mg relationship discussed in Chapter three (section 3.3.3), MgO + CaO content is thought to be more reliable to employ into the subdivision. Fig.4.1 shows the covariance of SiO_2 against MgO + CaO and how the rocks are subdivided on this basis.

Since the immobile elements Zr, Nb, Y, La and Ce show positive and linear trends against SiO_2, and Zr and Ti are probably the most immobile elements, the following chemical scheme of subdivision is proposed for all the volcanic rocks in the area which corresponds to the basis in Fig. 4.1:

Basic (basaltic) rocks:

$Zr < 200$ ppm
$Nb < 15$ "
$Y < 60$ "
$La < 13$ "
$Ce < 30$ "

$Zr/TiO_2\% < 120$ or $Zr \times 10^3/Ti$ ppm < 20

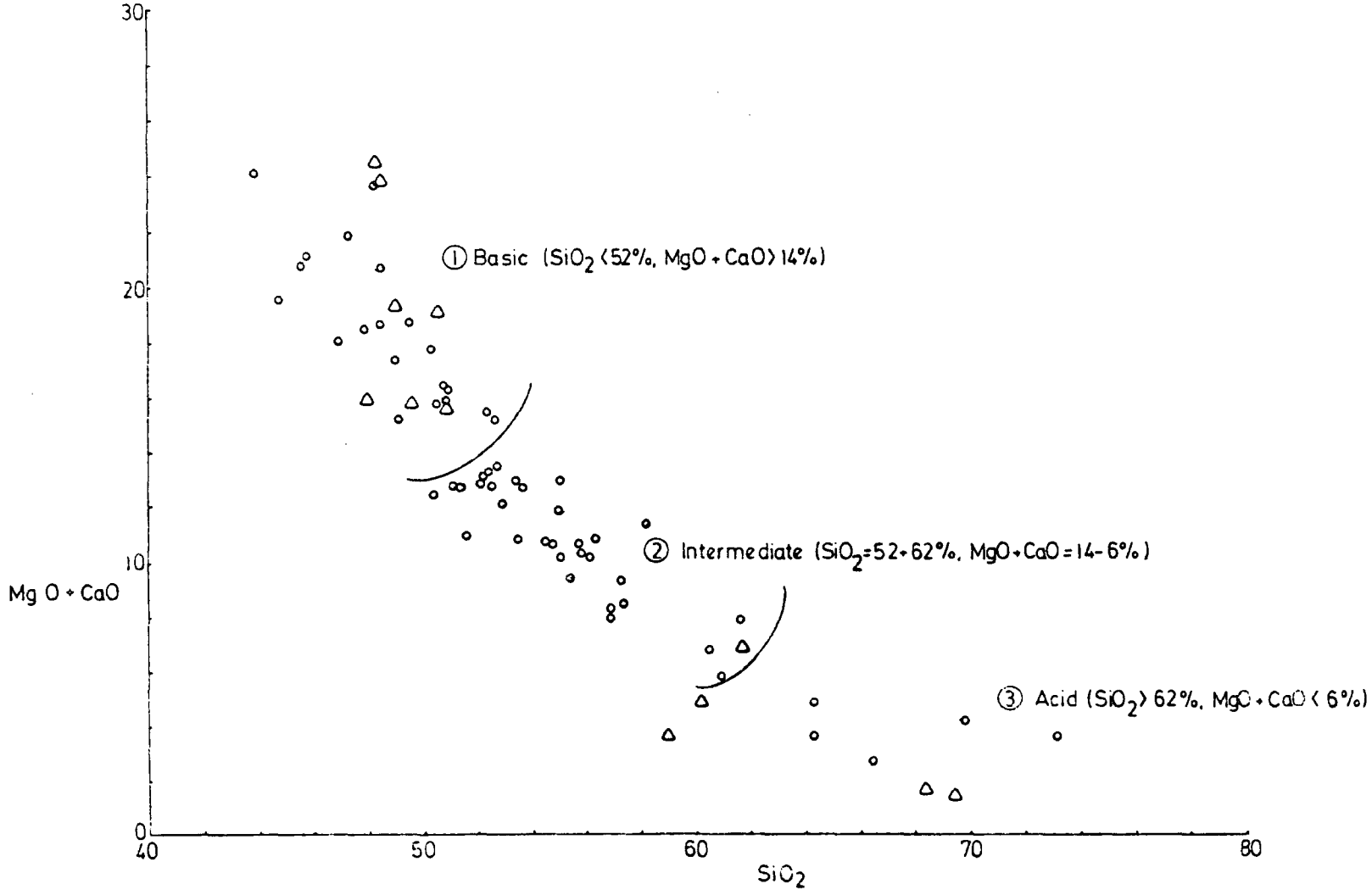


Fig.4.1. Variation of CaO+MgO with SiO_2 and the subdivision of the rocks (Group A).

o : volcanics and △ : hypabyssal rocks.

Intermediate (andesitic) rocks:

Zr	=	200-400 ppm
Nb	=	15- 25 "
Y	=	60- 90 "
La	=	13- 25 "
Ce	=	30- 55 "

Zr/TiO_2% = 120-500 or $Zrx10^3/Ti$ ppm = 20-80

Acid (dacitic) rocks:

Zr	>	400 ppm
Nb	>	25 "
Y	>	90 "
La	>	25 "
Ce	>	55 "

Zr/TiO_2% > 500 or $Zrx10^3/Ti$ ppm > 80

4.2.2.2 Comparison with other chemical schemes of subdivision

Discrimination of differentiation products of different magma series on the basis of immobile trace elements and their ratios has also been proposed by Winchester and Floyd (1977) and successfully applied to some altered and metamorphosed rocks (Floyd & Winchester 1978). In their classification, not only do they discriminate between sub-alkaline and alkaline rock series, but also discriminate the basalts, andesites, dacites and rhyolites within the sub-alkaline magmatic rocks. Their discrimination diagrams, utilising the trace element ratios Zr/TiO_2 and Nb/Y and Ce have been employed for the Polusagi rocks in Figs. 4.2 and 4.3 for comparison with the scheme of classification proposed above. These plots clearly indicate the sub-alkaline character of the Polusagi rock suite and exhibit total agreement on the discrimination of basalts and andesites. However, although almost all the andesites plot into the appropriate fields in the diagrams, dacitic rocks tend to plot into the fields reserved for more acidic rocks such as rhyodacites and rhyolites. This can be expected as the andesite and rhyolite fields on these diagrams are based on the calc-alkali suite of rocks (Winchester and

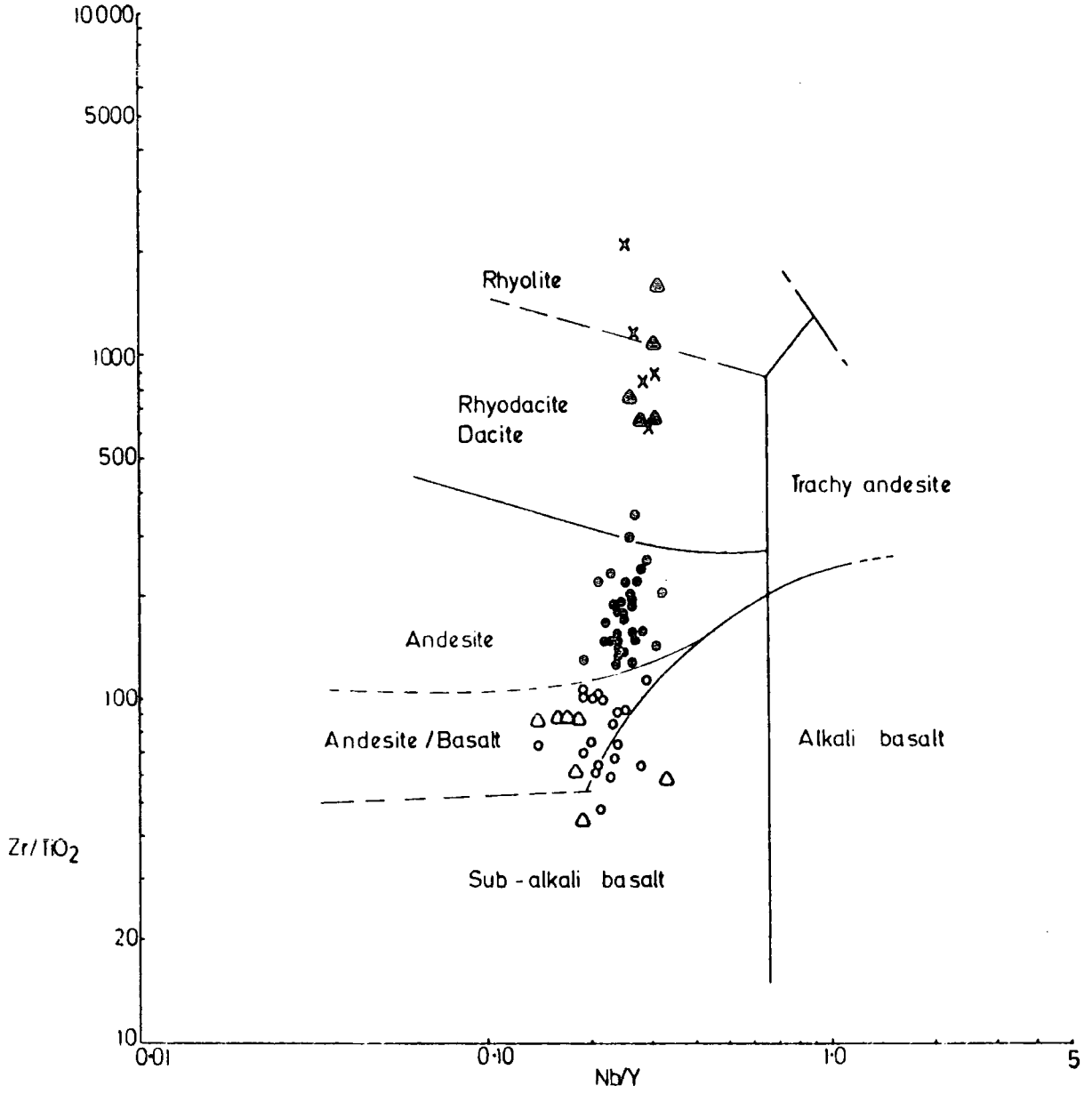


Fig.4.2 Zr/TiO_2-Nb/Y discriminant diagram showing the Polusagi rocks and the fields delimited by Winchester and Floyd (1977).

o : Basalt

o : Andesite

x : Dacite

△ : Gabbro

▲ : Plagiogranite

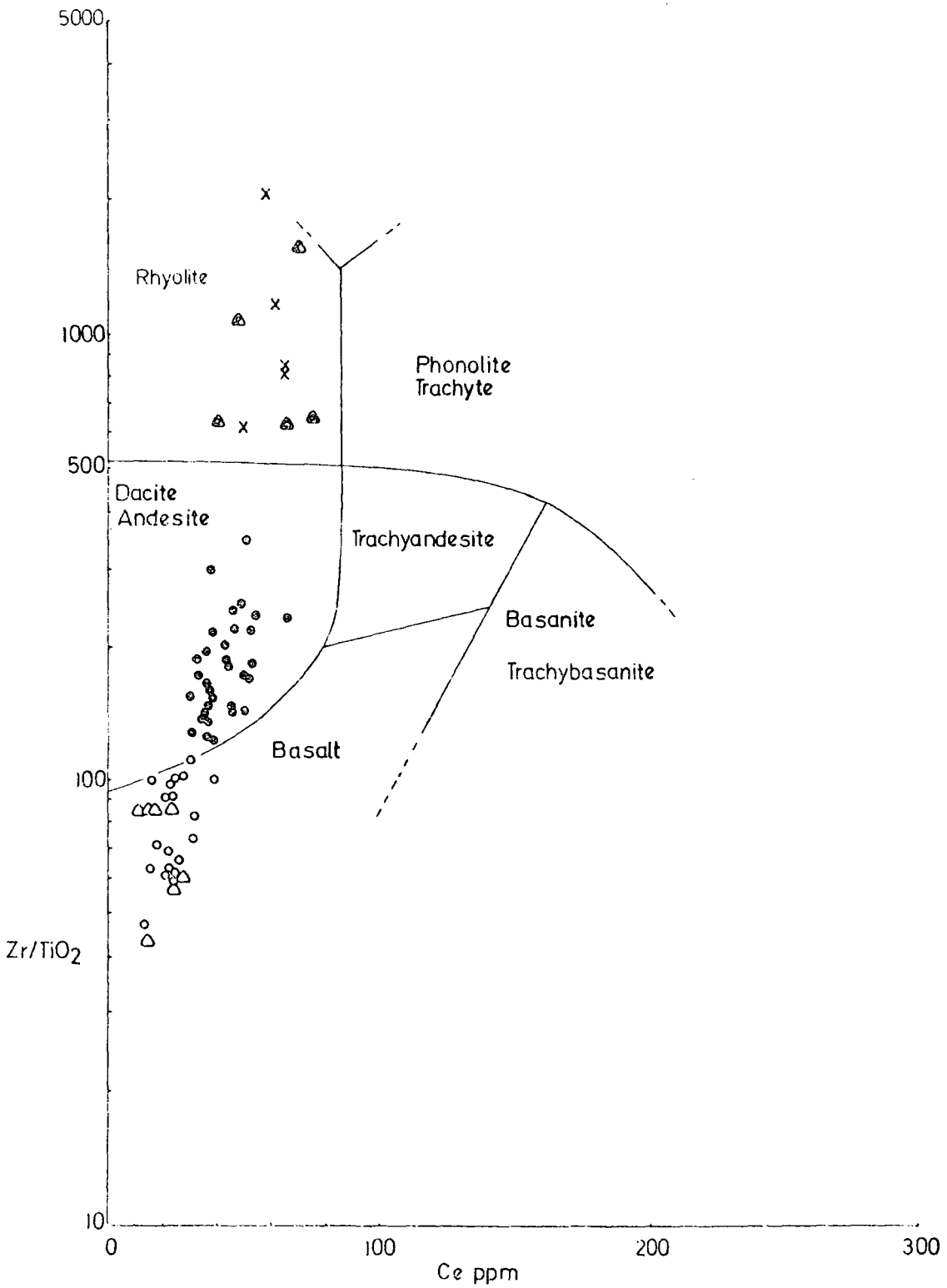


Fig.4.3 Cr/TiO_2-Ce diagram showing the Polusagi rocks and the fields defined by Winchester and Floyd (1977).

Symbols as in Fig.4.2.

Floyd, 1977), while the Polusagi rock series is of tholeiitic nature (see section 4.2.3) and Zr concentrations in the tholeiitic andesites and dacites of the Polusagi rock suite are higher than most of their counterparts in other areas (see section 4.3.5).

Normative parameters such as colour index and normative plagioclase composition have been used to discriminate basalts from andesites. Various delimiting values for these parameters have been suggested (Streckeisen, 1980; and see Coats, 1968, for a review). Irvine and Baragar (1971), in their chemical classification of common volcanic rocks, proposed a diagram plotting normative colour index against normative plagioclase composition, thus making use of both parameters as a simple and satisfactory diagram for subdividing all sub-alkaline rocks into differentiation products. As a further test and comparison, the Polusagi rocks were plotted in this diagram in Fig. 4.4 and it shows a high degree of agreement. All the basalts, 90% of andesites and all the dacites plot into the appropriate fields defined by Irvine and Baragar (op cit). Furthermore, andesites plot into the tholeiitic andesite field i.e. having more sodic plagioclase at the equivalent colour index than normal andesites.

4.2.2.3 Subdivision of the hypabyssal rocks

The chemical classification of the hypabyssal rocks is virtually the same as proposed for the volcanic rocks and the hypabyssal rocks have also been plotted in the diagrams used when dealing with the volcanic rocks (Figs. 4.1, 4.2, 4.3 and 4.4). It is apparent that the basic and acid hypabyssal rocks (having $<$ 52% SiO_2 and $>$ 62% SiO_2 respectively) are the chemical equivalents of the basalts and dacites. Nomenclature for the coarse grained equivalent of basalts and dacites is "gabbro" and "granodiorite" (Hatch et al 1972, Carmichael et al, 1974). As far as the rocks of the studied area are concerned there is no plutonic equivalent to the andesites.

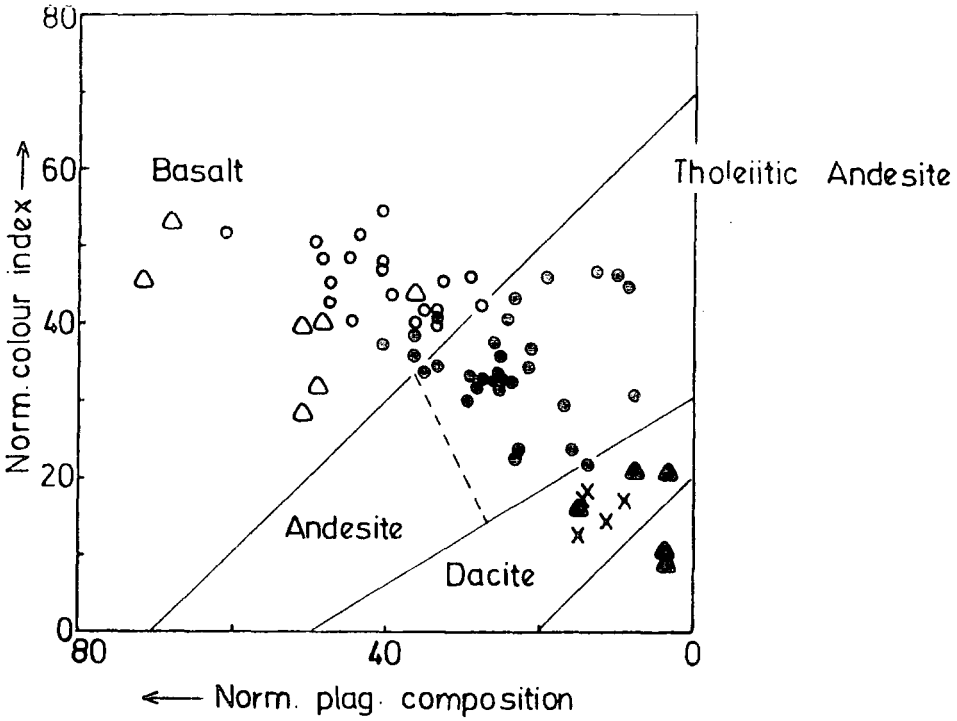


Fig.4.4 Normative colour index vs. normative plagioclase composition. The defined fields are for the sub-division of sub-alkaline rock suites (Irvine and Baragar, 1971).

$$\text{Normative (cation norm.) plag. composition} = \frac{100\ An}{An+Ab+5/3\ Ne}$$

Normative (cation norm.) colour index = Ol+cpx+opx+Mag+Ilm

o : Basalt

⊙ : Andesite

x : Dacite

△ : Gabbro

▲ : Plagiogranite

Although the nomenclature for the basic hypabyssal rocks (gabbro) is not ambiguous, this is not so for the acid hypabyssal rocks. In ophiolites, such leucocratic rocks seem to be common and where modal analyses of these rocks are available, Coleman (1977) reports that they plot near the quartz-plagioclase boundary on the Q-P-A triangle of Streckeisen (1976). Various names have been given to such rocks depending on the mafic mineral content such as granodiorite, quartz-diorite, tonalite and trondhjemite. For example, Whitten and Brooks (1972) define trondhjemite as "potash feldspar-free granodiorite". The Polusagi acid hypabyssal rocks contain extremely low values of K_2O (average = 0.02%), hence extremely small normative orthoclase (always $<$ 0.3%), and the normative An content of plagioclase varies from 2.4 to 11.7%. SiO_2 ranges from 59% to 70%, Na_2O is high and restricted - from 7.5% to just over 8%. For such rocks associated with ophiolites, Coleman and Peterman (1975) gave the name "oceanic plagiogranite" as a descriptive and collective name : "high silica, low to moderate alumina, low total iron-magnesium and extremely low K_2O characterise the oceanic plagiogranites and their associates. Normative orthoclase is usually less than 4 mol% and normative An content of plagioclase ranges from An_{21} - An_{61}" (Coleman,1977).The Polusagi acid hypabyssal rocks are thus termed "plagiogranite" and they are distinct from tonalites and trondhjemites and in general richer in normative Ab content of plagioclase than the oceanic plagiogranites of Coleman (1977), see Fig. 4.5.

4.2.2.4 Further considerations of the subdivided rocks

Chemical classification, proposed in the preceding pages, of 129 lavas and hypabyssal rocks produces 46 samples of basalt, 57 samples of andesite, 14 samples of dacite, 7 samples of gabbro and 5 samples of plagiogranite. Average major and trace element abundances of the basalts, andesites and dacites of group A rocks and of the gabbro and plagiogranite samples are

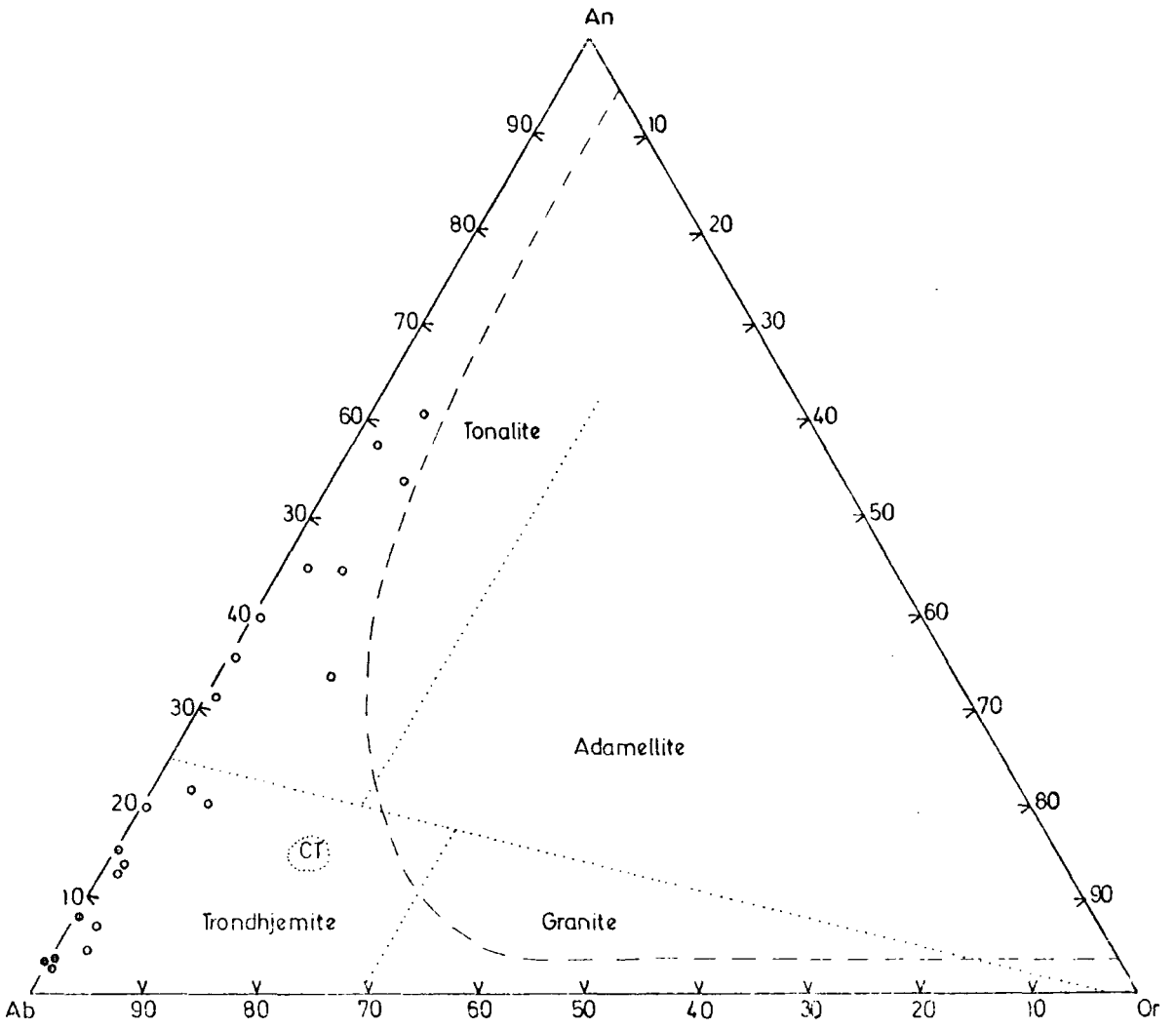


Fig.4.5 Triangular diagram of normative contents of Ab, An and Or for the Polusagi plagiogranites (●) and the oceanic plagiogranites (o) of Coleman (1977). From broken line to Ab corner: low pressure feldspar field. Dotted lines separate various rock types on the basis of their feldspar ratios. CT = continental trondhjemite.

presented in Tables 4.1 and 4.2 respectively, together with ranges and standard deviations. Individual rock analyses are listed in Appendix III.2. The following discussion will only take the group A volcanics and the hypabyssal rocks into consideration.

a) Basalts - They are all olivine normative, olivine ranging from 5.9 to 27.4%. Despite the very low SiO_2 content of some of the basalts, they are not picritic-basalts. A picritic-basalt, by definition, contains a large proportion of modal olivine which should reflect itself in high normative olivine. Irvine and Baragar (1971) put 25% normative-olivine as a practical minimum and MacDonald and Katsura (1964) delimit the sum of Ab+An+Or to less than 30% for picritic basalts. There is only one basaltic sample out of 19 with normative olivine $>$ 25% and none of the basalt samples contains Ab+An+Or less than 35%.

A certain distinction amongst the basaltic samples is possible and indeed inevitable as 6 basaltic samples (P66, P140, P214, P252, P282 and P286) consistently appear to be more primitive or more basic than the rest of the basalts: as a group these 6 basalts contain the lowest Zr, Nb, Y, La, Ce, TiO_2 and P_2O_5 and the highest Ni and Cr concentrations amongst the group A basalts. Considering the points raised in Chapter five, these 6 samples amongst the group A volcanics are termed here as the "more primitive" and the rest the "more differentiated" basalts. Their average major and trace element concentrations are presented and contrasted in Table 4.2. The "more primitive" basalts also have higher K_2O, MgO, CaO and SiO_2 and lower Na_2O and Fe_2O_3 contents than the "more differentiated" basalts.

b) Gabbros - The same kind of distinction as for the basalts is duplicated in the gabbroic rocks. The samples P272, P277 are "more primitive" than the other 5 gabbro samples and the chemical differences between the "more primitive" and the rest of the gabbros are

TABLE 4.1

Group A Rock Compositions

	BASALTS (19 samples)			ANDESITES (32 samples)			DACITES (5 samples)			GABBROS (7 samples)			OCEANIC PLAGIOGRANITES (5)			
	Range	MEAN	Std.Dev.	Range	MEAN	Std.Dev.	Range	MEAN	Std.Dev.	Range	MEAN	Std.Dev.	Range	MEAN	Std.Dev.	
SiO_2 wt%	43.78-52.63	48.51	2.46	50.43-61.69	54.83	2.93	64.27-73.19	67.64	3.86	47.97-50.89	49.19	1.16	59.13-69.61	64.06	4.68	SiO_2 wt%
Al_2O_3	12.93-15.77	14.13	0.89	13.09-18.78	15.86	1.24	11.95-16.31	14.35	1.79	13.65-18.91	15.86	1.75	15.05-17.79	16.00	1.13	Al_2O_3
Fe_2O_3	10.02-14.90	12.85	1.14	8.55-13.61	11.33	1.32	5.37- 8.74	7.13	1.51	8.12-15.10	10.60	2.55	5.65-10.67	7.61	2.18	Fe_2O_3
MgO	6.96-13.43	9.35	1.91	3.10-10.02	7.06	2.29	0.67- 2.72	1.63	0.89	6.98-14.77	10.23	3.03	0.83- 2.51	1.64	0.71	MgO
CaO	6.61-13.96	9.40	2.02	1.23- 8.34	3.91	1.64	1.20- 3.47	2.17	0.97	7.87-10.59	8.93	0.94	0.64- 4.93	2.04	1.86	CaO
Na_2O	2.07- 5.01	3.58	0.78	3.00- 6.24	4.57	0.85	5.44- 7.34	6.02	0.77	1.52- 3.76	2.79	0.89	7.38- 8.03	7.73	0.27	Na_2O
K_2O	0.00- 0.78	0.18	0.24	0.00- 0.71	0.15	0.21	0.00- 0.82	0.21	0.34	0.39- 1.83	0.87	0.48	0.00- 0.05	0.02	0.02	K_2O
TiO_2	0.78- 2.10	1.59	0.32	0.91- 2.11	1.59	0.25	0.30- 0.74	0.60	0.19	0.44- 2.63	1.16	0.81	0.38- 0.74	0.60	0.17	TiO_2
MnO	0.14- 0.33	0.21	0.04	0.09- 0.41	0.22	0.07	0.04- 0.16	0.10	0.05	0.15- 0.22	0.18	0.03	0.02- 0.11	0.05	0.04	MnO
S	0.00- 0.07	0.02	0.02	0.00- 0.17	0.02	0.04	0.00- 0.02	0.00	0.01	0.00- 0.10	0.02	0.04	0.00- 0.01	0.00	0.01	S
P_2O_5	0.09- 0.38	0.23	0.08	0.23- 0.73	0.44	0.10	0.04- 0.28	0.15	0.09	0.04- 0.37	0.17	0.12	0.10- 0.47	0.25	0.16	P_2O_5
Nb ppm	3- 14	9	3	13- 25	19	3	27- 35	32	3	3- 15	6	4	26- 33	31	3	Nb ppm
Zr	56-211	128	44	220-387	288	49	452-627	571	73	19-157	79	44	454-596	495	58	Zr
Y	21- 70	42	12	58-100	74	10	89-116	105	11	15- 51	29	13	82-121	106	15	Y
Sr	38-339	144	74	27-388	120	79	52-275	138	87	137-361	237	80	34-320	144	132	Sr
La	4- 19	10	3	10- 27	18	4	27- 32	30	2	1- 11	7	3	21- 39	29	7	La
Ce	13- 39	24	6	30- 65	42	8	49- 65	60	7	12- 26	19	5	40- 76	60	15	Ce
Rb	2- 17	4	4	1- 7	3	2	1- 8	3	3	5- 22	11	5	1- 2	1	1	Rb
Ba	35-210	88	50	25-468	99	98	19-162	80	62	113-329	185	76	29- 47	39	8	Ba
Zn	11-352	78	79	5-504	155	115	0-397	131	162	33- 85	50	17	0- 1	0	0	Zn
Cu	0- 99	34	30	0-583	50	132	1-246	102	127	9-106	35	35	0- 11	4	4	Cu
Ni	6-213	42	52	0- 19	6	6	0- 1	0	0	20-240	107	87	0- 2	1	1	Ni
Cr	26-454	117	121	5-101	29	23	3- 31	11	11	48-492	205	173	4- 10	7	3	Cr

TABLE 4.2

Average compositions of subdivided basalts, andesites and gabbros. Numbers in parantheses are number of samples.

	BASALTS		GABBROS		ANDESITES	
	More Primitive(6)	More diff-erentiated(13)	More Primitive(5)	More diff-erentiated(2)	Basaltic(20)	Acid(12)
SiO_2 wt%	47.49	48.98	49.36	48.78	53.47	57.10
Al_2O_3	14.05	14.16	16.42	14.46	15.70	16.11
Fe_2O_3	12.33	13.05	9.22	14.04	11.97	10.27
MgO	10.15	8.98	11.35	7.45	7.97	5.55
CaO	10.96	8.68	9.13	8.43	4.17	3.48
Na_2O	3.13	3.79	2.54	3.40	4.27	5.05
K_2C	0.30	0.12	1.00	0.55	0.12	0.20
TiO_2	1.20	1.77	0.70	2.30	1.65	1.49
MnO	0.22	0.20	0.17	0.21	0.23	0.19
S	0.02	0.02	0.00	0.05	0.03	0.01
P_2O_5	0.16	0.26	0.11	0.34	0.43	0.46
Nb ppm	7	10	4	12	17	22
Zr	85	147	56	134	255	343
Y	30	47	22	48	68	84
Sr	122	154	276	140	112	132
La	7	11	7	9	16	21
Ce	18	27	16	25	33	50
Rb	6	4	13	7	3	3
Ba	70	96	193	164	69	149
Zn	67	83	46	59	158	149
Cu	43	30	36	30	71	16
Ni	95	18	140	25	6	6
Cr	254	53	265	54	35	19

qualitatively the same as those for the two groups of basalts, but even more extensive (Table 4.2). It is clear that the gabbro samples P272 and P277 are related to the "more differentiated" basalts and the other 5 gabbro samples to the "more primitive" basalts, thus they are termed as the "more differentiated" and the "more primitive" gabbros respectively. The relation is discussed in section 5.4.2. The "more primitive" gabbros seem even more basic than the "more primitive" basalts in having lower averages of Zr, Y, Nb, Ce, TiO_2, P_2O_5, Fe_2O_3 and Na_2O and higher averages of Ni, Cr, K_2O and MgO contents.

Normative mineralogy of the gabbros is very similar to that of basalts.

c) Andesites - They are mostly quartz-normative (up to 14%); only 2 samples out of 32 show small amounts of normative olivine. Plagioclase composition is largely dominated by albite, and orthoclase is present in small amounts, generally less than 2%. 19 samples are corundum normative with a range 2-14%.

Average silica content of the andesites (54.83%) is lower than those of average tholeiitic andesite (57.40%), calc-alkaline andesite (59.64%) and low-potassium andesite (59.05%), reported by Jakes and White (1972). Basaltic andesites are defined as transitional rocks between basalts and andesites (Coats,1968; Carmichael et al, 1974). For comparative purposes, the Polusagi andesites have been further divided into "basaltic andesites" and "acid andesites" at a Zr content of 300 ppm, which corresponds to a dividing SiO_2 content of 56%. The basaltic andesites approximate to Jakes & White's (op cit) low-silica andesites in having an average SiO_2 content around 54% (Table 4.2)

4.2.3 The Polusagi magma type - sub-alkaline or alkaline?

Various diagrams discriminating the sub-alkaline and alkaline magma types on major element chemistry are available in the literature e.g.

total alkali vs. SiO_2, tetrahedral diagram with apices at the compositional points Ol, Cpx, Ne and Q or a ternary diagram of Ol-Cpx-Opx (Chayes, 1966). However because it has been customary to use the total alkali vs. silica diagram as it permits a direct use of analytical data, and also that doubts as to the effectiveness of the ternary diagram have been expressed (Irvine and Baragar, 1971), only the total alkali vs. silica diagram has been used for the evaluation of the nature of the Polusagi rocks (Fig.4.6). Only 3 out of 68 analyses plot into the alkaline field of Irvine and Baragar (1971), indicating that the rocks are of sub-alkaline nature.

Sub-alkalinity of the suite can be further verified by using the immobile trace elements. In general, alkalic basalts are all enriched in Ti, Y, Zr and P relative to sub-alkaline tholeiitic basalts (Manson, 1968; Prinz, 1968). Pearce & Cann (1973) used the Y/Nb ratio to distinguish between the two magma types, where Y/Nb ratio decreased with increasing alkalinity of the basalts. The Y/Nb ratio of tholeiitic basalts is >2, while it is <1 for alkalic basalts. The basic Polusagi rocks have Y/Nb ratios from 3 to 7.5 with an average of 5, suggesting a sub-alkaline and furthermore a tholeiitic nature.

The ratios Y/Nb and Zr/P_2O_5 together with the immobile elements Ti, Zr and P have been incorporated into a series of discriminant diagrams by Floyd and Winchester (1975) to separate alkaline basalts from tholeiitic basalts. Their diagrams, employed for the basic rocks of Polusagi in Fig. 4.7 confirm the sub-alkaline nature of the rock suite. However, these diagrams do not adequately discriminate between oceanic and continental types of either tholeiites or alkali basalts. Also, as the construction of their diagrams excluded calc-alkali basalts and island arc tholeiites (Floyd and Winchester, 1975), the possibility of the Polusagi basic rocks being calc-alkaline is not eliminated, despite the strong affiliation to tholeiitic basalts suggested by the Y/Nb ratios and Fig. 4.7.

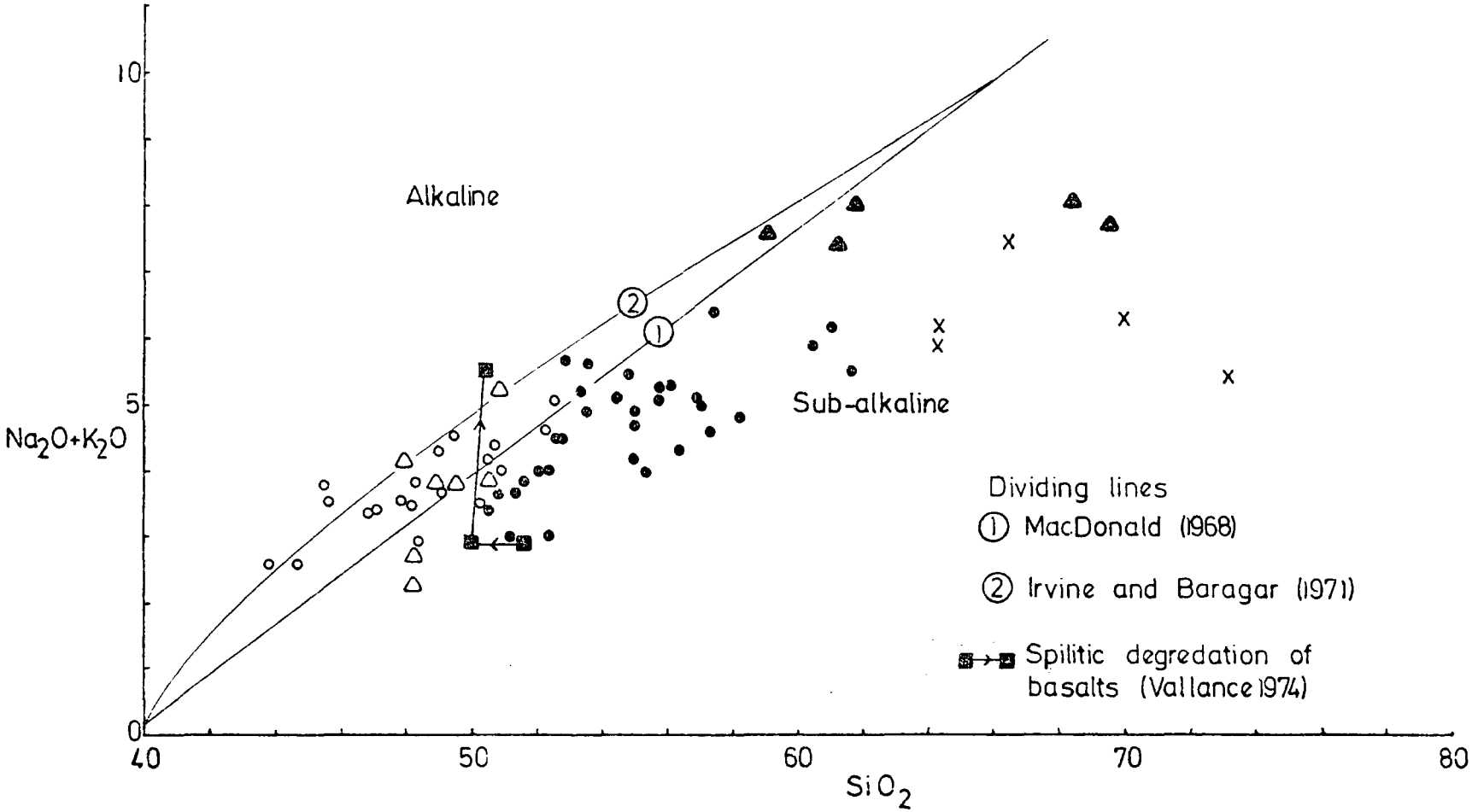


Fig.4.6. Total alkali vs. SiO_2 diagram for the Polusagi rock suite.

o :Basalt, ● :Andesite, x :Dacite, △ :Gabbro, ▲ :Plagiogranite.

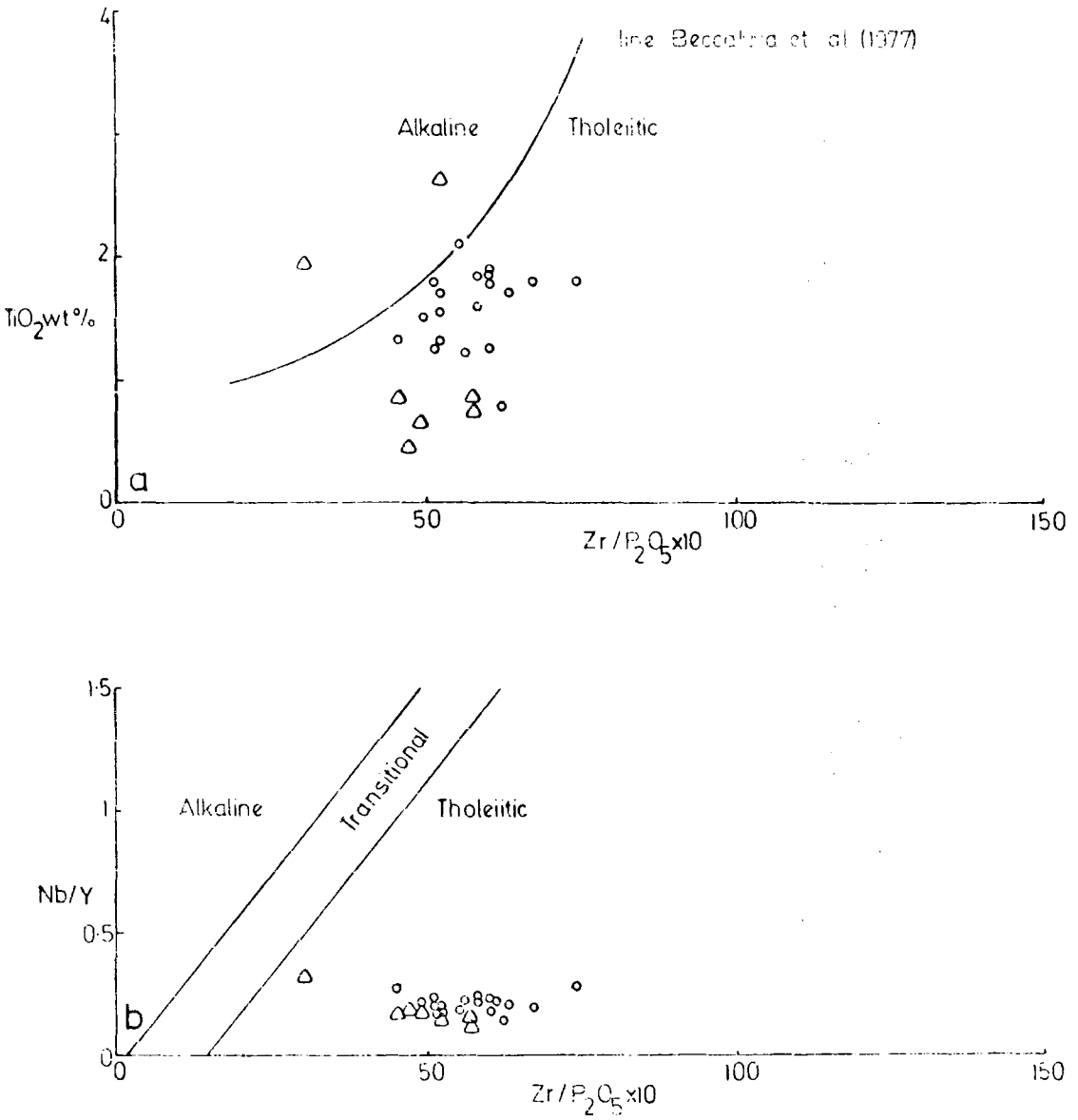


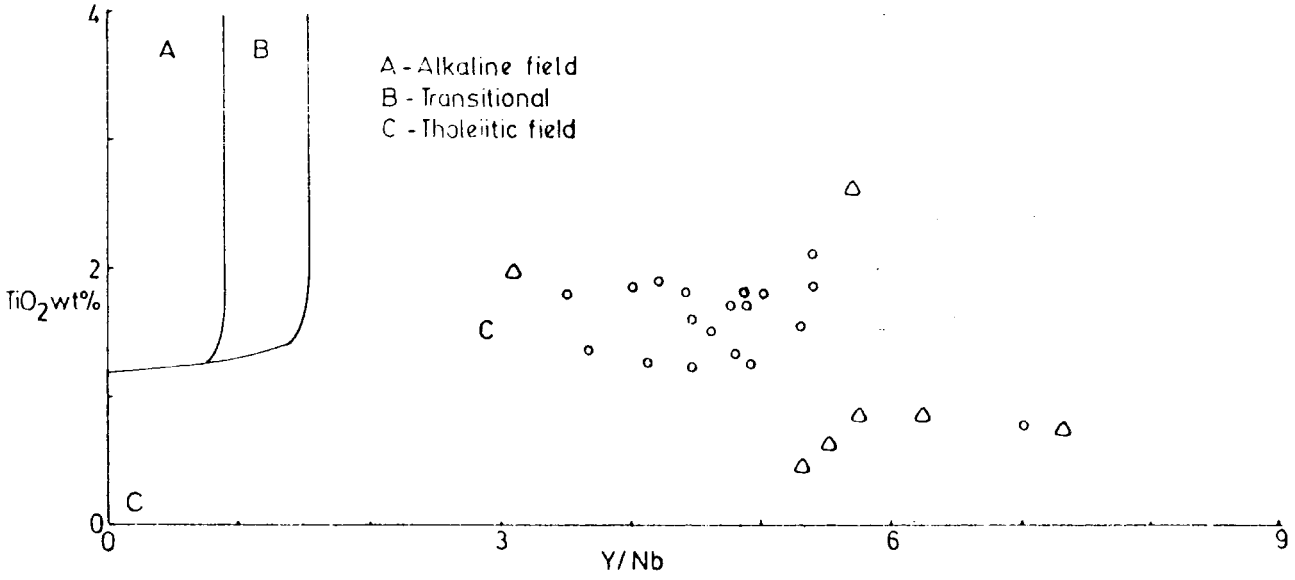
Fig.4.7. Discriminant diagrams for the magma types. See Floyd and Winchester, 1975. Basalt: (o), gabbro:(Δ).

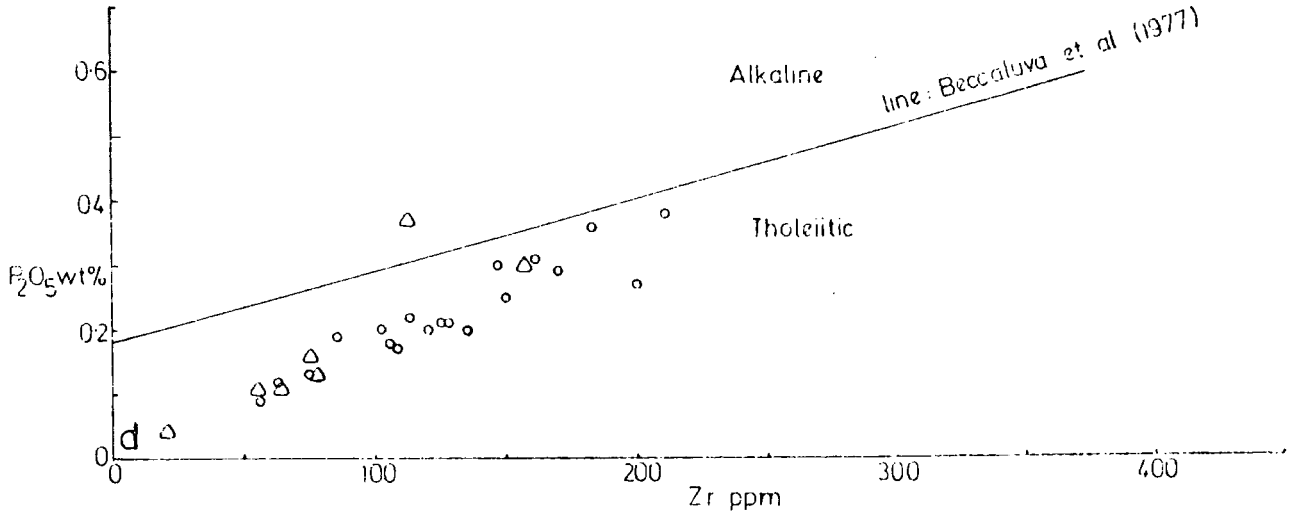
a) TiO_2 vs. Zr/P_2O_5x10

b) Nb/Y vs. Zr/P_2O_5x10

c) TiO_2 vs. Y/Nb

d) P_2O_5 vs. Zr


A
B
A - Alkaline field
B - Transitional
C - Tholeiitic field
C
C
4
2
0
0
3
6
9
TiO2wt%
Y/Nb


Alkaline
line : Beccaluva et al (1977)
Tholeiitic
d
0·6
0·4
0·2
0
0
100
200
300
400
P2O5wt%
Zr ppm

4.2.4 The Polusagi subalkaline rock series: tholeiitic or calc-alkaline?

In distinguishing the tholeiitic and calc-alkaline rock series, the degree of iron-enrichment in the course of differentiation of the magma has usually been taken as the major factor (Kuno, 1968; Jakes and Gill, 1970; Kushiro, 1979), the calc-alkali rocks being characterised by the lack of iron enrichment. Kuno (1965) showed that the lavas of the tholeiitic rock series segregated iron-rich residual liquid whereas those of calc-alkaline rock series segregated silica-rich residual liquid. The degree of iron-enrichment within tholeiitic magmas however, can vary. It can be high (e.g. the Skaergaard intrusion) or moderate to low (e.g. the Palisade diabase sill). The degree of iron enrichment in ophiolites is not high (Coleman, 1977) and moderate to low in the alpine ophiolites (Laurent et al, 1980).

The iron enrichment trends of magmatic series are usually displayed by AFM diagrams. In Fig. 4.8 the Polusagi rocks have been plotted in an AFM diagram which is presented with a dividing line between calc-alkali and tholeiitic rock series suggested by Irvine and Baragar (1971) together with the trends of ophiolitic tholeiites and olivine tholeiites of Laurent et al (1980) proposed for the Eastern Mediterranean ophiolites. The separation of the rock suite into calc-alkaline and tholeiitic types by the dividing line is not very effective. Although basic and acid rocks dominantly plot into the tholeiitic field, most of the andesites fall into the calc-alkaline field, but close to the boundary line. The behaviour of the Polusagi rocks is very likely to be realistic as the rocks involved are the least altered rocks. Since K_2O contents are very low (see Table 4.1), possible deviations from the original trend brought about by its mobility is probably negligible. Thus, it will not be incorrect to state that the Polusagi rock suite displays a moderate to

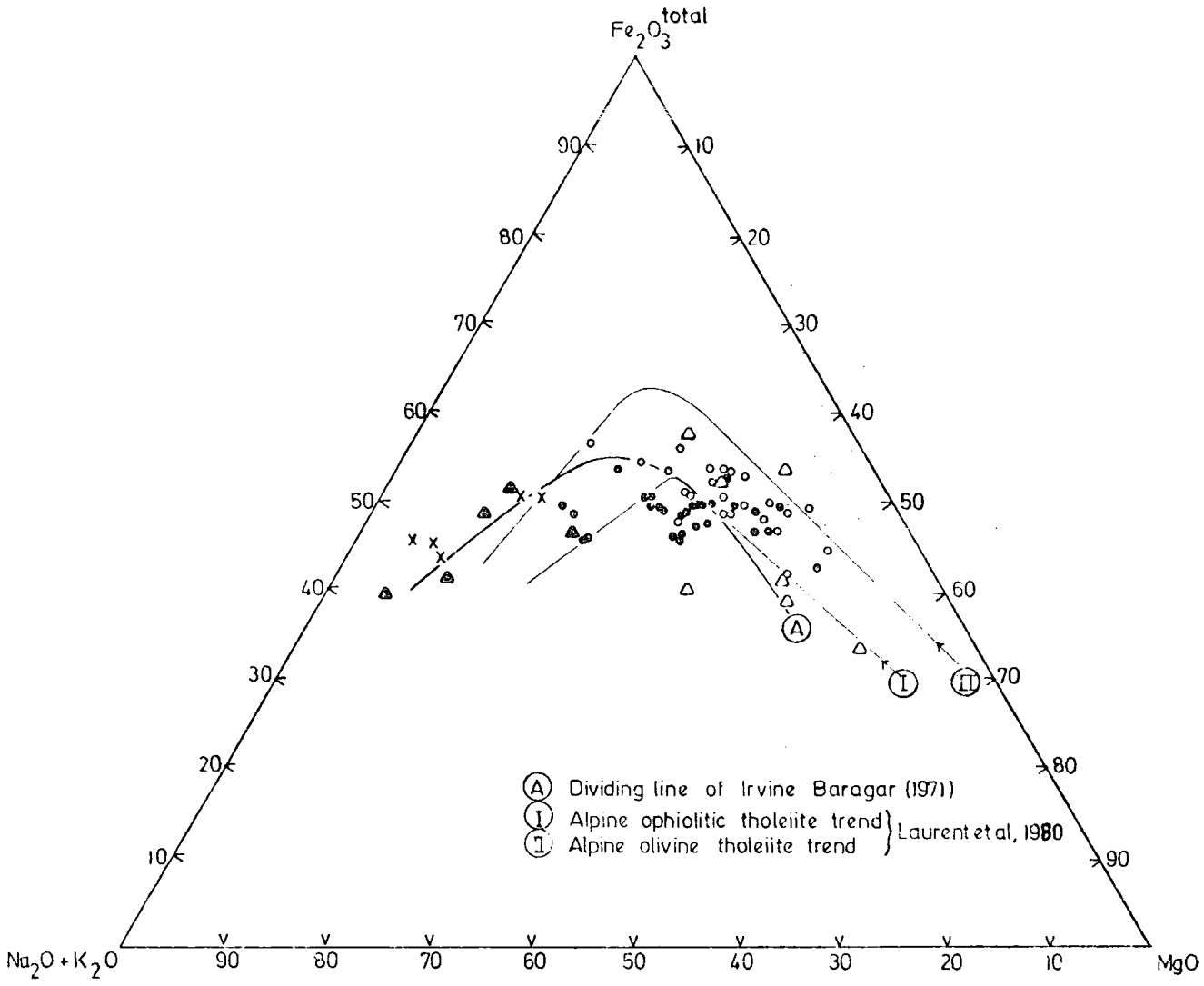


Fig.4.8. AFM diagram showing the degree of iron-enrichment in the Polusagi rock suite as compared with the trends of some Alpine tholeiitic rocks.

o : Basalt

⊙ : Andesite

x : Dacite

△ : Gabbro

◬ : Plagiogranite

low iron-enrichment, similar to many ophiolites. This trend is also similar to that of the island arc tholeiitic series which shows iron enrichment less than that of the abyssal tholeiites (Jakes and White, 1972).

Rocks of the tholeiitic suites are not only characterised by the enrichment in iron during differentiation, but also by the enrichment in TiO_2 and by a slower rate of increase in silica as opposed to the calc-alkalic rocks which have a monotonous decrease in TiO_2 and a faster rate of increase in silica (Miyashiro, 1973,74,75 a,b; Miyashiro and Shido, 1975). Miyashiro (op cit) produced a series of discriminant diagrams demonstrating the different trends of FeO* (means total Fe as FeO), TiO_2 and SiO_2 with progressive differentiation which he measured by an increase in FeO*/MgO ratio.

The iron and TiO_2 enrichment trends (with maxima) of Polusagi rock suite can best be displayed by using Zr as differentiation index (see Chapter five, Fig. 5.5), but for purposes of comparison the rocks have also been plotted in the Miyashiro diagrams (Fig. 4.9). It is clear from Fig. 4.9 that the FeO* and TiO_2 trends are typical of tholeiitic rock series and furthermore, the basic rocks occupy fields of the ocean floor tholeiitic rock series. However, the tholeiitic nature of the rock series is not as clear in the SiO_2 vs. Fe*/MgO diagram. Initial stages of differentiation seem to show a sharper than usual rate of increase in SiO_2 for tholeiitic rocks; and the andesites mostly plot into calc-alkaline field. This, however, does not necessarily suggest mildly calc-alkaline character, since this diagram cannot satisfactorily discriminate the two series below a FeO*/MgO ratio of 2 (Miyashiro op cit) and all the Polusagi basic rocks, and 92% of the andesites that fall into midly calc-alkaline field have FeO*/MgO ratios < 2.

The calc-alkaline basalts and andesites are generally high alumina types, containing 16-20% Al_2O_3, whereas their tholeiitic counterparts

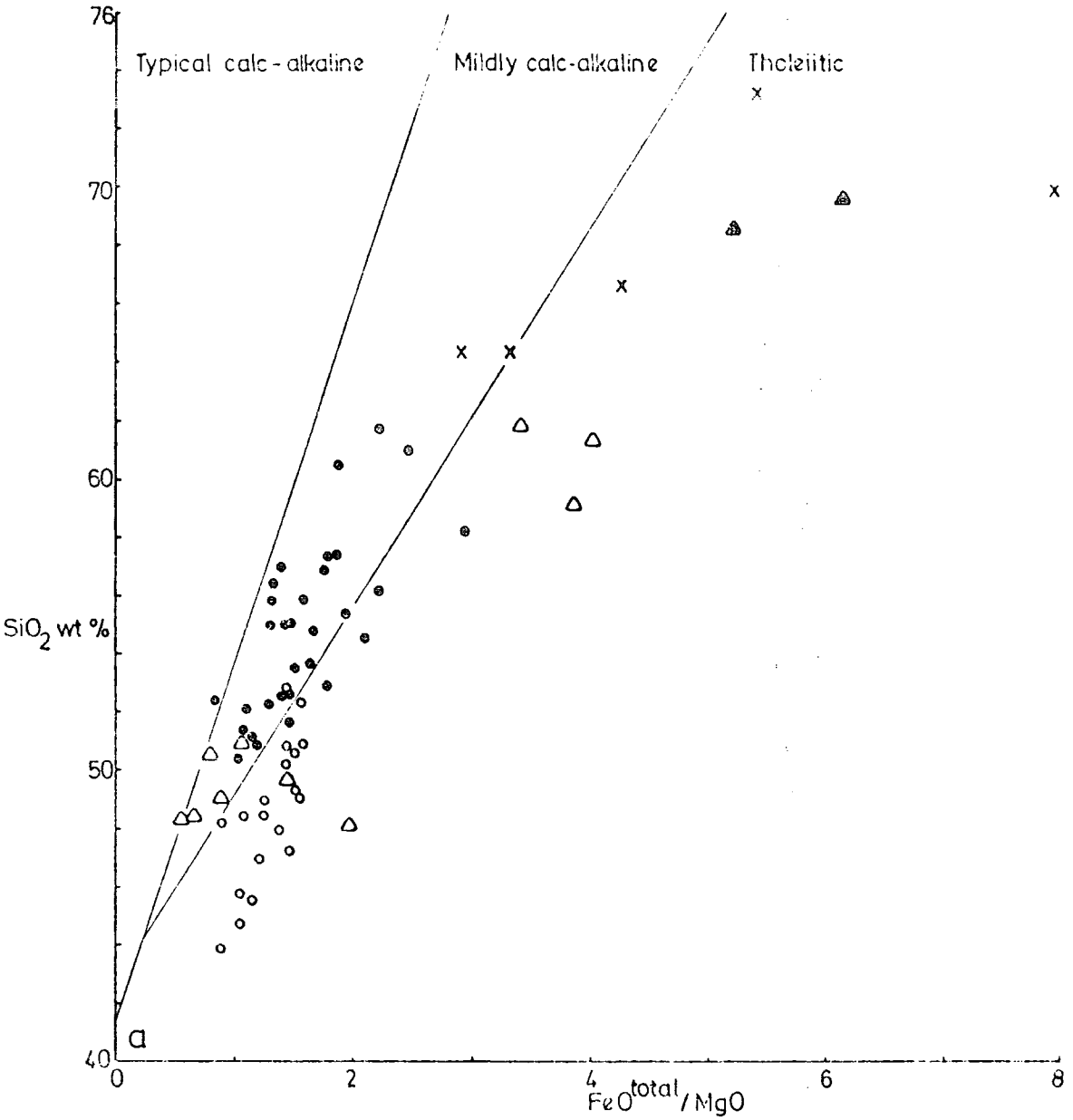
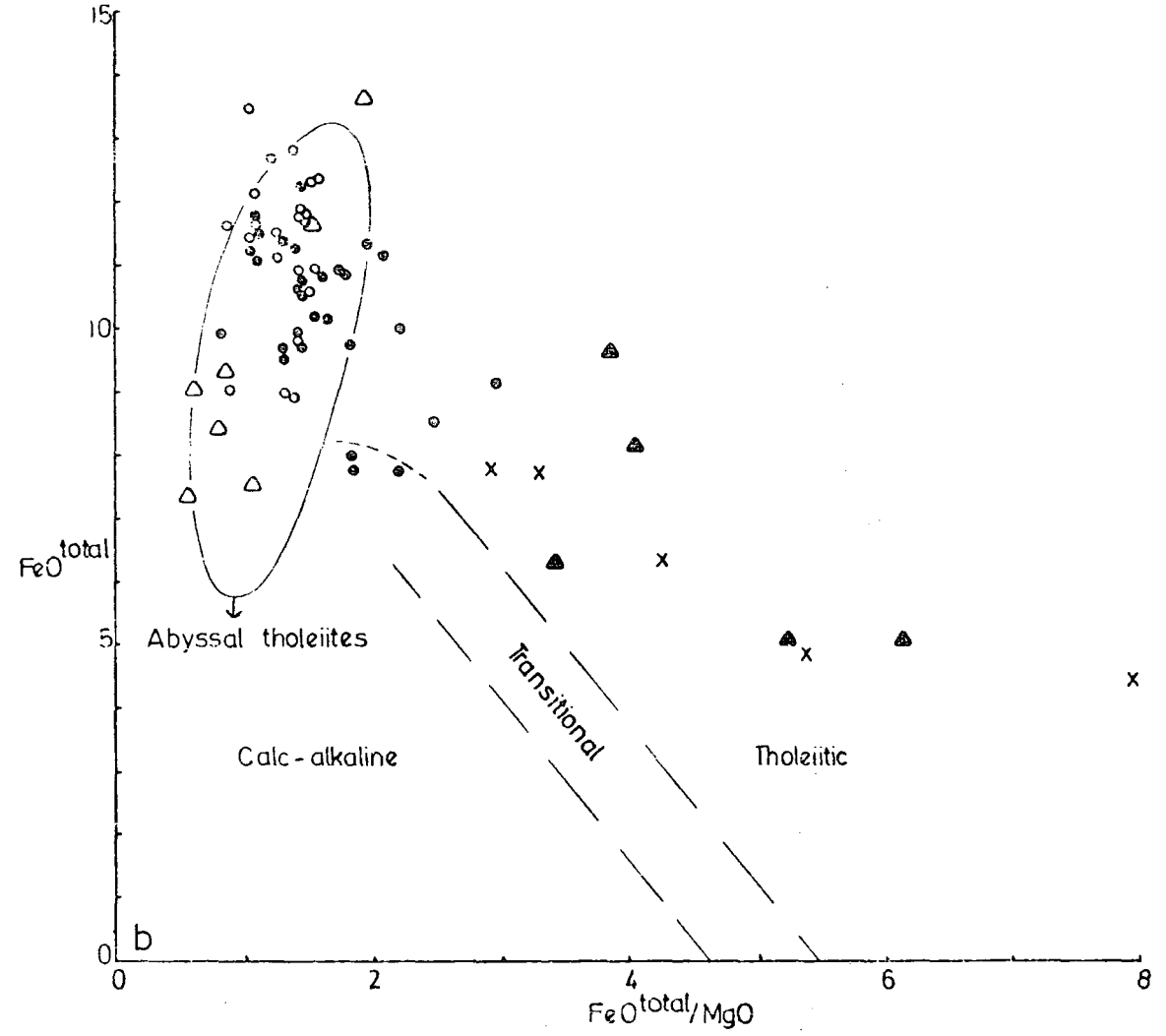


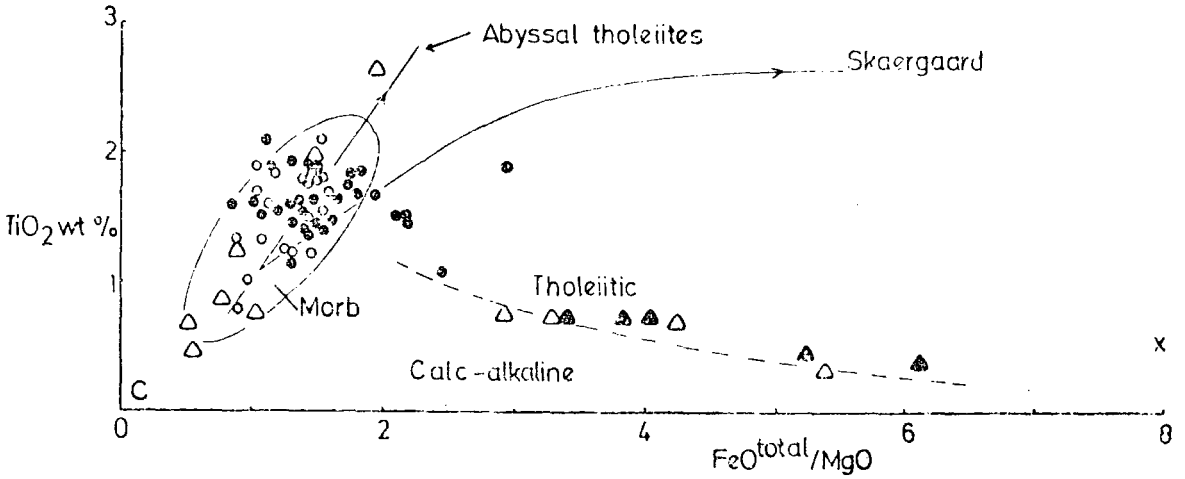
Fig.4.9. The Polusagi rocks plotted on discriminant diagrams of Miyashiro (1973,74,75a,b). Basalt(o), andesite (●), dacite (x), gabbro (△), plagiogranite(▲).

a) SiO_2 vs. FeO^{total}/MgO

b) Feo^{total} vs. FeO^{total}/MgO

c) TiO_2 vs. FeO^{total}/MgO


15
10
5
0
FeO total
Abyssal tholeiites
Transitional
Calc - alkaline
Tholeiitic
b
0
2
4
6
8
FeO total/MgO


3
2
1
TiO2 wt %
Abyssal tholeiites
Skaergaard
Morb
Tholeiitic
Calc - alkaline
c
0
2
4
6
8
FeO total/MgO

have lower Al_2O_3 content at 12-16% (Irvine and Baragar 1971). This difference in chemistry has been utilised to discriminate calc-alkaline and tholeiitic rocks by Irvine and Baragar (op cit) into a plot of normative plagioclase composition vs. Al_2O_3 which, they claim, should separate especially the more basic members of the two series more effectively than the AFM diagram. This plot (Fig.4.10) places the basic rocks of the Polusagi suite almost entirely into the tholeiitic field. Similarly, Jensen (1976) developed a triangular discriminant diagram to distinguish "komatiitic";tholeiitic and calc-alkali rock series, exploiting the chemical differences in iron and titanium enrichment trends and Al_2O_3 and MgO contents. The Polusagi rocks exhibit a clear tholeiitic i.e. iron and Ti enrichment trend (Fig.4.11).

In general, tholeiitic and calc-alkali rock series differ in silica mode, K_2O content and Na_2O/K_2O ratios (Jakes and Gill, 1970). Although some tholeiitic rock series may show silica range (45-70%) similar to calc-alkali rock series (53-70%), the SiO_2 mode is at 53% for tholeiitic rocks as opposed to 59% in calc-alkali rocks. Tholeiitic rocks have much lower contents of K_2O and higher Na_2O/K_2O (> 4) than calc-alkali rocks (Jakes and Gill, op cit). The Polusagi rock series have close similarities with tholeiitic rocks in having a silica mode at 54%, with a range 44-74%; very low K_2O contents (see Table 4.1) and an overall average Na_2O/K_2O ratio of 19. In general, calc-alkali rocks have lower Ni (0-30 ppm) and Cr (0-50 ppm) concentrations as opposed to tholeiitic rocks, where they are 0-200 ppm and 0-400 ppm respectively. Ni and Cr concentrations in the Polusagi rocks resemble those of tholeiitic rocks (Table 4.1).

It is concluded that the Polusagi rock suite is of tholeiitic nature.

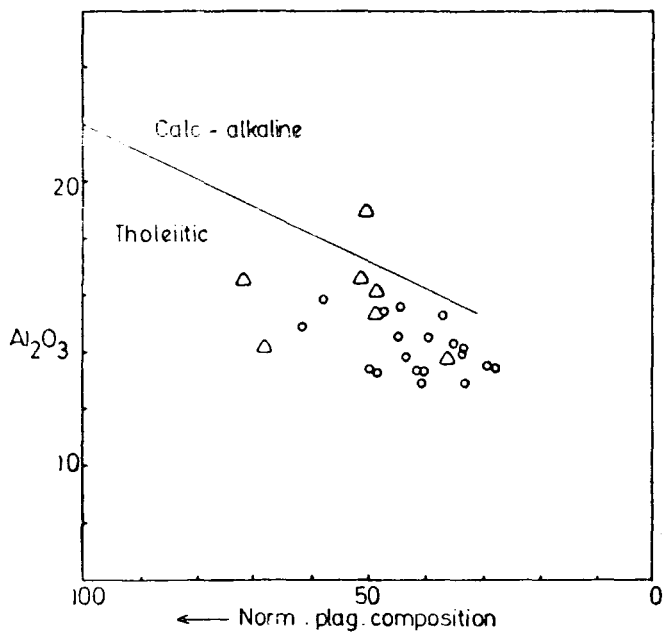


Fig.4.10 Al_2O_3 wt% vs. normative plagioclase composition (See Fig.4.4) diagram for the basic rocks (after Irvine and Baragar, 1971). Basalt: o , Gabbro: Δ

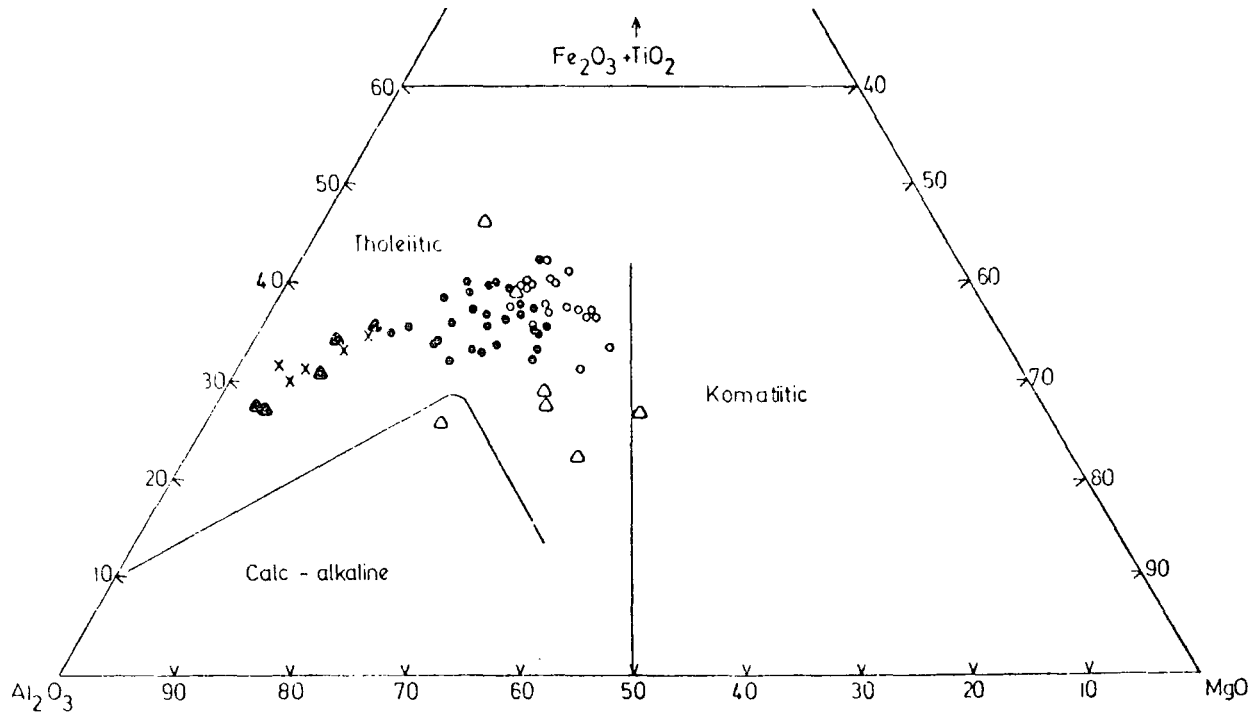


Fig.4.11. MgO-Al_2O_3-(Fe_2O_3+TiO_2) triangular diagram (after Jensen, 1976) showing Fe-Ti enrichment in the Polusagi rock suite. Symbols as in Fig.4.9.

4.3 Tectonic setting of the Polusagi tholeiitic rock suite

4.3.1 Introduction

With the development of the theory of global tectonics and rapid increase in the number of chemical analyses of various volcanic rock types in recent years, there has been much interest shown for chemical classification of major magma types into various tectonic environments. Especially using the immobile elements such as Ti, Y, Zr, Nb, P, Cr, Ni and the rare earth elements, which show systematic differences from one tectonic environment to the other, some success has been achieved in tectonic setting characterisation of volcanic rocks (Pearce and Cann, 1971,73; Bickle and Nisbet, 1972; Pearce, 1975; Floyd and Winchester, 1975; Pearce and Gale, 1977, Smith and Smith, 1976; Church and Coish, 1976). The principal behind the identification of the original tectonic setting of basic volcanic rocks from the past, particularly where this cannot unambiguously be deduced from the geology, is the comparison of the concentrations or ratios of the immobile elements of the rocks in unknown settings with those of the present day volcanic rocks of known settings.

The most promising scheme of classifying the basic volcanic rocks into different tectonic environments came from Pearce and Cann (1973), who defined four basaltic groups considering the major tectonic settings related to plate motions:

a)	Volcanic arc basalts)	
	)	Plate margin basalts
b)	Ocean-floor basalts)	
c)	Ocean island basalts)	
	)	Within plate basalts
d)	Continental basalts)	

Volcanic arc or island arc basalts are produced at converging plate margins and contain low-K tholeiites, calc-alkali basalts and shoshonites (Jakes and Gill, 1970; Gill, 1970; Jakes and White, 1972).

These three magma types appear to be related to the trench in terms of time and space. Rocks of the island arc tholeiitic series are predominantly basaltic and occur as the earliest eruptions closest to the trench, usually on oceanic crust. They are followed in time by calc-alkaline and then by shoshonitic rocks. Calc-alkaline rocks are predominantly andesitic and further away from the trench, while shoshonites are predominantly basaltic and occur furthest behind the trench and may also represent the last phase of the volcanic arc evolution.

Ocean-floor basalts are produced at accreting plate margins and are predominantly tholeiitic basalts, though small amounts of transitional and alkalic basalts also occur. They are associated with dolerite dykes, gabbros, ultramafics and plagiogranites. Such rocks have been dredged from mid-ocean ridges, marginal basins or back arc basins.

Ocean island basalts and continental basalts range from tholeiitic to highly alkaline suites of rocks and are termed "within plate basalts" as no geochemical method has been devised to distinguish them (Pearce and Cann, 1973). This type of volcanic activity is generally attributed to plumes of hot material from the mantle to explain their occurrences in the ocean islands and continental rift environments.

In practice, analysed rocks do not always clearly belong to a particular tectonic setting and may suggest transitional forms.

4.3.2 Tectonic Setting

The Polusagi rocks are tholeiitic in nature but each of the tectonic settings listed above is capable of producing tholeiitic basalts. Initially, all the possible tectonic settings for the Polusagi tholeiitic basalts will be considered.

In general, "within plate basalts" are distinguished geochemically by their higher concentrations of most lithophile elements, with few exceptions such as Y and Cr, in relation to "plate margin basalts"

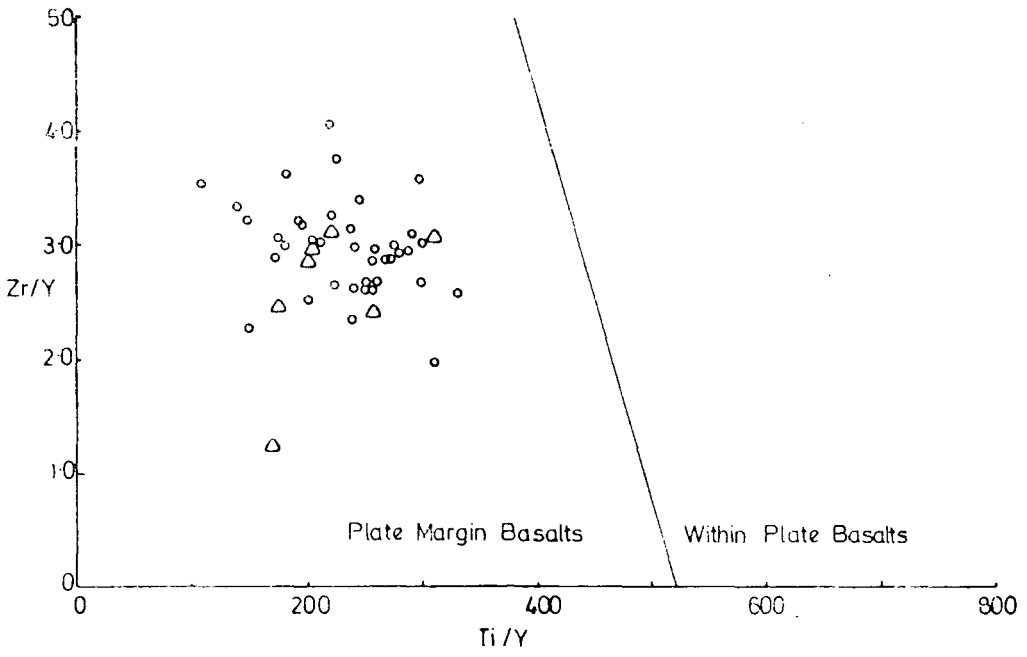


Fig.4.12 Polusagi basalts(o) and gabbros (Δ) plotted in the Zr/Y-Ti/Y diagram (Pearce and Gale,1977) separating plate margin basalts and within plate basalts.

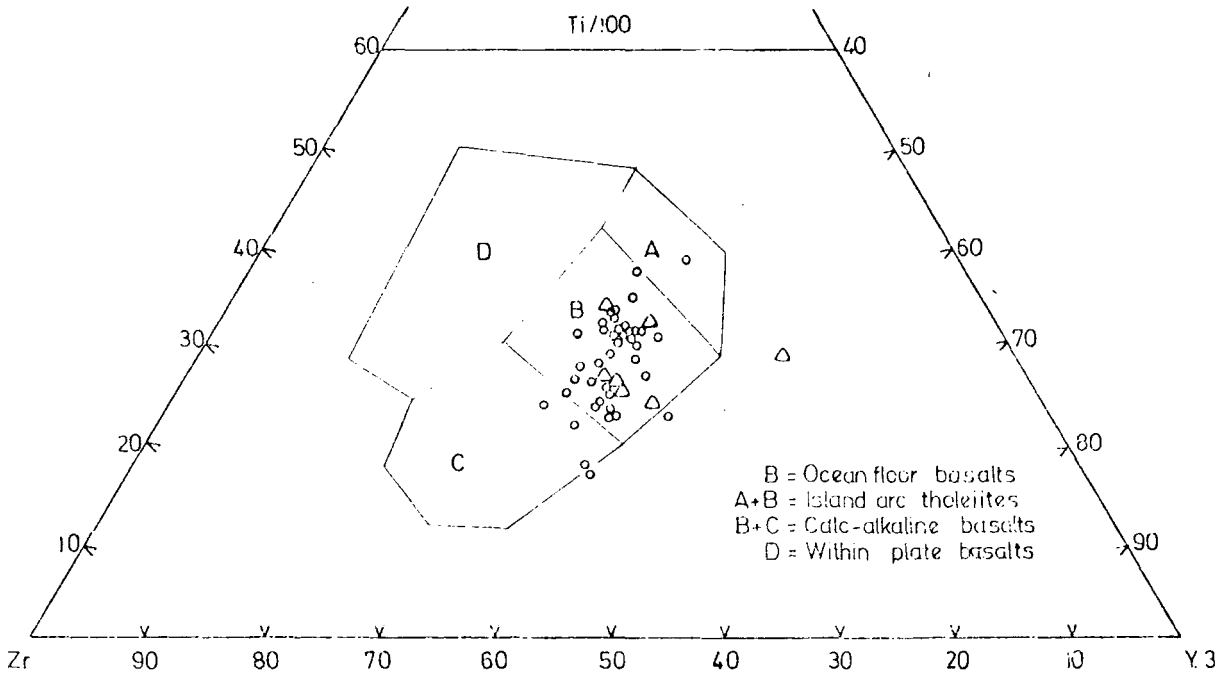


Fig.4.13 Ti-Zr-Y triangular discriminant diagram (Pearce and Cann, 1973), separating basic rocks from various tectonic settings. Symbols as above.

(Pearce and Gale, 1977). The distinctive enrichment of "within plate basalts" in Zr and Ti, but not in Y, has been successfully used to discriminate them from plate margin basalts (Pearce and Cann, 1973; Pearce, 1975; Pearce and Gale, 1977). Fig.4.12 is a plot of Zr/Y vs. Ti/Y for the Polusagi basic rocks and all of the analyses fall into the plate margin basalt field. Fig.4.13 is a triangular plot of Ti, Zr and Y, and again it clearly eliminates the possibility of a within plate tectonic environment for the Polusagi basic rocks. Fig.4.14 suggests an ocean-floor tectonic environment as the rocks overwhelmingly fall into field B. But field B is also shared by some of the calc-alkaline basalts and island arc tholeiites. Since the Polusagi rocks are tholeiitic, the possibility of the rocks being calc-alkaline can be disregarded. However, this diagram, like the Zr-Ti-Y diagram, cannot adequately discriminate between the ocean-floor and island arc tholeiitic basalts. Rather, the data points cover the fields of basalts from both tectonic settings.

Island arc tholeiites share many chemical characteristics with ocean-floor basalts, but differ from them in that they have lower concentrations of FeO, MgO, Ni, Cr, Ti, Zr and Nb and higher concentrations of K, Rb, Ba and Sr (Jakes and Gill, 1970), and these differences appear to be critical. They also have lower P_2O_5 and REE as compared with ocean floor basalts (Hawkins, 1980). These chemical differences seem to be more pronounced in the more fractionated basaltic members of the two series and the least fractionated basalts of island arc tholeiitic series probably converge into the ocean-floor basaltic compositions (Gill, 1970; Hawkins, 1980).These chemical differences can be employed in discriminant diagrams to help to distinguish the island arc tholeiites from ocean-floor basalts.

A triangular diagram of Zr, Ti and Sr, which is claimed to be very effective in distinguishing the plate margin basalts (Pearce and Cann, 1973; Pearce, 1975) cannot be used for the Polusagi basic rocks, since Sr is a highly mobile element.

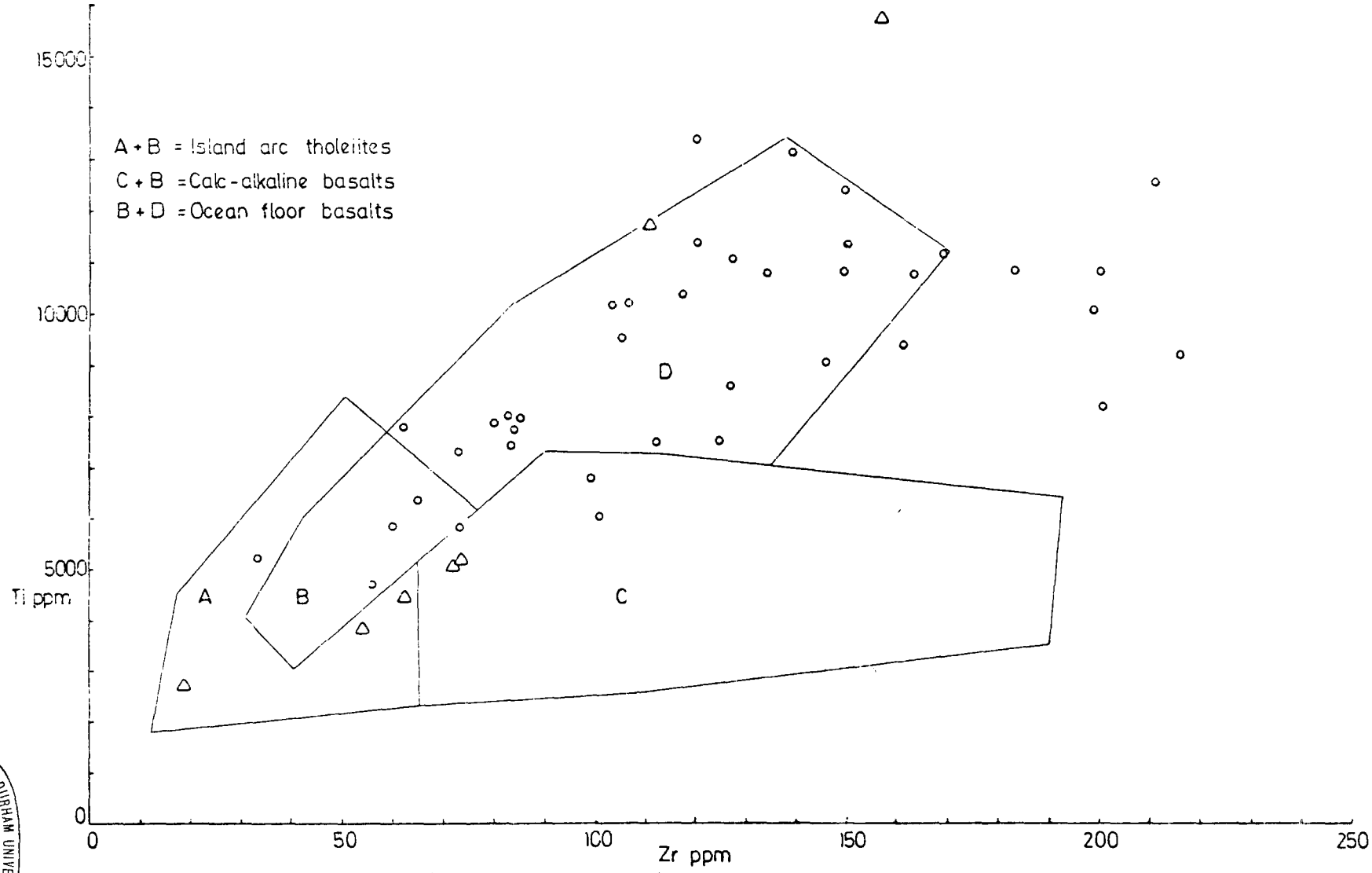


Fig.4.14 Polusagi basalts (o) and gabbros (Δ) plotted in Ti-Zr diagram of Pearce and Cann (1973).

DURHAM UNIVERSITY
23 SEP 1982
SCIENCE LIBRARY

Cr is apparently a very useful element in distinguishing ocean-floor basalts from island arc tholeiites since at any given Ti concentration ocean-floor basalts will always have higher Cr than island arc tholeiites (Pearce, 1975; Pearce and Gale, 1977); this is also the case for Ni. Figs. 4.15 and 4.16 are discriminant diagrams based on these observations. The majority of the Polusagi basic rocks fall into the island arc tholeiite field, while a considerable number of points plot into the ocean-floor basalt field. It is interesting to note that the majority of the points that fall into the ocean-floor basalt field in both diagrams are those basalts and gabbros that were separated from the others as being "more primitive" in section 4.2.2.4. Thus, these diagrams indicate an ocean-floor affinity for "more primitive" basalts and gabbros, and island arc affinity for the "more differentiated" ones. Apparently, the Eastern Mediterranean ophiolites e.g. the Troodos, Vourinos, Pindos and Othyrs amongst others, also plot into the island arc tholeiite fields of these diagrams (Pearce, 1975; Beccaluva et al, 1979, 80; Upadhyay and Neale, 1979).

La vs. Nb diagram of Saunders et al (1980) in Fig. 4.17 suggests that the La/Nb ratios of the Polusagi basic rocks are similar to ocean-floor basalts with some tendency towards island arc tholeiites. The same observation is made when the P content is considered e.g. in the P_2O_5 vs. TiO_2 diagram of Hawkins (1980).

Thus, it is clear that the Polusagi tholeiitic basalts and gabbros do not consistently show the major geochemical characteristics of either island arc tholeiites or ocean-floor basalts, but exhibit transitional chemical properties inbetween the two tectonic environments. Especially the low Cr on Ni contents of "more differentiated" basalts and gabbros and higher Cr and Ni contents of "more primitive" basalts and gabbros favour a transitional tectonic environment, one which evolves from the

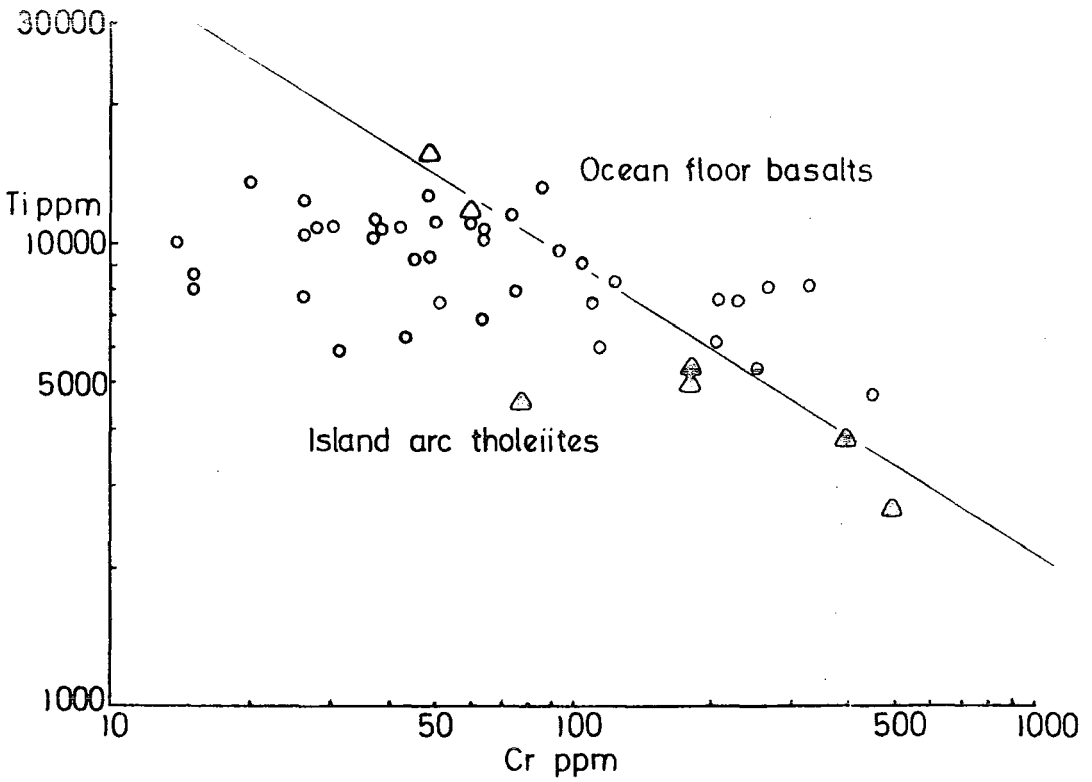


Fig.4.15 Group A and B basalts and gabbros plotted in Ti-Cr diagram of Pearce (1975).

o : "More primitive" basalts

o : "More differentiated" basalts

△ : "More primitive" gabbros

△ : "More differentiated" gabbros

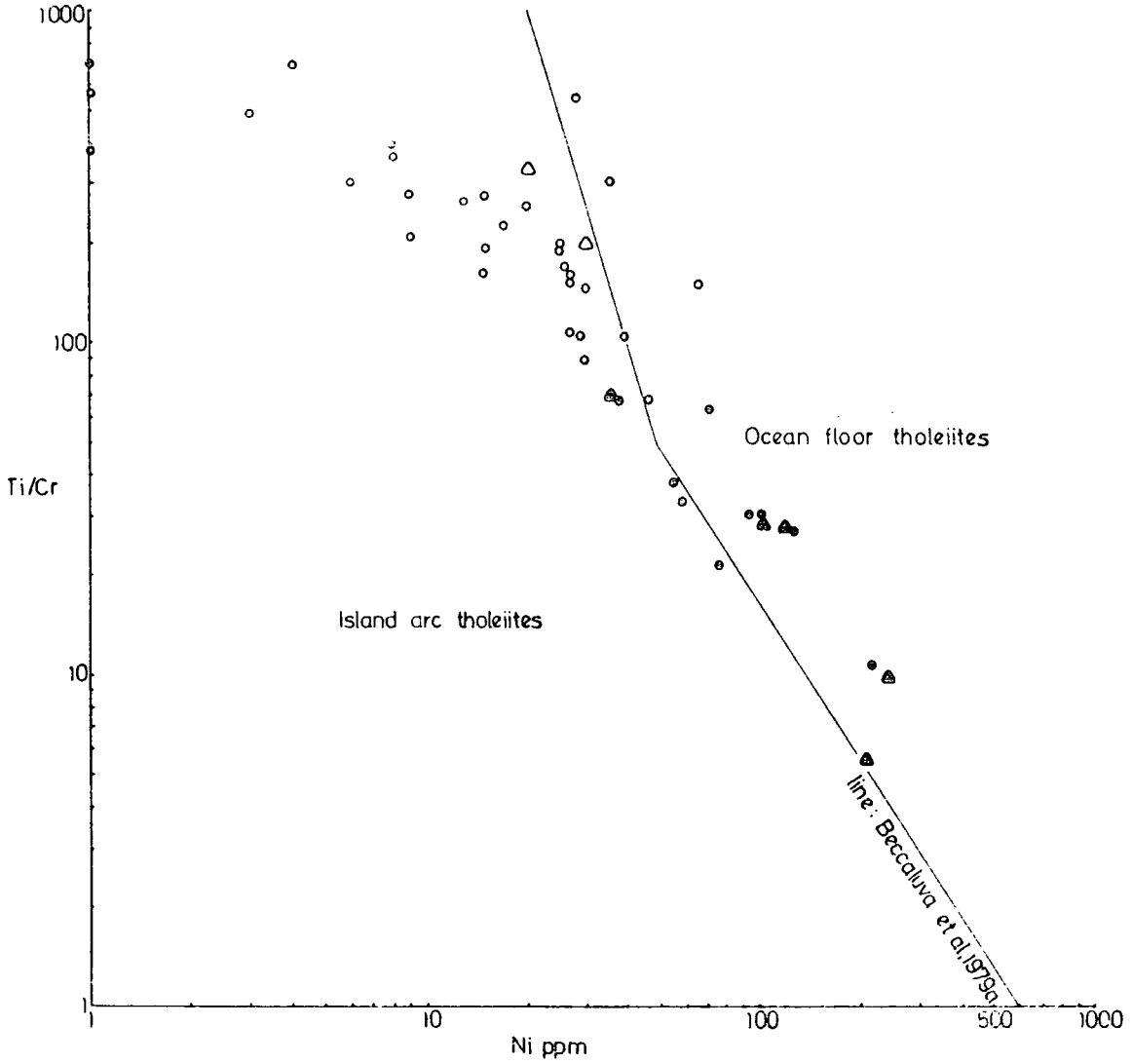


Fig.4.16 Ni vs. Ti/Cr for the group A and B basalts and gabbros. Dividing line after Beccaluva et al (1979). Symbols as in previous diagram.

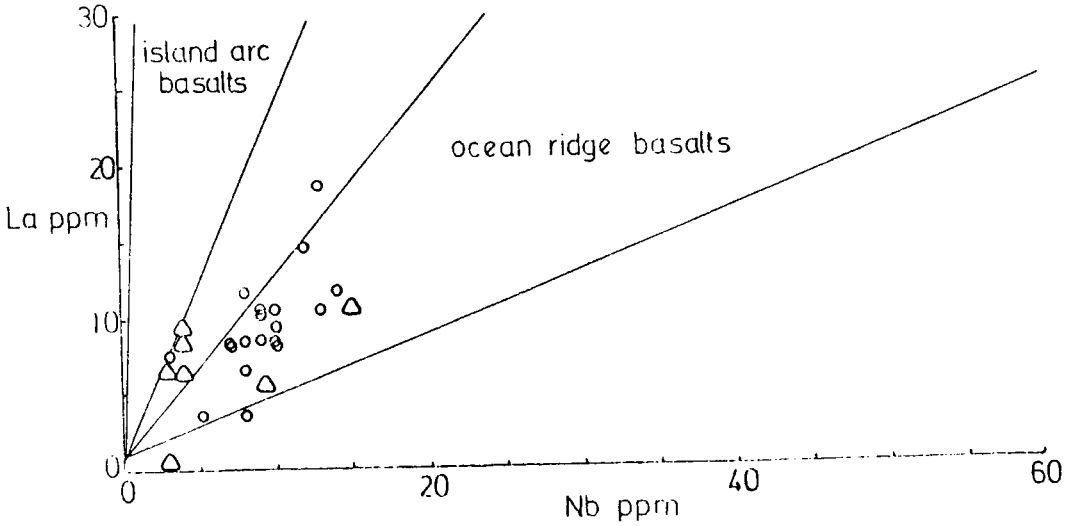


Fig.4.17 La vs. Nb. Defined fields are after Saunders et al, 1980. o : basalts and Δ : gabbros.

ocean-floor environment into the early stages of an island arc tectonic setting in the Tethyan ocean floor.

4.3.3 A discussion

Until recently, it was widely held that ophiolites represented obducted oceanic crust formed at mid-ocean ridges (See Coleman, 1977, for a review). However, mid-ocean ridges are not the only locations where oceanic crust can be generated. It can also be generated at back-arc basin (marginal basin of Karig, 1971) spreading centres, island arcs, intra-plate volcanic centres, transform faults that have a dilational component of motion etc. In recent years the idea that some, if not most, ophiolitic complexes were formed in back-arc basins has been gaining popularity (Dewey and Bird, 1971; Dewey, 1974, 76; Pearce, 1975; Saunders et al, 1980; Hawkins, 1980; Upadhyay and Neale, 1979). Some ophiolites can also form at the base of island arc complexes (Jakes and Gill, 1970; Ewart and Bryan, 1979; Miyashiro, 1973,75a,b,c; Hawkins, 1980) or in island arc/ marginal basin systems (Pearce, 1975,80).

Dewey (1974) and Hawkins (1976) have suggested that the lithosphere of marginal basins is more likely to be obducted than normal ocean-floor lithosphere because of the more buoyant nature of the mantle under back-arc marginal basins. This view is supported by Saunders et al (1979) on the basis of greater chance of arc-arc and arc-continent collision than that of continent-continent collision.

So, the tholeiitic nature and strong geochemical affinities of the Polusagi basic rocks to ocean-floor basalts and island arc tholeiites does not necessarily imply an original tectonic site such as mid-ocean ridges for generation, since basalts, chemically very similar to mid-ocean ridge basalts, have been recovered from back-arc basins where similar ocean-floor spreading takes place. In the back-arc basins, some island arc tholeiites have geochemical overlap with the back-arc basin basalts which in turn are very much like mid-ocean ridge basalts (Hawkins, 1980).

The island arc tholeiitic series has been postulated to be characteristic of the early stages of arc evolution (immature island arcs) that would form part of the root zone of island arc complexes (Jakes and Gill, 1970; Gill, 1970; Mitchell and Reading, 1971; Ewart and Bryan, 1972; Miyashiro, 1974,75a,b,c; Hawkins, 1980).

Therefore, what may have initially appeared as a geochemical conflict that the Polusagi basic rocks exhibit island arc tholeiitic as well as ocean-floor basaltic characteristics can be explained by a tectonic setting in the Tethyan ocean which involves a marginal basin plus an immature island arc system.

4.3.4 Further considerations of the tectonic setting

In recognising the above proposed tectonic environment for the formation of the Polusagi rocks, only the basic igneous members have been considered so far. Additional support for this proposition can be gained by considering the other differentiation products and rock types in the area.

It was shown in detail in Chapter two that the Polusagi pillowed and massive lavas are associated and interlayered with sedimentary and pyroclastic formations. This is an invariable common feature of the higher levels of ophiolitic complexes and such successions are not known to exist on any of the present-day major ocean-floors (Upadhyay and Neale, 1979). On the other hand some of the present-day marginal ocean floors indicate several seismic layers that may be interpreted as analogous to the observed sedimentary/volcanoclastic successions at the top of the ophiolite complexes (see Upadhyay and Neale, 1979, for references), probably indicating the existence of nearby arc complexes or an island arc.

Polusagi tholeiitic rock suite is mostly andesitic. Out of 129 analysed lavas and hypabyssal rocks 53 rocks are basic (46 basalts, 7

gabbros), 57 rocks are andesites and 19 rocks are acidic (14 dacites and 5 plagiogranites). Even if a silica content of 54% was adopted to divide the basalts and andesites, a large proportion (51 out of 129) of rocks would still be andesitic or acidic. Such large proportions of differentiated rocks are not known to occur either in marginal basin or mid-ocean ridge type tholeiitic assemblages. Although silicic rocks have been recovered from ocean-floors (Engel and Fisher, 1975; Coleman and Peterman, 1975), their proportions to basaltic rocks, to date, are very small. On the other hand, island arc tholeiitic rock assemblages have much larger proportions of differentiated magmatic products (e.g. Miyashiro, 1974).

In general, immature island arcs tend to have larger proportions of tholeiitic basalt, while more mature island arcs are richer in andesite (Baker, 1968). In Fig.4.18 the proportions of volcanic rocks in the South Sandwich island arc, which is considered to be immature, and the Lesser Antilles, which represent later stages of island arc evolution (Baker, 1968) are compared with those of the Polusagi rock suite. For this comparison, the Polusagi rocks have been re-classified on the same basis (basalts have $SiO_2 < 54\%$ etc.). The rock type proportions of the Polusagi rock suite and the immature South Sandwich island arc are evidently very similar.

Current theories of plate tectonics relate the island arc volcanism with trenches, back-arc basins and oceanic crust descending into the upper mantle along the Benioff zones (see Chapter five, 5.1). It has been shown by many workers that island arc volcanic rocks become more alkalic across the arc as it moves towards the adjacent continent with the arc's development in time (Kuno, 1959,60,66; Sugimura, 1960,68; Jakes and White, 1972). The well known total alkali vs. SiO_2 diagram of Kuno (1959), Fig.4.6, makes use of the observation that at a given SiO_2 there is a continuous increase in the alkali content of the island arc volcanic

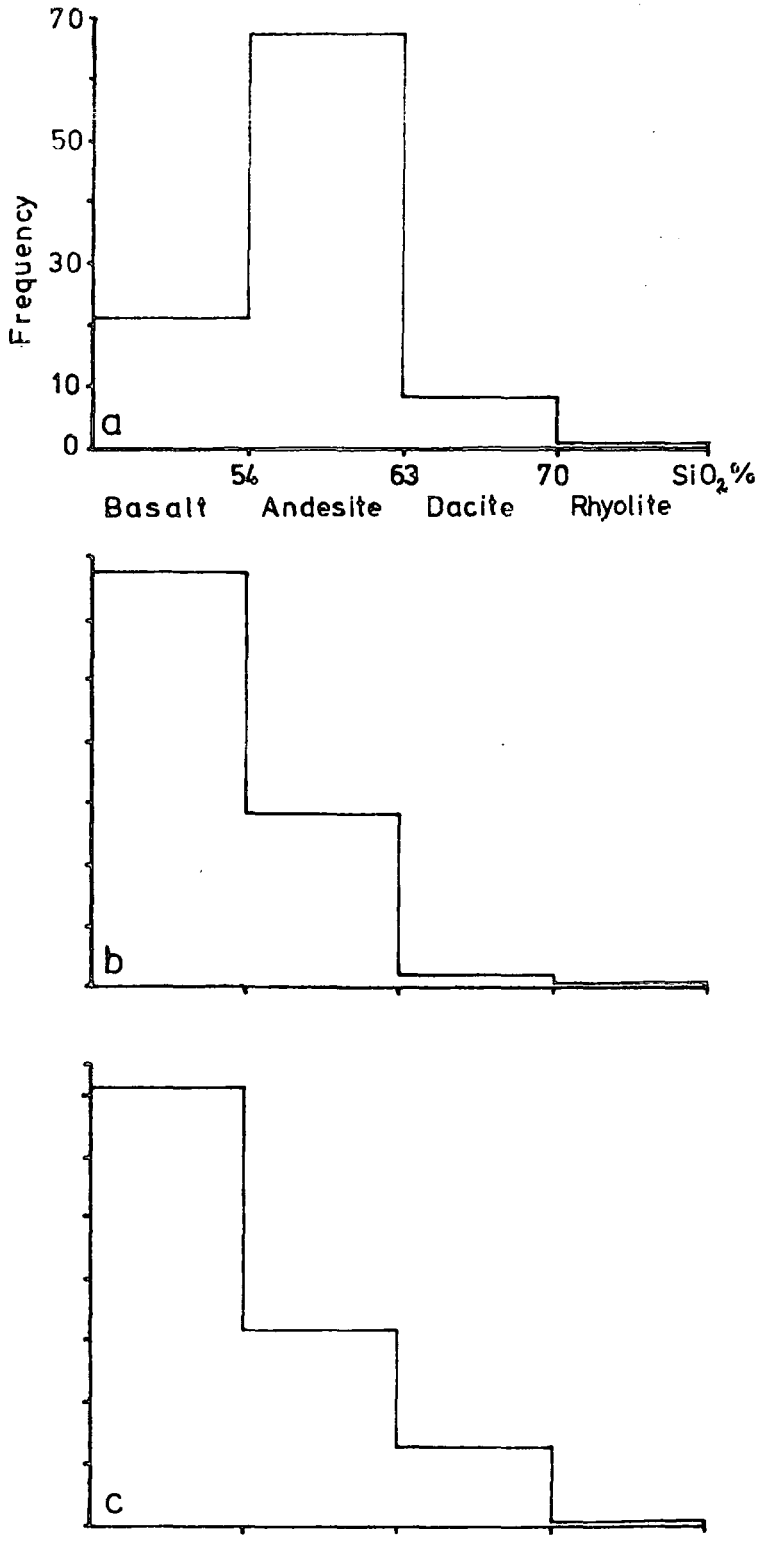


Fig.4.18 Comparison of proportions of volcanic rock types occurring in modern island arcs and Polusagi:

a) Lesser Antilles (mature arc)

b) South Sandwich Islands (immature arc)

c) The Polusagi volcanics

rocks from tholeiitic to high-alumina to shoshonitic rock series. Kuno (op cit) also showed that in the Pacific volcanic arcs, these three rock series appear to occur above earthquake foci of depths 100 km, 100-200 km and 200 km respectively. A later study on the Kurile volcanic arc showed a similar trend (Gorshkov, 1969). Hatherton and Dickinson (1968, 69), Dickinson (1968) and Dickinson and Hatherton (1967) related K_2O content of the volcanics at a given SiO_2 value, rather than the total alkali, with the depth of the Benioff zone and suggested that the K_2O content increased more regularly with increasing depth of the Benioff zone beneath the point of eruption. Ninkovich and Hays (1972), in addition to the K_2O content, showed that Rb could also be used to estimate the depth of the Benioff zone beneath the island arcs. They produced curves of equal earthquake focal depths based on the previous works in the Indo-Pacific region. Figs.4.19a and 4.19b show the trends of K_2O and Rb contents of the Polusagi volcanic rocks, respectively. As expected from a tholeiitic island arc volcanic rock series, the diagrams suggest relatively shallow depths for the Benioff zone, around or below 120 km. Another interesting observation is that although the volcanic rocks from the Indo-Pacific region and the Tyrrhenian and Aegean seas all show increasing K_2O and Rb contents with increasing SiO_2 (Ninkovich and Hays, 1972), the Polusagi volcanics display decreasing K_2O and Rb trends with increasing SiO_2, thus suggesting shallowing depths above the assumed downgoing Tethyan oceanic crust. The trends cannot be solely due to mobility, and the decreasing depth with differentiation i.e. rising magma is consistent with the ideas put forward in the next chapter. Therefore, it is concluded that the Polusagi volcanics were erupted above the Benioff zone which was probably not deeper than 100-120 km from the point of eruption.

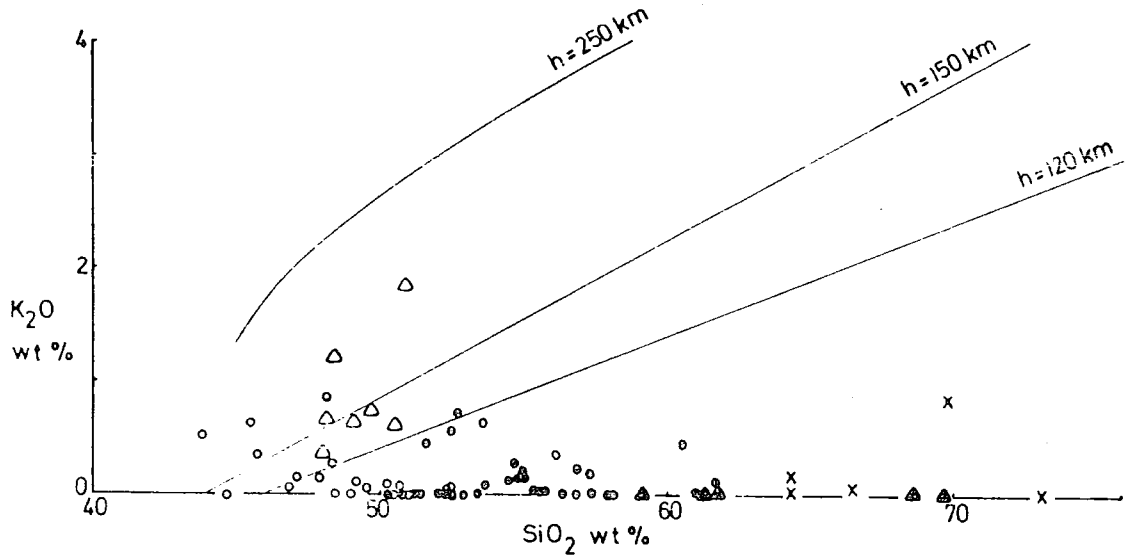


Fig.4.19a K_2O vs. SiO_2 contents of the Polusagi rock suite. Curves represent depth (h) to inclined Benioff zone beneath point of extrusion and are taken from Ninkovich and Hays (1972). Symbols as in following diagram.

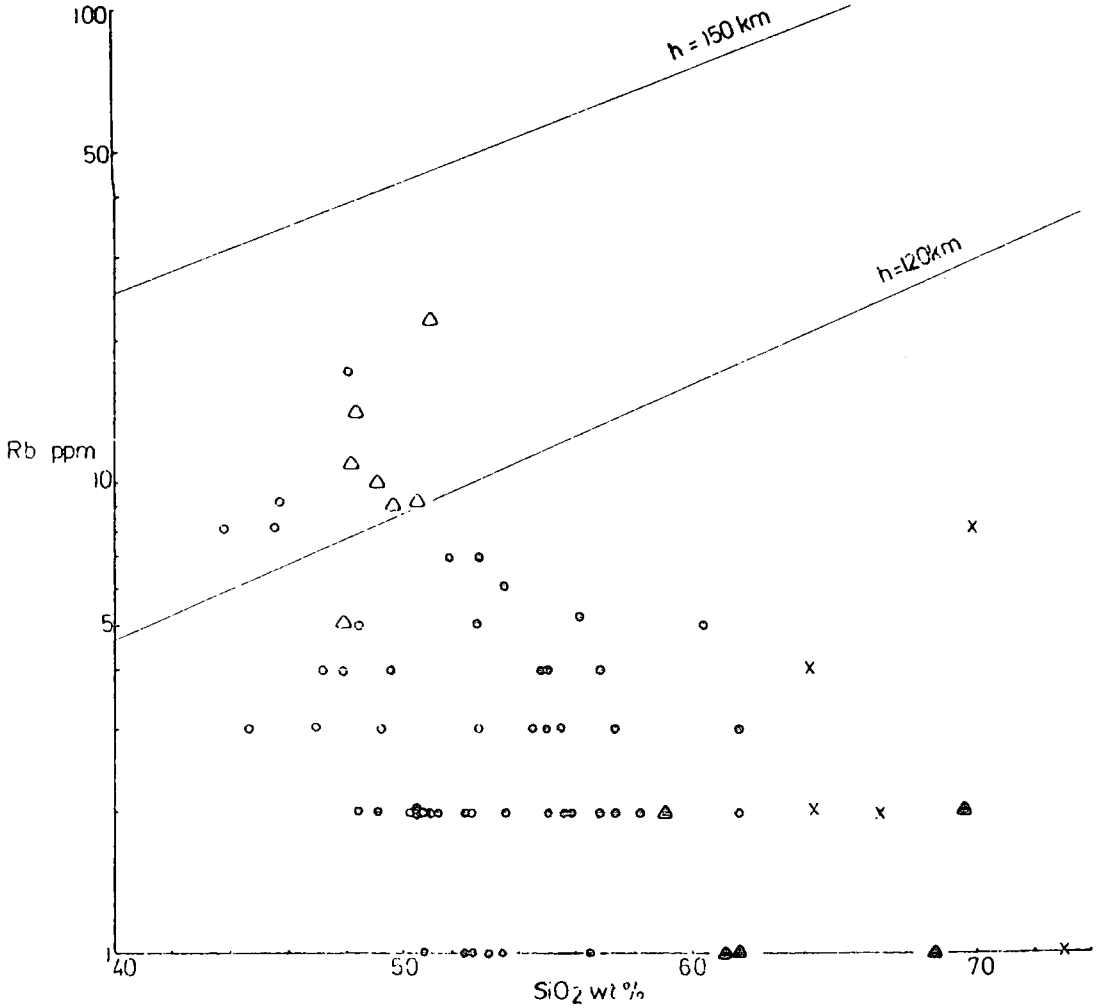


Fig.4.19b Rb vs SiO_2 for the Polusagi rocks. Depth curves are after Ninkovich and Hays (1972). Symbols = o : basalt, o : andesite, x : dacite, △ : gabbro, ▲ : plagiogranite.

4.3.5 Chemical comparison with rocks from known tectonic settings and from ophiolites

4.3.5.1 Introduction

Since the Polusagi rock suite is proposed to have formed in a Tethyan marginal basin-island arc complex, it will be useful to compare chemically the rock types with similar rocks elsewhere in the world. To do this, chemical analyses of similar rocks have been selected firstly from present day marginal basin and island arc tholeiitic rock series where the tectonic settings are known; and secondly from ophiolite complexes and especially from the Tethyan ophiolites of the eastern and western Mediterranean. The comparative data taken from various sources and all recalculated to 100% on a volatile free basis, total iron being represented as Fe_2O_3, is given in Table 4.3.

4.3.5.2 Chemical comparison of the basalts with those from known tectonic settings

Since the "more primitive" (MP) basalts show stronger chemical affinity towards ocean-floor tholeiites and the "more differentiated" (MD) basalts towards island arc tholeiites, they are respectively compared with present day marginal basin basalts and island arc tholeiites. In a similar fashion to Pearce (1980), all data were normalised to the average mid-ocean ridge basalt (MORB) composition and similarly plotted on logarithmic scale, such that all comparisons are relative to average MORB composition.

The present back-arc (marginal) basins have received much attention in recent years. Basaltic rocks recovered from marginal basins like the Mariana (Hart et al, 1972), Lau (Hawkins, 1976), Parace Vela (Ridley et al, 1974), South Sandwich and Drake Passage (Tarney et al, 1977; Saunders and Tarney, 1979) have been relatively well studied. Average chemical analyses of basalts from these basins and the MP basalts are compared in

TABLE 4.3

Comparative chemical data from known tectonic settings and ophiolites

MORB = Average composition of mid-ocean ridge basalts (mid-Atlantic ridge, Kolbeinsey ridge, East Pacific Rise and Indian Ocean ridge) compiled from Engel et al, 1965; Fisher et al, 1968; Nicholls and Islam, 1971; Melson and Thompson, 1971; Erlank and Kable, 1976; Baragar et al, 1977 and Sun et al, 1979.

A = Polusagi 'MP' basalt (6), this study.

B = Polusagi 'MD' basalt (13), this study.

C = Polusagi basaltic andesite (20), this study.

D = Polusagi acid andesite (12), this study.

E = Polusagi dacite (5), this study.

Marginal basin basalts:

1 - South Sandwich back arc basin basalt (9); Saunders and Tarney, 1979.

2 - South Sandwich spreading centre basalt (9); Saunders and Tarney, 1979; Tarney et al, 1977.

3 - Drake Passage basalt (2); Saunders and Tarney, 1979.

4 - Lau Basin basalt (11 least altered basalt average); Hawkins, 1976.

5 - Mariana basin basalt (5); Hart et al, 1972.

6 - Parace Vela Basin basalt (2); Ridley et al, 1974.

Ophiolitic basalts I (Western Mediterranean and Chilean):

7 - N.Apennine; Beccaluva et al, 1980.

8 - Corsican; Beccaluva et al, 1980.

9 - Calabrian; Beccaluva et al, 1980.

10 - Sarmiento ophiolite basalt (5); Saunders et al, 1979.

Ophiolitic basalts II (Eastern Mediterranean):

11 - Upper pillow lavas, Troodos; Beccaluva et al, 1980; x from Pearce, 1980 and * from Kay and Senechal, 1976.

12 - Lower pillow lavas, Troodos; Beccaluva et al, 1980; x from Pearce, 1980 and * from Kay and Senechal, 1976.

13 - Krapa, Vourinos; Beccaluva et al, 1980.

14 - Asprokampo, Vourinos; Beccaluva et al, 1980.

15 - Pontid 'arc' tholeiitic basalt; Egin et al, 1979.

Island arc tholiites (SiO_2 < 52%):

16 - St.Kitts, Lesser Antilles (27); Brown et al, 1977; X from Hawkesworth and Powell, 1980.

17 - South Sandwich Islands (11); Baker, 1968, 78.

18 - Eua, Tongan Islands (sample E7); Ewart and Bryan, 1972.

Island arc basaltic andesites (SiO_2 = 52-56%):

18 - South Sandwich Islands (8); Baker, 1978.

21 - Eua, Tongan Islands (3); Ewart and Bryan, 1972.

Island arc acid andesites (SiO_2 = 56-62%):

22 - St.Kitts, Lesser Antilles (86); Brown et al, 1977.

23 - South Sandwich Islands; Baker, 1978.

24 - Eua, Tongan Islands; Ewart and Bryan, 1972.

25 - Viti Levu (4 samples: 68.48, 68.52, 68.54 and 68.60); Gill, 1970.

26 - Pontid 'arc', Lower Basic Series (27); Egin et al, 1979.

Island arc dacites and rhyolites (SiO_2 > 62%):

27 - St.Kitts, Lesser Antilles (25); Brown et al, 1977.

28 - South Sandwich Islands (3); Baker 1978.

29 - Eua, Tongan Islands; Ewart and Bryan, 1972.

30 - Viti Levu (sample: 68.50); Gill, 1970.

31 - Pontid 'arc', Lower Volcanic series; Egin et al, 1979.

			MARGINAL BASIN BASALTS						OPHIOLITIC BASALTS (I)					OPHIOLITIC BASALTS (II)				
	A	MORB	1	2	3	4	5	6	7	8	9	10	B	11	12	13	14	15
SiO_2 wt%	47.49	49.37	51.05	52.14	50.21	48.72	49.81	49.31	51.35	51.58	49.30	51.34	48.98	54.44	53.66	55.56	56.33	53.59
Al_2O_3	14.15	15.80	16.74	16.70	15.52	16.37	16.92	17.47	16.53	16.77	18.90	15.66	14.16	15.19	15.69	16.72	15.12	16.41
Fe_2O_3	12.33	10.55	8.77	9.03	10.44	9.68	9.62	5.83	9.77	9.40	9.71	10.03	13.05	8.86	9.34	11.11	9.06	10.80
MgO	10.15	8.34	7.45	6.75	7.28	8.59	6.72	6.32	6.57	6.63	5.91	6.99	8.98	8.12	7.32	5.82	7.30	5.52
CaO	10.96	11.78	10.96	10.79	11.33	12.58	11.41	11.61	8.22	7.99	8.76	8.24	8.68	10.66	9.23	4.66	9.07	9.95
Na_2O	3.13	2.54	3.08	2.88	2.83	2.40	3.22	3.22	5.11	4.70	4.54	4.60	3.79	1.20	2.55	4.66	2.61	1.78
K_2O	0.30	0.19	0.39	0.35	0.28	0.18	0.47	0.32	0.29	0.75	0.80	0.40	0.12	0.97	0.85	0.62	0.16	0.49
TiO_2	1.20	1.17	1.24	1.09	1.74	1.20	1.52	1.07	1.84	1.87	1.70	1.65	1.77	0.48*	1.12*	0.80	0.31	1.01
MnO	0.22	0.17	0.16	0.16	0.18	0.20	0.14	0.16	0.18	0.18	0.16	0.18	0.20	0.15	0.13	-	-	0.19
P_2O_5	0.16	0.08	0.17	0.15	0.20	0.08	0.16	0.11	0.26	0.24	0.21	0.25	0.26	0.05*	0.09*	0.04	0.02	0.14
Nb ppm	7	3.5	5	3.7	4	-	-	2.5	6	6.5	5.5	5	10	2*	3*	-	-	2
Zr	86	94	105	90	129	-	-	69	177	171	127	155	147	22*	57*	41	22	62
Y	30	34	25	25	39	-	-	25	47	48	39	47	47	11*	26*	19	8	30
Sr	122	120	208	175	157	118	186	178	238	155	237	218	154	79*	124*	84	90	280
La	7	4	5	7.5	8	-	6	-	6.6	8.7	6.5	4.4	11	1.4*	2.5*	-	-	-
Ce	18	9	14	15	15	-	18	8	17	21	16	13	27	4.9*	11.7*	-	-	-
Rb	6.3	3	5	4.7	4	2	4.5	6.5	7	17.5	19	8	3.6	29	8	7	5	14
Ba	70	23	65	63	47	34	3.6	23	-	-	-	-	96	19*	24*	-	-	205
Zn	67	67	68	70	81	61	-	-	92	71	103	98	83	-	-	94	86	135
Cu	43	83	-	-	-	97	-	-	63	56	59	68	30	55	72	84	75	60
Ni	96	127	66	56	76	173	69	169	101	95	117	110	18	170	47	33	82	6
Cr	254	367	255	217	279	387	-	-	217	205	227	240	53	530*	90*	61	281	104

Table 4.3 - cont'd.

	ISLAND ARC THOLEIITES (SiO_2 < 52%)				ISLAND ARC BASALTIC ANDESITES (SiO_2=52-56%)				ISLAND ARC ACID ANDESITES (SiO_2=56-62%)						ISLAND ARC DACITES AND RHYOLITES (SiO_2 > 62%)					
	B	16	17	18	C	19	20	21	D	22	23	24	25	26	E	27	28	29	30	31
SiO_2 wt%	48.98	49.95	49.57	49.79	53.47	54.11	53.05	54.25	57.10	59.26	57.85	60.66	57.30	61.16	67.74	64.23	66.67	67.08	73.40	72.44
Al_2O_3	14.16	19.86	18.38	20.86	15.70	19.20	16.26	16.60	16.12	17.47	16.58	17.30	17.56	16.15	14.35	16.39	13.94	16.18	13.97	15.19
Fe_2O_3	13.05	9.80	10.60	9.30	11.97	8.97	12.48	11.88	10.27	7.80	10.12	7.25	9.33	7.40	7.13	6.20	8.22	4.74	3.87	2.66
MgO	8.98	4.66	6.57	6.00	7.97	3.07	4.53	4.76	5.55	2.56	2.74	3.12	3.23	2.67	1.63	1.67	0.98	2.29	0.77	0.53
CaO	8.68	11.46	11.82	11.92	4.17	9.68	9.22	8.80	3.48	7.88	7.61	6.12	6.68	7.70	2.17	6.49	4.13	3.29	3.63	2.28
Na_2O	3.79	2.70	1.89	1.23	4.27	3.27	2.65	2.68	5.05	3.42	3.31	3.87	4.02	2.48	6.02	3.50	4.03	5.48	4.72	2.69
K_2O	0.12	0.31	0.21	0.24	0.12	0.51	0.49	0.18	0.20	0.60	0.71	0.39	0.55	1.29	0.21	0.76	1.18	0.31	0.90	3.67
TiO_2	1.77	0.99	0.73	0.43	1.65	0.93	1.03	1.01	1.49	0.70	0.88	0.64	1.03	0.81	0.60	0.52	0.56	0.47	0.50	0.33
MnO	0.20	0.18	0.16	0.18	0.23	0.17	0.20	0.26	0.19	0.18	0.15	0.13	0.19	0.15	0.10	0.15	0.13	0.09	0.12	0.06
P_2O_5	0.26	0.10	0.05	0.04	0.43	0.10	0.09	0.11	0.46	0.11	0.16	0.11	0.26	0.16	0.15	0.10	0.16	0.06	0.12	0.10
Nb ppm	10	2	-	-	17	1	-	-	22	1	-	-	-	3	32	2	-	-	-	4
Zr	147	58	80	20	255	79	-	50	343	94	-	110	70	83	571	105	-	100	71	106
Y	47	20	-	12	68	24	-	30	84	25	-	29	30	30	105	23	-	27	43	21
Sr	154	286	135	115	112	299	-	113	132	297	-	137	197	252	138	292	-	135	116	149
La	11	-	-	-	16	-	-	-	21	-	-	-	2.6	-	30	-	-	-	2.7	-
Ce	27	8.5*	-	-	38	-	-	-	50	-	-	-	10	-	60	-	-	-	7.2	-
Rb	3.6	5	11	1.2	2.6	10	-	1.4	3.5	12	-	2.4	5.3	43	3.4	14	-	1.7	6.8	99
Ba	96	109	62	14	69	146	-	46	149	173	-	68	103	366	80	205	-	60	128	559
Zn	83	66	-	-	158	67	-	-	149	66	-	-	-	82	131	54	-	-	-	30
Cu	30	60	139	51	71	59	-	106	16	33	-	54	33	15	102	17	-	7	0	1
Ni	18	14	14	25	6	4	-	28	6	3	-	5	0	7	0.2	2	-	3.5	0	1
Cr	53	22	34	75	35	6	-	44	19	10	-	15	3	22	11	7	-	30	0	8

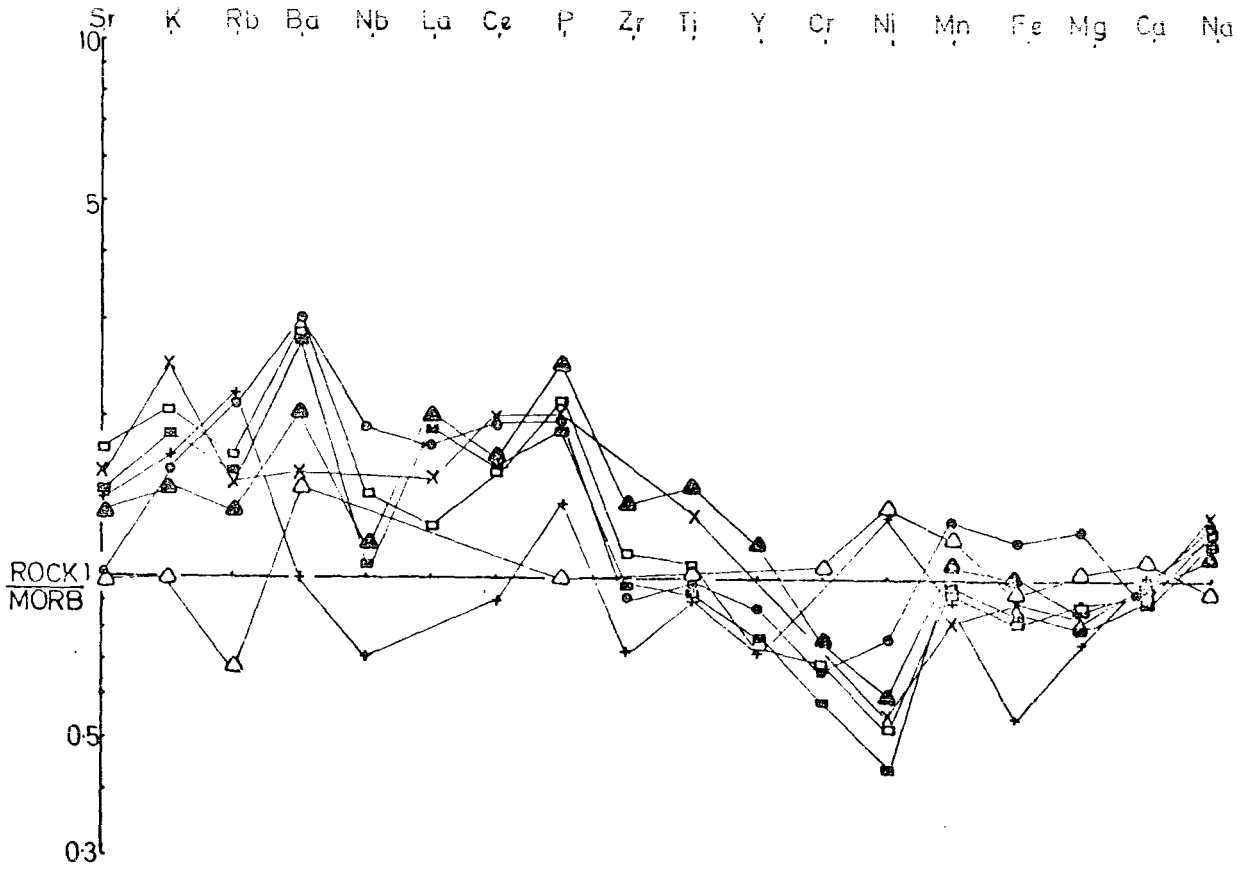


Fig.4.20 Geochemical patterns of some present day marginal basin and back arc basin basalts as compared with the Polusagi "more primitive" basalts.

- ⊙ : Polusagi - "more primitive" basalts
- □ : South Sandwich back-arc basin basalts
- ▣ : South Sandwich spreading centre basalts
- ◭ : Drake Passage basalts
- △ : Lau Basin basalts
- x : Mariana Basin basalts
- + : Parace Vela inter-arc basalts

Fig. 4.20. Chemical patterns displayed by the marginal basin basalts are in good general agreement with that of the MP basalts. Although they are all chemically very similar to MORB, the following distinctive features are apparent:

1) The Polusagi MP basalts are very similar to basalts from the South Sandwich spreading centre, the South Sandwich back-arc basin, the Drake Passage spreading centre and the Mariana basin. Relative to average MORB, they are all enriched in the immobile elements Nb, La, Ce and P as well as in the alkali elements Sr, K, Rb and Ba, and all depleted in Cr and Ni. The average Na contents of all basalts are higher than MORB average.

2) The MP basalts tend to be less depleted in Cr and Ni and more enriched in Nb, La, Ce, P and the alkali elements than the marginal basin basalts. The basalts from the marginal basins have similar or lower concentrations of MnO, Fe_2O_3 and MgO as compared with the MORB, but those of the MP basalts are consistently higher.

3) The MP basalt average is similar in SiO_2 but lower in Al_2O_3 when compared with either the marginal basin basalts or the MORB.

4) Basalts from the Lau basin and the Parace Vela basin do not conform with the above general pattern and show much closer chemical similarities with the MORB average. This could be a manifestation of the longer history of these basins, as basalts from basins having a relatively longer history tend to be chemically much closer to MORB (Tarney et al, 1977). The Polusagi MP basalts, being formed during the early stages of the development of a Tethyan marginal basin-island arc complex, show closer chemical affinity with basalts from the younger basins.

Average chemical analyses of island arc tholeiites from St. Kitts in the Lesser Antilles (Brown et al, 1977; Hawkesworth and Powell, 1980), from the South Sandwich islands (Baker, 1968,78) and Eua in the Tongan Islands (Ewart and Bryan, 1972) are compared with the Polusagi MD basalts

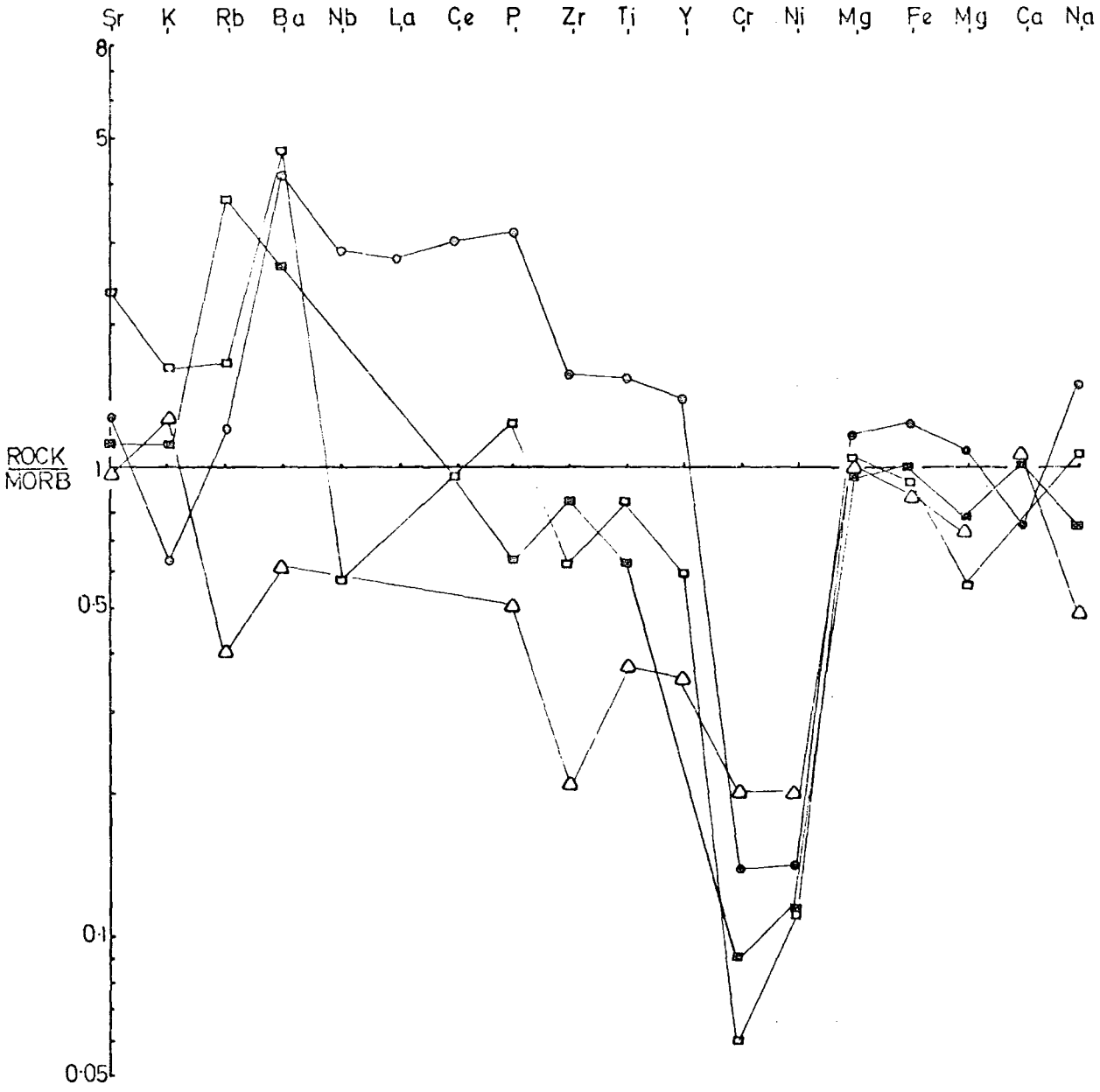


Fig.4.21 Geochemical patterns of some present day island arc tholeiites as compared with the "more differentiated".

● : Polusagi - "more differentiated" basalts

□ : St. Kitts, Lesser Antilles

▣ : South Sandwich Islands

△ : Eua, Tongan Islands

in Fig.4.21. In general, present day island arc tholeiites have lower Zr, Nb, Y, La, Ce and P_2O_5 contents than the average MORB, a feature not exhibited by the MD basalts. Although the Polusagi MD basalts display the characteristic low Cr and Ni concentrations of island arc tholeiites, they have much higher concentrations of Nb, Zr, Y, La, Ce, P_2O_5, TiO_2, MnO, total Fe, MgO and Na_2O than both the island arc tholeiites and the MORB. This feature seems to be distinctive of the Polusagi MD basalts and may be a result of the MD basalts being formed close to the spreading ridge in the Tethyan marginal basin with a fast spreading rate, as suggested by Pearce (1980) for some Tethyan ophiolitic lavas exhibiting island arc tholeiitic characteristics.

The MD basalts have similar SiO_2 but lower Al_2O_3 and K_2O contents than the present day island arc tholeiites. The alkali elements Sr, Ba and Rb do not show a systematic pattern; variations being within the variations of other island arc tholeiites.

4.3.5.3 Chemical comparison of the basalts with ophiolitic basalts

That the Tethyan ophiolites in the Mediterranean area fall into two distinct groups on the basis of pronounced chemical and petrological grounds is well established (e.g. Rocci et al, 1975; Beccaluva et al, 1977; Beccaluva et al, 1979, 80; Laurent et al, 1980; Pearce, 1980; Cameron et al, 1980). These are now briefly considered:

Group I - Western Mediterranean ophiolites: These ophiolites, such as those of Corsica, the Northern Apennines, Calabria and the Eastern Alps, are of early to middle Mesozoic age. The extrusive sequences represent Tethyan oceanic crust formed either at oceanic ridges or in marginal basins or incipient oceans. Intrusive complexes are mainly composed of gabbroic rocks, and scarce plagiogranites.

Group II - Eastern Mediterranean ophiolites: These ophiolites, like those of Vourinos, Greece; Troodos, Cyprus; Baer Bassit, Syria and the

Semail Nappe, Oman; are of upper Cretaceous age. Their extrusive sequences range from basalts to rhyolites, with abundant basaltic andesites. The basic members show only low iron and titanium enrichment. The intrusive complexes consist of well developed ultramafic cumulates (dunite, clinopyroxenite, olivine-clinopyroxenite), gabbroic rocks and relatively abundant diorites and plagiogranites.

The tectonic setting for the eastern Mediterranean ophiolites is controversial, a point which is highlighted by the controversy over Troodos (see Miyashiro, 1973,75 a,b,c; Hynes, 1975; Moores, 1975; Gass et al, 1975). Three theories for the origin of the Troodos ophiolite complex have been put forward:

a) Mid-ocean ridge environment (e.g. Moores and Vine, 1971; Gass and Smewing, 1973)

b) Marginal Basin environment (e.g. Pearce, 1975; Sun and Nesbitt, 1978; Sun et al, 1979)

c) Island arc environment (Miyashiro, 1973)

There are serious objections to the conventionally accepted theory of a mid-ocean ridge spreading centre origin for Troodos both on petrological grounds (Cameron et al, 1980) and chemical grounds (Miyashiro, 1975 a,b,c; Beccaluva et al, 1977; Pearce, 1980).

It has been generally recognised in recent years that the Troodos, Vourinos and Semail Nappe, Oman, ophiolites are chemically affiliated to island arc tholeiites and marginal basin basalts. Alabaster et al (1980) recognise that the lowermost lavas (the Geotimes Unit) of the Oman ophiolite have ocean crust characteristics while the upper Lasail and Alley Units have island arc tholeiite characteristics. They propose an "island arc" component in an incipient arc-basin complex setting for the formation of these rocks. According to Beccaluva et al (1979), the Troodos and Vourinos ophiolites include island arc tholeiites and were probably formed in or near immature arcs by spreading processes above a

subduction zone, while Pearce (1975) sees the relationship between the Lower pillow-lavas and the Upper pillow-lavas of Troodos as a transition from marginal basin basalts to island arc tholeiites. Pearce (1980) extends his interpretation of the Troodos complex to the "ophiolitic" and the overlying "non-ophiolitic" upper Cretaceous lavas in general for all the Tethyan ophiolites.

In Fig. 4.22 the Polusagi MP basalts are compared with the extrusives of western Mediterranean ophiolites and with the basalts from the Sarmiento ophiolite in Southern Chile, which is similarly thought to have formed in a marginal basin (Jurassic) by Saunders et al (1979). The chemical pattern of the Polusagi MP basalts is expectedly similar to those exhibited by the basalts from these ophiolites. It is also noteworthy that the patterns in Fig.4.22 are very similar to those exhibited by the modern marginal basin basalts shown in Fig.4.20. Nevertheless, as was the case against the modern marginal basin basalts, the Polusagi MP basalts are in general richer in Mn, Fe, Mg and Ca and poorer in Na, P, Zr and Ti concentrations than the ophiolitic basalts with which they are compared.

The Polusagi MD basalts are compared with the basalts from the eastern Mediterranean ophiolites, including the Lower and Upper pillow-lavas of Troodos, Vourinos (Krapa and Aspro) and with tholeiitic rocks from NE Turkey, which Egin et al (1979) interpret as the product of upper Cretaceous island arc volcanism, the Pontid 'arc', in Fig. 4.23. It is apparent that the rocks from the compared areas are generally depleted in Nb, La, Ce, P, Zr, Ti, Y, Mn, total Fe and Mg as compared with MORB and with the Polusagi MD basalts which show considerable enrichment in these elements even relative to MORB. The Cr and Ni values of the MD basalts are similar to those of the Troodos Lower pillow-lavas, Krapa (Vourinos Ophilite Complex) and the Pontic arc tholeiites, but are much lower than those of the Troodos upper pillow-lavas and Asprokampo

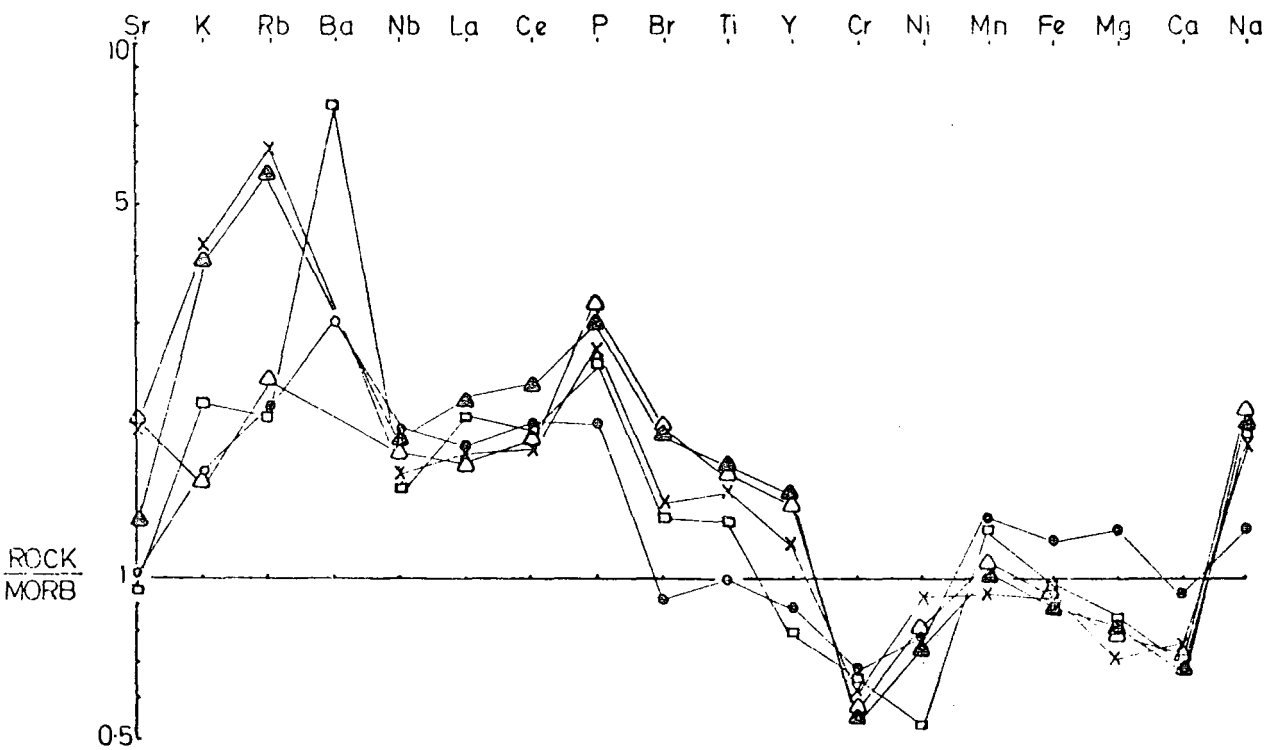


Fig.4.22 Geochemical patterns of Western Mediterranean ophiolitic basalts, compared with the "more primitive" basalts.

- ● : Polusagi - "more primitive" basalts
- △ : N.Apennine ophiolites
- ▲ : Corsican ophiolites
- x : Calabrian ophiolites
- □ : Sarmiento ophiolites, Chile.

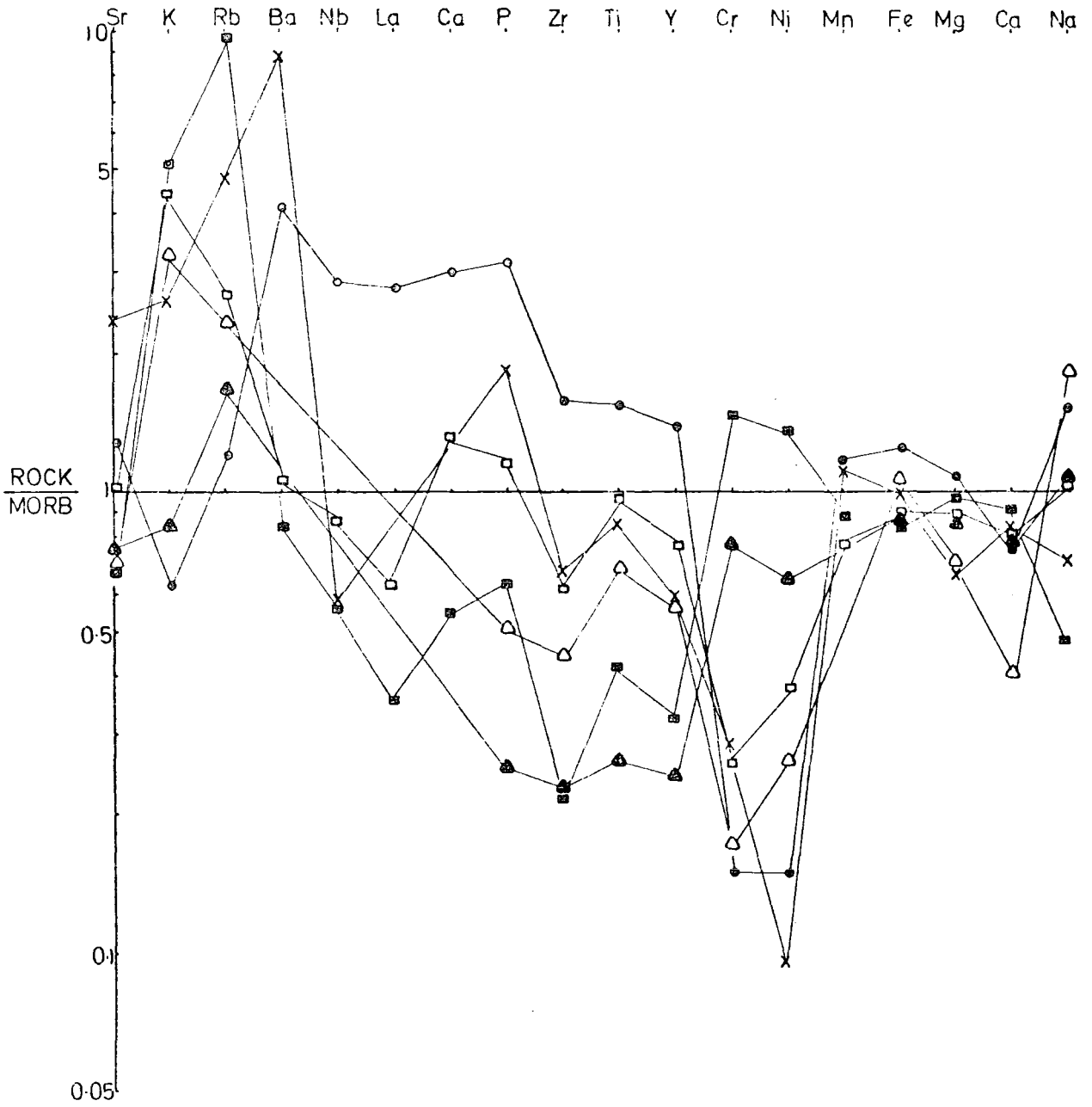


Fig.4.23 Geochemical patterns of basaltic rocks from Eastern Mediterranean ophiolites as compared with the "more differentiated" basalts.

- ⊙ : Polusagi - "more differentiated" basalts
- x : Pontid 'arc' tholeiitic basalts
- □ : Lower pillow lavas, Troodos
- ▣ : Upper pillow lavas, Troodos
- △ : Krapa, Vourinos
- ▲ : Asprokampo, Vourinos

(Vourinos). The lavas from the Troodos Upper pillow unit and Asprokampo are also distinctive in having the most depleted Ba, Nb, La, Ce, P, Zr, Ti, Y and the highest Cr and Ni concentrations in the group of lavas considered, and this is in complete contrast to the Polusagi MD basalts. Thus, although island arc environments have been suggested for the origin of the Vourinos and Troodos Upper pillow lavas, this cannot be a viable environment for the generation of the Polusagi MD basalts as far as the immobile element concentrations are concerned. Other element concentrations of the Polusagi MD basalts such as Na, Ca and the alkali elements, are comparable to the other lavas under consideration.

4.3.5.4 Chemical comparison of the Polusagi andesites and dacites

The average chemical compositions of the Polusagi basaltic andesite, acid andesite and dacite and of similar rocks from the Pontid arc, NE Turkey, and modern island arcs are presented in Table 4.3. The essential features of the comparison of these chemical analyses are very similar to those observed while comparing the Polusagi basalts with their modern and past counterparts. On the whole the Polusagi andesite averages seem to be much richer in Mg, Na, Ti, P, Nb, Zr, Y, La and Ce, much poorer in Ca and poorer in Al and K than similar rocks from tholeiitic suites of island arcs; other elements being comparable. The Polusagi dacites follow a similar pattern to the andesites when compared with dacitic members of the same rock suites.

4.3.5.5 Conclusion

The most basic volcanic rocks of the Polusagi suite, the MP basalts, show very similar and comparable chemistry to modern marginal basin basalts and basalts from the western Mediterranean Tethyan ophiolites. These basalts are all enriched in alkali elements (K, Rb, Ba and Sr), Nb, La, Ce, P and Na, but depleted in Cr, Ni and Ca relative to MORB. Furthermore, the Polusagi basalts are enriched in Mg, Mn and Fe as compared with

MORB. However, as the composition of the Polusagi volcanics moves to more acidic compositions (by fractional crystallisation, Chapter five, 5.3 and 5.5), some distinctive and systematic chemical differences are observed when they are compared with the equivalent or comparable rock types from modern and past island arc tholeiite suites : The Polusagi volcanic rocks are richer in Mg, Na, Ti, P, Nb, Zr, Y, La and Ce and poorer in Al, Ca and K contents.

CHAPTER FIVE

ORIGIN AND PETROGENESIS OF THE POLUSAGI THOLEIITIC MAGMA

5.1 Introduction

The current theory of plate tectonics proposes that the island arc rock suites are typical of collision boundaries, and island arcs are related to zones of subduction. Along the oceanic trenches where the oceanic crust is thrust under another section of the oceanic crust which may include continental crust to greater or lesser extents, a complex process of tectonic and magmatic activity occurs. A major role in this process has been advocated for the downgoing oceanic slab in explaining the origin and development of island arc magmas. In addition, the location of the subducted oceanic plate is generally assumed to be coincident with the earthquake zone, or Benioff zone.

The downgoing oceanic crust is initially cold relative to the upper mantle at the subduction zone, and this may be a contributing factor to its descent (Ringwood, 1972). To explain the heat source which is necessary to provide the melting and magmatic activity which gives rise to island arc volcanism and spreading in back-arc basins, two processes have been proposed (Fig. 5.1):

a) Frictional heating model (e.g. Matsuda and Uyeda,1971): This model assumes that large quantities of heat are being generated along the slip zone and the heat is effectively transformed into the mantle, causing partial melting and the rise of magma plumes. This model finds it necessary that heating takes place at depths greater than 60 km. from the surface.

b) Secondary flow model (Sleep and Toksöz, 1973; Toksöz and Bird,1977): This model assumes that the upper mantle wedge above the subducted oceanic slab is capable of sustaining convective flow forced by the descending slab as shown in Fig.5.1. This way heat from the lower parts of the mantle is transferred to shallow depths, tensional force is exerted

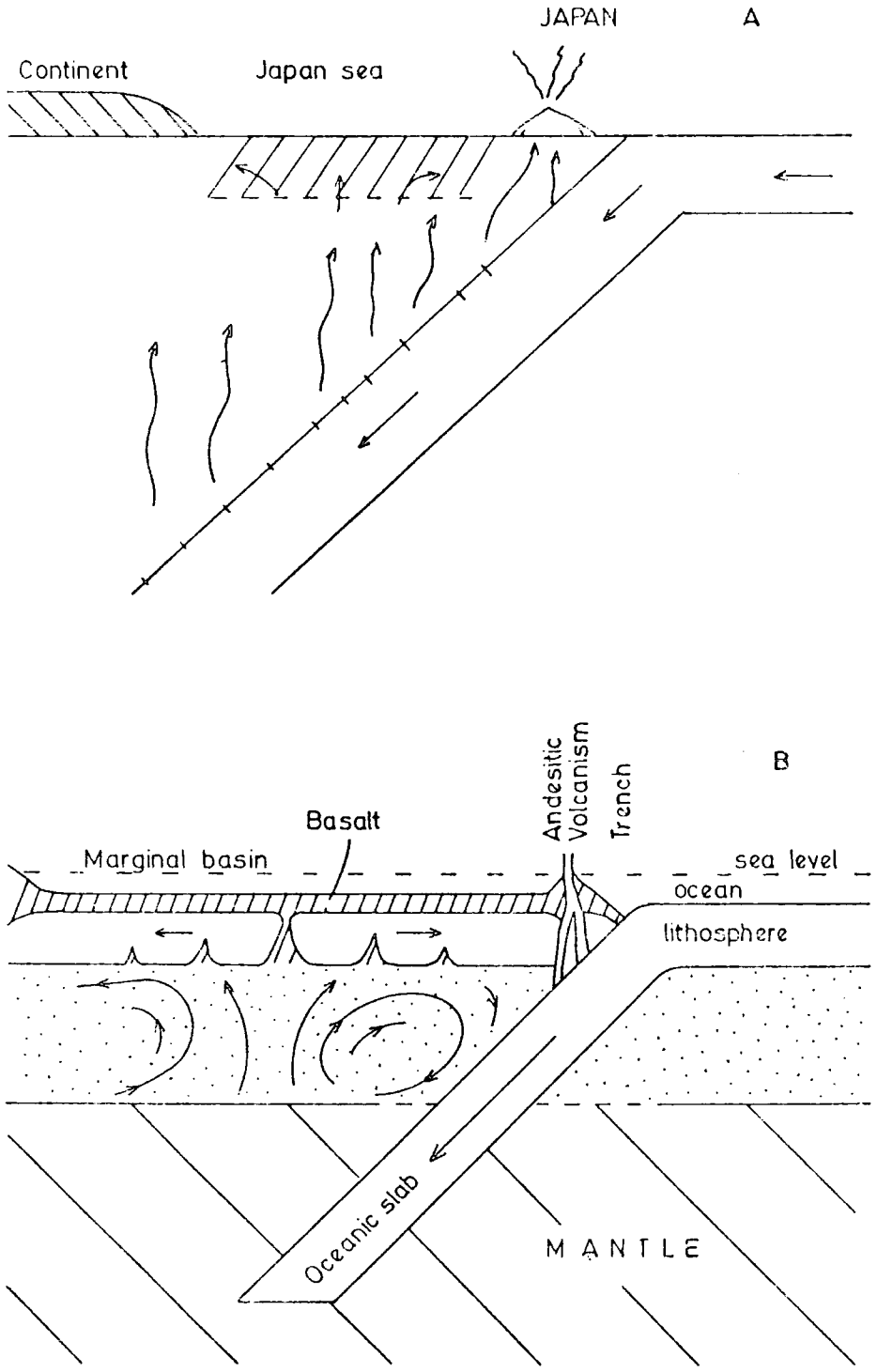


Fig.5.1 Two possible mechanisms of back-arc opening:
A) Frictional heating model (Matsuda and Uyeda, 1971)
B) Secondary flow model (Sleep and Toksöz, 1973; Toksöz and Bird, 1977)

at the bottom of the crust in the back-arc area which leads to the opening of the basin by spreading.

The explosive nature of island arc volcanism, as seen in the abundance of pyroclastic rocks and the occurrence of hydrous minerals in island arc rock suites, as well as other petrogenetic considerations (see e.g. Ringwood, 1974,77), suggests that water must have played an important role during the production and evolution of island arc magmas. Yet the water contents of the mantle is thought to be low and around o.1% (Ringwood, 1975). Thus an alternative source for the required amounts of water is necessary. It is generally agreed that this water is provided by the subducted oceanic crust (Ringwood, 1974,77; Arculus, 1973).

The structure of oceanic crust is generally compared with those of fully developed ophiolite sequences. It is believed to be composed, from top to bottom, of sediments (layer 1), basaltic flows and pillow-lavas (layer 2) passing down to the upper mantle through dyke swarms and layered gabbros (Davies,1971; Cann, 1970). The layer 2 basalts are normally metamorphosed to greenschist facies. As subduction begins, the sediments of layer 1 would probably be scraped off (Dewey and Bird,1970). The "wet" greenschists of layer 2, upon subduction into the mantle, would transform into amphibolites releasing water and volatiles. It is at this stage of the process that the role of the water, driven off the subducted oceanic crust, may be crucial in the development of island arc magmas. For instance, Hill and Boettcher (197o) have shown that if P_{H_2O} approaches P_{total} at mantle pressures, considerable quantities of silicate melt would be produced. The process of dehydration of descending oceanic crust can take place up to a depth of 100 km according to Wyllie (1973), or at a range of 80-100 km according to Ringwood (1977). Amphibolite would decompose at greater depths and this, Fitton (1971) suggests, would lead to the generation of island arc tholeiitic magmas. However, there is evidence that magmas giving rise to island arc volcanism can be generated at depths

greater than 100 km , extending sometimes to 150 km. (Ringwood,1977). Because amphibolite would break down before reaching such great depths, some different "carrier" of water to such depths must be operative, and Ringwood (1977) suggests that serpentinite within the oceanic crust is capable of taking water to depths well above 100 km.

Although the mechanism for the generation of island arc magmas is still debated, there seems to be a general agreement that such magmas, on the whole originate either from the mantle wedge overlying the subducted oceanic slab, or from the oceanic slab itself, by partial melting. Brown et al (1977), studying the geochemistry of the Lesser Antilles volcanic island arc, suggest partial melting of subducted oceanic crust for the origin of the calc-alkaline and tholeiitic rocks of the southern magmatic suite (Dominica and St.Kitts islands respectively). On the other hand, they propose partial melting of a garnet lherzolite source for the origin of the northern (Grenada) magmatic suite of the island arc. Gill (1970) extends Green and Ringwood's (1968) suggestion that calc-alkaline magmas represent the partial melts of a downgoing slab, and puts forward the same mechanism for the generation of the tholeiitic and shoshonitic magmas of the Viti Levu island arc. A similar proposal for the origin of island arc magmas comes from Fitton (1971). Variations in island arc magma compositions may be due to the degree of interaction of the two source regions i.e. the mantle wedge and the subducted slab. Alternatively, a two stage magma generation may be operative as suggested by Ringwood (1974,77), providing explanations for the differences observed during the development of island arcs in space and time (see section 4. 3.1). Ringwood (op cit) proposes, on the basis of work by Nicholls and Ringwood (1973), that at a depth interval of 80-100 km , a large amount of water is released from the descending slab by dehydration of amphibolite and by partial dehydration of serpentinite. This water rises into the upper mantle wedge causing a "drastic decrease in viscosity", partial melting and uprise of the "pyrolite" from the Benioff zone. Thus partial melting occurs under high water

pressures leading to the generation of hydrous tholeiitic magma. This magma, by separation mainly of olivine but also of pyroxene and possibly amphibole, produces the island arc tholeiitic rock series, during the early stages of island arc development. An important feature of this stage is that the subducted oceanic slab contributes mainly water to the mantle wedge, together with very small amounts of silica. In the second stage, or the mature phase of island arc magmatism, oceanic crust will be converted into quartz-eclogite at greater depths. Partial melting of quartz-ecologite will then occur under high water pressures and above about 750°C, leading to the generation of calc-alkaline magmas.

The origin of andesites and andesitic magmas has also been a matter of considerable debate: are they partial melts from the upper mantle, or are they lower pressure differentiation products of basaltic melts? Kushiro and Yoder (1969)and Kushiro (1972) maintain that andesitic and dacitic magmas might be produced by partial melting of upper mantle under high water pressures at depths ranging from 70 km to 100 km. Thus they imply that andesites and dacites can directly be produced at Benioff zones as a result of introduction of water into the mantle wedge. Mysen and Boettcher (1975) hold a similar view that andesitic liquids can be formed by partial melting of mantle peridotite at least up to 25kbars under hydrous conditions. On the other hand, for example, Nicholls and Ringwood (1973) conclude their experiments by stating that it is improbable that andesitic and dacitic magmas (60-65% SiO_2) can be produced as primary magmas by direct partial melting of mantle at depths greater than 40 km. Instead, these authors suggest that it is possible to produce magmas with compositions varying from olivine-tholeiite to quartz-tholeiite by partial melting of mantle under water saturated conditions at a depth range 70-100 km. Such magmas, upon ascent, can differentiate to basaltic andesite or even to andesite (maximum 58% SiO_2) by olivine fractionation. Further fractionation into more acidic compositions can be governed by separation

of amphibole ± pyroxene and, at very low pressures, plagioclase may become a dominant fractionating phase (Nicholls and Ringwood, 1973).

5.2 Origin of the Polusagi magma

From the preceding account it is clear that two main processes must be considered as possible mechanisms for generation of the Polusagi magma: a) Partial melting of an upper mantle wedge, b) Partial melting of a mafic oceanic crust subducted along a Benioff zone..

It was pointed out earlier (section 4. 4.1) that the most basic volcanic members of the Polusagi rock suite, the "more primitive" (MP) basalts, are similar in composition to the basalts from marginal basins and mid-ocean ridges, but have similar or higher incompatible element concentrations. This suggests that, if the MP basalts are the products of melting of an oceanic slab, then the melting could not have been complete. On the other hand, the MP basalts have similar or lower SiO_2 and higher MgO contents than the oceanic tholeiites. In all experiments, whether under dry or hydrous conditions, the partial melts produced from basaltic compositions are consistently more silicious than the parental material (Green and Ringwood, 1967). In order to get partial melts from the subducted oceanic crust with similar SiO_2 contents, the melting must be either complete or nearly so. This is in total contradiction to the suggestions made by the incompatible element abundances. Furthermore, it is hard to envisage a partial melt of the oceanic slab giving rise to magmas having more MgO than the oceanic tholeiites.

The above arguments assume that the MP basalts represent relatively unmodified partial melts of the source rock (see section 5.4. for discussion). Even when it is assumed that the MP basalts represent basaltic liquids modified after fractional crystallisation of mainly olivine, there are serious difficulties. Although the relatively higher concentrations of the incompatible elements in the MP basalts can, then, be explained as being due to fractionation (mainly olivine) of the partial melts of the

oceanic slab; the same process cannot explain the higher MgO contents of the MP basalts. The MP basalts are aphyric rocks and do not contain cumulus olivine or its pseudomorphed forms. Therefore the high MgO content is not due to "cumulus" olivine. Since the fractionation would deplete the residual "modified" liquids in MgO, it follows that the MP basalts must have had even higher MgO contents in their "unmodified" forms. This again points towards a source rock whose partial melts contain MgO values well above those of oceanic tholeiites. In conclusion, partial melting of a source rock, poorer in SiO_2 and richer in MgO than the MP basalts i.e. upper mantle, must be proposed for the origin of the Polusagi basaltic magma.

So far, only the origin of the MP basalts has been discussed. As pointed out earlier, all the rock types in Polusagi from basalts to dacites, could conceivably be produced by direct partial melting of the upper mantle. However, all the rock types in Polusagi are mineralogically and chemically gradational, and all the samples come from a relatively restricted area. Therefore, it is reasonable to assume that the other rock types are also of upper mantle origin, representing either a) different partial melts of the upper mantle or b) products of fractional crystallisation of a mantle partial melt. The possibilities will now be examined.

5.3 Fractional crystallisation vs. progressive partial melting

Progressive partial melting of upper mantle would produce variations in incompatible trace element concentrations in the melts, depending on the degree of partial melting. O'Hara (1968) has shown that variations in the amount of initial partial melting of a peridotite source may produce a variation in the incompatible trace element abundances by a factor of 3 for melts within the range 0 - 3% of the source. Fig. 5.2 illustrates the enrichment factors resulting from an increasing amount of partial melting of a peridotite source. Generally the initial concentractions of the incompatible trace elements, resulting from a small

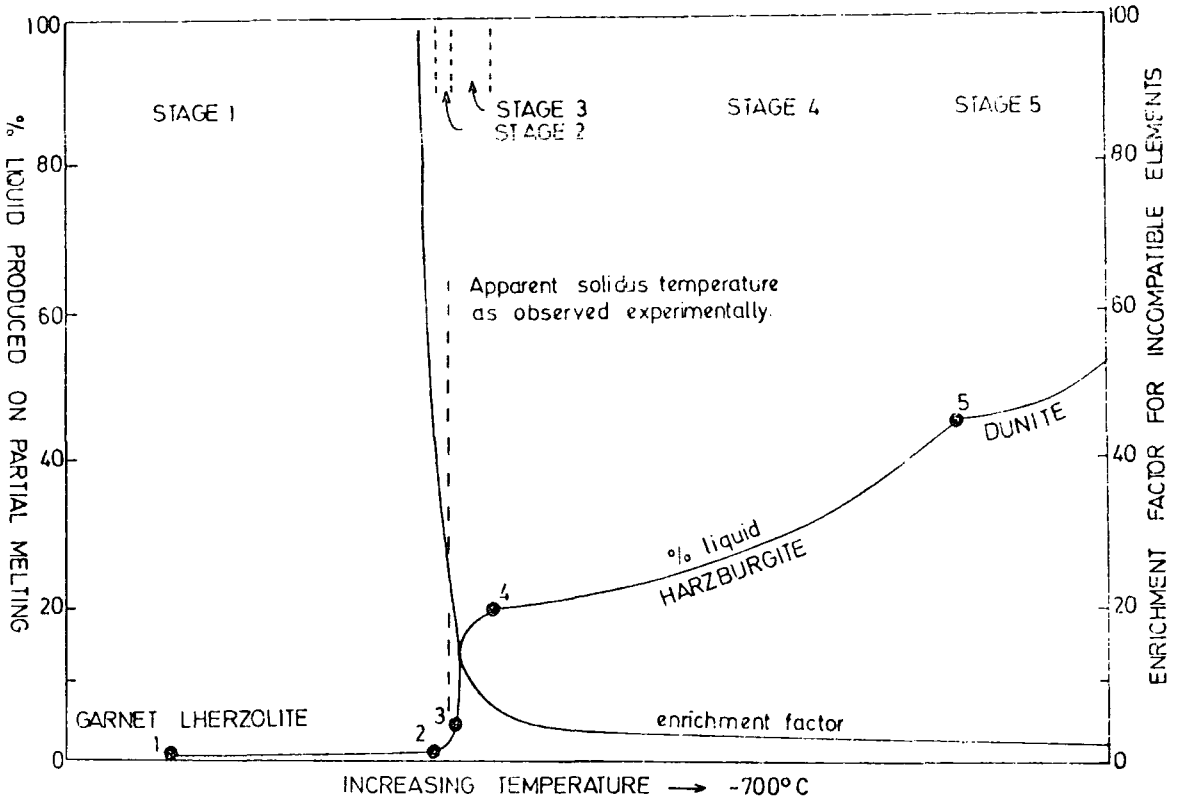


Fig.5.2. Variations in the partial melt composition and enrichment factors of incompatible elements as a result of melting of a garnet lherzolite source (after O'Hara, 1968)

Five main stages are:

1) Extreme enrichment in incompatible trace elements with small amount ($\sim$1%) of partial melting between temperatures 1 and 2.

2) Between temperatures 2 and 3, a sharp increase in the amount of liquid to 2-5%. Major element concentrations are strongly controlled by the major solid phases present and substantial variations in the Fe/Mg/Ni, Ca/Na and Al/Cr ratios are expected within a small temperature interval ($\sim 10^{o}$C). A marked dilution of incompatible trace element abundances takes place so that their absolute concentrations and ratios to major oxides vary rapidly but ratios to each other vary only slightly.

3) This stage between temperatures 3 and 4 is marked by a sharp rise in the volume of liquid to 15%. Very marked dilution, by a factor of 4, of the incompatible trace elements occurs with rising temperature, but only small changes in the ratios between them or in the ratios between the major elements.

4)Gradual increase in the volume of liquid with gradual dilution of incompatible trace elements. Concentrations of MgO, FeO and SiO_2 will increase with dilution of CaO, Al_2O_3 and Na_2O leaving residual harzburgite mineralogy.

5) Continuing increase in the volume of liquid and dilution of incompatible trace elements, leaving residual dunite mineralogy.

degree of partial melting, will be relatively high. These concentrations will be diluted by progressive partial melting at the same pressure, though the enrichment factor may not have an inverse linear relationship to the degree of partial melting. If the effects of possible fractionation can be disregarded, it seems possible, as a first approximation, to relate the trace element abundances to the initial variations in the melt composition, which in turn might reflect the degree of partial melting of the mantle source.

The Mg-rich end members of the solid solution series minerals in the upper mantle would melt at higher temperatures than the Fe-rich end members of the same series. Consequently, those initial partial melts, relatively small in volume percentage and lower in temperature of melting, would be comparatively richer in Fe and poorer in Mg. This would mean that the Fe/Mg ratios of the initial partial melts would be higher than those of progressively later melts, representing higher degrees of melting at higher temperatures. Another expected result of such a progressive partial melting would be the association of high Fe/Mg ratios with high incompatible trace element abundances.

The abundances of Zr, an incompatible element, in the Polusagi rocks show a positive correlation with Fe/Mg ratios (Fig.5.3). If progressive partial melting was responsible for the chemical variations in the Polusagi rock suite, then the acidic members must represent the first upper mantle partial melts, and the intermediate and basic members progressively increasing volumes. Production of andesitic and dacitic compositions by direct partial melting of the upper mantle is considered possible by some workers, under hydrous conditions. However, it is unlikely that compositions as silicious as some of the acidic members of the Polusagi rock suite (e.g.P65, SiO_2 = 69.91%; P223, SiO_2= 73.19%; and P270, SiO_2 = 69.61%; all group A rocks) can be produced in such a way, especially at depths >40 km (Nicholls and Ringwood, 1973). The

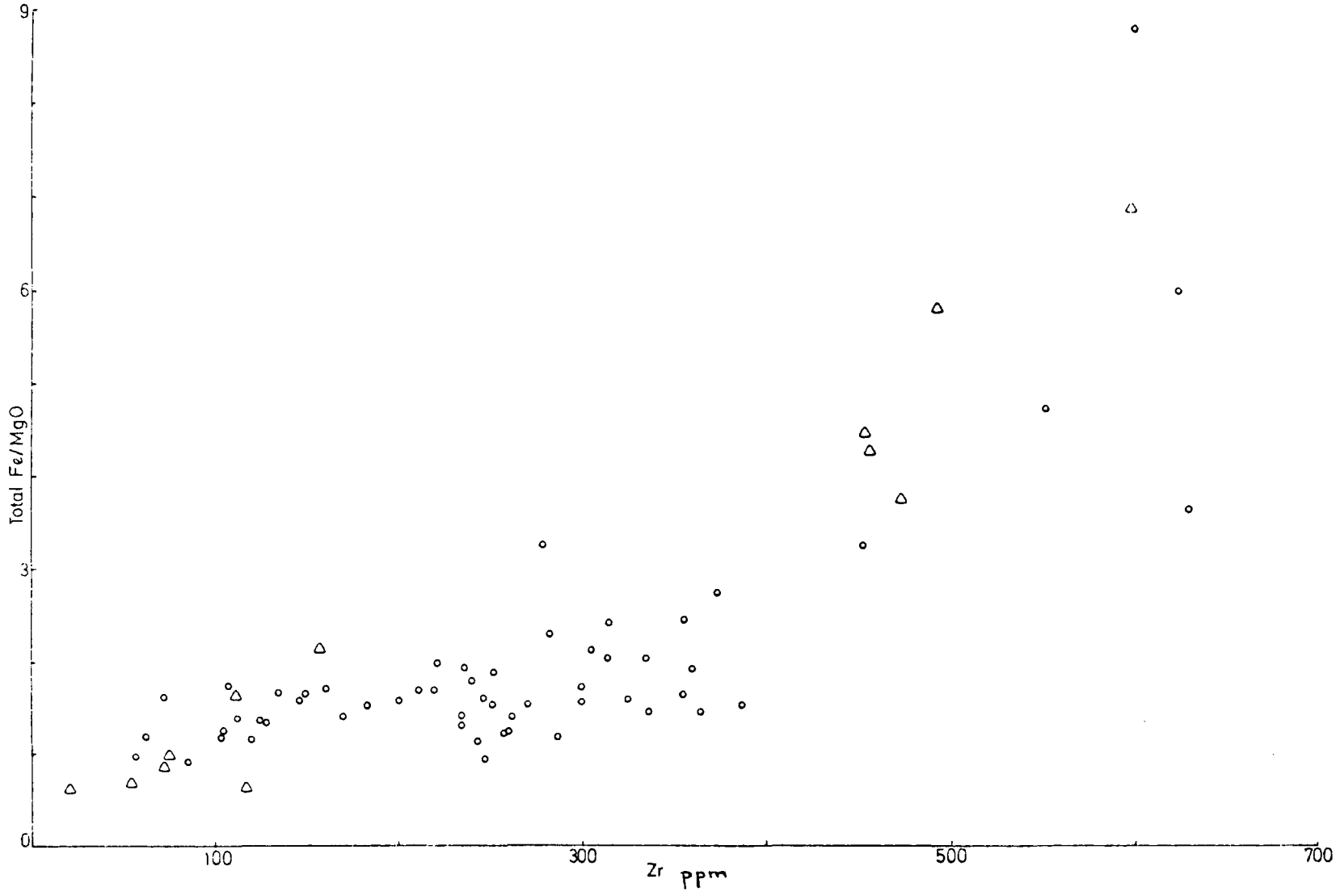


Fig.5.3. Zr vs. total Fe/Mg ratio for the Polusagi rocks. o :Volcanic rocks and △ : hypabyssal rocks.

correlation between Fe/Mg ratios and the incompatible trace elements can be better explained by a process of fractional crystallisation of an upper mantle partial melt with a composition not far from the average composition of the Polusagi MP basalts.

Considerations of the behaviour and abundances of Cr and Ni, which are considered to be immobile in the rocks concerned, and of the incompatible elements Ti and P mitigate against a progressive partial melting model and favour fractional crystallisation. The mineral/liquid partition coefficients of Cr and Ni (Table 5.1) indicate that these elements will be strongly partitioned into mafic minerals such as olivine and pyroxene. Consequently, following the initial stages of progressive partial melting, Cr and Ni concentrations in the partial melts from the upper mantle will be relatively high, and especially Cr should vary very little (Pearce and Norry, 1979). Thus relatively high values of Cr and Ni should be expected, at least in the intermediate and basic members of the Polusagi rock suite. This is not the case, Cr and Ni values are high only in the most basic members, the MP basalts, and rapidly decrease towards basaltic andesite compositions. At acid compositions, Cr and Ni concentrations are very low and on average 11ppm and 0.2 ppm in dacites respectively. The data thus suggest that an initial partial melt of the upper mantle was followed by fractional crystallisation of mafic phases into which Cr and Ni were strongly partitioned. The chemical behaviour of these elements cannot be explained by a progressive partial melting model.

Ti and P generally behave as incompatible elements (Sun and Nesbitt, 1977, 78; Sun et al, 1979) and for initially small degrees of partial melting, these elements should be enriched in the melt. This is not seen in the Polusagi rocks, where the most acidic members which contain some of the highest concentrations of incompatible elements and high Fe/Mg ratios, have some of the lowest T and P concentrations.

It can now be concluded that, although a progressive partial melting

model can account for some of the chemical variations in the Polusagi rock suite, this model cannot account for all the variations. Instead, a model in which a basaltic partial melt of upper mantle origin has evolved through fractional crystallisation producing progressively more siliceous compositions must be proposed. This model is capable of explaining the chemical variations in the Polusagi rock suite and assumes that the most primitive i.e. least modified compositions of the rock suite are represented by the MP basalts and gabbros. These 'least modified' compositions then may provide clues as to the degree of partial melting of the upper mantle.

5.4 Partial melting of upper mantle in Polusagi

5.4.1 Partial melt composition

A commonly used method to decide whether a basaltic liquid would be in equilibrium with the mantle (in this case the mantle olivine) is provided by Roedder and Emslie (1970). They define the partition coefficient, K_D, of Fe^{2+} and Mg between the liquid and the olivine as follows:

$$K_D = \left(\frac{Fe}{Mg}\right)_{olivine} \times \left(\frac{Mg}{Fe}\right)_{liquid} = 0.3$$

Therefore, if Fe^{2+} and Mg contents of the mantle olivine can be estimated, the Fe^{2+} and Mg contents of the partial melt in equilibrium with the olivine can also be estimated by the above equation. Mysen (1975) assumes that the mantle olivine has a Mg-number $\left(\frac{Mg \times 100}{Mg + Fe^{2+}}\right)$ of about 91. Coleman (1977), on the other hand, gives values mainly varying from 93 to 89.5 for olivines from ophiolite peridotites. The liquids which would be in equilibrium with these mantle olivines would thus have Mg-numbers in the range 72 to 80. The MP basalts from Polusagi have Mg-numbers varying from 61 to 72 with an average of 67, while the MP gabbros vary from 68 to 80 and average 75. In these calculations, a fixed Fe^{3+}/Fe^{2+} of 0.3 has been assumed (see section 3.1). Data on K_D, reported by Nicholls and Lorenz (1973) determined at pressures of 2-10 kbars

and under hydrous conditions, suggests an average value of 0.4. This value requires the liquids in equilibrium with the mantle olivine to have Mg-numbers ranging from 77 to 84. Whether the K_D assumes a value of 0.3 or 0.4, it is clear that the compositions of the Polusagi MP basalts and gabbros cannot have been highly modified by fractional crystallisation and can be taken as roughly approximating to the compositions of the mantle partial melts. Sun et al (1979) suggests that olivine-normative basalts from the mid-ocean ridges with Mg-numbers from 59 to 68, lower than those of Polusagi MP rocks, have experienced little fractional crystallisation. Therefore for further discussion, it seems reasonable to treat the compositions of the MP basic rocks of Polusagi, especially those with very high Mg-numbers, as relatively little modified upper mantle partial melt compositions.

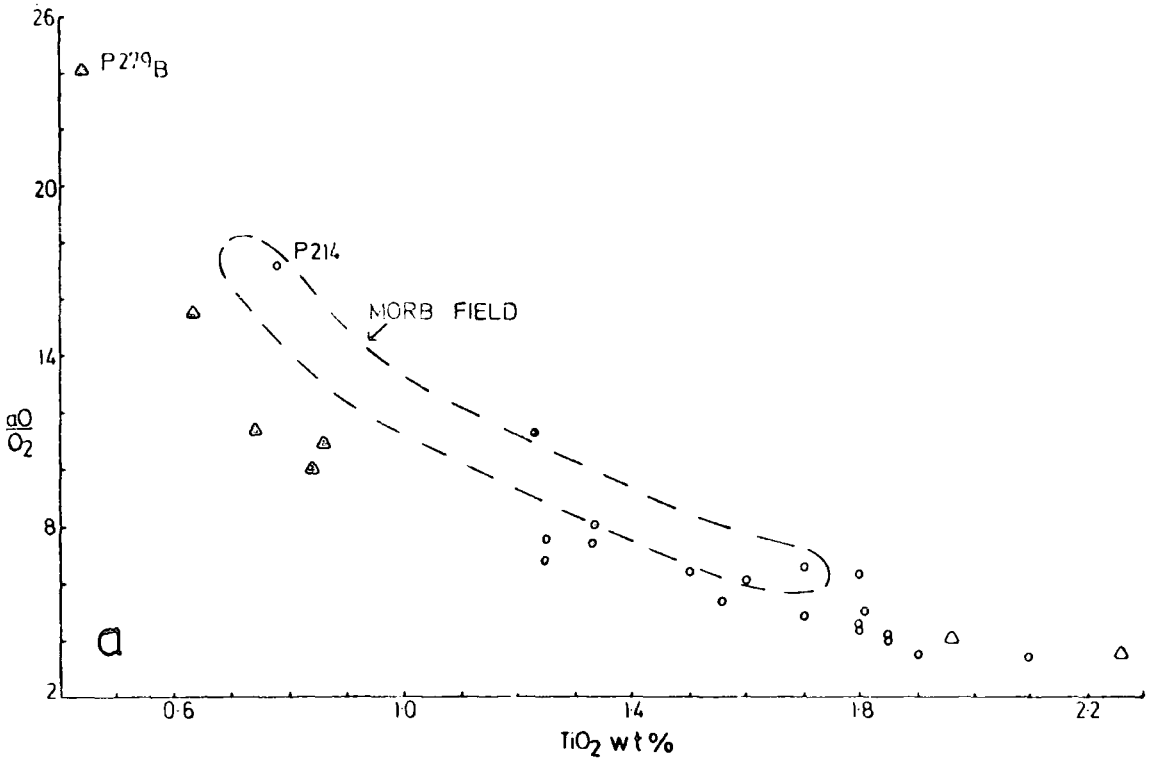
5.4.2 Degree of partial melting

It follows from the arguments raised in section 5.3 that the MP basalts and gabbros cannot have been products of a small degree of partial melting as they contain high MgO and low incompatible trace element concentrations. This can be more closely examined using the CaO, Al_2O_3 and TiO_2 contents as suggested by Sun and Nesbitt (1977) and Sun et al (1979). If the assumption that samples with high Ni and Cr concentrations and high Mg-numbers approximate to the primary liquids is correct, then the incompatible elements such as Ti and P offer a means of estimating the degree of partial melting necessary to produce these liquids. These authors suggest that as the degree of melting increases, TiO_2 should decrease, and the ratios, CaO/TiO_2 and Al_2O_3/TiO_2 should increase up to limiting values of 17 and 20 respectively, these being very close to chondritic values. Thus, at low degrees of partial melting of mantle ($\leqslant$15%), practically all the Ti, but only a proportion of the Ca and Al, would go into the melt, the rest of the Ca and Al being held in the residual phases such as pyroxene, garnet, plagioclase and spinel. As the proportion of melt increases, Ti concentrations would be diluted while Ca

and Al retaining phases would become progressively exhausted. Consequently, the CaO/TiO_2 and Al_2O_3/TiO_2 ratios would increase in the melt and continue increasing until all the Ca and Al is incorporated at high degrees of melting ($\sim$ 25%). At this stage, they argue, CaO/TiO_2 and Al_2O_3/TiO_2 ratios could not increase anymore, having reached limiting values of 17 and 20 respectively. Further increases in the amount of melting would dilute the concentrations of CaO, Al_2O_3 and TiO_2, but the above ratios would remain unchanged.

According to the above reasoning, primary MORB, having low TiO_2 ($\sim$ 0.7%), high Al_2O_3 ($\sim$ 16%) and CaO ($\sim$ 12%), and high Al_2O_3/TiO_2 ($\sim$ 20) and CaO/TiO_2 ($\sim$17) ratios is generated by a large degree of partial melting ($\sim$ 25%) of an upper mantle source. On the other hand basalts with high TiO_2 ($\sim$1.5%), and low Al_2O_3/TiO_2 ($\sim$ 10) and CaO/TiO_2 ($\sim$7) ratios are generated by small degrees of partial melting ($\lesssim$15%) of a similar source.

The Polusagi MP basalts and gabbros, all belonging to the least altered group of rocks i.e. group A (section 3.3.2), are plotted in Sun and Nesbitt - type diagrams in Figs. 5.4a and 5.4b. The MD basalts and gabbros are included in the diagrams for comparison. The MP basalts plot into or around the MORB field but the MP gabbros generally plot outside, and some of them have CaO/TiO_2 and Al_2O_3/TiO_2 ratios well above the chondritic limiting values, 17 and 20 respectively. They may merit separate interpretation. However, before doing this, it must be noted that these diagrams were originally designed to show the effects of different degrees of partial melting on the MORB compositions; and it is already pointed out (section 5.3) that the Polusagi rock types are related to one another by fractional crystallisation (section 5.5). Thus the trends shown by the basic Polusagi rocks in Figs. 5.4a and 5.4b , which agree fairly well with the MORB trends, should not be taken as due to varying degrees of partial melting, but due to varying degrees of fractional crystallisation (see section 5.5.2). Although the MP basalts and gabbros are relatively



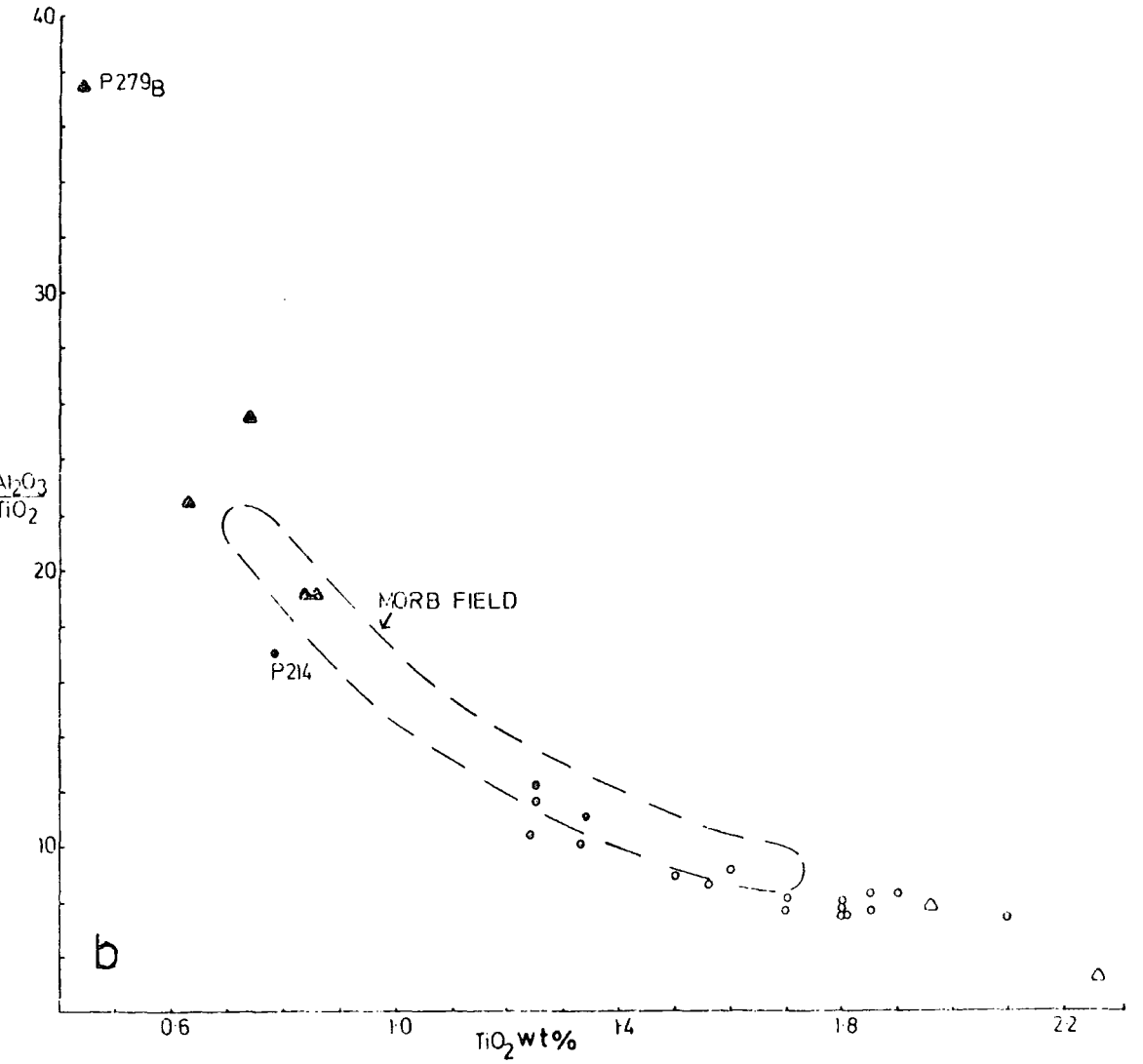


Fig.5.4a and b. a) CaO/TiO_2 vs. TiO_2 and b) Al_2O_3/TiO_2 vs. TiO_2. MORB field after Sun and Nesbitt (1979).

● :"MP" basalts, ○ : "MD" basalts,

▲ :"MP" gabbros and △ : "MD" gabbros.

little affected by fractional crystallisation processes as a group, their least modified members will, therefore, be taken to estimate the degree of partial melting of the upper mantle.

Amongst the MP basalt sample P214 shows the highest Mg-number, 72, and CaO/TiO_2 and Al_2O_3/TiO_2 ratios, about 17 in each case. These are coupled with the lowest Zr (56 ppm), Nb (3ppm), Y (21 ppm), TiO_2 (0.84%) and P_2O_5 (0.09%) abundances and the highest Ni (213 ppm) and Cr (454 ppm) concentrations found in all the group A basalts. This sample thus seems to be the least modified and represent a mantle partial melt with a high degree of melting, probably around 25%.

The MP gabbro sample, P279B, seems to be the least modified gabbro sample, containing the lowest Zr (19ppm), Nb (3ppm), Y (16 ppm), La (1ppm), Ce (14 ppm), TiO_2 (0.46%), P_2O_5 (0.11%) and total iron (Fe_2O_3 = 8.12%) concentrations and the highest Mg-number (80), the last being the highest in the Polusagi rock suite. The CaO/TiO_2 and Al_2O_3/TiO_2 ratios of this sample are very high, 24 and 37 respectively. When compared with P214, these chemical features suggest a higher degree of partial melting but this is not thought to be the case. Sun and Nesbitt (1978) point out that such high CaO/TiO_2 and Al_2O_3/TiO_2 ratios cannot be generated by variable degrees of partial melting of mantle, as they are well above chondritic values. When compared with P214, P279B does not have particularly higher Al_2O_3 and CaO contents, but its TiO_2 content is considerably lower. It is unlikely that the low TiO_2 content is due to Ti being held in phases such as ilmenite during partial melting. An alternative and more plausible explanation would be that the MP gabbros represent a later episode of partial melting of the same upper mantle source rock as that of MP basalts. If this is so, then after the removal of the first partial melt that generated the Polusagi volcanic rocks, the second phase of partial melt would be depleted in incompatible elements, but relatively enriched in compatible elements. The degree of depletion or enrichment would depend

on the efficiency with which previous partial melts (high degree) are removed. Such an explanation is not only supported when the least modified members of the MP basalts (P214) and of the MP gabbros (P279B) are compared, but also by the lower average incompatible element concentrations of the MP gabbros as a whole (see table 4.3). A process of remelting of mantle, after the extraction of a first partial melt, would give rise to a new magma with different element concentrations, but unaffected incompatible element ratios (Sun and Nesbitt, 1978), a feature which is shown by the Polusagi rock suite. The incompatible trace element ratios in the Polusagi rocks are quite constant; illustrated, for example, by linear trend in the Y, Nb, La and Ce vs. Zr variation diagrams, Fig . 5.5. A two stage partial melting of the mantle, with a first partial melt generating the volcanic rocks, and a second the hypabyssal rocks, is not only supported by the chemical continuity of both types of rocks but also by field relations. It was mentioned in Chapter two that the gabbro, as well as the plagiogranite bodies, intrude the volcanic rocks i.e. were emplaced later. When it is considered that the MP gabbros are more basic (i.e. lower incompatible element contents and higher Mg-numbers) than the MP basalts and the rest of the volcanics, it is difficult to envisage a process where a single partial melt would produce more basic compositions by fractional crystallisation.

A similar two stage melting of the source rock has been proposed by Sun and Nesbitt (1978) to account for the low - Ti ($<0.4\%$) basalts from ophiolites, e.g. from the Troodos and Betts Cove ophiolites, and from island arcs and inter-arc basins which may have Al_2O_3/TiO_2 and CaO/TiO_2 ratios up to 60.

5.5 Fractional crystallisation of the Polusagi magma

5.5.1 Introduction.

The Polusagi rock suite exhibits a tholeiitic differentiation trend with low to moderate iron and titanium-enrichments (section4.2.3).

According to Ringwood (1974,77), iron-enrichment in the early stages of evolution of tholeiitic magmas is caused by separation of olivine and pyroxene, having much lower Fe/Mg ratios than the liquids from which they crystallise. An alternative mechanism is advocated by Osborn (1959,62,69) to explain the differences between tholeiitic and calc-alkaline fractionation trends. This mechanism is based on differences in oxygen fugacity during crystallisation of the magmas. Osborn argues that if the system is open to oxygen, i.e. Po_2 is kept constant and high during crystallisation, magnetite crystallises early, followed by silicates such as olivine and pyroxene. The early precipitation of magnetite results in the accumulation of silica in the residual liquid, thus causing a calc-alkaline fractionation trend. But if the Po_2 is low, then silicates like olivine and pyroxene separate before magnetite, resulting in iron-enrichment and a relatively lower rate of silica enrichment i.e. a tholeiitic trend. The high oxygen fugacity required in Osborn's model for the early precipitation of magnetite which would lead to siliceous residual melts (dacitic and/or andesitic), may be caused by dissociation of water produced by the dehydration of descending oceanic crust. This could be accompanied by excess oxygen liberated from weathered rocks brought down from the ocean floor (Miyashiro, 1974).

Under conditions of low oxygen fugacity, magnetite would not be an early precipitating phase and some other mechanism for silica enrichment must be operative during fractional crystallisation. Ringwood (1974,77) states that tholeiitic partial melts of upper mantle, under water saturated conditions at depths 70-100 km , would be depressed below the 1 atm. liquidus. As such melts rise, and load pressure and water pressure drop, olivine precipitates. This produces basaltic andesites or even andesites upon ascent to within 30 km of the surface. However, olivine precipitation would not be capable of driving the residual liquids beyond a composition having 58% SiO_2. Beyond this, olivine would be in reaction relationship

with the liquids; and would be replaced by amphibole at intermediate pressures or by pyroxene at lower pressures. Fractionation of these phases would be able to produce residual liquids as siliceous as rhyodacites. At very low pressures, plagioclase separation could produce rhyolitic compositions. Ringwood (1974,77) suggests that the rocks, thus produced, would show the trace element characteristics of island arc tholeiitic rock series. Boettcher (1973), similarly, states that in the pressure range 12-20 kbars (40-65 km), amphiboles with low SiO_2 contents (<44%) exist at, or close to, the temperatures of water saturated basaltic liquids. Fractionation of these sub-siliceous amphiboles could be a very effective mechanism for the silica enrichment in the residual liquids.

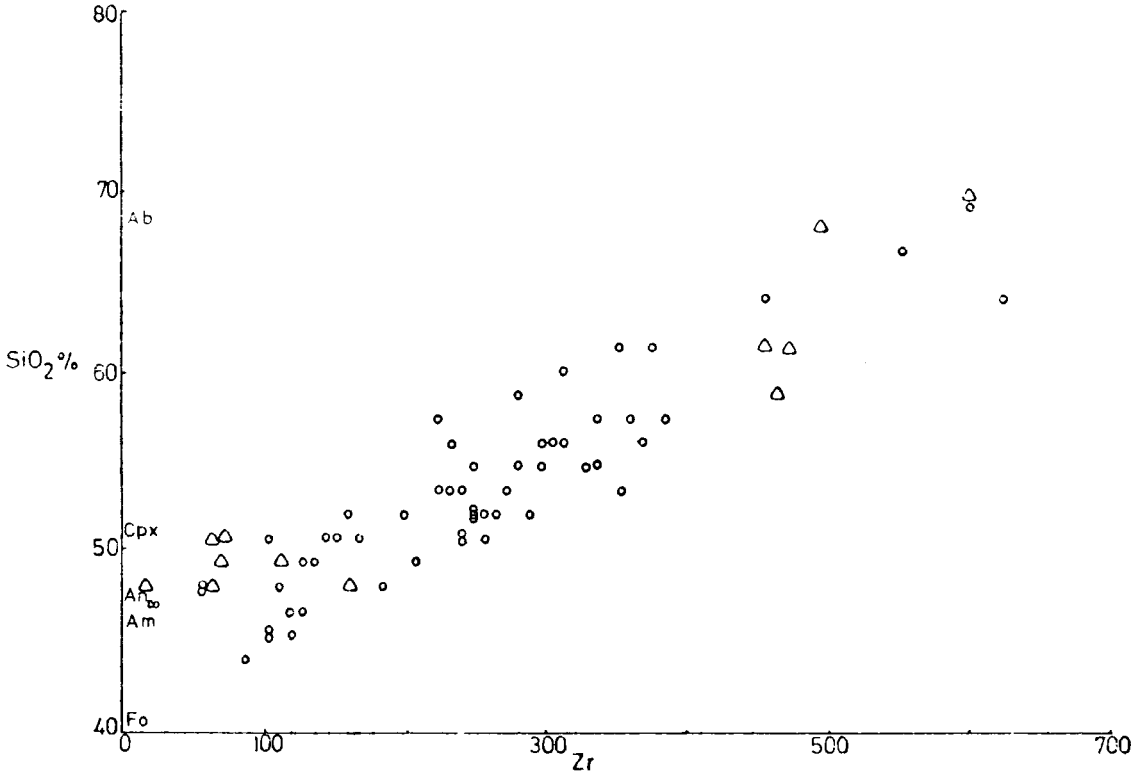
Church and Riccio (1977) report that those ultramafic sequences in ophiolite complexes associated with low-Ti (<0.6% TiO_2) basalts have olivine-orthopyroxene cumulate sequences, while the high-Ti basalts are associated with olivine-clinopyroxene (or plagioclase) cumulates. The Polusagi basaltic rocks are high-Ti types and can thus be expected to be associated with olivine-clinopyroxene-plagioclase cumulates.

The most likely phases to have fractionated during differentiation of the Polusagi magmas, therefore, are olivine, clinopyroxene, plagioclase, amphibole and magnetite. The predominantly aphyric nature of the volcanics, and subsequent metamorphism and alteration, do not facilitate direct petrographic observation of fractionation phases as phenocrysts in the rocks, although there are few microphenocrysts of clinopyroxene and plagioclase (Chapter six). Many studies of the fractionation phases of tholeiitic island arc volcanic series have shown that the predominant phases crystallising are olivine, clinopyroxene and plagioclase (e.g. Pearce and Norry, 1979) with amphibole and/or magnetite (Brown et al, 1977).

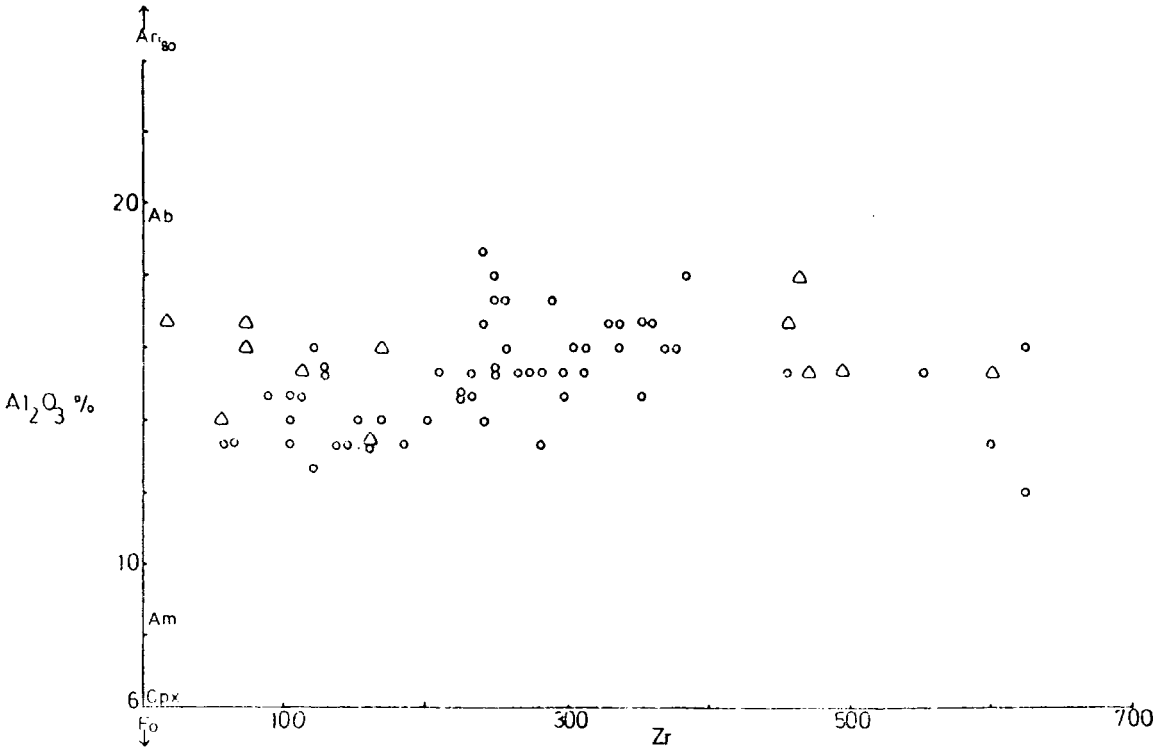
Chemical variations in major and trace element concentrations in the Polusagi rock suite are shown in Fig. 5.5. The concentration of Zr has

Fig.5.5 Element variation trends with increasing Zr concentrations in the Polusagi rock suite. o : volcanic rocks and △ : Hypabyssal rocks. Fo = Olivine (Fo_{90}), Cpx = Clinopyroxene, Am = amphibole, Ab = albite, An_{80} = plagioclase, Mag = Ti-rich magnetite and Ap = apatite.

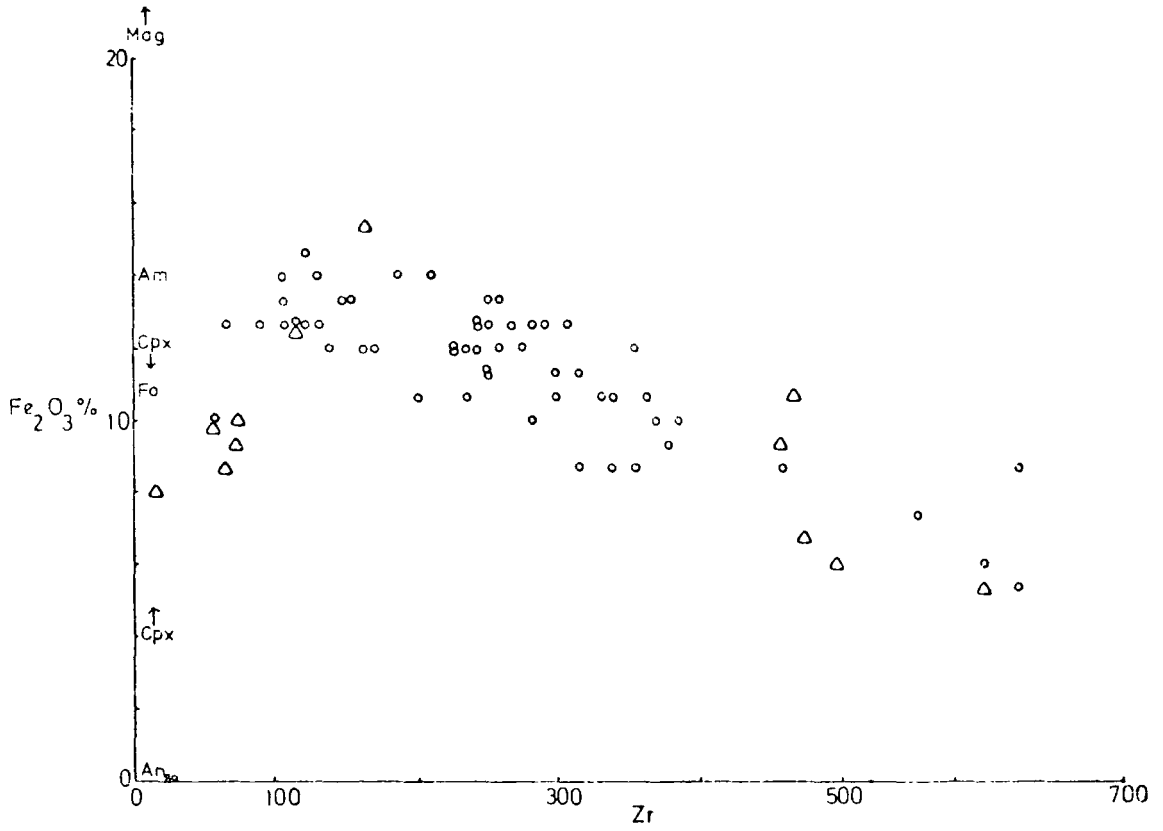
1 - SiO_2 wt% vs. Zr ppm
2 - Al_2O_3 wt% vs. Zr ppm
3 - $Fe_2O_3^{total}$ wt% vs. Zr ppm
4 - MgO wt% vs. Zr ppm
5 - CaO wt% vs. Zr ppm
6 - Na_2O wt% vs. Zr ppm
7 - K_2O wt% vs. Zr ppm
8 - MnO wt% vs. Zr ppm
9 - S wt% vs. Zr ppm
10 - TiO_2 wt% vs. Zr ppm
11 - P_2O_5 wt% vs. Zr ppm
12 - Nb ppm vs. Zr ppm
13 - Y ppm vs. Zr ppm
14 - La ppm vs. Zr ppm
15 - Ce ppm vs. Zr ppm
16 - Sr ppm vs. Zr ppm
17 - Rb ppm vs. Zr ppm
18 - Ba ppm vs. Zr ppm
19 - Zn ppm vs. Zr ppm
20 - Cu ppm vs. Zr ppm
21 - Ni ppm vs. Zr ppm
22 - Cr ppm vs. Zr ppm


80
70
60
50
40
SiO_2 %
Ab
Cpx
Ab
Am
Fo
0
100
300
500
700
Zr

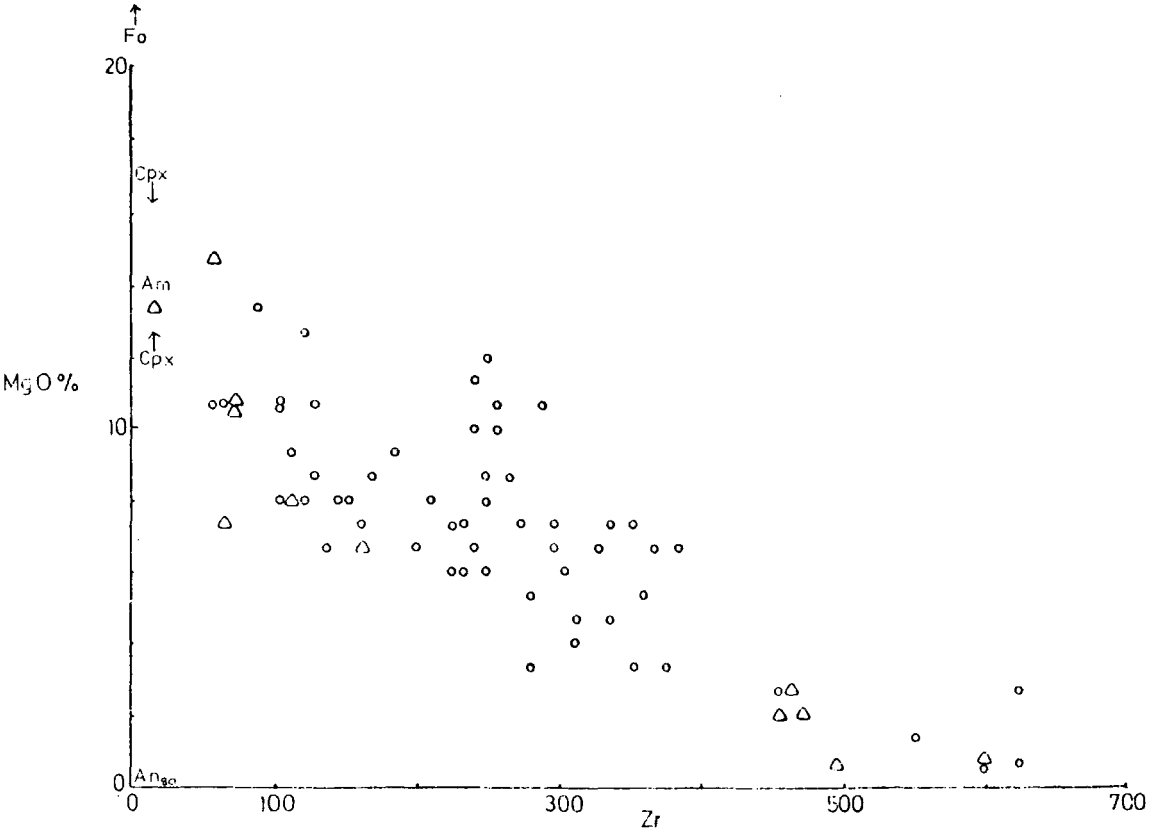
1


Ab
20
10
6
Al_2O_3 %
Ab
Am
Cpx
Fo
100
300
500
700
Zr

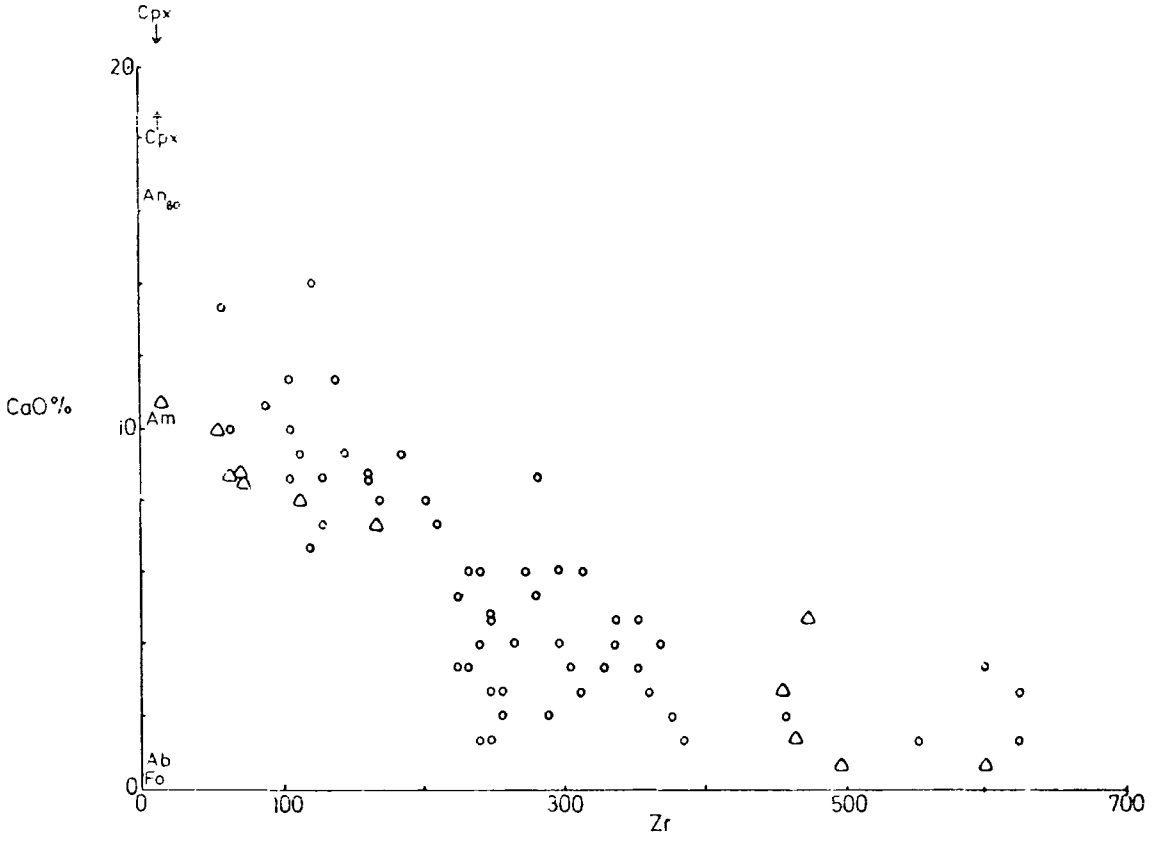
2


Mag
20
Am
Cpx
Fo
Fe_2O_3 %
10
Cpx
0
An_{30}
0
100
300
500
700
Zr

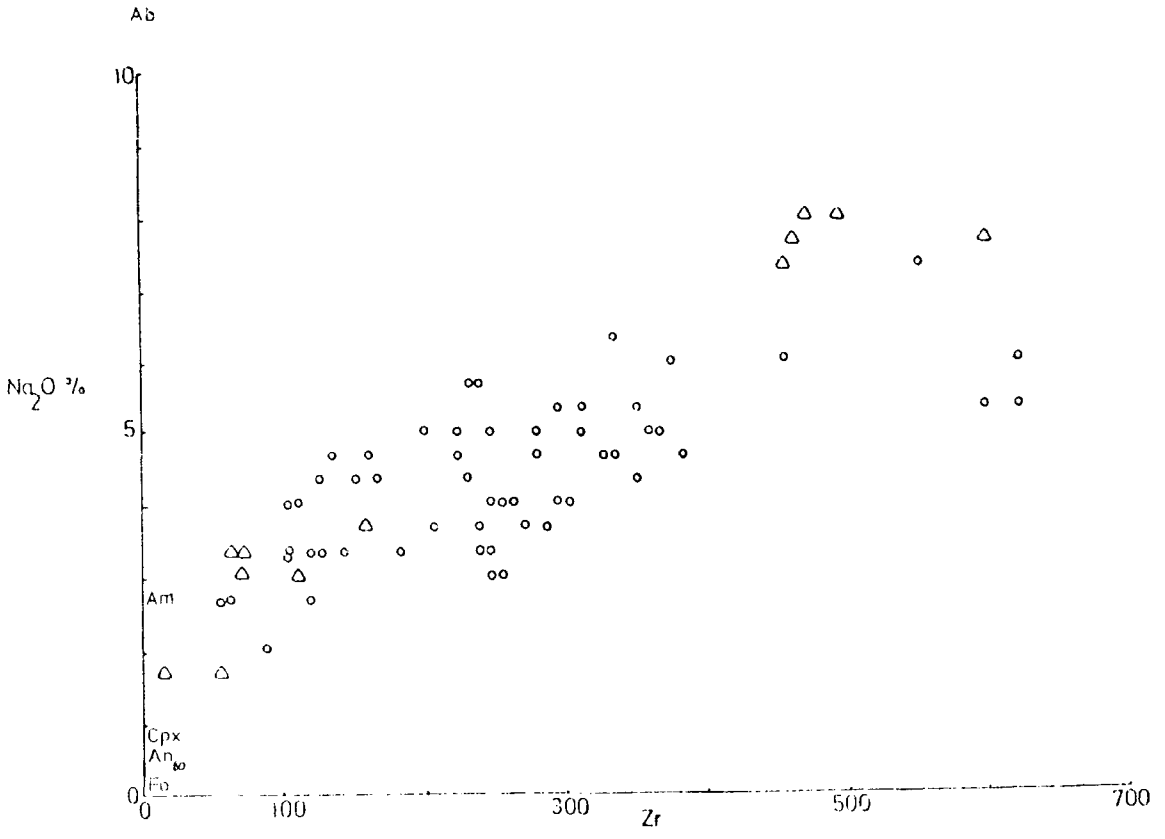
3


Fo
20
Cpx
Am
Cpx
MgO %
10
0
An_{30}
0
100
300
500
700
Zr

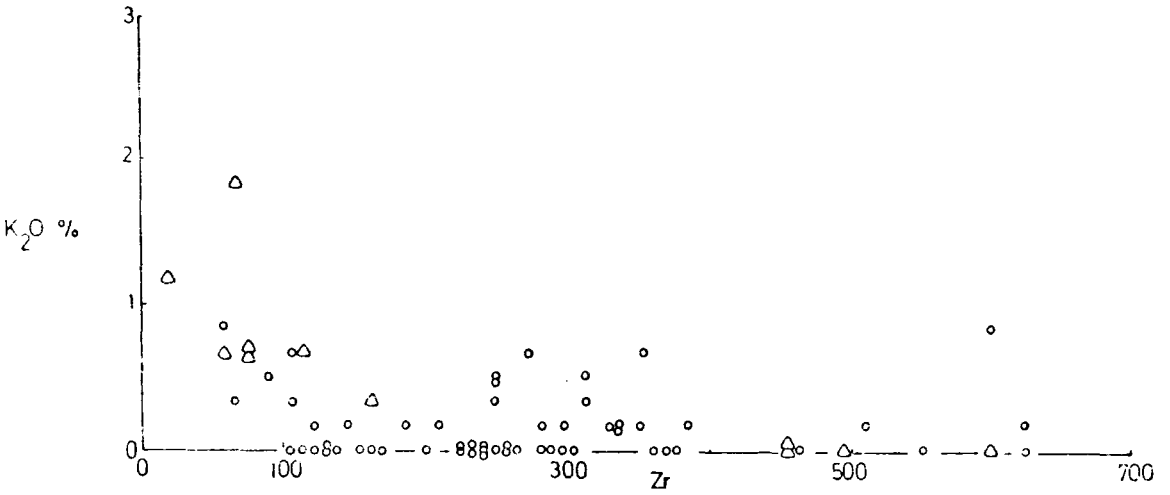
4


Cpx
20
Cpx
An80
CaO%
10
Am
Ab
Fo
0
0
100
300
500
700
Zr

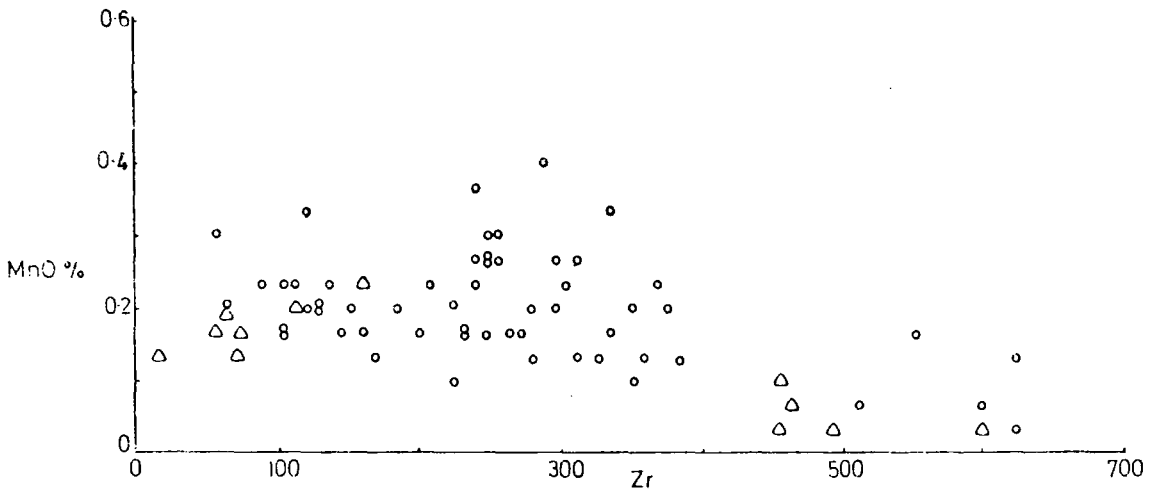
5


Ab
10
Na2O %
5
Am
Cpx
An80
Fo
0
0
100
300
500
700
Zr

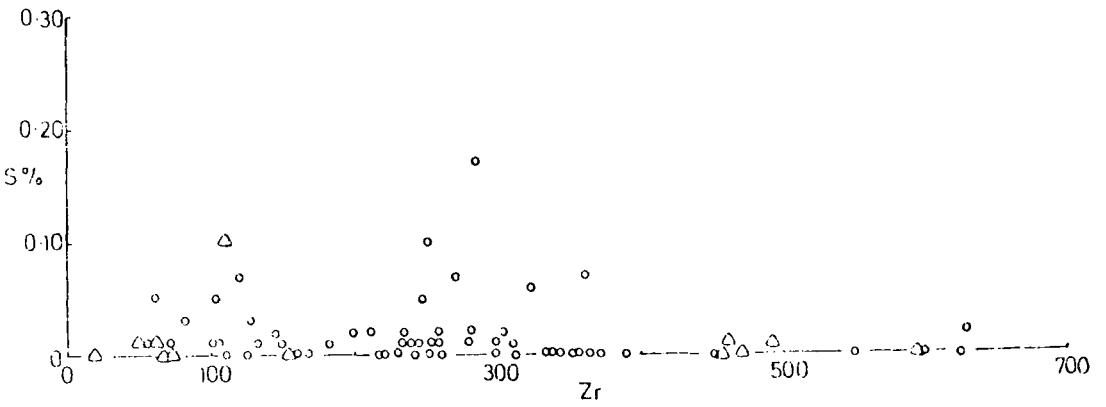
6


3
2
1
0
K_2O %
0
100
300
500
700
Zr

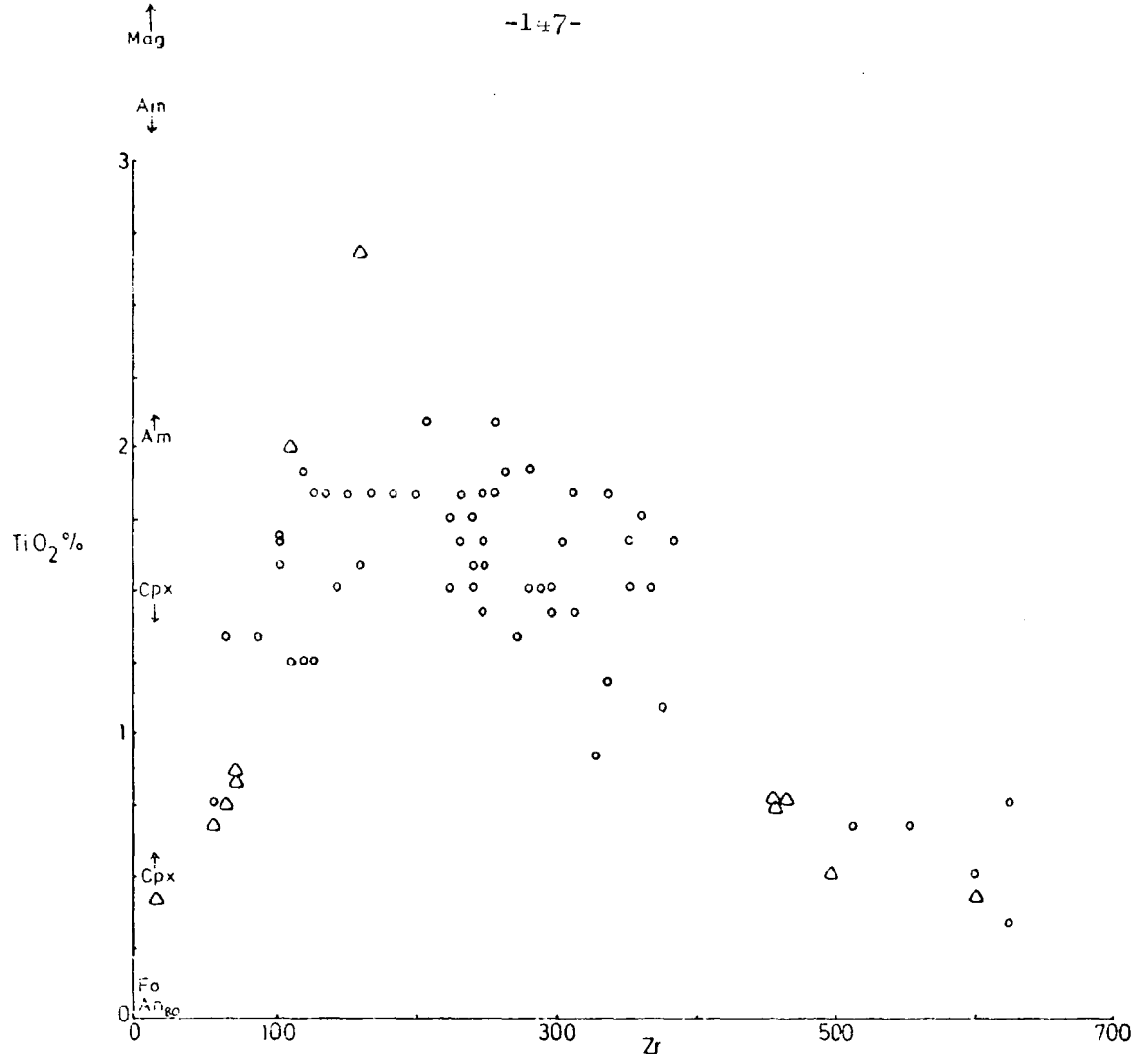
7


0·6
0·4
0·2
0
MnO %
0
100
300
500
700
Zr

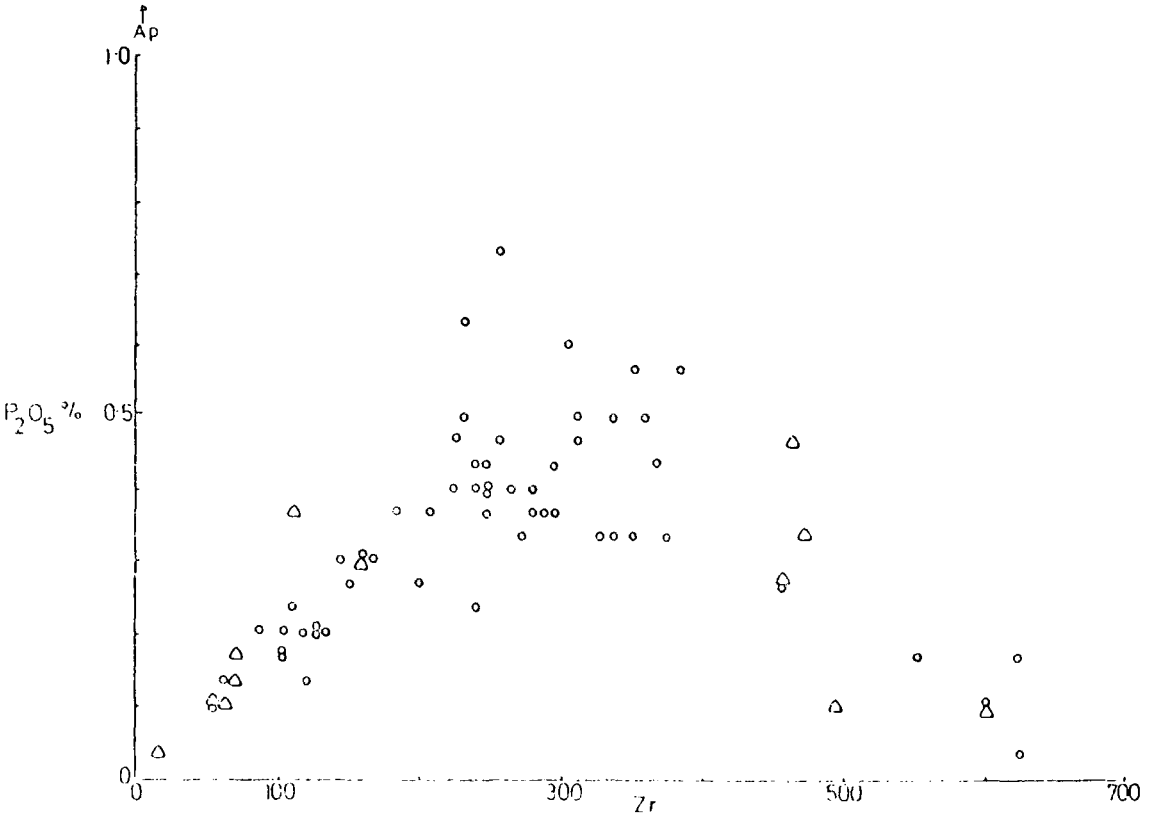
8


0·30
0·20
0·10
0
S %
0
100
300
500
700
Zr

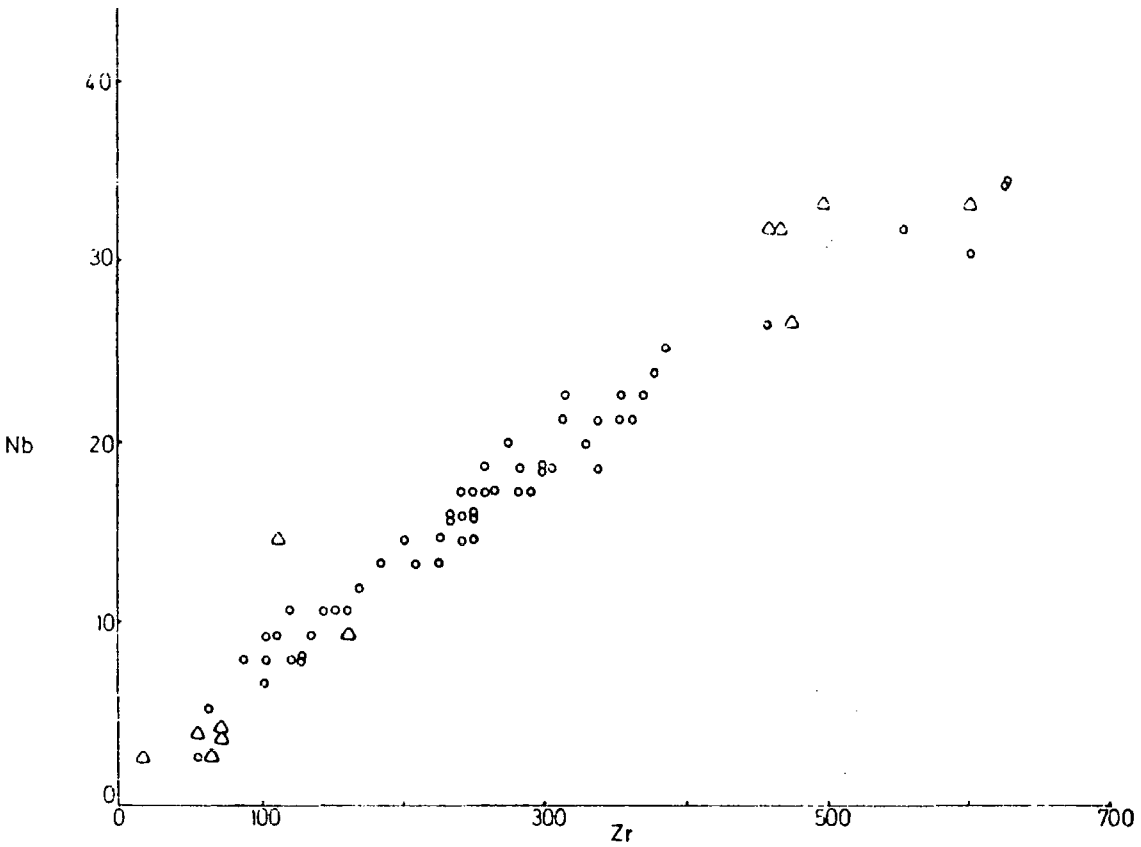
9


Mag
Ain
Am
Cpx
Cpx
Fo
An80
TiO2 %
3
2
1
0
0
100
300
500
700
Zr

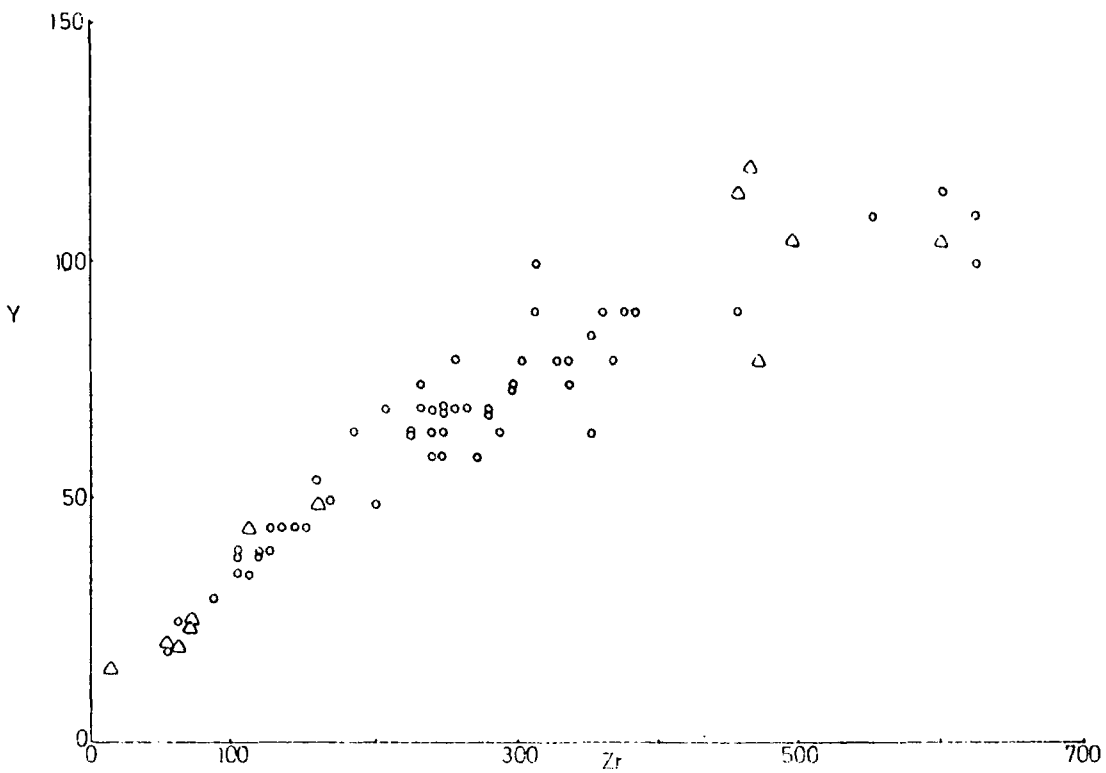
10


Ap
1·0
0·5
0
P2O5 %
0
100
300
500
700
Zr

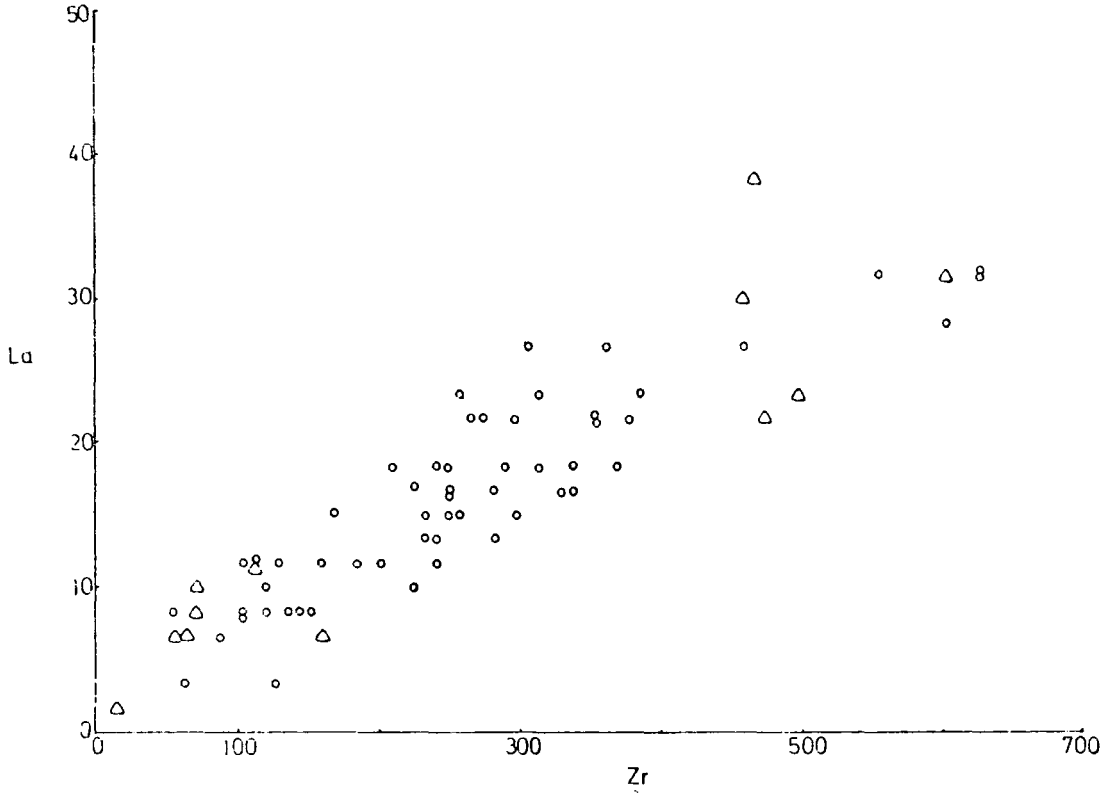
11


40
30
20
10
0
Nb
0
100
300
500
700
Zr

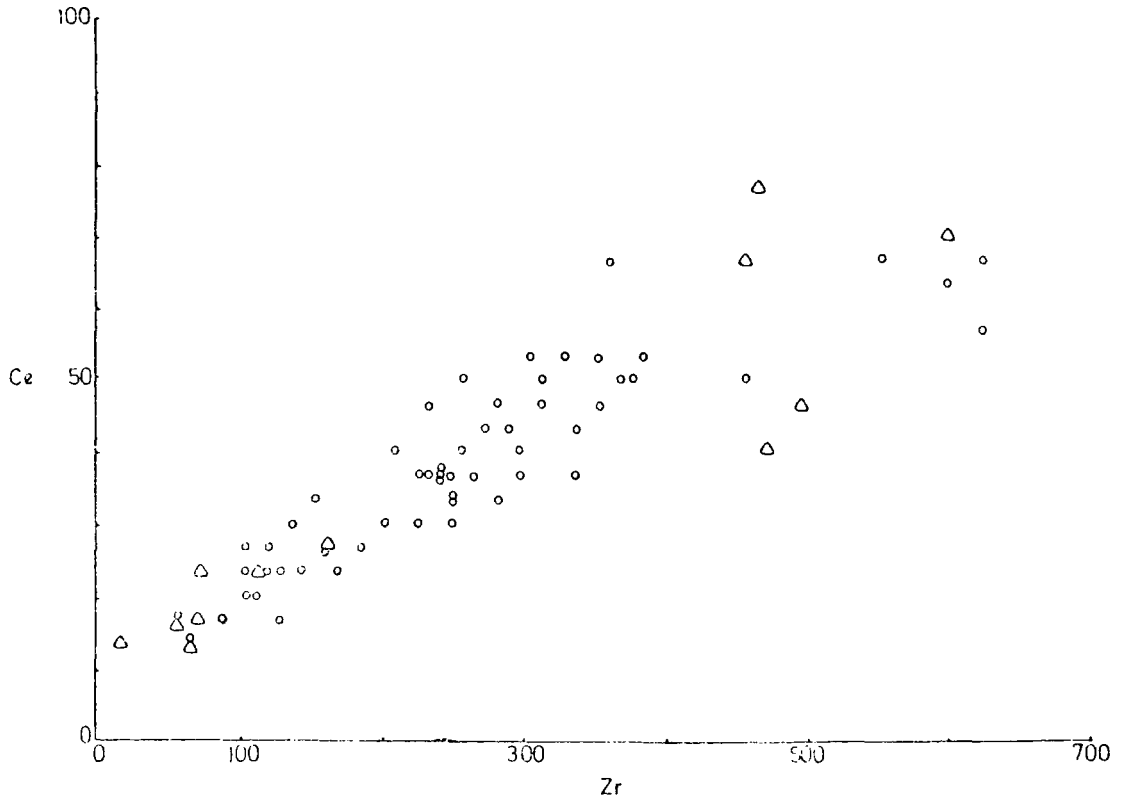
12


150
100
50
0
Y
0
100
300
Zr
500
700

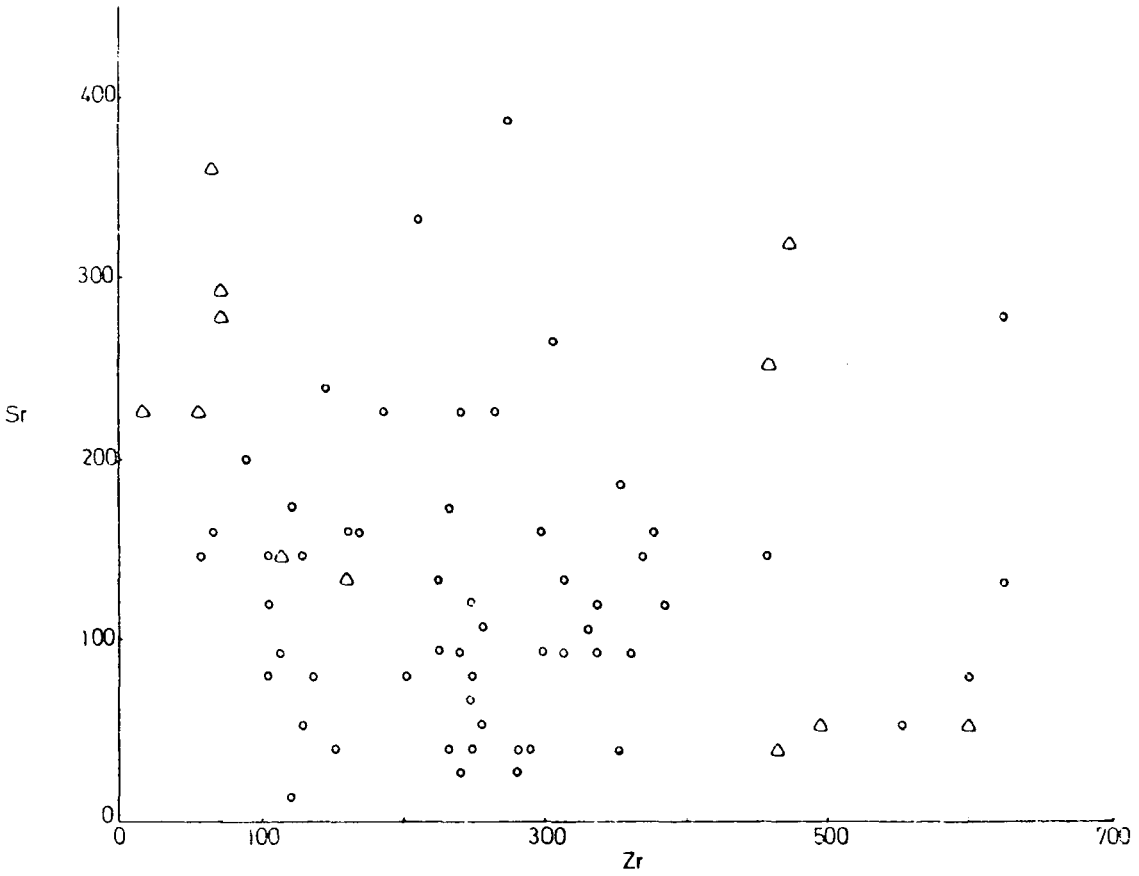
13


La
50
40
30
20
10
0
0
100
300
500
700
Zr

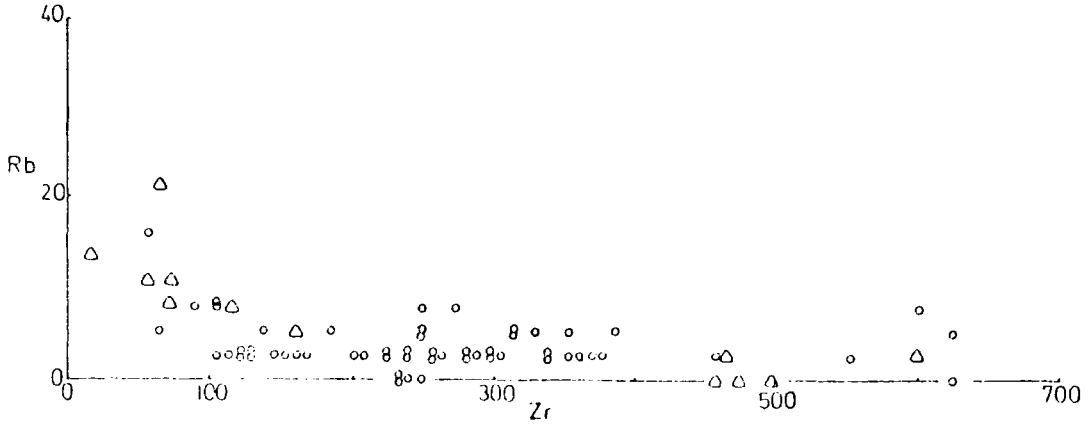
14


Ce
100
50
0
0
100
300
500
700
Zr

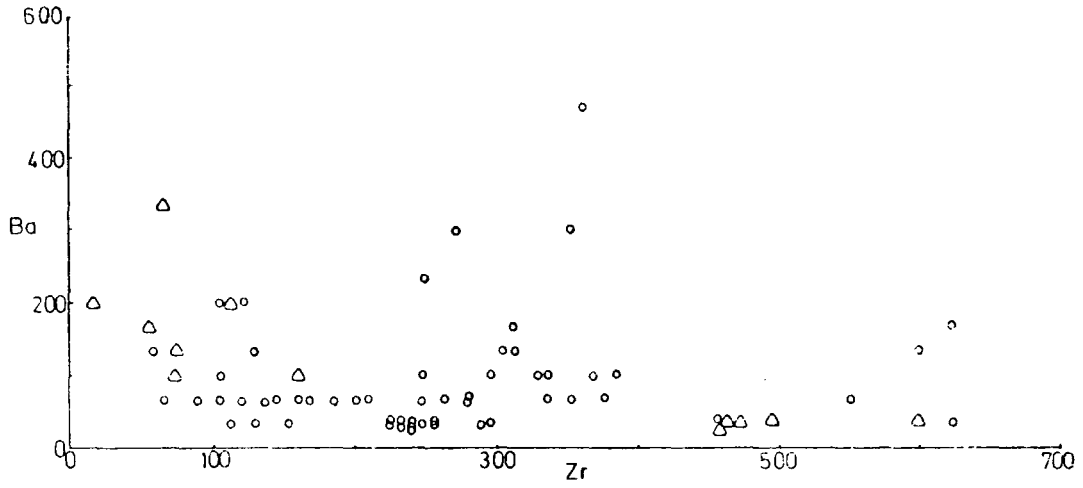
15


Sr
400
300
200
100
0
0
100
300
500
700
Zr

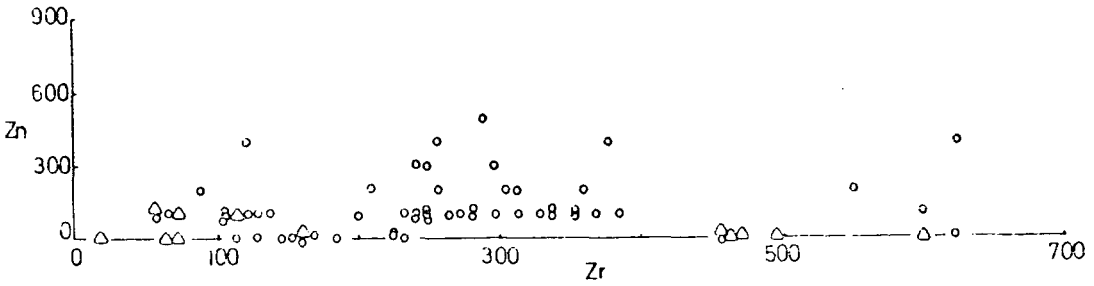
16


Rb
40
20
0
0
100
300
500
700
Zr

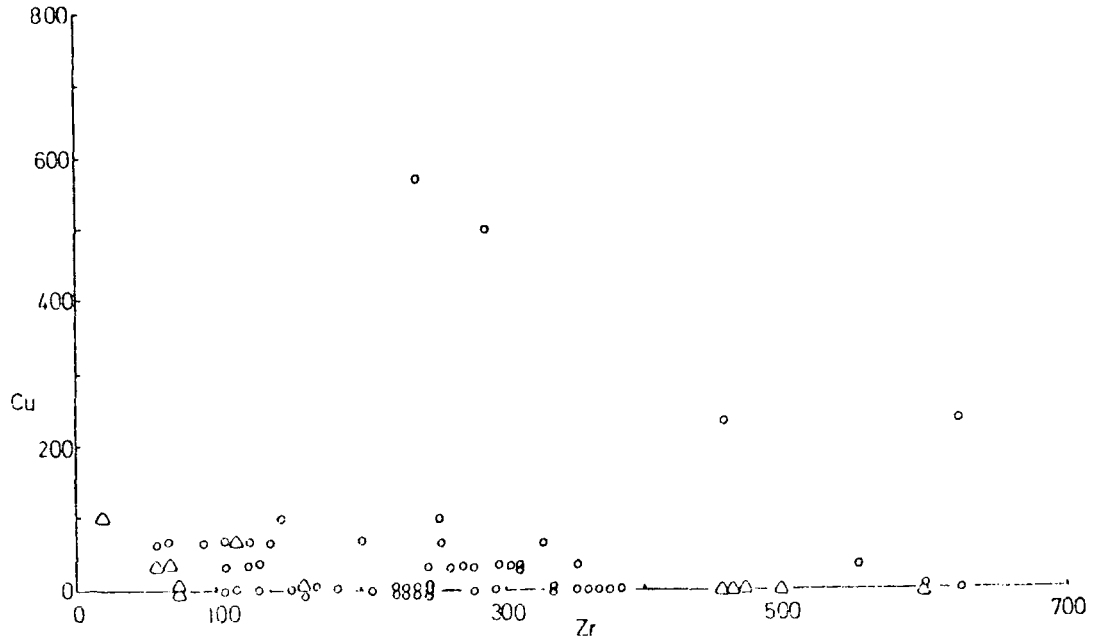
17


600
400
Ba
200
0
0
100
300
Zr
500
700

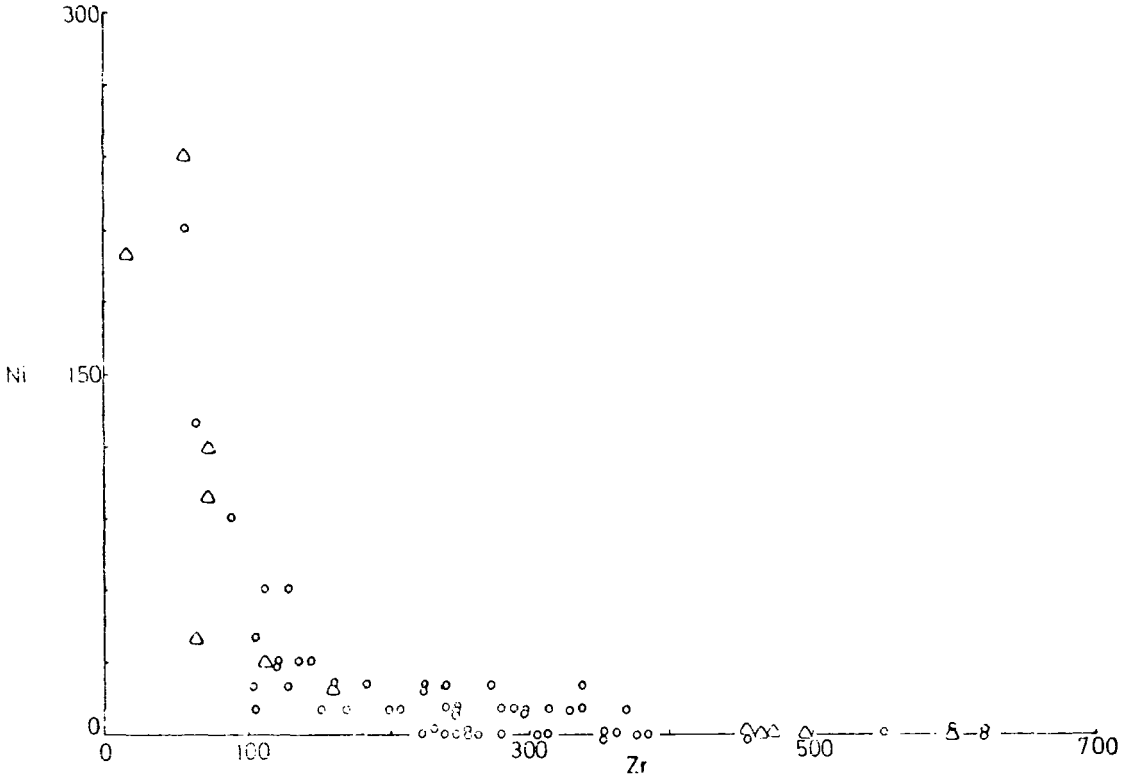
18


900
600
Zn
300
0
0
100
300
Zr
500
700

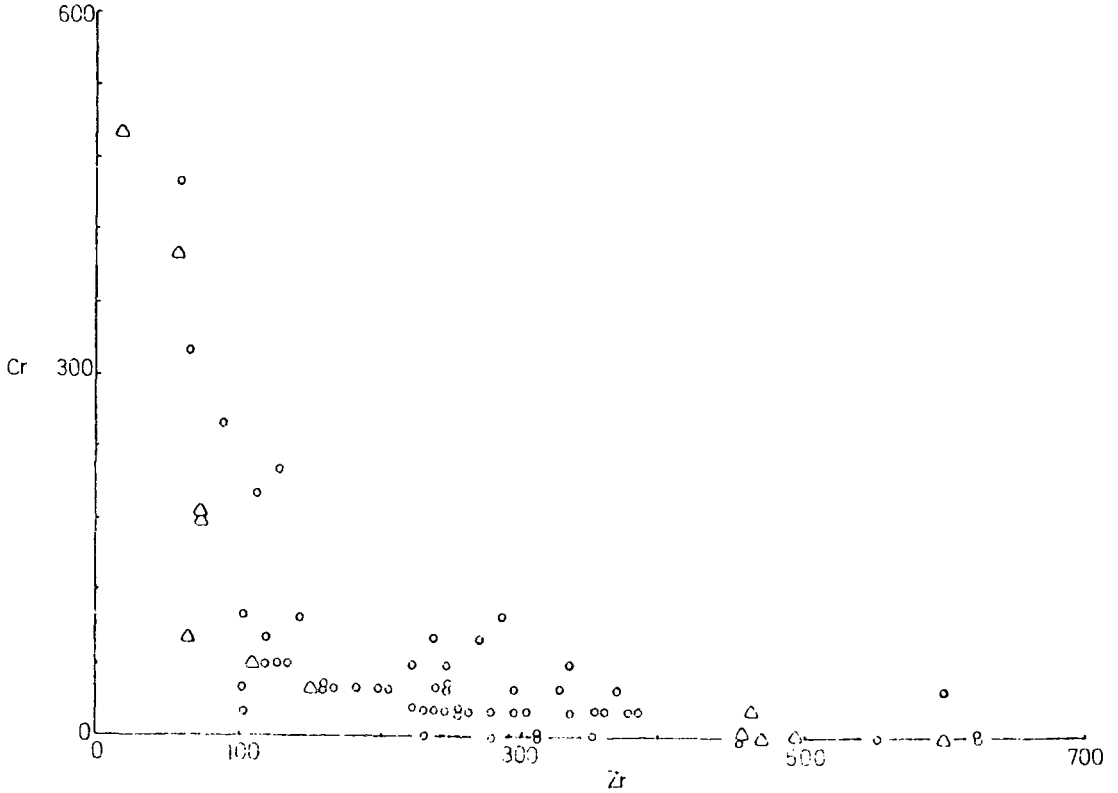
19


800
600
400
Cu
200
0
0
100
300
Zr
500
700

20



21



22

been used as a differentiation index (see section 3.3.1). Apart from the mobile elements, S, Sr and Ba and to a lesser extent Rb and K_2O, all elements exhibit clear variation trends with increasing Zr. The scatter of data points is especially tight with the immobile elements Ti, P, Y, Nb, La, Ce, Cr and Ni. The major element variation diagrams also include the positions of possible fractionating phases. This allows a test of their influence on the observed chemical trends by means of graphical methods described by Cox et al (1979, Chapter six). They state that the liquid fractionation path must project into the "extract polygon" defined by the fractionating phases (or a line in the case of 2 separating phases). For clinopyroxene and amphibole, average compositions of the Polusagi augites and brown hornblendes(Chapter six)have been used respectively. However, because the Polusagi rocks contain no olivine or unaltered plagioclase, the composition of olivine is assumed to be Fo_{90} and of plagioclase An_{80}. Plagioclase compositions averaging An_{77} are reported from the tholeiitic basalts of Eua in the Tongan Islands (Ewart and Bryan,1972). In South Sandwich Islands, tholeiitic basalts contain plagioclases with bytownite cores and labradorite margins (Baker, 1978) and tholeiitic basalts from St.Kitts in the Lesser Antilles have calcic plagioclase (bytownite) (Hawkesworth and Powell, 1980).

5.5.2 Chemical variations in major oxides

As seen in Fig.5.5 , SiO_2 varies from about 44% to 73% and shows a smooth increase from basic to acid rock types. Al_2O_3 contents do not exhibit a wide range, but a weak trend of rise with increasing Zr is suggested in the basic range reaching a plateau in the intermediate range and subsequently decreasing in the acid rocks. The shape of the trend would be in line with fractionation of relatively Al-poor phases such as olivine and clinopyroxene from the basaltic melts. The intermediate compositions seem to be influenced by plagioclase whose dominant role during fractionation at acid compositions may have given rise to an inevitable decrease of

the Al_2O_3 contents.

Total iron and TiO_2 increase continuously up to 200 ppm Zr (~52% SiO_2), thereafter decreasing smoothly through the intermediate and acid compositions, as typically seen in the fractionation of tholeiitic rock series (Pearce and Norry, 1979). Dominant fractionation in the basaltic melt must have involved a phase poor in iron and Ti, probably forsteritic olivine. Plagioclase is unlikely to be a dominant phase at this stage as this would not explain the Al_2O_3 trend. Subsequently, precipitation of a major phase (or phases) rich in both Fe and Ti, for example Ti-rich magnetite, must have controlled their variations in the residual liquid.

Fractionation of Ti-rich magnetite from residual liquids of intermediate and acid compositions is supported by the fractionation trend of MnO, as MnO concentrations show a continuous decrease towards and into the most siliceous compositions. Mn^{2+} is chiefly camouflaged by Fe^{2+} (Ringwood, 1955), thus, Ti-rich magnetite should concentrate Mn^{2+} more than the residual liquid, resulting in the evidently similar iron, Ti and Mn fractionation trends.

Both MgO and CaO contents decrease continuously with fractionation from basic to acid compositions. In the early basaltic stages of fractionation, decrease in the MgO content of the residual liquid can be attributed mainly to olivine which may later be joined by clinopyroxene and amphibole. The decrease in the CaO content cannot be interpreted as mainly due to calcic plagioclase, since the major oxide trends examined so far exclude plagioclase as a major or dominant phase separating from the basaltic liquid. Therefore, CaO depletion must be due to clinopyroxene and possibly to amphibole precipitating alongside olivine. At intermediate and acid compositions, however, plagioclase may well be a major crystallising phase, which together with clinopyroxene and amphibole, fractionates alongside Ti-rich magnetite.

Na_2O contents increase from about 1.5% to 8% by a SiO_2 value of

about 65%, when the smooth increase tends to level off. This variation is consistent with the separation of such Na-poor phases as olivine, clinopyroxene and amphibole. Only at acid compositions, dominated by relatively Ab-rich plagioclase, is there a levelling off of the fractionation trend.

So far, amphibole has been considered as a possible fractionating phase. The possibility that it plays a major role is unlikely as some of the brown hornblendes contain more Na_2O than the host rocks. Precipitation of high proportions of such amphiboles would deplete Na_2O, or at least reduce the rate of increase during fractionation. Major amphibole fractionation is also discredited by the graphical methods. It requires highly varying proportions of fractionation to explain the variations in different major oxide variation diagrams.

P_2O_5 contents increase sharply until a residual magma composition containing $\sim$ 56% SiO_2 is reached. This is followed by an equally sharp decrease with further fractionation. This trend can be simply interpreted as due to apatite. This is a crystallising phase at the transitional composition from basaltic andesite to acid andesite and goes on crystallising until the most siliceous compositions are reached.

K_2O, being mobilised during metamorphism, does not show a clear trend and cannot be reliably utilised for petrogenesis.

5.5.3 Chemical variations in trace elements

The mobile elements, Sr, Rb, Ba, Zn and Cu are not considered here : only the immobile elements, Zr, Y, Nb, La, Ce, Cr and Ni are used in the following discussion.

With advancing fractionation, the incompatible elements Y, Nb, Ce and La present linear trends whereby their concentrations regularly increase with increasing Zr. At acidic compositions, there is a somewhat slower rate of increase in the concentrations of these elements with increasing Zr. Table 5.1 contains some mineral/liquid distribution coefficients for elements including Zr, Y, Nb, Ce, La, Cr and Ni, compiled from

various sources. Most of the distribution coefficients are composition dependent and increase with increasing SiO_2 content of the liquid (Pearce and Norry, 1979). Thus, the slower rate of increase in Nb, Y, Ce and La concentrations with respect to the increase in Zr at acidic compositions may partly be due to a faster increase in the distribution coefficients of these elements relative to Zr for crystallising phases such as magnetite; and partly due to new phases such as apatite. Both, magnetite and apatite, are capable of concentrating these elements into their structures. It is apparent from table 5.1 that, especially at basic and intermediate compositions, olivine, clinopyroxene, magnetite, plagioclase and apatite fractionations, in the order suggested by the major element trends, would continually enrich the residual liquids in Zr, Nb, Y, Ce and La. Therefore, the trends exhibited by these incompatible trace elements are in complete agreement with the course of fractional crystallisation determined in the preceding section.

The possibility that amphibole was a major crystallising phase at any stage during the fractionation of the Polusagi magma can now be ruled out on the basis of the distribution coefficients of incompatible elements between amphibole and the liquid (Table 5.1). They predict that extensive amphibole separation would reduce incompatible trace element concentrations into the acidic compositions, contrary to the observed trends. Schentzler and Phillpotts(1970) state that extensive amphibole crystallisation should result in some increase in Ce, and a marked increase in Ce/Y ratio. In the Polusagi rocks, Ce/Y ratios are substantially constant as opposed to variations in the Ce (Fig. 5.6) or Zr concentrations. It appears that amphibole did not play a major role during the fractional crystallisation of the Polusagi magma.

Cr and Ni show similar fractionation trends, concentrations decreasing exponentially with increasing Zr concentrations from basic to acidic compositions. Average values for Cr and Ni are 254 ppm and 95 ppm

TABLE 5.1

MINERAL/LIQUID DISTRIBUTION COEFFICIENTS -

BASIC ROCKS	Olivine	Plagioclase	Clinopyroxene	Amphibole	Magnetite	Apatite
Mn	0.9	0.07	0.8	-	-	-
Ti	0.02	0.04	0.3	1.5	7.5	-
Zr	0.01	0.01	0.1	0.5	(0.1)	-
Y	0.01	0.03	0.5	1.0	(0.2)	-
Nb	0.01	0.01	0.1	0.8	(0.4)	-
Ld_g	0.01	-	0.02	0.78	-	-
Ce	0.001	0.10	0.10	0.20	0.08	-
Cr	0.2	0.01	10	12	10	-
Ni	10	0.01	2	3	5	-
INTERMEDIATE ROCKS						
Ti	0.03	0.05	0.4	3.0	9.0	-
Zr	0.01	0.03	0.25	1.4	0.2	-
Y	0.01	0.06	1.5	2.5	0.5	20
Nb	0.01	0.025	0.3	1.3	1.0	-
Ce	-	0.3	0.5	1.3	-	35
ACID ROCKS						
Ti	(0.04)	0.05	0.7	7.0	12.5	(0.1)
Zr	(0.01)	0.1	0.6	4.0	0.8	(0.1)
Y	(0.01)	0.1	4.0	6.0	2.0	40
Nb	(0.01)	0.06	0.8	4.0	2.5	(0.1)

Mn : from Sun et al, 1979; Ce, Cr and Ni ; from Cox et al, 1979;

Ce : estimated from Gast, 1968.

All others from Pearce and Norry, 1979.

Parenthesis means inferred.

in the MP basalts, respectively, dropping sharply to 23 ppm and 6 ppm in andesites, and to 11 ppm and zero in dacites. The sharp decrease in Ni values at basic compositions can only be attributed to extensive olivine fractionation, since olivine is the only mineral capable of severly depleting the basic magma in Ni at this stage (see Table 5.1). Magnetite cannot be responsible for Ni depletion, as it only enters into the fractionation as a major crystallising phase after a SiO_2 content of $\sim$52% is reached. Similar reasoning shows that the sharp drop in Cr contents at the basaltic stage must be due to clinopyroxene separation.

The variations of Cr and Ni contents in the basaltic rocks with fractionation can also indicate the relative importance of olivine and clinopyroxene during the early stages of fractionation. The partition coefficents in Table 5.1 show that relatively more extensive clinopyroxene separation would result in a higher rate of decrease in Cr than Ni, while relatively more extensive olivine crystallisation would cause Ni to decrease at a higher rate than Cr. In Fig.5.7 the Cr/Ni ratios of the basic rocks are plotted against Zr. The ratio rises from under 2 to 4, as silica varies from about 46% to 50%. This confirms the previous suggestions that olivine is a more dominant fractionating phase than clinopyroxene in the basaltic melts.

At intermediate and acid compositions, Cr and Ni concentrations continue to decrease, but at much reduced rates. These trends are explicable by magnetite separation (Table 5.1), perhaps accompanied by some olivine any clinopyroxene in the intermediate stages.

Additional support for the outlined course of crystal fractionation during the evolution of the Polusagi magma is provided by the variations of Ti, Zr and Y, following the technique devised by Pearce and Norry (1979). Distribution coefficients have allowed them to compute theoretical fractionation vectors for both single phases and selected phase assemblages. The Polusagi rocks are plotted in their Y-Zr, TiO_2-Zr and Nb-Zr type diagrams in Fig. 5.8. The trends exhibited by the Polusagi rocks are all

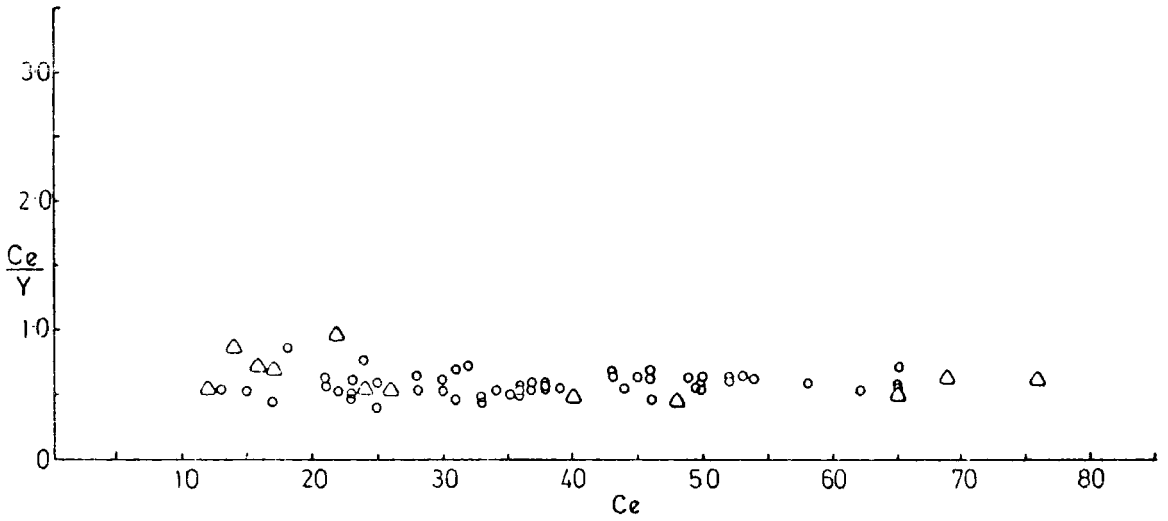


Fig.5.6. Ce vs. Ce/Y ratio in the Polusagi rock suite.
o : volcanic rocks and △ : hypabyssal rocks.

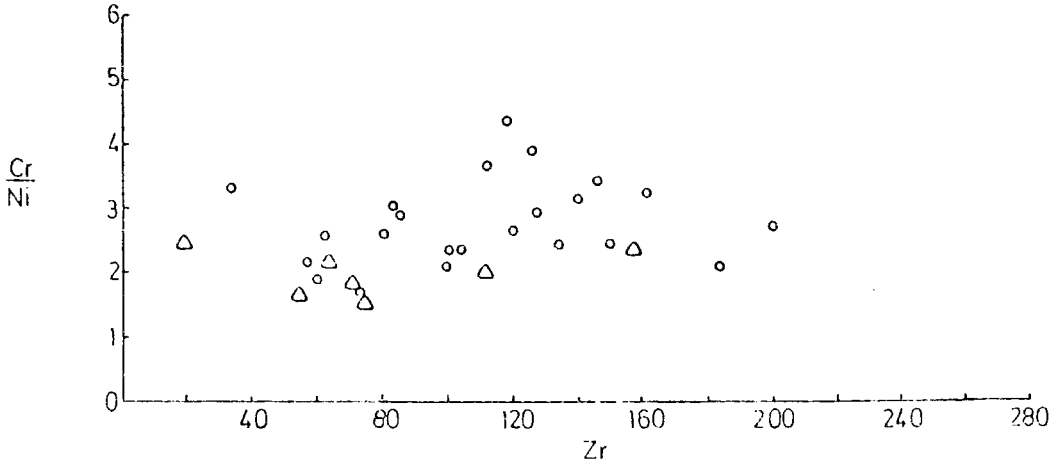
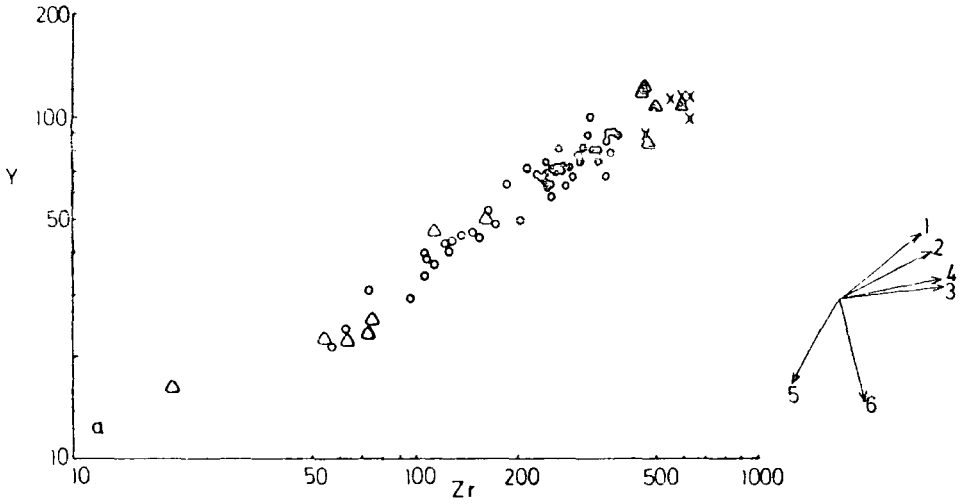
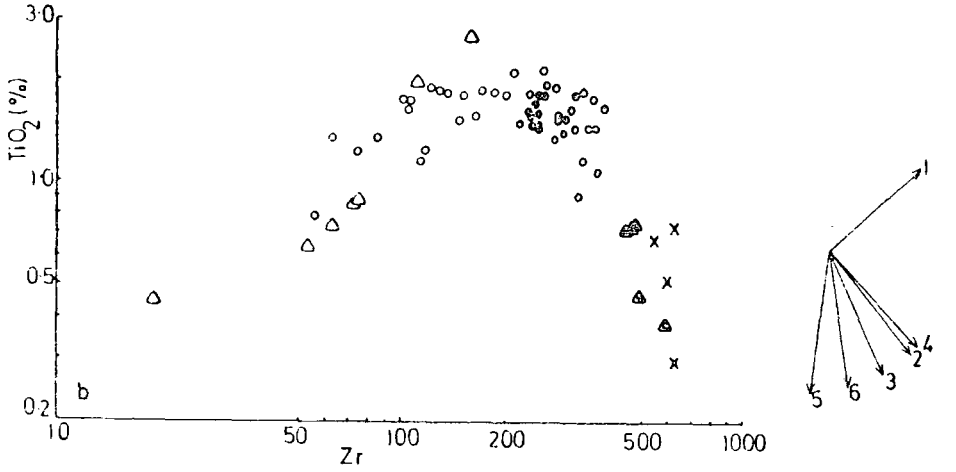
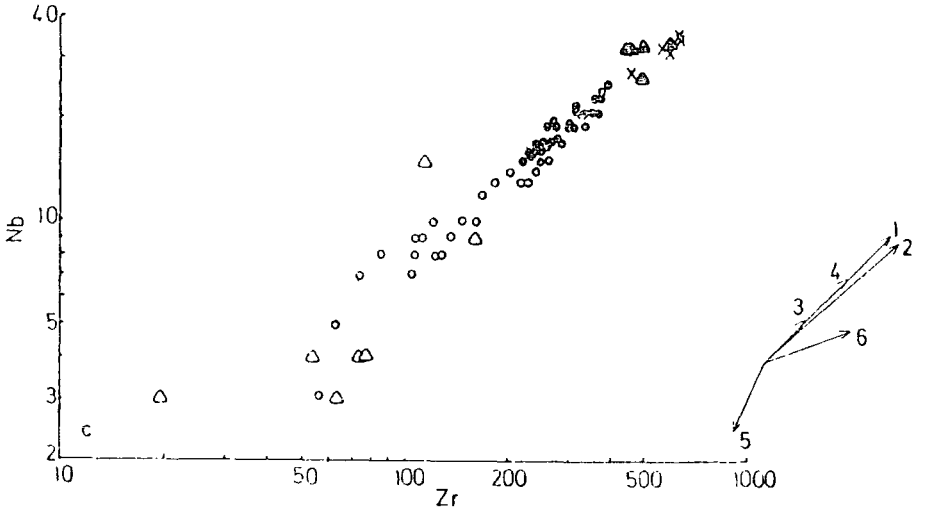


Fig.5.7. Zr vs. Cr/Ni ratio for the basic rocks.
o : basalts and △ : gabbros.


200
100
50
10
Y
a
10
50
100
200
500
1000
Zr
1
2
4
3
5
6


3·0
1·0
0·5
0·2
TiO2 (%)
b
10
50
100
200
500
1000
Zr
1
4
2
3
5
6


40
10
5
3
2
Nb
c
10
50
100
200
500
1000
Zr
1
2
4
3
6
5

consistent with their modelled trend-1 for basic compositions and the trend-2 for intermediate and acid composition. The former trend involves fractionation of olivine, clinopyroxene and plagioclase, while the latter is similar, but with additional magnetite . These theoretical assemblages are thus the same assemblages as those deduced from major and trace element variations. It is also interesting that theoretical trends 3,4,5 and 6 (Fig. 5.8) are those involving amphibole fractionation, and that they do not match the observed trends of the Polusagi rocks.

5.5.4 Major and trace element variations in the hypabyssal rock

Chemical data for the Polusagi gabbros and plagiogranites have also been plotted in the diagrams used for the Polusagi volcanic rocks. It is clear that these hypabyssal rocks are chemically similar to their volcanic counterparts and closely follow the trends exhibited by the volcanic rocks.

5.6 Summary and conclusions

The Polusagi volcanic rocks and hypabyssal rocks originate from two successive high degree (≈ 25%) partial melts of the same upper mantle source above the Benioff zone in a Tethyan marginal basin. The composition of the first partial melt approximates to that of the most basic MP basalt and the second to most basic MP gabbro. The volcanic rock types and the hypabyssal rock types are products of fractional crystallisation processes which followed a very similar path in the respective melts. The major phases that controlled the crystal fractionation during the generation of the Polusagi rock suite are olivine, clinopyroxene, plagioclase, Ti-rich magnetite and apatite. Amphibole was not a major crystallising phase. The early stages of fractionation were basically governed by olivine precipitation, but towards the later stages of basaltic liquid compositions, olivine was joined by clinopyroxene. The iron and Ti enrichments i.e. the Polusagi tholeiitic trend, are thus caused by separation of olivine and clinopyroxene, with lower Fe/Mg ratios than the

remaining basaltic liquid. Silica enrichment, from basaltic or basaltic andesite compositions, has been achieved by the entrance into fractionation of Ti-rich magnetite as a major crystallising phase at $\sim$52% SiO_2, and not by amphibole separation. At intermediate compositions there was also major plagiclase separation, joined by apatite at a composition of $\sim$56% SiO_2. Fractionation at acid compositions are dominated by relatively Ab-rich plagiclase, although magnetite and apatite were still precipitating.

The absence of magnetite as a crystallising phase at basaltic compositions implies that the oxygen fugacity was initially low, but subsequently increased causing magnetite precipitation i.e. the system was not far from theoretical, open-system fractionation. Such an increase in the oxygen fugacity, after 52% SiO_2 values were reached, can be explained by larger contributions (and probable dissociation) of water into the magma provided by the dehydrating and descending Tethyan oceanic crust along the Benioff zone.

CHAPTER SIX

PETROGRAPHY AND MINERALOGY

6.1. Introduction

The Polusagi rocks are variably altered and metamorphosed. Alteration and metamorphic processes affect the mineralogy, texture and composition of the rocks to various extents producing different, sometimes patchy, mineral and textural assemblages. The only igneous remnants are the relict clinopyroxene and a late stage magmatic product in gabbros - the brown hornblendes- , in addition to the igneous textures exhibited by now albitised plagioclases. Metamorphic minerals include amphibole, chlorite, epidote, prehnite, pumpellyite, calcite, quartz, sphene and leucoxene. Therefore, it is desirable to divide the area into zones where the mineralogy and textural relationships are relatively uniform. Amongst the metamorphic minerals, the most conspicuous feature is the distribution of amphibole, prehnite and pumpellyite. On this basis two zones can be recognised and defined as follows:

Zone A = The rocks contain prehnite $\pm$ pumpellyite, but no amphibole.

Zone B = This zone includes all the rocks with amphibole and is further divided into sub-zones B_1 and B_2.

Sub-zone B_1 = The rocks contain amphibole and prehnite $\pm$ pumpellyite.

Sub-zone B_2 = The rocks contain amphibole, but no prehnite or pumpellyite.

These zones are believed to represent increasing grade of metamorphism passing from prehnite-pumpellyite facies to greenschist facies from A to B. The details are discussed in sections 6.10. and 6.11. of this chapter.

In this chapter the mode of occurrence and chemistry of minerals will be examined and the possibility of metamorphic minerals having different optical or chemical properties in different zones will be considered.

This will be followed by descriptions of textural relationships amongst the minerals and of the conditions and nature of metamorphism.

All analyses of minerals are by electron microprobe, which returns total iron as Fe^{2+}. The procedure, analytical conditions and method of estimating Fe^{3+} and water contents, in appropriate minerals, are described and the analyses are presented in Appendix IV.

6.2. Clinopyroxene

6.2.1. Mode of occurrence

Clinopyroxene, as the only form of pyroxene, occurs chiefly in basalts and gabbros. Some basaltic andesites also contain minor amounts of clinopyroxene, but it is completely absent from the more acidic andesites and acid rocks. The proportion of clinopyroxene (cpx) in basalts and gabbros, where it is not extensively replaced by secondary minerals, may constitute up to 20% of the rocks and these are generally the "more primitive" types defined in section 4.2.2.4.Two different modes can be recognised:

a) Groundmass clinopyroxenes : This is by far the dominant mode of occurrence. They are generally fine grained, 0.3 mm or less in size, but in some cases they may be up to 0.5 mm across. They usually occur amongst the albite laths, filling the interstices, showing anhedral or subhedral grain boundaries. Some thin sections of lavas (e.g. samples P252, P286) may show that all the cpx have low-birefringence. However, sections of these samples taken at another orientation, will show that nearly all cpx grains have normal birefringence. This is taken to suggest flow alignment of cpx.

b) Microphenocrysts : These are relatively rare and generally vary from 1-3 mm in size. In rare cases, they may reach up to 5-6 mm across (sample $P279_B$). Although they show anhedral outlines, they tend to be cracked, the cracks being filled by secondary minerals, but in most cases uniform extinction is maintained. Usually the microphenocrysts are



Plate 6.1 : Clinopyroxene (white), being replaced by brown amphibole (grey). Black is magnetite which is being replaced by chlorite (patch dark grey). Sample: P281, X80.

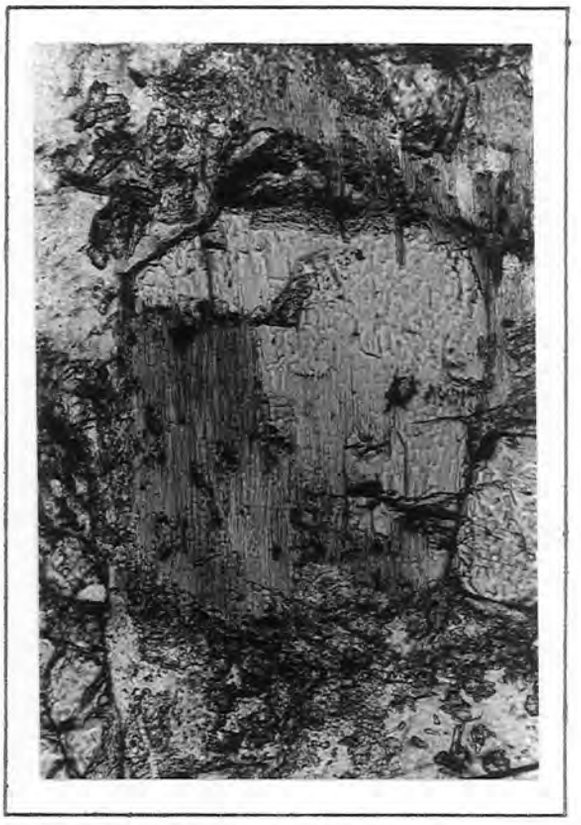


Plate 6.2 : Fibrous amphibole (grey, striated) replacing euhedral clinopyroxene. Sample: P252, X200.

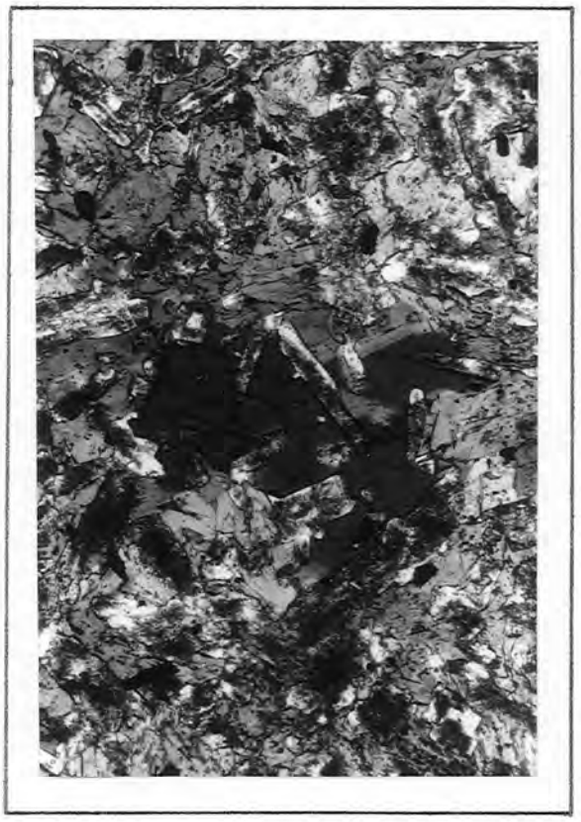


Plate 6.3 : Large euhedral brown amphibole (dark grey), being replaced by chlorite (patchy lighter grey) around the margins. Note the enclosed altered plagioclase laths. Sample: P282, X50.



Plate 6.4 : Brown amphibole (dark grey), being gradually taken over by green amphibole (lighter grey). Patchy black to dark grey areas are chlorite. Sample: P246, X50.

surrounded by plagioclase laths, and in some cases they are completely enclosed and isolated by clusters of plagioclase grains.

They do not contain any opaque inclusions.

Zoning and twinning : Although rare, some cpx grains display zoning and three types of zoning can be recognised:

Type a) : Zoning is demonstrated by a continuous variation in the extinction angle from core to margin.

Type b) : Zoning is demonstrated by a thin rim around the grain which abruptly extinguishes at a different angle from that of the core where extinction is uniform.

Type c) : Shows hour-glass structure.

It is interesting to note that all the samples where zoned cpx grains are observed are relatively more basic basalts.

6.2.2. Chemistry

87 clinopyroxene analyses (57 in basalts, 13 in andesites and 17 in gabbros) are listed in Appendix IV.2.1. Analyses are largely of groundmass mode with some microphenocrysts.

6.2.2.1. Nomenclature

The analyses of clinopyroxenes from the volcanics and gabbro samples are plotted on the conventional pyroxene quadrilateral in Figs.6.1a and 6.1b, respectively. It is evident that analyses from both rock types do not show any systematic difference and the same nomenclature should be applicable to all the pyroxenes analysed. According to the nomenclature of Deer et al (1974), they are predominantly augites. However about half of the analyses from 'MP' basalts and gabbros plot into the diopside-augite end of the endiopside compositional field, the other half plotting into the augite field. Furthermore, the analyses from basaltic andesites on the whole are the most iron-enriched. Thus, the evolution of pyroxene chemistry is from the diopsidic endiopside to augite with advancing fractionation of the Polusagi magma. No Ca-poor pyroxene is observed in the studied rocks.

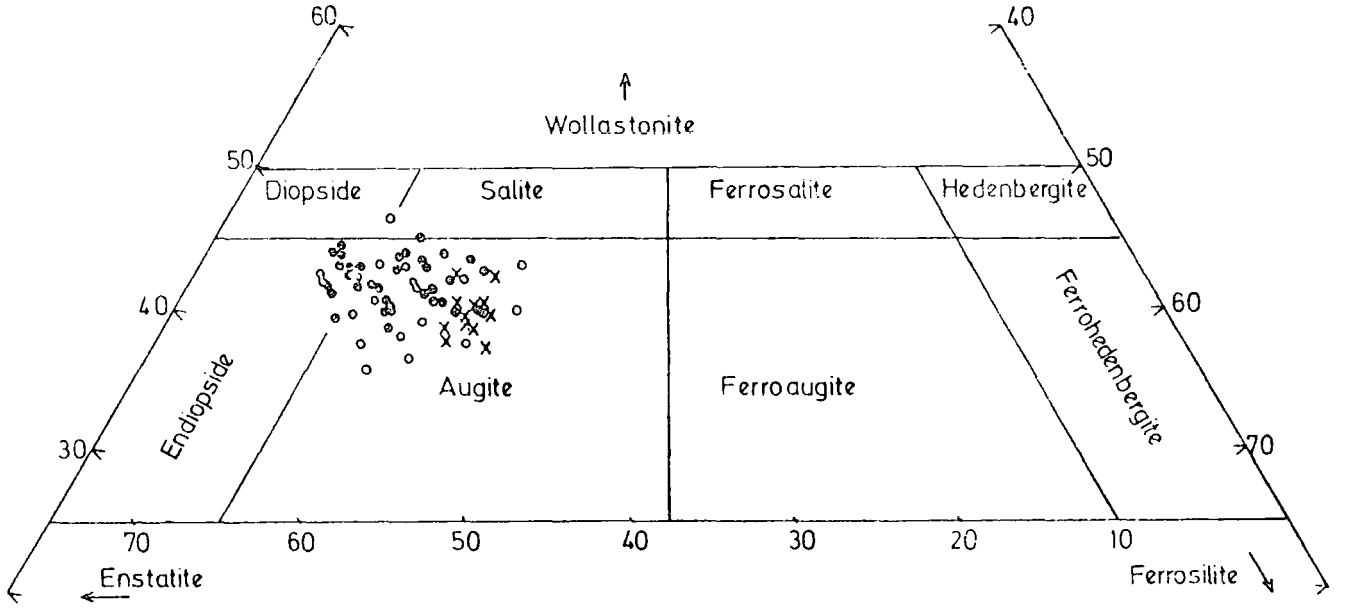


Fig.6.1 a. Classification and chemical variation of clinopyroxenes from basalts (⊙) and andesites(×) in the system Diopside-Hedenbergite-Ferrosilite-Enstatite.

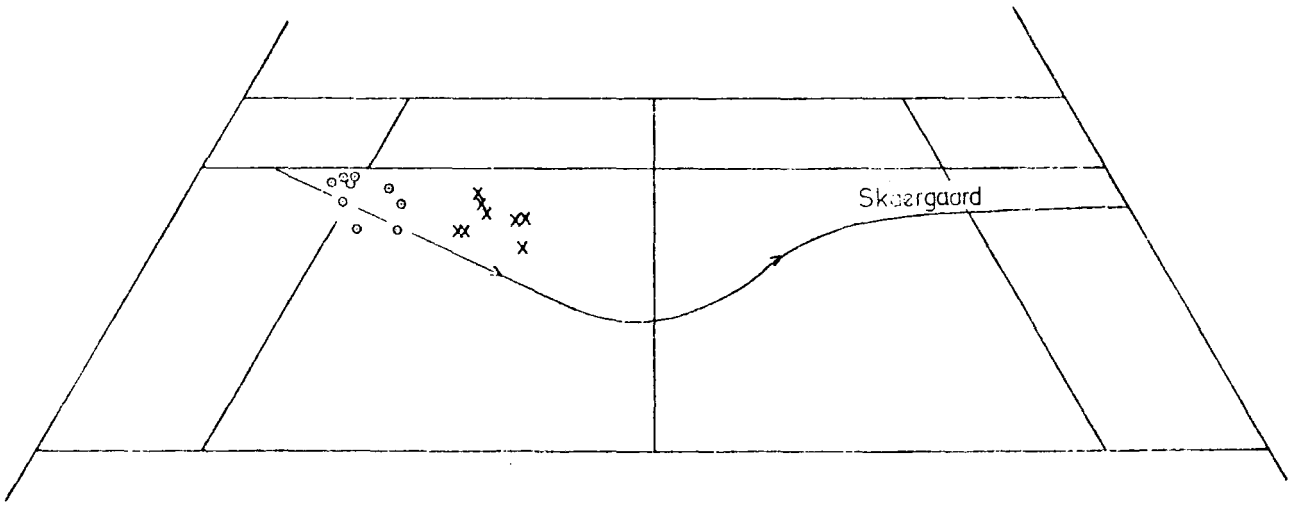


Fig.6.1b. Same as above for clinopyroxenes from the "more primitive" gabbros (⊙) and "more differentiated" gabbros(×). Fractionation trend of the Skaergaard pyroxenes is shown for comparison.

6.2.2.2. Chemical variation

What is also evident in Figs.6.1a and 6.1b is that the analyses occupy a restricted field , showing a limited amount of iron-enrichment with differentiation, as compared, for instance, with the well known tholeiitic trend of the Skaergaard intrusion. This is a reflection of the relatively low to moderate iron enrichment trend of the Polusagi magma (section 4.2.4) upon the clinopyroxene chemistry. This could also be due to relatively early separation of Ti-rich magnetite from the melt, and to the relatively restricted compositions of the rocks (all basic) in which cpx is found.

Chemical variation in relation to Mg-number $\frac{100 \times Mg}{Mg + Fe^{2+}}$, a measure of degree of fractionation, is shown in Fig.6.2. The plots show that Ti,Mn and Na increase, to a lesser extent Ca and Al decrease with advancing fractionation or decreasing Mg-number. Ti and Mn tend to level off at the latest stages of the given range of fractionation of the Polusagi magma. Si and Al exhibit unclear trends. With all the analyses included, there is a tendency of Si and Al trends to go through a minimum and maximum respectively at a Mg-number of approximately 75. This is probably an artefact created by the analyses from the zoned cpx grains, since when these analyses are excluded the trends do not have the minimum and maximum around Mg-number = 75. Instead the data points, much scattered, show signs of increase and decrease for Si and Al respectively at the very latest stages of fractionation. The nature of zoned cpx grains will be discussed presently. Fe^{3+} (estimated) and K are absent in most of the analyses and when present are in negligable amounts. The absence of Fe^{3+} may indicate a non-oxidising environment which is in line with the early stages of evolution of the Polusagi magma discussed in Chapter five.

A comparison of the chemical variation trends of all the elements, perhaps with the exception of Al and possibly Si, (Fig.6.2), with those of the whole-rock major element trends for the given differentiation range

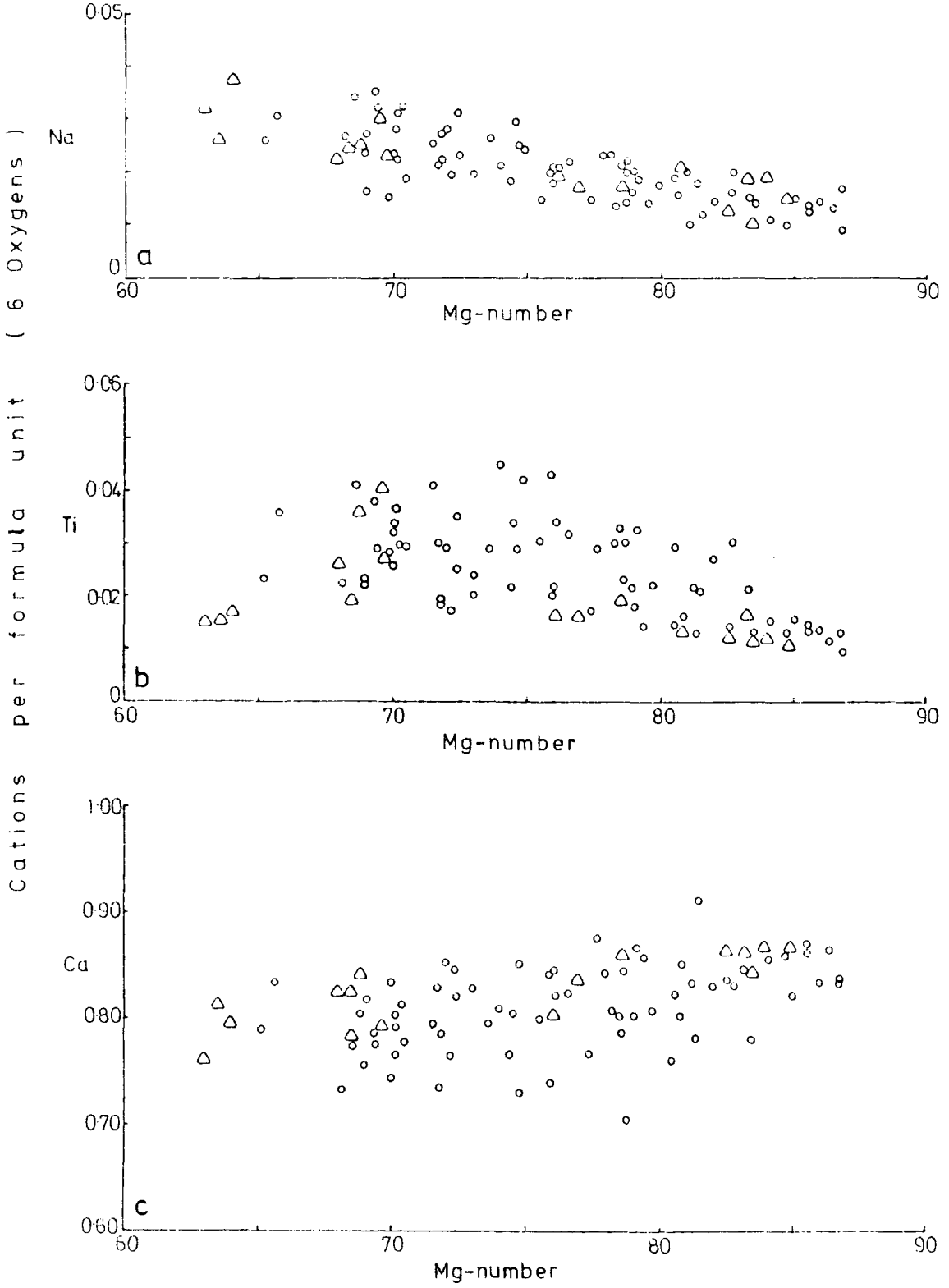
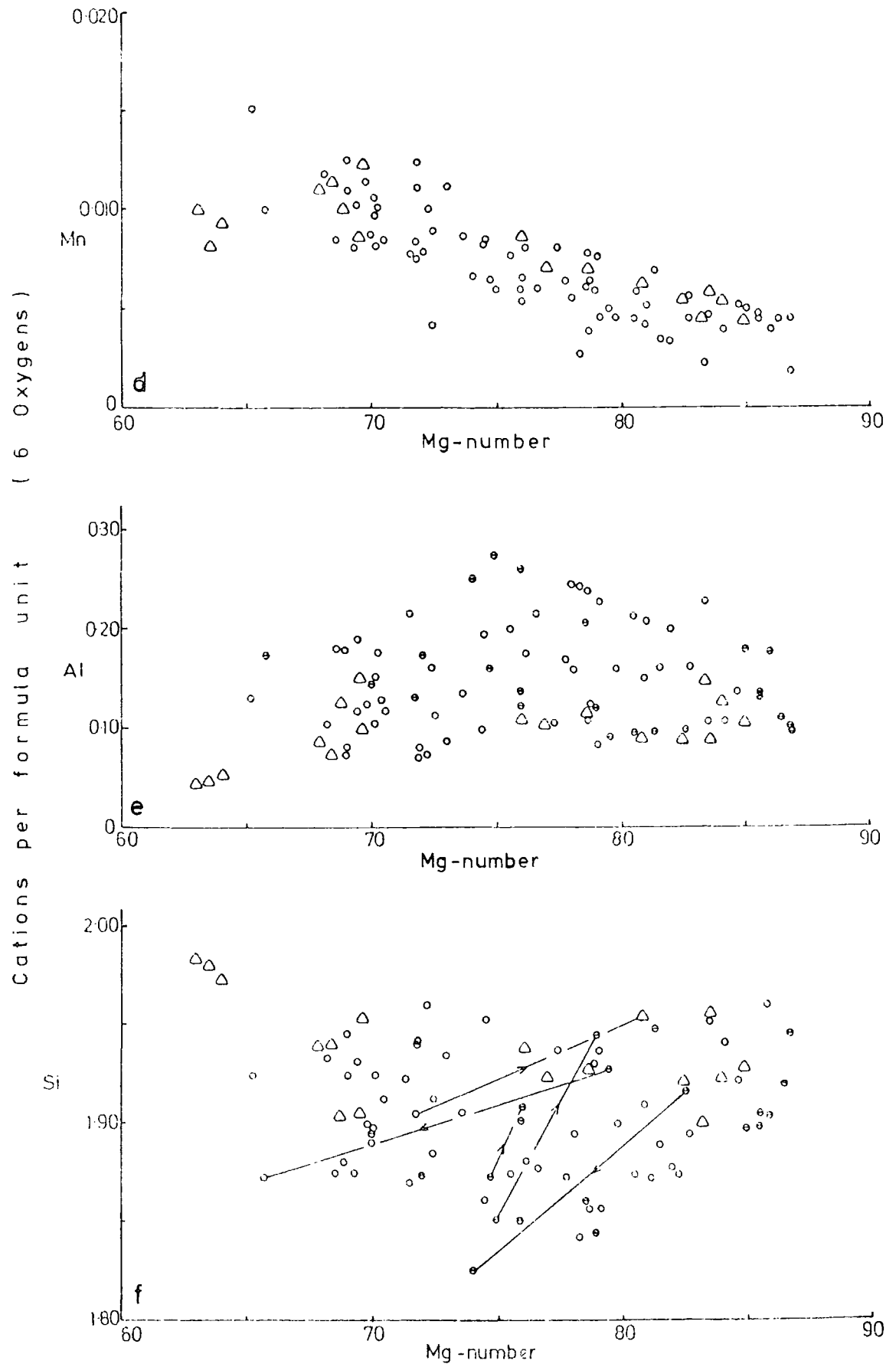


Fig.6.1. Chemical variation in clinopyroxenes from volcanics (o) and gabbros(△) with Mg-number: a) Na, b) Ti, c) Ca, d) Mn, e) Al and f) Si (cations per formula unit, on basis of 6 oxygens). Symbol (●) in diagrams e) and f) indicate analyses from zoned grains, and solid lines in diagram f) join core and margin analyses of zoned grains.


Cations per formula unit (6 Oxygens)
0·020
0·010
0
Mn
d
60
70
80
90
Mg-number
030
0·20
0·10
0
Al
e
60
70
80
90
Mg-number
2·00
1·90
1·80
Si
f
60
70
80
90
Mg-number

(see Chapter five, Fig.5.5) shows that the respective trends are very similar or comparable. This suggests that the cpx chemistry closely followed the continuing chemical variation within the host magma. This point will be returned to in section 6.2.3 of this chapter.

Chemical variation in zoned grains:

It was pointed out earlier that zoned grains occur only in the relatively more primitive basalts i.e. representing relatively early magmatic liquids. The analyses from these basalts show extremely variable chemical range. In some cases, the chemical variation of cpx analyses from one sample (e.g. P66 or P286) may cover nearly all the variation displayed by the cpx analyses from all samples. As a result, the chemical correlation between the zoned cpx and the host rock is poor. Table 6.1. contains representative core and margin analyses from the three types of zoned cpx grains (mentioned in section 6.2.1). It is apparent from this table that type a) zoning is a normal one where from core to margin there is Fe, Ti, Mn, Al and Na enrichment and Si and Mg depletion i.e. the same trend of variation with host magma chemistry, with differentiation. However, type b) zoning is chemically opposite to that of type a). There,from core to margin, Fe, Ti, Mn, Al and Na decrease and Mg and Si increase, which is unexpected. Such chemical differences can not simply be explained by the general trend of element variations in the host magma. The possibility that the rims could have grown at a stage where extensive and rapid separation of Fe-Ti-Al rich spinels from the magma may have given rise to such a chemical change,is ruled out; because the available evidence (Chapter five, 5.5) shows that the spinel as a major fractionation phase was Fe-Ti rich and did not start separating until intermediate compositions were reached. The mechanism for type b) zoning is not understood, but in any case it indicates a complex history for cpx crystallisation. Analyses of different sectors in the type c) hour-glass zoning indicate that each sector

TABLE 6.1

Chemical analyses of zoned cpx grains

	Type a) zoning		Type b) zoning		Type c) zoning	
	Core	Margin	Core	Margin	Sector I	Sector II
Analyses	$P161_{1A}$	$P161_{1B}$	$P286_{1D}$	$P286_{1C}$	$P66_{2A}$	$P66_{2B}$
SiO_2%	51.96	49.14	50.84	53.21	51.75	49.05
TiO_2	0.52	1.25	1.06	0.53	0.51	1.62
Al_2O_3	2.06	3.83	2.95	2.01	2.17	5.72
FeO^{total}	7.38	11.47	9.81	6.95	6.45	8.83
MnO	0.16	0.31	0.26	0.19	0.18	0.21
MgO	15.99	12.32	13.93	16.18	17.18	14.14
CaO	21.61	20.46	20.69	20.94	21.12	20.32
Na_2O	0.14	0.41	0.28	0.22	0.22	0.29
K_2O	0.00	0.00	0.00	0.00	0.00	0.00
Total	99.82	99.19	99.82	100.23	99.58	100.18
Atomic proportions O=6						
Si	1.927	1.872	1.905	1.953	1.916	1.824
Ti	0.014	0.036	0.030	0.015	0.014	0.045
Al	0.090	0.172	0.131	0.087	0.095	0.251
Fe^{3+}	—	—	—	—	—	—
Fe^{2+}	0.229	0.366	0.307	0.213	0.200	0.275
Mn	0.005	0.010	0.008	0.006	0.006	0.007
Mg	0.884	0.670	0.778	0.885	0.948	0.784
Ca	0.859	0.835	0.831	0.823	0.838	0.810
Na	0.010	0.030	0.021	0.016	0.016	0.021
K	—	—	—	—	—	—

is chemically different from the other. Similarly Fe, Ti, Mn, Al and Na behave in antipathy with Mg and Si in this type of zoning.

6.2.2.3. Crystal chemistry

The above observed chemical variations are governed by single or charge balancing coupled substitutions. The most obvious and important single substitution is $Mg \rightleftharpoons Fe^{2+}$ which moves to the right during differentiation, indicated by a decrease in Mg-number from about 57 to about 63. Small but increasing amounts of replacement of Mg by Mn is also indicated by a negative correlation of Mn with Mg-number.

Fig.6.3. is a plot of Si vs. Al which shows that all the analyses plot above the line Si+Al = 2 (saturation line of Kushiro, 1960). This means that Al is the only element substituting for Si in the Z site. Furthermore, it indicates that the entrance of Al into the Z site (which is more than 50% of Al on average) is to a large extent compensated for by the entrance of excess Al into the Y site, hence the positive correlation of Al^{iv} with Al^{vi} (Fig.6.4). However, Al^{vi} is not totally sufficient to compensate for Al^{iv}, and the charge balance must be maintained. This is done by Ti which shows a positive correlation with Al^{iv}, indicated by Fig. 6.10. Ti also shows positive correlation with Na (Fig.6.5), but there is no appreciable correlation between Na and Al^{vi} (Fig. 6.6). This suggests that it is Ti which is largely compensating the replacement of Ca by Na. This is also indicated by positive correlations of Ti and Na with Mg-number (Fig.6.2a and b).

The general decrease of Ca, below 1 atom per formula unit, with decreasing Mg number is not totally due to its being increasingly substituted by Na, since on average Ca drops from 0.87 to 0.75 while Na increases from 0.01 to 0.035. Rather, negative correlations of Mg and Ca and positive correlation of Fe^{2+} with Mg-number imply that Fe^{2+} in relation to Mg is being preferentially and increasingly incorporated into the X site with advancing differentiation.

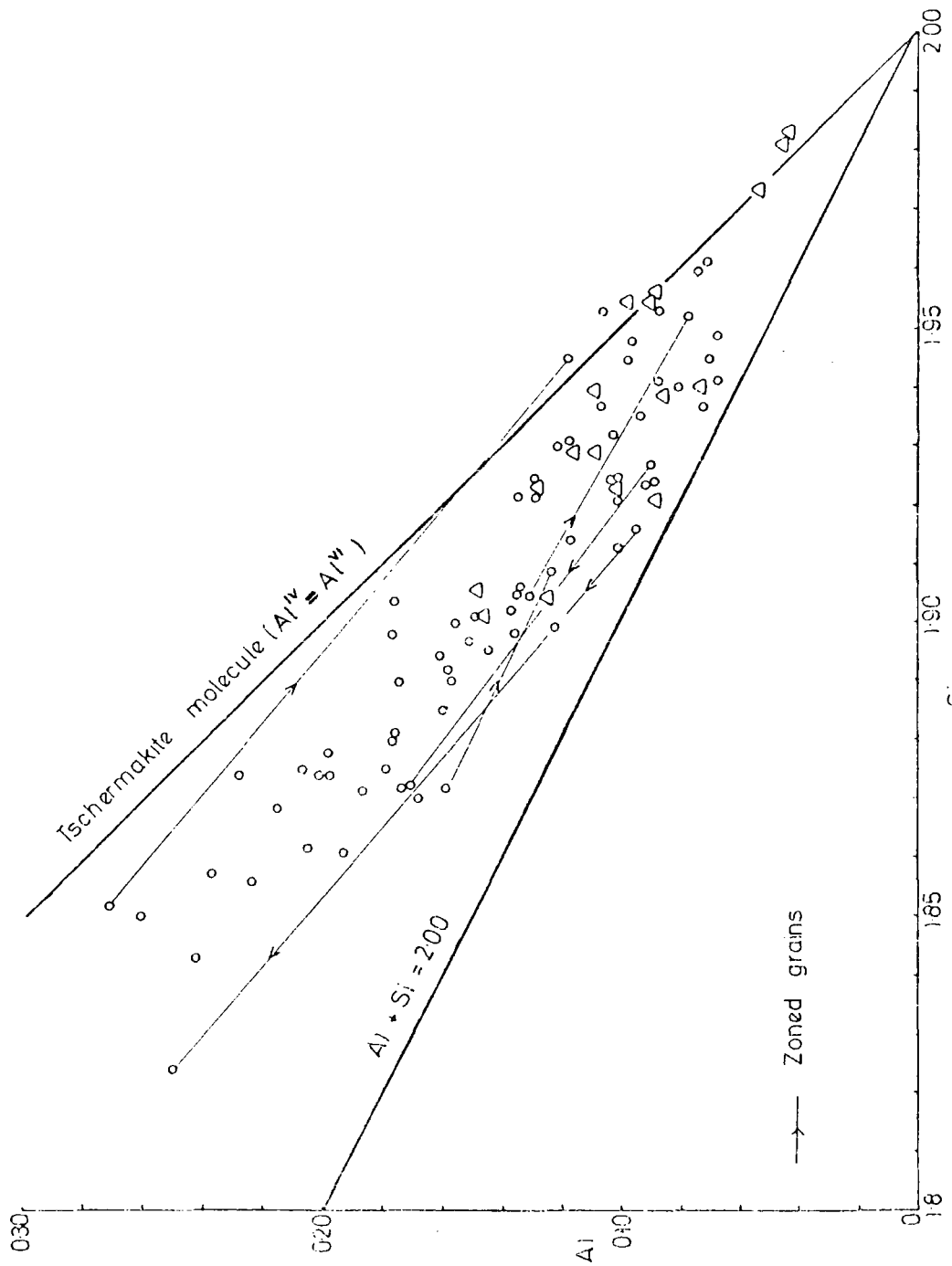


Fig.6.3. Si vs. Al in clinopyroxene from volcanic (o) and gabbro (Δ) (cations per formula unit, 6 oxygens).

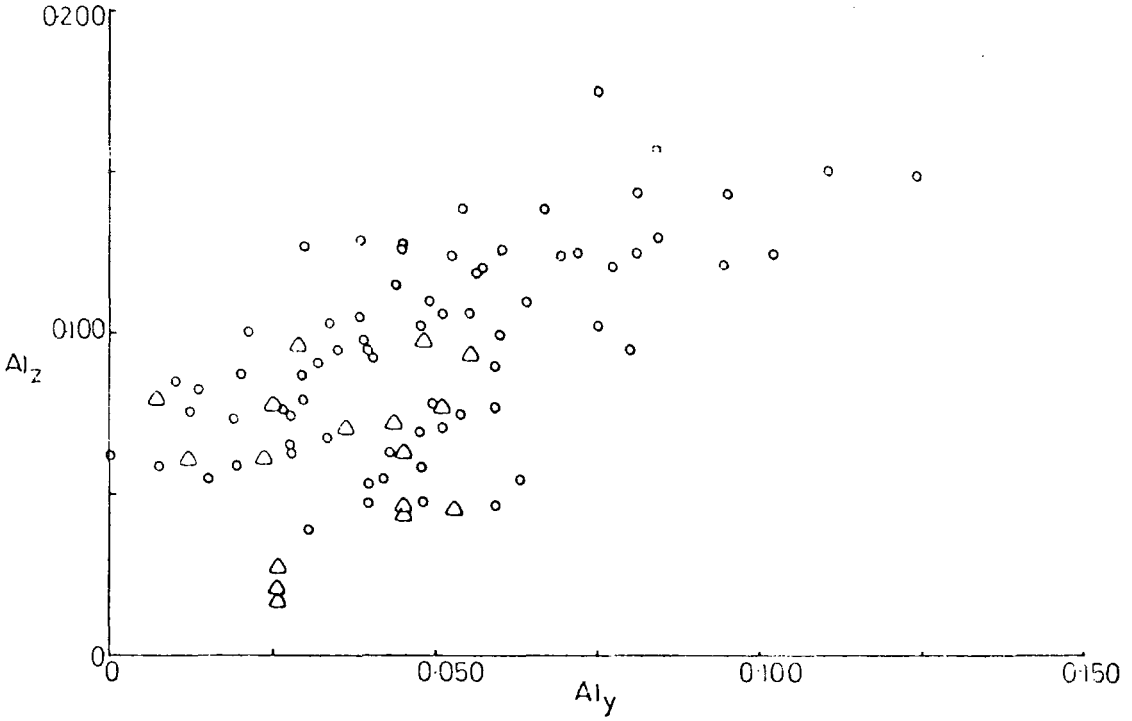


Fig.6.4. Tetrahedrally co-ordinated Al vs. octahedrally co-ordinated Al in clinopyroxenes from volcanics (o) and gabbros (△).

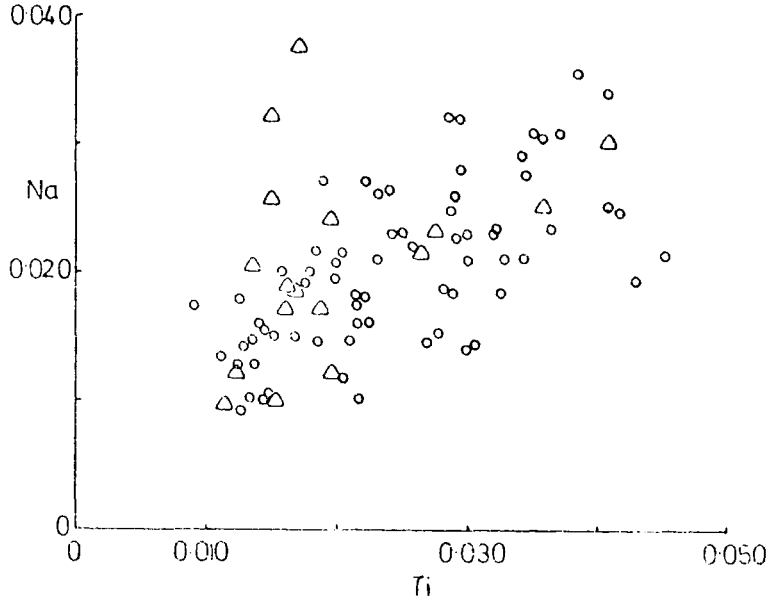


Fig.6.5. Ti vs. Na in clinopyroxenes (cations per formula unit, 6 oxygens). Symbols as above.

6.2.3 Factors controlling the chemical variations

a) Physical factors: It is apparent from the foregoing chemical variation diagrams that clinopyroxenes from lavas and hypabyssal rocks are chemically very similar and there is no appreciable chemical difference. Therefore, the mode of occurrence of the host rocks i.e. the load pressure does not seem to be an important factor controlling the chemistry. A similar conclusion is reached by Le Bas (1962).

Brown (1968) states that Al content of cpx varies according to pressure and temperature and the type of magma. The possibility of temperature dependence of tetrahedrally coordinated Al is considered by Kushiro (1960). However, Le Bas (1962) considers such a control as unlikely for two reasons: 1) Although temperature normally falls with differentiation, the Al^{iv} goes up in some magma types and yet falls in others, 2) At similar degrees of differentiation, although there appears to be no great difference between the temperatures and ranges of crystallisation, Al^{iv} does vary. Le Bas (1962) also points out that partial pressure of oxygen has no great effect on Al relations in cpx.

Mevel and Velde (1976) studied the cpx compositions in the Mesozoic pillow-lavas from the French Alps and found that the cpx compositions from the core and margin of pillow lavas are different. They attributed this to the differences in cooling rate of the host. Therefore, it is possible that some of the observed chemical differences of the Polusagi cpx may be due to the differential cooling rates of the host lavas.

b) Chemical factors : Fig. 6.7 is a plot of Mg-numbers of cpx against those of the host rocks. In order to have a meaningful variation, only the Group A samples (section 3.3.1) have been used and the samples P66 and P286, which contain zoned cpx analyses showing widely varying Mg-numbers, have been excluded. The plot demonstrates a strong positive correlation i.e. the control of host rock composition over cpx composition. An observation was made in section 6.2.2.2 that the respective

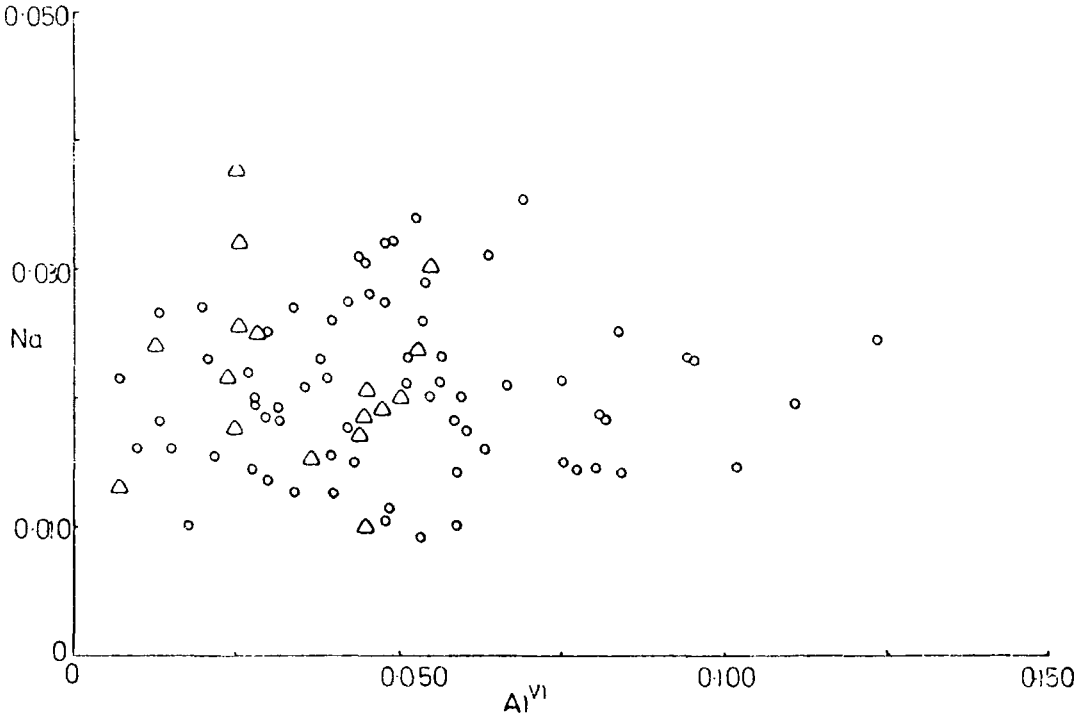


Fig.6.6. Na vs. octahedrally co-ordinated Al in clinopyroxenes from volcanics (o) and gabbros(Δ). (Cations per formula unit, 6 oxygen).

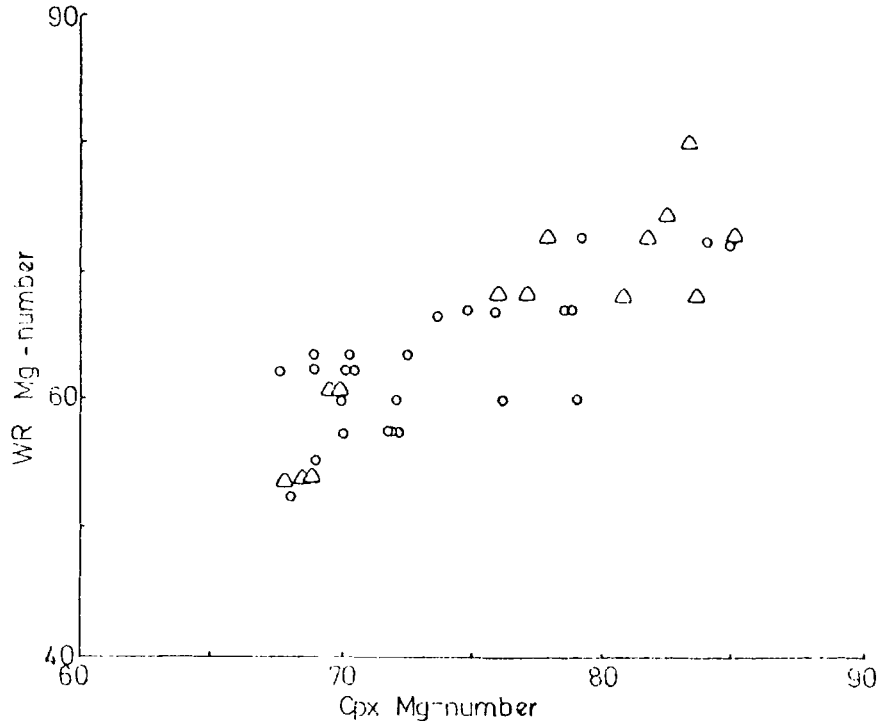


Fig.6.7. Whole-rock Mg-number vs. clinopyroxene Mg-number . Symbols as above.

element variation trends of total Fe, Ti, Mn, Mg, Ca and Na, with differentiation, in cpx and in the host rocks were either very similar or comparable. These strongly suggest that the dominant factor controlling the cpx chemistry is that of host magma composition. Similar suggestions are made by Kushiro (1960), Le Bas (1962), Coombs (1963) and Fodor et al (1975).

However, it is also suggested by Kushiro (1960) and Le Bas (1962) that the concentration of Si in the host magma appears to determine the Si in the Z site of cpx, and the deficiency is made up by Al. Therefore, the distribution of Al in cpx should reflect the degree of Si-saturation in the host magma. Such a control of Si activity of the host magma is not clearly demonstrated by the Polusagi cpx. Despite that there are signs that Si in the Z site tends to increase in the latest stages of basic magma compositions (Fig.6.2f), the silica activity in Polusagi magma was probably variable for most of the basaltic range of differentiation. This conclusion is not contradicted by the magmatic trend of silica for the range under consideration (Chapter five, Fig.5.5.).

Using the same comparative criteria, it is clearly seen that Al in cpx is not effectively controlled by the Al concentrations in the host magma, but rather, it depends on the amount of Si in cpx. It is also possible that there is some control of physical factors i.e. temperature and pressure over the Al content of cpx (Kushiro 1960; Brown 1968).

In summary, a strong host rock chemical control is apparent on the Polusagi clinopyroxenes.

6.2.4. Petrogenetic implications of clinopyroxene chemistry

6.2.4.1. Introduction

Chemical compositions of cpx have been used to recognise the nature of host magmas (Kushiro, 1960; Le Bas, 1962; Coombs, 1963; Vallance, 1974b; Fodor et al , 1975; Barron, 1976) and the tectonic environment of the host magma (Nisbet and Pearce, 1977). This is made possible by the

intimate relationship of cpx and host magma chemistry and has useful applications where the host rocks are altered.

Diagrams designed by Nisbet and Pearce (1977) put some constraints on the tectonic environment of eruption but they can not satisfactorily differentiate ocean floor basalts from volcanic arc and within plate basalts, due to extensive overlap of the defined respective fields. A method to recognise the nature of host magma by cpx composition is suggested by Coombs (1963) using the CIPW norms obtained from cpx chemistry in much the same way as the whole rock norms, and Vallance (1974b) showed that this method has useful applications in studying the spilitised rocks. Fodor et al (1975), studying the pyroxenes from Hawaii, report that Wollastonite contents of cpx from tholeiitic, alkalic and nephelinitic rocks vary within the range Wo_{30-40}, Wo_{38-48}, and Wo_{47-54} respectively.

A statistical study by Kushiro (1960) distinguished three magma types: tholeiitic, feldspathoid free alkalic and feldspathoid bearing alkalic, using atomic proportions of Si, Al and Ti in the cpx. He showed that Al and Ti increase and Si decreases in going from tholeiitic rocks to feldspathoid bearing alkalic rocks with some overlap between the respective rock types. Le Bas (1962), in a similar study, confirms Kushiro's findings and recognises three magma types:

a) Non-alkaline : includes the tholeiitic, high-alumina and calc-alkaline series

b) Normal alkaline

c) Per-alkaline

on the basis of variations of SiO_2 against Al_2O_3 and TiO_2 against Al^{iv} in the clinopyroxene. These three magma types are also distinct when plotted in a ternary, $Ca+Na+K : Mg : Fe^{2+}+Fe^{3+}+Mn$. Le Bas (op.cit) also states that the respective fields in his plots are better defined, if only groundmass cpx analyses are used. If phenocrystic grains are included, there is some

overlap between the neighbouring fields.

6.2.4.2 The Polusagi magma type as indicated by cpx chemistry

Because the cpx composition is defined to a large extent by the composition of the Polusagi magma, it can be utilised to recognise the nature of the host magma.

In Fig.6.8, the cpx analyses are plotted in the ternary diagram of Le Bas (1962). The majority plot into the tholeiitic field but there is a considerable overlap with the alkaline field. Fig. 6.9 is the plot of SiO_2 vs. Al_2O_3 and puts a greater majority of the analyses into the non-alkaline field. However nearly all analyses plot into the ocean-floor basalt field defined by Nisbet and Pearce (1977) which is superimposed into Fig.6.9. The TiO_2 vs. Al_z, Al_z being defined by Le Bas (1962) as $Al^{iv} \times \frac{100}{Z}$ where Z = 2, is shown in Fig.6.10. It predicts that the clinopyroxenes predominantly belong to a non-alkaline type host magma. It also supports Le Bas's (op cit) suggestion that the trend of differentiation is towards decreasing Al_z and increasing TiO_2 in the non-alkaline rocks. Some of the analyses plotting into the alkaline fields in these diagrams are those of zoned cpx grains or from samples containing zoned cpx grains. This suggests that exclusion of analyses from phenocrystic cpx would result in less overlap between fields as suggested by Le Bas (1962). Despite the overlap, these plots suggest a non-alkaline and probably a tholeiitic magma as the host for the cpx. This supports the conclusion reached in Chapter four, that the Polusagi rock suite is a tholeiitic rock suite.

Further common characteristics of the Polusagi cpx with those from other non-alkaline rocks can be found. Le Bas(1962)reports that on average 70% of total Al is taken up into the tetrahedral site of cpx from non-alkaline rocks, while the percentages are 90 and almost 100 in alkaline and per-alkaline rocks respectively. It can be inferred from Fig.6.3 that on average 70% of total Al is tetrahedrally coordinated in the

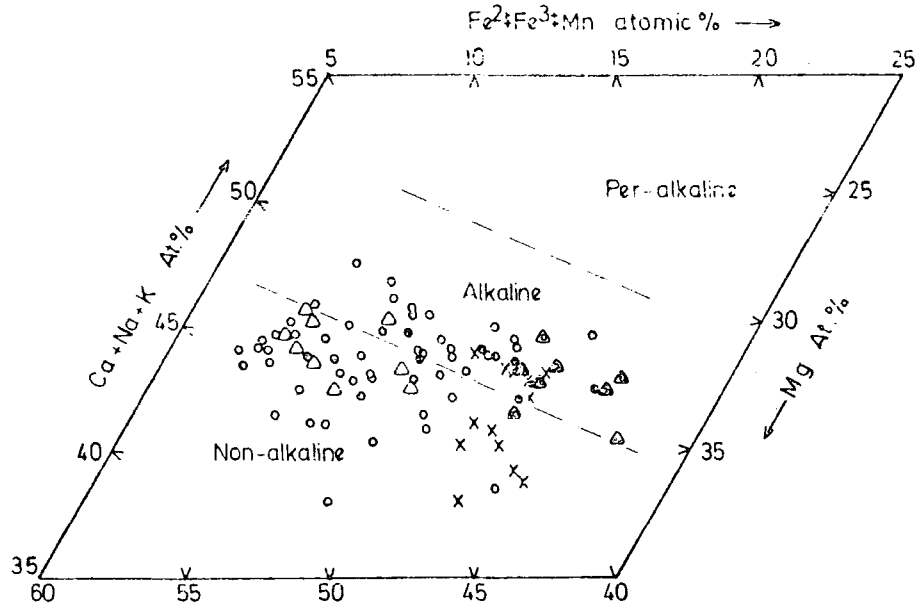


Fig.6.8. Clinopyroxene analyses plotted in the ternary diagram of Le Bas (1962). ○ : from 'MP' basalts, ⊕ : from 'MD' basalts, × : from andesites, △ : from 'MP' gabbros and ⊛ : from 'MD' gabbros.

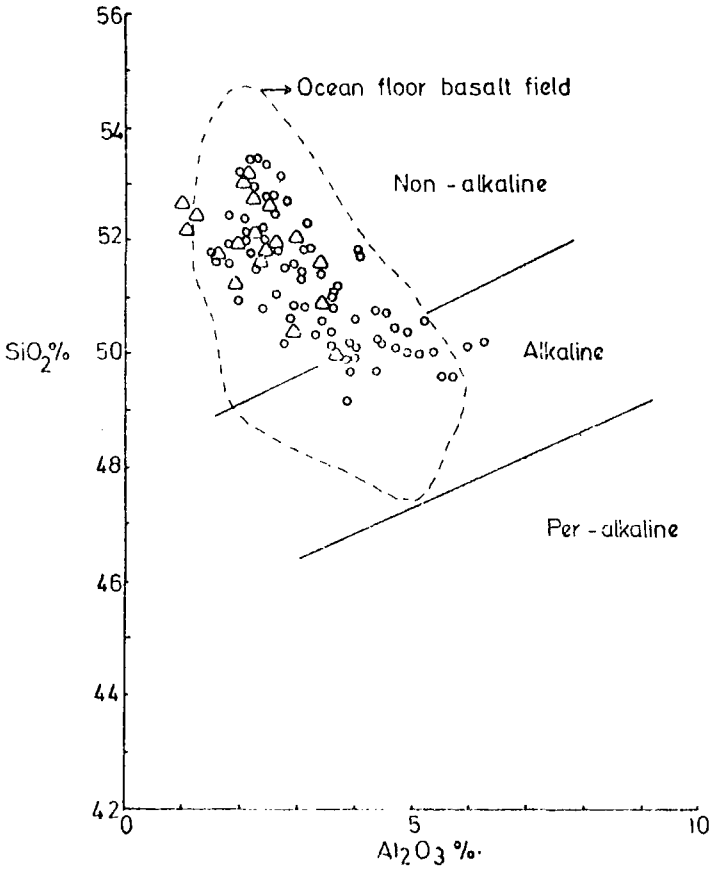


Fig.6.9. SiO_2 vs. Al_2O_3 for clinopyroxenes from volcanics (○) and gabbros(△). Solid dividing lines are after Le Bas (1962) and ocean floor basalt field after Nisbet and Pearce (1977).

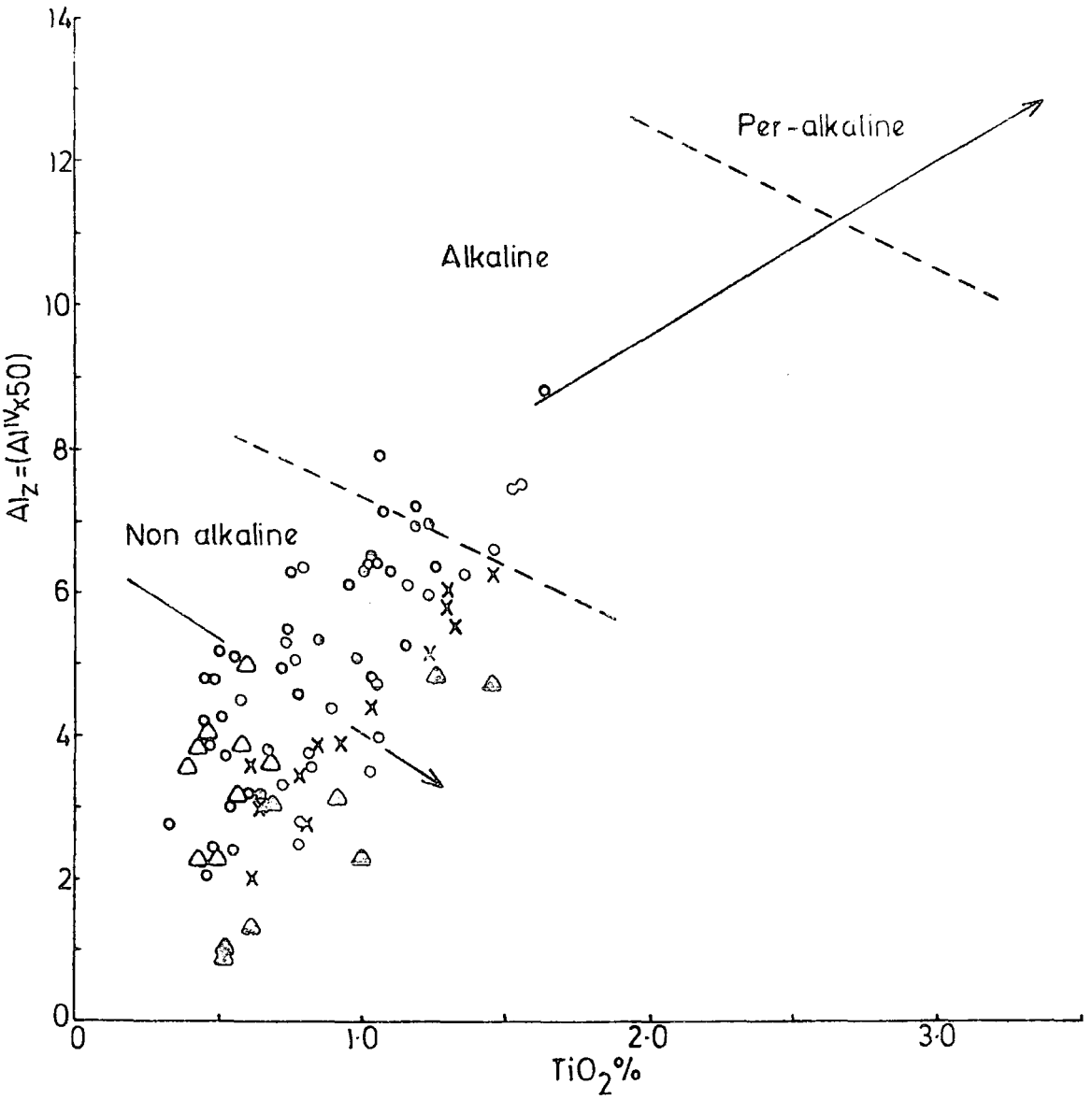


Fig.6.10 Clinopyroxene analyses plotted in Al_z vs. TiO_2 diagram of Le Bas (1962). Symbols: (o): from 'MP' basalts, (⊙): from 'MD' basalts, (×): from andesites, (△): from 'MP' gabbros and (△): from 'MD' gabbros. Arrows show general trend of variation in clinopyroxene chemistry with differentiation.

Polusagi cpx, the range being approximately 50-80%. The average soda content of the Polusagi cpx is 0.3%, the range being 0.1-0.5%, which indicates a non-alkaline magma (average 0.35%), rather than a normal-alkaline (average 0.55%) or a per-alkaline (average 0.70% magma type (Le Bas, 1962).

6.3 Amphibole

6.3.1 Mode of occurrence

Amphibole chiefly occurs in basalts and gabbros and to a lesser extent in basaltic andesites and plagiogranites that form the zone B rocks. Optically and texturally 3 types of amphiboles have been recognised:

a) Brown amphibole : This is confined to the MP gabbro samples and thought to be a late magmatic product. It is generally coarse grained and sometimes up to 2 mm across (Plate 6.3) and shows perfect amphibole cleavages. The pleochroism is strong, from light-brownish to deep-brown colours. Grain boundaries are well defined and show euhedral to subhedral forms. It sometimes has inclusions of sphene and albitised plagioclase. The only phase this type of amphibole replaces is the relict igneous clinopyroxene (Plate 6.1). It is also not in equilibrium relation with the other types of amphibole.

b) Green Amphibole : This amphibole chiefly occurs as a replacement product after the brown amphibole (Plate 6.4). However, it may also be formed replacing the relict igneous cpx. The grain size may be up to 2 mm, mimicking the brown amphibole. The grains generally show euhedral to subhedral forms. Pleochroism is strong from colourless or very light green to deeper green with or without a brownish or bluish tint.

This amphibole type is intimately related to the brown amphibole. The replacement of brown amphibole by this green variety can be observed at various stages. At the early stages of the process, the green amphibole tends to have a brownish tint, but in the advanced stages the brownish tint disappears and greenish pleochroism dominates. In some instances,

patches of relict brown amphibole are observable within the green amphibole, exhibiting optical continuity. In fact the green amphibole, at any stage of the replacement process, inherits the same cleavage patterns of brown amphibole in addition to the optical continuity. The uniform extinction and non-fibrous form of green amphibole distinguish it from the fibrous amphibole, when the pseudomorphing process of brown amphibole by the green amphibole is complete. In such grains, there may be areas where the colour is a deep bluish green.

c) Fibrous amphibole : Due to its fibrous form, the grains are anhedral but elongated with irregular ends. The size varies a great deal, largest grains may be 2 mm long and 1 mm wide. However they are usually around 0.3 to 0.7 mm long. The extinction is wavy and non-uniform. The pleochroism is strong from colourless or slightly greenish to deeper and darker green colours. Unlike some of the green amphibole grains, the fibrous amphiboles have no brownish tint.

The fibrous amphibole grows largely at the expense of chlorite and cpx (Plate 6.2). Where chlorite normally occurs in the non-amphibolised rocks of zone A, is largely taken over by the fibrous amphibole in the zone B rocks. They also replace prehnite, pumpellyite and sometimes epidote, quartz and albitised plagioclase.

Amongst all the amphibole types described above, the fibrous variety is the most common one occurring in the amphibolised rocks. Its abundance increases from sub-zone B_1 to B_2, and in the latter case, it dominates the rocks together with albite.

6.3.2 Chemistry

6.3.2.1 Introduction

56 amphibole analyses (12 brown, 15 green and 29 fibrous types) are presented in Appendix IV.2.2. In the calculation of the standard amphibole formula, the following general procedure is followed : 1) Tetrahedral site

(Z) occupancy = 2.000, includes Si, then Al, then Fe^{3+}; 2) Y site = 5.000, includes excess Al, Fe^{3+} from Z site then Ti, Mg, then Fe^{2+}, then Mn; 3) X (M_4) site = 2.000, includes excess Fe^{2+}, Mn from Y site, then Ca, then Na; 4) A site = 0-1.000, includes excess Na from M_4 site, then K.

Water determination can not be made by microprobe which also returns total Fe as Fe^{2+}. The Fe^{3+}/Fe^{2+} ratio is important in the amphibole classification and a correct knowledge of Fe^{3+} proportion is essential, for instance, in the correct calculation of Na in M_4 site. As will be discussed in section 6.3.3.2, the Na (M_4) content of amphiboles is believed to be pressure dependent.

Therefore, in this study, in order to estimate the Fe^{3+}/Fe^{2+} ratio, perfect amphibole stochiometry was assumed i.e. exactly 2 hydroxyl ions in the basic amphibole formula $A_{0-1}X_2Y_5Z_8O_{22}(OH)_2$, and the analyses were calculated on the basis that total number of oxygen anions combined with the total number cations must be 24 and any deficiency from O=24.000 was made up by coverting Fe^{2+} to Fe^{3+}. The main objection to this method may be that it ignores the possibility of hydrogen deficiency such as occurs in oxyamphiboles which is balanced by high Fe^{3+}, or due to halogen replacement of the hydroxyl ions. However the occurrence of oxyamphibole is relatively rare and many metamorphic hornblendes do not contain sufficient Fe^{3+} to balance their apparent hydrogen deficiency in the manner postulated for oxyhornblendes (Binns, 1965).

Some of the Fe^{3+}/Fe^{2+} ratios obtained by this method were also compared with those obtained using an unpublished computer program developed by R.Phillips (1972, personal communication). The agreement is satisfactory and in the case of brown amphiboles, it may even be perfect.

However, in order to have a better insight into the problem, the basic amphibole formula is also calculated on water-free basis to 23 oxygen, assuming 2 (OH) and total Fe = Fe^{2+}. In Table 6.2 the results by the two

TABLE 6.2

	BROWN AMPHIBOLE		GREEN AMPHIBOLE		FIBROUS AMPHIBOLE	
	24 O; H_2O and Fe^{3+} estimated	23 O, Total Fe= Fe^{2+}	24 O, H_2O and Fe^{3+} estimated	23 O Total Fe= Fe^{2+}	24 O, H_2O and Fe^{3+} estimated	23 O total Fe= Fe^{2+}
Analyses	P282 1B	P282 1B	P282 1A	P282 1A	P276 1D	P276 1D
SiO_2	44.80	44.80	47.47	47.47	50.25	50.25
TiO_2	3.20	3.20	1.33	1.33	0.43	0.43
Al_2O_3	9.36	9.36	6.82	6.82	4.08	4.08
Fe_2O_3	2.93	14.49	4.68	16.33	3.90	20.16
FeO	11.85		12.12		16.65	
MnO	0.17	0.17	0.23	0.23	0.32	0.32
MgO	12.00	12.00	12.12	12.12	10.29	10.29
CaO	10.70	10.70	11.13	11.13	11.19	11.19
Na_2O	2.64	2.64	1.81	1.81	0.55	0.55
K_2O	0.24	0.24	0.16	0.16	0.07	0.07
H_2O^+	2.04	-	2.04	-	2.02	-
Total	99.94	97.61	99.91	97.40	99.74	97.33
Atom.prop.						
Si	6.588	6.637	6.978	7.059	7.463	7.535
Al^{iv}	1.412	1.363	1.022	0.941	0.537	0.465
Al^{vi}	0.212	0.272	0.160	0.254	0.178	0.256
Ti	0.354	0.357	0.147	0.149	0.048	0.049
Fe^{3+}	0.324	-	0.518	-	0.434	-
Mg	2.630	2.650	2.656	2.687	2.277	2.299
Mn	0.022	-	0.029	-	-	-
$Fe^{2+}(M_4)$	-	0.073	-	0.120	0.007	0.132
$Mn(M_4)$	-	0.022	-	0.030	0.040	0.041
Ca	1.686	1.699	1.753	1.773	1.780	1.797
$Na(M_4)$	0.314	0.206	0.247	0.077	0.156	0.030
Na(A site)	0.438	0.539	0.268	0.436	-	0.128
K(A site)	0.044	0.045	0.031	0.031	0.013	0.013

methods are compared for representative amphibole analyses for each type of amphibole.

It is important to note that the method (1) followed in this study tends to maximise the Fe^{3+}, while the method (2) where total Fe=Fe^{2+}, assumes no Fe^{3+} present. Comparison shows that method (1) produces lower cation ratios, therefore, there is slightly more Al in Z site; less divalent ions (Fe and/or Mn), but more Na in the X site; hence less A-site occupancy than those calculated by method (2). Another interesting observation is that method (1) may allocate up to 0.15 Fe^{3+} atoms into the Z site (in the hornblendes and the green amphiboles only), while method (2) calculations avoid the need of allocating Fe^{3+} into Z, but they considerably increase the amount of Fe^{2+} and Mn in the X site.

In the following pages determinations made by method (1) will be used, however, references will be made to those by method (2) where necessary.

6.3.2.2. Nomenclature

Figs.6.11 and 6.12 are commonly used amphibole classification diagrams. All the amphiboles, having (Ca+Na) in the X site $\geqslant$ 1.34 and Na in the X site $<$ 0.67, are also plotted in Leake's (1978) classification system for the calcic-amphibole group (Figs.6.13 and 6.14). The fibrous and green amphiboles have Na+K in the X site $<$ 0.50 and Ti $<$ 0.50 while they are $\geqslant$ 50 and $<$ 0.5 for the brown amphiboles respectively. It will be shown in a proceeding section (6.3.2.4) that it is most likely that the calculated amounts of Fe^{3+} is more or less correct and there is much Fe^{3+} exceeding the amount of Al^{vi} (average = 0.22) in the amphiboles. Therefore, the brown amphiboles are plotted in a separate classification diagram of Leake(1978)than for the fibrous and green amphiboles (Fig. 6.14).

Brown amphibole : Considering the Figs. 6.11 and 6.12, it is evident that these primary amphiboles have a considerable chemical variation,

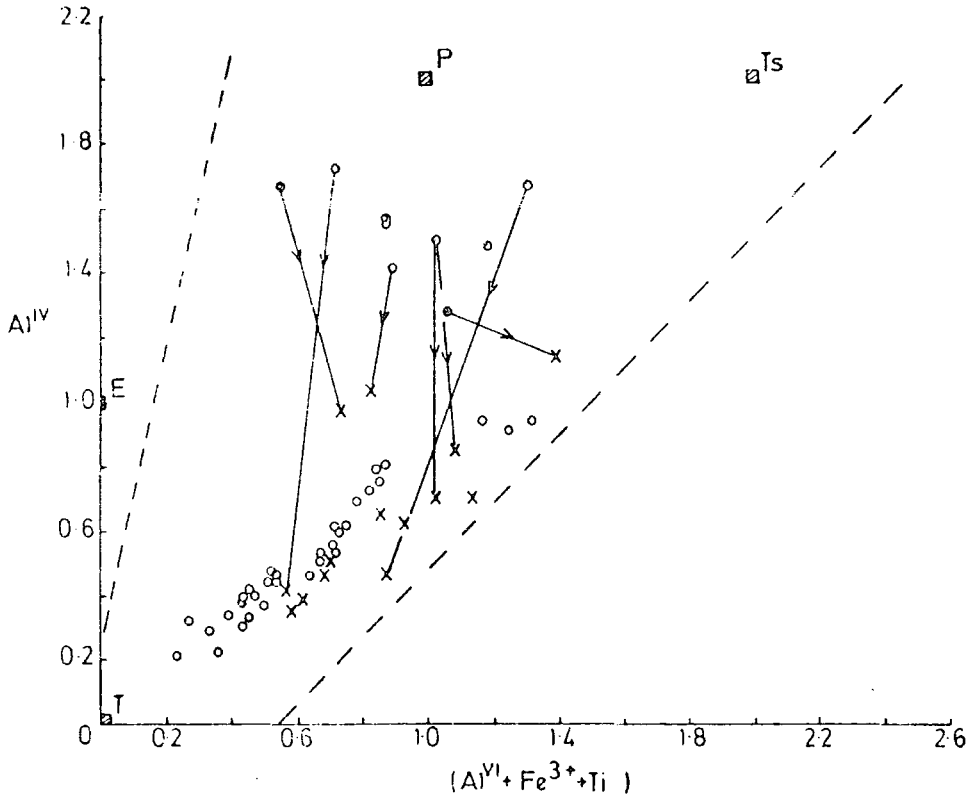


Fig.6.11 Al^{iv} vs. $(Al^{vi} + Fe^{3+} + Ti)$ classification diagram for amphiboles. ⊙: brown amphibole, x: green amphibole and o: fibrous amphibole.

P = Pargasite, Ts = Tschermakite, E = Edenite and T = Tremolite. Tie-lines join the related brown and green amphiboles.

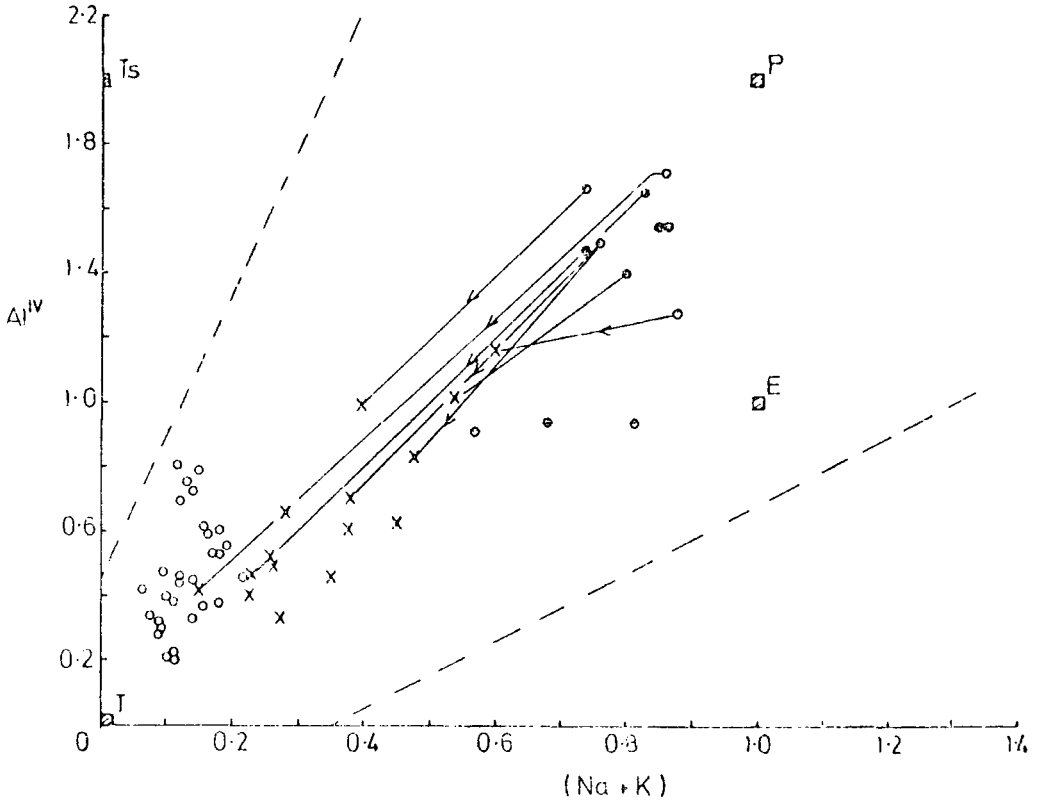


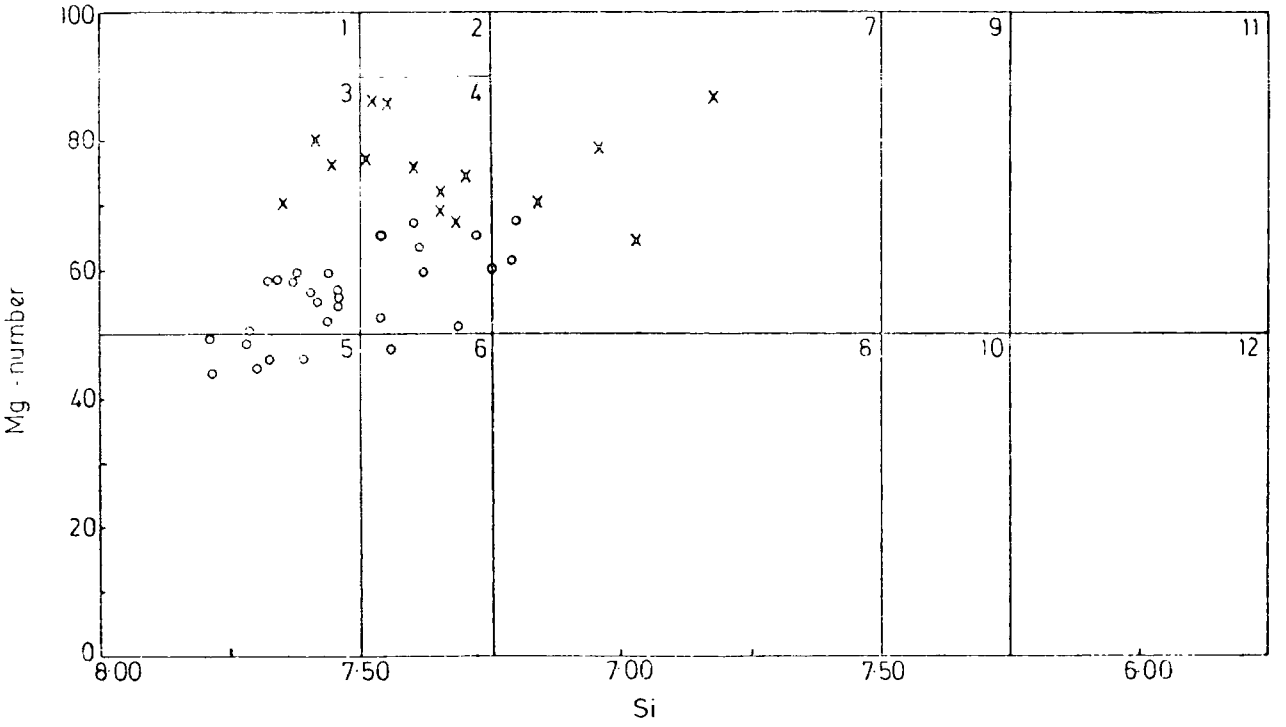
Fig.6.12 Al vs. (Na+K) classification diagram for amphiboles. Symbols as above.

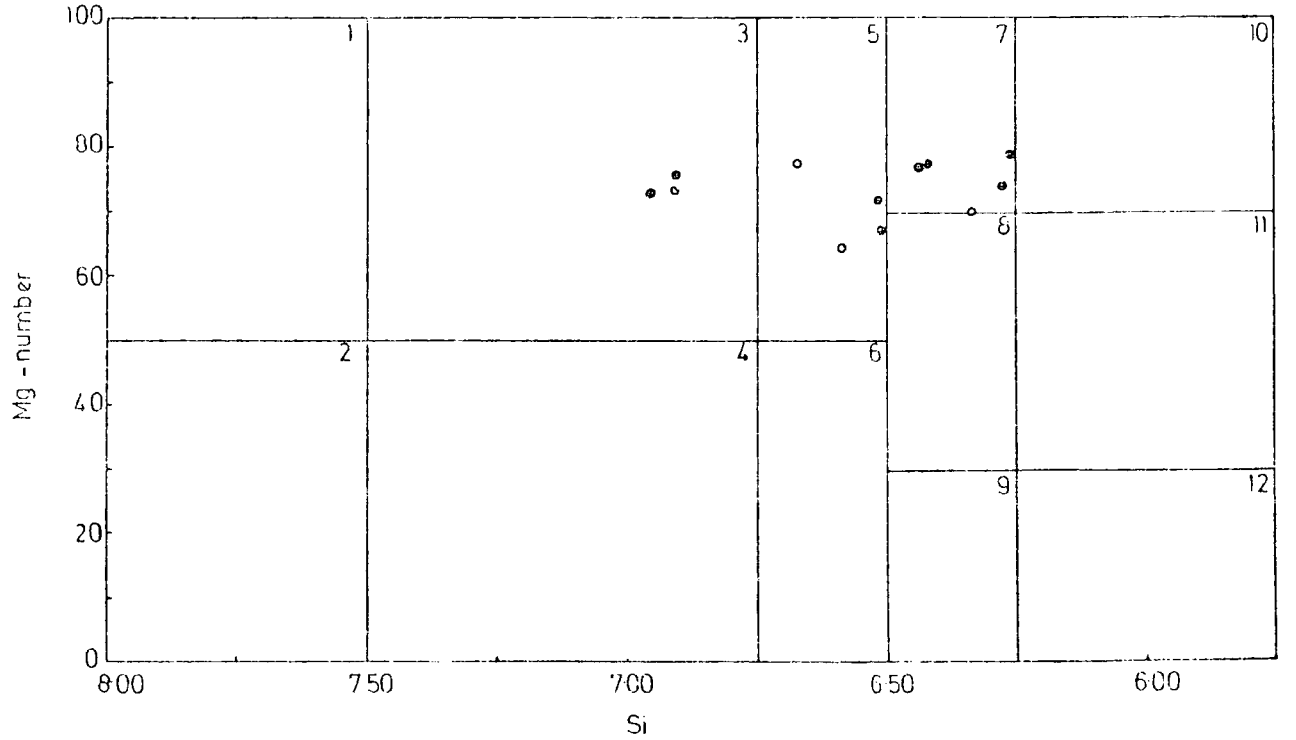
extending from edenite to pargasite and common hornblende. Similarly, Leake's scheme (Fig.6.14) identifies these amphiboles in a range, varying from magnesio-hastingsitic hornblende to edenitic hornblende, 3 analyses falling into the edenite field. Thus, it seems that no single name would be sufficient to cover all the brown amphibole analyses. But generally they are edenitic to hastingsitic hornblendes. The conclusion that these hornblendes are hastingsitic rather than pargasitic is also indicated by an average $\frac{100 \times Mg}{Mg+Fe^{2+}+Fe^{3+}+Mn}$ value of 63 with a range from 57 to 70 (Deer et al, 1974; Fig. 64, p.172).

Fibrous Amphibole: It is apparent from the classification diagrams that these amphiboles are best described as belonging to the tremolite-ferroactinolite series. In Leake's classification diagram (Fig. 6.13), which takes a Si value of 7.50 to separate the tremolite-ferroactinolite series from hornblendes, the fibrous amphiboles are classified as actinolite to actinolitic hornblendes. However, in this study a Si value of 7.20 is preferred as the boundary between tremolite-ferroactinolite series and hornblendes following Miyashiro (1973). Then all fibrous amphiboles are classed as belonging to the tremolite-ferroactinolite group.

To further classify the group, Leake (1978) uses Mg-numbers of amphiboles $\frac{Mg \times 100}{Mg + Fe^{2+}}$ at 50 and 90 to distinguish ferroactinolites, actinolites and tremolites respectively, while Deer et al(1974,Fig.59, p.164) takes $\frac{Mg \times 100}{Mg+Fe^{2+}+Fe^{3+}Mn}$ values at 20 and 80 respectively. According to the Leake's scheme, most of the Polusagi fibrous amphiboles, and according to Deer et al's scheme all of them, are actinolites.

Green amphibole : As discussed in the next section, the chemistry of these amphiboles falls between the other two types. This is also clearly


100
80
60
40
20
0
Mg - number
1
2
3
4
5
6
7
8
9
10
11
12
8·00
7·50
7·00
6·50
6·00
Si


100
80
60
40
20
0
Mg - number
1
2
3
4
5
6
7
8
9
10
11
12
8·00
7·50
7·00
6·50
6·00
Si

demonstrated in the classification diagrams referred to presently. The tie lines drawn in Figs. 6.11 and 6.12 connect the hornblendes and their direct alteration products : the green amphiboles. Where the alteration of the hornblendes is at an advanced stage (as observed in thin sections), the green amphiboles are affiliated to the actinolites and where this is not so, their chemistry and thus nomenclature, occupies fields gradational from the hornblendes to the actinolites. Therefore, a single descriptive name for this type of amphibole will not be used,but simply referred to as the 'green amphibole' hereafter.

6.3.2.3 Chemical variation

Chemical variations in all amphiboles against Mg-number are presented in Fig.6.15. The tie lines are between green amphiboles and their parental brown hornblendes. The following features are apparent:

1) Chemically the actinolites are very different from hornblendes. Actinolites are distinctly richer in Si, total Fe, and Mn, but equally poorer in Al, Na and Ti. There is no systematic difference in Ca. Hornblendes, on average, are richer in Fe^{3+}.

2) Progressive alteration of hornblende into the green amphibole involves enrichment in Si, Fe^{3+} and Mn and depletion in Al, Na, Ti and to a lesser extent Ca. Therefore the alteration of hornblende is towards acquiring an actinolitic chemistry.

Mg, and Fe^{3+} contents of the green amphiboles seem to move away from the actinolite compositional field while altering from the hornblendes; acquiring higher Mg-numbers and Fe^{3+}. This is certainly an effect of the host rock chemistry discussed in section 6.3.3.1, since the host rocks for the green amphiboles have very high Mg-numbers, 68 to 80, while the Mg-numbers of the host rocks for actinolites vary from 40 to 72. The increased Fe^{3+} contents of the green amphiboles indicate a stronger oxidising environment during metamorphism than was prevailing during the

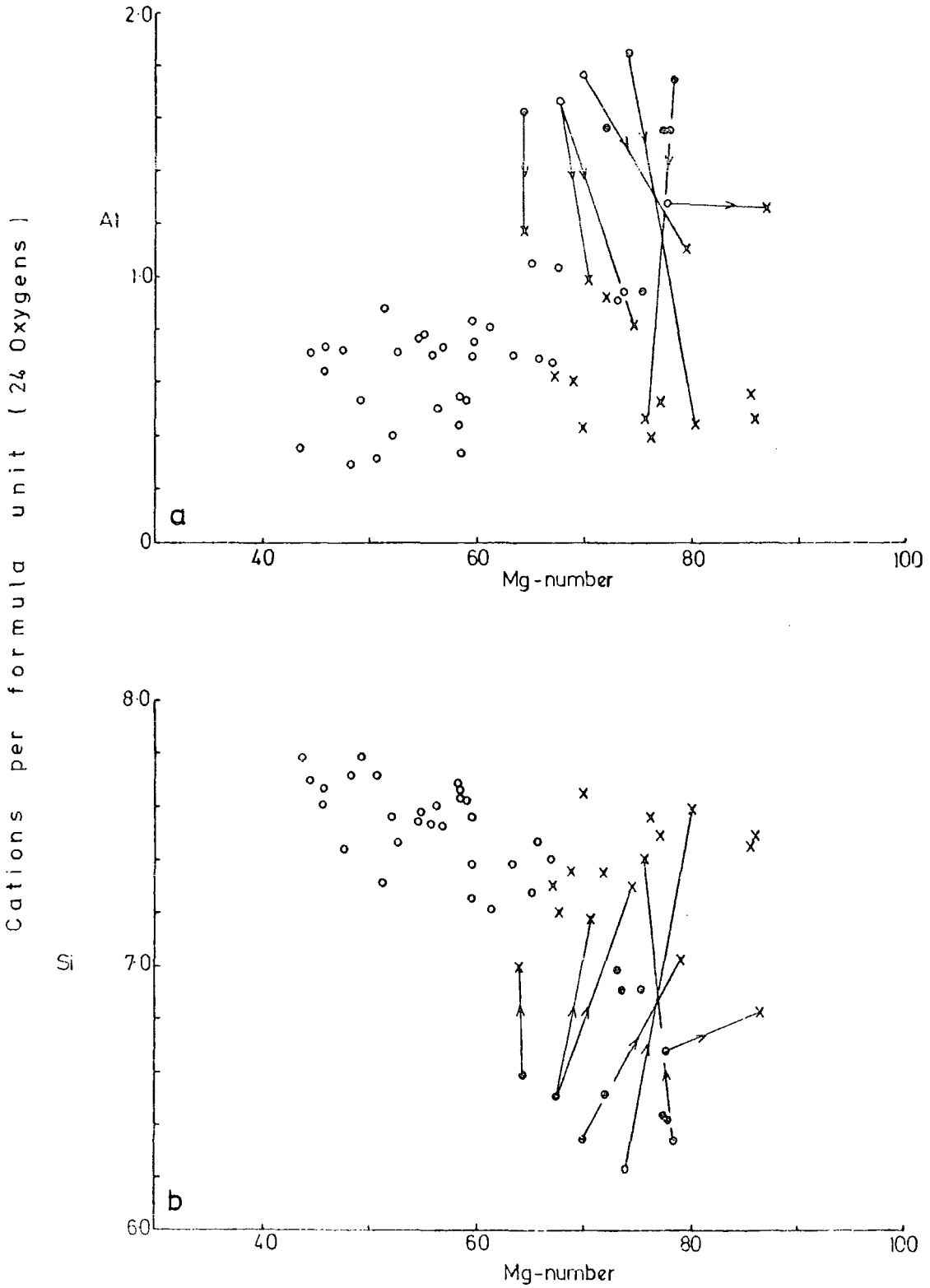
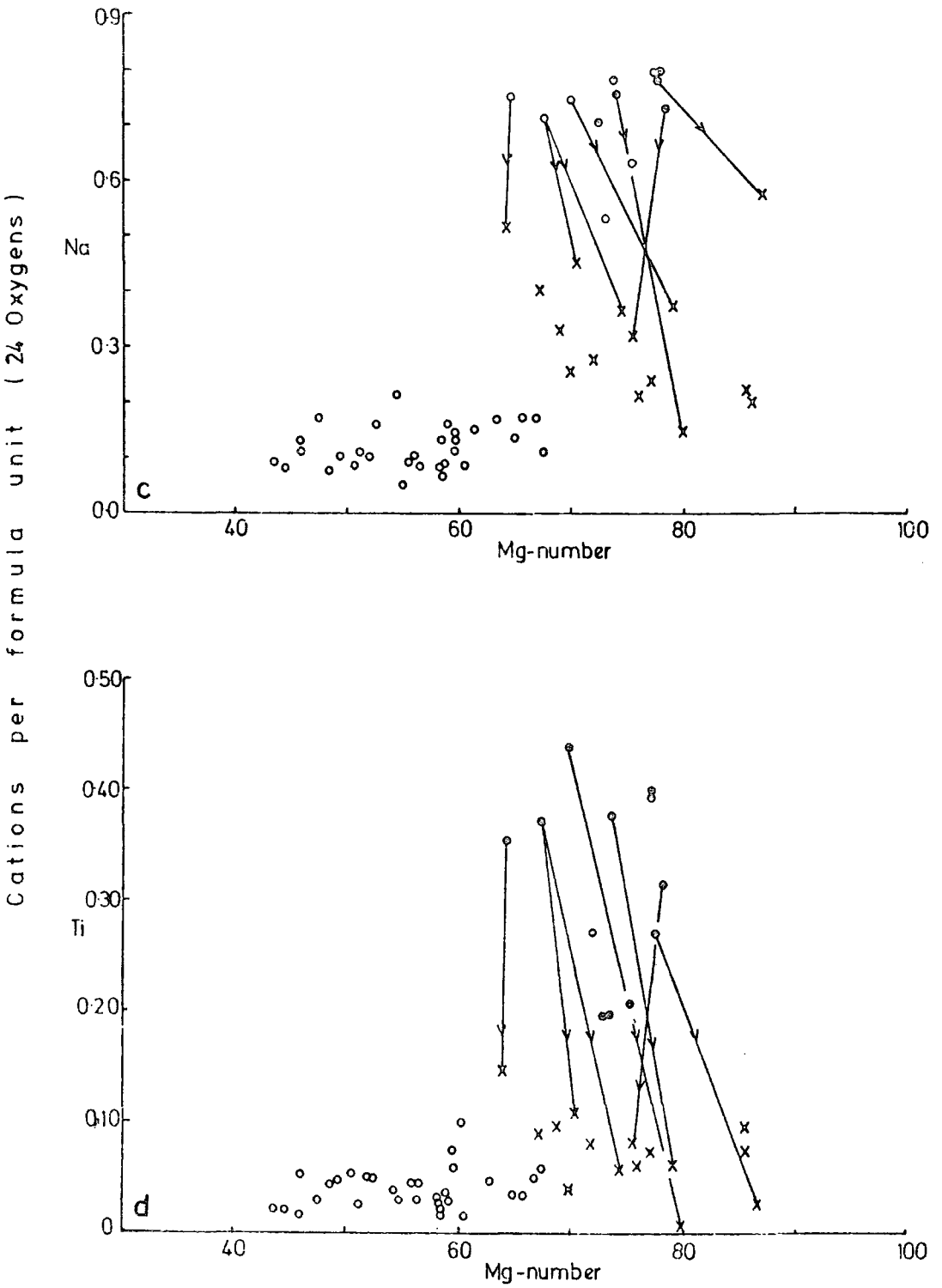
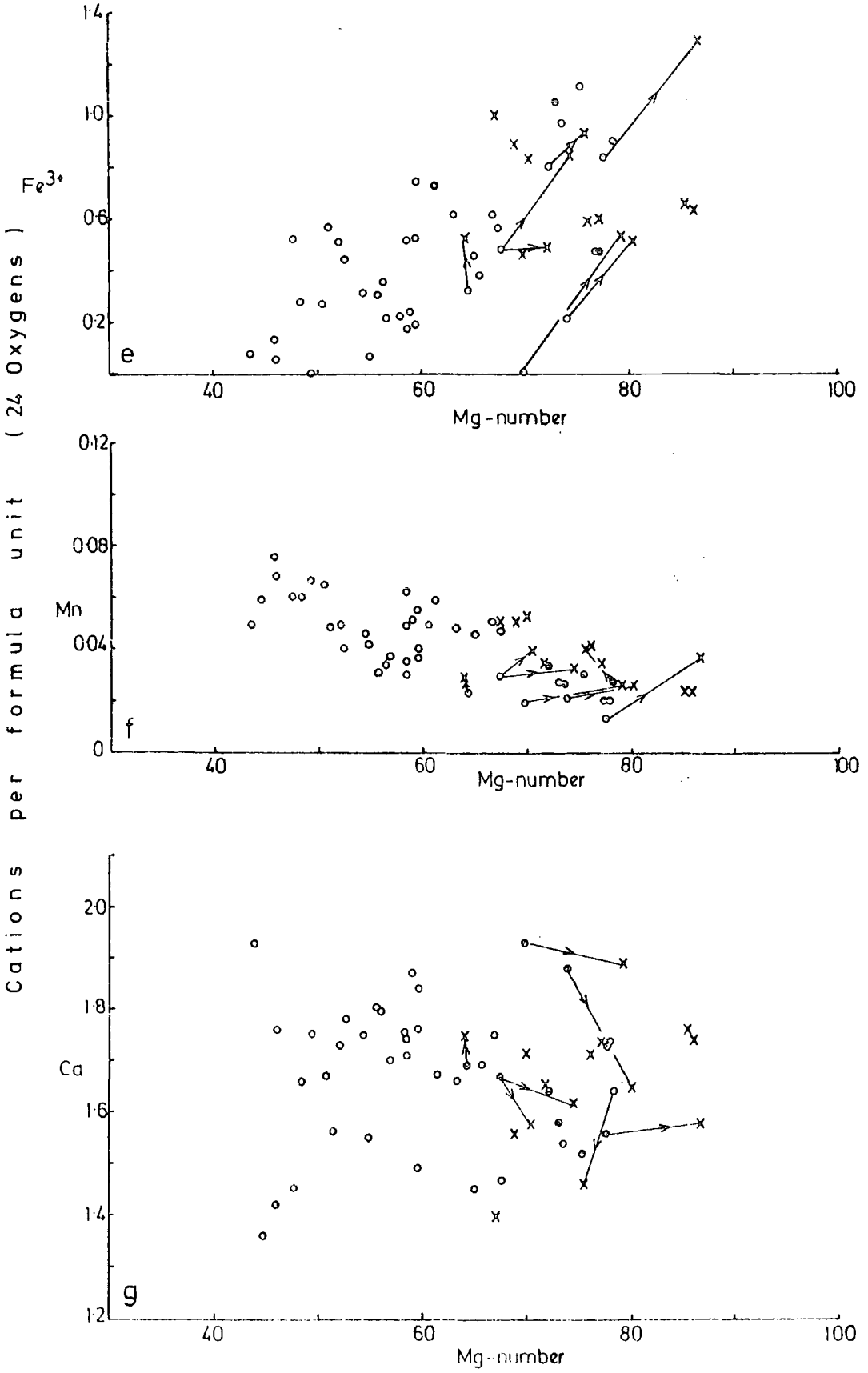


Fig.6.15 Chemical variation in amphiboles with Mg-number : a) Al, b) Si, c) Na, d) Ti, e) Fe^{3+}, f) Mn and g) Ca.

o :actinolite, x : green amphibole and ⊙ : brown amphibole. Tie lines join related hornblende and green amphibole analyses.


Cations per formula unit (24 Oxygens)
Na
0·9
0·6
0·3
0·0
c
40
60
80
100
Mg-number
Ti
0·50
0·40
0·30
0·20
0·10
0
d
40
60
80
100
Mg-number


Cations per formula unit (24 Oxygens)
Fe3+
1·4
1·0
0·6
0·2
e
40
60
80
100
Mg-number
0·12
0·08
Mn
0·04
0
f
40
60
80
100
Mg-number
2·0
1·8
Ca
1·6
1·4
1·2
g
40
60
80
100
Mg-number

crystallisation of magmatic hornblendes.

3) In actinolites and hornblendes Fe^{3+}, in general, decreases while Si and Mn increase with decreasing Mg-numbers. Al,Ca,Na and Ti do not exhibit any systematic change in any of the amphibole types.

It is of interest to note that the Si trend, in relation to decreasing Mg-number, is qualitatively very similar to the trend of the same component exhibited in the host rocks with advancing fractionation (Chapter five, Fig.5.5).

6.3.2.4 Crystal chemistry

In half the hornblendes, green amphiboles and a couple of actinolites, the available Al is not totally sufficient to make up the Z site to 8.000, and up to 0.15 atoms of Fe^{3+} may be assigned to the Z site. The Al^{iv}/Al^{vi} ratios are high; >7 in the hornblendes and vary from around 1 to over 8 in the actinolites. Al^{iv} and Al^{vi} values range from 0.9 to 1.7 and from 0 to 0.2 in the hornblendes and from 0.2 to 0.8 and from 0 to 0.4 in actinolites respectively. The presence of Fe^{3+} in the Z site can be disputed however, in any case, what is unambiguously clear is that especially in the hornblendes much of the iron must be present in ferric state in the Y site compensating for the tetrahedral Al and tetrahedral Fe^{3+} when present. Since the chemistries of the actinolites and the hornblendes are different, they will be examined separately.

Actinolites : The dominant incorporation of total Al into the Z site is largely compensated for by the tschermakite-ferritschermakite type coupled substitution: $Al^{iv} + (Al^{vi},Fe^{3+},Ti) \rightleftharpoons Si + (Mg,Fe^{2+})$ (Fig.6.11). As Fig. 6.16 shows, however, this type of reaction is not totally sufficient to compensate for the Al^{iv} and a small amount of deficiency is apparent. As the A site is virtually vacant in actinolites the edenitic charge balancing substitution ($Na+Al^{iv} \rightleftharpoons \square+Si$) could not be operative. Instead,a glaucophane-riebeckite type substitution [$Na+(Al^{vi},Fe^{3+},Ti) \rightleftharpoons Ca+(Mg+Fe^{2+})$] is indicated by Fig.6.17 to be responsible in maintaining the charge

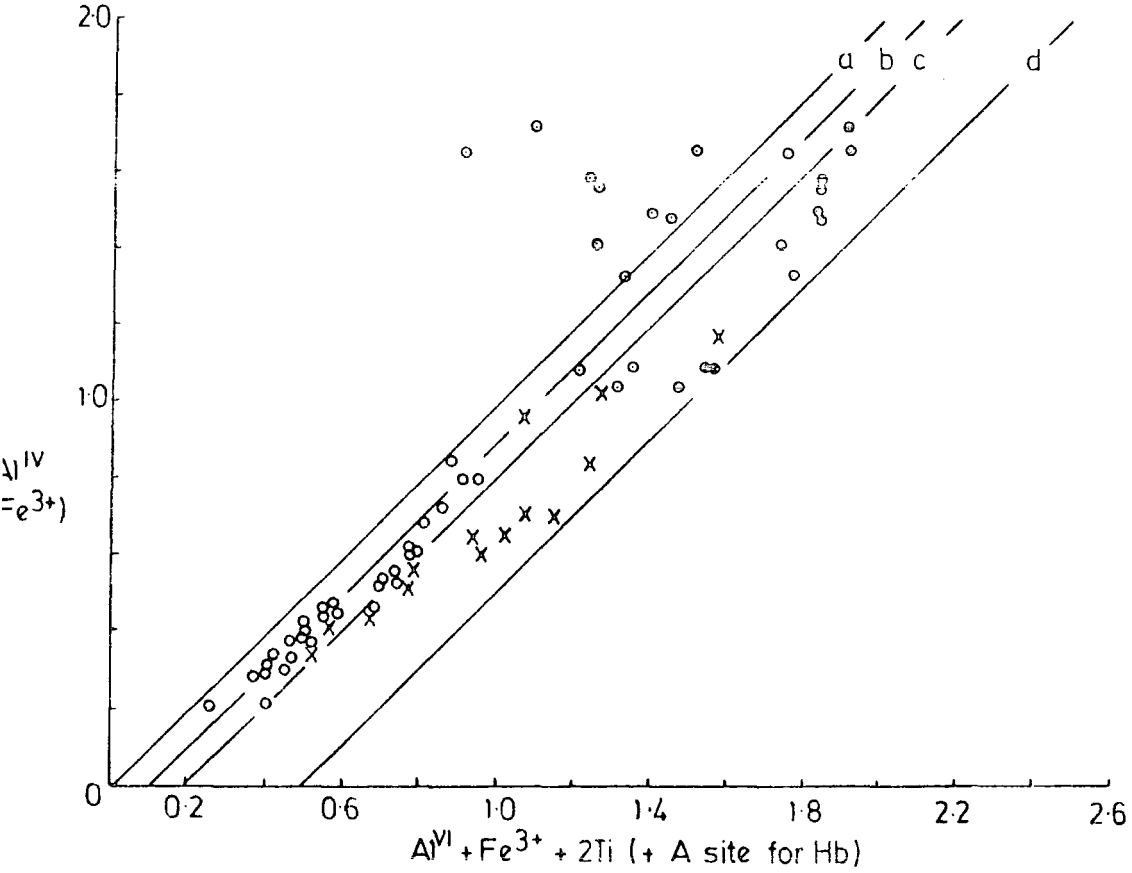


Fig.6.16 Al^{iv} vs. ($Al^{iv}+Fe^{3+}+2Ti$) in amphiboles (all cations per formula unit on a basis of 24 oxygens). o : Actinolites, x : green amphibole, ⊙ : brown hornblende and ● : A site occupancy added to ($Al^{iv}+Fe^{3+}+2Ti$) for brown hornblendes. Solid lines: $[Al^{vi}+Fe^{3+}+Ti$(+A site for hornblende)$]-[Al^{iv}(+Fe^{3+})]=$ a) 0.00, b) 0.10, c) 0.20 and d) 0.50.

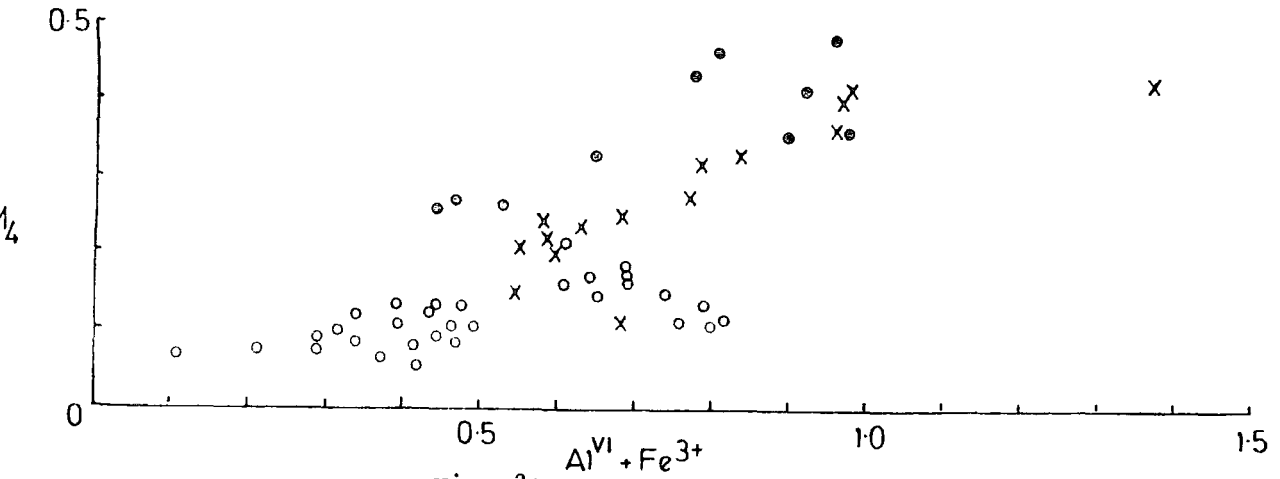


Fig.6.17 Na_{M4} vs. ($Al^{vi}+Fe^{3+}$) in amphiboles (all cations per formula unit, 24 oxygens). Symbols as above.

balance.

Hornblendes : These amphiboles have A site occupancies varying from 0.1 to 0.7 and averaging to 0.5. The diagrams used presently for actinolites indicate that in addition to the major ferritschermakite-tschermakite and minor glaucophane-riebeckite type coupled substitutions, hornblendes also exhibit considerable edenitic substitution. Richteritic substitution, $Na_A + Na_{M4} \rightleftharpoons \square + Ca$ is discredited as the partitioning of Na into the A and X sites is not positively correlated (Fig.6.18). It is interesting that the A site occupancy seems to be positively correlated with Ti (Fig. 6.19) and not with $Al^{vi} + Fe^{3+}$ in the Y site which suggests a substitution of a type : $Na_A + Ti \rightleftharpoons \square + (Mg, Fe^{2+})$.

The green amphiboles, in general, show all the above named substitution reactions to various degrees depending on their composition, whether they are closer to the actinolites or the hornblendes.

That the substitution reactions accounted for above satisfy the charge balance requirements of the amphibole chemistry is demonstrated in Fig.6.20. The plot is based on the assumption that any deficiency due to the tschermakite-ferritschermakite type substitution is balanced by the charge difference between edenitic and glaucophane-reibeckite type coupled substitutions i.e. $(Al^{vi} + Fe^{3+} + 2Ti)_Y - (Al^{iv} + Fe^{3+})_Z = (Na_{M4}$ - A site occupancy) or (Y-Z)-(X-A) = 0. The plot shows that the charge balancing is very good in hornblendes, good in actinolites and fair in green amphiboles. The departures from the ideal situation is created by cation deficiencies in the X sites, where the occupancy varies from 1.95 to 2.00 for the actinolites and the green amphiboles.

The extent of replacement reaction $Mg \rightleftharpoons Fe^{2+}$ is demonstrated by the variations of Mg-numbers in the range 43-68 in the actinolites, 64-74 in the hornblendes, and 64-87 in the green amphiboles.

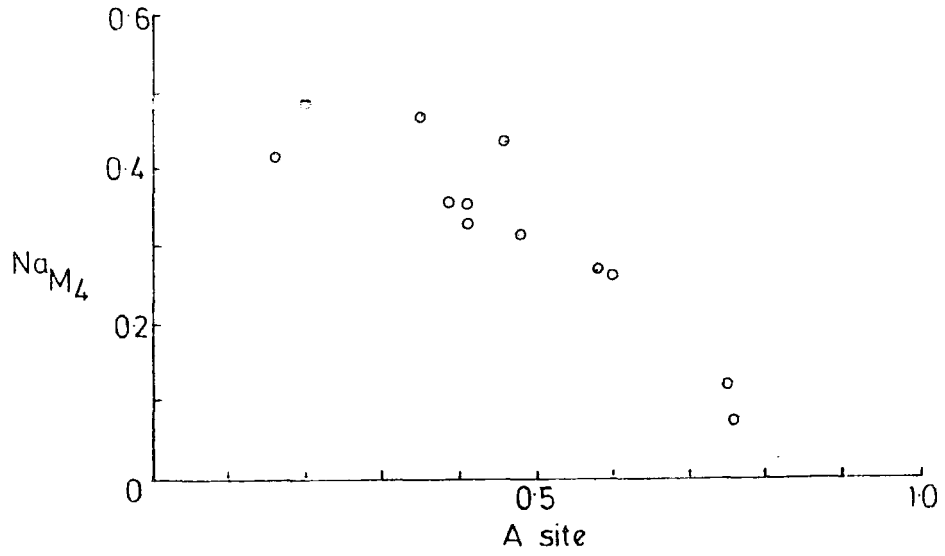


Fig.6.18 Na_{M_4} vs. A site occupancy in brown hornblendes (all cations per formula unit, 24 oxygens).

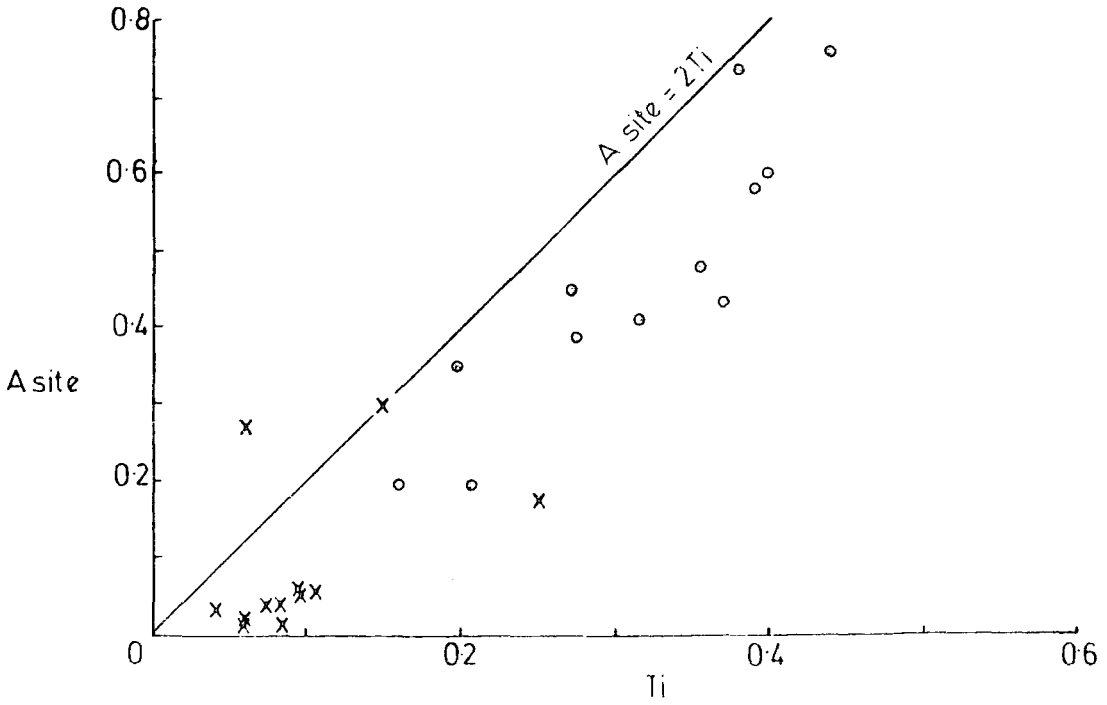


Fig.6.19. A site occupancy vs. Ti in brown hornblendes (o) and green amphiboles(x) (all cations per formula unit, 24 oxygens).

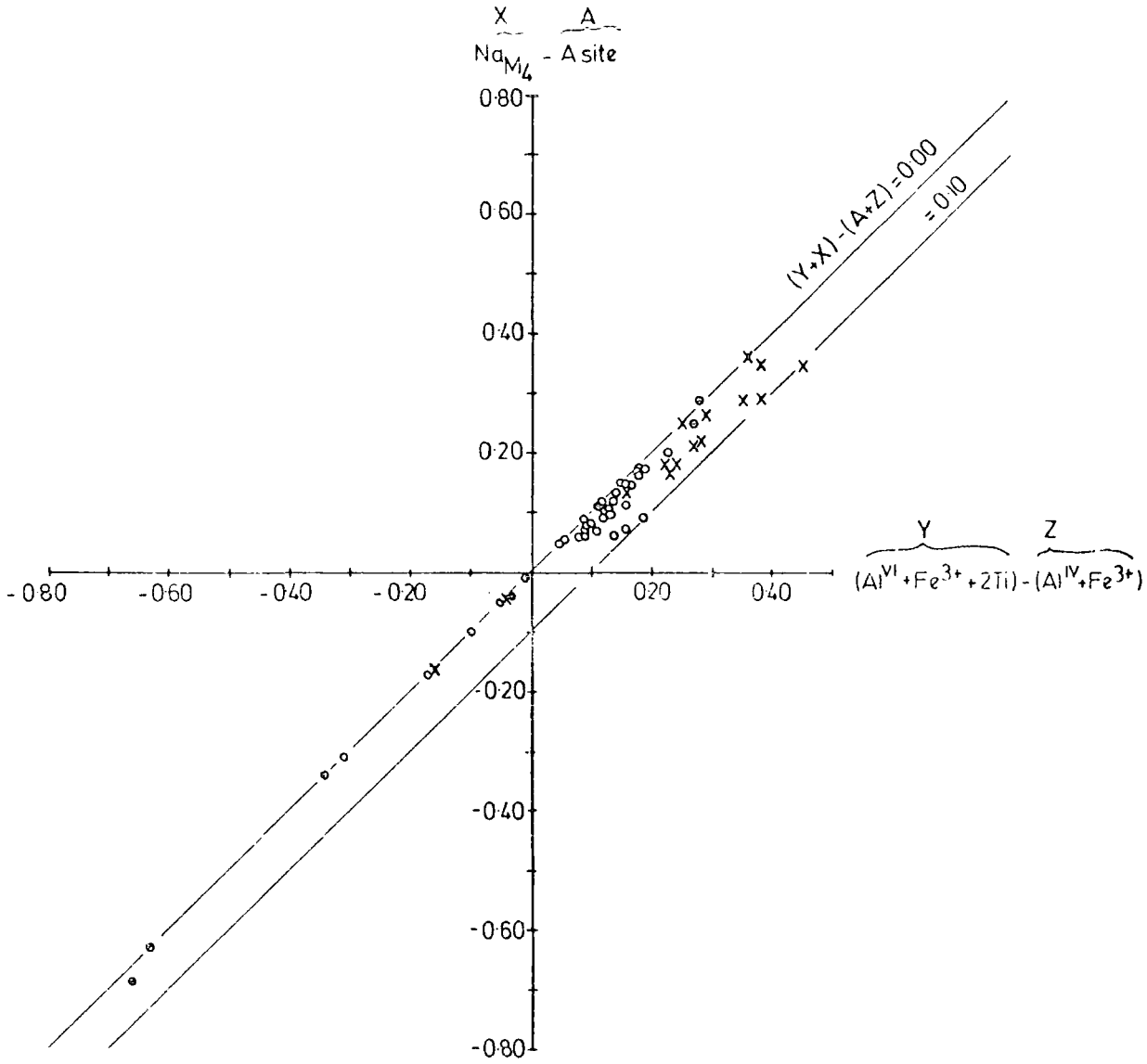


Fig.6.10 Diagram showing the charge balancing as a result of coupled substitution reactions in amphiboles. Ideally (Y+X)-(A+Z) = 0.00. o :brown hornblendes, o : green amphiboles and x : actinolites.

6.3.3. Factors controlling the chemical variations

6.3.3.1. Chemical factors

It was noted previously (Section 6.3.2.3) that chemical variation of Si in the actinolites and hornblendes, in relation to decreasing Mg-number, is positively correlated with the same element variation in the parent rocks. Fig.6.21 is a plot of the host rock Mg-number against the amphibole Mg-number and demonstrates a positive correlation. Mn falls in sympathy with iron both in the amphiboles and the host rocks. Therefore, it is concluded that variations of Si, Mg, total Fe and Mn in the amphiboles are largely controlled by the host rock compositions. Similar findings are reported, for example, by Shido and Miyashiro (1959) and Binns (1965).

However, the host rock chemistry does not seem to affect the concentrations of Ti,Al,Na and Ca in the amphiboles, thus, factors other than chemical may be operative.

6.3.3.2 Physical factors

Temperature and pressure of formation may have some bearings on the distributions and concentrations of Ti, Al and Na. It is recognised by many workers that partitioning of Al into the octahedral and tetrahedral sites; partitioning of Na into the X and A sites and the mere concentrations of Ti in amphiboles are pressure and/or temperature dependent and may serve as indicators of the physical conditions of formation e.g. grade of metamorphism.

Titanium : Ti content of metamorphic amphiboles steadily increases with increasing grade of metamorphism (Shido and Miyashiro,1959; Binns, 1965; Cooper and Lovering,1970; Raase, 1974). Rising Ti, and also the amount of Fe^{3+}, reflect themselves on the metamorphic hornblendes as changing colours from blue-green to green to brownish, for example in the Willyama complex amphibolite-granulite facies described by Binns (1965). Raase (1974) provides the following maximum Ti values (as cations per formula unit) for hornblendes of various metamorphic grades:

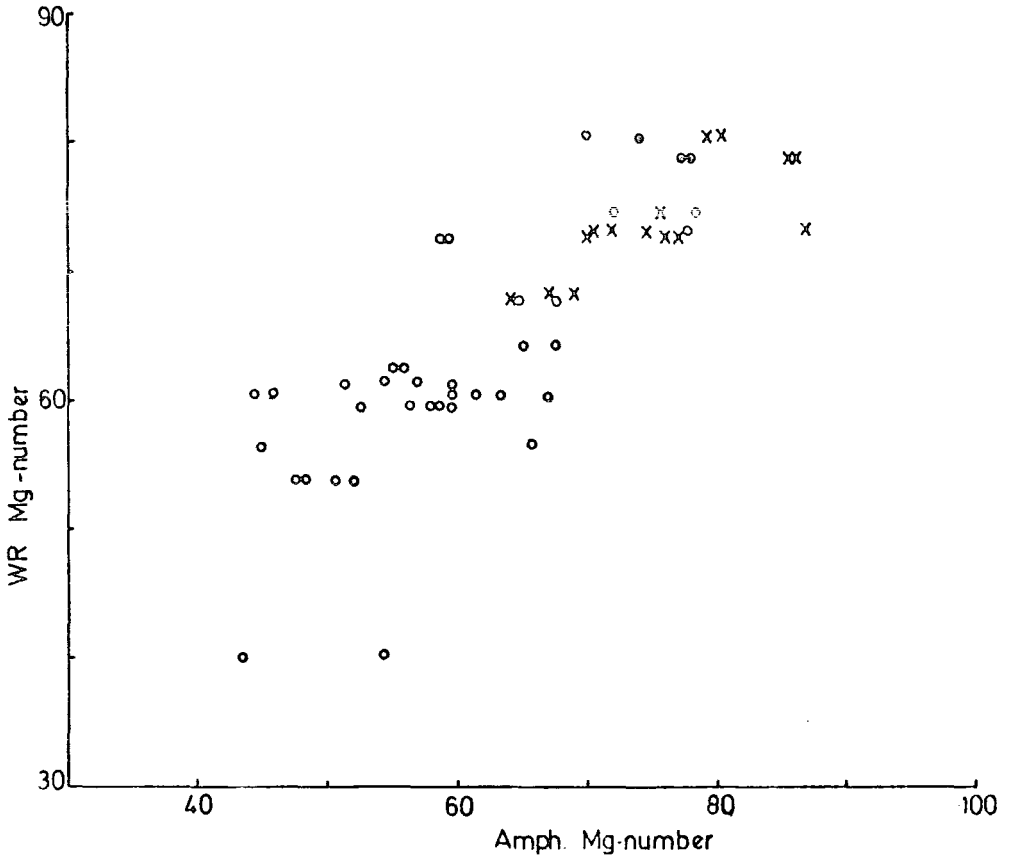


Fig.6.21 Whole-rock Mg-number vs. amphibole Mg-number.
⊛ : brown hornblendes, x : green amphiboles
and o : actinolites.

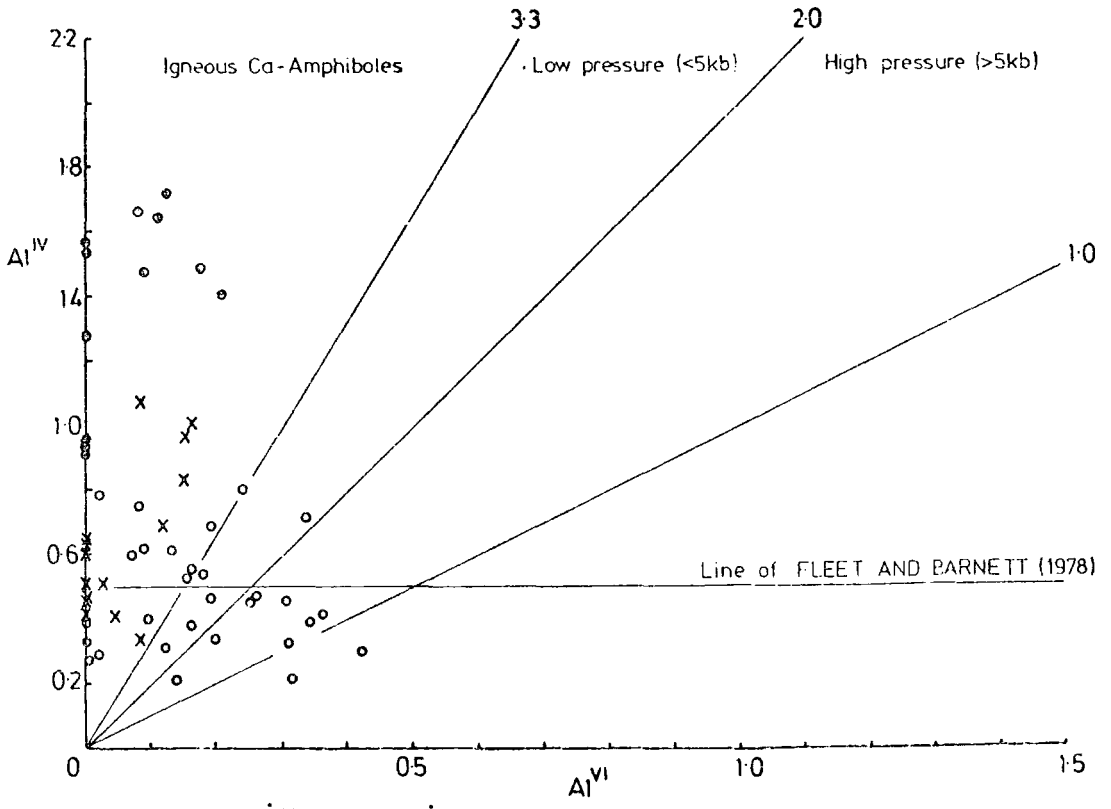


Fig.6.22 Al^{iv} vs. Al^{vi} in amphiboles. Defined areas, on the basis of Al^{iv}/Al^{vl} ratios, are after Fleet and Barnett (1978). Symbols as above.

1) Greenschist - amphibolite transition facies - 0.08

2) Low-grade amphibolite facies - 0.13

3) High-grade amphibolite facies - 0.22

4) Hornblende-granulite facies - 0.29

Raase also states that the amount of Ti is largely a measure of temperature, rather than pressure.

The Polusagi actinolites contain up to 0.08 cations of Ti per formula unit, excluding 1 analyses which has 0.10, while the hornblendes may have up to 0.44 Ti. Therefore, the Ti contents suggest that metamorphic grade may be up to greenschist-amphibolite transition facies and that the hornblendes formed at temperatures above those attained by hornblende-granulite facies.

Aluminium : Leake (1965,1971) pointed out that the hornblendes from magmatic and contact metamorphic rocks have generally low Al^{vi} and Si contents than those from regional metamorphic rocks and suggested that Al^{vi} was pressure dependent. Binns (1965) noted that while the Al^{vi} increased with metamorphic grade, Al^{iv} showed much the same range in hornblendes from New South Wales. Raase (1974), using published data, devised a plot of Al^{vi} vs. Al^{iv} in which he defined fields for low and high pressure environments, below and above 5 kbars respectively, for the formation of metamorphic amphiboles. Fleet and Barnett (1978) showed that increases in Al^{iv} and Al^{vi} are coupled with increases in temperature and pressure respectively and produced a plot of Al^{iv} vs. Al^{vi}. They proposed that the boundary between high-pressure (> 5 kbars) and low-pressure (< 5 kbars) assemblages should be at $Al^{iv}/Al^{vi} = 2.0$, which is more or less equivalent to the 5 kbars line of Raase (1974).

The Polusagi amphiboles are presented in the last mentioned plot in Fig.6.22. The actinolites fall into the low pressure field defined by Fleet and Barnett (1978). However, most of the actinolites, having $Al^{iv} < 0.5$, plot below the range of Al^{iv} values used in the construction of

their diagram. Hornblendes plot into the field normally assigned for igneous amphiboles i.e. $Al^{iv}/Al^{vi} > 3.3$ and indicate similar pressures to (< 5 kbars), but much higher temperatures of formation than the metamorphic amphiboles.

Sodium : In greenschist facies, where calcic amphiboles are present, Na content shows correlation with load pressure. This feature is used by Brown (1977) to establish a tentatively calibrated plot of the crossite content of amphiboles (defined as the amount of Na in the M_4 site) against Al^{iv} which, as was discussed previously, can be used as a temperature indicator. Brown (1977) states that the crossite content of actinolites is pressure dependent only in assemblages which include albite, chlorite and iron-oxides. Then the crossite content is buffered by a reaction :

Crossite+Epidote+H_2O = Ca-amphibole+Albite+Chlorite+Iron-oxides. Therefore, at any given temperature and pressure the $Na(M_4)$ content is fixed, as long as other phases are present.

The problem with this method is that the amount of $Na(M_4)$ in the structural formula is dependent on the method used to determine the Fe^{3+}/Fe^{2+} ratio as pointed out in section 6.3.2.1. For this reason, in Fig. 6.23, the Na (M_4) contents of the Polusagi actinolites- which have the required assemblage of minerals-calculated by method (1) as well as method (2) have been plotted. The diagram, in any case, suggests pressures below 3 kbars and probably around or lower than 2 kbars for the metamorphism, which does not contradict the value estimated by the Al method.

Calcium - The Ca content of the amphiboles probably reflects the amount of Na and divalent ion (e.g. Fe^{2+}) substitutions into the X site and does not seem to be influenced by the physical conditions.

In the Polusagi amphiboles, Ti, Al and Na variations do not follow any systematic patterns related to the metamorphic zones defined at the beginning of this chapter. This is most likely to be due to the rather limited temperature and pressure ranges across the zones since the indicators are not sensitive to such relatively small variations in the physical

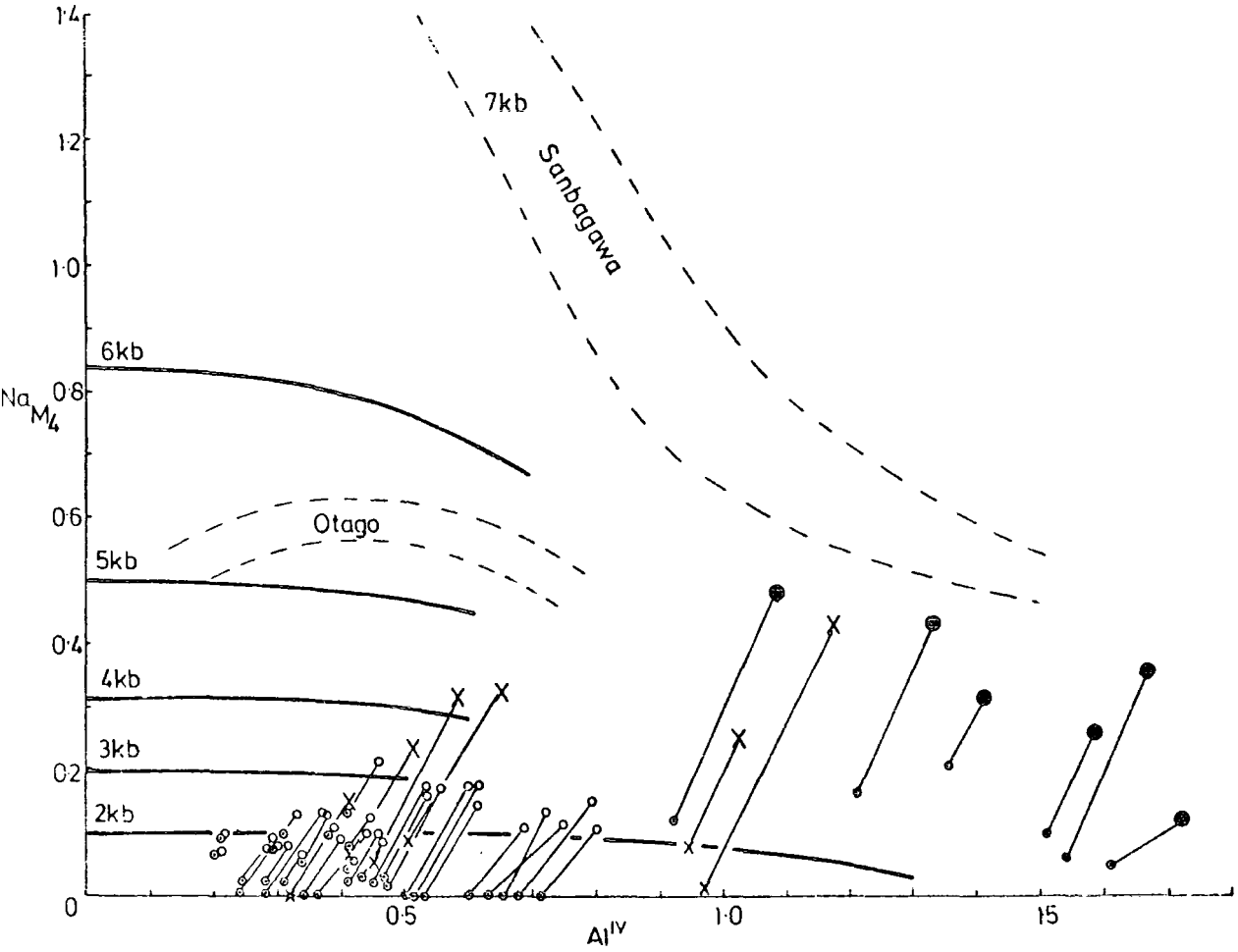


Fig.6.23 Actinolites plotted in Crossite content (Na_{M_4}) vs. Al^{iv} diagram of Brown (1977). Green amphiboles and brown hornblendes are plotted for comparison.

⊙ : Actinolites
x : Green amphiboles
⊖ : Hornblendes
} Variables calculated by the Method 1 i.e. 24 oxygens, Fe^{3+} and H_2O estimated.

○ : Actinolites
X : Green amphiboles
● : Hornblendes
} Variables calculated by the Method 2 i.e. water free bases, 23 oxygen and all Fe as Fe^{2+}

Tie-lines are between points of the same analyses calculated by the two methods.

conditions within the prehnite-pumpellyite and lower greenschist facies metamorphism.

In conclusion, the amphibole chemistry indicates that the pressure during the metamorphism was less than 3 kbars and probably around or even less than 2 kbars. It emphasises the different physical conditions for the formation of the actinolites and the primary hornblendes, the latter having a higher temperature environment of formation.

Further support for the above conclusion comes from the fact that the A site is vacant in the actinolites and on average half filled in the hornblendes. This feature points to their different environment of formation as the increased occupancy of the A site is a matter of higher grade physical conditions (Cooper and Lovering,1970). As it was shown, the hornblendes show considerable edenitic substitution while the actinolites are characterised by tschermakitic substitution and the absence of edenitic substitution. This again indicates that the two amphibole types belong to high and low grade environments respectively (Binns, 1965).

6.4 Chlorite

6.4.1 Mode of occurrence

Chlorite is an ubiquitous metamorphic phase in all the studied rocks of igneous origin. However its abundance decreases from basic and intermediate rocks to acid rocks as well as from zone A to zone B. This is in line with the general recognition that chlorite abundance decreases with increased grade (Winkler,1974). Textural relations of the metamorphic minerals, discussed later in this chapter, suggest that chlorite was one of the earliest phases formed under metamorphism.

It is found in two locations in the rocks:

a) Groundmass : It occurs as decomposition product of the fine-grained or glassy matrix (Plate 6.5). Not only does it replace the groundmass, but it also acts as the chief replacing phase for the albitised

plagioclase laths, sometimes completely pseudomorphing them. This mode of occurrence is more common than the next described.

b) Amygdales and small veins : Some amygdales, up to 2 mm in diameter, may be entirely filled with chlorite. In other cases, chlorite shares the gas vesicles with calcite, quartz and sometimes epidote and prehnite and rarely with pyrite (Plate 6.6). In the latter case, chlorite is an early phase and may form thin coats around the margins of otherwise calcite and/or quartz filled amygdales. Some thin veins may be simply chlorite filled, or the space shared by the above mentioned phases.

Chlorite occurs predominantly as fine-grained poly-crystalline aggregates. Individual grains are rarely greater than 0.1 mm across, and usually show fibrous and radiating forms. In rare cases, well crystallised, euhedral, lath shaped grains are seen to have grown in some amygdales filled with coarse poly-crystalline quartz. These chlorite crystals show stronger pleschroism and higher birefringence colours and are rare.

In the fine-grained and fibrous chlorites, the colour, pleochroism and birefringence colours are very variable. There is a continuous gradation of the birefringence colours from greenish to bluish then to brownish, and on this basis the chlorites can be divided into 3 major types :

a) Greenish chlorites : Birefringence colours vary from light grey-green or yellowish-green to green.

b) Bluish chlorites : These have various shades of grey-blue, light blue or purplish birefringence colours.

c) Brownish chlorites : Birefringence colours grade from light purplish-brown to somewhat deeper brown.

In going from the greenish to the bluish chlorite types, light bluish-green or greenish-blue shades can be recognised, although rather arbitrarily. The colour and the strength of pleochroism also vary from the greenish to the bluish, then to the brownish chlorites. The greenish chlorites have relatively weak pleochroism and the colour varies from



Plate 6.5 : Albitised plagioclase laths (white) and chlorite groundmass (grey). Black is Ti-rich magnetite. Sample: P137, X80, crossed-polars.



Plate 6.6 : Gas vesicle filled with precipitation of chlorite (dark margin) followed by epidote (grey core). Note the alignment of fine albite laths around the vesicle. Sample: P193, X30, crossed-polars.



Plate 6.7 : Phenocrystic plagioclase, albitised then replaced by chlorite, sericite (dark patches) and prehnite (light patches). Sample: P53, X30, crossed polars.



Plate 6.8 : Typical amygdoidal prehnite. Note the radial extinction in some grains. Sample: P213, X40, crossed-polars.

nearly colourless to slightly greenish, while in the brownish chlorites pleochroism is stronger and generally varies from light-greenish to greenish.

In general, each rock sample contains one or the other type of chlorites. However, this is not always true and some samples clearly contain two or more types especially distinctly seen in the gas vesicles, though not confined to them. Then the fine grained aggregates of chlorite show zonation of birefringence colours from the margin to the core of the chlorite filled amygdales. Invariably, the zonation from the margin to the core is either from the greenish to the bluish chlorites or from the bluish to the brownish chlorites.

6.4.2 Chemistry

6.4.2.1 Introduction

76 chlorite analyses (6 from gabbros, 8 from plagiogranites, 3 from dacites, 24 from andesites and 35 from basalts) are presented in Appendix IV.2.3. They include 9 brownish, 36 bluish and 31 greenish chlorite types, 24 of which come from volcanic rocks which are either mineralised or occurring immediately in the vicinity of 'stockwork' type sulphide mineralisation.

The structural formula was calculated by assuming 16 (OH) ions and the oxygen combined with the total cations = 36 in the basic chlorite formula $Y_{12}Z_8O_{20}(OH)_{16}$. The water content is thus estimated and any deficiency from O = 36 is attributed to the presence of ferric iron. The analyses totals vary from 85.5% to 88% without water and from 96% to 100% with the estimated water content. Although some totals look rather low, they are comparable to other chlorite analyses carried out by the electron micro-probe (e.g. Hietanen, 1974; Beddoe-Stephens, 1977). The possible causes of low totals may be that there is more water than estimated in the chlorite structure or some analytical inaccuracies due to the relatively

high and volatile water content.

The chlorite chemistry does not seem to be simple and the variations observed can not be explained in a simple manner without taking into account the host rock compositions, grade of metamorphism, and the extent of sulphide mineralisation the rocks might have undergone. Therefore, while examining the chemistry, each type of chlorite i.e. greenish, bluish and brownish, will be treated separately and those from mineralised rock samples will be given some consideration where necessary. This is also important since the chlorites are unique amongst the metamorphic minerals in that they occur relatively abundantly in almost every rock sample of igneous origin across the metamorphic zones and show a fair degree of chemical variation. The albitised plagioclases, though of as widespread occurrence, show very little chemical variability. Therefore, the variation in the chlorite chemistry may be useful to demonstrate the variations in and due to the metamorphic conditions and provide clues as to the nature of sulphide mineralisation.

6 .4.2.2 Nomenclature

The chlorites are plotted in the conventional classification diagram of Hey (1954) in Fig. 6.24. Only 3 analyses indicate minor amounts of Fe^{3+}, therefore they are all classified as unoxidised chlorites. Over 90% of the chlorites, irrespective of the type, plot into the pycnochlorite field; a few are scattered into the brungsvigite and diabantite fields, but still very close to the pychochlorite field.

6.4.2.3 Crystal chemistry

The simple but extensive substitution $Mg \rightleftharpoons Fe^{2+}$ (Fig.6.27) is operative in the chlorites and the extent is indicated by widely varying Mg-number, from 73 down to 34. Small amounts of divalent ions, such as Mn, may also occupy the Y site, probably preferably replacing Fe^{2+}. The substitution of Si by Al^{iv} is compensated for by Al^{vi} (Fig.6.25) with a coupled substitution of the type : $Al^{iv}+Al^{vi} \rightleftharpoons Si+(Mg,Fe)$, indicated in Fig.6.26.

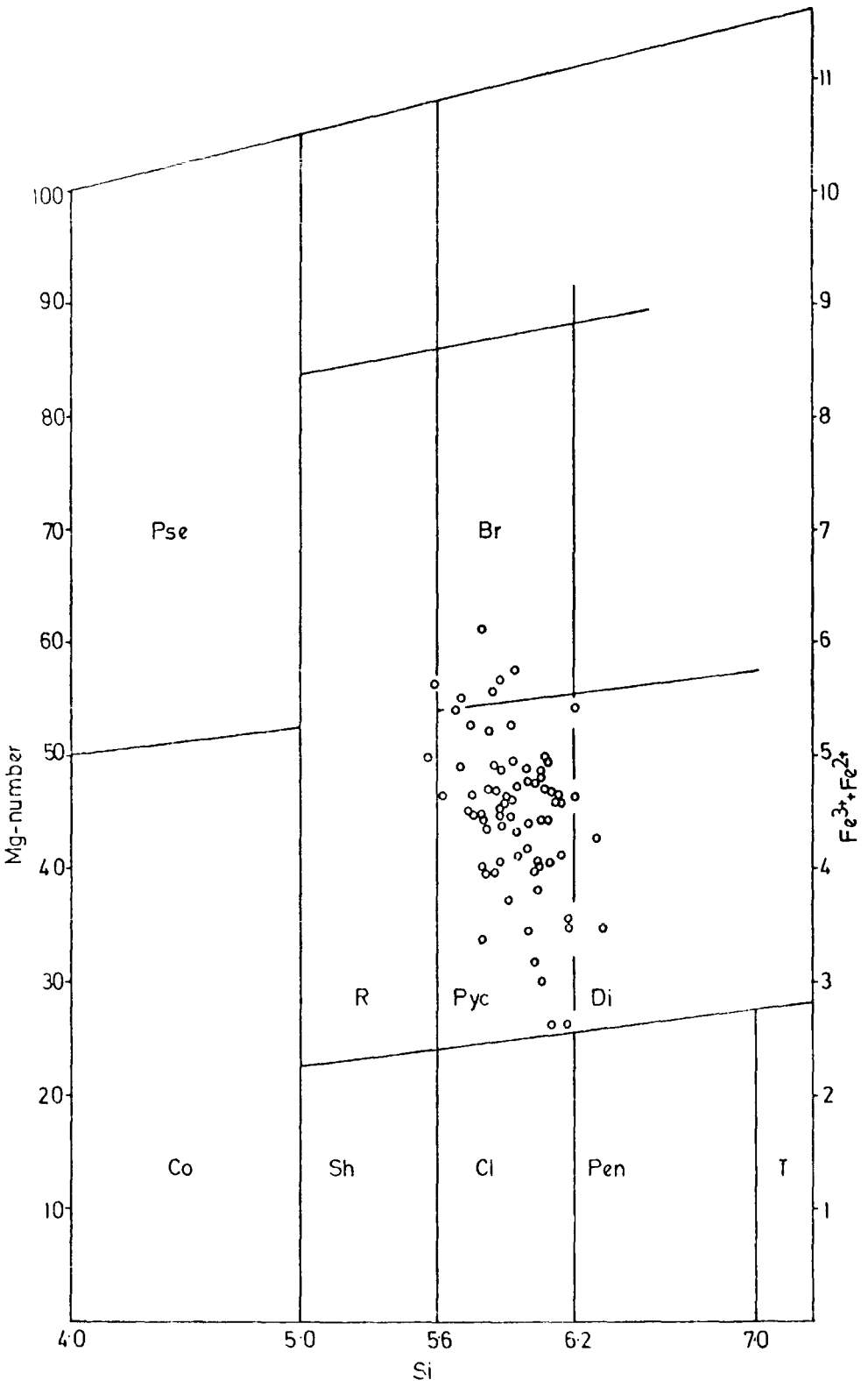


Fig.6.24 Diagram for the nomenclature of unoxidised chlorites (after Hey, 1954).

Pse = Pseudothuringite	Br = Brungsvigite
Co = Corundophilite	R = Ripidolite
Pyc = Pycnochlorite	Di = Diabantite
Sh = Sheridanite	Cl = Clinoclore
Pen = Penninite	T = Talc-chlorite

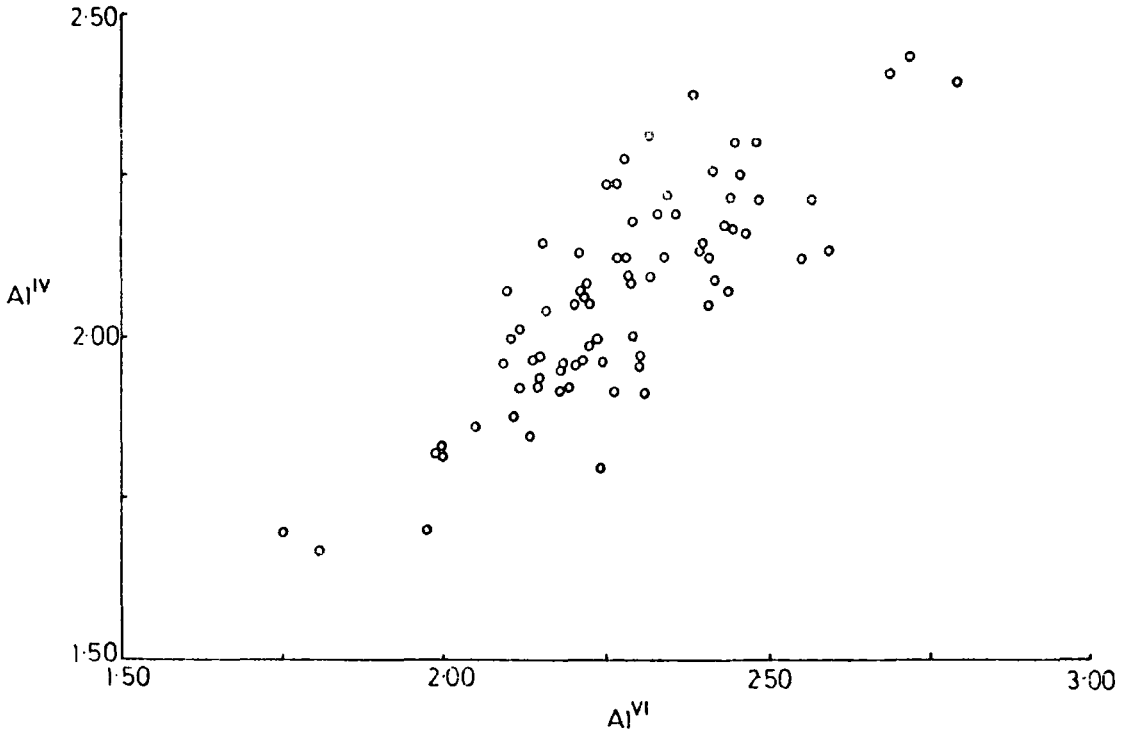


Fig. 6.25 Al^{iv} vs. Al^{vi} in chlorites.

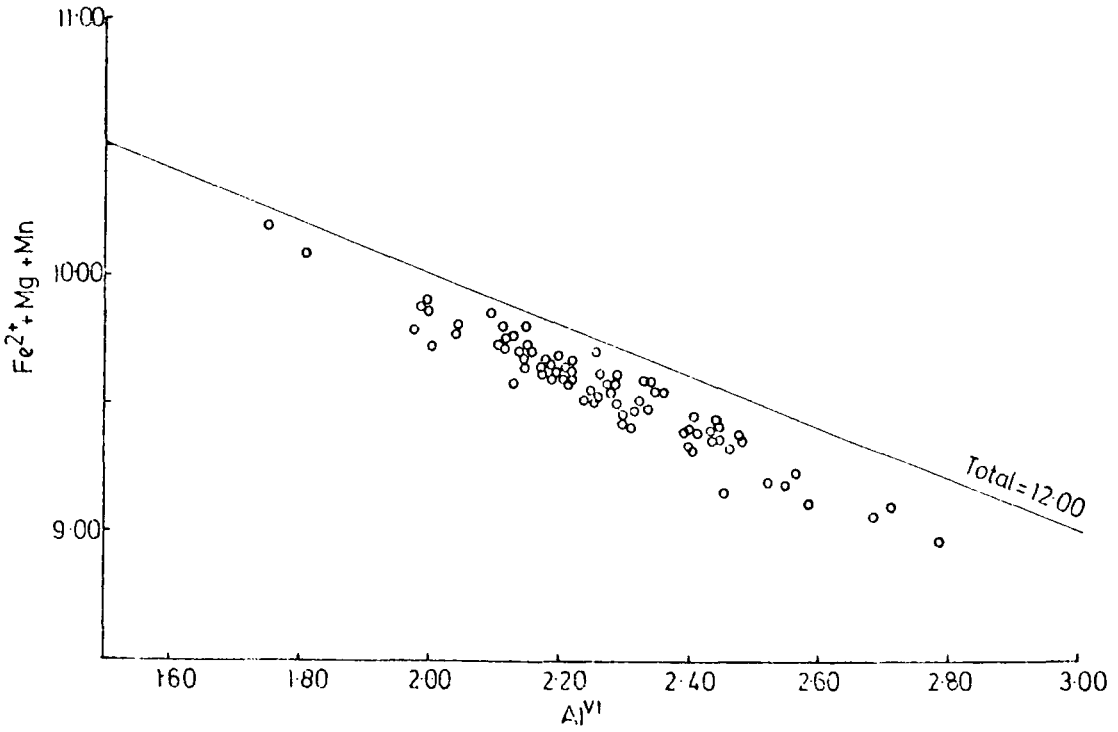


Fig.6.26 Al^{vi} vs. $(Fe^{2+}+Mg+Mn)$ in chlorites.

Solid line represents $Al^{vi}+(Fe^{2+}+Mg+Mn) = 12.00$.

6.4.2.4 Chemical variation

Ignoring the minor amounts of Fe^{3+} indicated in only 3 analyses, it seems that all iron is in the ferrous state. It varies from 6.1 to 2.6 (atoms per formula unit), while Mg ranges from 3.1 to 7.2 in going from the greenish to the bluish then to the brownish chlorites. This is the most conspicuous chemical distinction between the chlorite types as shown in Fig. 6.27. It is clear that the three optically defined chlorite groups can also be chemically defined on the basis of the extent of Fe^{2+} substitution for Mg as follows:

a) Greenish chlorites : $Mg < 4.9$, $Fe^{2+} > 4.1$, or Mg-number < 51.

b) Bluish chlorites : $4.9 < Mg < 6.2$, $3.5 < Fe < 4.1$, or Mg-number in the range $\simeq 51$-64.

c) Brownish chlorites : $Mg > 6.2$, $Fe < 3.5$, or Mg-number > 64.

These chemical boundaries, however, cannot be strictly applied since the transition from one type to the other is gradational and occurs within a Mg-number range of ± 2 from the defined values, and also because the Mg and Fe^{2+} contents are not the only chemical parameters describing the groups.

The Si and Al contents of the chlorites range from 6.3 to 5.5 and 3.5 to 5.2 atoms per formula unit respectively. With decreasing Mg-number, they do not exhibit clear trends unless the Si and Al contents of the greenish, bluish and brownish chlorites are treated separately. Fig.6.28 is a plot of Si (or Al^{iv}) against the Mg-number, and Fig.6.29 demonstrates the variation of total Al with the Mg-number. From these figures the following features are apparent:

a) Each type of the chlorite groups exhibits decreasing Si (or increasing Al^{iv}) and increasing total Al trends with decreasing Mg-numbers.

b) At a given total Al or Si value the Mg-number increases in going from the greenish to the bluish then to the brownish chlorites.

c) At a given Mg-number, Si decreases and total Al increases in the

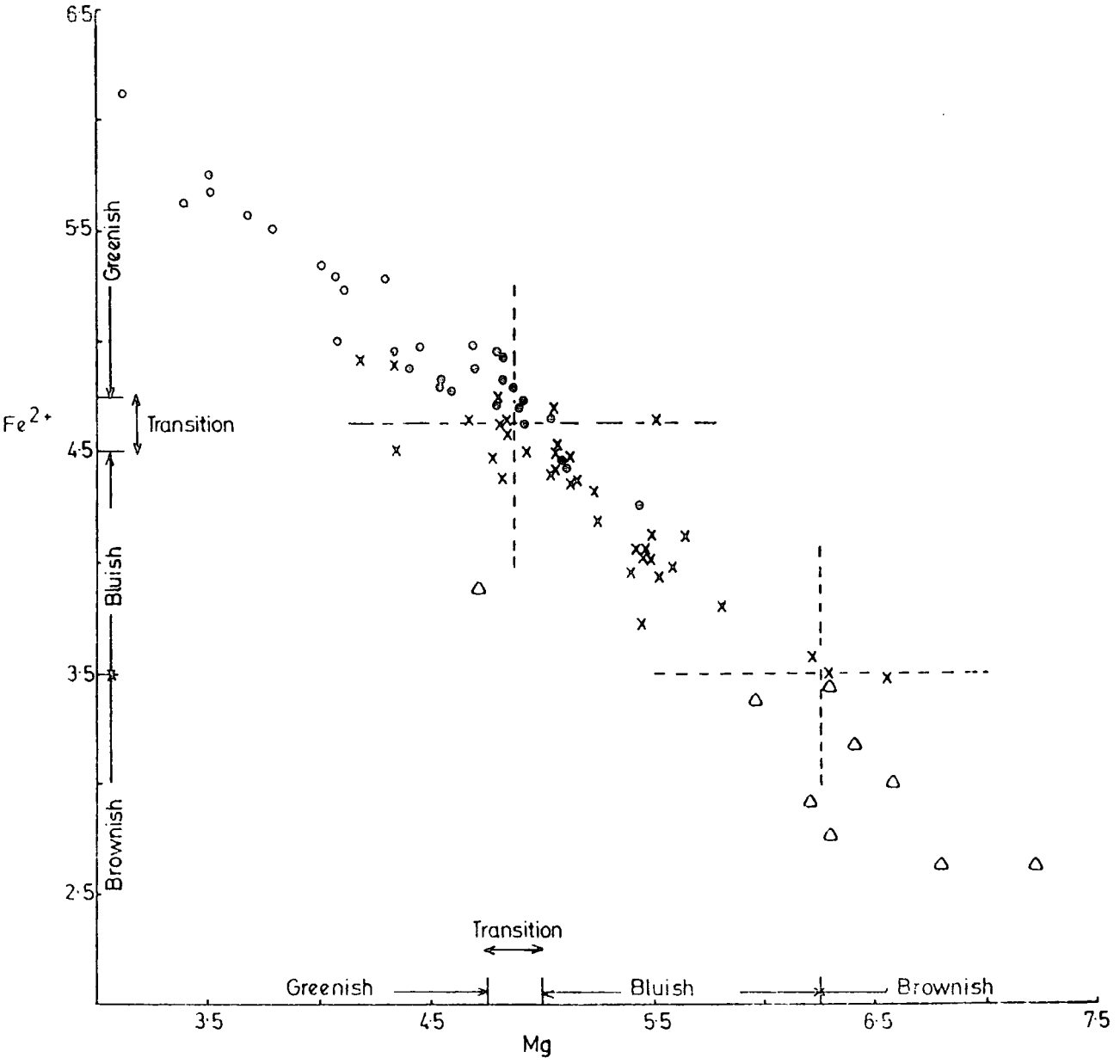


Fig.6.27. Fe^{2+}-Mg variation in chlorites (all cations per formula unit, 36 oxygens).

o : Greenish chlorites

x : Bluish chlorites

△ : Brownish chlorites

Broken lines show how the three types are separated with transitional boundaries.

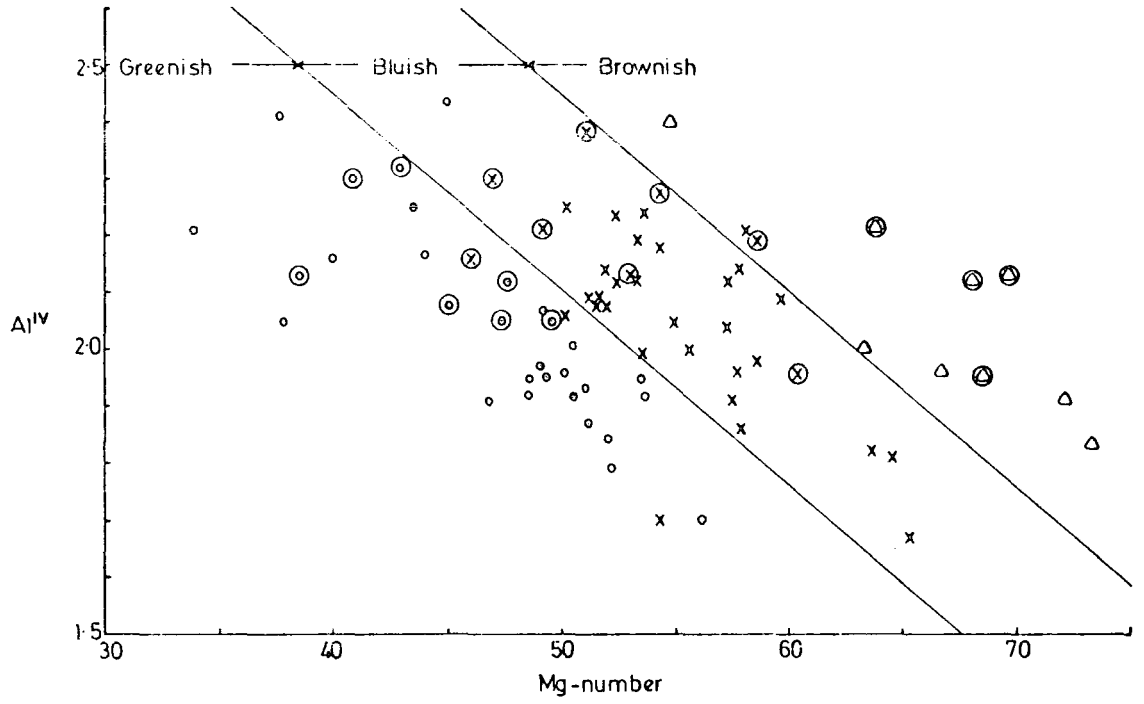


Fig.6.28 Variation of Al^{iv} with Mg-number in chlorites.
⊛ : greenish chlorites, x : bluish chlorites and △ : brownish chlorites. Circled symbols indicate analyses from mineralised samples. Solid lines define the fields for the three types.

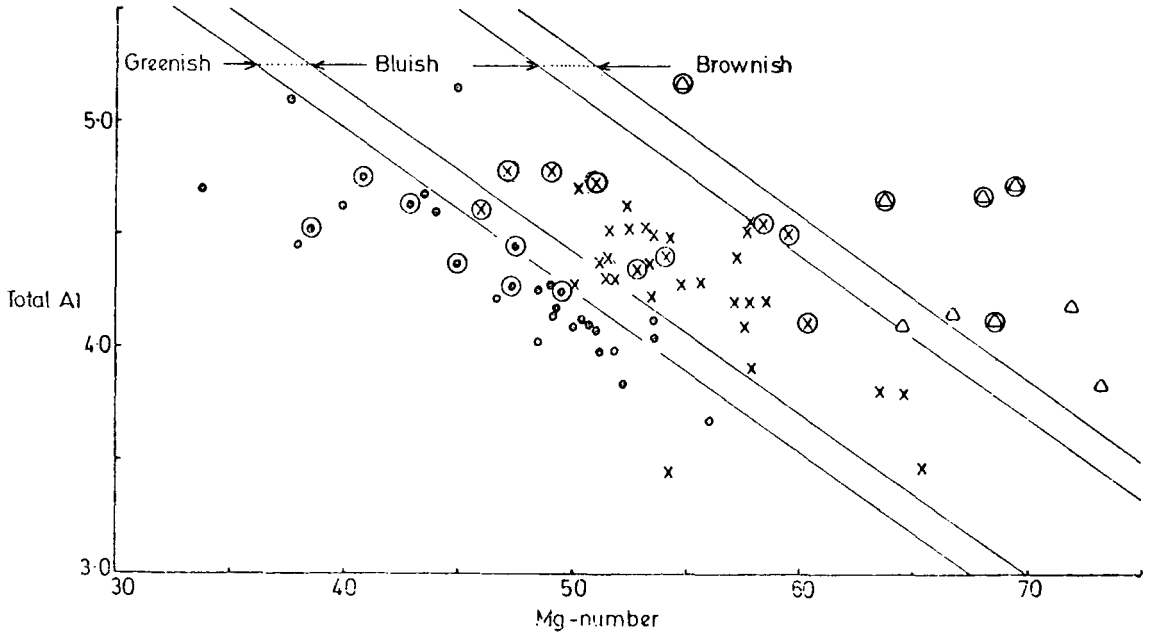


Fig.6.29 Variation of total Al with Mg-number in chlorites.
All symbols as above.

order from the greenish to the bluish then to the brownish chlorites. Therefore, each type of the chlorite can be fully defined only when Si, Al, Mg and Fe contents are considered.

d) The brownish chlorites occurring in the volcanic rocks are associated with sulphide mineralisation i.e. they occur in association with the stockwork mineralisation or in lavas from the immediate vicinity of the mineralisation.

e) In each group of chlorites those from the mineralised lava samples have lower Si (or higher Al^{iv}) and higher total Al than the rest of their types at a given Mg-number.

It is perhaps worth noting here that the Si and Al trends with decreasing Mg-number, exhibited by each group of the chlorites, are not similar to the trends of these elements exhibited in the host rocks with advancing differentiation. Therefore, their concentrations are not directly influenced by the whole-rock composition.

Mn content of the chlorites does not show a regular trend with the Mg-number. However Mn contents of the chlorites occurring in the non-mineralised rock samples are low and mostly in the range 0.04 to 0.10 atomic cations i.e. 0.3 to 0.6 wt % respectively, and those from the mineralised lavas are higher and in the range 0.10 to 0.40 (or 0.6 to 2 wt%). Increases in the Mn content of the rocks during hydrothermal metamorphism, which lead to the mineralisation, was also noted in Chapter three.

Ca is present in small amounts varying from 0.01 to 0.13 (0.05 to 0.60 wt% respectively) in all the chlorites. The chlorites from the mineralised rocks are much lower in Ca than average, most having Ca contents around 0.02 atoms per formula unit. Depletion in the Ca content of the mineralised rocks was also noted in chapter three. Therefore, it seems that the Mn and Ca contents of the chlorites in the mineralised rocks are affected by the concentrations of these elements in the mineralising solutions.

Ti, Na and K contents are very small. Most of the chlorites have less than 0.01 (0.06 wt%) Ti and less than 0.04 (0.12 wt%) total alkali contents.

6.4.3 Factors controlling the chemical variation

6.4.3.1 Chemical factors

Mg-numbers of the chlorites and the host rocks, plotted in Fig.6.30, are positively correlated in a general way. The correlation is stronger for the chlorites from the hypabyssal rocks and the data points for the chlorites from the volcanic rocks are rather scattered, although they show some degree of positive correlation. Therefore, it is reasonable to assume that the Mg and Fe contents of the chlorites from the hypabyssal rocks are dominantly controlled by the host rock composition. However, this is only partly so for the chlorites from the volcanic rocks and there may be other factors involved in the process. The apparent deviation in the behaviour of the chlorites from the two different rock settings may be caused by the following considerations:

a) All the hypabyssal rock samples studied belong to group A rocks, therefore by definition, the alteration is relatively uniform and they show little element mobility. The volcanic rocks, on the other hand, belong to rock groups A,B or C i.e. the alteration is variable and the rocks exhibit relatively high element mobility (Chapter three).

b) The hypabyssal rocks are confined to the greenschist facies metamorphism,i.e. zone B, and due to relative uniformity of the physical conditions their influence may be masked by the influence of the host rock compositions. The volcanic rocks however, are present in all the metamorphic zones. Thus the physical conditions of metamorphism were somewhat more variable for the volcanic rocks, from prehnite-pumpellyite facies to greenschist facies.

Therefore, in considering the physical condition of metamorphism as

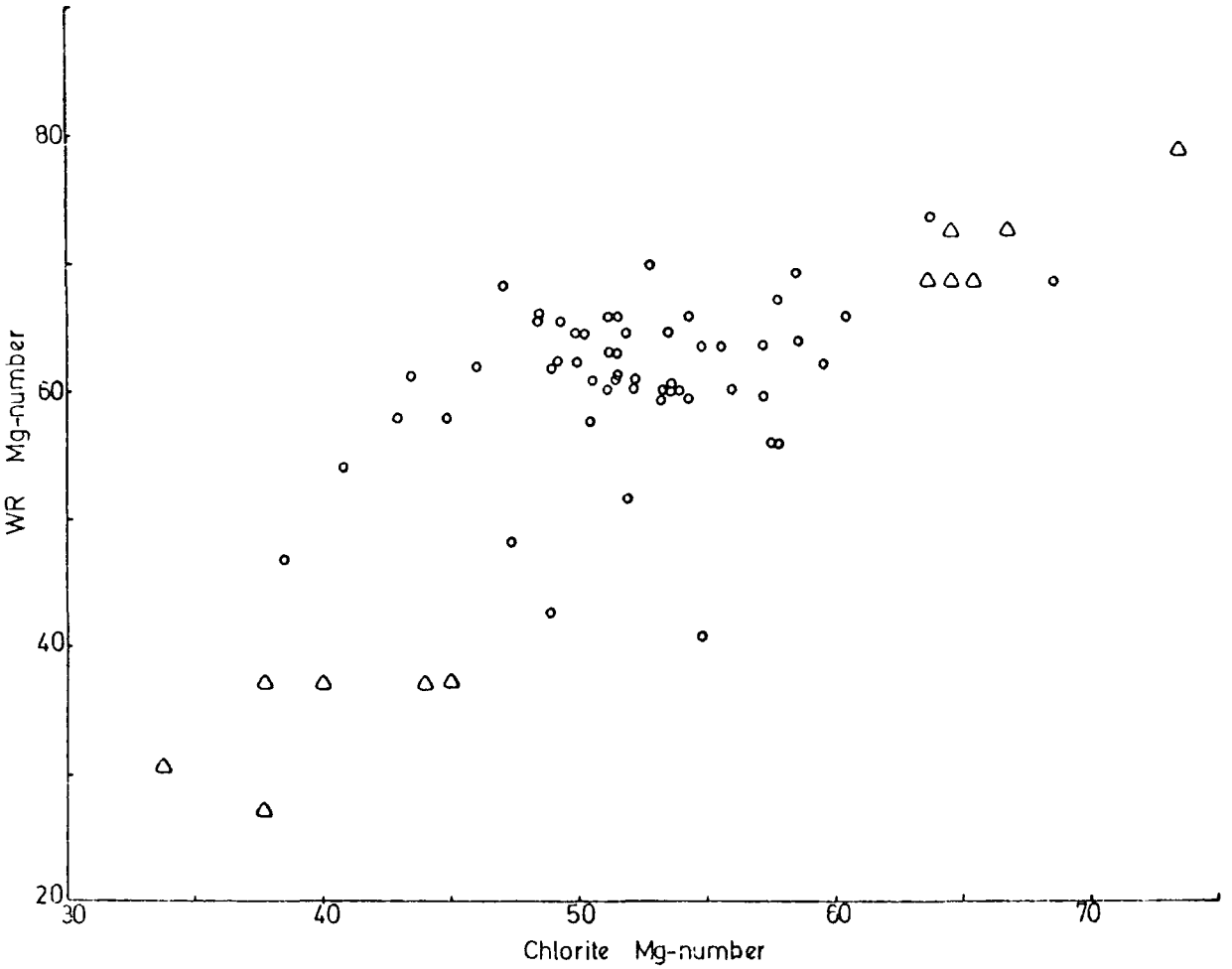


Fig.6.30 Whole-rock Mg-number vs. chlorite Mg-number.
o : analyses from volcanics and △ : from hypabyssal rocks.

additional controls over chlorite Fe and Mg contents as well as over the Si and Al contents, only the chlorites from volcanic rocks will receive further attention below.

6.4.3.2 Physical factors or grade of metamorphism

Increases in Al contents of chlorites with increasing metamorphic grade have been reported by Pincent (1974), Kuniyoshi and Liou (1976) and Beddoe-Stephens(1977). Also, Mg-rich chlorites are stable to higher temperatures than the Fe-rich chlorites (Turnock 1959,1960). Therefore, the Al contents and the Mg-numbers of the chlorites should be influenced by the temperature of metamorphism as the pressure during the Polusagi metamorphism is indicated to be low.

In Figs.6.31a and6.31b Si (or Al^{iv}) and total Al contents of the chlorites are plotted against their Mg-numbers respectively. Chlorite analyses in these diagrams are plotted according to the general metamorphic zones in which they occur. When studied in conjunction with the observations made on the chemical variations of the chlorites in section 6.4.2.3, the following features are observed:

a) The greenish chlorites are typical of zone A and are confined to this zone.

b) Zone B lavas contain only the bluish and brownish chlorite types.

c) Zone A lavas, in addition to the greenish chlorites, also contain the bluish and the brownish varieties which are typical of zone B. The volcanic samples in zone A, containing the typical zone B chlorites are mineralised or at least come from exposures in the vicinity of exposed sulphide mineralisation (stockwork type).

d) Ignoring the chlorites associated with sulphide mineralisation, the general trend from zone A to zone B chlorites involves increases in Mg-number and total Al and decrease in Si.

From these observations the following conclusions are, therefore, drawn:

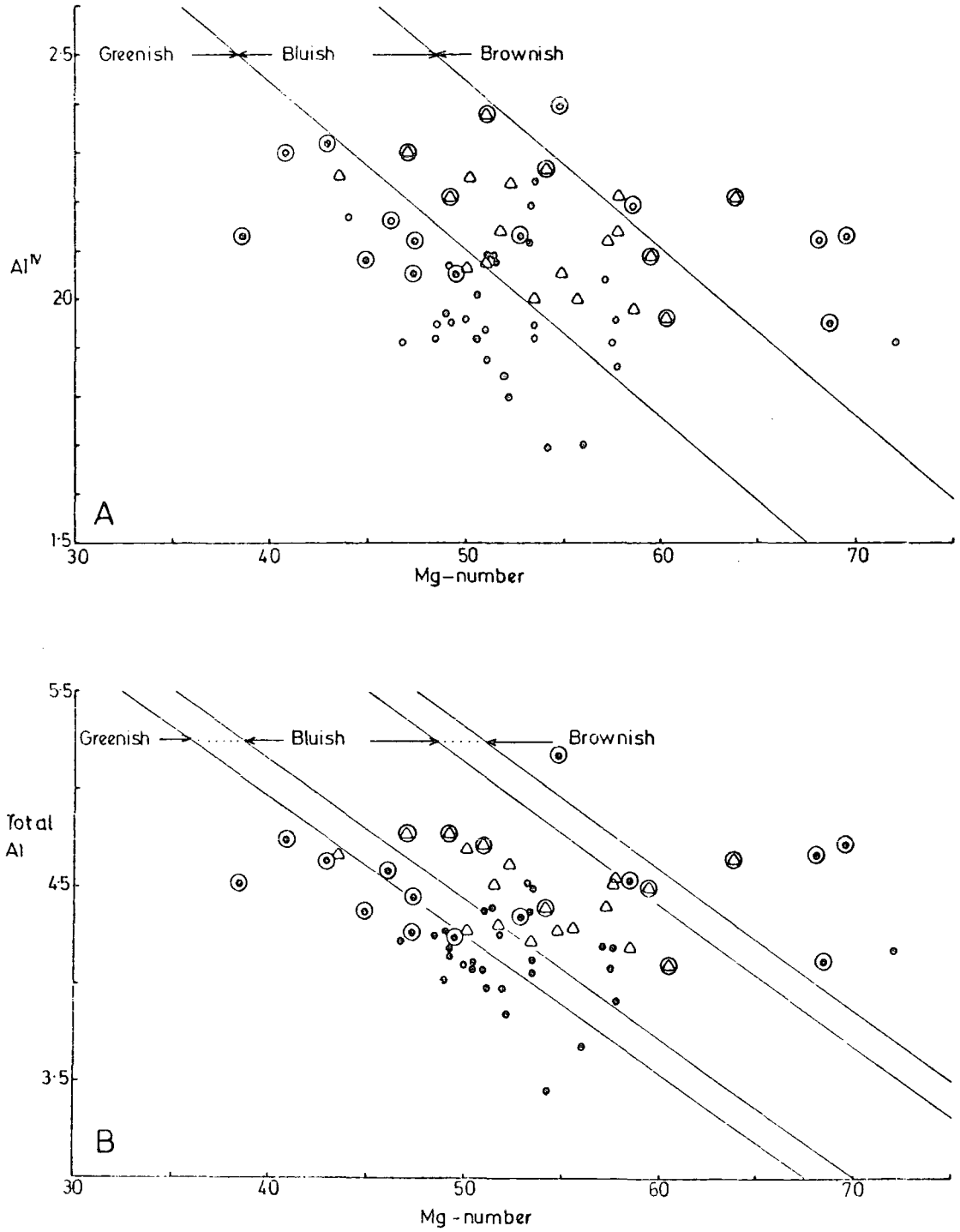


Fig.6.31a and b - A) Al^{iv} vs. Mg-number and B) Total Al vs Mg-number in chlorites.

o : Chlorites from Zone A rocks.

Δ : Chlorites from Zone B rocks.

Circled points indicate mineralised host rock.

Solid lines are reproduced from Figs.6.28 and 6.29 respectively.

a) The physical conditions of metamorphism, mainly the temperature, govern the distributions of Si and total Al in the chlorites. Mg and Fe contents of the chlorites are influenced by the temperature as well as the host rock compositions. Increasing temperature leads to decreasing Si and increasing total Al and Mg-numbers.

b) Prehnite-pumpellyite facies conditions typically produce the greenish chlorites, while greenschist facies the bluish and the brownish.

c) Amygdales filled with zoned chlorite aggregates indicate that metamorphism was a progressive one.

d) Although,in general, prehnite-pumpellyite facies metamorphism prevailed in zone A, there were areas with localised higher temperature conditions where the stockwork sulphide mineralisation took place.

e) The chlorite compositions and the optical properties ,therefore, can be used as a guide to the localised areas in zone A where higher temperature conditions existed and thus to the possibility of unexposed mineralisation. As an application of this method, it is suggested that outcrops of the samples P76 and P93, - containing higher grade forms of chlorites yet not obviously mineralised,may not be far away from some unexposed sulphide mineralisation albeit a stockwork type.

6.5 Plagioclase

6.5.1 Mode of occurrence

Plagioclase usually is the most abundant mineral in the rocks. It shows itself in two modes:

a) Groundmass plagioclases - These invariably occur in lath-like forms with serrated or split ends in the volcanic rocks. The size of the laths is variable in the general range from a few tens of microns to about 1 mm in length and 0.1 mm in width; in rare cases the laths may be as long as 7 mm. However, in each rock sample the variation in size is

relatively restricted. In some cases, when they occur with the clinopyroxenes, they tend to cluster around the clinopyroxene grains in the groundmass. In the lavas, the plagioclase laths are sometimes clearly aligned, probably due to the flow structures present in the lavas.

b) Phenocrystic plagioclases: Some volcanic rocks do have some plagioclase phenocrysts, but they are relatively rare. These plagioclases show euhedral forms and are equidimensional as opposed to the lath-shaped groundmass plagioclases and generally 2-3 mm in diameter.

The gabbro and plagiogranite samples also have 2 different sizes of coarser plagioclases. The smaller grains may show similar forms to the groundmass plagioclase, but are o.5 to 1 mm in size. The larger plagioclase grains are coarse and may be 7 mm in diameter in the plagiogranite.

As will be shown in the next heading, both the groundmass and phenocrystic plagioclases are almost totally pseudomorphed by albite and most have dusty, cloudy and speckled appearances, sometimes darkened by the fine inclusions of other minerals. In many cases they show uneven extinction. The cloudy, unclear nature of the plagioclase in thin sections is due to replacement and the formation of some fine grained metamorphic phases within the plagioclase grains. These phases may be sericite, calcite, chlorite, epidote, prehnite, pumpellyite and probably some fine particles of iron-oxides, see plate 6.7. The replacement of plagioclase by the other phases is somewhat irregular and varies from sample to sample with the probable exception of the sericitic and chloritic clouding.

In most of the gabbro samples, there seems to be a new growth of clear plagioclase rim replacing the cloudy and darkish core, but this phenomenon is relatively uncommon compared with the above described unclear plagioclases.

Texturally, nearly all plagioclases exhibit primary igneous relations. Only in very rare cases were irregular-shaped small plagioclase aggregates observed along some veins. It seems that metamorphic albite simply

pseudomorphed the igneous plagioclase , largely retaining the igneous textures and even preserving the typical plagioclase twinning.

6.5.2 Chemistry

85 plagioclase analyses (21 in basalts, 41 in andesites, 4 in dacites, 7 in gabbros and 12 in plagiogranites) are presented in Appendix IV.2.4. The anorthite, albite and orthoclase proportions of the analyses are plotted in the conventional ternary diagram in Fig.6.32. Compositionally, all the analyses, excepting the 5 from the gabbro samples P246 and P258, are albites. All An contents are less than 6%, and 75% of the analyses have less than 2% An. However, 3 analyses from P246 and 2 from P258 have oligoclase and andesine compositions respectively. These calcic plagioclase compositions are those of the clear and late growth plagioclase rims replacing the cloudy albite cores.

All plagioclase analyses contain less than 1.5% orthoclase component, excepting 4 analyses where the range is 2 to 4%. The Fe content is variable and small, up to 0.03 atoms per formula unit (0.86 wt%), but mostly in the range 0 to 0.008 (0 - 0.24 wt%). Mn, Mg and Ti contents are negligible.

There is a chemical zonation from An_{1-2} in the cores to An_{4-5} in the margins observable in single albite grains from zone B rocks. It is interesting to note (Fig.6.32) that the albite grains from zone A rocks having An contents in the range 3 to 6 are those associated with the mineralised rocks, or the rocks not far from the zone A-subzone B_1 boundary.

6.5.3 Factors controlling the chemistry

The fact that almost all plagioclase compositions are of albite, despite the large range of host rock composition within which they occur, indicates that the host rock compositions had little, if any, effect on the plagioclase chemistry.

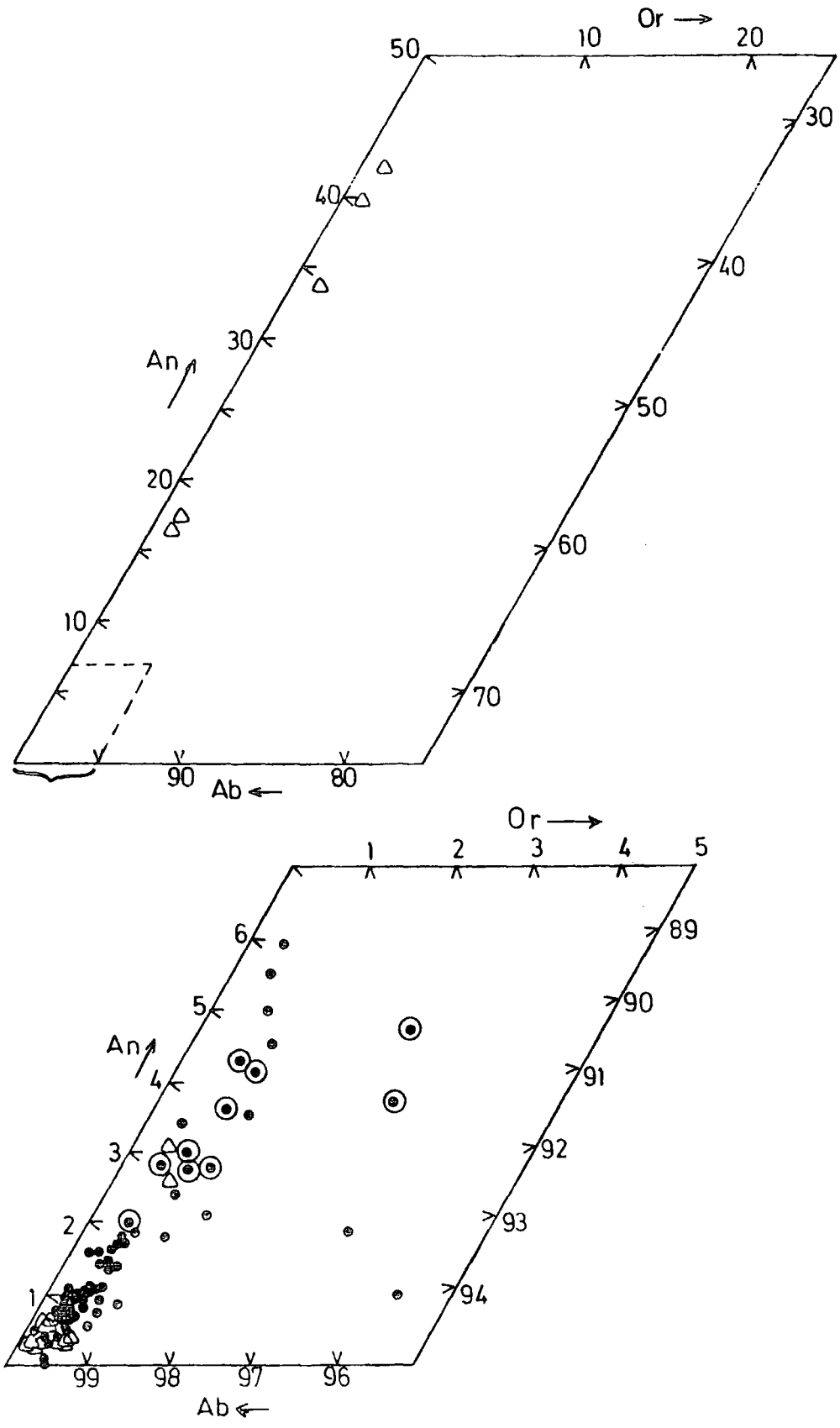


Fig.6.32 Plagioclase analyses plotted in ternary feldspar diagram. The lower diagram is the exposed Ab corner of the upper diagram.

⊙ : Analyses from volcanics.
△ : Analyses from hypabyssal rocks.

Circled points indicate mineralised host rock.

It is well established that albite is the only stable plagioclase in the prehnite-pumpellyite and greenschist facies (or "very low grade" and "low grade") metamorphism, regardless of the CaO contents of the rocks (e.g. Miyashiro, 1973; Winkler 1974). With increasing metamorphic grade, An content increases. At higher temperatures, as metamorphic grade moves into the amphibolite facies (or the medium grade metamorphism of Winkler, 1974), there occurs a jump in the plagioclase composition from about An_5 to An_{17} which is governed by the peristerite unmixing. The temperature at which this "abrupt and universal" jump takes place is estimated to be 20°C to 40°C lower than the temperature of transition from the low grade to the medium grade metamorphism defined by Winkler (1974). The formation of the more calcic plagioclase ($An > 17$) involves a reaction of Ab with Ca and/or Al rich phases such as epidote, calcite, chlorite, prehnite and pumpellyite, and it is supposed to be influenced by the temperature and pressure of metamorphism and mineral assemblages (Miyashiro, 1973). Higher temperatures lead to higher An content of the calcic plagioclase; however, higher pressures may retain Ab up to amphibolite facies.

Therefore, the physical conditions prevailing in zone A (prehnite-pumpellyite facies) and zone B (greenschist facies) must have been the major factors transforming the unstable igneous plagioclases into the stable albite. The release of the An content from the igneous plagioclase would then produce Ca-rich and probably Al-rich metamorphic phases such as epidote, calcite, chlorite, prehnite and pumpellyite, which are all found in the Polusagi rocks.

The "abrupt compositional jump" from the cloudy albite cores ($An < 6$) to clear plagioclase rims of oligoclase and andesine in some gabbro samples, albeit not common, suggests that the metamorphic temperatures in zone B must have approximated to the temperatures of the transitional condition from the greenschist facies to amphibolite facies in certain localities.

Since the pressure during the Polusagi metamorphism is believed to be low (section 6.3.3.2), and probably did not vary a great deal, the increase in the An content of the albites may be related to the increasing temperature. This would mean that the mineralised rock samples of zone A must have undergone higher local temperatures than the non-mineralised rocks - a conclusion also reached in previous sections.

6.6 Epidote

6.6.1 Mode of occurrence

Compared with the other mineral phases dealt with so far epidote is relatively scarce in the Polusagi rocks. Its distribution is somewhat erratic and may be abundant in some volcanic rock samples, especially along cracks, in amygdales as well as in isolated areas. Although present in all the rocks of the suite it seems to be comparatively more abundant in the rocks of zone B. Epidote is colourless to yellowish with greenish-yellow pleochroism. It may be in the form of relatively coarse fibrous sheaves or well-crystallised euhedral to subhedral grains or sometimes irregular fine-grained masses. Some euhedral grains may show slight optical zonation and be up to 1 mm across. It occurs in amygdales or cracks with chlorite and quartz and in the groundmass chiefly as a phase replacing the plagioclase. The replacement of plagioclase by epidote is generally observed as fine epidote grains or sometimes irregular masses within the cloudy plagioclase laths and phenocrysts. To a lesser extent it replaces the clinopyroxene and sometimes the chlorite.

6.6.2 Chemistry

40 epidote analyses (8 in basalts, 18 in andesites, 6 in dacites, 2 in gabbros and 6 from plagiogranites) are included in Appendix IV.2.5. The structural formula is calculated on the basis of 8 cations and by

assuming 1 hydroxyl ion to estimate the water content. Any deficiency from O=13 is made up by converting the ferrous iron into ferric iron.

6.6.2.1 Nomenclature

In the epidote group minerals the chemical variations are mainly due to substitutions of ferric iron and/or trivalent Mn for Al between the end-members zoisite/clinozoisite ($Ca_2Al_3Si_3O_{12}.OH$) and epidote ($Ca_2Fe^{3+}Al_2Si_3O_{12}.OH$) and the Mn-rich piemontite. The chemical boundary between epidote (or the so-called pistacite) and clinozoisite is rather arbitrary and is taken at 10% Fe^{3+} end-member i.e. the pistacite percentage (Ps%) by Miyashiro and Seki (1958). Winkler (1974) indicates a boundary at Ps% = 15. In natural occurrences, the Ps content rarely exceeds 1 atom Fe^{3+} per formula unit corresponding to a Ps% = 33, but values up to Ps% = 40 are recorded.

In the Polusagi epidotes, the Ps% varies from 17 to 37 with an average value of 29. Even when all iron is assumed to be in the ferric state, the Ps% is still high and in the range 21 to 39. Therefore, whatever the value of Ps% used to distinguish clinozoisite from epidote may be, the Polusagi analyses fall into the epidote field.

6.6.2.2 Chemical variation and crystal chemistry

Si contents of the epidotes do not depart significantly from the ideal 3 atoms per formula unit and average to 3.04 with a range from 2.97 to 3.14. Thus, there are extremely small amounts of Al substituting for Si, even then only in about one-quarter of the epidotes analysed.

Al ranges from 2.10 to 1.82 atoms (22-19 wt%) while total Fe (calculated $Fe^{3+}+Fe^{2+}$) from 0.63 to 1.16 atoms per formula unit (14-19 wt%). It is indicated that most of the iron is in the ferric state and up to 24% of the total Fe may be in the ferrous state. Fig.6.33 shows that although the calculated Fe^{3+} is negatively correlated with Al, the R^{3+} site occupancy is up to 0.25 atoms deficient from the ideal 3 atoms. The

addition of Fe^{2+} into the R^{3+} site, already occupied by $Al+Fe^{3+}$, brings the occupancy to 3.00 $\pm$ 0.10 atoms (Fig.6.34). This means that either all the calculated ferrous iron is incorporated into the R^{3+} site or that nearly all total iron is in ferric state i.e. the calculated amounts of Fe^{3+} is erroneous. The latter is more likely as the entrance of Fe^{2+} into R^{3+} site would cause charge imbalance which cannot possibly be fully compensated by the small Ti content, which is present in R^{3+} site only up to 0.03 atoms or 0.5 wt%, or by possible trivalent Mn. The R^{3+} site occupancy in one analysis, even when total Fe = Fe^{3+} is assumed, is rather low, but this analysis is also unusually rich in Mg (0.21 atoms) - far in excess required to fill the R^{2+} site- and contains 1.97 atoms of Ca. This would suggest that some degree of divalent ions, in this case Mg, may possibly be incorporated into the R^{3+} site.

The R^{2+} site on the Polusagi epidotes is largely occupied by Ca. The Ca in the R^{2+} site varies from 1.85 to 2.04 atoms with an average of 1.95. Total alkali content in the epidotes is very small and averages to 0.008 atoms or 0.6 wt%. Mg and Mn contents are mostly small, but may be up to 0.2 (1.7 wt%) and 0.07 (1 wt%), averaging to 0.02 (0.2 wt%) and 0.02 (0.3 wt%) atoms respectively.

Analyses of one optically zoned epidote grain ($P240_{1B}$ for the margin and $P240_{1c}$ for the core) indicate that the margin is slightly richer in Al, Mn and Mg and slightly poorer in total Fe and Ca. The Ps% in the margin is 31.6 and in the core 34.1. Similar but stronger chemical zonation in epidotes has been reported, for example, by Brown (1967).

6.6.3 Factors controlling the chemistry

6.6.3.1 Chemical factors

Despite their occurrences in the compositionally varied host rocks the Si and Ca contents are relatively constant indicating that host rock composition was not an effective factor over the epidote chemistry. The

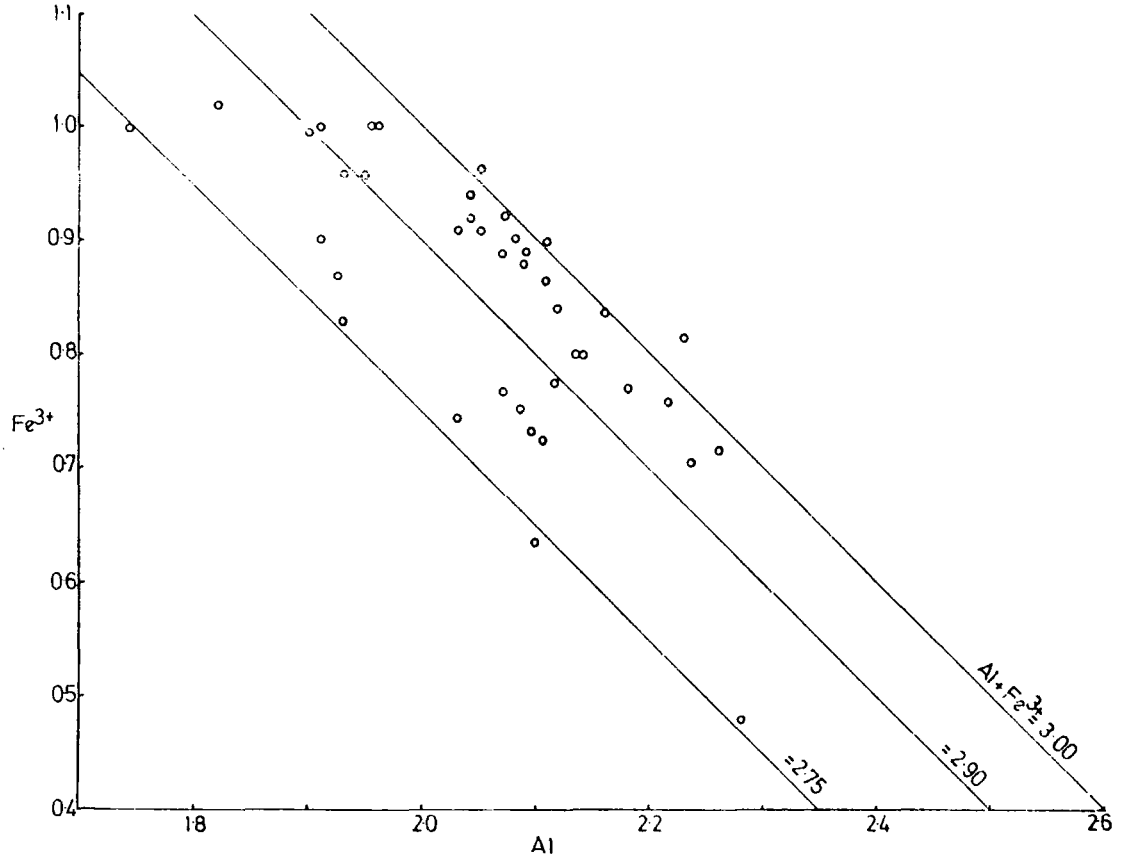


Fig.6.33 Fe^{3+} vs. Al in epidotes (cations per formula unit, 13 oxygens).

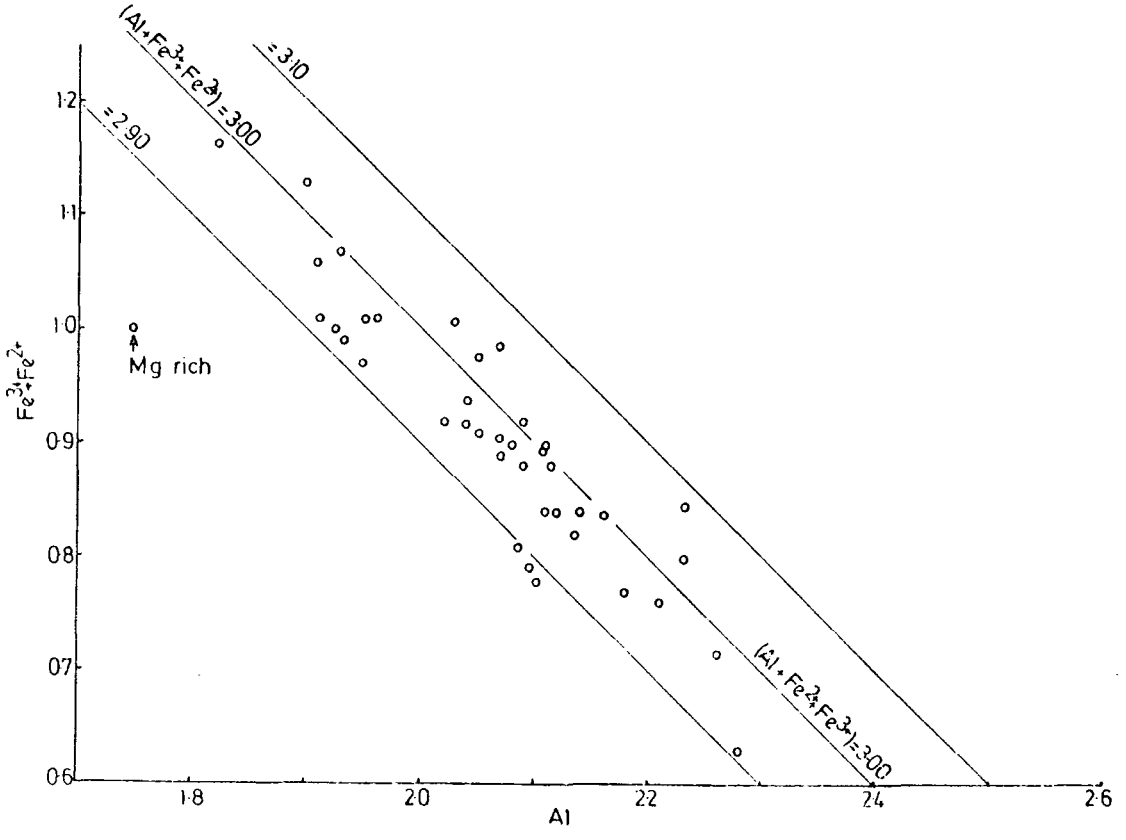


Fig.6.34 Total Fe (as $Fe^{3+}+Fe^{2+}$) vs. Al in epidotes (cations per formula unit, 13 oxygens).

same is true for total Fe and Al contents as the Ps% and the host rock $\frac{Fe^{total}}{Fe^{total}+Al_2O_3}$ ratios are not correlated. Therefore the main chemical variation in the epidotes i.e. the extent of Fe^{3+} substituting for Al, may have been influenced by other factors.

6.6.3.2. Physical factors

Chemical variations with metamorphic grade in epidotes is complex. Miyashiro and Seki (1958) report that in the Kanto Mountains, Japan, the epidotes from the lowest grade metamorphic rocks have a Ps% range 20 to 35 with maximum frequency at 30 and the range becomes 0 to 50 in the higher actinolite-greenschist facies. Kuniyoshi and Liou (1976) point out that the Ps% of the epidotes from prehnite-pumpellyite facies decreases slightly from around 30 to around 26 as metamorphic grade increases to epidote-amphibolite facies.

The above observations are not contradicted by the Polusagi epidotes. Although in a general sense the epidotes from zone A show slightly more restricted Ps% range than those of zone B, clearer observations are hampered by the fact that only 10 epidote analyses are from zone A rocks most of which are mineralised samples. Hence, they may not represent the temperatures typical of zone A metamorphic conditions.

The Ps% of epidotes seems also to be a function of the oxygen fugacity. The shift in the Ps content of the Fe-rich epidotes towards Fe-poor epidotes with increasing metamorphic grade is attributed to a decrease in the oxygen fugacity by Beddoe-Stephens (1977) who shows that the Ps content of the epidotes in the Rossland volcanic suite, British Columbia, is related to, and positively correlated with, the Fe^{3+}/Fe^{2+} ratio of the host rocks. Thus the high Ps content of the Polusagi epidotes raises the point that the oxygen fugacity may have been relatively high during metamorphism, which is supported by the high oxidation ratios of the rocks

(Appendix II). There is a suggestion however, that the zone A metamorphism may have experienced higher oxygen fugacity conditions than the zone B metamorphism since the epidotes with the highest and lowest total Fe, therefore Fe^{3+}, contents are from zone A and zone B rocks respectively.

6.7 Prehnite

6.7.1 Mode of occurrence

Prehnite occurs in zone A rocks in small amounts and in even smaller amounts in sub-zone B_1 rocks irrespective of the rock compositions. By definition, it is absent from sub-zone B_2 rocks.

It occurs along small veins with other phases such as chlorite, calcite, epidote or quartz. In the amygdales they are associated with quartz and calcite and sometimes with pumpellyite. The general form is as poly-crystalline aggregates associated with amygdales, the aggregates being up to 2mm across and each individual grain about 0.1 mm (Plate 6.8). However, it also occurs in the groundmass as individual crystals, up to 1 mm in diameter, with generally non-fibrous forms showing uneven extinction. In some amygdales it shows sheaf-like, radiating, fibrous forms with radial extinction. It has a low relief and is colourless, sometimes with anomalous birefingence.

Those grains occurring in the groundmass are generally there as a plagioclase - replacing phase associated with calcite, epidote and chlorite. They are relatively stable in zone A rocks, rarely showing textures suggestive of replacement by chlorite, but in sub-zone B_1 rocks, they are unstable and chiefly replaced by actinolites.

6.7.2 Chemistry

20 analyses of the prehnite (12 in basalts and 8 in gabbros) are presented in Appendix IV.2.6. The structural formula is calculated on the basis that total cations = 24 and OH = 4. Any deficiency from 24

oxygen is attributed to Fe^{3+} and the water content is estimated with the assumption that H=4.

6.7.2.1 Chemical variation and crystal chemistry

The Si content of the Polusagi prehnites is relatively uniform and approximates to the ideal 6 atoms per formula unit. The variation is in the range 5.97 to 6.15 averaging to 6.06. Only in 3 analyses small quantities of Al replacing Si are indicated. The R^{2+} site contains Ca in the range 3.78 (24.8 wt%) to 4.11(27.4 wt%) with an average of 3.96. The alkali content (Na+K), assumed to be replacing Ca is therefore expectedly low and up to 0.04 atoms (0.16 wt%). Mn and Mg contents are very low and up to 0.03 (0.3 wt%) and 0.16 (0.8 wt%) atoms respectively. Ti, when present, is in negligible quantities.

The most important chemical variation in the prehnites is seen in total Fe and Al concentrations. This is governed by a solid-solution series between the two ideal end members $Ca_4Al_4Si_6O_{20}(OH)_4$ and $Ca_4Fe_4Si_6O_{20}(OH)_4$ i.e. by iron substituting for Al. Total Fe which is indicated to be dominantly in the ferric state in most of the analyses, continuously substitutes for Al up to 0.9 atoms per formula unit (Fig.6.35). Similar but higher degrees of Fe substitution of Al in prehnites is reported by Surdam (1969).

6.7.3 Factors controlling the chemistry

The main chemical variation in prehnites i.e. total iron substituting for Al is not related to the concentrations of total Fe and Al in the host rocks. However, the suggestion that most of the total Fe in prehnites is in the ferric state and the high Fe^{3+}/Fe^{2+} ratios of the host rocks (Appendix II) indicate that perhaps the extent of $Fe \rightleftarrows Al$ substitution reaction is related to the iron oxidation ratio in the host rocks.

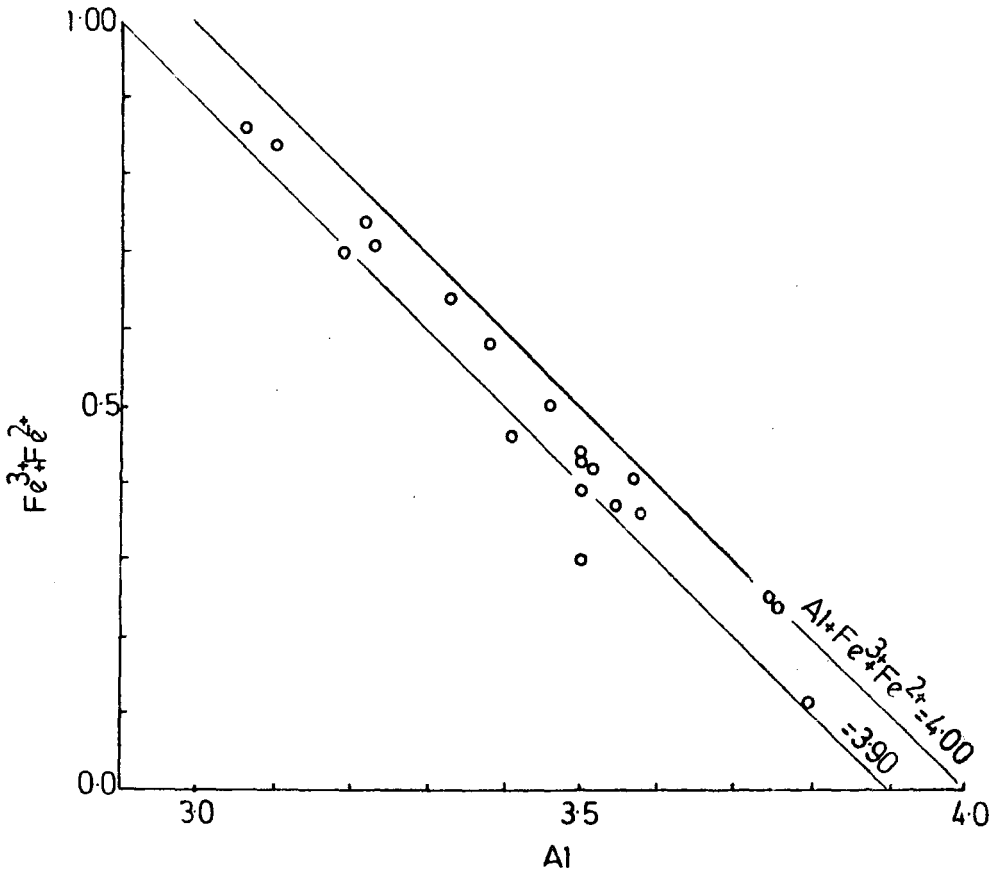


Fig.6.35 ($Fe^{3+}+Fe^{2+}$) vs. Al in prehnites (cations per formula unit, 24 oxygens).

The correlation of the degree of Fe substitution for Al with the metamorphic zones is not clear for the Polusagi prehnites. This may be due to the relatively restricted range of metamorphic conditions under which the prehnites have formed. However, amongst the prehnite analyses from zone A rocks, 4 analyses from a mineralised sample (P213) consistently contain the highest total Fe contents. If it is assumed that this mineralised sample underwent a relatively higher temperature of metamorphism than the non-mineralised samples from zone A, this would suggest that the replacement of Al by Fe is temperature dependent, increasing with increasing temperature. It may also be due to higher amounts of Fe^{3+} available, i.e. higher oxygen fugacity, during the metamorphism of mineralised rocks. However, such conclusions can only be tentative in this study and need verification by more detailed work.

6.8 Pumpellyite

6.8.1 Mode of occurrence

Pumpellyite is a rare phase and the least abundant metamorphic mineral observed in the Polusagi rocks. Apart from 1 basalt sample in subzone B_1 it is confined to the basaltic rocks of zone A. It is associated with prehnite, quartz, epidote and chlorite and occurs as an amygdale filling phase (Plate 6.9). The form is generally fibrous with radiating sheaf-like structures, where it shows radial extinction. Some non-fibrous varieties are cloudy with yellowish or brownish tints occurring in the groundmass.

6.8.2 Chemistry

6.8.2.1 Introduction

9 analyses of pumpellyite from 3 basalt samples are presented in Appendix IV.2.7. The calculation of the structural formula is based on

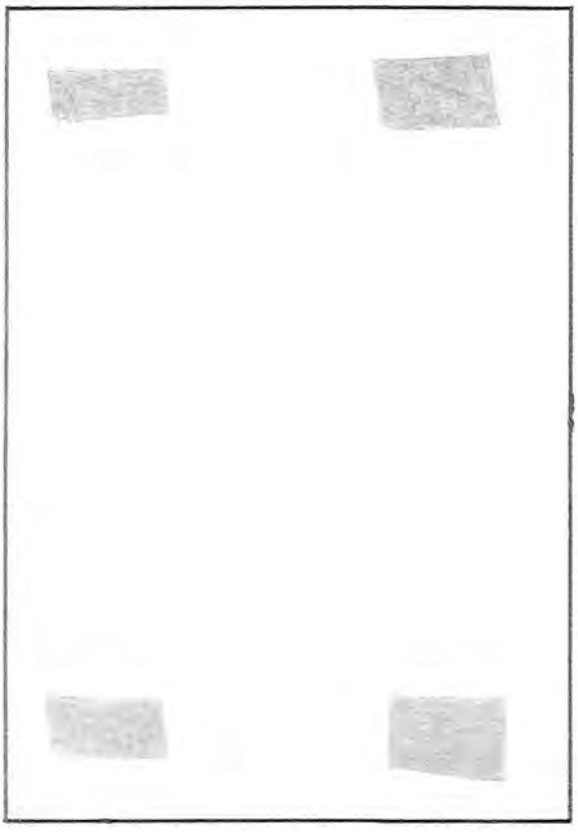


Plate 6.9 : Gas vesicle filled with pumpellyite showing radial extinction. Note the thin coat of quartz (white) around the margin. Sample: P48, X200, crossed-polars.



Plate 6.10 : Calcite with opaque inclusions (iron-oxide). Sample: P24A, X200, crossed-polars.



Plate 6.11 : Round quartz grains (white) within chlorite (patch light grey areas). Note the opaques (black) and the albitised plagioclase laths. Sample: P219, X50.



Plate 6.12 : Ti-rich magnetite (black) being replaced by fibrous amphibole (striated, dark grey). Sample: P277, X80, crossed-polars.

the assumption that total cations = 16, and it contains 7 hydrogens associated with 2 water molecules and 3 OH ions which are used to estimate the water content. Oxygen deficiency from 28 is made up by converting iron into the ferric state.

Coombs et al (1976) suggest that the general formula of pumellyite is $W_4X_2Y_4Z_6O_{(20+x)}(OH)_{8-x}$, where W=Ca, Mn, Fe^{2+}; X = $(Mg,Fe^{2+},Mn)_{2-x'}$, $(Fe^{3+}, Al)_{x'}$; Y=Fe^{3+},Al and Z = Si,Al. The allocation of the cations into various sites in the Polusagi pumpellyites is carried out by the following procedure (Passaglia and Gottardi , 1973):1)Z=6 contains Si, then Al if the sum of octahedral cations (Al,Ti,Fe^{3+},Mg,Fe^{2+},Mn) > 6; 2)Y=4 contains Al, Ti and then Fe^{3+}; 3)X=2 contains excess Al and/or Fe^{3+} from Y site and then Mg, Fe^{2+} and Mn; 4)W=4 contains excess Mn and Fe^{2+} from X site and then Ca, Na and K. These calculations for the Polusagi pumpellyites are listed in Table 6.3.

6.8.2.2 Nomenclature

In this study, the scheme of nomenclature suggested by Passaglia and Gottardi (1973) is adopted as it seems to be gaining popularity (e.g. Coombs et al, (1976); Offler et al,(1981)). According to this classification, the Polusagi pumpellyites are iron-rich pumpellyites, since Al is predominant in the Y site and total Fe is the dominant component of the X site. Due to the uncertainties in the oxidation-state of the iron in the X-site, they cannot be further classified into pumpellyite-Fe^{3+}or pumpellyite - Fe^{2+}, but both names are indicated by the estimated iron oxidation ratios.

6.8.2.3. Chemical variation and crystal chemistry.

The Z site is fully occupied by Si which averages to 6.12 atoms per formula unit. Ca in the W site is relatively uniform, but more varied than Si, in the range 3.73 to 4.02 with an average value of 3.85 atoms. In addition to Ca, up to 0.05 atoms of Fe^{2+} and 0.04 atoms of Mn are allocated into the W site alongside total alkalis up to 0.13 atoms.

TABLE 6.3

Chemical Formula calculations for the Pumpellyites.

Analyses	P76-2A	P76-2B	P76-3B	P76-3C	P213-3A	P213-4A	P213-4B	P213-4C	P271-1B
Si	6.163	6.098	6.169	6.137	6.161	6.077	6.039	6.043	6.157
Z total	6.163	6.098	6.169	6.137	6.161	6.077	6.039	6.043	6.157
Ti	0.003	0.004	0.004	0.004	0.007	0.005	0.001	0.004	0.004
Al	3.997	3.996	3.794	3.996	3.993	3.837	3.763	3.803	3.996
Fe^{3+}	-	-	0.202	-	-	0.158	0.236	0.193	-
Y total	4.000	4.000	4.000	4.000	4.000	4.000	4.000	4.000	4.000
Al	0.240	0.186	-	0.192	0.324	-	-	-	0.329
Fe^{3+}	0.464	0.627	0.789	0.537	0.348	0.882	0.948	0.933	0.394
Mg	0.522	0.516	0.520	0.548	0.021	0.556	0.583	0.647	0.101
Fe^{2+}	0.774	0.657	0.621	0.671	1.264	0.469	0.371	0.405	1.176
Mn	-	0.014	0.027	0.025	0.043	0.018	0.014	0.011	-
X total	2.000	2.000	1.957	1.973	2.000	1.925	1.916	1.996	2.000
Fe^{2+}	0.031	-	-	-	-	-	-	-	0.052
Mn	0.019	0.017	-	-	0.037	-	-	-	0.028
Ca	3.762	3.873	3.740	3.874	3.808	3.958	4.018	3.936	3.725
Na	0.019	0.013	0.130	0.023	0.003	0.039	0.026	0.024	0.035
K	0.002	0.000	0.002	0.000	0.001	0.002	0.000	0.000	0.004
W total	3.833	3.903	3.872	3.897	3.849	3.999	4.044	3.960	3.844

The dominant and important variations in pumpellyites are those of total Fe, Al and Mg, occupying the octahedral X and Y sites (Coombs et al 1976) The total Fe,Al and Mg contents of the Polusagi pumpellyites in these sites vary in the range 1.61 to 1.24, 3.76 to 4.32 and 0.02 to 0.65 atoms respectively. These variations are plotted in Fig. 6.36, and compared with the pumpellyites from other areas. The Polusagi pumpellyites are similar to those reported from the prehnite-pumpellyite facies metamorphic rocks of Upper Wakatipu, Vancouver Island, Olympic Peninsula, Janestown and to some reported from Taiwan Ophiolites.

The dominant substitution reactions in the pumpellyites are $Fe^{2+} \rightleftharpoons$ Mg and $Fe^{3+} \rightleftharpoons$ Al indicated in a plot of total Fe i.e. $Fe^{3+} + Fe^{2+}$, against Al+Mg (Fig.6.37).

6.8.3 Factors controlling the chemistry

All the pumpellyite analyses are from 3 samples and Si,Al,total Fe and Mg contents are rather varied even in the analyses from one sample. Therefore, the chemical or physical factors that may have affected the chemistry are very hard to assess. In general,the effects of the various factors seem to be complex. Jolly (1980) reports that the iron contents of pumpellyites increases with increasing iron content of the host rocks. On the other hand, such a host rock compositional influence is shown to be non-operative by Offler et al (1981) in the pumpellyites from low-grade metamorphic terrains in Newcastle, New South Wales, Australia. These authors state that the more important factors are "the intensity of alteration and the chemistry of the fluids in contact with the solid phases forming the domain where the pumpellyite has nucleated". Schiffman and Liou (1980) point out that the compositional variations between Fe- and Al-rich pumpellyites are dependent on metamorphic grade as well as rock composition. According to these authors, pumpellyites with <10 wt%

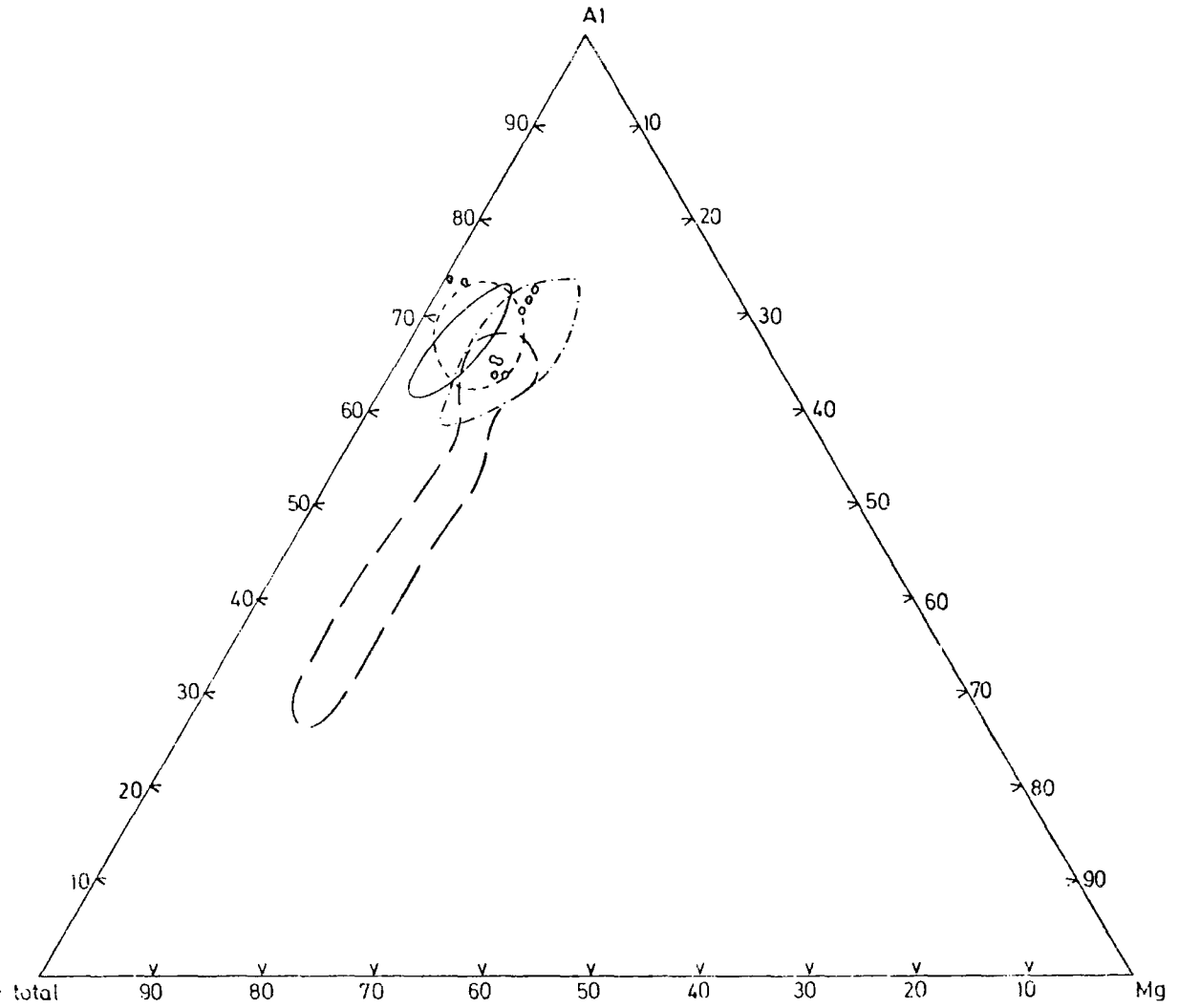


Fig.6.36 Mg-Al-Fe^{total} triangular diagram showing the compositional variation in pumpellyites.
Compositional fields after Coombs et al (1976) and Schiffman and Liou (1980)

— — : Taiwan ophiolites (Liou, 1979)

——— : Vancouver Island (Surdam, 1969 and Kuniyoshi and Liou, 1976)

– – – – : Upper Wakatipu, New Zealand (Kawachi, 1975).

—·—·— : Olympic peninsula (Glassley, 1975) and Janestown Park (Zen, 1974).

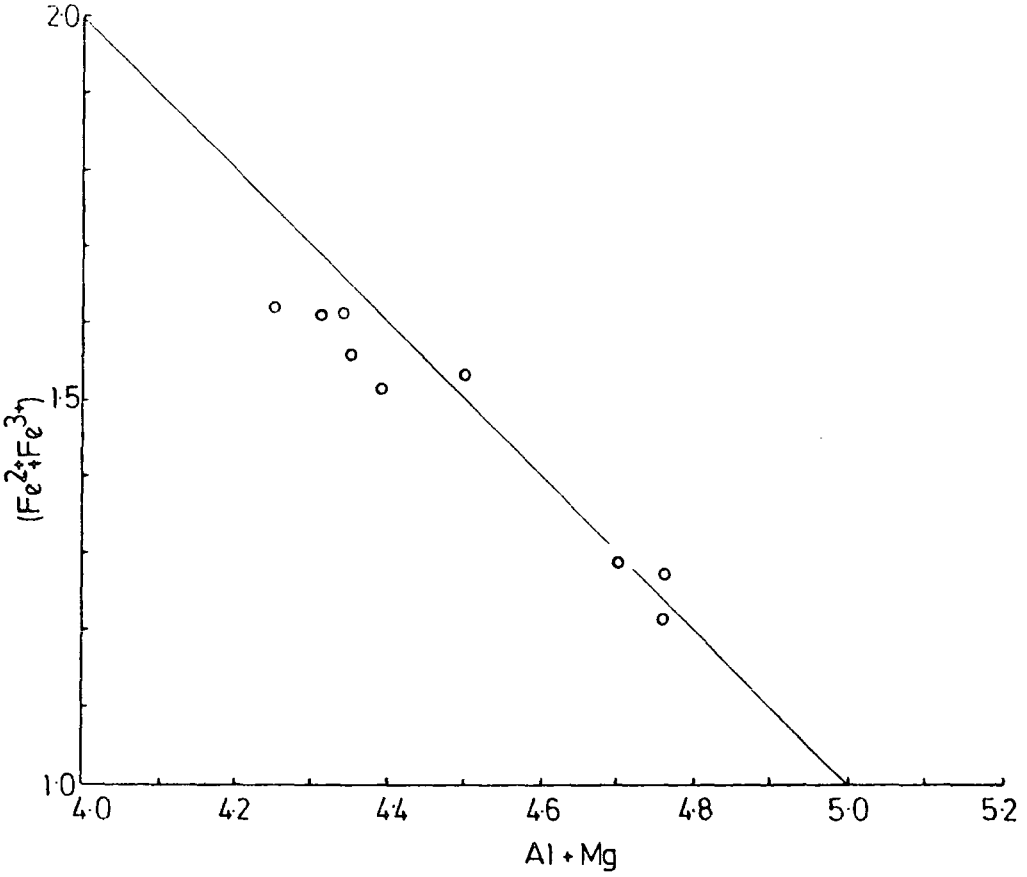


Fig.6.37 $(Fe^{3+}+Fe^{2+})$ vs. (Al+Mg) in pumpellyites (cations per formula unit, 28 oxygen).

total Fe (as Fe_2O_3) are associated with pumpellyite-actinolite or blueschist facies and those with >10 wt% total Fe with zeolite or prehnite-pumpellyite facies metamorphism. However, the Polusagi pumpellyites, having about 9-12 wt% total Fe and being associated with prehnite-pumpellyite facies (zone A), seem to have transitional total Fe contents. Schiffman and Liou (op cit) also consider that the crystallisation of high iron-rich pumpellyites under low-grade conditions may be a process strongly influenced by solution chemistry and oxygen fugacity.

6.9 Other mineral phases

Calcite, quartz, opaque oxide phases and sphene-leucoxene are the other phases worth consideration in the Polusagi rocks. Minerals of economic value, sulphides, sulphosalts and related minerals will be described in the next chapter.

6.9.1 Calcite

It occurs in appreciable amounts only in the basaltic rocks of zone A and is rather scarce in the other rock types. It is present in small quantities in sub-zone B_1 and absent in sub-zone B_2. Calcite is generally a vein and amygdale filling phase, sometimes together with other phases such as chlorite, prehnite and quartz. It is also commonly found as a decomposition product after plagioclase. In the latter case, it is not coarse-grained but rather fine and may form numerous isolated patches within the albitised plagioclase laths or phenocrysts. In some basaltic rocks of zone A the calcite filled amygdales also contain iron-oxides where calcite may also be associated with patches of hematite (Plate 6.10).

6.9.2 Quartz

This is a common metamorphic mineral and its abundance increases from basic to acid rock types of zone A; it is relatively scarce in zone B rocks. It is practically impossible to distinguish the primary quartz occurrences from the metamorphic ones and it seems that most, if not all, of the primary quartz has been mobilised and recrystallised. In the rocks from the stockwork mineralisation the development and/or introduction of secondary quartz into the rocks is most intense and in many cases it becomes the dominant mineral phase together with pyrite. In the lavas it occurs as an amygdale filling phase on its own or together with chlorite, calcite and prehnite. It is also found as a phase replacing plagioclase and less commonly clinopyroxene. Its relation with chlorite, especially in andesitic and dacitic rocks of zone A, is conspicuous in that spherical quartz grains around 0.1 mm in diameter are intimately related to chlorite. These round grains sit in the middle of chlorite aggregates (plate 6.11) and may be single crystals or polycrystalline. This relation is commonly seen where plagioclase seems to be replaced by chlorite.

6.9.3 The opaque oxides, sphene and leucoxene

The opaques in the Polusagi rocks are predominantly Ti-rich magnetites. In the gabbro and plagiogranite samples ilmenite also occurs either as exsolution lamellae in the Ti-rich magnetite or as separate grains. These opaque minerals are not found as phenocrysts or microphenocrysts and the size of the grains are within the range of the average grain size of the rocks within which they are found. Ilmenite in the hypabyssal rocks sometimes shows skeletal forms. Both Ti-rich magnetite and ilmenite are extensively altered. Alteration is such that numerous micro-veins of silicates invade the grains, and the surface of the phases under the reflected-light microscope is clouded by the silicate replacement. The chief phases replacing the opaques, especially

the Ti-rich magnetite are chlorite (Plate 6.12) and actinolite. On the other hand they are also oxidised and altered into hematite, sphene and leucoxene. Sphene occurs in all rocks as an ubiquitous but minor phase fixing the Ti-released from the opaques and the Ca-released during the albitisation of plagioclase.

One relatively clear patch of Ti-rich magnetite analysed by electron microprobe gave the following result with a total of 93%: Fe^{total} = 62.2%, Ti = 22.2%. Si = 2.9%, Ca=2.4%. Al = 2.2%, Mn = 1.0% which demonstrates the presence of silicates in microscopic scale due to alteration.

6.10 General features and textural relations in the metamorphic zones

6.10.1 Introduction

Some textural inter-relations have already been mentioned during the examination of the individual mineral phases. Here, general inter-relations of minerals with respect to the zones and the general features of the rocks will be discribed. The textural variations in the rocks are not only present between the metamorphic zones but also, when studied in detail, amongst different samples within a zone. Therefore, emphasis will be given to the more common and significant features. The zones A, B_1 and B_2 are shown on the map in Fig.6.38.

6.10.2 General features of metamorphic zones

Each zone contains basic, intermediate and acid rock compositions. Most of the volcanic rocks in the studied area are in zone A and zone B embraces all the gabbroic and plagiogranitic occurrences as well as the rest of the volcanics. Thus the zones are not composition bound. It seems therefore that the mineralogical variations are mainly due to the variations in the metamorphic conditions they have undergone,

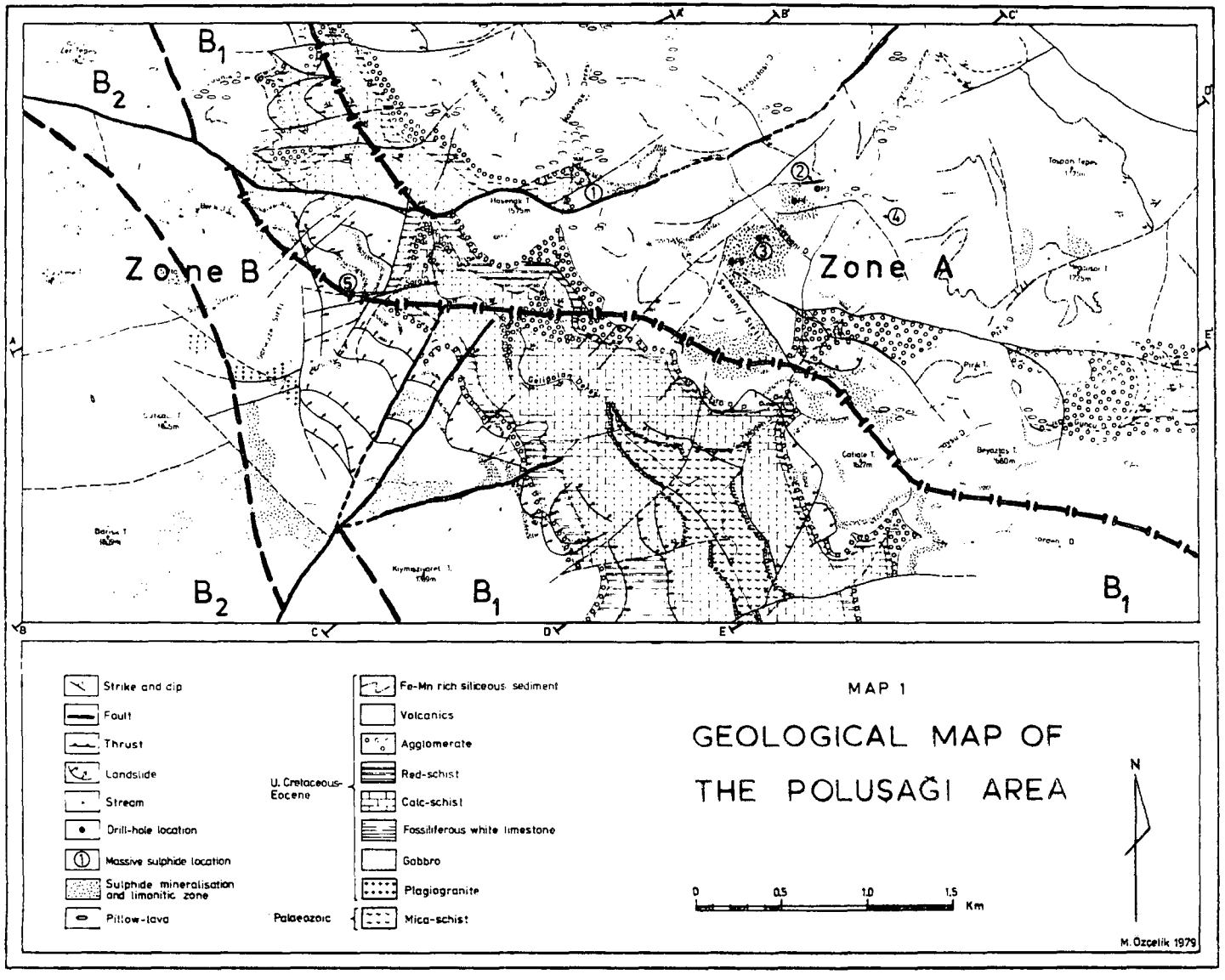


Fig. 6.38. Metamorphic zones in the Polusagi area.

: Boundary between zones A and B. : Boundary between sub-zones B_1 and B_2 .

although the compositional variations of the rocks in different zones may have influenced the relative abundances of the metamorphic minerals. The boundary between zone A and zone B is comparatively better defined than the boundary between sub-zones B_1 and B_2 which is rather irregular. In a general sense, the boundaries run in a NW-SE direction. Zone A is situated to the NE covering about half the studied area and includes most of the apparent Cu-Zn mineralisation and almost all the Fe-Mn rich sedimentary chert bands. The boundaries between the zones are roughly parallel to the general strike direction of the volcano-sediments and the volcanics. This suggests that the zones, therefore the grade of metamorphism, are depth controlled i.e. with increasing depth zone A passes into sub-zone B_1 then to B_2.

6.10.3 Mineral relations and abundances across the zones

Clinopyroxene, being an igneous relict phase, shows no signs that it replaces any other phase. On the contrary, it is unstable under the metamorphic conditions and variably replaced by the metamorphic phases. In zone A, it largely survives the metamorphic conditions and tends to retain its igneous form. Its decomposition product is mainly greenish chlorite and to a lesser extent calcite. In the basaltic andesites of this zone minor amounts of quartz also replace it. In zone B, cpx is largely replaced by actinolite (Plate 6.2) and to a lesser extent by the bluish or brownish chlorite and epidote. The extent of decomposition of cpx is variable in this zone : it is progressively replaced, mainly by actinolite, from sub-zone B_1 towards B_2 and in sub-zone B_2 it is completely overtaken. A good example of such a progressive replacement of clinopyroxene is demonstrated by the basalt samples P252 in sub-zone B_1 and P253 which is situated a few hundred meters to the SW into the sub-zone B_2. P252 contains a lot of relict clinopyroxenes which are clearly attacked and replaced by

actinolites, while in P253 the destruction is complete and there is no clinopyroxene present. The progressive disappearance of clinopyroxene is considered to be a result of the increasing metamorphic grade from zone A towards sub-zone B_2.

The index minerals prehnite and pumpellyite are not only present in zone A, - by definition-, but also are stable. They are not replaced by the other metamorphic phases in zone A. But in sub-zone B_1 they are replaced progressively and extensively by actinolite and to some extent by the bluish and brownish chlorites i.e. they are present in sub-zone B_1 as unstable phases. The progressive decomposition of prehnite and pumpellyite is completed in the SW corner of the mapped area and this, by definition, separates the sub-zones B_1 and B_2.

Zone B is defined by the presence of actinolite which becomes progressively more abundant towards the SW from the boundary with zone A. In sub-zone B_2, actinolite is the dominant phase together with albite. Textural relations suggest that actinolite and the green amphibole are the latest metamorphic phases to have formed. Actinolite develops at the expense of almost every other phase, that is mainly clinopyroxene, prehnite, pumpellyite, albite, chlorite and to a lesser extent quartz and brown hornblende. In the gabbroic samples, brown hornblende replaces clinopyroxene (Plate 6.1) but is replaced chiefly by green amphibole and actinolite and to some extent by chlorite and quartz. Clearly the brown hornblende is neither stable under the zone B metamorphic conditions nor is it a product of the igneous conditions that produced the clinopyroxene. It is thought that the brown hornblende belongs to a late magmatic stage.

Not only do chlorites change physically and chemically from zone A to zone B i.e. from greenish to bluish and brownish types, but their abundance also decreases in the direction towards the SW corner of the studied area. In zone A, chlorite is the major phase occupying the groundmass and there it replaces albite and the opaques. In zone B it retains its role

as the major groundmass phase and the decomposition product after albite and the opaques, but in reduced proportions. Additionally, it replaces prehnite, pumpellyite and the brown hornblende in the gabbroic rocks. In this zone, it replaces clinopyroxene more extensively than in the volcanic rocks of zone A.

Albite is almost totally confined to the previous plagioclase sites and does not replace any other phase. In zone A, chlorite is the main phase replacing it but phases such as calcite, epidote, prehnite and quartz also form after it. In zone B, replacement by epidote and actinolite becomes more important in addition to that by chlorite. In the gabbroic rocks, some clear rims of metamorphic calcic-plagioclase develop around and at the expense of albite grains.

Epidote occurs in all zones but its abundance is relatively higher in zone B. Sphene does not show any preference to the zones. Calcite, as already stated, is present in appreciable amounts only in the basaltic rocks of zone A and is scarce in zone B.

The above observations are summarised in Fig.6.39.

6.10.4 General order of crystallisation in gas vesicles

The gas vesicles and the veins in the volcanic rocks are filled with metamorphic mineral phases such as chlorite, quartz, calcite, prehnite, pumpellyite, epidote and pyrite. Albite is very rare and actinolite is not present in the amygdales. The order of crystallisation of these minerals follows a general sequence. The most interesting is the relationship of chlorites and quartz. When present together in the gas vesicles and veins, the deposition of chlorites always follows the same order i.e. from greenish to bluish, then to brownish varieties. In others, deposition of chlorites may be alternately followed or preceded by deposition of quartz in the amygdales so that a sequence such as:

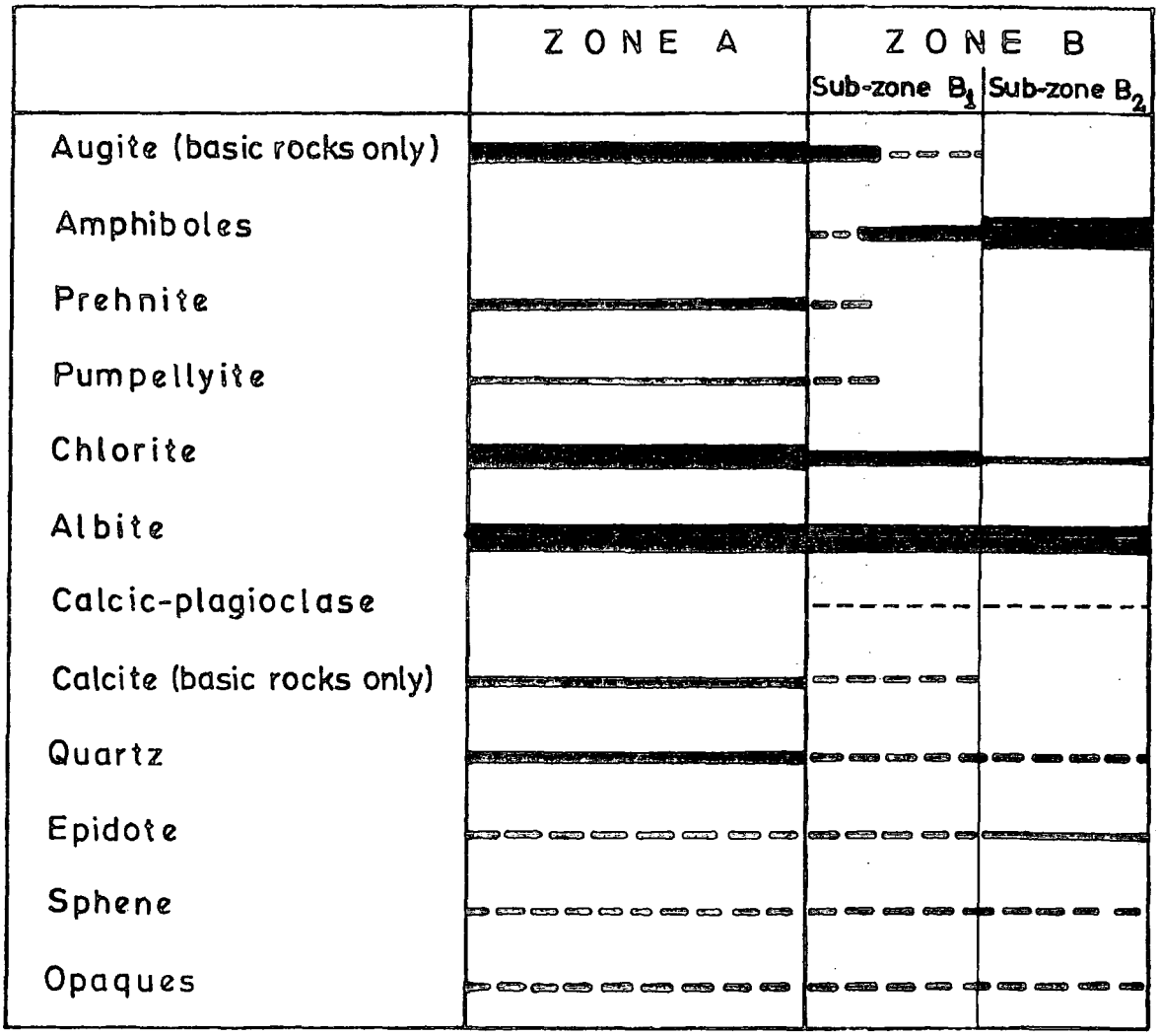


Fig.6.39 Mineral abundances in the metamorphic zones.

quartz→greenish chlorite→quartz→bluish chlorite→quartz

may be observed from the rim to the core. These alternations and the general order with which other phases crystallise in the gas vesicles and veins show that chlorite and quartz are early phases followed by prehnite and pumpellyite. These again may be followed by some chlorite and/or quartz. Epidote, calcite, pyrite and hematite seem to be the later phases filling the amygdales and veins. No systematic variation is observed in the order of crystallisation in the volcanics of zones A and B.

6.11 Evaluation of metamorphic conditions

6.11.1 Introduction

Relict igneous phases and textures, lack of penetrative metamorphism and the evidence discussed in this chapter indicate that pressure during the metamorphism of the Polusagi rocks was low i.e. less than 3 kbars and probably even less than 2 kbars. Therefore the main factor that determined the variation in metamorphic grade can be taken to be the variation in temperature.

6.11.2 Zone A

The mere fact that zeolites are not present in the rocks of the studied area shows that the grade in zone A was higher than the zeolite facies metamorphism. The presence of the index minerals prehnite and pumpellyite shows that the metamorphic conditions in zone A were of prehnite-pumpellyite facies which is recognised as a transitional facies between zeolite and greenschist facies metamorphism and reported from many areas (E.g. Coombs et al, 1959, 70, 76 ; Jolly, 1970; Miyashiro, 1978). The same facies is termed "prehnite-pumpellyite-chlorite zone" of the "very low grade metamorphism" by Winkler (1974). The typical assemblage of zone A is albite+chlorite +prehnite $\pm$ pumpellyite $\pm$ calcite

$\pm$ quartz $\pm$ epidote which is common in prehnite-pumpellyite facies metamorphic conditions (e.g. Miyashiro 1978).

Nitsch (1971) estimates the temperature of the appearance of prehnite +pumpellyite+chlorite+albite in the range 350-400°C. According to the experiments of Liou (1971), prehnite-pumpellyite facies is stable, at pressures exceeding 2 kbars and around 3 kbars in the temperature range 250-380°C and he suggests a maximum temperature for crystallisation of prehnite to be 403°C at 3 kbars where fluid pressure = total pressure. Glassley (1974) considers that quartz-pumpellyite would disappear before prehnite-chlorite with advancing metamorphism at 1 and 2 kbars. Similarly Schiffman and Liou (1980) indicate that in general pumpellyite is more stable at lower temperatures than prehnite. The rarity of pumpellyite in relation to prehnite in the Polusagi rocks therefore may indicate that the lower thermal boundary for zone A may have been higher than the generally considered temperaturesi.e. $>$ 250°C. Thus it seems reasonable to suggest a temperature range of 300-400°c for the prehnite-pumpellyite facies metamorphism of zone A.

6.11.3 Zone B

The typical mineral assemblage of this zone is albite+actinolite+epidote+chlorite$\pm$quartz which is typical of basalts and andesites that have undergone greenschist facies metamorphism (e.g. Miyashiro, 1978) or the "low grade metamorphism" of Winkler (1974). The unstable nature of prehnite or its absence in this zone suggests a lower thermal boundary at 400°C (e.g.Raith et al, 1977). Winkler (1974) estimates the temperature of transition of the greenschist actinolites into hornblende at about 500°C and 3 kbars rising only slightly with increasing pressure and marking the transition of greenschists into amphibolites. Although a change from actinolites to hornblende is not encountered in this zone

there are signs that the transition temperature into amphibolites was not far away : i.e. the bluish tint in some of the actinolites and green amphibole and the observed jump from albite composition to more calcic plagioclase compositions which Winkler (1974) states takes place 20-40°C lower than the temperatures attained at the transition from "low grade" to "medium grade" metamorphism.

Liou et al (1974) indicate an upper thermal boundary of the greenschist assemblage albite+chlorite+actinolite at 475°C and the lower limit of the amphibolite assemblage plagioclase+hornblende at 550°C. According to Liou et al (op cit) the transitional assemblage plagioclase +actinolite+chlorite, which is attained in some gabbroic samples in Polusagi, occurs within the range 475-550°C.

Therefore, a general temperature range 400-500°C seems reasonable for the Polusagi zone B greenschist facies conditions.

Two further conclusions can be drawn from the above discussion :

a) The conclusion that in general the temperature range in zone A was 300-400°C would mean that some local temperatures around and above 400°C must have existed along certain zones where stockwork mineralisation took place (see section 6.4.3.2).

b) Since prehnite and pumpellyite seem to have developed and become unstable later in zone B, it follows that prehnite-pumpellyite facies metamorphic conditions must have been prevailing in zone B prior to greenschist facies metamorphic conditions. This indicates a rise in temperature during the evolution of metamorphic processes from about 300-400°C to 400-500°C which may be a result of burial under increasingly thickening rock pile during submarine volcanism.

The possible cause of the metamorphism will now be considered.

6.12 Nature of metamorphism.

6.12.1 Introduction

Incomplete metamorphic recrystallisation plus the non-penetrative and low pressure nature of the Polusagi metamorphism suggest that the rocks escaped the high or medium pressure type regional orogenic metamorphism that may have been present during the transport of the rocks from the Tethyan marginal basin to the present location on land. The gabbroic and plagiogranitic intrusions are metamorphosed to the same grade as the surrounding volcanic rocks. This indicates that contact metamorphism due to the heat released by the intrusives was not the major cause of metamorphism, but that the process was controlled externally. Burial metamorphism as defined by Coombs (1961) is taken by Miyashiro(1978) as a category to include parts of both low-grade regional metamorphism and ocean-floor metamorphism. Although "burial metamorphism" must have played a part in the process of the Polusagi metamorphism, it is considered more likely on the whole that the process was a result of ocean floor hydrothermal activities for the reasons explained below. At this point, it is beneficial to summarise the now widely accepted hypothesis of ocean floor hydrothermal metamorphism (Elder 1965,1967,1977, Spooner and Fyfe 1973, Spooner et al 1977 a,b; Gass 1980).

Elder's theoretical work (op cit) showed that the hydrothermal convection of sea-water through the newly formed hot oceanic-crust was not only possible but likely. Spooner and Fyfe (op cit) suggested that metamorphism takes place in sub-sea-floor geothermal systems and such systems are an integral part of the sea-floor spreading processes where the oceanic-crust is hydrated and oxidised. These predictions are justified by the ubiquitous presence of hydrated and oxidised meta-basalts, meta-gabbros and serpentinites in many ocean floor dredge hauls.

The hypothesis of ocean floor hydrothermal metamorphism proposes a sea-water-basalt interaction during hydrothermal convection of sea-water through the oceanic-crust along permeable zones of structural weakness

created by tectonic movements or permeable pillow lava piles. During the convection, circulating sea-water is heated up and modified by leaching metals like Fe, Mn, Cu, Zn, Pb, Ni, Co, Ag and Au and redistributes other elements including Si. The circulation of hot brine through the oceanic crust imposes a hydrothermal metamorphism whose grade increases downward from zeolite to greenschist to amphibolite facies. In such a sub-sea floor geothermal system, the hot hydrothermal solutions undergo chemical and thermal evolution before they finally are discharged into the sea-water. During their return to the ocean floor the fluids are directed along discrete localised channels such as faults along which precipitation takes place in response to decreasing temperature as fluids rise. On the sea-floor, a reaction between the heavy metal-enriched hot brine and the sea-water occurs, resulting in precipitation of sulphides or Fe-Mn oxide or hydroxide-rich sediments. In favourable sites, these accumulate and form ore bodies. An important feature of this hypothesis is that it requires abnormally high thermal gradients on the oceanic crust for activation, such as ocean floor spreading centres.

Circulation of hot brine in such geothermal systems not only causes intense metamorphism, but also provides an important mechanism for transporting and depositing a variety of heavy metals from the oceanic-crust to the ocean floor.

Metamorphic events resulting from ocean floor hydrothermal activities are now recognised in many ophiolites including those from Troodos (Spooner et al, 1977 b; Gass, 1980), E.Liguria, Italy (Spooner and Fyfe, 1973; Spooner et al, 1977a), East Taiwan (Liou and Ernst, 1979), Betts Cove (Coish, 1977), Sarmiento, Chile (Elthon and Stern, 1978) and Southern Cordillera, Chile (Stern et al, 1976). The Cyprus cupriferous pyrite deposits are identified with the sites of discharge of the hot brines (Spooner et al 1977b). Oxygen and strontium isotope geochemistry of the E.Ligurian and Troodos ophiolites (Spooner et al 1977 a,b) and the

lead and strontium isotope geochemistry of the metalliferous sediments of Troodos; Baer Bassit (Syria) and Semail Nappe (Oman) ophiolites support the hypothesis of ocean floor hydrothermal metamorphism (Gale et al,1981).

In recent years, such geothermal systems connected with ocean floor spreading processes have been discovered in many locations on the sea-floor such as the East Pacific Rise and the Galapagos rift, where hydrothermal vents with fluid temperatures up to 400°C actively precipitating sulphides and Fe-Mn rich sediments have been observed (MacDonald et al, 1980 ; Bischoff,1980; Francheteau et al, 1979; Hekinian,et al,1980;rise project group, 1980; Corliss et al, 1979; Edmond, 1981).

6.12.2 The Polusagi metamorphism

It is proposed that the Polusagi rocks have undergone an ocean floor hydrothermal metamorphism which took place at the Tethyan marginal ocean basin crust by considering the following criteria:

1) Miyashiro et al (1971) assume that the crust beneath the normal ocean basins is about 6 km thick and estimate that the temperature at the base would be in the order of 120-180°C. During the greenschist facies metamorphism in the Polusagi rocks temperatures as high as 500°C are indicated. Therefore, even if it is assumed that the Polusagi greenschist facies metamorphism took place at the bottom of the Tethyan oceanic crust, the temperatures and hence the thermal gradient, are still abnormally high. High thermal gradient associated with the metamorphism is also evident from the fact that the vertical thickness of the rocks studied is in the order of 2 km within which a metamorphic temperature variation in the order of 200°C is indicated. The fact that the temperature increases from top to bottom in the studied area suggests that the dominant heat source must have been the underlying magma and less importantly the heat of the volcanic or hypabyssal rocks.

2) The Polusagi rocks have been hydrated to various degrees during metamorphism. The water content of 34 analysed samples (Appendix II) shows an average value of 2.6% and a range 0.9 to 4%, which is incorporated mainly into the metamorphic minerals such as chlorite, prehnite, pumpellyite and actinolite. The average water content of ocean floor basalts is quoted as 0.3% by Spooner et al (1977 a,b) who consider the hydration as a clear evidence of alteration by water-rock interaction. Therefore, the hydrated nature of the Polusagi rocks is consistent with a progess of water-rock interaction.

3) The Polusagi rocks exhibit Fe_2O_3/FeO ratios from 0.3 to 1.6 (Appendix II), the same ratio is as low as 0.15 in the average ocean floor basalt (Spooner et al 77a). The Polusagi rocks are therefore oxidised to varying degrees and on average the Fe_2O_3/FeO ratio decreases from zone A rocks(average 0.78) to zone B rocks (average 0.55). Such a decrease of ferric iron proportion i.e. oxygen fugacity, with depth is also indicated by epidote chemistry (section 6.6.3.2). These observations suggest that in the upper parts of the metamorphosed Polusagi rocks, solutions responsible for the hydration were also relatively more oxygenated than the lower parts. The solutions producing such alteration could not have been juvenile water as it would be reduced and hydrogen enriched (Spooner and Fyfe 1973). These suggest that the fluid responsible for the metamorphism of Polusagi rocks was introduced from the top which predominantly circulated downward and oxygen was progressively consumed with depth. The most obvious source in a sub-marine environment is the then existing Tethyan sea-water.

4) The suggestions made above are also consistent with the occurrence of calcite predominantly in zone A i.e. upper levels of the metamorphosed rocks. During the sea-water-rock interaction in the Tethyan marginal basin crust, the sea-water, which must have contained some

dissolved Ca^{2+} and HCO_3^-, would penetrate into the rocks, get heated and enriched in Ca which is released by the breakdown of plagioclase to albite. Further downward movement of this brine, now enriched in Ca, would result in a further increase in temperature and since the solubility of Ca decreases drastically with increasing temperature (Coish, 1977; Holland and Malinin, 1979) calcite would precipitate rapidly at the upper sections of the rocks, with the lower sections being largely devoid of it.

5) The dominently down-going hot brine must be discharged upwards towards the sea-floor along channels and zones such as faults passing through the upper parts i.e. the zone A rocks at Polusagi. This would not only lead to a decrease in the temperature of the metal enriched brine, thus resulting in stockwork mineralisation along the discharge channels and subsequently heavy metal rich precipitates or sediments on mixing with sea-water on the sea-floor, but also cause a higher grade hydrothermal metamorphism of the rocks adjacent to the discharge channels. Therefore the observation made earlier in this chapter that in zone A the mineralised rocks or the rocks adjacent to the mineralised areas generally indicate higher temperatures of metamorphism, is explicable by these mineralised rocks being altered by fluids introduced from below zone A having higher temperatures than generally attained in the zone. In other words these localised areas represent the discharge channels or zones for the hydrothermal solutions that caused the metamorphism and produced the stockwork mineralisation, where temperatures around or above $400^{\circ}C$ were attained.

CHAPTER SEVEN

ORE MINERALISATION

7.1. Introduction

The general relations of ore mineralisation to enclosing rocks in the Polusagi and Canakci areas have been discussed in Chapter two and the presence of 'disseminated', 'stockwork' and 'massive' ore types in the volcanic rocks of the Polusagi area was emphasised. It was shown in the foregoing chapter that the Polusagi rocks were hydrothermally metamorphosed to prehnite-pumpellyite facies grade, passing downward to greenschist facies grade in a geothermal system operating on the Tethyan marginal basin. There it was suggested that the stockwork mineralisation represented channels along which the metal-bearing hydrothermal solutions moved upwards in the volcanic pile towards distinct discharge outlets on the sea-floor, having temperatures $> 400^{o}C$ on entrance into the now prehnite-pumpellyite facies grade metamorphosed volcanic rocks. Considering the transitional relationship of the massive ore mineralisation with the underlying stockwork mineralisation (Chapter two), it is reasonable to assume that the massive ore mineralisation and the overlying Fe-Mn-oxide-rich and sometimes sulphide-rich sedimentary cherty levels are direct products of the hydrothermal activity that took place near or at the sea-floor. Such a perspective will be kept in mind when discussing and evaluating the ore mineralisation in the following pages.

In this chapter, textural, mineralogical and chemical features of the ore minerals and the mineralisation in general will be examined in both areas studied, with special emphasis on the Polusagi area. The general characteristics of the 5 exposed massive sulphide outcrops in the Polusagi area (Chapter two) are similar, and will altogether be referred

to as the "massive sulphide" mineralisation.

All the ore mineral samples were collected from the surface outcrops with the exception of some samples taken from short adits in the massive ore occurrences in Locality 1, and small excavations in Localities 2 and 3 of the Polusagi area. About 100 polished ore samples and 50 polished thin or ordinary thin sections from both areas have been examined and a number of microprobe analyses of ore minerals have been made. The analyses, analytical conditions and procedures are presented in Appendix IV.3.

7.2 Ore mineralisation in Polusagi

7.2.1. Sulphide mineralisation

7.2.1.1. Introduction

As was discussed in Chapter two, sulphide mineralisation in general takes three distinct forms:

a) Fracture filling, normally pyritic, stockwork mineralisation where a certain amount of sulphide mineralisation has replaced the surrounding rocks.

b) Compact, poly-mineralic, massive sulphide mineralisation which shows mineralogical banding and is generally associated with the Fe-Mn rich cherts. The massive sulphides are normally underlain by the stockwork mineralisation.

c) Disseminated or semi-massive sulphide mineralisation occurring at the top of some stockwork mineralisation or as broadly stratified disseminated pyritic horizons not obviously underlain by a stockwork type mineralisation. The sulphide horizons may sometimes show mineralogical banding.

Type c) mineralisation is taken to be a transitional stage between the 'stockwork' and 'massive' type ore mineralisation, therefore in the

following pages this type will be treated as such and discussion will concentrate on stockwork mineralisation 'grading' into massive ore mineralisation.

The major constituents of the ore mineralisation in Polusagi are pyrite, chalcopyrite and sphalerite. Pyrite is ubiquitous, while the presence and the relative proportions of chalcopyrite and sphalerite depend on the type of mineralisation. The minor ore mineral phases include galena, fahlore and bornite. Trace amounts of magnetite and hematite and small amounts of supergene minerals, idaite and covellite occur within the sulphide mineralisation. Malachite, cuprite, native copper and some hematite have been identified within the country rocks.

General mineralogical and textural features of the sulphide mineralisation are now presented and their genetic implications are discussed.

7.2.1.2 Zonation

Mineralogical and textural zonation exists vertically from the stockwork type grading into the massive type mineralisation. In the stockwork mineralisation the dominant ore mineral is pyrite which is typically coarse, up to 3 mm in diameter, generally euhedral to subhedral and relatively free of inclusions. Characteristically the mineralisation is fracture filling disseminated pyrite in a siliceous matrix. As this type of mineralisation develops upward into the massive poly-metallic sulphide mineralisation, pyrite in general changes to a finer grained porous, subhedral to anhedral forms. Although in the massive ore pyrite may be coarse and euhedral, this is not typical.

With the transition of stockwork mineralisation upward into the massive sulphide mineralisation, the ore mineral content changes through first an increase in the amount of chalcopyrite associated with pyrite, followed by the appearance and increase in the amount of sphalerite, coupled with a decrease in the gangue mineral content i.e. increasing

sulphide/gangue ratio. The massive ore overlying the stockwork mineralisation is dominated by pyrite (with a lot of inclusions), chalcopyrite and sphalerite whose relative proportions vary as a result of strong mineralogical banding. The massive ore body, especially towards the uppermost levels i.e. away from stockwork mineralisation, is associated with reddish or brownish, Fe- and/or Mn-oxide rich cherty sedimentary horizons which also form a blanket over the massive sulphides. The massive sulphides are not only richer in chalcopyrite and sphalerite than the disseminated stockwork mineralisation, but also contain minor amounts of galena, fahlore and bornite which are not present in the stockwork mineralisation. Finally, two iron oxides, magnetite occurring in sphalerite as minute inclusions and hematite, are found in trace amounts associated with massive sulphides and increasingly towards the top but especially near the reddish cherty sedimentary bands in the massive ore. The overlying cherty horizon may contain thin sulphide bands. In summary, the following vertical upward zonation, from top to bottom, can be generalised :

1) Cherty or muddy sediments, rich in hematite and Mn-oxides, containing thin sulphide bands.
2) Massive ore (consisting of pyrite, chalcopyrite, sphalerite and minor galena, fahlore and bornite) + traces of magnetite and hematite + minor Fe-Mn rich cherty sedimentary fragments or thin bands.
3) Massive ore + lesser magnetite and hematite traces.
4) Pyrite + chalcopyrite + minor sphalerite.
5) Pyrite + minor chalcopyrite + traces of sphalerite.
6) Pyrite.

The zonation of ore minerals is accompanied by a zonation in the gangue minerals. In the typically pyritic stockwork mineralisation, the gangue is mainly fine grained quartz forming the matrix. Fine anhedral quartz grains are typically 30-40 microns across. However, coarser quartz

grains around 0.5 mm in diameter occur especially associated with the later developed thin veins. In the silicified matrix, the disseminated pyrite mineralisation is associated with brownish or bluish chlorites and sometimes with epidote. The gangue minerals in the massive ore are dominantly quartz, calcite and barite with some bluish or brownish chlorite and lesser epidote. Much of the quartz is fine and recrystallised around sub-hedral pyrite grains. Barite may be coarse, in some cases forming pools up to a few centimeters in diameter, and contains a lot of fine opaque inclusions. Fragments or bands of cherty sedimentary material in the massive sulphide are not uncommon. Thus, the zonation of gangue minerals from stockwork to massive type mineralisation involves mainly the confinement of calcite and barite rich gangue to the massive ore.

7.2.1.3 Factors controlling the zonation

Such a zonation of the ore and gangue minerals strongly suggests that solubilities of chalcopyrite, sphalerite and barite species decreased with the upward movement of the hydrothermal solutions, and the saturation for Cu was reached before those of Zn and barite. It also suggests that at the higher levels, where massive ore deposition was taking place, solutions moved from an essentially reducing environment to an essentially oxidising environment where hematite deposition took place in the cherty sediments. Therefore it is reasonable to assume that the vertical zonation of the ore and gangue minerals is essentially due to a reduction in the solubilities where different mineral species reached saturation at different stages, and that an increase in the oxygen fugacity played an important role in the zonal precipitation.

Amongst many factors, variations in a) temperature, b) pH and oxygen fugacity and c) concentration of the mineral species are the most important factors controlling the ionic solubilities in hydrothermal solutions. These factors will now be considered.

a) The effects of temperature on solubility are complicated,but in most cases a decline in temperature will cause a reduction in the solubility products of the ore minerals and lead to precipitation of ore minerals (Skinner, 1979). It is thought that the heat loss from the hot metalliferous solutions to the surrounding rocks would be minimal as the flow during discharge to the sea-floor must be rapid. But due to the reduction in pressure as the solutions travel upwards i.e. from lithostatic to hydrostatic pressures, adiabatic expansion could take place and this would lead to a decrease in temperature (Skinner, 1979; Bischoff, 1980). However the most dramatic decrease in the temperature of the solutions must take place during mixing with the cold sea-water near or on the sea-floor. It is generally accepted that Cu-sulphides are less soluble than the Zn and Pb sulphides (Finlow-Bates and Large, 1978; Solomon et al,1980). According to Holland and Malinin (1979) barite can precipitate during the simple cooling of most hydrothermal solutions. Its solubility in water at 500 bars increases from cooling at temperatures $>300^{o}C$ to about $100^{o}C$, then starts decreasing. In the presence of NaCl the maximum shifts towards higher temperature, and at any given temperature and NaCl concentration, the solubility increases with increasing pressure.

Therefore the vertical zonation involving the early appearance of chalcopyrite precipitation with respect to sphalerite in the stockwork zone and the confinement of barite to the massive ore can be attributed to the gradual decrease in the temperature of the hydrothermal solutions during adiabatic expansion in the stockwork zone for the former, and to mixing with cold sea-water near or on the sea-floor for the latter. On the sea-floor, abrupt decrease in temperature of the solutions during mixing with the cold sea-water would increase the supersaturation of the sulphide minerals by several orders of magnitude leading to the massive sulphide deposition on site, as well as to barite formation probably around

or below 100°C.

The presence of calcite as a gangue mineral associated with the massive rather than the stockwork mineralisation cannot be explained by precipitation due to decreasing temperature of the solutions, since calcite is more soluble at lower temperatures (Holland and Malinin, 1979; Coish,1977). However, calcite precipitation could take place from the dissolved calcite constituent of the cold sea-water during temperature rise upon mixing with the hot hydrothermal solutions. This again implies that massive ore mineralisation must have occurred near or on the sea-floor.

The solubility of silica below 750 bars goes through a maximum and the temperature at which quartz has its maximum solubility decreases with decreasing pressure (Holland and Malinin, 1979; Bischoff, 1980). For instance, the maximum solubility at 200 bars is at a temperature around 330°C (Holland and Malinin, 1979, Fig.9.6). Therefore much of the dissolved silica in the hydrothermal solutions, having temperatures $>400^{o}C$ to start with, would be retained until abrupt temperature decreases during mixing with the sea-water take place. This is further supported by the slow rate of cooling until mixing starts and low pressures around the mere hydrostatic pressure of the water-column. Provided that the hydrothermal solutions had relatively high exit temperatures on reaching the sea-floor, the solubility behaviour of silica would explain the presence of the silica rich sediments overlying the massive ore.

b) The hydrothermal solutions formed by the sea-water-basalt interaction at elevated temperatures would be slightly acid (Bischoff and Dickson, 1975; Bischoff and Seyfried, 1978). In the East Pacific Rise, for instance, the hydrothermal solutions, jetting out at temperatures around 350°C, have an in situ pH of 4.7 (Edmond, 1981). If it is assumed that the solutions which gave rise to the mineralisation at Polusagi had similar pH

values and that they had lower oxygen fugacity than the relatively more oxygenated sea-water (Chapter six, section 6.12.2), then it follows that upon mixing with the neutral and oxygenated sea-water the pH as well as the oxygen fugacity of the hydrothermal solutions would rise towards values equal to those of the sea-water. According to Large (1977), a reduced and slightly acid metalliferous brine could precipitate chalcopyrite, sphalerite and galena due to increasing pH around the sea-water-rock interface, where changes in oxygen fugacity will also affect the chalcopyrite solubility. Similarly, on the sea-floor itself, changes in pH of the environment of deposition will affect the Cu-solubility. Large (1977) also states that in a reduced environment, the cherty or muddy sediments will be pyrite-rich whereas in an oxidised environment they will be hematite-rich. Thus dilution of the hydrothermal solutions by the sea-water, apart from lowering the temperature, would increase the pH and oxygen fugacity which affect the precipitation of sulphides. Further mixing or dilution could result in the formation of the silica and Fe-Mn-rich sediments if the solutions contained more iron than could be fixed as iron-sulphides or iron-copper sulphides.

c) According to Taylor (1963), referred to in Large (1977), the relative abundances of ore metals in the hydrothermal solutions are a major factor in determining the order of sulphide mineral deposition. Therefore, provided that the solubilities under specific conditions are not too dissimilar, metals with the highest abundances in the solutions can be expected to precipitate earlier than those with lesser abundances. Such a process could have played a part in the vertical zonation of the ore minerals in the Polusagi area where solutions must have contained relatively high Fe, Cu, Zn and low Pb abundances.

7.2.1.4 Banding in the massive sulphide mineralisation

7.2.1.4.1. Introduction

Mineralogical and to some extent textural banding in some parts of the massive ore mineralisation is common and characteristic. Gross mineralogical banding, conspicuous in the hand specimen scale, was described in Chapter two, and it was pointed out that the bands could be classified into crudely 4 monomineralic categories : pyrite-rich, chalcopyrite-rich, sphalerite-rich and siliceous-hematitic bands. These bands which do not follow any regular sequences will now be examined microscopically.

7.2.1.4.2 Pyrite-rich bands

Although pyrite is the dominant ore mineral in these bands, it is always accompanied by chalcopyrite, sphalerite and gangue minerals in varying proportions, forming the matrix in between pyrite crystals or occurring as inclusions in them. The distribution of these matrix minerals is not random and they form broad or well defined, in many cases continuous, chalcopyrite- or sphalerite- or gangue-rich micro-bands. The thickness of such one mineral dominated miniature stratification within the broadly pyrite-rich bands can vary from a few tens of microns to hundreds of microns.

There are also fine horizons within these bands where similar forms of pyrite,- i.e. framboidal or porous or well crystalline pyrite, see next section - or roughly equal-sized coarser pyrite grains are aligned parallel or sub-parallel to the general banding forming microscopic bands(plates 7.1, 7.5, and 7.6).

7.2.1.4.3 Chalcopyrite-rich bands

In these bands the dominant chalcopyrite is accompanied by pyrite, sphalerite and gangue minerals, each forming its own distinct micro-stratification within the bands parallel or sub-parallel to the general banding. Some very fine anhedral or subhedral pyrite grains form 'strings' within the chalcopyrite matrix, Plates. 7.2, 7.3 and 7.5.

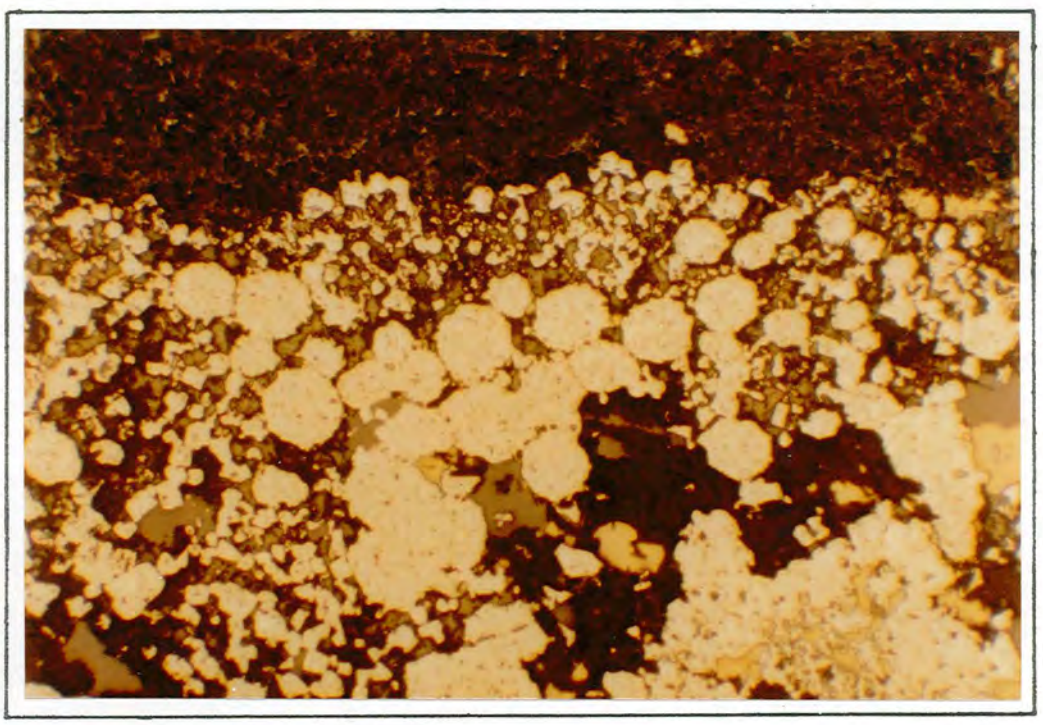


Plate 7.1 : Fe-Mn rich sedimentary band (dark) and framboidal pyrite band boundary. Denser yellow is chalcopyrite and grey is sphalerite. Note the chalcopyrite inclusions in the porous pyrite (lower right hand corner). Sample: P212, X225.

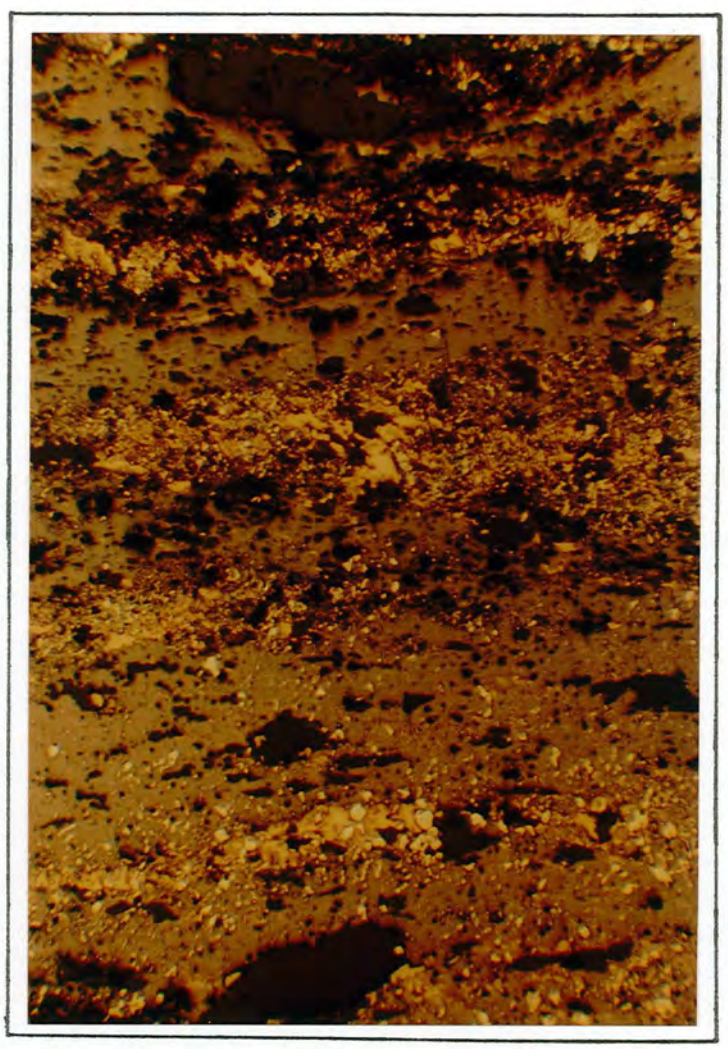


Plate 7.2 : Microbands of chalcopyrite (+ pyrite) and gangue in sphalerite rich matrix. Sample: P72D, X70.

7.2.1.4.4. Sphalerite-rich bands

In a similar manner to the pyrite and chalcopyrite-rich bands, the sphalerite-rich bands accommodate fine micro-bands dominated by chalcopyrite or pyrite or gangue minerals (Plates 7.2,7.3. and 7.6). Fine pyrite grains may be aligned to form 'strings' within the sphalerite matrix in the same way as is seen in chalcopyrite in Plate 7.5. In some samples, the sphalerite rich bands are full of tiny irregular chalcopyrite grains whose general alignment is parallel to the coarse mineralogical banding (Plate 7.4). Such fine chalcopyrite grains in sphalerite are probably due to unmixing and they are sometimes oriented to show regular 3 directional exsolution textures (Plate 7.23).

7.2.1.4.5. Siliceous-hematitic bands

These bands may be present within the upper levels of massive sulphide mineralisation as micro-bands or as coarse bands. They can, in turn, contain somewhat isolated and elongated sulphide-rich areas conformable with the general banding. However the most obvious alignment is that of extremely fine-grained hematite microcrystals into crudely hematite-rich and hematite-poor micro-bands (Plate 7.28.).

The transition from one essentially monomineralic coarse band to the other is generally very sharp, within a distance of a few or a few tens of microns (Plates 7.1 and 7.3) or relatively 'gradual', within a distance of a few hundreds of microns. However in some micro-bands the transition may be over a distance comparable with the thickness of the microbands.

The minor ore minerals, galena, fahlore and bornite are mostly anhedral small grains occurring within the matrix minerals or in the pyrite grains as inclusions. They are not present in all massive sulphide samples, but when present, they tend to occur together, probably along very broad horizons. However, galena may be present in some of the stratified, but not quite massive, sulphide horizons in large enough quantities as to

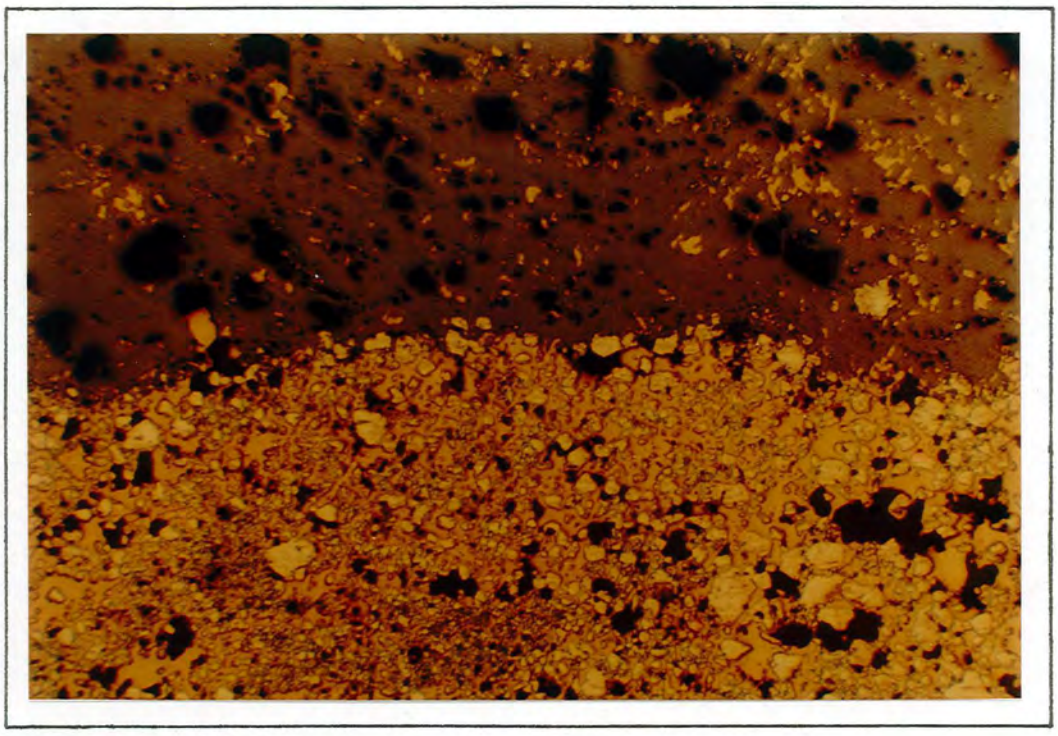


Plate 7.3 : Sharp boundary between the coarse sphalerite (+ chalcopyrite) rich band and chalcopyrite (+ pyrite) rich band. Black is gangue. Sample: P211A, X100.

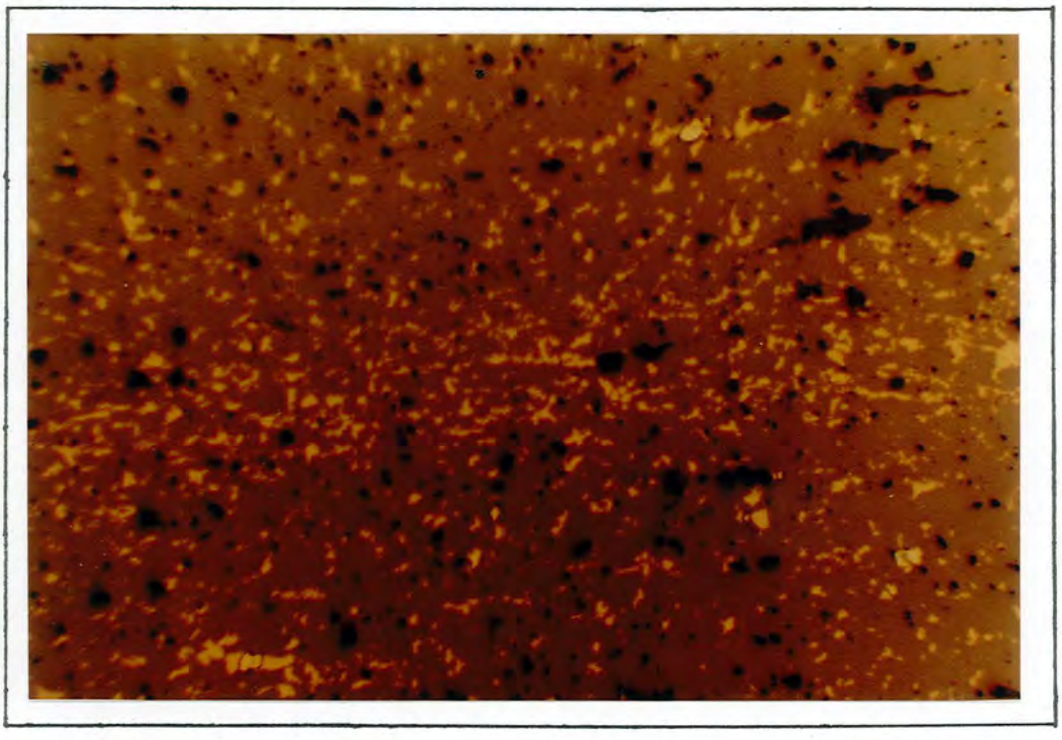


Plate 7.4: Aligned chalcopyrite exsolution in sphalerite rich matrix. Black is gangue. Sample: P72D, X70.

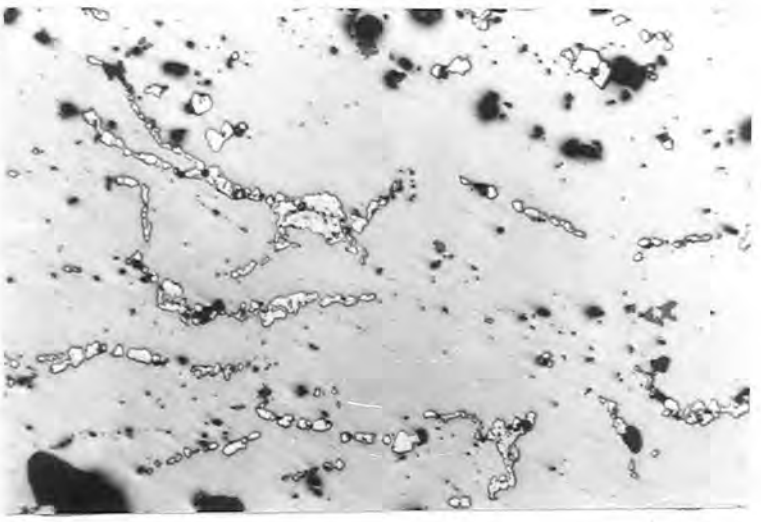


Plate 7.5:"Strings" of fine grained pyrite in chalcopyrite matrix. Sample: P156A, X100.

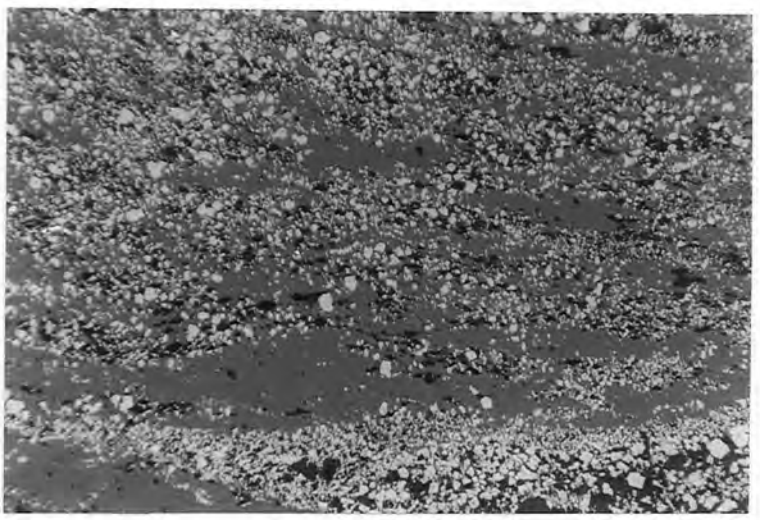


Plate 7.6: Alternating, fine pyrite and sphalerite (grey) rich micro-stratifications. Sample: P210B, X70.

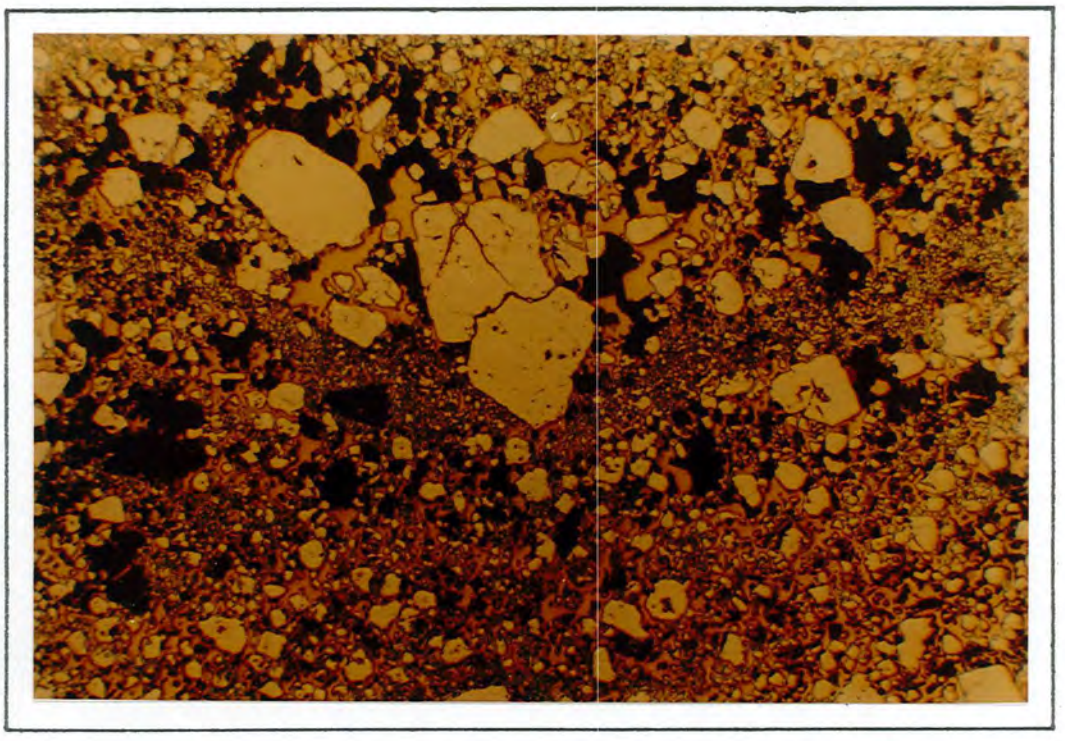


Plate 7.7 : Warping of fine grained delicate pyrite and gangue rich bands in chalcopyrite matrix (deeper yellow) by large and competent pyrite grains. Sample: P211A, X100.

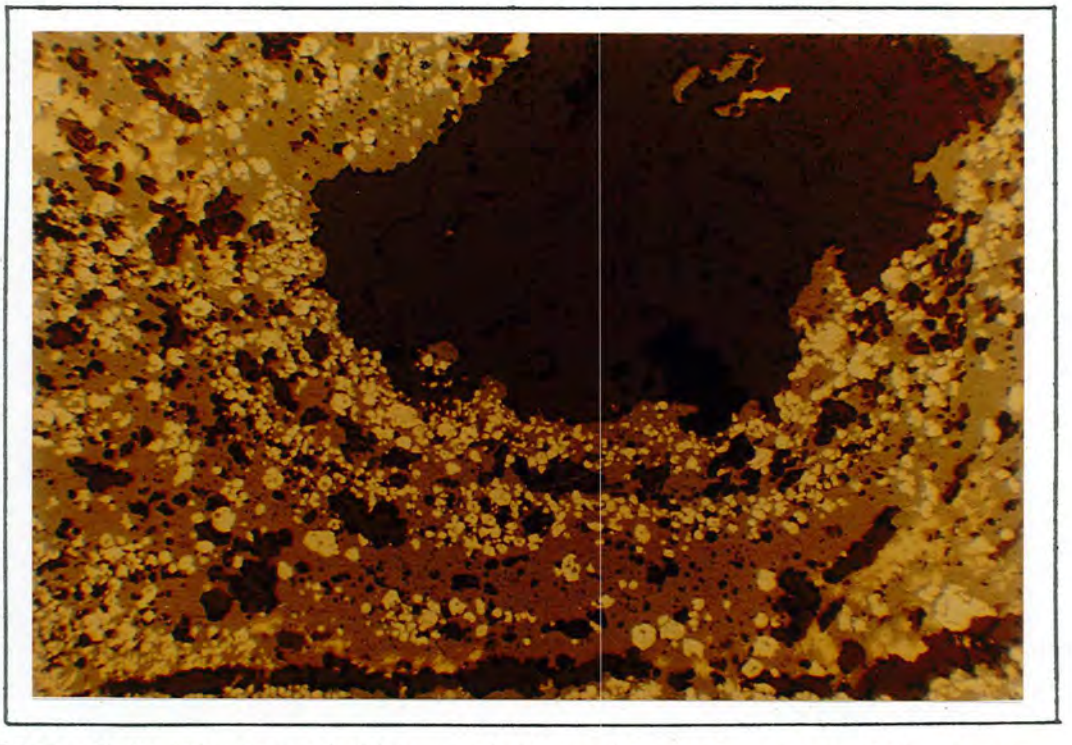


Plate 7.8: Warping of fine grained pyrite and gangue rich micro-bands in sphalerite matrix by a large fragment of gangue material (dark). Sample: P211BC, X70.

define bands alongside with pyrite, chalcopyrite and sphalerite at the higher levels of the stockwork mineralisation where the typical massive ore does not occur.

Similar to the disturbances in the regular, coarse mineralogical banding described in Chapter two, irregularities and distortions in the otherwise typical microscopic bands exist in the massive sulphides. These microscopic distortions generally manifest themselves as warping in the microbands brought about by larger, not in situ occurrences of either much coarser pyrite grains or larger fragments of gangue minerals, as demonstrated by Plates 7.7 and 7.8. In such instances the same side of the disturbed micro-bands may consistently be warped by similarly large and isolated grains. On the other hand, some short distances (e.g. 500 microns) away from the distorted micro-band traces of warping disappear. This suggests that some irregularities in the mineralogical banding may have been due to 'rains' of mechanically transported but already compact fragments into the unconsolidated newly formed massive sulphide bodies. Such an environment for the precipitation of the banded massive ore is most likely to be an open space aqueous environment such as the sea-floor itself. This conclusion is also strongly supported by the nature of the banding in the massive ore described above.

7.2.1.5. Factors leading to banding in the massive sulphide ore

The mineralogical banding in the sulphides is very unlikely to be brought about by precipitation from contemporaneous and essentially monometallic hydrothermal solutions. Therefore a mechanism which would lead to repeated differential precipitation of pyrite, chalcopyrite and sphalerite from a poly-metallic hydrothermal solution on to the sea floor must be considered.

It was pointed out earlier in this chapter that factors which have important bearings on the solubility and precipitation of the ore and

gangue minerals are basically the changes in temperature, pH, oxygen fugacity and the ionic concentrations at the site of deposition. Therefore fluctuating changes, which were probably of local extent, should be capable of producing the banding seen in the massive sulphides, in any or a certain combination of these changing factors. Changes in pH could result with differential precipitation of sulphides (Lambert and Bubela, 1970) and, for example, changes in the pH of an oxidised, acid to alkaline brine on the sea floor will only affect the Cu-solubility and not Zn or Pb-solubility at high ($>270^{o}C$) to low temperatures (Large, 1977).

Since the banded massive sulphide samples may have numerous coarse or micro-bands even in one hand specimen, it is unlikely that the possible fluctuations in the metal contents of the initially hot and reduced solutions could have played a major role in the differential precipitation of the banded ore. It follows that fluctuations in the temperature, pH and oxygen fugacity of the solutions must have been the major factors behind the mechanism leading to the banded ore formation on the sea-floor. However, the relative roles of these factors could not be assessed here.

Such proposed fluctuations in temperature, pH and oxygen fugacity may be the consequences of non-homogenous mixing of the solutions with the sea-water; of bottom currents or some weak turbulances which are indicated by the distortions in some coarse and micro-bands as discussed above.

Stanton (1960) considers that some crude banding in metamorphosed sulphide deposits may have originated by metamorphic differentiation. Although, as will be discussed in the next section, the Polusagi massive ores are metamorphosed and metamorphism was of low grade, many clearly non-metamorphic bands , such as of framboidal pyrite , would preclude a metamorphic origin for the banding.

Lambert and Bubela (1970) on the basis of their experiments consider

that ionic migration processes can cause the formation of very thin (up to 50 microns thick) sulphide bands within homogenous layers of unconsolidated sediments or slowly settling suspensions. It is possible that some of the very thin micro-bands in the massive ore may have been produced this way, but on the whole, such a mechanism is unable to produce the thicker bands in the massive sulphide ore. This is also emphasised by Lambert and Bubela (1970) : "It is questionable whether the ionic migration process can produce thicker sulphide bands....".

7.2.1.6 Sulphide mineral textures

7.2.1.6.1 Pyrite forms

The grain size, form and crystallinity of pyrite is extremely variable and on this basis 4 types of pyrite can be recognised : euhedral pyrite, crystalline pyrite, porous pyrite and framboidal pyrite.

Euhedral pyrite exhibits well-crystalline, cubic forms and typically occurs as coarse grains, up to 3mm across but mostly from 0.5 to 1 mm, in the stockwork mineralisation and chalcopyrite, sphalerite poor stratified pyritic horizons. In the massive sulphides, the euhedral pyrite is not typical but where it is found,it is not as coarse and generally around 0.5 mm in diameter.

Crystalline pyrite exhibits subhedral and anhedral and sometimes euhedral forms. Nevertheless it is well crystalline and is common in the upper levels of the stockwork mineralisation and massive sulphides. The typical grain size is 0.1-0.5 mm in diameter (Plates 7.11,7.12,7.17 and 7.18).

Porous pyrite is extremely fine grained and occurs in aggregates which are full of tiny inclusions of gangue material giving it a porous, dusty or cloudy appearance. Characteristically, each pyrite grain is in the order of few microns or few tens of microns, the spotty gangue material being in the same order of size. This type of pyrite is normally associated

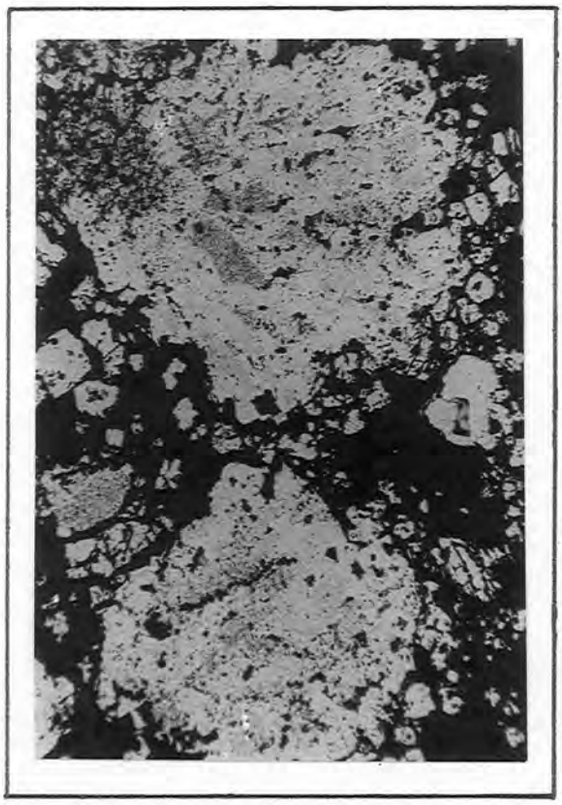


Plate 7.9 : Large aggregates of porous pyrite composed of fine pyrite crystals and gangue material. Sample: P136E, X70.

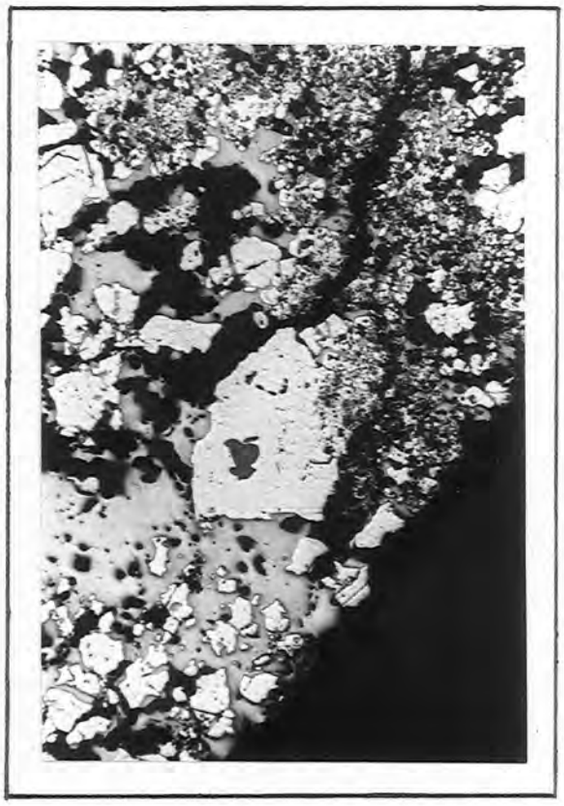


Plate 7.10 : Fine porous pyrite, chalcopyrite and gangue (upper right corner) grading into coarser pyrite in a dominantly chalcopyrite matrix (lower left corner). Sample: P136D, X225.

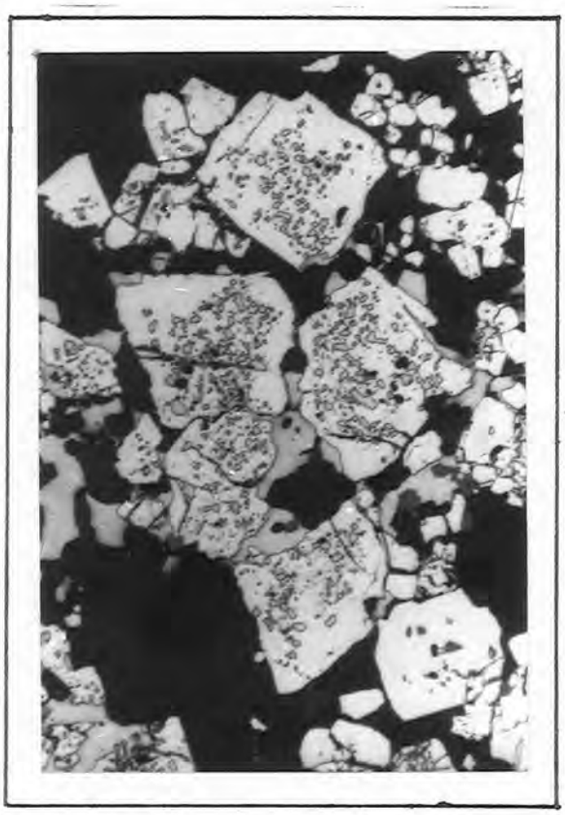


Plate 7.11 : Crystalline euhedral pyrite in a gangue rich matrix containing numerous chalcopyrite inclusions. Sample: P208B, X225.

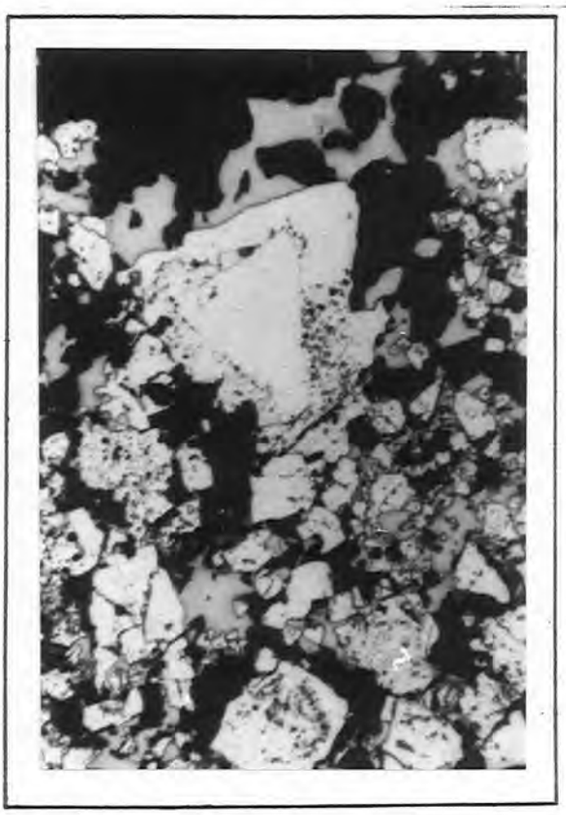


Plate 7.12 : Euhedral pyrite with chalcopyrite, sphalerite and gangue inclusions along growth zones. Note also the smaller porous pyrite aggregates with mostly gangue 'dust' Sample: P208B, X225.

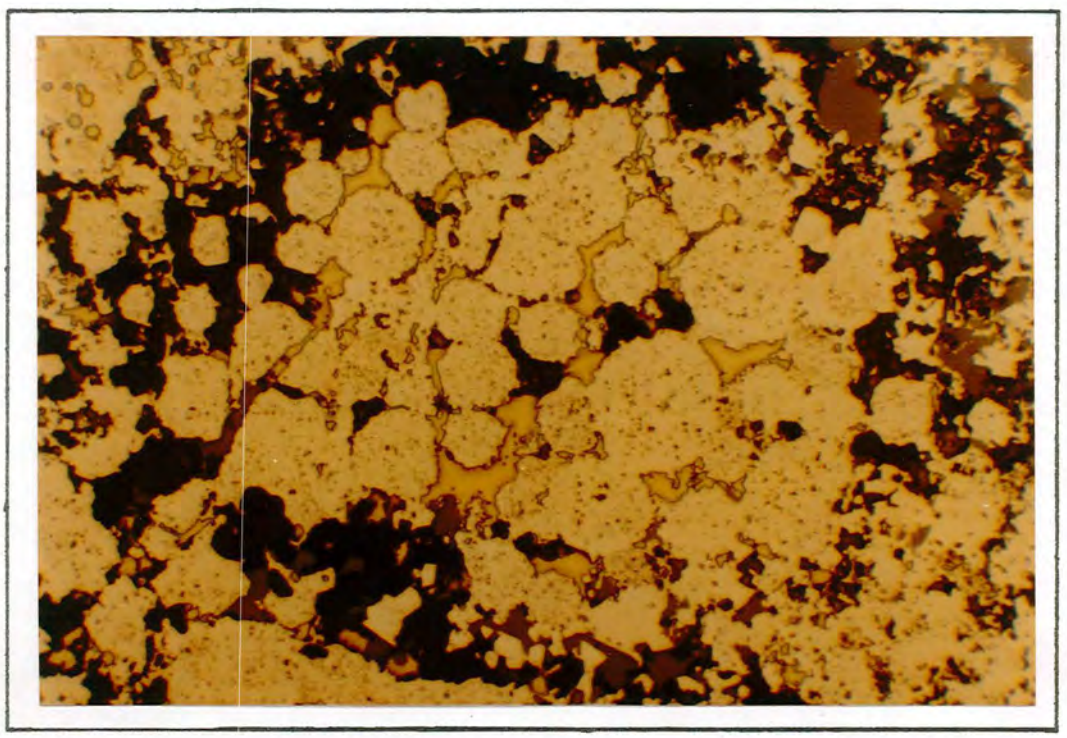


Plate 7.13 : Framboidal pyrite (note the fine silicate inclusions) starting to recrystallise with chalcopyrite (denser yellow) filling the interstices. Dark grey is sphalerite and black is gangue. Notice the various inclusions in porous pyrite at the lower right and upper left corners. Sample: P212, X225.

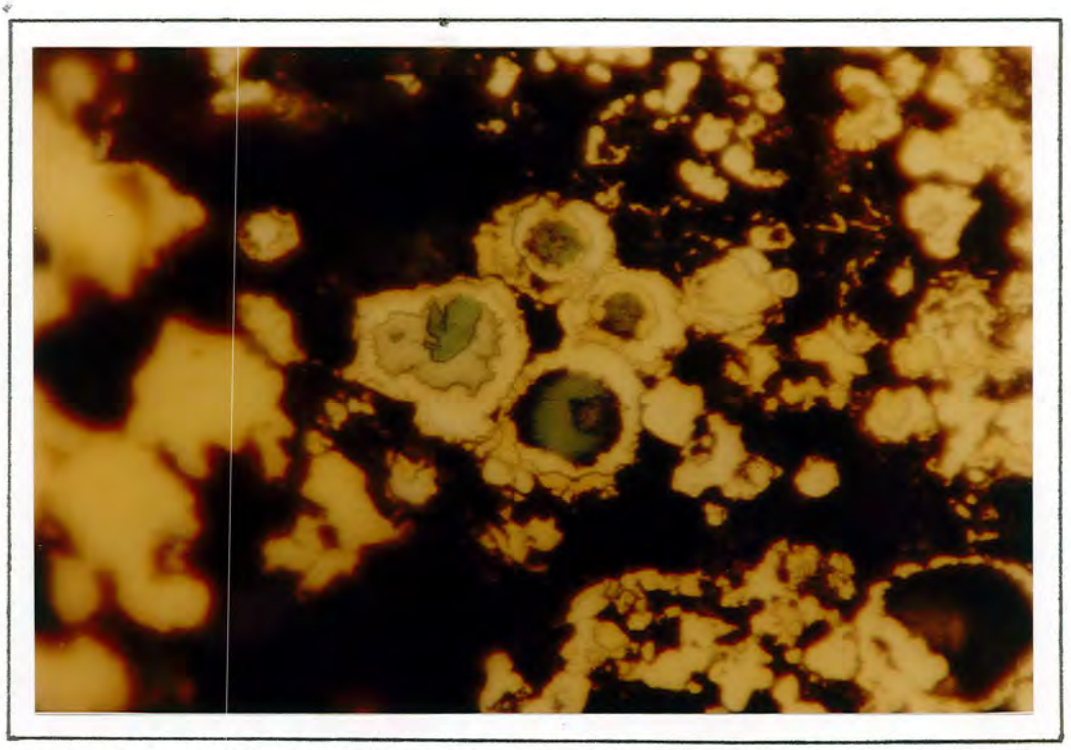


Plate 7.14 : 'Rosettes' or 'spheroids' of pyrite with hematite (greenish-grey), galena (creamy-grey) and chalcopyrite (denser yellow) cores. Black is gangue. Sample: P212, X1000, under oil.

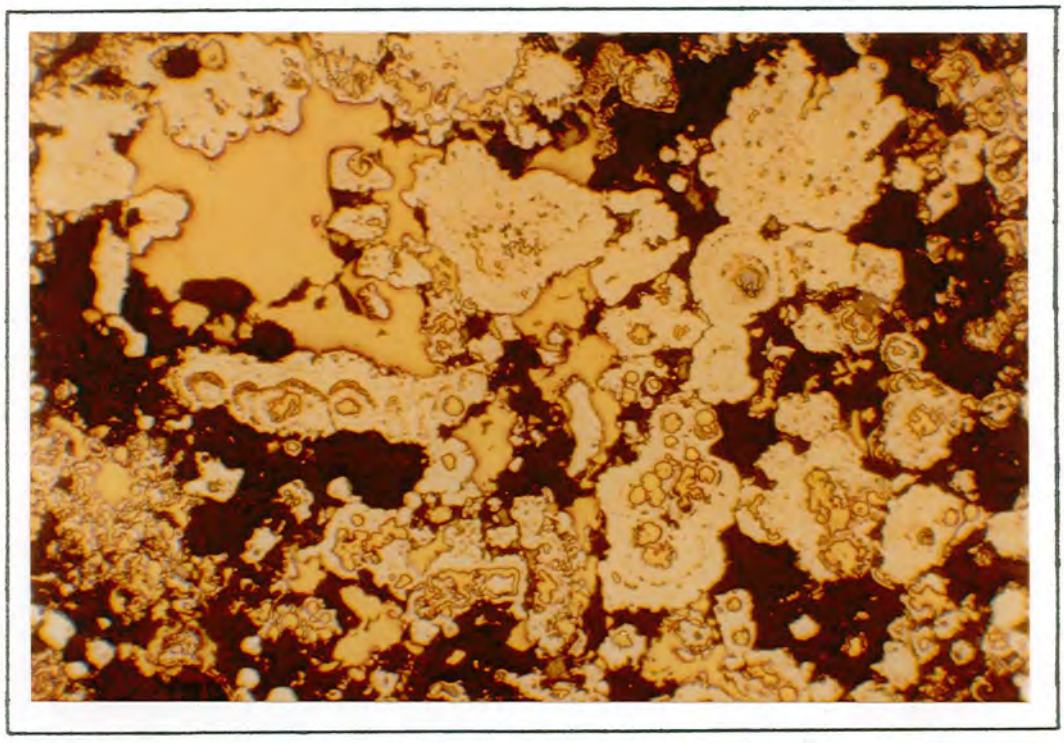


Plate 7.15 : Porous and colloform fine grained pyrite in chalcopyrite (denser yellow) and gangue (black) rich matrix, showing concentric and radial growth surfaces. Hematite (light grey) and chalcopyrite may form the cores of such pyrite. Sample: P212, X225.

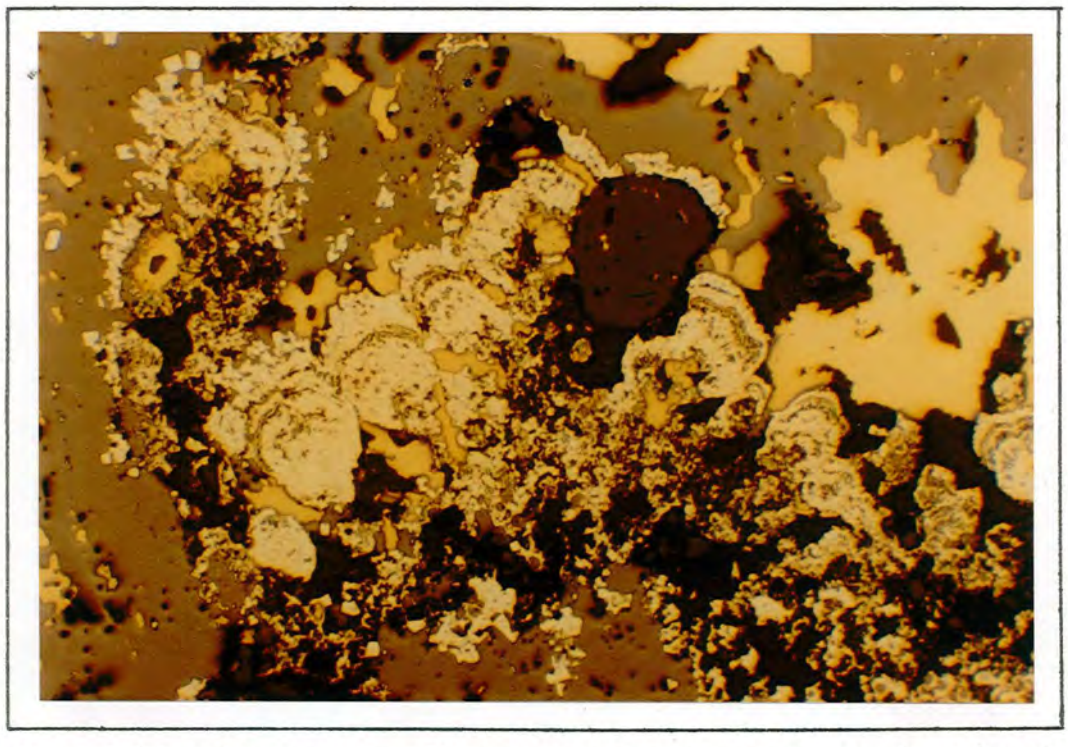


Plate 7.16 : Porous and colloform pyrite in sphalerite (grey) and chalcopyrite (denser yellow) rich matrix. Pyrite is selectively replaced along growth surfaces by chalcopyrite. Sample: P212, X225.

with the massive ores and may show colloform growths within the fine grained aggregates (Plates 7.9,7.10 and 7.16).

Framboidal pyrite, forming'raspberry' looking spheroidal shapes, occurs normally in the massive sulphides especially near the muddy, siliceous gangue rich bands or near the overlying hematitic cherty horizons. Framboids are generally 40-60 microns across but some may be as coarse as 100 microns in diameter (Plates 7.1 and 7.13). Each spherical or subspherical framboid consists of very fine microcrystals of pyrite, size being in the range of a few microns or a few tens of microns, surrounded by dusty, equally fine gangue material. Apparently pyrite framboids of this size and nature are a common form of framboidal pyrite (Rickard,1970). The pyrite microcrystals are not organised into any recognisable patterns and therefore would be classed as low-ordered framboids according to Skripchenko and Barberyan (1975) who also state that the cement for the pyrite micro-crystals could be gel-pyrite and carbonised organic matter. Some framboids have hematite, chalcopyrite or galena rich cores, probably representing nuclei around which the pyritic spherules have formed and some framboids show a concentric structure due to alignment of the fine non-sulphide material (Plate 7.14).

The framboidal pyrite is always associated with the porous sulphide and in many cases the two grade into one another. The distribution of the fine dusty material in the porous pyrite aggregates may show concentric forms suggesting an intimate association with pyrite framboids or radial and calloform structures (Plate 7.15). In some cases,the concentric bands in the framboidal and porous pyrite as well as the calloform and radial traces may be filled with chalcopyrite, and to a lesser extent sphalerite.

The origin of calloform textures is extensively discussed in the literature (e.g. Rickard, 1970; Kribek, 1975) with the general acceptance that they are produced by open space precipitation. This is in agreement

with their dominant occurrence in the massive sulphides formed on the sea-floor. The framboidal pyrite are characteristic of many modern sediments, and are commonly found in the sedimentary or meta-sedimentary rocks (Rickard, 1970; Ostwald and England, 1979), but not restricted to sedimentary rocks as some may occur in magmatic rocks (Rickard, 1970; Farrand, 1970). The origin of framboidal pyrite is disputable. It has been interpreted as mineralised or pyritised micro-fossils of sulphate reducing bacteria, supported by the organic remains within the framboids (see Ramdohr, 1980; and Farrand, 1970). But this mechanism can not explain the occurrence of framboids in the magmatic rocks. A more widely accepted view is that framboidal pyrite is colloidal in origin and precipitated from an iron and sulphur rich gel or suspension, biogenically or abiogenically (Rickard, 1970; Skripchenko and Barberyan, 1975; Ostwald and England, 1977, 79). Indeed framboidal pyrite has now been produced experimentally (Farrand, 1970; Kribek, 1975). Kribek (1975), discussing the origin of framboidal pyrite concludes that it is formed "by sulphidation of metastable spherical grains of sulphur arisen either in an organic way by oxidation of H_2S or in a metabolic way by the action of micro-organisms". The form and gradational nature of "some extremely fine grained pyrite aggregates" and pyrite framboids described by Chen (1978) seem to be similar to the porous and framboidal pyrite types and their gradational forms in the Polusagi area. Such features are considered to be due to chemical precipitation by Chen (op.cit.). Thus, it is more than likely that the porous pyrite and the framboids associated with it represent chemical precipitates from solutions in an unrestricted environment with or without the involvement of sulphur reducing bacteria. Furthermore, they indicate a low temperature environment (Rickard, 1970; Ostwald and England, 1979), since rapid crystal growth and recrystallisation would destroy the primary framboidal or colloform growth. Therefore, it is

plausable to assume that the framboidal and porous pyrite types are the primary forms of pyrite precipitated from solutions upon mixing with the sea-water.

Not only the framboidal and porous pyrite types grade into one another, but also there is a complete gradation of these pyrite types into the generally coarser crystalline pyrite and euhedral pyrite types. While the former gradation does not involve any coarsening of grain size, the latter does. This is demonstrated in Plates 7.9, 7.10, 7.11, and 7.12. Such a gradation of fine grained pyrite into coarser grained crystalline pyrite is very common and was observed in almost every massive sulphide sample studied. In some crystalline pyrite grains, the remains of framboidal pyrite is still preserved (Plate 7.12). Very similar gradational textural relationships between fine primary forms of pyrite and euhedral pyrite have been observed by Love and Amstutz (1966), Wheatley (1978), Chen (1978) and Ostwald and England (1979). The study of the last mentioned authors indicates that "whole framboids pass through a more compact intermediate form to form euhedral pyrite". The coarsening of grain size is considered to be due to partial recrystallisation. It is widely accepted that under conditions of increasing metamorphism, sulphide rich assemblages tend to recrystallise, becoming progressively coarser grained (Vokes, 1968, 69; McDonald, 1967; Suffel et al, 1971; Shadlun, 1971; Lawrence, 1972; Krivtsov, 1974). The fact that the reorganisation of the fine grained pyrite into the coarser crystalline pyrite is not complete, and the primary depositional textures e.g. banding, framboidal or colloform structures are preserved, suggest that the metamorphism was of low grade and recrystallisation was a partial one (McDonald,1967; Vokes,1969; Shadlun, 1971).

7.2.1.6.2. Inclusions in pyrite crystals or aggregates

Probably the most distinct feature of pyrite, common to all types,

is the numerous inclusions within single grains or aggregates. However, the inclusions show variations in size, form, distribution and mineral content from the fine grained primitive types to coarser recrystallised euhedral and subhedral types.

In the porous and framboidal pyrite types, the inclusions are very fine grained giving them a spotty or dusty appearance. The size of the inclusions is typically similar to the individual pyrite microcrystals or smaller. Many are of sub-micron sizes. The distribution of the inclusions is generally random but crudely homogenous. However, some inclusions may form circular, concentric, radial or colloform banding patterns. The inclusions appear mostly to be gangue or transparent minerals.

In the crystalline pyrite and its gradational forms to the porous and framboidal types the inclusions are larger and may be up to several 100's of microns in diameter in the very coarse,crystalline pyrite grains. The size of the inclusions is dependent on the degree of crystallinity, increasing with the increase in the size of the host pyrite grain. The shapes of the inclusions are in general round, sub-round or lobate. The mineral content of the inclusions is variable even in a single pyrite grain. The infilling phases can be chalcopyrite, sphalerite, bornite, galena, fahlore, gangue minerals and even hematite in some cases. Some single inclusions may have a combination of mineral phases i.e. bornite + chalcopyrite, galena+chalcopyrite, sphalerite+bornite etc. In the latter cases the ratios of the minerals in the inclusions is very variable. However one well-maintained general rule is that the content of the inclusions is the same as that of the matrix, i.e. pyrite "porphyryblasts" contain a lot of chalcopyrite inclusions in a chalcopyrite-rich band or sphalerite inclusions in a sphalerite-rich band etc... As to the distribution of the inclusions, it is very variable and the following are the common forms :

a) The inclusions are concentrated around the centre of the

grains, and the margins are relatively clear and homogenous or vice versa e.g. Plates 7.11 and 7.12.

b) The inclusions are gathered in certain parts of the grains, other parts being relatively free of inclusions e.g. Plate 7.19.

c) Some fine inclusions in euhedral pyrite grains, mostly of gangue minerals, follow cubic growth zones demonstrating the internal zonation which is sometimes revealed by slight variations in reflectance as well e.g. Plate 7.18.

d) In the compact aggregates, the inclusions follow the individual grain boundaries (Plate 7.12). This may be so in some apparently large single crystals. As pointed out in section 7.4.2.1, the pyrite is slightly anistropic, which helps to distinguish single crystal outlines along which fine grained inclusions form 'strings' or 'chains'.

e) In rare cases, the inclusions in crystalline pyrite may simply be the remains of framboidal pyrite, Plate 7.20.

The above described features suggest that they are manifestations of different degrees of partial recrystallisation of a variable sulphide assemblage undergoing low-grade metamorphism. During recrystallisation, not only would the sulphide grain size increase, but also the original mineral inclusions would be segregated into larger pools or expelled as a result of partial "self-purification" (Anger, 1971; Shadlun, 1971) leading to relatively clear portions in the grains. This would be accompanied by further inclusion of the matrix minerals during the coarsening of pyrite "porphyryblasts" (Vokes,1969). These inclusions would tend to assume rounded shapes, the state of lowest surface-free energy (Stanton,1972).

The internal textures in the coarse and euhedral pyrites, such as growth zonation revealed by very fine grained traces of inclusions, cannot be explained by metamorphism or partial recrystallisation since such processes would tend to obliterate the internal fabrics especially if metamorphism or deformation is of high grade (McDonald, 1967; Vokes,1969;

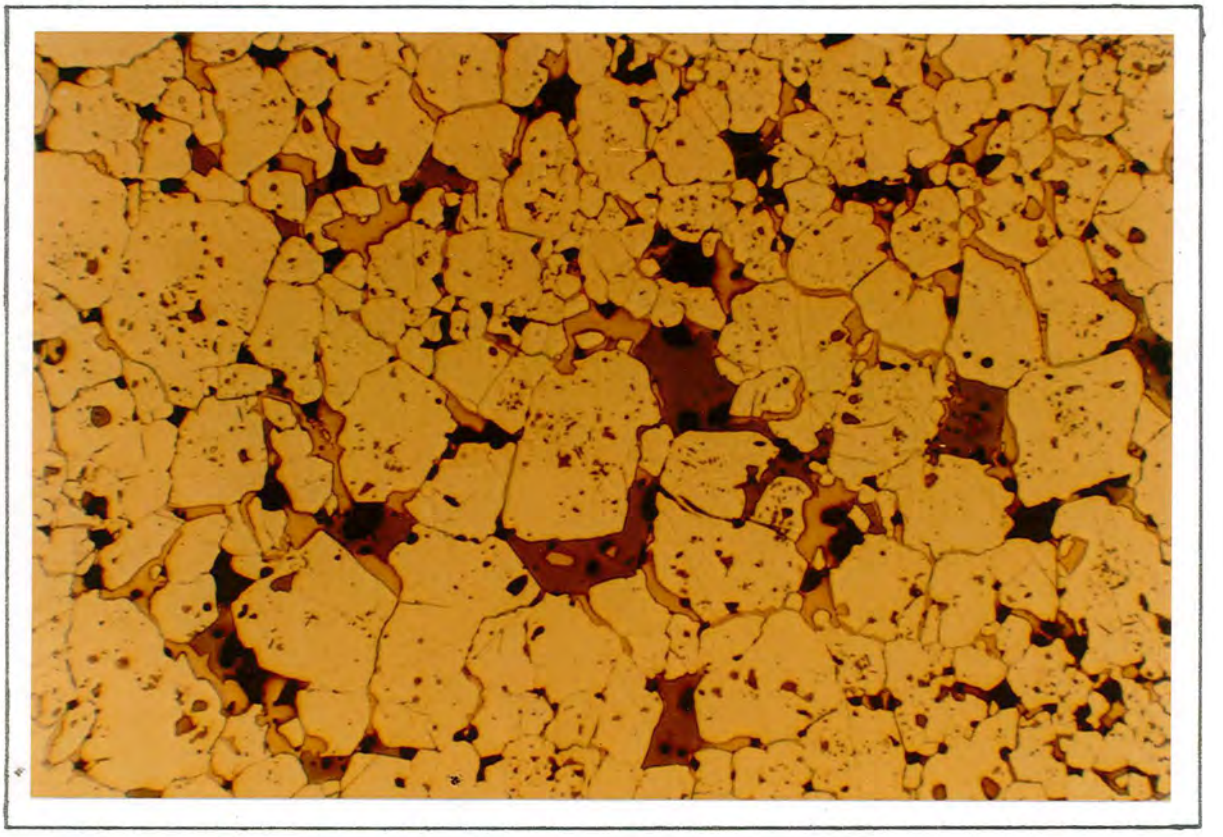


Plate 7.17 : A general view of massive sulphides at Polusagi. Euhedral to subhedral pyrite grains contain numerous inclusions of chalcopyrite (denser yellow) and sphalerite (grey) which also occur in the matrix together with some gangue minerals (black). Sample: P72, X120.

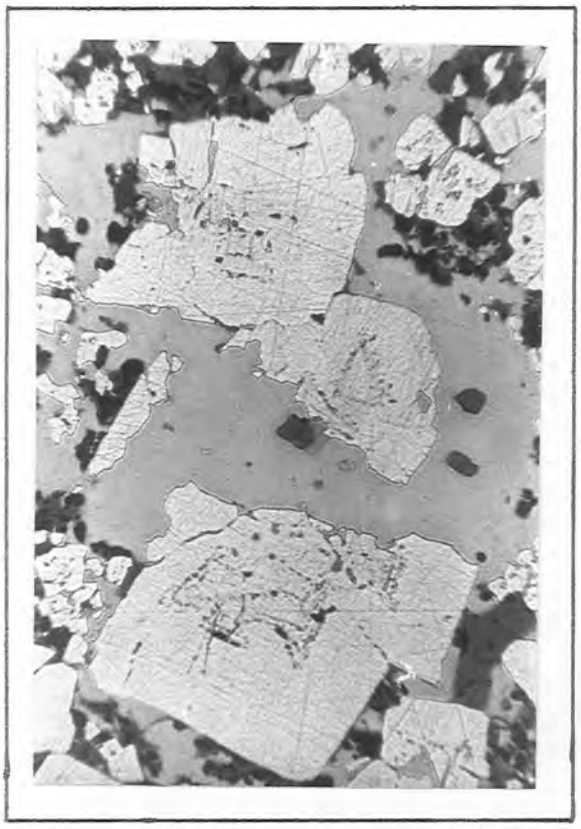


Plate 7.18 : Fractured euhedral pyrite grains (whitish) with inclusions along cubic growth zones, embedded in chalcopyrite (grey) which fills the cracks without apparent replacement. Sample: P211BA, X225.



Plate 7.19 : Large euhedral pyrite with sphalerite, chalcopyrite and gangue inclusions concentrated along grain boundaries of pyrite. Grey is chalcopyrite and dark grey is gangue. Sample: P136A, X225.

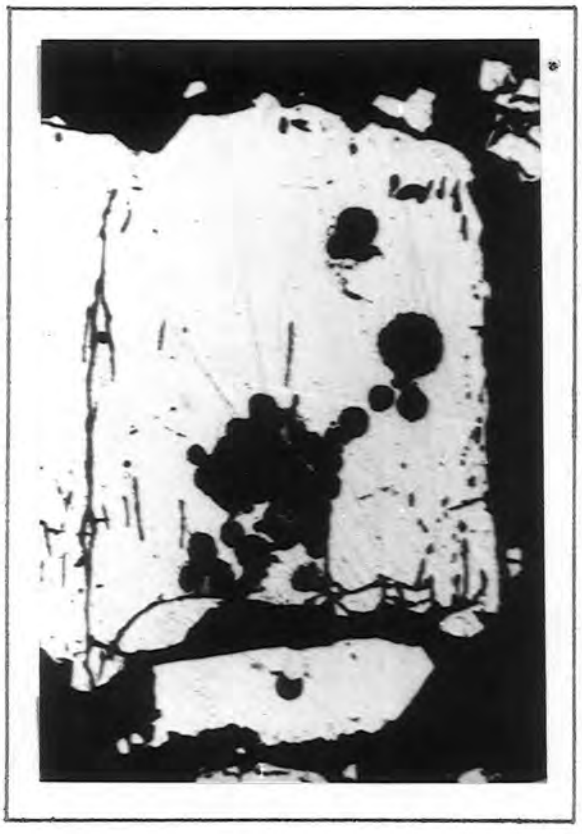


Plate 7.20 : Etched euhedral pyrite with framboidal pyrite remains, now black due to etching. Sample: P143A, X225.

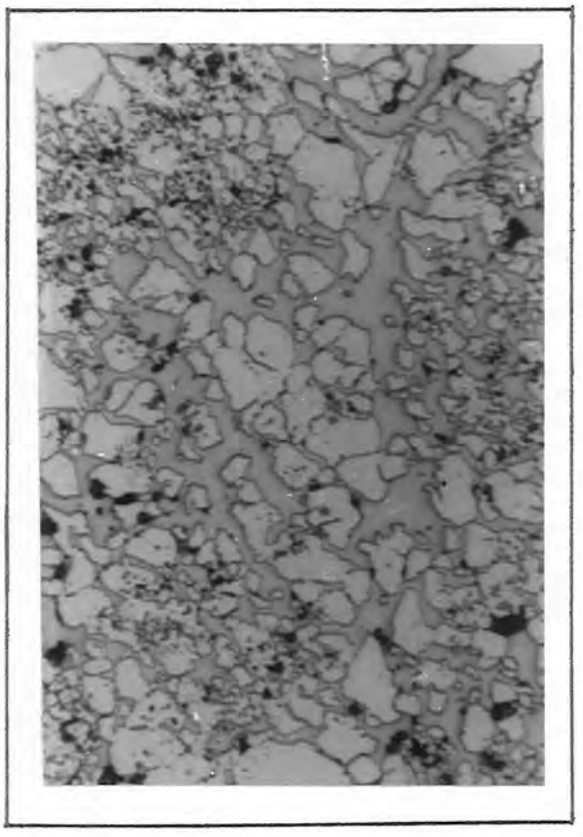


Plate 7.21 : Porous pyrite transforming into better crystalline coarser pyrite within the "soft" chalcopyrite matrix. Sample: P208, X225.

Shadlun, 1971). Therefore the presence of such internal fabrics not only shows that metamorphism of the sulphides was of low grade, but also that some of these coarse pyrite grains may be primary or of diagenetic origin. Then, the oriented fine inclusions may represent periods of decreased crystal growth or interruptions during the crystal growth (Ramdohr,1980).

The coarse grained generally euhedral pyrite associated with the stockwork mineralisation is relatively free of larger inclusions. The inclusions are very small and generally of gangue material. They may concentrate along cubic growth zones. Some chalcopyrite and sphalerite may occur in the euhedral pyrite as inclusions despite the lack of chalcopyrite and sphalerite in the siliceous matrix. These suggest that the coarse euhedral pyrite in the stockwork was largely precipitated from solutions, rather than being a product of coarsening during metamorphism, which enclosed fine grained gangue minerals, chalcopyrite and sphalerite as inclusions along growth surfaces.

7.2.1.6.3 Interrelations of pyrite, chalcopyrite and sphalerite

In many cases the large pyrite grains are fractured and cracked and may even tend to form cataclastic textures. These cannot be due to some fault brecciation since such shattering of the coarse pyrite does not seem to be affecting the delicate bands in the massive ores. Therefore they are likely to be due to load pressure and stress or to shrinkage. Some radial cracks in the zoned pyrite grains show textures similar to those described by Anger (1971, Fig.16,18, and 29) as shrinkage cracks. The cracks are filled with chalcopyrite, sphalerite and less commonly by gangue minerals, depending on the nature of the phases forming the matrix. However the relationship of these pyrite "fragments" now completely surrounded by sphalerite or chalcopyrite, or the relationship of these crack filling sulphides to pyrite, do not exhibit any convincing evidence of replacement.

The chalcopyrite- or sphalerite-rich bands in the massive ore are generally associated with the crystalline pyrite rather than porous pyrite. Where, for example, a chalcopyrite rich band occurs next to a porous pyrite-rich band there is a tendency for the pyrite grains to be coarsening towards the chalcopyrite-rich band where the pyrite grains may already be termed as "crystalline". See Plate 7.22. These relations suggest that chalcopyrite and sphalerite were largely mobilised during metamorphism and perhaps acted as heat-conductors for the fine pyrite grains enclosed by them to grow into coarse, crystalline pyrite. The chalcopyrite and sphalerite do not exhibit any textures that can be attributed to primary precipitation apart from some exsolution textures.

The above features are attributed to be results of low-grade metamorphism and deformation. Gill (1969) has shown experimentally that plastic flow occurs very quickly in sulphides such as chalcopyrite and galena and to a lesser extent sphalerite, at temperatures within the range generally assumed for greenschist facies under pressures less than 1.7 kbars. Under these conditions pyrite fails by fracture, if at all. Response to deformation and metamorphism depends on the level of form-energy which decreases in the order : pyrite, sphalerite, chalcopyrite, galena (McDonald,1967; Vokes,1969). Accordingly, obliteration of original textures will be completed earlier for the 'softer' sulphides such as galena, chalcopyrite and sphalerite, than pyrite (Shadlun, 1971).

Thus, it is suggested that during the metamorphism at Polusagi, under the load pressure,pyrite failed by fracturing while chalcopyrite and sphalerite were mobilised and "flew" into the cracks or around more competant pyrite grains (see Plate 7.21). The survival of the chalcopyrite exsolution in sphalerite points to the fact that mobilisation of these minerals must have been only of partial or local extent.

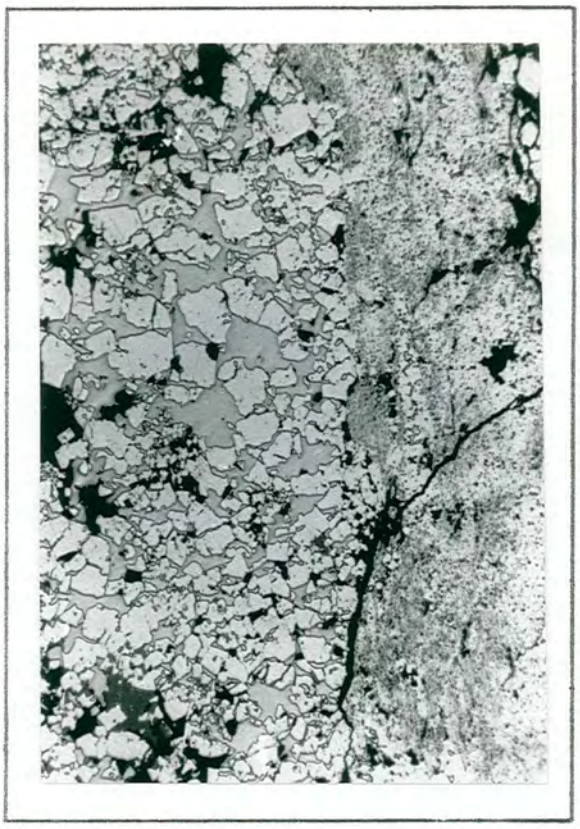


Plate 7.22 : Porous pyrite (right sector) becoming progressively coarser towards the chalcopyrite rich matrix. Chalcopyrite may have played a role as heat conductor for the re-crystallisation. Sample: P209A, X100.



Plate 7.23 : Oriénted chalcopyrite exsolution in sphalerite. Sample: P211B, X1000, under oil.

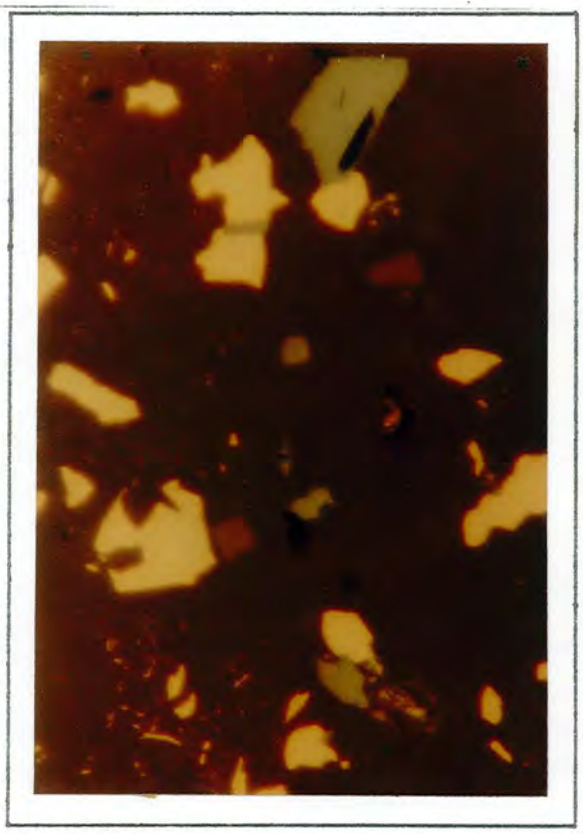


Plate 7.24 : Hematite (grey), euhedral magnetite (brown) and chalcopyrite (yellow) inclusions in sphalerite matrix. Sample: P212, X1000, under oil.



Plate 7.25 : Hematite laths (grey) in chalcopyrite. Lighter yellow is pyrite. Sample: P211, X750.

7.2.2 Fe-Mn oxide mineralisation

7.2.2.1 Introduction

The Fe-Mn rich cherty sediments and their relations with the sulphide mineralisation were discussed in Chapter two. Here their microscopic and chemical features will be examined and its origin in relation to sulphide mineralisation will be discussed.

The cherty sediments are extremely fine grained mixtures of silica, hematite and Mn-oxides in varying proportions. The grain size is generally around or less than 1 micron. The silica shows textures where sub-micron sized grains form spherical bodies which are no more than 50 microns and on average 15 microns in diameter, or polygonal concentric bodies which look like honey-comb in appearance having sizes similar to those of framboidol pyrite (Plates 7.26 and 7.27). However most silica seems to be in amorphous form. Hematite occurs in this siliceous matrix either as sub-micron dust intimately mixed with silica or as microcrystalline laths, in many cases forming fine microbands (Plate 7.28) within the coarse bands, described in Chapter two. Such fine hematite dust in the silicous matrix causes a deep-red to pink-reddish internal reflection. These features suggest that the Fe-Mn rich cherty sediments are produced by chemical precipitation from hydrothermal solutions on the sea-floor much the same way as the porous and framboidol pyrite, but obviously under different sets of physical and chemical conditions.

It was pointed out in Chapter two that the cherty horizon contained more sulphides in the vicinity of sulphide mineralisation, and more Mn away from it. 4 Fe-Mn rich chert samples which were taken at various distances from the obvious centres of sulphide mineralisation have been analysed by XRF for a number of major and trace elements as presented in Appendix III.2.

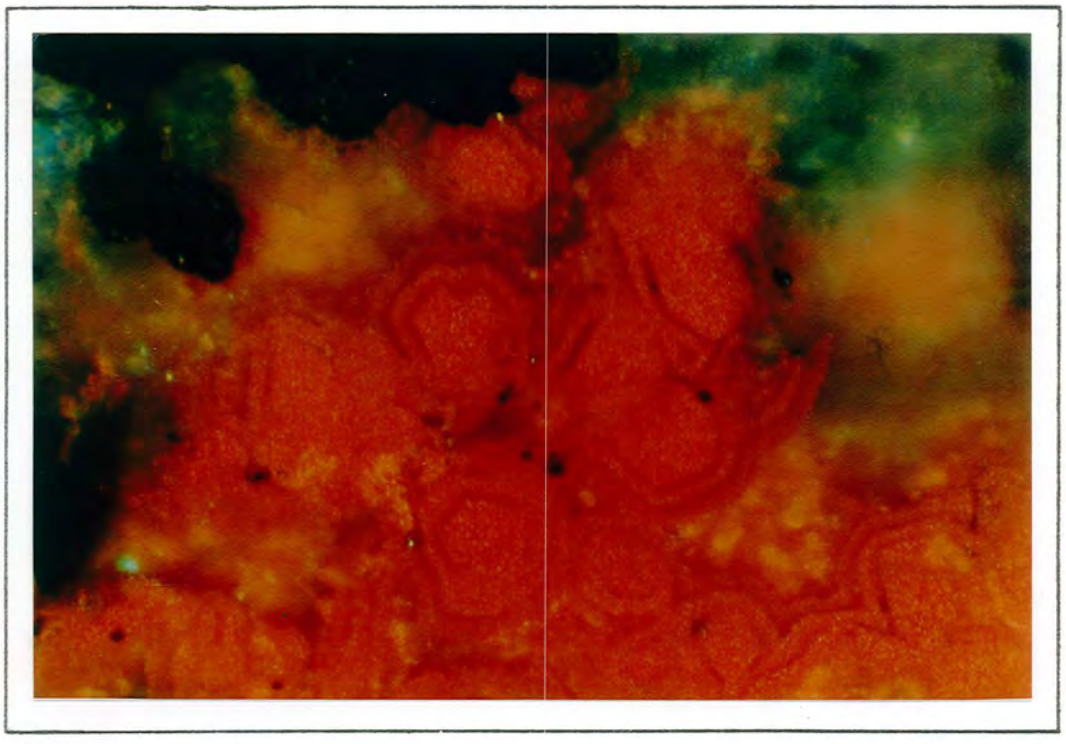


Plate 7.26 : 'Honeycomb' textured colloform growth of silica in the Fe-Mn rich siliceous sediments. The red colour is due to the fine hematite 'dust' within silica. Sample: P72C, X225, crossed-polars.

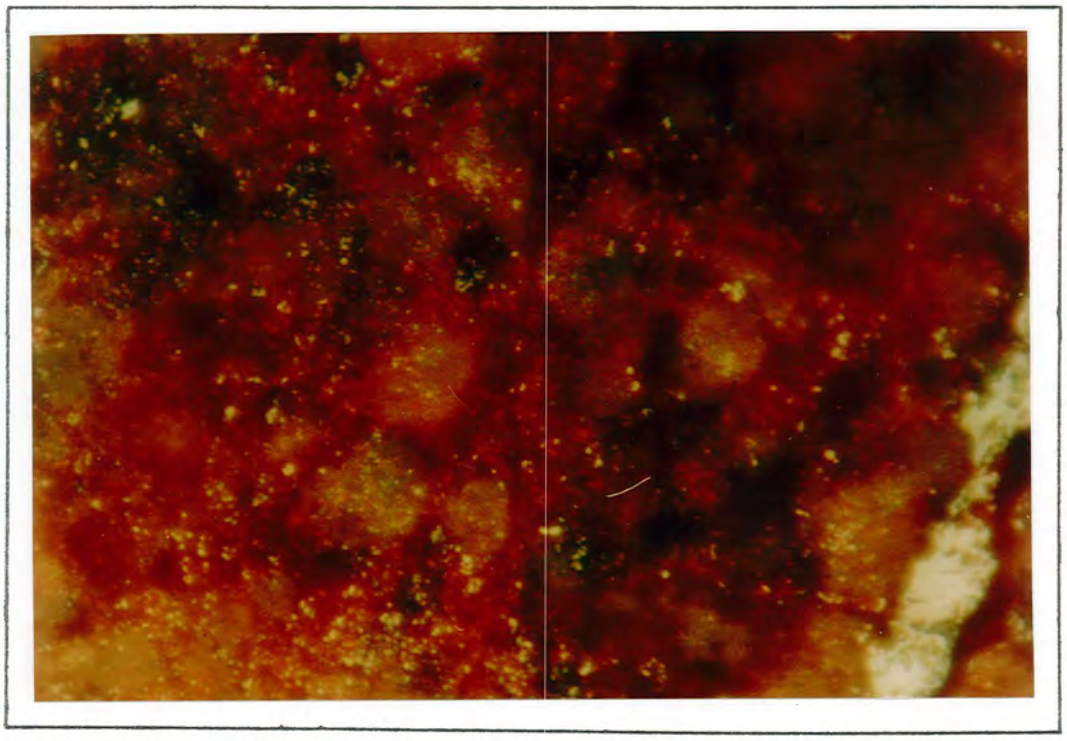


Plate 7.27 : Extremely fine grained silica spheroids in the siliceous matrix. Red colour is due to internal reflection of fine hematite 'dust' and the greyish-white specks are micro-crystals of hematite. Note the hematite-rich vein at the lower right corner. Sample: P235, X1000, crossed-polars, under oil.

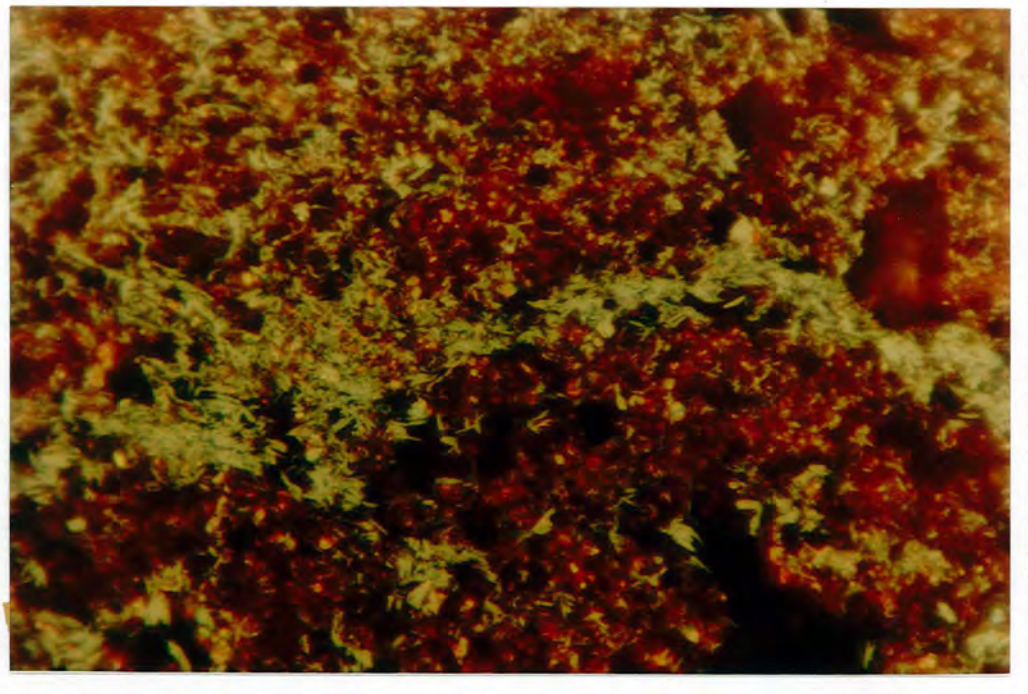


Plate 7.28 : Extremely fine hematite micro-crystals (greyish-white) aligned in bands in the siliceous matrix of Fe-Mn rich sediments. Red colour is due to internal reflection of hematite 'dust' within the matrix. Sample: P212, X1000, crossed-polars, under oil.

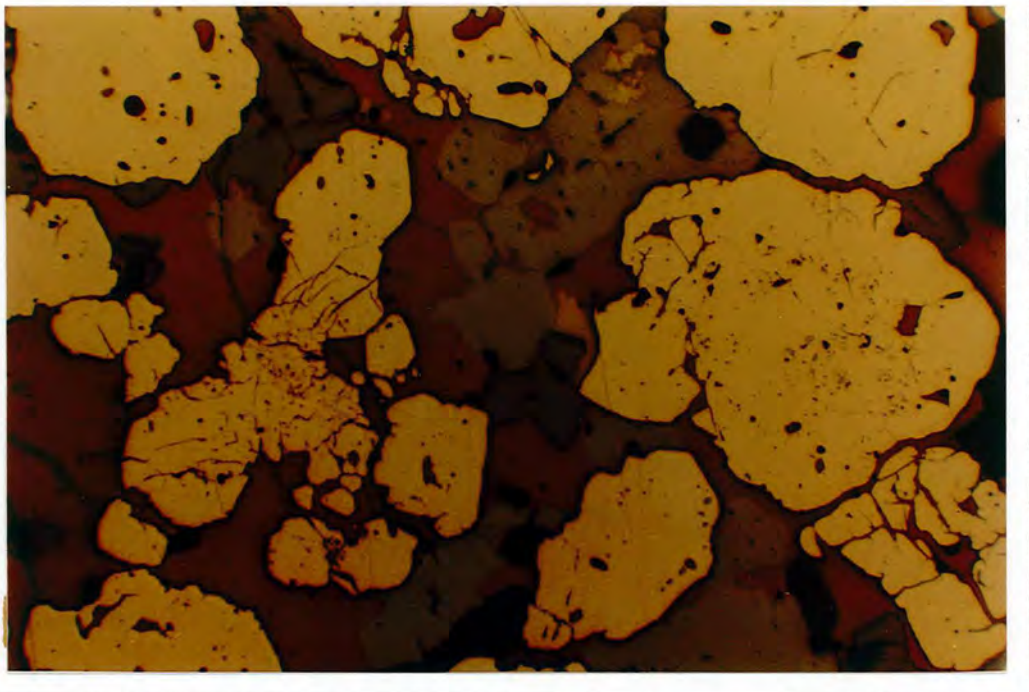


Plate 7.29 : A typical view of the Canakci massive sulphides. Anhedral to subhedral pyrite grains are in a matrix composed of bornite (brown), fahlore (grey), sphalerite (dark grey), galena (creamy-grey) and gangue (black). Note the inclusions in pyrite which are mostly bornite, chalcopyrite and gangue. Sample: E1-6A, X100.

Table 7.1 shows some of the major and trace element variations as a function of distances from the apparent centres of sulphide mineralisation. Despite the small number of samples analysed, they suggest certain and probably lateral chemical variations. As one moves away from the massive sulphide mineralisation i.e. sites at which the hydrothermal solutions entered the sea-floor, the following chemical changes occur in the Fe-Mn-rich cherts:

a) Si, S, Ba, Cu and probably Fe concentrations decrease.

b) Mn, Ca, and Ni concentrations increase.

In terms of minerals, this would mean an increase in Mn-oxide minerals and calcite and a decrease in quartz, barite and possibly pyrite and chalcopyrite away from the hydrothermal vents. Ni is probably affiliated to Mn-oxides and distribution of sphalerite is unclear.

7.2.2.2. Factors controlling the formation and distribution of minerals

As was pointed out when discussing the formation of sulphide deposits, the metalliferous high temperature, acid and reducing solutions, upon ascending, would mix with the ambient sea-water. Consequent decrease in temperature and increase in the oxidation potential and pH would lead to sulphide deposition. Progressive mixing would deposit much silica and barite around the vents. At advanced stages of mixing, the solutions would be so diluted as to contain only a small percentage of the original fluid. They would become cool, oxidising and poorer in silica and barite and very poor in metals such as Fe, Cu, and Zn which are already precipitated as sulphides at the earlier stages of mixing. The composition of the highly diluted, cool and oxidising solutions would depend on the initial composition of the original high temperature solutions. For instance, if iron was in excess of the amount that could be fixed as sulphides, some iron would be expected to remain dissolved in the highly diluted solutions to be precipitated as iron-oxides in the now highly

TABLE 7.1

CHEMICAL COMPOSITION OF Fe-Mn RICH CHERTS

Increasing column number indicates increasing distance from the centres of mineralisation.

wt%	1	2	3	4
SiO_2	43.47	87.01	28.12	28.98
Fe_2O_3	49.63	12.38	30.34	27.92
MnO	0.01	0.03	22.58	13.39
CaO	0.40	0.03	14.46	27.23
S	0.47	0.01	0.02	0.01
ppm				
Ba	6386	29	238	27
Zn	199	-	327	73
Cu	289	62	11	14
Ni	-	-	693	429

oxidised environment. Toth (1980), studying the deposition of sub-marine crusts rich in Mn and Fe, states that chemical stability limits of dissolved silica and oxides of Fe and Mn indicate that Si and Fe will precipitate before Mn, in the case of an ascending fluid, on the sea-floor i.e. an environment of increasing pH and oxygen fugacity and decreasing temperature. Therefore the chemical variation of the Fe-Mn rich cherty sediments can be explained by the degree of progressive mixing of the hydrothermal solutions with the sea-water. It is plausible to assume that further away from the sites of hydrothermal solutions entering the sea-floor, the progressively diluted solutions would be cooler and more oxidising. This would in turn mean precipitation of progressively less silica and Fe-oxides and more Mn-oxides. Since, at extreme dilution the flow rate is expected to be sluggish, fine chemical precipitates stand a chance of accumulation with continuous but localised banding. The very high Si,Mn and Fe contents of the final formation indicate that the hydrothermal solutions were originally rich in these elements.

7.3. Sulphide mineralisation in Canakci

7.3.1 Introduction

Two types of ore mineralisation, the polymetallic massive mineralisation and the disseminated pyrite mineralisation (Chapter two), are distinct in terms of ore and gangue mineral contents and textures. General features and the differences of the two types of mineralisation will now be discussed and compared with the 'massive' and 'stockwork' mineralisation occurring in the Polusagi area.

7.3.2 Ore and gangue mineral contents

7.3.2.1 Massive sulphides

Pyrite is the dominant ore mineral. Second most abundant ore mineral is bornite, the abundence of which varies from one sample to another.

Sphalerite, fahlore and galena occur in appreciable but variable quantities(Plate 7.29). Chalcopyrite is a very minor phase. Trace amounts of mawsonite, hexastannite, colusite and native gold have been identified. Minor amounts of supergene ore minerals include covellite, digenite and idaite. The gangue minerals are mostly silica, barite and some calcite. Fragments of red hematitic-chert, as it occurs in Polusagi, have been identified in the massive ore, but are rare.

It is clear that the massive sulphide ore is mineralogically very similar to the massive sulphide ore of the Polusagi area. The important mineral phases are the same in both areas i.e. pyrite, chalcopyrite, sphalerite, bornite, fahlore and galena, although relative amounts can vary significantly. For example, the main Cu-sulphide at Polusagi is chalcopyrite, while it is bornite at Canakci. Magnetite and hematite, found at Polusagi, are not observed in Canakci; while mawsonite, hexastannite, colusite and native gold,occurring only in trace amounts, are not encountered in the Polusagi massive sulphides. The gangue mineral contents of massive sulphides of both areas are qualitatively identical.

7.3.2.2. Disseminated pyrite mineralisation

Pyrite is almost the sole ore mineral. Chalcopyrite and sphalerite do occur, but only in trace amounts and rarely as minor phases alongside the major ore mineral, pyrite. The sulphide content varies from disseminated types to more massive types. The gangue is dominantly siliceous with fine, interlocking quartz grains. The mineralisation is clearly comparable with the stockwork mineralisation of the Polusagi area.

7.3.3. Banding in the massive sulphides

No clear-cut mineralogical banding of the type seen at the massive sulphide mineralisation of the Polusagi area is observed. However, there are horizons, up to a few mm thick and parallel to each other, which are

identified with coarse pyrite grains, up to 2mm in diameter, in a matrix of finer grained pyrite (average diameter 0.3 mm). In such cases the coarse grained pyrite "band" is accompanied by bornite, with some sphalerite, galena and fahlore, forming the matrix while the latter minerals are scarce outside the band. Similarly, bornite or sphalerite or fahlore may be enriched along some bands within the broadly pyritic background.

7.3.4 Mineral textures

7.3.4.1 Pyrite forms

The same forms of pyrite as identified in the mineralisation at Polusagi exist although in different proportions. Clearly framboidal forms are not observed but framboidal shapes outlined by tiny inclusions are identified within the crystalline pyrite grains and taken to represent now recrystallised remains of previous framboidal pyrite. Porous pyrite, slightly recrystallised versions of that at Polusagi occurs both in the massive and disseminated sulphide mineralisations, containing numerous tiny inclusions. However, porous pyrite is not as common and tends to occur in the massive ore more than it does in the disseminated sulphides. The crystalline pyrite is by far the dominant form in the massive sulphides with round, sub-round, subhedral and anhedral shapes. The grain size is variable from 0.1 to 2 mm in diameter. On average they are more closely packed and coarser than their counterparts at Polusagi. Similar to its occurrence in Polusagi, the euhedral pyrite is typical of the disseminated pyrite mineralisation where its size varies, in general, from 0.5 to 1.5 mm in diameter. As compared with the similar sized crystalline pyrite in the massive ore, the euhedral pyrite is relatively free from large sulphide inclusions but may have fine inclusions of gangue concentrated along growth zones, or in the centres of the grains.

It is concluded that the forms of pyrite observed from the massive and disseminated ore mineralisation are very similar to those of the

massive and stockwork ore mineralisation of Polusagi respectively. The relatively less common occurrences of framboidal and porous pyrite and the dominance of crystalline pyrite as well as the coarser sizes of the pyrite grains observed at Canakci, is attributed to a higher grade or a more prolonged period of metamorphism than occurred at Polusagi.

7.3.4.2 Inclusions in pyrite

As was the case at the Polusagi mineralisation, pyrite of all forms contains numerous inclusions of varied size, form, distribution and mineral content (Plate 7.30). What was said for the inclusions in the pyrite grains of Polusagi area (section 7.2.1.6.2) is equally valid for the pyrite grains occurring at Canakci area, with two deviations. Firstly, since the crystalline pyrite grows through recrystallisation of the finer porous or framboidal pyrite, it encloses inclusions from the matrix and consequently the pyrite "porphyryblasts" at Canakci have more bornite, galena and fahlore but less chalcopyrite inclusions due to relative variations in the abundances of these minerals as compared with those at Polusagi. Secondly the internal textures, such as growth zoning, are less pronounced in the crystalline pyrite as a result of a higher degree of metamorphism (McDonald, 1967; Vokes, 1969; Shadlun, 1971).

7.3.4.3. Inter-relations of ore minerals in the massive sulphides

Pyrite, along the fractures in the massive ore (Chapter two), shows excellent cataclastic textures due to fault brecciation where angular grains ground down to sub-micron sizes are partially cemented by gangue minerals but little bornite, chalcopyrite and sphalerite. However, away from these fractures, in the compact ore, pyrite grains are also commonly cracked. The orientation of the cracks is commonly irregular but may be broadly radial or concentric (Plate 7.31). The cracks are invaded and filled with the matrix sulphides : mostly bornite and less commonly sphalerite, fahlore, galena and rarely chalcopyrite and sometimes gangue minerals. These cracks are thought to be due to the

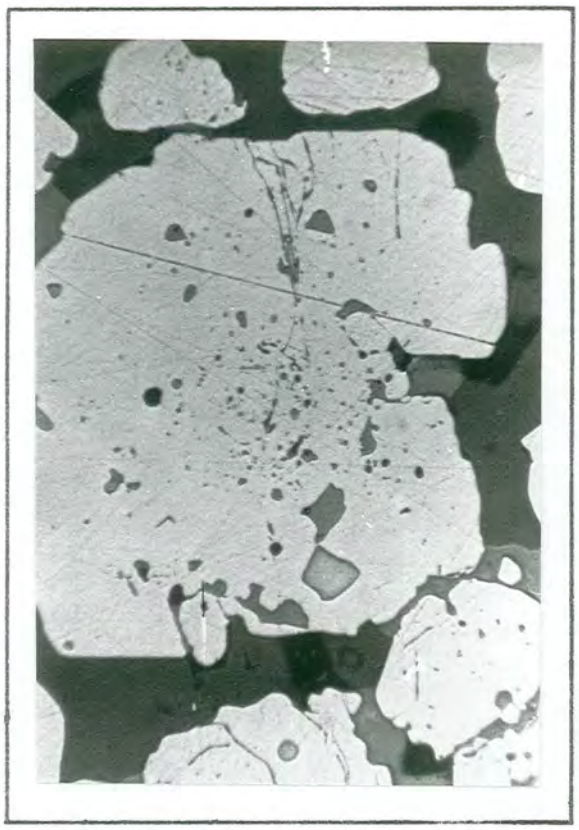


Plate 7.30 : Large euhedral pyrite with inclusions of galena, sphalerite, bornite and some chalcopyrite, concentrating in the centre. Dark is gangue. Sample: E1-7, X225.



Plate 7.31 : Pyrite grain with concentric "shrinkage" cracks now filled with bornite which is partially replaced by digenite. Sample: E5-B, X225.



Plate 7.32 : Cataclastic texture of pyrite with a preferred orientation of shattering. Sample: E3-A-3, X70.

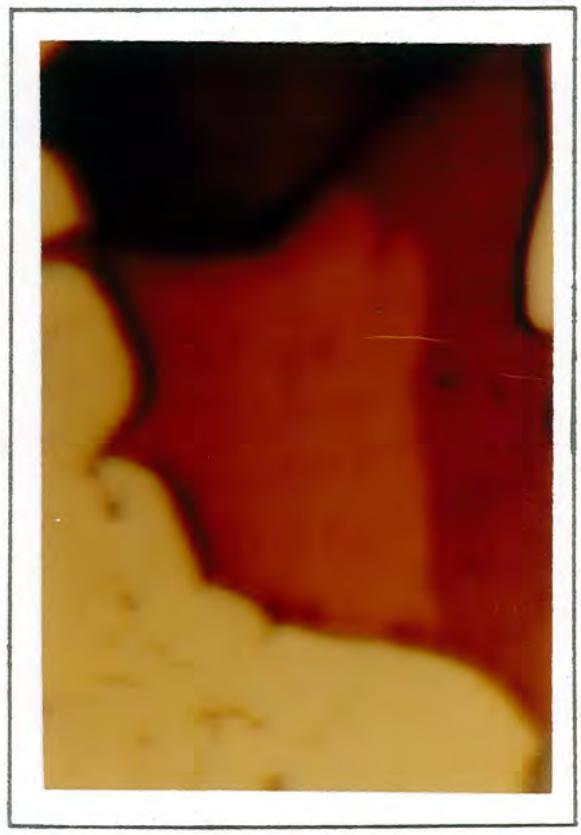


Plate 7.33 : Mawsonite (orange) in bornite (brown). Yellow is pyrite. Sample: E1-6-1B, X1000, under oil.

load pressure after formation, or due to shrinkage in case of the originally coarse pyrite grains. Some pyritic samples exhibit textures where pyrite grains are fractured and brecciated with a certain directional fabric, suggesting directional high pressure stress (Plate 7.32).

In the areas within the massive ore where the matrix minerals are abundant and form mineralogical "bands", pyrite grains are generally separated from one another; coarser than average and completely surrounded by the matrix minerals. In pyrite dominated areas, pyrite may form a compact granular texture where grains touch one another, but not quite developing triple junctions described by Stanton (1972) to be due to annealing. In the latter case, only small amounts of matrix minerals are present and they concentrate along grain boundaries.

The relationship of pyrite with the surrounding and invading matrix minerals, and indeed the interrelations of the matrix minerals, do not provide evidence for replacement. The only replacement observed is between the matrix minerals and the supergene ore minerals such as covellite, digenite and idaite replacing bornite.

Considering the points raised during the discussion of the effects of metamorphism on the sulphide assemblages of the Polusagi area, the above features are attributed to metamorphism. Under the increasing temperature and pressure recrystallisation would be followed by fracture failing of the competent pyrite grains and mobilisation and flow of the "softer" matrix minerals around pyrite and into the cracks so developed. The granular texture of the compact pyrite grains approximating to annealing textures and the directional pattern in the brecciation of some pyritic samples indicate that metamorphism (particularly pressure) was of higher grade than that of Polusagi.

7.3.5 A discussion of the origin of mineralisation

The above account of the mineralisation at the Canakci area clearly

demonstrates that the polymetallic massive ore and disseminated pyrite mineralisation are mineralogically and texturally very similar to the massive and stockwork type mineralisation of the Polusagi area respectively. Although the host rocks for the mineralisation at each area are quite different, both are products of sub-marine volcanogenic processes (Chapter two). Therefore, it is reasonable to assume a similar origin of deposition for the mineralisation at the Canakci area as that proposed for the mineralisation at the Polusagi area, discussed earlier in this chapter and summarised at the end. However, the differences between the mineralisations must also be considered.

Unlike the mineralisation at Polusagi, the field relations do not permit a direct recognition of a vertical mineralogical zonation or gradation from the disseminated to the massive types of sulphide mineralisation. This can be explained by the probable tectonic displacement of the massive ore as well as some of the disseminated mineralisation (Chapter two). The Fe-Mn rich cherty sediments associated with the sulphide mineralisation at Polusagi are not observed. However, identical but discontinuous bands, up to 0.5 m thick, of Fe-Mn rich cherty horizons a few km SW of the Canakci area and around the village of Gevenis, 7 km to the west, have been observed within tuffaceous and agglomeratic volcanogenic formations by the present author while studying the Canakci area and mapping the area around the village of Gevenis (unpublished work, 1979). Furthermore, rare red-cherty fragments do occur within the gangue of the massive ore. These suggest that similar conditions to those that produced the Fe-Mn rich cherty sediments at Polusagi must have existed during the formation of the massive ore, but probably somewhat modified.

Mineralogically, the most significant differences are that the major Cu-sulphide is bornite in the Canakci massive ore while it is chalcopyrite in that of Polusagi and that some rare minerals, namely mawsonite, hexastannite, colusite and native gold (see proceeding sections) occur

in the Canakci massive sulphides, albeit in trace amounts. These differences can be explained in terms of a higher grade metamorphism that the massive sulphides at Canakci have undergone.

As extensively discussed in review papers on the metamorphism of sulphide deposits by McDonald (1967) and Vokes(1969), high grade metamorphism can alter the sulphide mineralogy. Pyrite is the dominant iron-sulphide in low grade metamorphic sulphide assemblages; however at high grades, it may be transformed into pyrrhotite which releases sulphur, thus increasing the sulphur fugacity. An increase in sulphur fugacity could result in transformation of chalcopyrite to bornite plus pyrite. E. Horikoshi, in a personal communication (1968) with Vokes (1969), considers that the pyrite+chalcopyrite assemblage is the primary association of the Japanese strata-bound sulphide deposits occurring in the central metamorphic belt. This assemblage tends to change to pyrrhotite+chalcopyrite under normal high grade metamorphism. However, under conditions of the glaucophane schist facies i.e. high pressures and moderate temperatures, the new stable assemblage is bornite+pyrite rather than pyrrhotite+chalcopyrite.

Pyrrhotite is not observed in the massive sulphides of Canakci area, where chalcopyrite and bornite abundances have an inverse relationship i.e. chalcopyrite occurs in minor amounts in bornite-poor samples, and is virtually non-existent in the bornite-rich samples. Therefore, it is possible that the original massive sulphides could have contained chalcopyrite as the dominant Cu-sulphide, as in the Polusagi area, which subsequently transformed into bornite under moderate temperatures and high pressures (which is implied by mineral textures) during metamorphism.

According to McDonald(1967), increasing thermal metamorphism and especially "dynamic" metamorphism would lead to an increasingly complex sulphide mineralogy since deformation and the subsequent recrystallisation of the sulphides would remove the "foreign" ions from the structure,

forming new additional mineral phases. Such a mechanism under high pressures and moderate temperatures could account for the occurrence of trace amounts of mawsonite , hexastannite, colusite and native gold, all of which mainly occur within the "soft" minerals capable of plastic flow under these circumstances.

7.4. Ore minerals

7.4.1 Introduction

Since the general forms and textural relations of the ore minerals associated with the massive and disseminated 'stockwork' types of sulphide mineralisations have been discussed earlier in this chapter, the following pages will concentrate on the chemistry of these minerals and on more descriptive accounts of those minerals not already discussed in the order : primary sulphides, sulphosalts, native elements, oxides, and supergene sulphides and other minerals.

7.4.2 Primary ore minerals

7.4.2.1 Sulphides

7.4.2.1.1 Pyrite

Pyrite from both deposits is slightly anisotropic from orange-brownish to greyish-bluish tints; especially notable when the analyser is not completely crossed. This is not a polishing effect, as some pyrite grains in the same section show complete isotropy. Similar slight anisotropy has also been observed by Taylor (1981), and Bayliss (1977) proposes a triclinic structure to account for this. This feature is found to be useful in identifying single crystals in the composite grains.

67 spot analyses of pyrite from the Polusagi mineralisation - both porous and crystalline grains - were carried out (Appendix IV.3.1) for Fe

and S and the trace elements Co, Ni, Mn, Cu, Zn and Se, and their ranges and averages are presented in Table 7.2.

There are no systematic variations of major or trace elements between the porous and crystalline pyrite grains. Although a number of zoned pyrite grains have been analysed at regular intervals from core to margin, significant systematic variations in major or trace elements could not be established.

The greatest trace element variations are seen in the Cu and Zn contents. Zn values up to 5% and Cu values up to 0.6% are indicated. However, such high values are most probably due to admixtures of minute sphalerite and chalcopyrite grains (Fleischer, 1955) respectively.

Considerable amounts of Co and Ni can substitute for Fe in pyrite (Stanton 1972). The amounts of both substitutions seem to depend on the origin of pyrite formation. Fleischer (1955) reports that sedimentary pyrite is characterised by low Co contents (< 100 ppm) and Co/Ni ratio < 1, whereas pyrites of hydrothermal origin have high Co values (400-2400 ppm) and Co/Ni ratio > 1. Bralia et al (1979) consider the Co/Ni ratio of pyrite to be a reliable and useful geochemical tool in ore genesis, and on the basis of Price's (1972) work distinguish pyrites from 3 distinct environments of formation :

a) Sedimentary pyrites are characterised by generally low values of Co and Ni, but mainly by a low value of their ratio (average 0.63).

b) Pyrites from hydrothermal veins show highly variable Co and Ni contents as well as highly variable Co/Ni ratios, average of which = 1.17.

c) Pyrites from massive sulphides and volcanogenic exhalative mineral deposits are characterised by Co/Ni ratios varying from 5 to 50.

Co/Ni ratios have been successfully used in distinguishing environments of formation by Loftus-Hills and Solomon (1967) and Willan and Hall (1980) and claimed to be reliable indicators. The Co content of pyrites from Polusagi is consistently high (average 1250 ppm) and that of Ni very

low (average 60 ppm). The Co/Ni ratio average is 21. Therefore the Co and Ni contents and their ratios suggest a volcanogenic exhalative mode of formation - fully compatible with the proposed origin.

Similarly the S/Se ratio of pyrite has been proposed as a possible indicator of ore genesis (Fleischer, 1955; Stanton, 1972) : the ratio is generally $\leq$22000 for pyrite from hydrothermal exhalative sources, and around 100000 for sedimentary pyrite. However this ratio as an indicator may not be as reliable as Co/Ni ratio (Willan and Hall, 1980). The Polusagi pyrites, having S/Se ratios $<$22000, are indicated to have a hydrothermal exhalative source which provides further support for the proposed origin of deposition.

7.4.2.1.2 Chalcopyrite

As one of the major ore constituents at Polusagi, chalcopyrite occurs as a matrix mineral on its own or with sphalerite, forming very fine exolution textures (Plates 7.4 and 7.23), or as inclusions of sizes down to sub-micron scale in sphalerite and pyrite. It is a rather minor phase at Canakci, probably due to its transformation to bornite as a result of high pressure and moderate temperature metamorphism (section 7.3.5.).

17 analyses of chalcopyrite from Polusagi are listed in Appendix IV. 3.2. They are analysed for Fe, Cu, S and trace elements Co, Ni, Mn, Zn and Se. The ranges and averages of the elements are presented in Table 7.2. They are very poor in Ni, Mn and Se and poor in Co, but the indicated abundances are comparable to those reported by Hawley and Nichol (1961) for chalcopyrite from various deposits. 13 analyses contain high concentrations of Zn, in the range 0.4 to 2.1%. This is almost certainly due to extremely fine inclusions or exsolution of sphalerite in chalcopyrite.

TABLE 7.2

Range and average element concentrations in pyrite, chalcopyrite and sphalerites.

PYRITE			CHALCOPYRITE		SPHALERITE				
	Polusagi Mineralisation		Polusagi Mineralisation		Polusagi Mineralisation			Canakci Mineralisation	
wt%	Range	Average(67)	Range	Average(17)	wt%	Range	Average(29)	Range	Average(11)
Fe	42.86- 47.94	46.59	29.67- 31.96	30.37	Zn	63.55- 67.33	65.83	64.71- 66.88	66.09
S	50.20- 53.84	52.72	33.53- 34.62	34.14	S	31.89- 32.84	32.39	31.95- 32.83	32.48
Cu	0.06- 0.19	0.12	0.00- 0.12	0.05	Fe	0.05- 1.94	0.78	0.03- 0.99	0.45
Ni	0.00- 0.09	0.01	0.00- 0.03	0.00	Mn	0.00- 0.08	0.02	0.00- 0.12	0.02
Mn	0.00- 0.29	0.02	0.00- 0.04	0.01	Cu	0.00- 1.44	0.39	0.00- 1.19	0.28
Cu	0.00- 0.58	0.10	3.52- 34.75	34.07	Se	0.00- 0.14	0.05	0.00- 0.10	0.04
Zn	0.00- 5.25	0.20	0.00- 2.11	0.75	Ag	0.00- 0.04	0.00	0.00- 0.00	0.00
Se	0.00- 0.38	0.07	0.00- 0.13	0.01	Cd	0.11- 0.36	0.20	0.26- 1.18	0.67
Total	99.05-101.00	99.82	98.27-100.70	99.40	Total	98.95-100.67	99.65	98.52-100.84	100.04

7.4.2.1.3. Sphalerite.

Sphalerite is one of the major ore minerals at Polusagi and an important ore constituent at Canakci, occurring chiefly as a matrix mineral in both areas. It is interesting that sphalerite, in the sphalerite-rich bands of massive sulphides of the Polusagi mineralisation, show subtle colour variations from brownish to bluish tints of grey. Despite a number of microprobe analyses made on the areas with different colour shades, a systematic chemical variation in the abundances of elements could not be established. Sphalerite from both areas does not show the more common reddish or yellowish-brown internal reflection, but rather a milky and yellowish-white internal reflection is observed. This is probably due to its low iron content (Ramdohr, 1980).

40 microprobe analyses of sphalerite, 29 from Polusagi and 11 from Canakci, carried out for Zn, S and the trace elements Fe, Mn, Cu, Se, Ag and Cd are listed in Appendix IV.3.3. Ranges and averages of the element concentrations of sphalerite from each area are shown in Table 7.2.

Mn and Se concentrations are very similar in sphalerites from both areas with averages 0.02% and 0.045% respectively. The Ag concentrations are very low and mostly below the detection limit.

Cd often substitutes for Zn (Ramdohr, 1980) and up to 4.4% Cd has been reported to have substituted for it (Fleischer, 1955). Sphalerite analyses from Canakci contain up to 1.2% Cd (average = 0.67%) whereas those from Polusagi contain up to 0.4% Cd (Average 0.20%). Cadmium content of sphalerite seems to be independent of the conditions of formation and a clear indication of systematic differences in sphalerites from high-temperature and low-temperature deposits does not exist (Fleischer, 1955). Therefore, the differences in Cd concentration of sphalerite from the two areas under consideration can be attributed to the differences in the abundances in the original hydrothermal solutions. The high Cd

concentrations could prove to be a valuable economic by-product of the ore, especially at Canakci.

Fe and Cu contents of the sphalerites from both areas are positively correlated. Cu values in some analyses are high, up to well over 1% and much higher than those reported by Fleischer (1955). Even different parts of the same grain show great variations in Fe and Cu concentrations. Therefore, almost certainly, the high Fe values which are coupled with high Cu values are due to minute chalcopyrite exsolution or inclusions present in sphalerite. At reasonably low Cu abundances i.e 0.1%, the Fe content varies in the ranges 0.3 to 2% and 0.03 to 0.60% for the sphalerite analyses from Polusagi and Canakci areas respectively. Thus, the Canakci sphalerites are characterised by lower iron contents. This can be explained by the higher grade (mainly higher pressure) metamorphism that prevailed over the mineralisation at Canakci, since higher pressures would decrease the iron contents of sphalerite (Willan and Hall, 1980). The iron content of sphalerite has been suggested as a geothermometer (Barton and Toulmin, 1966) and applied to ore genesis problems (Urabe, 1974; Willan and Hall, 1980). No attempt, however, was made to use the iron content of the sphalerites as a geothermometer since there is no pyrrhotite occurring in the deposits, as well as there is the probability of the Fe contents of the sphalerite being modified during subsequent metamorphic events.

7.4.2.1.4 Galena

Galena is a minor phase in Polusagi,only gaining importance amongst the ore minerals at some banded and semi-massive mineralisation away from the massive ores. In the massive ore it is normally associated with the chalcopyrite-rich bands and occurs as irregular and individual grains up to 0.3 mm in diameter, but normally much finer. It is also found within sphalerite and as inclusions in the crystalline pyrite. It is absent in the

stockwork mineralisation.

In the Canakci area, galena is not found in the disseminated pyritic mineralisation, but is one of the major ore mineral phases of the massive ore. Its form, similarly, is anhedral and the grains may be up to 0.5 mm in diameter. It is normally accompanied by bornite and fahlore.

35 analyses of galena (26 from Polusagi and 9 from Canakci) were made for Pb, S and the trace elements Mn, As, Se, Ag, Cd, Sb, Te and Bi (Appendix IV3.4). The ranges and averages of these elements are presented in Table 7.3.

The abundances of Mn, As, Cd, Sb, Te and Bi in galenas from both areas are very similar and within the same range as those reported by Fleischer (1955), Malakhov (1969) and Urabe (1977), except Cd. The Cd concentration of galenas from both deposits are higher than most of the reported concentrations which are well below 0.02%. Malakhov (op cit) tentatively suggests that Bi and Sb contents of galena can be used as indicators of conditions of ore formation. The abundances of these elements in the galenas from both mineralisations are compatible with the abundances in galenas from deposits formed under medium temperatures and associated with effusive and subvolcanic formations (Malakhov, 1969, Fig.6.).

Se can substitute for S, up to as much as 18% (Ramdohr, 1980). Most galena analyses from Canakci have Se in the range 0.2 to 0.9%, while they have a great deal of variation in Polusagi. In Polusagi most galena analyses show Se contents below the detection limit or $\leq$0.0.1% while the analyses of different galena grains from two samples repeatedly indicate Se concentrations around 0.4% for one, and around or above 1.2% for the other. Such high Se concentrations are quoted by Fleischer (1955) and may be due to a solid solution with clausthalite (PbSe).

Ag is reported to be almost always present in galena, up to a few per cent, as silver bearing solid solution phases such as argentite and fahlore (Ramdohr, 1980). While the average Ag contents of galenas from

TABLE 7.3

Range and average element concentrations in galenas and bornite

GALENA					BORNITE		
	Polusagi Mineralisation		Canakci Mineralisation			Canakci Mineralisation	
Wt%	Range	Average(26)	Range	Average (9)	Wt %	Range	Average (4)
Pb	85.20- 86.94	86.24	85.77- 86.67	86.27	Fe	11.39-12.58	11.74
S	12.53- 13.62	13.28	13.08- 13.43	13.23	Cu	60.39-63.09	62.01
Mn	0.00- 0.05	0.01	0.00- 0.01	0.00	S	24.14-25.20	24.92
As	0.00- 0.06	0.01	0.00- 0.05	0.02	Zn	0.00- 0.13	0.06
Se	0.00- 1.64	0.23	0.00- 0.87	0.34	Ag	0.00- 0.04	0.02
Ag	0.00- 0.32	0.05	0.01- 0.07	0.04	Total	98.28-99.38	98.76
Cd	0.04- 0.18	0.12	0.12- 0.16	0.14			
Sb	0.00- 0.06	0.01	0.00- 0.07	0.02			
Te	0.00- 0.16	0.06	0.00- 0.09	0.04			
Bi	0.00- 0.14	0.03	0.00- 0.04	0.01			
Total	99.05-100.90	100.03	99.64-100.66	100.17			

both deposits are similar and low, occasional grains in Polusagi may have Ag contents well above the average values, e.g. 0.3%.

7.4.2.1.5. Bornite

Bornite is one of the major ore constituents and matrix minerals occurring in the Canakci massive sulphide mineralisation (Plate 7.29). However, it is a minor sulphide phase in Polusagi, gaining importance only at the massive ore locality 4 (Chapter two). It alters to covellite and idaite in both deposits, but the alteration into digenite is exclusive to, and common in the massive ore at Canakci.

The average abundances of Fe , Cu, S, Zn and Ag from 4 analyses (Appendix IV.3.5) are shown in Table 7.3. As, Sb, Ge and Sn were not detected. The average composition gives a formula : $Cu_{5.02}$ $Fe_{1.08}$ $S_{4.00}$ on the basis of 4 sulphur atoms per formula unit. i.e. close to the theoretical formula.

7.4.2.1.6 Mawsonite or 'orange bornite' and hexastannite or 'stannite jaune'

7.4.2.1.6.1. Introduction

Two tin-sulphides, mawsonite and related hexastannite, occur in trace quantities exclusively within the massive sulphide ore at Canakci. These ore minerals have been identified for the first time in Turkey (see Cagatay A., 1979, for a complete list of known ore minerals of Turkey).

Mawsonite occurs as minute grains, up to 60 microns in diameter, within the bornite matrix and is difficult to spot at first sight in the freshly polished bornite background (Plate 7.33). It has, however, a strong bireflection between tints of brownish-orange colours and very strong anisotropy. Anisotropy colours change from light orange-yellow to greenish-blue. As compared with freshly polished bornite, mawsonite shows a lighter yellowish-orange colour.

Hexastannite is very rare and related to mawsonite. It occurs with mawsonite in the same environment i.e. in bornite. Grains reaching sizes of 10-15 microns are extremely rare. It is browner with no yellowish tint as compared with mawsonite, and has a similarly strong anistropy.

7.4.2.1.6.2 Chemistry

Mawsonite was first described by Markham and Lawrence (1965) from Mt.Lyell, Tasmania, and Tingha, New South Wales, and a formula $Cu_7 Fe_2 Sn S_{10}$, and a structure similar to that of renierite were suggested. Most of the "orange bornites" described in literature since the beginning of this century seem to be equivalent to mawsonite (Uytenbogaardt and Burke, 1971). The original formula given by Markham and Lawrence (1965) was revised on the basis of improved chemical analyses and the formula $Cu_6Fe_2Sn S_8$ now seems to have gained acceptance (Springer, 1968; Lee et al, 1975; Kissin and Owens, 1979).

It was Ramdohr (1944, 1960) who first described the mineral 'stannite (?) I' and later named it hexastannite. Kato (1969) named a mineral 'stannoidite' and later suggested that it was equivalent to hexastannite. According to Levy (1966), 'stannite (?)I' and hexastannite may also be 'stannite jaune' whose formula he gives as $(Cu,Sn)_3 Fe S_4$. However a more accepted formula today is $Cu_8 (Fe,Zn)_3 Sn_2S_{12}$ (Springer, 1968; Lee et al, 1975; Kissin and Owens, 1979).

Levy (1966) pointed out that hexastannite ('stannite jaune') and mawsonite may be part of a solid solution series, but Springer (1968) considers this unlikely on the basis of the metal/sulphur ratios being higher than 1 and different for each phase and because of the different structures.

Appendices IV.3.6 and IV.3.7 include 10 mawsonite and 2 hexastannite analyses from Canakci , carried out for the elements Fe, S, Cu, Zn, Ag and Sn and the atomic proportions calculated on the basis of 17 and 25 atoms

respectively. No Ge was detected in any of the analyses. In Table 7.4 the ranges and the averages of the elements for the mawsonite and hexastannite analyses are presented and the averages are comparable with those of the equivalent minerals reported by various sources. Analyses of the mawsonites approximate closely to the generally accepted formula : $Cu_{5.99}Fe_{2.06}Sn_{1.09}S_{7.83}$. This is also so for the hexastannite : $Cu_{8.05}(Fe_{2.15}Zn_{1.02})_{3.17}Sn_{2.03}S_{11.75}$. It is interesting to note that the Fe/Zn ratio in the hexastannite is nearly 1 and relatively constant, while Kissin and Owens (1979) report variations in Fe/Zn ratios of hexastannite in the range 2 to 3.

The association of mawsonite and hexastannite with bornite is considered by Lee et al (1975) who synthesized mawsonite and hexastannite ('stannoidite') and discussed their genesis in ore deposits. They conclude that mawsonite forms below 390°C and it is always accompanied by bornite and/or 'stannoidite'. Above 390°C, mawsonite decomposes into a fine mixture of 'stannoidite', bornite and chalcopyrite. Therefore, the association bornite+mawsonite+hexastannite in the Canakci massive ore should represent temperatures below 390°C, which suggests that the metamorphism could not have attained higher temperatures than 390°C i.e. compatible with relatively high pressure prehnite-pumpellyite facies conditions.

7.4.2.1.7 Colusite

7.4.2.1.7.1. Introduction

This mineral phase occurs as round or sub-round grains in pyrite and frequently in bornite, exclusively within the massive sulphide ores of the Canakci area. In bornite, it is sometimes associated with mawsonite and hexastannite. The grain size is similar to the tin-bearing phases and no more than 50 microns in diameter (Plate.7.34). The colour

TABLE 7.4

Comparative chemical data on mawsonite and hexastannite

	MAWSONITE					HEXASTANNITE					
wt%	(A)	(B)	(1)	(2)	(3)	(C)	(D)	(4)	(5)	(6)	wt%
Fe	11.23- 14.05	13.10	13.51	12.55	12.40	9.16- 9.23	9.20	11.84	10.75	10.00	Fe
S	27.83- 28.89	28.53	29.82	31.15	30.42	28.76-28.88	28.82	29.81	29.73	29.2	S
Cu	41.18- 45.00	43.27	43.59	44.30	43.79	38.90-39.32	39.11	37.52	39.78	38.65	Cu
Zn	0.00- 1.41	0.21*	0.08	-	0.02	5.03- 5.15	5.09	2.70	1.68	3.05	Zn
Ag	0.00- 0.06	0.02	-	-	-	0.02- 0.05	0.03	-	-	-	Ag
Sn	13.59- 16.26	14.72	13.82	12.48	12.66	18.30-18.48	18.39	20.12	16.38	18.45	Sn
Total	98.91-100.37	99.85	100.82	100.50	99.02	100.27-101.00	100.64	102.01	99.45	99.90	Total

Numbers in parentheses=number of analyses averaged.

(A) Present study, element range.

(B) Present study, mawsonite average (10).

(1) 'Orange bornite' average (9); Levy,1966.

(2) Mawsonite average (4); Levy, 1966.

(3) Mawsonite average (5); Springer, 1968.

* with exclusion of one analysis (Zn=1.41%), Zn average = 0.07%.

(C) Present study, element range.

(D) Present study, hexastannite average (2).

(4) 'Stannite jaune' average (9); Levy; 1966.

(5) Hexastannite average (4); Springer; 1968.

(6) 'Stannoidite' average (2); Kissin and Owen,1979.



Plate 7.34 : Colusite (grey), associated with bornite (brown) and pyrite (yellow). Black is gangue. Sample: E4-1, X1000, under oil.

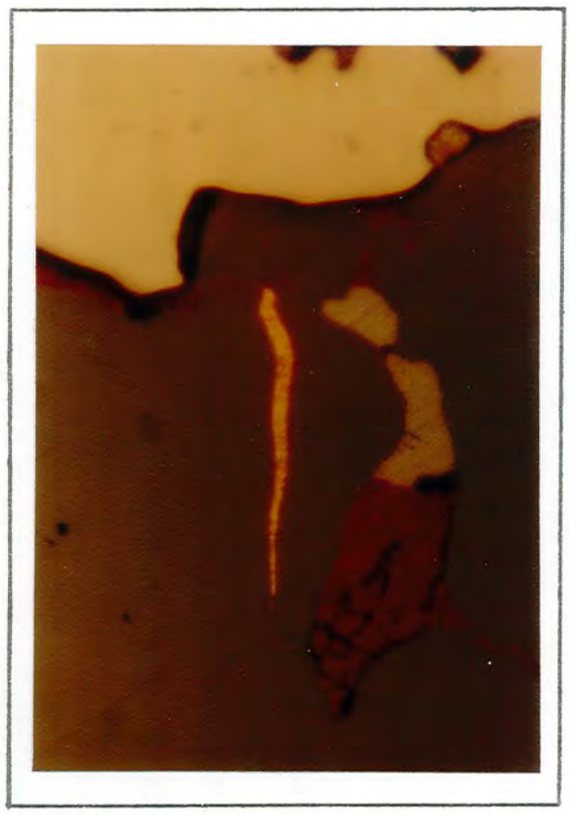


Plate 7.35 : Gold streak (orange-yellow) in tennantite. Yellow is pyrite, brown is bornite, blue is digenite and grey is galena. Sample: E2-4, X1000, under oil.

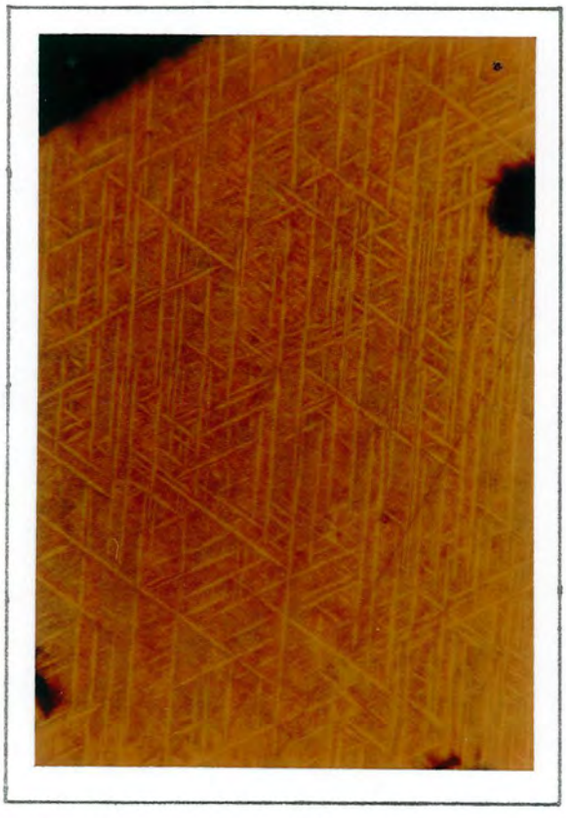


Plate 7.36 : Extremely fine intergrowth of chalcopyrite (the spindles) and idaite. Sample: E-3, X2250, under oil.

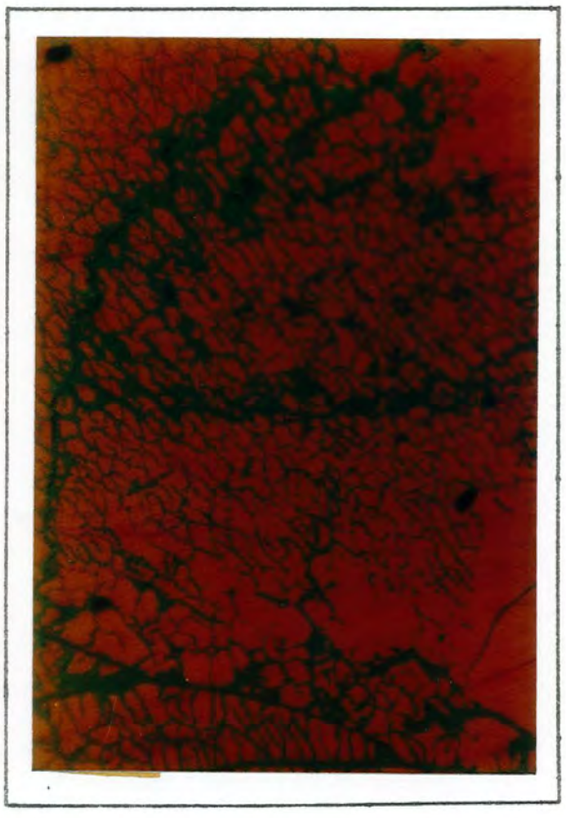


Plate 7.37 : Bornite, being replaced by digenite (blue) along numerous veins with a "mosaic" texture. Sample: E1-6B, X1000, under oil.

is a brownish-creamy yellow colour. The reflectance seems to be lower than pyrite and higher than bornite and it is isotropic. Although it occurs in trace amounts, its occurrence is more common than those of mawsonite and hexastannite. Like mawsonite and hexastannite, colusite has not previously been reported from Turkey.

7.4.2.1.7.2 Chemistry

17 spot analyses of the mineral were made (Appendix IV.3.8) for the elements Fe, S, V, Cu, Zn, Ga, Ge, As, Ag and Sn and the range and averages of element abundances are shown in Table 7.5. It is a Cu, As, Ge, V, Fe and Sn sulphide with traces of Zn, Ga and Ag. The following ore minerals similar in some optical and chemical aspects are considered :

a) Sulvanite, Cu_3VS_4 : Dolanski (1974) reports the fourth occurrence in the world of this rare primary vanadium sulphide and reviews much of the existing literature. The colour of sulvanite in the polished section is creamy-white.

b) Arsenosulvanite, Cu_3AsS_4 : This mineral shows a complete solid solution series with sulvanite and has been reported by Sclar and Drovenik (1960) under the name 'lazarevicite' (reference from Uytenbogaardt and Burke, 1971). The colour of the As-end member of the series is a distinct yellow-brown tint and the members seem to get browner with increasing As-content.

c) Colusite, $Cu_3(As,Sn,V,Fe)S_4$, has the advantage of being found in association with hexastannite ('stannite jaune')- mawsonite series, as reported by Uytenbogaardt and Burke (1971) where its colour is given as 'coppery-cream to creamy tan'.

d) Germanite, $Cu_3(Fe,Ge)S_4$, may contain some Ga, Zn, As and V, and is pinkish violet-grey in colour (Uytenbogaardt and Burke 1971).

All the above mentioned ore minerals are cubic and have reflectances in the range between bornite and pyrite. Some representative compositions

of these minerals are also included in Table 7.5. Cu and S values of the mineral occurring in Canakci agree with those of the 4 minerals considered; however the other important elements, As, Ge, V, Fe and Sn show considerable variations. Therefore, the formula in analogy to the above minerals may be calculated with S=4 or total number of atoms = 8. On the basis of S=4, the average chemical analyses gives:

$$Cu_{3.24}(As_{0.47}V_{0.24}Ge_{0.18}Fe_{0.16}Sn_{0.03})_{1.08}\ S_{4.00}$$

and on the basis of total number of atoms = 8 it becomes :

$$Cu_{3.11}(As_{0.45}V_{0.23}Ge_{0.17}Fe_{0.15}Sn_{0.03})_{1.03}\ S_{3.84}$$

If the slight excess in Cu is ignored both formulae closely approximate to a type Cu_3 X S_4 which is extensively studied by Levy (1966) where X = As,V,Ge,Fe,Sn and trace amounts of Ga and Zn. Therefore, it seems possible that this mineral represents a member of a complex solid-solution series with end members : Cu_3 As S_4, Cu_3V S_4, Cu_3 (Ge,Fe)S_4 and Cu_3 Sn S_4 in the crude proportions 15 :7 :6 : 1 respectively.

Commonly, the mineral 'colusite' appears to accommodate As, Sn, V and Fe into the X position (Levy,1966), and it is found in association with hexastannite-mawsonite series. Perhaps the mineral found in the Canakci massive sulphide ore can then be best described as a Ge bearing-colusite.

It is noteworthy that amongst the members of the X site of the Canakci colusite, As shows minimal variation and the content is very close to 0.5 atom per formula unit. The range of atomic contents of the important elements are as follows (S=4) : As = 0.401 - 0.509, V = 0.153 - 0.269, Ge = 0.107 - 0.225, Fe = 0.012 - 0.364 and Sn = 0.007 - 0.066. Therefore, the formula also approximates to an ideal Cu_6 (V,Ge,Fe,Sn) As S_8. Such a constancy of As content around 0.5 atoms in colusite formula is also observed by Levy (1966). This provides further support for the suitability of the name 'colusite' for the mineral under consideration.

TABLE 7.5

Composition of colusite and related sulphides

	(A)	(B)	(1)	(2)	(3)	(4)
Fe	0.17- 5.19	2.18	1.00	-	7.53	-
S	29.70- 31.46	31.04	30.65	36.5	33.20	32.56
V	1.98- 3.34	2.98	2.28	14.6	-	-
Cu	48.96- 52.89	50.53	47.99	50.4	45.27	48.41
Zn	0.00- 3.03	0.22	-	-	0.93	-
Ga	0.00- 0.12	0.03	-	-	-	-
Ge	1.96- 4.01	3.15	-	-	9.60	-
As	7.59- 9.18	8.62	9.54	-	3.37	19.02
Ag	0.00- 0.09	0.02	-	-	-	-
Sn	0.20- 1.96	0.89	6.71	-	-	-
Others	--------	-	1.45	-	-	-
Total	98.22-101.38	99.66	99.71	101.5	99.9	99.99

Numbers in parentheses = number of analyses averaged.

(A) Present study, element range.

(B) Present study, colusite average (17).

(1) Colusite; Levy, 1966.

(2) Sulvanite; Levy, 1966.

(3) Germanite average (3); Levy, 1966.

(4) Arsenosulvanite, theoretical composition.

7.4.2.2 Sulphosalts.

7.4.2.2.1 Fahlore group minerals

7.4.2.2.1.1 Introduction.

The German term "fahlerz", long used to describe the group of related sulphosalt minerals of which tetrahedrite and tennantite are the most common examples, is now commonly used by various authors in the anglisized form "fahlore". Following Ramdohr (1980), the Sb, As, Ag, Te and Bi rich members of the group are termed tetrahedrite, tennantite, freibergite, goldfieldite, and annivite respectively. Minerals of this group are probably the most abundant sulphosalts in the earth's crust and are the only sulphosalts found in the deposits being described.

They occur only in trace amounts in the massive sulphides of Polusagi, but constitute one of the major phases occurring in the matrix of the Canakci massive sulphides in association with bornite, sphalerite and galena (Plate 7.29). In each area, the fahlore is anhedral, but the grain sizes are different. At Polusagi, it is found within chalcopyrite - and/or sphalerite-rich bands as grains up to 0.3 mm in diameter, but most grains are much smaller. At Canakci, it is coarser and grains around 0.5 mm in diameter are common.

Despite the earlier doubts on the chemical formula, in recent years a formula $Cu_{12}(As,Sb)_4S_{13}$ has been widely accepted for the fahlore group as an ideal formula based on its crystal structure. However, it contains many elements such as Fe, Zn, Ag in solid solution and the majority of fahlore from various localities has been considered to correspond to the general formula $(Cu,Ag)_{10}(Fe,Zn)_2(As,Sb)_4S_{13}$ (see Springer,1969; Yui,1971; Tatsuka and Morimoto, 1973; Charlat and Levy, 1974; Wu and Petersen,1977; Shikazono and Kouda, 1979). Furthermore, less frequent substitutions of

Hg, Ni and Co for Cu, of Te, Bi and to a lesser extent Sn and Ge for As and Sb can take place (Springer, 1969; Ramdohr, 1980).

7.4.2.2.1.2 Chemistry.

66 microprobe analyses of fahlore (40 from Polusagi and 26 from Canakci) were carried out for Fe, S, Cu, Zn, As, Ag, Sb, Te and Bi (see Appendix IV.3.9) and the averages and the ranges of element concentrations are presented in Table 7.6 for fahlores from each area. The elements Hg, Sn, Ge, Co and Ni were analysed for in some samples but found to be low ($<0.01\%$) or below detection limit. The atomic proportions were calculated on the basis that total number of atoms, excluding S, = 16 (see Table 7.6).

The chemical formula for the average fahlore from Polusagi, therefore, is :

$$(Cu_{9.77}\ Ag_{0.01})_{9.78}\ (Zn_{1.84}Fe_{0.45})_{2.29}(As_{3.04}Sb_{0.87}Te_{0.00}Bi_{0.00})_{3.92}\ S_{12.66}$$

and that from Canakci :

$$(Cu_{10.08}Ag_{0.01})_{10.09}\ (Zn_{1.83}\ Fe_{0.11})_{1.94}\ (As_{3.72}Sb_{0.12}Te_{0.10}Bi_{0.02})_{3.96}\ S_{12.65}.$$

These formulae approximate very closely to the widely accepted theoretical formula in the form $A_{10}\ B_2\ C_4\ S_{13}$ where A = Cu, Ag, B= Zn, Fe, C= As, Sb, Te and Bi. Thus, there is a general deficiency in S, and in the Polusagi fahlore there is a deficiency in Cu and an excess in Zn+Cu.

Considering the fact that fahlore is one of the major silver-bearing mineral groups, and that it can contain as much as 50% silver (Ramdohr, 1980), the fahlores from both areas are very poor in Ag, the contents on average being 0.04% in each case. Despite the uniformly low Ag values, all the other elements show either significant or remarkable chemical variations, excepting S. The extent and significance of these variations are summarised in the following points :

a) Single grains from both deposits show only insignificant chemical variation and are relatively uniform. This is contrary to reports

TABLE 7.6

Range and average element concentrations in fahlores

	Polusagi mineralisation		Canakci mineralisation	
wt%	Range	Average(40)	Average(26)	Range
Fe	0.07- 5.91	1.73	0.52	0.08- 2.57
S	25.56- 28.07	27.00	27.41	26.33- 27.83
Cu	39.40- 44.21	41.42	43.29	41.49- 44.69
Zn	4.75- 10.66	8.01	8.09	6.98- 9.18
As	8.01- 19.28	15.23	18.83	15.94- 19.71
Ag	0.00- 0.19	0.04	0.04	0.00- 0.08
Sb	1.01- 16.97	7.05	0.96	0.05- 3.47
Te	0.00- 0.12	0.03	1.15	0.14- 1.85
Bi	0.00- 0.69	0.03	0.23	0.09- 1.05
Total	99.14-101.56	100.53	100.25	99.12-101.55
Atomic proportions				
S	12.153- 13.282	12.626	12.647	12.041- 12.972
Cu	9.466- 10.296	9.778	10.076	9.798- 10.322
Ag	0.000- 0.026	0.006	0.005	0.000- 0.011
Zn	1.1021- 2.439	1.836	1.830	1.596- 2.068
Fe	0.018- 1.605	0.464	0.113	0.022- 0.690
As	1.633- 3.754	3.044	3.717	3.192- 3.827
Sb	0.122- 2.129	0.871	0.117	0.007- 0.427
Te	0.000- 0.015	0.004	0.101	0.016- 0.216
Bi	0.000- 0.049	0.002	0.017	0.006- 0.075

that most of the single grains of fahlore (mostly tetrahedrite) are heterogenous due to strong chemical zonation (Springer,1969; Yui, 1971; White, 1972; Charlat and Levy, 1974; Wu and Petersen, 1977). This may be a result of metamorphism i.e. obliteration of zoning during recrystallisation. However, in general, the extent of chemical variation increases when comparison is made between : the analyses from different grains in the same sample, different samples from the same location, samples from different locations in the same area, and, finally, between samples from the two areas.

b) The C site occupancy of fahlores from both areas is dominantly As; therefore they are called tennantite hereafter. However, there are important differences between the Polusagi and Canakci tennantites. The Polusagi tennantites contain extremely small amounts of Te and Bi, nearly always zero or less than a combined 0.4% of the C site occupancy, and As constitutes between 40%and 90% of the C site occupancy, the rest being Sb. On the other hand, the Canakci tennantites are nearly the pure As-end member of the solid solutions in the fahlore group; As comprising consistently well over 90% of the C site occupancy. Furthermore, the rest of the C site on average is equally occupied by Te+Bi and Sb. The variation in As as opposed to Sb (and+Te+Bi, in the case of Canakci), is shown in Fig. 7.1., which also clearly demonstrates the strong negative correlation due to the substitution of Sb (and Te and Bi) for As in the basic tennantite formula.

c) The Zn and Fe , as expected , show a negative correlation in all tennantites. But the Polusagi tennantites have a much greater range of Fe and Zn contents and the B site occupancy is up to 0.75 atoms in excess of that required, see Fig. 7.2. This excess is positively correlated with the deficiency of Cu in the A site; therefore, it follows that some of the Zn and Fe present in the Polusagi tennantites must be in the A site. On the other hand, the Canakci tennantites have a limited range of Zn and Fe

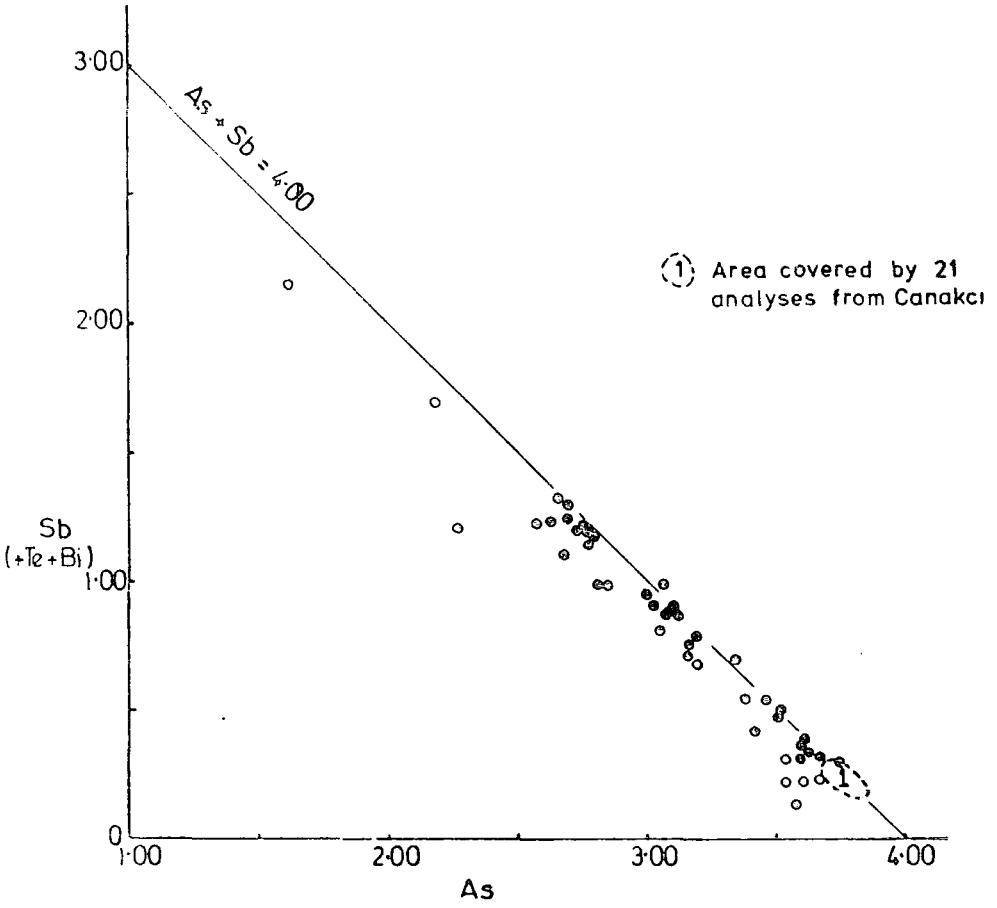


Fig.7.1. As vs. Sb (+Te+Bi for Canakci) diagram for the fahlore group. ● :Tennantites from Polusagi and ○ : tennantites from Canakci.

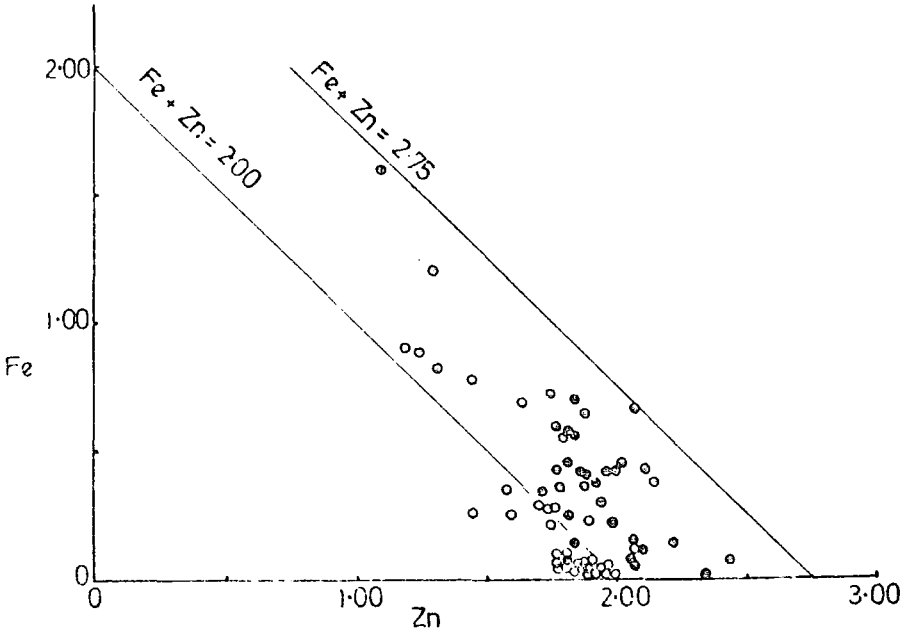


Fig.7.2. Fe-Zn variation diagram for the fahlore group.

● : tennantites from Polusagi and ○ : from Canakci.

contents and the occupancy of the B site is generally not complete (Fig.7.2). With similar reasoning it can be shown that some Cu may be present in the B site but this is comparatively insignificant. That Cu may be present in the B site of the tetrahedrite-tennantite series is also suggested by Charlat and Levy (1974).

d) The B site in the tennantites from both areas is dominated by Zn. On the basis of B site occupancy the tetrahedrite-tennantite series is defined here (Fig.7.3) as either Zn-rich or Fe-rich. It is clear from Fig.7.4 that all tennantites plot into the Zn-rich field, and all can be labelled as Zn-rich tennantites. But there are systematic differences between tennantites from the two areas. The Canakci tennantites have higher Zn/Fe ratios (atomic), most being >10, while the Zn/Fe ratio for most of the tennantites from Polusagi is less than 10. Nevertheless, the ratio in tennantites from both areas may reach values around 100.

d) The various substitutions involving As,Sb,Te and Bi in the C site and Cu, Zn, Fe in the A and B sites are not independent. In Fig.7.4. As occupancy of the C site and Zn occupancy of the B site (in percentages) are plotted. It shows that there is a certain degree of positive correlation between the two which becomes stronger if the analyses from 1 single grain is ignored. Similar conclusions, that such different substitutions are not independent, have been reached by other workers. Yui (1971) and Wu and Petersen (1977) have observed a positive correlation between Ag and Sb i.e. higher Ag contents in tetrahedrites, which may help to explain the poor silver content of the Polusagi and Canakci tennantites. Charlat and Levy (1974) found an affinity of Cu for As and Fe, and of Ag for Sb and Zn in the tetrahedrite-tennantite series.

In conclusion, the Polusagi tennantites can be represented by an ideal formula, $(Cu,Zn,Fe)_{10}\ (Zn,Fe)_2\ (As,Sb)_4\ S_{13}$, and they are Zn rich members of the simple tetrahedrite-tennantite solid solution series. On the other hand, the Canakci tennantites can be represented by an ideal formula,

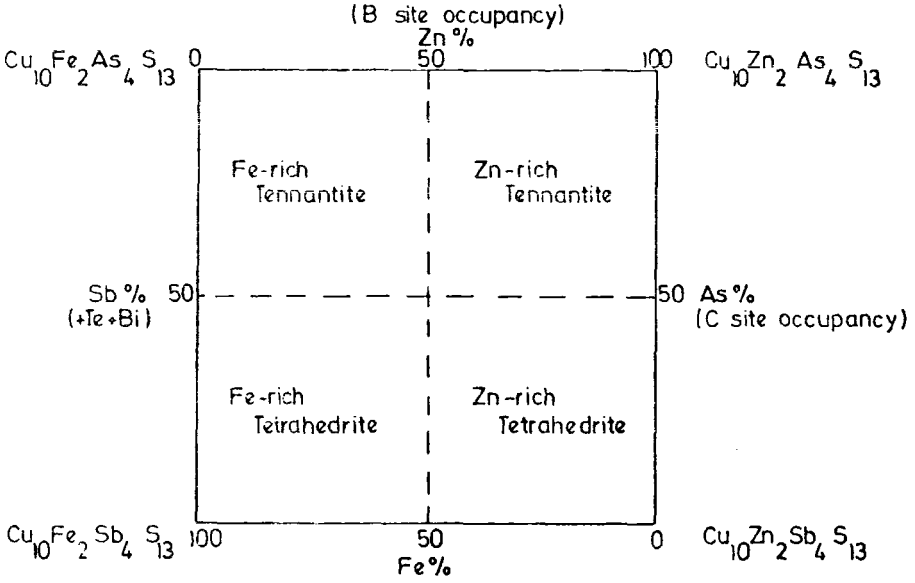


Fig.7.3. Classification diagram for tetrahedrite-tennantite series on the basis of relative proportions of Fe and Zn in the 'B' site.

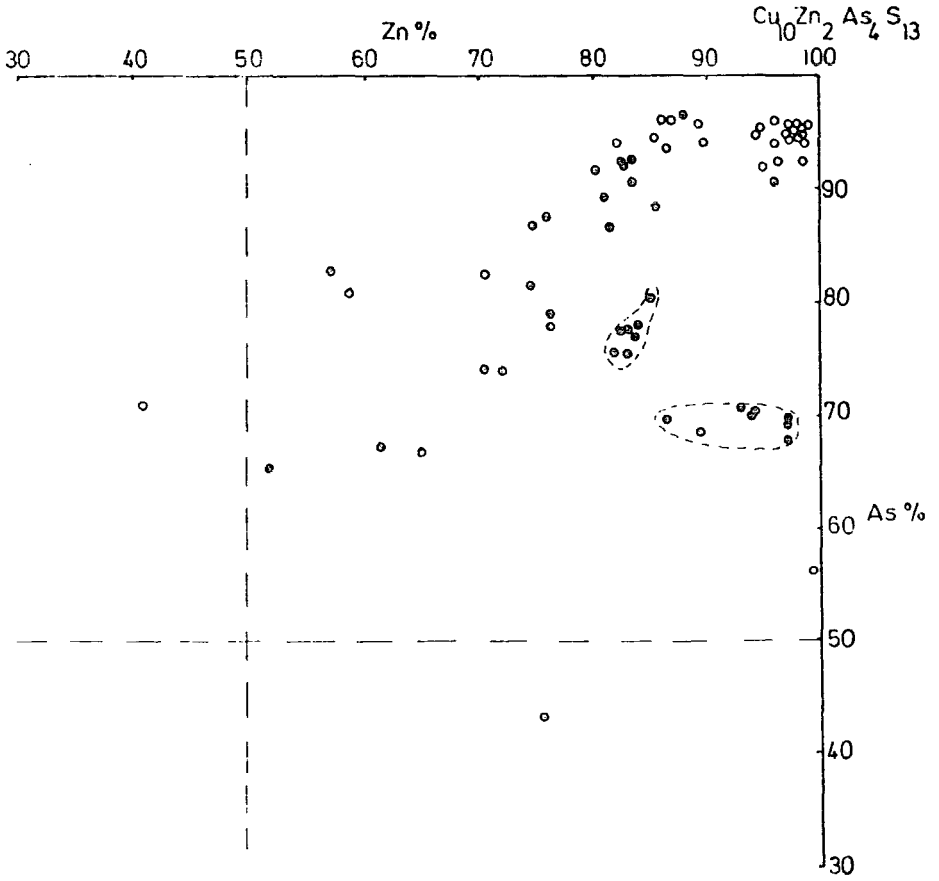


Fig.7.4. Tennantite analyses from Polusagi (●) and Canakci (○) plotted in the above diagram. Broken lines encircle analyses from single grains.

$Cu_{10}(Zn,Fe)_2(As,Sb,Te,Bi)_4S_{13}$ and they are mostly near Zn and As rich end-members of the complex tetrahedrite-tennantite-goldfieldite-annivite solid solution series with approximate proportions of the end members 3 : 92 : 3 : 2 respectively.

Shikazono and Kouda (1979) who studied the chemical composition of tetrahedrite-tennantite minerals in relation to the chemical environment of some Japanese ore deposits, state that there are systematic variations in the chemistry of the elements Cu, Ag, Zn, Fe, Sb and As in different types of ore deposits. They consider that the Zn/Fe ratio is largely dependent on oxygen fugacity as well as pH and S activity and "has a maximum value at the boundary between the predominance field of oxidised sulphur species and that of reduced sulphur species at constant other variables". The high Zn/Fe ratios of the Polusagi and Canakci tennantites, therefore, would agree with and provide further support to their formation on the sea-floor where "reduced" hydorthermal solutions mixed with the "oxidised" sea water.

7.4.2.3. Oxides

7.4.2.3.1 Magnetite

Magnetite is the only spinel found in association with the Polusagi massive sulphide mineralisation and confined to it. It occurs in trace amounts in sphalerite-rich bands as tiny, round and sometimes euhedral grains, sizes being no more than 6-7 microns in diameter. It is not very easy to spot due to its very fine and scattered nature, but under oil the colour contrast and the higher reflectance against sphalerite become apparent (Plate 7.24). The relative abundance increases towards the upper levels of the massive sulphides where it is sometimes accompanied by hematite.

Despite the very small grain sizes, two magnetite grains were analysed

by the microprobe and the analyses are close to the magnetite end-member composition of the spinels (Appendix IV.3.10). The high Zn contents (3-4%) are thought to be due to contamination from the surrounding sphalerite.

7.4.2.3.2. Hematite and Mn-oxides

In the Polusagi mineralisation,hematite, as a primary phase, occurs in trace amounts in the upper levels of the stockwork mineralisation from where its abundance increases upward through the massive sulphides, but still in trace quantities, and finally becomes one of the major phases comprising the Fe-Mn rich cherty chemical precipitates overlying the massive sulphides as well as occurring as separate discrete or continuous horizons. In the massive sulphides it is found sometimes together with magnetite within sphalerite or chalcopyrite as euhedral or subhedral plates and laths, up to sizes 60 microns long (Plates7.24, 7.25). In the Fe-Mn-rich cherts, it is very fine grained, mostly in sub-micron scale, sometimes showing a banded alignment (Plates 7.26, 7.27m 7.28). It is in the cherty sediments that the Mn-oxides with extremely small grain sizes are present, as indicated by up to 23% MnO content.

In the Canakci massive sulphides, both hematite and Mn-oxides are presumed to be present in the rare red-cherty fragments, in analogy to those from Polusagi.

Well crystalline hematite, in the form of sheaves, up to 1 mm long, were found in a thin quartz vein (< 0.5 m) in Polusagi, with no apparent spacial relation to either the Fe-Mn rich sediments or the sulphide mineralisation.

7.4.2.3.3. Chromite

This spinel is found only within the serpentinite in Canakci, in pod-like or fragmentary small bodies of chromitite (Chapter two). Microscopically,

it is massive and the grains are subhedral, reaching sizes a few mm in diameter.

8 spot analyses of cores and margins on 4 relatively coarse grains (Appendix IV.3.11) show that they are chemically uniform and the average composition is as follows : Cr_2O_3 = 59.17%, MgO = 13.69%, FeO = 12.37% , Fe_2O_3 = 3.18%, MnO = 0.79%, SiO_2 = 0.17%, TiO_2 = 0.13%, Ni = 0.13%, V = 0.07%, and the total = 100.52%. The Fe^{3+} content was calculated by assuming perfect stochiometry i.e. O = 4.000. On the basis of 4 oxygen in the spinel structure, the atomic proportions are calculated (Appendix IV.3.11) and ignoring minor Si, Ti, Ni and V, the average formula is :

$$(Mg_{0.65}\ Fe^{2+}_{0.33}\ Mn_{0.02})_{1.00}\ (Cr_{1.50}\ Al_{0.41}Fe^{3+}_{0.08})_{1.99}\ O_{4.00}$$

Therefore, it is (sensu stricto) an aluminian-chromite, according the R^{3+} site occupancy and a magnesio-chromite, according the R^{2+} site occupancy.

High chromium content and massive nature of the chromite are indicative of a dunite host lithology (Dick,1977). The 100 x Cr/Cr+Al ratio is high, average = 78. According to Irvine (1967) and Coleman (1977,Fig.9.), this ratio should indicate a stratiform chromite deposit as parental to the fragmentary massive chromite blocks of Canakci, since it is $\rangle$ 58. The above ratio, the 100 x Mg/Mg+Fe^{2+} ratio (average = 66) and the composition in general fall into the compositional fields of those chromites from the Troodos complex (Greenbaum, 1977), Vavdos complex, Greece (Christodoulou, 1980), and the Alpine type deposits in general (Irvine and Findlay,1972).

7.4.2.4. Native metals

7.4.2.4.1 Gold

It is found only within the matrix minerals, tennantite and bornite, in the Canakci massive sulphides. It occurs in trace amounts and is the least abundant identified ore mineral. The denser yellow colour and higher

reflectance help to distinguish it from chalcopyrite. It shows a strong anomalous anisotropy from greyish-white to a brown tinted yellowish colour. The grains are generally extremely small, in the order of few microns, and irregularly shaped. A relatively large grain, 50 microns long and up to 3 microns wide occurring in tennantite is shown in Plate 7.35.

3 spot analyses of the grain in Plate 7.35 were carried out (Appendix IV.3.12) which gave the following average composition : Au = 51.42% , Cu = 23.76%, Ag = 6.00%, Zn = 3.55%, Fe = 0.70%, Bi = 0.14%, and S = 16.53%. Total = 102.10%. Pt was not detected. Due to the very narrow width of the analysed grain, being almost the same as that of the microprobe electron beam, there was contamination from tennantite during analyses. If Cu and Ag are excluded from the average composition, the elements in the rest of the analyses have atomic proportions crudely approximating to those of tennantite. Thus it seems that the 'gold' is not rich in Cu but contains some Ag, probably around 10%, since the tennantites are very poor in Ag.

7.4.3 Secondary ore minerals

7.4.3.1 Sulphides

7.4.3.1.1 Idaite

7.4.3.1.1.1 Introduction

Although present in the massive sulphide ores of both areas, idaite is very rare in Polusagi, only found in a few isolated small grains in sphalerite and in inclusions within pyrite, whereas in Canakci it is more common and occurs as one of the important sulphide phases in a few samples. The form and associated minerals, however, are identical : always found as intimate and extremely fine, orientated, lamellar intergrowths with chalcopyrite (Plate 7.36) and is associated with bornite and covellite. The size of the

individual idaite and chalcopyrite phases in the intergrowth is in the order of no more than a few microns, but usually smaller. In some cases, the chalcopyrite may occur as slightly coarser spindles in the intergrowth or may form chalcopyrite enriched areas. The proportion of each phase in the fine intergrowth judging by optical means seems roughly of equal amounts. In certain grains bornite may occur next to the intergrowth and the textural relations suggest that the chalcopyrite-idaite intergrowth may be a decomposition product of bornite. This is supported by the fact that the idaite-rich samples have relatively little bornite in Canakci and that idaite abundance is proportional to that of bornite in the ore deposits of each area. Covellite, as a much later phase, occurs along cracks, penetrating through bornite as well as the intergrowth in much the same way, described by Ramdohr (1980) as the "crack-disease" in idaite.

Optically, the colour of idaite is similar to that of bornite, but there is a certain amount of bireflectance with shades of orange-brown and more reddish brown colours. Like bornite, it tarnishes to darker colours. The most spectacular optical property is its extreme anisotropy : whitish with greenish tint which easily distinguishes it from bornite. These properties are similar to those described by Uytenbogaardt and Burke(1971) and Ramdohr (1980), except the bireflectance, these authors indicate it to be much stronger. This may be due to the difficulty of observing it in such fine intergrowth with chalcopyrite.

The general associated minerals and the mode of occurrence of the idaite is very similar to other occurrences reported elsewhere (e.g. Krause, 1965; Sillitoe and Clark, 1969; Constantinou1975) and to a specimen kept in the collection at Durham University, from Ida mine, S.W. Africa, where idanite was first described by Frenzel (1959).

7.4.3.1.1.2. Chemistry

Chemical composition of idaite has been a much discussed controversy.

Frenzel (1959), in his original description of idaite, was unable to obtain pure material for chemical or x-ray analysis but, on the basis of its similarities to a synthetic material, considered the formula to be $Cu_5Fe\ S_6$. Frenzel and Ottemann(1967) analysed a coarse grained "idaite-like" mineral from Fiji, and agreed with the above formula, which is also given to be correct by Ramdohr (1980). On the other hand, Levy (1966) proposed that the correct formula was Cu_3FeS_4. This was supported by the analyses carried out by Sillitoe and Clark (1969) on some idaites from Chile, who stated that the Chilean idaite was "quite distinct" in nature from that originally described by Frenzel (1959). They proposed it to be a new phase. More recently, idaite was described and analysed from the Skouriotissa massive sulphide ore body by Constantinou (1975) who showed the formula to be very close to $Cu_3Fe\ S_4$. Ottemann and Frenzel (1971), on the basis of 11 probe analyses of idaite from different localities, concluded that idaite showed chemical compositions from $Cu_3Fe\ S_4$ to $Cu_5\ Fe\ S_6$. Recently, an attempt to clarify the controversy over idaite was made by Rice et al (1979). These authors drew attention to the fact that there seems to be at least two distinct phases currently referred to as idaite, — phase I is the "idaite" described by Levy (1966) with a formula $Cu_3\ Fe\ S_4$, and Phase II is the "idaite" from Fiji and Chile, with a formula $Cu_5Fe\ S_6$-, and proposed the name "nukundamite for the Fijian "idaite" to distinguish it from the "idaite" of Ida mine.

Microprobe analysis of the Polusagi or Canakci idaite, as an individual phase, proved to be practically impossible since it forms too fine intergrowths with chalcopyrite to be adequately resolved by the electron beam. However, by diffusing the beam into several orders of magnitude of the focussed beam, 3 analyses from Polusagi and 21 analyses from Canakci were carried out for Fe, Cu and S in relatively uniform looking areas of the intergrowth. This way, representative combined compositions of chalcopyrite and idaite intergrowth were achieved and the results are presented

in Appendix IV.3.13. The analyses are remarkably consistent and the average composite compositions from Polusagi and Canakci are very similar. The averages are : Fe = 15.97%, Cu = 50.05% and S = 33.13% (total = 99.16%) for Polusagi, and Fe = 15.66%, Cu = 50.04% and S = 33.81% (total 99.51%) for Canakci.

If the formula $Cu_3Fe\ S_4$ is assumed for idaite, a mixture of idaite and chalcopyrite with a respective proportion 9:1 would produce a calculated composite composition very close to the analysed composite composition. On the other hand, an equally close agreement between the calculated and analysed composite compositions is achieved by assuming an approximate 1 : 1 proportion for the idaite and chalcopyrite and the chemical formula, Cu_5 $Fe\ S_6$ for idaite. Since on the basis of optical observations crudely equal amounts of idaite and chalcopyrite appear to be present in the intergrowth, it is suggested that the formula $Cu_5Fe\ S_6$ is more likely to be correct for the idaites from Polusagi and Canakci. This would mean that these idaites, according to Rice et al's (1979) proposal, are "idaite", sensu stricto, and not "nukundamite".

Idaite in general is considered to be a supergene product of decomposing bornite. This view is supported by the relations of idaite with bornite from the presently described areas. Frenzel (1959) suggested a supergene origin for idaite through the oxidation of bornite by chlorite-rich ground-water under acid conditions and pointed out that the action of inorganic acids on bornite produced idaite and chalcopyrite. It was Sillitoe and Clark (1969) who emphasised the importance of ferric sulphate-bearing solutions in the oxidised zone above the water table for the formation of idaite by the oxidation of bornite in the Copiapo district of northern Chile. Ugarte and Burkin (1975) studied the nature of reaction of synthetic bornite with ferric sulphate solutions and reported that at low temperatures ($\sim 40^{\circ}C$) idaite formed by the leaching of Cu out

of bornite. Constantimou. (1975) considers that the Skouriotisso idaite was formed during oxidative leaching of chalcopyrite by descending ferric sulphate bearing acid solutions, produced during the submarine oxidation of pyrite. In analogy to the above summarised proposals, it is probable that the disintegration of bornite into idaite and chalcopyrite and subsequently all phases to covellite is a result of highly oxidised and acid conditions following the formation of the massive sulphides on the Tethyan sea-floor.

7.4.3.1.2. Covellite

This Cu-sulphide occurs both in the Polusagi and the Canakci massive sulphides, forming after chalcopyrite. It follows that its occurrence is more common in the Polusagi sulphides where it is coarser, and especially in locality 4 chalcopyrite is extensively replaced by it. In both areas it displays the characteristic and extremely strong reflection pleochroism, bireflection and anistropy. The formation of covellite is clearly a low temperature, supergene process; in Polusagi, for instance, it mostly occurs in association with hematite formed by the oxidation of pyrite.

7.4.3.1.3. Digenite

Digenite, a grey-blue and isotropic Cu-sulphide, is commonly found in the Canakci massive ore, replacing bornite. It is not found in Polusagi. The replacement of bornite by digenite in the Canakci massive sulphides takes place along veins or cracks, and in many cases takes the form of a mosaic texture where numerous fine digenite veins cut across bornite, isolating the bornite 'islands' from one another (Plate 7.37). The veins replacing bornite stop against pyrite grains and in most cases against tennantite, sphalerite and galena. It is thought that digenite is a higher temperature secondary sulphide phase as opposed to covellite.

7.4.3.2 Miscellaneous minerals

7.4.3.2.1 Hematite and goethite

As low temperature secondary minerals, hematite and geothite form after pyrite in the oxidised sulphide outcrops in both areas. Hematite is also occasionally found as crystalline sheaves ($\ll 5$ mm) in lavas in Polusagi, and in agglomerates in Canakci.

7.4.3.2.2 Cuprite, native copper and malachite

The combination of these three copper phases was found in an oxidised thin vein in Polusagi, away from the mineralised areas. However, malachite is a common supergene mineral occurring in small quantities scattered over a few restricted areas in the pillow lavas and lavas in Polusagi and in the calc-schists and 'red' schists in Canakci. In the latter area, its occurrence follows the stratigraphic horizon containing the pyritic mineralisation. It is here that some azurite was also identified.

7.5 Some further considerations of the ore mineralisation.

Bethke and Barton (1971) carried out experimental studies on the distribution of Cd amd Mn between coexisting sphalerite and galena in the temperature range 600-800°C and of Se at 395-595°C. They state that the partitioning of these minor elements between sphalerite and galena is basically a function of temperature and can be used to estimate temperature of formation. Urabe(1977) applied this phenomenon with some success in certain Japanese epithermal Pb-Zn vein type deposits. Bezmen et al (1978) experimentally determined the Co distribution between coexisting pyrite and chalcopyrite at 300-500°C and used the distribution coefficients to estimate temperature of formation in some copper deposits in the U.S.S.R.

In both deposits under study, a considerable number of coexisting

sphalerite and galena were analysed for Mn, Cd and Se and coexisting pyrite and sphalerite for Co. Application of the techniques developed by the above cited works indicated unrealistically high temperature of formation for both deposits (800-1000°C). This is probably a result of the mobilisation of these minor elements in the considered sulphides during the metamorphism after the mineralisation.

Temperatures of the hydrothermal solutions in the upper parts of a submarine geothermal system are constrained by the boiling points which depend on pressure. When the total vapour pressure of a hydrothermal solution exceeds the total confining pressure plus the strength of the rocks boiling takes place which leads to explosion breccia associated with the subsequent mineralisation. Therefore, the hydrostatic pressure, hence the depth of water, largely controls the boiling of hydrothermal solutions and the experimental curves relating boiling points of saline solutions to pressure can be used to put constraints on the depth of the water column above the sites of mineralisation on the sea-floor (see: Ridge, 1973,74; Finlow-Bates and Large, 1978; Plimer, 1981). According to Ridge (1973), typical hydrothermal solutions (5-20%NaCl) with temperatures at 220-230°C cannot reach a sea-floor on which the depth of water is $<$ 180m without subsurface boiling taking place. For example, solutions with temperatures $\pm$300°C will reach the sea-floor in fluid state only if the depth of water is $>$ 915m. Finlow-Bates and Large (1978) indicate limits at $>$ 1000m and $>$ 1700m for solutions (5%NaCl) with temperatures 300°C and 330°C respectively to reach the sea-floor without boiling. They state that at shallow depths ($<$500m), typical solutions would boil before reaching the sea-floor and the least soluble species (chalcopyrite) would precipitate in the stockwork zone as a result of temperature decreases. In deep water settings the solutions upon reaching the sea-floor in fluid state would precipitate the least soluble

species (e.g. chalcopyrite) within the stratiform ore and not in the stockwork.

Neither of the two studied deposits show any evidence that boiling took place during the mineralisation. On the contrary the following points suggest that the hydrothermal solutions exhaled onto the sea-floor in fluid state :

a) The stockwork mineralisation is largely devoid of chalcopyrite and sphalerite which with pyrite are the dominant constituents of the massive banded ores.

b) There is no explosion breccia associated with the mineralisation and the fine mineralogical banding is well preserved both in the massive sulphides and the Fe-Mn-oxide rich cherty sediments.

Therefore the suggestion that the hydrothermal solutions at the Polusagi mineralisation reached the sea-floor in fluid state and probably at temperatures up to 400°C imply a water depth well above 1700m. Such an indicated sea-water depth above the sites of sulphide deposition at Polusagi is comparable with that estimated for sulphide deposits in Cyprus (2-3 km; Plimer, 1981). The recent data from the "black-smokers" of the East Pacific Rise also support great water depths above sites of sulphide mineral deposition on the sea-floor.

7.6 Summary of the model for sulphide formation

The mineralisations at both areas are considered to have originated from a similar process of sulphide formation, therefore, the following model is summarised for both deposits.

Following the submarine volcanic activity and the accumulation of extrusives on the Tethyan marginal basin floor, sea-water percolated through the volcanic pile along permeable zones such as fractures and faults. The magmatic heat initiated and set up a geothermal system within the marginal basin crust. The sea-water, now heated up to elevated

temperatures, interacted with the rocks leaching metals e.g. Cu, Fe, Zn and S from them. The solution at the lower parts of the geothermal system reached temperatures of up to 500°C. The discharge of the now hot, metal rich and probably acid hydrothermal solutions took place along distinct channels, such as pre-existing faults, which are now represented by the stockwork mineralisation. During their ascent, the temperature of the solutions decreased probably due to adiabatic expansion which resulted with some Cu followed by Zn sulphide deposition at the upper levels of the feeder zones. However, the drastic temperature drop accompanied by rises in the pH and oxygen fugacity took place upon mixing with the cold and oxidising sea-water at the sea-water-rock interface and on the sea-floor. This led to the supersaturation of sulphide species resulting with the precipitation of the massive ores. The uneven mixing with the sea-water provided a mechanism for fluctuations in temperature, pH and oxygen fugacity of the solutions which resulted with the banding in the massive sulphides. With further dilution the solutions, now cooler and largely devoid of metals like Zn and Cu and to a lesser extent Fe, became cool and oxidised, precipitating Fe-Mn-oxide rich siliceous sediment over and away from the massive sulphides.

REFERENCES

ALABASTER, T., PEARCE, J.A., MALLICK, D.I.J. and ELBOUSHI, I.M. (1980). The volcanic stratigraphy and location of massive sulphide deposits in the Oman ophiolite. In: A.Panayiotou (Ed.), Ophiolites: proceedings of international ophiolite symposium, Cyprus. Minist. Agric. Nat.Resour. Geol. Surv. Dep., Nicosia, Cyprus, pp.751-757.

AMSTUTZ, G.C. (1967). Spilites and spilitic rocks. In: H.H.Hess and A.Poldervaart(Eds.), Basalts, V.2, Interscience, New York, pp.737-754.

AMSTUTZ, G.C. (1974). Introduction. In: G.C.Amstutz (Ed.), Spilites and spilitic rocks, Springer-Verlag, Heidelberg, pp.1-4.

ANGER, G. (1971). Microfabrics in geosynclinal sulphide deposits. Clauhusthaler Hefte Zur Lagerstã Henkunde Und Geochernie Der Mineralischen Rohstoffe, Heft 10.

ARCULUS, R. J.(1973). The alkali-basalt, andesite association of Grenada, Lesser Antilles. Unpub. Ph.D. thesis, Univ. of Durham.

ATAMAN, G., BÜKET, E. and ÇAPAN, U.Z. (1975). The North Anatolian fault zone: new interpretation as a paleo-Benioff zone. M.T.A. Bull. 84, Ankara, pp.112-118.

BAILEY, E.B., CLOUGH, C.T., WRIGHT, W.B., RICHEY, J.E. and WILSON, G.V.(1924). Tertiary and post-tertiary geology of Mull, Loch Aline and Oban. Mem.Geol. Survey Scot., 445p.

BAKER, P.E. (1968). Comparative volcanology and petrology of the Atlantic island-arcs. Bull. Volcanol., 32, pp.189-209

BAKER, P.E. (1978). The South Sandwich Islands - II: Petrology and geochemistry. Brit. Antarct. Surv. Sci. Report, 93.

BARAGAR, W.R.A., PLANT, A.G., PRINGLE, G.J. and SCHAU, M. (1977). Petrology and alteration of selected units of Mid-Atlantic Ridge basalts sampled from sites 332 and 335 DSDP. Can. J. Earth Sci., 14, pp.837-874.

BARRON, B.J. (1976). Recognition of the original volcanic suite in altered mafic volcanic rocks at Sofala, New South Wales. Am. J. Sci., 276, pp.604-636.

BARTON, P.B. and TOULMIN, P. (1966). Phase relations involving sphalerite in the Fe-Zn-S system. Econ. Geol., 61, pp.815-849.

BATTEY, M.H. (1974). Spilites as weakly metamorphosed tholeiites. In: G.C.Amstutz (Ed.), Spilites and spilitic rocks. Springer-Verlag, Heidelberg.

BAYKAL, F. and ERENTÖZ, C. (1966). Explanatory text of the geological map of Turkey; Sivas sheet, 1:500000 scale. M.T.A.Institute publications, Ankara.

BAYLISS, P. (1977).
Crystal structure refinement of weakly anisotropic pyrite. Am.Miner., 62, pp.1168-1172.

BECCALUVA, L., OHNENSTETTER, D., OHNENSTETTER, M., and VENTURELLI, G.(1977).
The trace element geochemistry of Corsican ophiolites. Contrib. Mineral. Petrol., 64, pp.11-31.

BECCALUVA, L., OHNENSTETTER, D. and OHNENSTETTER, M. (1979).
Geochemical discrimination between ocean - floor and island - arc tholeiites ⟹ applications to some ophiolites. Can. J. Earth Sci., 16, pp.1874-1882.

BECCALUVA, L., PICCARDO, G.B. and SERRI, G. (1980).
Petrology of northern Apennine ophiolites and comparison with other Tethyan ophiolites. In : A.Panayiotou (Ed.), Ophiolites ; proceedings of international ophiolite symposium, Cyprus. Minist. Agric. Nat. Resour. Geol. Surv. Dep., Nicosia, Cyprus.pp.314-332.

BEDDOE - STEPHENS, B. (1977).
The petrology and geochemistry of the Rossland volcanic rocks, Southern British Columbia. Unpub. Ph.D. thesis, Univ. of Durham.

BETHKE, P.M. and BARTON, P.B. (1971).
Distribution of some minor elements between co-existing sulphide minerals. Econ. Geol., 66, pp.140-163.

BEZMEN, N.I., YEREMIN, N.I., NARAZAULI, I.G., POZDNYAKOVA, N.V. and SERGEYEVA, N.Ye. (1978).
Cobalt distribution and the pyrite-chalcopyrite geothermometer. Geochem. Inter., 15, no=2, pp. 44-48.

BICKLE, M.J. and NISBET, E. (1972).
The oceanic affinities of some alpine mafic rocks based on their Ti - Zr - Y contents. J . Geol. Soc., 128, pp. 267-271.

BINNS, R.A. (1965).
The mineralogy of metamorphosed basic rocks from Willyama Complex, Broken Hill District, New South Wales. Part I : Hornblendes. Min. Mag., 35, pp.306-326.

BISCHOFF, J.L. (1980).
Geothermal system at 21°N, East Pacific Rise : physical limits on geothermal fluid and role of adiabatic expansion. Science, 207, pp.1465-1469.

BISCHOFF, J.L. and DICKSON, F.W. (1975).
Sea-water basalt interaction at 200°C and 500 bars : Implications for origin of sea-floor heavy-metal deposits and regulation of seawater chemistry. Earth Planet. Sci. Lett., 25, pp.385-397.

BISCHOFF, J.L. and SEYFRIED, W.E. (1978).
Hydrothermal chemistry of seawater from 25°C to 350°C. Amer.J. Sci., 278, pp.838-860.

BOETTCHER, A.L. (1973).
Volcanism and orogenic belts - the origin of andesites, Tectonophysics, 17, pp.223-240

BOWEN, N.L. (1928).
The evolution of the igneous rocks. Princeton Univ. Press, Princeton, N.J., 334p.

BRALIA, A., SABATINI, G. and TROJA, F. (1979).
A revaluation of the Co/Ni ratio in pyrite as geochemical tool in ore genesis problems : Evidences from Southern Tuscany pyrite deposits. Mineral. Deposita, 14, pp.353-374.

BRINKMAN, R. (1972).
Mesozoic troughs and crustal structure in Anatolia. Geol. Soc. Am. Bull., 83, pp.819-826.

BROWN, E.H. (1967).
The greenschist facies in part of Eastern Otago, New Zealand. Contr. Mineral. Petrol., 14, pp.259-292.

BROWN, E.H. (1977).
The crossite content of Ca-amphiboles as a guide to pressure of metamorphism. J.Petr., 18, pp.53-72.

BROWN, G.M. (1968).
Mineralogy of basaltic rocks. In : H.H. Hess and A. Poldervaart, (Eds.), Basalts, V.2, Interscience, New York, pp.103-161.

BROWN, G.M., HOLLAND, J.G., SIGURDSSON, H., TOMBLIN, J.F. and ARCULUS, R.J. (1977).
Geochemistry of the Lesser Antilles volcanic Island arc. Geochim. Cosmochim. Acta, 41, pp.785-801.

BÜYÜKYANBOLU, N. (1969).
Malatya - Pütürge Ar. 3105 ve 42/153nolu bakır sahaları aramaları değerlendirme raporu. (In Turkish). Unpub. report to Etibank, Ankara.

ÇAĞATAY, A. (1977).
Guneydagu Anadolu bakır yatak ve zuhurlarının jeolojik-mineralojik etüdü sonunda elde edilen jenetik bulgular. Maden Tetkik ve Arama Enstitüsü Dergisi. (M.T.A. Bull.). No=84. ANK. pp.46-69.

ÇAĞATAY, A. (1979).
Maden mikroskopisi. TMMOB Jeoloji Mühendisleri Odası Yayınları : 2. ANK. 72 p.

ÇALGIN, R. (1976).
Siirt-Madenköy bakır yatağının jeolojisi ve mineralizasyonu hakkında ara rapor. Unpub. report to M.T.A. ANK.

CAMERON, W.E., NISBET, E.G. and DIETRICH, V.J. (1980).
Petrographic dissimilarities between ophiolitic and ocean-floor basalts. In: A. Panayiotou, (Ed.), Ophiolites : proceedings of international ophiolite symposium, Cyprus. Minist. Agric. Nat. resour. Geol. Surv. Dep., Nicosia, Cyprus. pp.182-192.

CANN, J.R. (1969).
Spilites from the Carlsberg Ridge, Indian Ocean. J.Petrol., 10, part 1, pp.1-19.

CANN, J.R. (1970).
Rb, Sr, Y, Zr and Nb in some ocean-floor basaltic rocks. Earth Planet, Sci. Lett., 10, pp.7-11.

CANN, J.R. (1971).
Major element variations in ocean-floor basalts. Phil. Trans. Soc. Land., A 268, pp.495-505.

CARMICHAEL, I.S.E., TURNER, F.J. and VERHOOGEN, J. (1974).
Igneous Petrology McGraw Hill, New York, 739p.

CHARLAT, M. and LEVY, C. (1974).
Substitutions multiples dans la serie tennantite-tetraedrite . En: G.Sabatier (Ed.), les solutions solides en mineralogie. Colloque International No=234, Bull. Soc. Franc. Min. Crist., 97 pp.241-250.

CHAYES, F. (1966).
Alkaline and sub-alkaline basalts. Amer. J. Sci., 264, pp.128-145.

CHEN, T.T. (1978).
Colloform and framboidal pyrite from the Caribou deposit, New Brunswick. Can. Min., 16, pp.9-15.

CHRISTODOULOU, C. (1980).
The geochemistry of podiform chromite deposits from two ophiolite complexes, Chalkidiki Peninsula, Northern Greece. Unpub. M.Sc. thesis, Univ. of Durham.

CHURCH, W.R. and COISH, R.A. (1976).
Oceanic versus island arc origin of ophiolites. Earth Planet. Sci. Lett., 31, pp.8-14.

CHURCH, W.R. and RICCIO, L. (1977).
Fractionation trends in the Bay of Islands ophiolite of Newfoundland : polycyclic cumulate sequences in ophiolites and their classification. Can. J. Earth Sci., 14, pp.1156-1165.

COATS, R.R. (1968).
Basaltic andesites. In : H.H. Hess and A. Poldervaart (Eds.), Basalts, V.2, Interscience ,New York, pp.689-736.

COISH, R.A. (1977).
Ocean floor metamorphism in the Betts Cove Ophiolites, Newfoundland. Contr. Mineral. Petrol., 60, pp.255-270.

COLEMAN, R.G. (1977).
Ophiolites - Ancient oceanic lithosphere? Minerals and Rocks, No=12,Springer-Verlag,Heidelberg, 229p.

COLEMAN, R.G. and PETERMAN, Z.E. (1975).
Oceanic plagiogranite. J.Geophys. Res., 80, pp.1099-1108.

CONSTANTINOU, G. (1975).
Idaite from the Skouriotissa massive sulphide orebody, Cyprus: Its composition and conditions of formation. Am. Min. 60, pp.1013-1018.

COOMBS, D.S.(1961).
The nature and alteration of some Triassic sediments from Southland, New Zealand. Trans. R. Soc. N.Z., 82, pp.65-109.

COOMBS, D.S. (1963).
Trends and affinities of basaltic magmas and pyroxenes as illustrated on the diopside-olivine-silica diagram. Min. Soc. Am., Special paper 1, Int. Min. Assoc., Papers, Third Gen. Meeting, pp.227-250.

COOMBS, D.S. (1974).
On the mineral facies of spilitic rocks and their genesis. In : G.C. Amstutz (Ed.), Spilites and spilitic rocks. Springer-Verlag, Heidelberg, pp.373-386.

COOMBS, D.S., ELLIS, A.J., FYFE, W.S. and TAYLER, A.M. (1959).
The zeolite facies, with comments on the interpretation of hydrothermal synthesis. Feochim. Cosmochim. Acta, 17, pp.53-107.

COOMBS, D.S., HERODYSKI, R.J. and NAYLOR, R.S. (1970).
Occurrence of prehnite-pumpellyite facies metamorphism in northern Maine. Am. J. Sci., 268, pp.142-156.

COOMBS, D.S., NAKAMURA, Y. and VAUGNAT., M. (1976).
Pumpellyite-actinolite facies schists of the Taveyanne formation near Loeche, Valais, Switzerland. J. Petrol., 17, pp.440-471.

COOPER, A.F. and LOVERING, J.F (1970).
Greenschist amphiboles from Haast River, New Zealand. Contr. Mineral. Petrol., 27, pp.11-24.

CORLISS, J.B., DYMOND, J., GORDON, L.I., EDMOND, J.M., van HERZEN, R.P., BALLARD, R.D., GREEN, K., WILLIAMS, D., BAINBRIDGE, A., CRANE, K. and van ANDEL, T.H. (1979).
Submarine thermal springs on the Galapagos Rift. Science, 203, No.4385, pp.1073-1082.

COX, K.G., BELL, J.D. and PANKHURST, R.J. (1979).
The Interpretation of Igneous Rocks. George Allen and Unwin, London, 450p.

DAVIES, H.L. (1971).
Peridotite-gabbro-basalt complex in eastern Papua : an over thrust plate of oceanic mantle and crust. Australian Bur. Min. Resor. Bull., 128, 48p.

DEER, W.A., HOWIE, R.A. and ZUSSMAN, J. (1962).
Rock forming minerals, Longman, London.

DEER, W.A., HOWIE, R.A., and ZUSSMAN, J. (1974).
An introduction to the rock forming minerals - Longman, London.

DEWEY, J.F. (1974).
Continental margins and ophiolite obduction : Appalachian Caledonian system. In : C.A. Burk, C.L. Drake (Eds.), New York : Springer, pp.933-950.

DEWEY, J.F. (1976).
Ancient plate margins - some observations. Tectonophysics, 33, No=314, pp.379-385.

DEWEY, J.F. and BIRD, J.M. (1970).
Mountain belts and the new global tectonics. J.Geophys. Res., 75, pp.2625-2647.

DEWEY, J.F. and BIRD, J.M. (1971).
Origin and emplacement of the ophiolitic suite Appalachian ophiolites in Newfoundland. J. Geophys. Res., 76, pp.3179-3206.

DICK, H. (1977).
Partial melting in the Josephine peridotite, the affect on mineral composition and its consequence for geobarometry and geothermometry. Amer. J. Sci., 277, pp.801-832.

DICKINSON, W.R. (1968).
Circum - Pacific andesite types. J. Geophys. Res., 73 pp.2261-2269.

DICKINSON, W.R. and HATHERTON, T. (1967).
Andesitic volcanism and seismicity around the Pacific. Science, 157, pp.801-803.

DIXON, C.J. and PEREIRA, J. (1974).
Plate tectonics and mineralisation in the Tethyan region. Mineral. Deposita, 9, pp.185-198.

DOLANSKI, J. (1974).
Sulvanite from Thorpe Hills, Utah. Am. Min., 59, pp.307-313.

EDMOND, J.M. (1981).
Hydrothermal activity at mid-ocean ridge axes. Nature, 290, pp.87-88

EĞIN, D., HIRST, D.M. and PHILLIPS, R., (1979).
The petrology and geochemistry of volcanic rocks from the northern Harşit River area, Pontid volcanic province, northeast Turkey. J.Volcanol., Geotherm. Res., 6, pp.105-123.

ELDER, J.W. (1965).
Physical processes in geothermal areas. Monogr. Ser. Amer. Geophys. Union, 8, pp.211-239.

ELDER, J.W. (1967).
Steady free convection in a porous medium heated from below. J. Fluid Mech., 27, pp.29-48.

ELDER, J.W. (1977).
Model of hydrothermal ore genesis. Geol. Soc. Lond. Spec. Pub., 2, pp.4-13.

ELTHON, D. and STERN, C. (1978).
Metamorphic petrology of the Sarmiento ophiolite complex, Chile. Geology, 6, pp.464-468.

ENGEL, A.E.J., ENGEL, C.G. and HAVENS, R.G.(1965).
Chemical characteristics of oceanic basalts and the upper mantle. Bull. Geol. Soc. Am., 76, pp.719-734.

ENGEL, C.F. and FISHER, R.L. (1975).
Granitic to ultramafic rock complexes of the Indian Ocean ridge system, western Indian Ocean. Geol. Soc. Am. Bull., 86, pp.1553-1578

ERLANK, A.J. and KABLE, E.J.D. (1976).
The significance of incompatible elements in Mid-Atlantic Ridge basalts from 45° N with particular reference to Zr/Nb. Contrib. Mineral. Petrol., 54, pp.281-291.

EWART, A. and BRYAN, W.B. (1972).
Petrology and geochemistry of the igneous rocks from Eua, Tongan Islands. Geol. Soc. Am. Bull., 83, pp.3281-3298.

FARRAND, M. (1970).
Framboidal sulphides precipitated synthetically. Mineral. Deposita, 5, pp.237-247.

FENNER, C.N. (1929).
The crstallisation of basalts. Am. J. Sci., 5th ser., 18, pp. 225-253.

FINLOW - BATES, T. and LARGE, D.E. (1978).
Water depth as a major control on the formation of submarine exhalative ore deposits. Geol. Jahrb., Reihe D, No.=30,pp.27-39.

FINLOW - BATES, T. and STUMPFL, E.F. (1981).
The behaviour of so-called immobile elements in hydrothermally altered rocks associated with volcanogenic submarine - exhalative ore deposits. Mineral. Deposita, 16 pp.319-328.

FISHER, R.L., ENGEL, C.G. and HILDE, T.W.C.(1968).
Basalts dredged from the Amirante Ridge, western Indian Ocean. Deep-Sea Res., 15, pp.521-534.

FITTON, J.G. (1971).
The generation of magmas in island arcs. Earth and Planet. Sci. Lett., 11,pp.63-67.

FLEET, E.M. and BARNETT, R.L. (1978).
Al^{iv}/Al^{vi} partitioning in calciferous amphiboles from the Frood mine, Sudbury, Ontario. Can. Min.,16, pp.527-532.

FLEISCHER, M. (1955).
Minor elements in some sulphide minerals. Econ. Geol., 50th Ann. Vol., pp.970-1024.

FLOYD, P.A. (1976).
Geochemical variation in the greenstones of S.W. England. J.Petr., 17, pp.552-545.

FLOYD, P.A. and WINCHESTER, J.A. (1975).
Magma type and tectonic setting discrimination using immobile elements. Earth Planet. Sci. Lett., 27, pp.211-218.

FLOYD, P.A. and WINCHESTER, J.A. (1978).
Identification and discrimination of altered and metamorphosed volcanic rocks using immobile elements. Chem. Geol., 21, pp.291-306.

FODOR, R.V., KEIL, K. and BUNCH, T.E. (1975).
Contribution to the mineral chemistry of Hawaiian rocks. IV. Pyroxenes in rocks from Haleakola and West Mauai volcanoes, Mauai, Hawaii. Contr. Mineral. Petrol., 50, pp.173-195.

FRANCHETEAU, J., NEEDHAM, H.D. and CHOUKROUNE, P. (1979).
Massive deep-sea sulphide ore deposits discovered on the East Pacific Rise. Nature, 277, No= 5697, pp.523-528.

FRENZEL, G. (1959).
Idait und "blaubleibender Covellin". Neues Jahrb. Mineral. Abh., 93, pp.97-132.

FRENZEL, G. and OTTEMANN, J. (1967).
Eine Sulfidparagenese mit Kupferhaltigen Zonarpyrit von Nukundam/ Fiji. Mineral. Deposita, 1, pp.307-316.

GALE, N.H., SPOONER, E.T.C. and POTTS, P.J. (1981).
The lead and strontium isotope geochemistry of metalliferous sediments associated with Upper Cretaceous ophiolite rocks in Cyprus, Syria and the Sultanate of Oman. Can. Earth Sci., 18, pp.1290-1302.

GANNSER, A. (1974).
The ophiolite melange, as a world-wide problem on Tethyan examples. Eclogae. Geol. Helv., 67/3, pp.479-507.

GASS, I.G. (1980).
The Troodos massif : its role in the unravelling of the ophiolite problem and its signficance in the understanding of constructive plate margin processes. In : A. Panayiotou (Ed.), Ophiolites : proceedings of international ophiolite symposium, Cyprus. Minist. Agric. Nat. Resour. Geol. Surv. Dept., Nicosia, Cyprus. pp.23-35.

GASS, I.G. and SMEWING, J.D. (1973).
Intrusion, extrusion and metamorphism at constructive margins : Evidence from the Troodos Massif, Cyprus. Nature, 242, pp.26-29.

GASS, I.G., NEARY, C.R., PLANT, J., ROBERTSON, A.H.F., SIMONIAN, K.O., SMEWING, J.D., SPOONER, E.T.C. and WILSON, R.A.M. (1975).
Comments on "The Troodos ophiolitic complex was probably formed in an island arc, "by A.Miyashiro and subsequent correspondence by A.Hynes and A. Miyashiro. Earth and Planet. Sci. Lett., 25, pp.236-238.

GAST, P.W. (1968).
Trace element fractionation and the origin of tholeiitic and alkaline magma types. Geochim. Cosmochim. Acta, 32, pp.1057-1086.

GILL, J.B. (1970).
Geochemistry of Viti Levu, Fiji, and its evolution as an island arc. Contr. Mineral. Petrol., 27, pp.179-203.

GILL, J.E. (1969).
Experimental deformation and annealing of sulphides and interpretation of ore textures. Econ. Geol., 64, pp.500-508.

GLASSLEY, W. (1974).
A model for phase equilibria in the prehnite-pumpellyite facies. Contr. Mineral. Petrol., 43, pp.317-332.

GLASSLEY, W. (1975).
Low variance phase relationships in a prehnite-pumpellyite facies terrain. Lithos, 8, pp.69-76.

GORSHKOV, G.S. (1969).
Geophysics and petrochemistry of andesite volcanism of the circum-Pacific belt. Oregon Dept. Geol. and Mineral Industries Bull., 65, p.91.

GREEN, D.H. and RINGWOOD, A.E. (1967).
The stability fields of aluminous pyroxene peridotite and garnet peridotite and their relevance in upper mantle structure. Earth Planet. Sci. Lett, 3, pp.151-160.

GREEN, D.H. and RINGWOOD, A.E. (1968).
Genesis of the calc-alkaline igneous rocks suite. Contr. Mineral., Petrol., 18, pp.105-162.

GREENBAUM, D. (1977).
The chromitferous rocks of the Troodos ophiolite complex. Econ. Geol., 72, pp.1176-1194.

GRIFFITTS, W.R., ALBERS, J.P. and ONER, O. (1972).
Massive sulfide copper deposits of the Ergani - Maden area, south eastern Turkey. Econ. Geol., 67, pp.701-716.

HART, S.R. (1969).
K, Rb, Cs contents and K/Rb, C/Cs ratios of fresh and altered submarine basalts. Earth Planet. Sci. Lett., 6, pp.295-303.

HART, S.R., ERLANK, A.J. and KABLE, E.J.D. (1974).
Sea floor basalt alteration : Some chemical and Sr isotopic effects. Contr. Mineral. Petrol., 44, pp.219-230.

HART, S.R., GLASSLEY, W.E. and KARIG, D.E. (1972).
Basalts and sea floor spreading behind the Mariana Island Arc. Earth Planet. Sci. Lett., 15, pp.12-18.

HATHERTON, T. and DICKINSON, W.R. (1968).
Andesitic volcanism and seismicity in New Zealand. J.Geophys. Res., 73, pp.4615-4619.

HATHERTON, T. and DICKINSON, W.R. (1969).
The relationship between andesitic volcanism and seismicity in Indonesia, the Lesser Antilles and other island arcs. J. Geophys. Res., 74 pp. 5301-5310.

HATCH, F.H., WELLS, A.K. and WELLS, M.K. (1972).
Petrology of the Igneous Rocks. Thomas Murby and Co., London, 551p.

HAWKESWORTH, C.J. and POWELL, M. (1980).
Magma genesis in the Lesser Antilles island arc. Earth Planet Sci. Lett., 51, pp.297-308.

HAWKINS, J.W. (1976).
Petrology and geochemistry of basaltic rocks of the Lau Basin. Earth Planet. Sci. Lett., 28, pp. 283-297.

HAWKINS, J.W. (1980).
Petrology of back-arc basins and island-arcs : their possible role in the origin of ophiolites. In : A Panayioutou (Ed.), Ophiolites : proceedings of international ophiolite symposium, Cyprus. Ministr. Agric. Nat. Resour. Geol. Surv. Dept., Nicosia, Cyprus. pp.244-254.

HAWLEY, J.E. and NICHOL, I. (1961).
Trace elements in pyrite, pyrrhotite and chalcopyrite of different ores. Econ. Geol., 56, pp.467-487.

HEKINIAN, R., FEVRIER, M., BISCHOFF, J.L., PICOT, P. and SHANKS, W.C. (1980), Sulfide deposits from the East Pacific Rise near 21°N. Science, 207, pp.1433-1444.

HEY, M.H. (1954).
A new review of the chlorites. Min. Mag, 30, pp.277-292.

HIETANEN, A. (1974).
Amphibole pairs, epidote minerals, chlorite and plagioclase in metamorphic rocks, Northern Sierra Nevada, California. Am. Min., 59, pp.22-40.

HILL, R.E.T. and BOETTCHER, A.L. (1970).
Water in the Earth's mantle : melting curves of basalt - water and basalt-water-carbon dioxide. Science, 167, pp.980-981.

HOLLAND, H.D., and MALININ, S.D. (1979).
The solubility and occurrence of non-ore minerals. In: H.L.Barnes (Ed.), Geochemistry of Hydrothermal Ore Deposits, Wiley Interscience, 2nd. Edn., pp.461-508.

HUGHES, C.J. (1972).
Spilites, Keratophyres and the igneous spectrum. Geol. Mag., 109, pp.513-527.

HUGHES, C.J. (1973).
Late pre-cambrian volcanic rocks of Avalon Newfoundland - a spilite - keratophyre province : recognition and implications. Can. J. Earth Sci., 10, pp.272-282.

HUMPHRIS, S.E., and THOMPSON, G. (1978a).
Hydrothermal alteration of oceanic basalts by sea-water. Geochim. Cosmochim. Acta, 42, pp.107-125.

HUMPHRIS, S.E., and THOMPSON, G. (1978b).
Trace element mobility during hydrothermal alteration of oceanic basalts. Geochim. Cosmochim. Acta, 42, pp.127-136.

HYNES, A. (1975).
Comment on "The Troodos ophiolitic complex was probably formed as an island arc, "by A.Miyashiro. Earth Planet. Sci. Lett., 25, pp.213-216.

İLERİ, S., SALANCI, B., BİTEM, M. and DOĞAN, R. (1976).
Ergani (maden) copper deposits and plate tectonics. Bull. Geol. Soc. Turkey, 19, pp.133-142.

ILHAN, E. (1971).
The structural features of Turkey. In: A.S.Campbell (Ed), Geology and History of Turkey. Petr. Expl. Soc. Libya, 1971, pp.159-170.

IRVINE, T.N. (1967).
Chromian-spinel as a petrogenetic indicator. Part II : Petrologic applications. Can.J.Earth Sci., 4, pp.71-103.

IRVINE, T.N. and BARAGAR, W.R.A. (1971).
A guide to the chemical classification of the common volcanic rocks. Can. J. Earth Sci., 8, pp.523-548.

IRVINE, T.N. and FINDLAY, T.C. (1972).
Alpine-type peridotite with particular reference to the Bay of Islands complex. Pub. Earth Physics Branch Dept. Energy, Mines res. Can., 42, pp.97-128.

JAKES, P. and GILL, J. (1970).
Rare earth elements and the island arc tholeiitic series. Earth Planet. Sci. Lett., 9, pp.17-28.

JAKES, P. and WHITE, A.J.R. (1972).
Major and trace element abundances in volcanic rocks of orogenic areas. Geol. Soc. Am. Bull., 83, pp.29-40.

JENSEN, L.S. (1976).
A new cation plot for classifying subalkalic volcanic rocks. Ontario Dep. Mines., Misc. Paper 66, 22p.

JOLLY, W.T. (1970).
Zeolite and prehnite-pumpellyite facies in South Central Puerto Rico. Contr. Mineral. Petrol., 27, pp.204-224.

JOLLY, W.T. (1980).
Development and degradation of Archaean lavas, Abitibi Area, Canada, in light of major element geochemistry. J.Petrol., 21, pp.323-363.

JOPLIN, G.A. (1965).
The problem of the potash-rich basaltic rocks. Mineral. Mag., 34, pp.266-275.

JOPLIN, G.A. (1968).
The shoshonite association : a review. J. Geol. Soc. Aust., 15, pp.275-294.

KARIG, D.E. (1971).
Origin and development of marginal basins in the Western Pacific. J. Geophys. Res., 76, pp.2542-2561.

KARSLIOĞLU, Y. (1976).
Unpublished geological map : Scale 1: 25000. Malatya L.41 - b4 paftasının jeolojisi ve Çanakcı Köyü bakır zuhurları. M.T.A. archive No=32612, Ankara.

KATO, A. (1969).
Stannoidite, $Cu_5(Fe, Zn)_2 Sn S_8$, a new stannite-like mineral from the Konjo Mine, Okayama Prefacture, Japan. Nat. Sci. Museum Bull., 12, pp.165-172.

KAWACHI, Y. (1975).
Pumpellyite - actinolite and contiguous facies metamorphism in part of upper Wakatipu district, South Island, New Zealand. N.Z. Jl. Geol. Geophys., 18, pp.401-441.

KAY, R.W. and SENECHAL, R.G. (1976).
The rare earth geochemistry of the Troodos ophiolite complex. J. Geophys. Res., 81, No=5, pp.964-970.

KENNEDY, W.Q. (1933).
Trends of differentiation in basaltic magmas. Am. J. Sci., 5th ser., 25, pp.239-256.

KETIN, I. (1966).
Tectonic units of Anatolia. Bull. Min. Res. Exp. Inst. of Turkey, No=66, pp.23-33.

KISSIN, S.A. and OWENS, D.R. (1979).
New data on stannite and related tin sulphide minerals. Can. Min., 17, pp.125-135.

KRAUSE, H. (1965).
Contributions to the mineralogy of Norway, No=33, Idaite, $Cu_5 Fe S_6$, from Konnerud near Drammen. Norsk Geol. Tidsskr., 45, pp.417-421.

KRAUSKOPF, K.B. (1979).
Introduction to Geochemistry. McGraw-Hill, 2nd. Edn, 617p.

KRIBEK, B. (1975).
The origin of framboidal pyrite as a surface effect of sulfur grains. Mineral. Deposita, 10, pp.389-396.

KRIVTSOV, A.I. (1974).
Metamorphism of pyritic deposits of the Southern Urals. Acad. Sci. USSR, Dokl., Earth Sci. Sect., 215, No=1-6, pp.132-134.

KUNIYOSHI, S. and LIOU, J.G. (1976).
Contact metamorphism of the Kermutsen Volcanics, Vancouver Island, British Columbia. J. Petrol., 17, pp.73-99.

KUNO, H. (1950).
Petrology of Hakone Volcano and the adjacent areas, Japan. Bull. Geol. Soc. Am., 61, pp.957-1020.

KUNO, H. (1959).
Origin of Cenozoic petrographic provinces of Japan and surrounding areas. Bull. Vokanologique ser.II, 20, pp.37-76.

KUNO, H. (1960).
High alumina basalt. J. Petrol., 1, pp.121-145.

KUNO, H. (1965).
Fractionation trends of basalt magmas in lava flows. J.Petrol., 6, pp.302-321.

KUNO, H. (1966).
Lateral variation of basalt magma across continental margins and island arcs. Bull. Volcanol., 29, pp.195-222.

KUNO, H. (1968).
Differention of basaltic magmas. In: H.H. Hess and A.Poldervaart (Eds.), Basalts, V2, Interscience, New York, pp.623-688.

KUSHIRO, I. (1960).
Si-Al relations in clinopyroxenes from igneous rocks. Am. J. Sci., 258, pp. 548-554.

KUSHIRO, I. (1972).
Effect of water on the composition of magmas formed at high pressures. J. Petrol., 13, pp.311-334.

KUSHIRO, I. (1979).
Fractional crystallisation of basaltic magma. In : H.S. Yoder Jnr. (Ed.), The evolution of the igneous rocks, 50th ann. perspectives, Princeton Univ. Press, N.J., pp.171-204.

KUSHIRO, I. and YODER, H.S. (1969).
Melting of forsterite and enstatite at high pressures under hydrous conditions. Carnegie Inst. Washington Yearbook, 67, pp.153-158.

LAMBERT, I.B. and BUBELA, B. (1970).
Banded sulphide ores : the experimental production of monomineralic sulphide bands in sediments. Mineral. deposita, 5, pp.97-102.

LARGE, R.R. (1977).
Chemical evolution and zonation of massive sulfide deposits in volcanic terrains. Econ. Geol., 72, pp.549-572.

LAURENT, R., DELALOYE, M., VAUGNAT, M. and WAGNER, J.J. (1980).
Composition of parental basaltic magma in ophiolites. In : A.Panayioutou (Ed.), Ophiolites : proceedings of international ophiolite symposium, Cyprus. Minist.Agric. Nat. Resour. Geol. Surv. Dept., Nicosia, Cyprus. pp.172-181.

LAWRENCE, L.J. (1972).
The thermal metamorphism of a pyritic sulphide ore. Econ. Geol., 67, pp.487-496.

LEAKE, B.E., (1965).
The relationship between tetrahedral aluminium and the maximum possible octahedral aluminium in natural calciferous amphiboles. Am. Min., 50, pp.843-851.

LEAKE, B.E. (1971).
On aluminous and edenite hornblendes. Min. Mag., 38, pp.389-407.

LEAKE, B.E. (1978).
Nomenclature of Amphiboles. Can. Min., 16, pp.501-520.

LE BAS, M.J. (1962).
The role of aluminium in igneous clinopyroxenes with relation to their parentage. Am. J. Sci., 260, pp.267-288.

LEE, M.S., TAKENOUCHI, S. and IMAI, H. (1975).
Syntheses of stannoidite and mawsonite and their genesis in ore deposits. Econ. Geol., 70, pp.834-843.

LEVY, C. (1966).
Contribution à la minéralogi des sulfures de cuivre du type Cu_3XS_4.
Ph. D. thesis, Univ. of Paris. Bur. Rech. Géol. Minières Mém., 178p.

LIOU, J.G. (1971).
Synthesis and stability relations of prehnite. Am. Min., 56, pp.507-531.

LIOU, J.G. (1979).
Zeolite facies metamorphism of basaltic rocks from the East Taiwan ophiolite. Am. Min., 64, pp.1-14.

LIOU, J.G. and ERNST, W.G. (1979).
Oceanic ridge metamorphism of the East Taiwan ophiolite. Contr. Mineral. Petrol., 68, pp.335-348.

LIOU, J.G., KUNIYOSHI, S. and ITO, K. (1974).
Experimental studies of the phase relations between greenschist and amphibolite in a basaltic system. Am. J. Sci., 274, pp.613-632.

LISITSYANA, N.A. (1968).
Geochemistry of weathering zones of basic rocks. Geochim. Int., 5, pp.210-244.

LOFTUS-HILLS, G. and SOLOMON, M. (1967).
Co-Ni and Se in sulphides as indicators of ore genesis. Mineral. Deposita, 2,pp.228-242.

LOVE, L.G. and AMSTUTZ, G.C. (1966).
Review of microscopic pyrite from the Devonian Chattanooga shale and Rammelsberg Banderz. Fortschr. Min., 43, pp.273-309.

MACDONALD, G.A. (1968).
Composition and origin of Hawaiian lavas. Geol. Soc. Am. Mem., 116, pp.477-522.

MACDONALD, G.A. and KATSURA, T. (1964).
Chemical composition of Hawaiian lavas. J. Petr., 5, pp.82-133.

MACDONALD, K.C., BECKER, K., SPEISS, F.N. and BALLARD, R.D. (1980).
Hydrothermal heat flux of the "Black smoker" vents on the East Pacific Rise. Earth and Planet. Sci. Lett., 48, pp.1-7.

MALAKHOV, A.A. (1969).
Bismuth and antimony in galenas as indicators of some conditions of ore formation. Trans. from : Geokhimiya, No=11, pp.1283-1296.

MANSON, V. (1968).
Geochemistry of basaltic rocks : major elements. In : H.H. Hess and A.Poldervaart (Eds.), Basalts, V.2, Interscience, New York, pp.215-269.

MARKHAM, N.L. and LAWRENCE, L.J. (1965).
Mawsonite, a new copper-iron-tin sulfide from Mt.Lyell, Tasmania and Tingha, New South Wales. Am. Min., 50, pp.900-908.

MATSUDA, T. and UYEDA, S. (1971).
On the Pacific - type orogeny and its model - extension of the paired belts concept and possible origin of marginal seas. Tectonophys., 11, pp.5-27.

MATTHEWS, D.H. (1971).
III. Weathered and metamorphosed basalts. Altered basalts from Swallow Bank, abyssal hill in the N.E. Atlantic and from a nearby seamount. Phil. Trans. Roy. Soc. Lond., A.268, pp.551-571.

McDONALD, J.A. (1967).
Metamorphism and its effects on sulphide assemblages. Mineral. Deposita, 2, pp.200-220.

MELSON, W.G. and THOMPSON, G. (1971).
Petrology of a transform fault zone and adjacent ridge sediments. Roy. Soc. Lond. Phil. Trans., A.268, pp.423-441.

MEVEL, C. and VELDE, D. (1976).
Clinopyroxenes in mesozoic pillow lavas from the French Alps : Influence of cooling rate on compositional trends. Earth. Planet. Sci. Lett., 32, pp.158-164.

MIDDLEMOST, E.A.K. (1972).
A simple classification of volcanic rocks. Bull. Volcanol., 36 pp.382-397.

MIDDLEMOST, E.A.K. (1975).
The basalt class. Earth Sci. Rev., 11, pp.337-364.

MIDDLEMOST, E.A.K. (1980).
A contribution to the nomenclature and classification of volcanic rocks. Geol. Mag., 117, pp.51-57.

MITCHELL, A.H. and READING. H.G. (1971).
Evolution of island arcs. J. Geol., 79, pp.253-284.

MIYASHIRO, A. (1973).
The Troodos ophiolite complex was probably formed in an island arc. Earth Planet. Sci. Lett., 19, pp.218-224.

MIYASHIRO, A. (1974).
Volcanic rock series in island-arcs and active continental margins. Am. J. Sci., 274, pp.321-355.

MIYASHIRO, A. (1975a).
Origin of the Troodos and other ophiolites : A reply to Hynes. Earth Planet. Sci. Lett., 25, pp.217-222.

MIYASHIRO, A. (1975b).
Origin of the Troodos and other ophiolites : A reply to Moores. Earth Planet. Sci. Lett., 25, pp.227-235.

MIYASHIRO, A. (1975c).
Classification, characteristics and origin of ophiolites. J. Geol., 83, pp.249-281.

MIYASHIRO, A. (1978).
Metamorphism and metamorphic belts. London : Allen and Unwin, 492p.

MIYASHIRO, A. and SEKI, Y. (1958).
Enlargement of the compositional field of epidote and piemontite with rising temperature. Am J. Sci., 256, pp.423-430.

MIYASHIRO, A. and SHIDO, F. (1975).
Tholeiitic and calc-alkaline series in relation to the behaviours of titanium, vanadium, chromium and nickel. Am. J. Sci., 275, pp.265-277.

MIYASHIRO, A., SHIDO, F. and EWING, M. (1971).
Metamorphism in the mid-Atlantic Ridge near 24° and 30°N. Phil. Trans. Roy. Soc. Lond., A.268, pp.289-603.

MOORES, E.M. (1975).
Discussion of "Origin of Troodos and other ophiolites : a reply to Hynes," by A. Miyashiro. Earth Planet. Sci. Lett., 25, pp.223-226.

MOORES, E.M. and VINE, F.J. (1971).
The Troodos Massif, Cyprus and other ophiolites as oceanic crust : evolution and implications. Phil. Trans. Roy. Soc. Lond., A.268, pp.443-466.

MOTTL, M.J. and HOLLAND, H.D. (1978).
Chemical exchange during hydrothermal alteration of basalt by sea-water - I. Experimental results for major and minor components of sea-water. Geochim. Cosmochim. Acta., 42, pp.1103-1115.

MOTTL, M.J., HOLLAND, H.D. and CORR, R.F. (1979).
Chemical exchange during hydrothermal alteration of basalt by sea-water - II. Experimental results for Fe, Mn and Sulfur species. Geochim. Cosmochim. Acta, 43, pp.869-884.

MYSEN, B. (1975).
Partitioning of iron and magnesium between crystals and partial melts in peridotite upper mantle. Contr. Mineral. Petrol. 52, pp.69-76.

MYSEN, B.O. and BOETTCHER, A.L. (1975).
Melting of a hydrous mantle : II Geochemistry of crystals and liquids formed by anatexis of mantle peridotite at high pressures and high temperatures as a function of controlled activities of water, hydrogen and carbon dioxide. J. Petr., 16 part 3, pp.549-593.

NAREBSKI, W. (1974).
A statistical study of specific petrochemical features of some spilitic rock series. In : G.C. Amstutz (Ed.), Spilites and spilitic rocks, Springer - Verlag, Heidelberg, pp.127-160.

NICHOLLS, G.D. and ISLAM, M.R. (1971).
Geochemical investigations of basalts and associated rocks from the ocean floor and their implications. Phil. Trans. Roy. Soc., Lond., A.268, pp.469-486.

NICHOLLS, J.A. and LORENZ, V. (1973).
Origin and crystallisation history of Permian tholeiites from the Saar - Nake trough, S.W. Germany. Contr. Mineral. Petrol., 40 pp.327-344.

NICHOLLS, J.A. and RINGWOOD, A.E. (1973).
Effect of water on olivine stability in tholeiites and the production of silica - saturated magmas in the island arc environment. J. Geol, 81, pp.285-300.

NINKOVICH, K. and HAYS, J.D. (1972).
Mediterranean island arc and origin of high potash volcanoes. Earth Planet. Sci. Lett., 16, pp.331-345.

NISBET, E.G. and PEARCE, J.A. (1977).
Clinopyroxenes in mafic lavas from different tectonic settings. Contr. Mineral. Petrol., 63, pp.149-160.

NITSCH, K.H. (1971).
Stabilitatsbeziehungen von Prehnit und pumpellyithaltigen Pargenesen. Contr. Mineral. Petrol., 30, pp.240-260.

OFFLER, R., AGUIRRE, L., LEVI, B. and CHILD, S. (1980).
Burial metamorphism in rocks of the Western Andes of Peru. Lithos, 13, pp.31-42.

OFFLER, R., BAKER, C.K. and GAMBLE, J. (1981).
Pumpellyites in two low grade metamorphic terranes north of Newcastle, N.S.W., Australia. Contr. Mineral. Petrol., 76 pp.171-176.

O'HARA, M.J. (1968).
The bearing of phase equilibria studies in synthetic and natural systems on the origin and evolution of basic and ultrabasic rocks. Earth. Sci. Rev., 4, pp.69-133.

OSBORN, E.F. (1959).
Role of oxygen pressure on the crystallisation and differentiation of basaltic magma. Am. J. Sci., 257, pp.609-647.

OSBORN, E.F. (1962).
Reaction series for sub-alkaline igneous rocks based on different oxygen pressure conditions. Am. Min., 47, pp.211-216.

OSBORN, E.F. (1969).
The complementariness of orogenic andesite and alpine peridotite. Geochim. Cosmochim. Acta, 33, pp.307-324.

OSTWALD, J. and ENGLAND, B.M. (1977).
Notes on framboidal pyrite from Allandale, New South Wales, Australia. Mineral. Deposita, 12, pp.111-116.

OSTWALD, J. and ENGLAND, B.M. (1979).
The relationship between euhedral and framboidal pyrite in base - metal sulphide ores. Min. Mag., 43, pp.297-300.

OTTEMANN, J., and FRENZEL, G. (1971).
Neue Mikrosonden Untersuchungen an Idait, Covellin und blaubleibendem Covellin. Neues Jahrb. Min. Mh., pp.80-89.

OZCELIK, M. (1977).
Geology and genesis of copper mineralisation in Madenkoy area, Province of Siirt, S.E. Turkey. Unpub. B.Sc. thesis, Univ. of London : Royal School of Mines, Imperial College, of Science and Technology.

PASSAGLIA, E. and GOTTARDI, G. (1973).
Crystal chemistry and nomenclature of pumpellyites and julgoldites. Can. Min., 12, pp.219-223.

PEARCE, J.A. (1975).
Basalt geochemistry used to investigate past tectonic environments on Cyprus. Tectonophys., 25, pp.41-67.

PEARCE, J.A. (1976).
Statistical analysis of major element patterns in basalts. J.Petr. 17, pp.15-43.

PEARCE, J.A. (1980).
Geochemical evidence for the genesis and eruptive setting of lavas from Tethyan ophiolites. In : A. Panayiotou (Ed.), Ophiolites : proceedings of international ophiolite symposium, Cyprus. Minist. Agric. Nat. Resour. Geol. Surv. Dep., Nicosia, Cyprus. pp.261-272.

PEARCE, J.A. and CANN, J.R. (1971).
Ophiolite origin investigated by discriminant analysis using Ti, Zr and Y. Earth Planet. Sci. Lett., 12, pp.339-349.

PEARCE, J.A. and CANN, J.R. (1973).
Tectonic setting of basic volcanic rocks determined using trace element analysis. Earth Planet. Sci. Lett., 19, pp.290-300.

PEARCE, J.A. and GALE, G.H. (1977).
Identification of ore-deposition environment from trace - element geochemistry of associated igneous host rocks. Geol. Soc. Lond. Spec. Pub., 7, pp.14-24.

PEARCE, J.A. and NORRY, M.J. (1979).
Petrogenetic implications of Ti, Zr, Y and Nb variations in volcanic rocks. Cont. Mineral. Petrol., 69, pp.33-47.

PINCENT, R.H. (1974).
The emplacement and metamorphism of the Blue River ultramafic body, Cassiar District, British Columbia, Canada. Unpub. Ph.D. thesis, Univ. of Durham.

PLIMER, I.R. (1981).
Water depth - a critical factor for exhalative ore deposits. BMR Jl. Aust. Geol. Geophys, 6, No=4, pp.293-300.

PRICE, B.G. (1972).
Minor elements in pyrites from the Smithers Map area, B.C. and exploration applications of minor element studies. Unpub. thesis, Univ. of British Columbia, 270.p.

PRINZ, M. (1968).
Geochemistry of basaltic rocks :trace elements. In : H.H. Hess and A.Poldervaart (Eds.), Basalts, V.1, Interscience, New York, pp. 271 - 323.

RAASE, P. (1974).
Al, Ti content of hornblende, indicators of pressure and temperature of regional metamorphism. Contr. Mineral. Petrol., 45, pp.231-236.

RAITH, M., HORMANN, P.K. and ABRAHAM, K. (1977).
Petrology and metamorphic evolution of the Penninic ophiolites in the Western Tauern window (Austria). Schweiz. Mineral. Petrogr. Mitt., 57, pp.187-232.

RAMDOHR, P. (1944).
Zum zinnkies problem. Abh. Preuss. Akad. Wiss., Math. -nat. Kl.4., pp.1-30.

RAMDOHR, P. (1960).
Die Erzmineralien und ihre Verwachsungen (3rd edition). Akademie-Verlag, Berlin.

RAMDOHR, P. (1980).
The ore minerals and their intergrowths. Pergamon Press, Oxford.

REED, J.C. Jr. and MORGAN, B.A. (1971).
Chemical alteration and spilitisation of the Catocin greenstones, Shenandoah National Park, Virginia. J.Geol., 79, pp.526-548.

RICE, C.M., ATKINS, D., BOWLES, J.F.W., and CRIDDLE, A.J. (1979).
Nukundamite, a new mineral, and idaite. Min. Mag., 43, pp.193-200.

RICKARD, D.T. (1970).
The origin of framboids. Lithos, 3, pp.269-293.

RIDGE, J.D. (1973).
Volcanic exhalations and ore deposition in the vicinity of the sea-floor. Mineral. Deposita, 8, pp.332-348.

RIDGE, J.D. (1974).
Note on boiling of ascending ore fluids and position of volcanic-exhalative deposits in the modified Lindgren classification. Geology, 2, pp.287-288.

RIDLEY, W.I., RHODES, J.M., REID, A.M., JAKES, P., SHIH, C. and BASS, M.N. (1974).
Basalts from leg 6 of the deep sea drilling project. J.Petrol., 15, pp.140-159.

RINGWOOD, A.E. (1955).
The principles governing trace element distribution during magmatic crystallisation. Part I : the influence of electronegativity. Geochim. Cosmochim. Acta, 7,pp.189-202.

RINGWOOD, A.E. (1972).
Phase transformations and mantle dynamics. Earth Planet. Sci. Lett., 14, pp.233-241.

RINGWOOD, A.E. (1974).
The petrological evolution of island arc systems. J. Geol. Soc. Lond., 130, pp.183-204.

RINGWOOD, A.E. (1975).
Composition and petrology of the Earth's mantle. McGraw-Hill, New York, 618p.

RINGWOOD, A.E. (1977).
Petrogenesis in island arc systems. In : M.Talwani and W.C.Pitman III (Eds.), Island arcs, deep sea trenches and back-arc basins, Maurice Ewing series 1, pp.311-324.

RISE PROJECT GROUP : SPIESS, F.N., MACDONALD, K.C., ATWATER, T., BALLARD, R., CARRANZA, A., CORDOBA, D., COX, C., GARCIA, V.M.D., FRANCHETEAU, J., GUERRERO. J., HAWKINS, J., HAYMON, R., HESSLER, R., JUTEAU, T., KASTNER, M., LARSON, R., LUYENDYK, B., MACDOUGALL, J.D., MILLER, S., NORMARK, W., ORCUTT, J. and RANGIN. C. (1980).
East Pacific Rise : Hot springs and geophysical experiments. Science, 207, pp.1421-1432.

ROCCI, G., OHNSTETTER, D. and OHNSTETTER, M. (1975).
Duality of Tethyan ophiolites. Petrologie, 1, pp.172-174.

ROEDDER, P.L. and EMSLIE, R.F. (1970).
Olivine-liquid equilibrium. Contr. Mineral. Petrol., 29, pp. 275-289.

SAUNDERS, A.D. and TARNEY, J. (1979).
The geochemistry of basalts from a back-arc spreading centre in the East Scotia Sea. Geochim. Cosmochim. Acta, 43, pp.555-572.

SAUNDERS, A.D., TARNEY, J., STERN, C.R. and DALZIEL, I.W.D. (1979).
Geochemistry of Mesozoic marginal basin floor igneous rocks from Southern Chile. Geol. Soc. Am. Bull., part 1, 90, pp.237-258.

SAUNDERS, A.D. TARNEY, J., MARSH, N.G. and WOOD, D.A. (1980).
Ophiolites as ocean crust or marginal basin crust : A geochemical approach. In : A.Panayiotou (Ed.), Ophiolites : proceedings of international ophiolite symposium, Cyprus. Minist. Agric. Nat. Resour. Geol. Surv. Dep., Nicosia, Cyprus. pp.193-204.

SCHENTZLER, C.C. and PHILLPOTTS, J.A. (1970).
Phenocryst-matrix partition coefficients for K, Rb, Sr and Ba with applications to anorthosite and basalt genesis. Geochim. Cosmochim Acta, 34, pp.307-322.

SCHIFFMAN, P. and LIOU, J.G. (1980).
Synthesis and stability relations of Mg-Al pumpellyite, $Ca_4Al_5Mg\ Si_6O_{21}(OH)_7$. J. Petrol., 21, pp.441-475.

SCLAR, C.B. and DROVENIK, M. (1960).
Lazarevicite, a new cubic copper-arsenic sulphide from Bar, Yugoslavia. Prog. Ann. Meet., Denver, 202. Also : Geol.Soc.Am.Bull, 71, 1970.

SEYFRIED, W.E. and BISCHOFF, J.L. (1979).
Low temperature basalt alteration by sea-water : An experimental study at 70°C and 150°C. Geochim. Cosmochim. Acta, 43, pp.1937-1947.

SEYFRIED, W.E. and BISCHOFF, J.L. (1981).
Experimental sea-water-basalt interaction at 300°C, 500 bars, chemical exchange, secondary mineral formation and implications for the transport of heavy minerals. Geochim. Cosmochim. Acta, 45, pp.135-147.

SHADLUN, T.N. (1971).
Metamorphic textures and structures of sulphide ores. Soc. Min. Geol. Jap., spec. issue 3, [Proc. IMA-JAGOD meetings, 1970, IAGOD vol] pp.241-250.

SHIDO, F. and MIYASHIRO, A. (1959).
Hornblendes of basic metamorphic rocks. J.Fac. Sci. Tokyo Univ., sec.2, 12, pp.85-102.

SHIKAZONO, N. and KOUDA, R. (1979).
Chemical composition of tetrahedrite-tennantite minerals and the chemical environments of some Japanese ore deposits. Min. Geol. (Soc. Min.Geol. Jap.), 29, No=153, pp.33-41 (Japanese, including English sum.).

SHILOV, V.N. (1974).
The pillow lavas of Sakhalin and the Kurile Islands and their significance for the solution of the spilite problem. In : G.C.Amstutz (Ed.), Spilites and spilitic rocks, Springer-Verlag, Heidelberg, pp.387-402.

SILLITOE, R.H. and CLARK, A.H. (1969).
Copper and copper-iron sulphides as the initial products of supergene oxidation, Capiapó mining district, Northern Chile. Am. Mineral., 54 pp.1684-1710.

SKINNER,B.J. (1979).
The many origins of hydrothermal ore deposits. In : H.L. Barnes (Ed.), Geochemistry of hydrothermal ore deposits, 2nd edition, Wiley-Interscience, pp.1-21.

SKRIPCHENKO, N.S. and BERBER'YAN, T.K. (1975).
The structure of framboidal pyrite. Int. Geol. Rev.,18, No=12, pp.1435-1439.

SLEEP, N. and TOKSÖZ, M.N. (1973).
Evolution of marginal basins. Nature, 233, pp.548-550.

SMITH, R.E. (1968).
Redistribution of major elements in the alteration of some basic lavas during burial metamorphism. J.Petrol., 9, pp.191-219.

SMITH, R.E. (1969).
Zones of progressive regional burial metamorphism in part of the Tasman geosyncline, Eastern Australia. J. Petrol, 10, pp.144-163.

SMITH, R.E. (1974).
The production of spilitic lithologies by burial metamorphism of flood basalts from the Canadian Keweenawan, Lake Superior. In : G.C. Amstutz (Ed.), Spilites and spilitic rocks. Springer-Verlag, Heidelberg, pp.403-416.

SMITH R.E. and SMITH, S.E. (1976).
Comments on the use of Ti, Zr, Y, Sr, K, P and Nb in the classification of basaltic magmas. Earth Planet. Sci. Lett., 32,pp.114-120.

SOLOMON, M., WALSHE, J.L. and PALOMERO, F.G. (1980).
Formation of massive sulphide deposits at Rio Tinto, Spain, Inst. Min. Metall. Trans., 89, pp.B16-B24.

SPIESS, ET AL (1980) - See under : RISE PROJECT GROUP.

SPOONER, E.T.C. and FYFE, W.S. (1973).
Sub-sea-floor metamorphism, heat and mass transfer. Contr. Mineral Petrol., 42, pp.287-304.

SPOONER, E.T.C., BECKINSALE, R.D., ENGLAND, P.C. and SENIOR, A. (1977a).
Hydration, ^{18}O enrichment and oxidation during ocean-floor hydrothermal metamorphism of ophiolitic metabasic rocks from E.Liguria, Italy. Geochim. Cosmochim. Acta, 41, pp.857-871.

SPOONER, E.T.C., BRAY, C.J.and CHAPMAN, H.J. (1977b).
A sea-water source for the hydrothermal fluid which formed the ophiolitic cupriferous pyrite ore deposits of the Troodos Massif, Cyprus, [Abstr.]. Geol. Soc. Lond. J., 134, Part 3, p.395.

SPRINGER, G. (1968).
Electronprobe analyses of stannite and related tin minerals. Mineral. Mag., 36, pp.1045-1051.

SPRINGER, G. (1969).
Electronprobe analyses of tetrahedrite. N.Jb. Miner. Monatsh. pp.24-32.

STANTON, R.L. (1960).
General features of the conformable "pyritic" ore bodies. Can. Min. Metall. Bull., 53, pp.24-39.

STANTON, R.L. (1972).
Ore petrology. McGraw Hill, New York, 713p.

STERN, C., de WIT, M.J. and LAWRENCE, J.R. (1976).
Igneous and metamorphic processes associated with the formation of Chilean ophiolites and their implications for ocean floor metamorphism, seismic layering, and magnetism. J.Geophys. Res., 50, pp.4370-4379.

STOCKLIN, J. (1974).
Possible ancient continental margins in Iran. In : G.A. Burke and C.L. Drake (Eds.), The geology of continental margins. Springer, New York, pp.873-887.

STONELEY, R. (1974).
Evolution of continental margins bounding a former Southern Tethys. In: C.A. Burke and C.L.Drake (Eds.), The geology of continental margins. Springer, New York, pp.889-903.

STRECKEISEN, A. (1976).
To each plutonic rock its proper name. Earth-Science Rev., 12, pp.1-33.

STRECKEISEN, A. (1980).
Classification and nomenclature of volcanic rocks, lamprophyres, carbonitites and melilitic rocks - IUGS sub-commission on the systematics of igneous rocks. Geologische, Rundschau, 69, No=1,pp.194-207.

SUFFEL, G.G. HUTCHINSON, R.W. and RIDLER, R.H. (1971).
Metamorphism of massive sulphides at Manitouwadge, Ontario, Canada. Soc. Min. Geol. Jap. Spec. Issue 3 [proc. IMA-IAGOD meetings, 1970, IAGOD vol.] pp.235-240.

SUGIMURA, A. (1960).
Zonal arrangement of some geophysical and petrological features in Japan and its environs. Univ. Tokyo Journ. Fac. Sci. Sect. 2, 12, pp.133-153.

SUGIMURA, A. (1968).
Spatial relations of basaltic magmas in island arcs. In : H.H. Hess and A. Poldervaart (Eds.), Basalts, V.2., Interscience, New York, pp. 537-571.

SUN, S-S, and NESBITT, R.W. (1977).
Chemical heterogeneity in the Archaen mantle, composition of the earth and mantle evolution. Earth Planet, Sci. Lett., 35, pp.429-448.

SUN, S-S. and NESBITT, R.W. (1978).
Geochemical regularities and genetic significance of ophiolite basalts. Geology, 6, pp.689-693.

SUN, S-S., NESBITT, R W. and SHARASKIN, A.V. (1979).
Geochemical characteristics of mid-ocean ridge basalts. Earth Planet. Sci. Lett., 44, pp.119-138.

SURDAM, R.C. (1969).
Electron microprobe study of prehnite and pumpellyite from Karmutsen group, Vancouver Island, British Columbia. Am. Mineral., 54, pp. 256-266.

TARNEY, J., SAUNDERS, A.D. and WEAVERS, S.D. (1977).
Geochemistry of volcanic rocks from the island arcs and marginal basins of the Scotia Sea region. In : M. Talwani and W.C. Pitman III (Eds.), Island arcs, deep sea trenches and back-arc basins. Maurice Ewing series, vol: 1, pp.367-378.

TATSUKA, K. and MORIMOTO, N. (1973).
Composition and polymorphism of tetrahedrite in the Cu-Sb-S system below 400°C. Am. Mineral., 58, pp.425-434.

TAYLOR, H.P. Jr. (1963).
Importance of chalcophile element abundances in determining the sequence of sulphide mineral deposition from monoascendent ore forming solutions. In: Symposium-Problems of post-magmatic ore deposition, Prague, Czechoslovakia Geol. Survey, 1, pp. 267-272.

TAYLOR, R.S. (1981).
Volcanogenic copper-zinc sulphide deposits and their geological setting, in the central portion of the Murchison Greenstone Belt, Northern Transvaal, South Africa. Unpub. Ph.D. thesis, Univ. of Durham.

THOMPSON, R.N., ESSON, J., and DUNHAM, A.C. (1972).
Major elemental chemical variation in the Eocene lavas of the Isle of Skye. J.Petrol., 13, pp.219-253.

THORNTON, C.P. and TUTTLE, O.F. (1960).
Chemistry of igneous rocks : part I, Differentiation index. Am. J. Sci., 258, pp.664-684.

TILLEY, C.E. (1950).
Some aspects of magmatic evolution. Quart. J. Geol. Soc. Lond., 106, pp.37-61.

TOKSÖZ, M.N. and BIRD, P. (1977).
Formation and evolution of marginal basins and continental plateaus. In : M.Talwani and W.C. Pitman III (Eds.), Island arcs, deep sea trenches and back-arc basins, Maurice Ewing series 1, pp.379-394.

TOMASSON, J. and KRISTMANNSDOTTIR, H. (1972).
High temperature alteration minerals and thermal brines, Reykjanes, Iceland. Contr. Mineral. Petrol., 36, pp.113-134.

TOTH, J.R. (1980).
Deposition of submarine crusts rich in manganese and iron. Geol. Soc. Am. Bull. Part I, 91, pp.44-54.

TURNER, F.J. and VERHOOGEN, J. (1960).
Igneous and metamorphic petrology. 2nd. Edition. McGraw-Hill, New York, 694p.

TURNOCK, A.C. (1959).
Stability range of iron-chlorite. Geol. Soc. Am. Bull., 70, pp.1690-1691.

TURNOCK, A.C. (1960).
The stability of iron-chlorites. Carnegie Inst. Washington Year-book, 59, pp.98-103.

UGARTE, F.J. and BURKIN, A.R. (1975).
Mechanism of formation of idaite from bornite by leaching with ferric sulphate solution. In : A.R. Burkin (Ed.), Leaching and reduction in hydrometallurgy, London (Inst. Mining Metall.), pp.46-53.

UPADHYAY, H.D. and NEALE, E.R.W. (1979).
On the tectonic regimes of ophiolite genesis. Earth Planet. Sci. Lett., 43, pp.93-102.

URABE, T. (1974).
Mineralogical aspects of the Kuroko deposits in Japan and their implications. Mineral. Deposita, 9, pp.309-324.

URABE, T. (1977).
Partition of Cd and Mn between co-existing sphalerite and galena from some Japanese epithermal deposits. Mineral.Deposita, 12, pp.319-330.

UYTENBOGAARDT, W. and BURKE, E.A.J. (1971).
Tables for microscopic identification of ore minerals. 2nd. revised edition. Elsevier Publ. Company, Amsterdam, 430p.

VALLANCE, T.G. (1960).
Concerning spilites. Proceedings of the Linnean Soc. of New South Wales, XXXV, part 1, pp.8-52.

VALLANCE, T.G. (1965).
On the chemistry of pillow lavas and the origin of spilites. Min. Mag., 34, (Tilley vol.), pp.471-481.

VALLANCE, T.G. (1969).
Spilites again: some consequences of the degradation of basalts. Proceedings of the Linnean Soc. of New South Wales, 94, part 1, pp.8-51.

VALLANCE, T.G. (1974a).
Spilitic degradation of tholeiitic basalts. J. Petrol., 15, part 1, pp.79-96.

VALLANCE , T.G. (1974b).
Pyroxene and the basalt : spilite relation. In : G.C.Amstutz (Ed.), Spilites and spilitic rocks. Springer-Verlag, Heidelberg, pp.59-71.

VAUGNAT, M. (1974).
A new appraisal of Alpine spilites. In : G.C. Amstutz (Ed.), Spilites and spilitic rocks. Springer-Verlag, Heidelberg, pp.417-427.

VOKES, F.M. (1968).
Regional metamorphism of the Palaeozoic geosynclinal sulphide ore deposits of Norway. Trans. Inst. Min. Metal., 77, B53-B59.

VOKES. F.M. (1969).
A review of the metamorphism of sulphide deposits. Earth-Science Rev., 5, pp.99-143.

WAGER, L.R., and DEER, W.A. (1939).
Geological investigations in East Greenland : part III, the petrology of the Skaergaard intrusion, Kangerdlugssuog, East Greenland. Medd. Grönland, 105, No=4.

WHEATLEY, C.J.V. (1978).
Ore mineral fabrics in the Avoca polymetallic sulphide deposit, south-east Ireland. In : W.J. Mervoerd (Ed.), Mineralisation in metamorphic terranes. Geol. Soc. South Africa, spec. publ. No=4, pp.529-544.

WHITE, J.S. (1972).
Tennantite-tetrahedrite from Naica, Chihuahua, Mexico. Min. Record, 3, pp.115-119.

WHITEHEAD, R.E.S., and GOODFELLOW, W.D. (1978).
Geochemistry of volcanic rocks from the Tetagouche group, Bathurst, New Brunswick, Canada. Can. J. Earth Sci., 15,pp.207-219.

WHITTEN, D.G.A. and BROOKS, J.R.V. (1972).
A dictionary of geology. Penguin Books.

WILKINSON, J F.G. (1968).
The petrography of basaltic rocks. In : H.H. Hess and A. Poldervaart (Eds.), Basalts, V.1, Interscience, New York, pp.163-214.

WILLAN, R.C.R. and HALL, A.J. (1980).
Sphalerite geobarometry and trace element studies on stratiform sulphide from McPhun's Cairn, Loch Fyne, Argyll, Scotland. Trans. Inst. Min. Metal., 89, pp.B31-B40.

WINCHESTER, J.A. and FLOYD, P.A. (1977).
Geochemical discrimination of different magma series and their differentiation products using immobile elements. Chem. Geol., 20, pp.325-343.

WINKLER, H.G.F. (1974).
Petrogenesis of metamorphic rocks. 3rd edition. Springer-Verlag, New York, 320 p.

WOOD, D.A., GIBBSON, I.L. and THOMPSON, R.N. (1976).
Elemental mobility during zeolite facies metamorphism of the Tertiary basalts of Eastern Iceland. Contrib. Mineral. Petrol., 55, op.241-254.

WOOD, D.A., VARET, T.J., SAUNDERS, A.D., BOUGAULT, H., JORON. J.L., TREUIL, M. and CANN, J.R. (1979).
Geochemistry of basalts drilled in the North Atlantic by IPOD Leg 49 : Implications for mantle heterogeneity. Earth Planet. Sci. Lett., 42, pp.77-97.

WU, I. and PETERSEN, U., (1977).
Geochemistry of tetrahedrite and mineral zoning at Casapalca, Peru. Econ. Geol., 72, pp.993-1016.

WYLLIE, P.J. (1973).
Experimental petrology and global tectonics - a preview. Tectonophysics, 17, pp.189-209.

YAZGAN, E. (1969).
Silan bölgesi jeolojisi ve bakir yataklari hakkinda. In : Büyükyanbolu, N., unpub. report to Etibank, ANK, (1969).

YAZGAN, E. (1972).

Étude géologique et pétrographique du complexe ophiolitique de la région située au sud-est de Malatya (Taurus oriental, Turquie) et de sa couverture volcano-sédimentaire. Thèse, Fac. Sc. Univ. Genève, Genève, 236p.

YUI, S. (1971).
Hetrogeneity within a single grain of minerals of the tennantite-tetrahedrite series. Soc. Min. Geol. Jap. Spec. Issue 2 [Proc. IMA-IAGOD meetings, 1970, Joint symp. vol],pp.22-29.

ZEN, E-AN. (1974).
Prehnite - and pumpellyite-bearing mineral assemblages, west side of Appalachian metamorphic belt, Pennsylvania to Newfoundland. J. Petrol., 15, pp.197-242.

APPENDIX 1

Sample collection and nomenclature

All the samples are surface samples and collected by the writer from the fields during mapping. On average, 1 kg of material was taken at approximately 100-300 m intervals but more frequently around the sulphide mineralisation.

The samples analysed for H_2O and FeO (App.II), whole rock composition (App.III) and silicate minerals (App.IV) are all from the Polusagi area and the sample locations are given on Map 3, included in the back-pocket. Each sample number is prefixed "P" for Polusagi, followed by the sample location number. Where more than one sample is collected from the same location, they were donated the letters A,B,C etc., such as P279A and P279B.

Numbering system for the electron microprobe analyses is as follows: sample number is accompanied by a number indicating the location on the polished sample. If there is more than 1 analyses from roughly the same location, they are distinguished from one another by letters A,B,C,D etc. For example, P245-3D means analysis D on location 3 of the polished section of sample 245 from Polusagi.

Electron microprobe analyses of ore minerals from the Canakci massive ore begin with the letter E, followed by two numbers, the first indicating the location of the sample in the ore body, and the second, number of the analysis from this sample. For example, E1-6-1A means the analysis A of the position 1 on the polished specimen of the 6th sample from location 1 in the Canakci massive sulphide ore body.

APPENDIX II

I.1 H_2O and FeO determinations

Total H_2O was determined for 34 samples by a gravimetric method similar to that described by Riley (1957)*. Water is driven off the sample by heating to 1100-1200°C and flushed by nitrogen through an absorption tube filled with $CaCl_2$. The tube is weighed before and after absorption.

FeO was determined for the same samples using the Ammonium Metavanadate method described by Wilson (1955)**.

The results are given in Table II.1.

---

* RIDLEY, J P. (1957).
Simultaneous determination of water and carbondioxide in rocks and minerals. Analyst, 83, pp.42-49.

** WILSON, A.D. (1955).
A new method for the determination of ferrous iron in rocks and minerals. Bull. Geol. Soc. Great Britain, 9, pp.56-58.

TABLE II.1

FEO AND WATER DETERMINATIONS BY WET CHEMICAL METHODS

SAMPLE	WT % H2O	FE2O3	FEO	FE2O3/FEO
P66	3.31	6.97	5.40	1.29
P78	2.76	5.85	3.84	1.52
P93	2.89	5.85	5.31	1.10
P95	1.62	5.57	3.79	1.47
P104	2.58	5.55	6.13	0.90
P109	2.32	4.35	10.83	0.40
P112	3.06	2.54	9.08	0.28
P118	0.88	4.25	8.30	0.51
P123	2.34	7.27	4.67	1.56
P124	1.52	4.49	6.94	0.65
P134	2.46	3.06	9.01	0.34
P137	2.90	3.30	8.33	0.40
P161	2.76	5.05	7.80	0.65
P167	2.36	3.24	7.42	0.44
P168	1.25	5.07	7.35	0.69
P170B	2.77	3.33	9.26	0.36
P 181	3.83	3.81	7.20	0.53
P185A	1.53	4.21	9.32	0.45
P188	2.27	3.75	6.09	0.62
P191	3.46	3.03	6.15	0.49
P204	3.98	4.52	8.59	0.53
P214	3.49	4.45	5.02	0.89
P219	2.24	4.22	7.23	0.58
P226	3.53	4.24	6.80	0.62
P238	2.03	3.92	7.35	0.53
P243	2.08	2.69	8.83	0.30
P251	3.21	5.05	6.56	0.76
P253	2.79	4.39	7.78	0.56
P255	2.52	2.99	5.70	0.53
P256	1.18	5.79	5.70	1.02
P271	3.91	4.83	8.44	0.57
P277	1.09	4.56	9.50	0.48
P282	2.31	3.02	8.94	0.34
P286	3.33	4.30	7.67	0.56

APPENDIX III

X-RAY FLUORESCENCE ANALYSES

III.1 Sample preparation and operating conditions.

Samples were fragmented using a Cutrock Engineering hydraulic splitter and the weathered material was removed. Further splitting into fragments, roughly 1cm, was carried out with a Sturtevant 2" x 6" Roll Jaw Crusher. The crushed samples were then ground to a fine powder using a Tema Laboratory Disc Mill with a tungsten-carbide grinding barrel. Grinding on average took around 1 minute. Between 50 and 150 gm of the powdered samples were pressed into briquettes using a hydraulic press operating at 6-7 tons/sq. inch. Between 6 and 10 drops of "Mowiol" were used as the binding agent.

The analyses were performed using a Philips PW 1400 X-Ray Spectrometer incorporating a 3kw generator and allowing a maximum 100 kV. A Rhodium tube enabled both major and trace elements to be analysed simultaneously. The operating conditions for the analysed elements are given in Table IV.1. The data were calibrated using the international standards, GA, GH, GR, G1, G2, GSP-1, AGV-1, W1, PCC-1, BR, SY-1, DTS-1 and BCR-1, the compositions of which were taken from Flanagan (1973)*. Data handing for the major elements was performed using a procedure described by Holland and Brindle (1966) **. Analytical count data for the trace elements were converted into concentrations (ppm) using the computer programme TRATIO, written by R.C.O. Gill, which incorporates contamination and interference corrections.

---

* FLANAGAN, F.G. (1973)
1972 values for international geochemical reference standards. Geochim. Cosmochim. Acta, 37 pp.1189-1200.

** HOLLAND and BRINDLE (1966).
A self-consistent mass absorption correction for silicate analysis by X-ray fluorescence. Spectrochim. Acta., 22, pp.2083-2093.

Table III.1

Operating conditions for PW 1400 X-ray spectrometer

Element	Line	Collimator(1)	Detector (2)	Crystal (3)	Upper Level	Lower Level	KV	mA	Angle	Background +	Offset -
Na	$K\alpha_1$	C	F	4	75	30	35	80	55.165	3.50	0.00
Mg	$K\alpha_1$	C	F	4	70	35	35	80	45.220	2.40	0.00
Al	$K\alpha_1$	C	F	3	75	30	35	80	145.225	0.00	0.00
Si	$K\alpha_1$	C	F	3	80	25	35	80	109.230	0.00	0.00
P	$K\alpha_1$	C	F	5	70	30	70	40	141.100	2.40	0.00
S	$K\alpha_1$	C	F	3	75	30	60	50	75.890	1.20	0.00
K	$K\alpha_1$	C	F	2	70	30	35	80	136.820	0.00	0.00
Ca	$K\alpha_1$	C	F	2	70	30	35	80	113.280	0.00	0.00
Ti	$K\alpha_1$	C	F	2	75	30	35	80	86.275	0.00	0.00
Mn	$K\alpha_1$	C	F	1	70	40	50	60	95.320	2.00	0.00
Fe	$K\alpha_1$	F	F	2	70	35	35	80	57.635	0.00	0.00
Ni	$K\alpha_1$	C	S	1	75	25	80	35	71.280	2.00	1.50
Cu	$K\alpha_1$	C	S	1	70	30	80	35	65.575	1.00	0.80
Zn	$K\alpha_1$	C	S	1	60	40	80	35	60.615	1.10	1.30
Rb	$K\alpha_1$	C	S	1	60	40	90	30	37.990	1.70	1.00
Sr	$K\alpha_1$	C	S	1	60	40	90	30	35.845	1.00	1.00
Y	$K\alpha_1$	C	S	1	60	40	90	30	33.905	1.00	0.90
Zr	$K\alpha_1$	C	S	1	60	40	90	30	32.095	0.90	1.20
Nb	$K\alpha_1$	C	S	1	60	40	90	30	30.450	0.50	0.00
Ba	$K\alpha_1$	F	S	1	60	40	90	30	15.575	1.50	0.90
La	$L\alpha_1$	C	F	1	70	30	35	80	139.095	2.00	2.00
Ce	$L\alpha_1$	C	F	1	70	30	35	80	111.840	2.00	2.00

(1) C - coarse; F - fine.

(2) F - flow; S - scintillometer

(3) 1 - LiF_{220}

2 - LiF_{220}

3 - PET

4 - ThAP

5 - Ge

III.2 Results

The analyses are presented in the following tables starting with "Table III.2". They are all on water free basis and normalised to 100%.

The normative calculations (Group A rocks only), presented in the tables starting with "Table III.3." were performed using the programme NORMCAL, written by R.C.O. Gill, with a fixed Fe_2O_3/FeO ratio of 0.3.

TABLE III.2.1A GROUP A BASALTS WHOLE ROCK ANALYSES

	P66	P93	P118	P140	P157	P183	P204	P210	P213	P214	P234	P252
WEIGHT %												
SIO2	47.17	49.45	45.50	43.78	49.08	50.90	46.92	44.72	45.72	48.19	52.63	48.98
AL2O3	12.93	13.57	14.48	14.87	15.56	13.07	15.36	15.77	13.82	13.32	13.92	15.28
FE2O3	12.96	11.74	13.46	12.89	13.67	13.69	14.05	14.90	12.71	10.02	10.92	12.37
MGO	7.98	6.99	10.84	13.43	8.11	7.87	10.72	12.94	10.95	10.42	6.96	8.95
CAO	13.96	11.43	9.86	10.68	7.15	8.42	7.29	6.61	11.16	13.42	8.25	8.47
NA2O	3.28	4.51	3.18	2.07	3.60	4.00	3.29	2.56	3.23	2.63	5.01	4.30
K2O	0.16	0.06	0.61	0.51	0.10	0.00	0.08	0.00	0.34	0.84	0.05	0.00
TIO2	1.23	1.80	1.60	1.34	2.10	1.70	1.85	1.90	1.70	0.78	1.80	1.25
MNO	0.19	0.24	0.23	0.22	0.23	0.18	0.20	0.33	0.18	0.29	0.18	0.19
S	0.01	0.01	0.05	0.03	0.02	0.01	0.03	0.07	0.01	0.01	0.02	0.00
P2O5	0.13	0.20	0.18	0.19	0.38	0.17	0.21	0.20	0.20	0.09	0.27	0.21
PPM												
NB	7	9	9	8	13	8	8	10	7	3	14	8
ZR	73	134	105	85	211	107	127	120	103	56	200	125
Y	31	45	40	29	70	38	43	42	34	21	49	39
SR	71	81	152	196	339	119	149	173	84	153	78	59
LA	9	9	11	7	19	9	12	10	9	8	12	4
CE	24	31	26	15	39	23	22	25	21	18	30	17
RB	3	4	8	8	3	2	3	3	9	17	3	2
BA	63	76	210	72	80	64	139	197	95	143	66	35
ZN	62	72	83	152	151	75	103	352	83	54	77	20
CU	75	58	37	59	9	53	22	41	9	52	53	6
NI	30	26	39	92	13	15	17	27	8	213	8	58
CR	51	64	93	265	48	37	50	72	26	454	30	227

TABLE III.2.1A GROUP A BASALTS WHOLE ROCK ANALYSES - CONT'D

	P253	P271	P276	P280	P282	P286	P287
WEIGHT %							
SIO2	50.54	47.91	52.34	50.24	48.37	48.43	50.75
AL2O3	14.24	13.48	13.38	13.36	13.35	14.55	14.11
FE2O3	13.03	14.20	12.13	13.05	12.94	12.81	12.14
MGO	7.89	9.36	7.09	8.28	10.85	9.26	8.70
CAO	7.86	9.12	8.39	9.58	9.85	9.40	7.68
NA2O	4.17	3.41	4.57	3.42	2.67	3.84	4.28
K2O	0.00	0.14	0.06	0.09	0.28	0.00	0.06
TIO2	1.80	1.81	1.56	1.50	1.33	1.25	1.85
MNO	0.21	0.21	0.16	0.16	0.20	0.22	0.14
S	0.01	0.01	0.00	0.02	0.05	0.00	0.00
P2O5	0.25	0.36	0.31	0.30	0.12	0.22	0.29
PPM							
NB	10	13	10	10	5	9	12
ZR	149	183	161	146	62	112	169
Y	44	63	53	46	24	37	48
SR	38	224	159	242	160	92	165
LA	9	11	11	9	4	11	15
CE	32	25	28	23	13	21	23
RB	2	4	2	2	5	2	2
BA	42	82	62	82	71	38	50
ZN	15	24	18	11	65	49	12
CU	0	2	4	99	61	4	0
NI	9	20	15	30	125	55	6
CR	39	42	49	103	324	203	37

TABLE III.2.1B GROUP A ANDESITES WHOLE ROCK ANALYSES

	P73	P78	P80	P82	P101	P104	P117	P133	P134	P137	P142	P154
WEIGHT %												
SIO2	56.85	58.17	57.35	60.49	56.08	54.49	55.06	61.07	51.22	55.44	50.43	55.01
AL2O3	16.58	13.09	16.42	15.76	15.16	15.16	16.55	16.04	17.10	16.05	18.78	14.76
FE2O3	10.84	10.11	8.85	8.60	11.10	12.35	10.81	9.47	13.06	12.55	12.53	10.95
MGO	5.65	3.10	4.35	4.24	4.53	5.36	6.79	3.46	10.51	5.86	11.21	7.04
CAO	2.54	8.34	4.09	2.54	5.69	5.43	3.42	2.18	2.25	3.56	1.23	5.91
NA2O	5.08	4.78	6.24	5.44	4.88	4.97	4.76	6.12	3.01	3.99	3.42	4.11
K2O	0.00	0.00	0.17	0.46	0.36	0.13	0.14	0.03	0.00	0.04	0.02	0.11
TIO2	1.76	1.89	1.86	1.81	1.45	1.50	0.91	1.08	1.80	1.66	1.71	1.54
MNO	0.15	0.13	0.18	0.14	0.28	0.21	0.15	0.21	0.30	0.24	0.26	0.19
S	0.07	0.01	0.00	0.00	0.01	0.02	0.06	0.00	0.02	0.02	0.01	0.01
P2O5	0.49	0.39	0.50	0.51	0.47	0.38	0.34	0.34	0.73	0.60	0.39	0.36
PPM												
NB	21	19	21	22	21	17	20	24	19	19	17	19
ZR	359	277	334	313	314	282	324	372	258	305	241	298
Y	90	70	80	88	100	72	80	90	80	81	70	74
SR	96	31	99	87	136	46	111	166	103	270	27	166
LA	26	16	19	19	24	13	16	21	24	27	11	15
CE	65	45	44	50	46	33	52	50	50	53	35	36
RB	2	2	3	5	6	3	4	2	2	3	2	3
BA	468	81	108	173	128	60	99	58	46	137	30	84
ZN	179	80	133	131	186	104	112	370	383	165	272	92
CU	14	3	10	23	24	26	65	3	88	18	0	23
NI	0	8	11	11	0	1	14	1	0	1	3	9
CR	12	7	14	8	8	22	30	10	13	16	26	36

TABLE III.2.1B GROUP A ANDESITES WHOLE ROCK ANALYSES - CONT'D

	P159	P170B	P181	P191	P195	P202	P205	P206	P224	P226	P238	P243
WEIGHT %												
SIO2	52.36	51.64	52.74	56.93	55.77	52.26	61.69	54.82	57.30	53.51	53.60	52.50
AL2O3	18.03	17.37	15.55	17.84	16.24	15.43	14.39	15.50	14.54	16.54	14.04	15.47
FE2O3	11.02	13.61	11.80	9.86	10.01	12.62	8.55	11.25	12.03	11.79	12.08	12.49
MGO	12.02	8.50	7.55	6.52	6.99	8.90	3.50	6.02	6.05	7.24	6.77	8.14
CAO	1.26	2.56	5.97	1.47	3.77	4.23	4.41	4.64	3.23	3.61	6.01	4.65
NA2O	3.00	3.39	3.77	4.83	5.08	4.01	5.43	5.15	4.59	4.26	5.50	3.99
K2O	0.00	0.46	0.71	0.21	0.02	0.03	0.10	0.29	0.01	0.63	0.07	0.56
TIO2	1.60	1.80	1.34	1.66	1.46	1.95	1.48	1.65	1.71	1.64	1.47	1.43
MNO	0.29	0.25	0.17	0.12	0.22	0.17	0.11	0.18	0.09	0.20	0.23	0.25
S	0.05	0.01	0.07	0.00	0.00	0.01	0.00	0.00	0.00	0.00	0.00	0.10
P2O5	0.38	0.41	0.32	0.56	0.44	0.40	0.33	0.41	0.46	0.58	0.23	0.42
PPM												
NB	16	15	20	25	23	17	21	16	13	23	14	17
ZR	247	246	270	387	364	261	355	251	221	355	241	251
Y	58	63	62	89	79	68	67	68	67	85	63	70
SR	45	80	388	116	152	220	46	69	94	193	87	121
LA	15	16	21	23	18	22	21	16	10	21	13	19
CE	30	34	43	54	49	36	46	38	31	52	36	33
RB	1	7	7	4	2	2	3	4	2	6	2	5
BA	37	67	292	93	93	64	50	86	39	310	40	217
ZN	310	115	90	107	50	72	90	107	20	123	82	117
CU	7	3	36	3	4	22	5	8	0	22	4	17
NI	7	7	19	0	7	1	3	7	0	1	12	3
CR	53	36	71	12	30	22	22	37	15	5	42	20

TABLE III.2.1B GROUP A ANDESITES WHOLE ROCK ANALYSES - CONT'D

	P245	P248	P250	P251	P256	P257	P263B	P289
WEIGHT %								
SIO2	55.01	53.40	56.40	52.09	52.91	50.76	51.40	55.84
AL2O3	15.81	14.44	15.36	15.83	14.59	16.50	17.34	15.14
FE2O3	10.78	11.94	10.61	12.29	12.13	12.82	12.44	11.31
MGO	7.46	7.49	7.40	10.07	6.23	9.75	10.67	6.56
CAO	4.44	5.45	3.48	2.86	5.88	4.16	1.99	3.80
NA2O	4.51	5.16	4.31	4.00	5.72	3.64	3.70	5.25
K2O	0.20	0.02	0.00	0.00	0.00	0.00	0.02	0.00
TIO2	1.14	1.50	1.63	2.11	1.86	1.55	1.52	1.40
MNO	0.33	0.19	0.18	0.26	0.17	0.37	0.41	0.26
S	0.00	0.00	0.01	0.01	0.00	0.02	0.17	0.00
P2O5	0.32	0.40	0.62	0.48	0.51	0.42	0.36	0.44
PPM								
NB	19	15	16	17	16	16	17	19
ZR	336	220	235	257	233	236	286	298
Y	74	66	73	70	68	62	66	77
SR	116	137	40	52	179	229	35	97
LA	17	16	15	15	14	18	19	21
CE	38	38	46	39	37	37	43	39
RB	2	1	1	2	1	1	2	2
BA	68	37	30	33	33	25	35	39
ZN	141	20	113	206	5	142	504	332
CU	5	5	2	62	3	583	511	12
NI	18	15	0	0	0	19	12	6
CR	65	57	8	17	20	71	101	26

TABLE III.2.1C GROUP A DACITES WHOLE ROCK ANALYSES

	P65	P71	P144	P218	P223
WEIGHT %					
SIO2	69.91	66.53	64.30	64.27	73.19
AL2O3	13.06	15.30	16.31	15.12	11.95
FE2O3	5.91	7.07	8.54	8.74	5.37
MGO	0.67	1.50	2.35	2.72	0.90
CAO	3.47	1.20	1.30	2.11	2.77
NA2O	5.47	7.34	5.98	5.89	5.44
K2O	0.82	0.06	0.16	0.03	0.00
TIO2	0.52	0.68	0.74	0.74	0.30
MNO	0.06	0.16	0.14	0.10	0.04
S	0.00	0.00	0.02	0.00	0.00
P2O5	0.10	0.16	0.17	0.28	0.04
PPM					
NB	31	32	34	27	35
ZR	599	552	627	452	624
Y	116	112	111	89	99
SR	78	52	132	151	275
LA	28	32	32	27	31
CE	62	65	65	49	58
RB	8	2	4	2	1
BA	128	50	162	40	19
ZN	83	164	397	13	0
CU	1	26	2	246	237
NI	0	0	1	0	0
CR	31	5	8	8	3

TABLE III.2.1D GROUP A GABBROS WHOLE ROCK ANALYSES

	P239	P246	P255	P258	P272	P277	P279B
WEIGHT %							
SIO2	48.98	48.19	50.48	50.89	49.58	47.97	48.26
AL2O3	16.51	14.14	16.05	18.91	15.26	13.65	16.48
FE2O3	10.30	9.99	9.32	8.37	12.98	15.10	8.12
MGO	10.81	14.77	10.77	7.19	7.92	6.98	13.20
CAO	8.51	9.76	8.38	8.40	7.87	8.99	10.59
NA2O	3.07	1.56	3.22	3.35	3.03	3.76	1.52
K2O	0.67	0.68	0.63	1.83	0.72	0.39	1.19
TIO2	0.86	0.63	0.84	0.74	1.96	2.63	0.44
MNO	0.16	0.16	0.15	0.21	0.21	0.22	0.15
S	0.00	0.01	0.00	0.01	0.10	0.00	0.00
P2O5	0.13	0.11	0.16	0.11	0.37	0.30	0.04
PPM							
NB	4	4	4	3	15	9	3
ZR	74	54	72	63	111	157	19
Y	25	22	23	22	46	51	16
SR	276	228	292	361	144	137	222
LA	10	7	9	7	11	6	1
CE	17	16	22	12	24	26	14
RB	10	11	9	22	9	5	14
BA	115	175	140	329	215	113	208
ZN	57	50	41	45	85	33	39
CU	9	21	16	30	52	9	106
NI	120	240	102	36	30	20	202
CR	185	391	180	77	60	48	492

TABLE III.2.1E GROUP A PLAGIOGRANITES WHOLE ROCK ANALYSES

	P254	P264A	P264B	P270	P274
WEIGHT %					
SIO2	61.78	59.13	61.30	69.61	68.48
AL2O3	15.30	17.79	16.40	15.05	15.44
FE2O3	6.99	10.67	9.00	5.65	5.73
MGO	1.86	2.51	2.02	0.83	0.99
CAO	4.93	1.10	2.89	0.64	0.66
NA2O	7.96	7.56	7.38	7.70	8.03
K2O	0.02	0.00	0.00	0.01	0.05
TIO2	0.74	0.72	0.72	0.38	0.46
MNO	0.11	0.05	0.04	0.02	0.03
S	0.00	0.01	0.00	0.00	0.01
P2O5	0.33	0.47	0.25	0.10	0.11
PPM					
NB	26	32	32	33	33
ZR	472	461	454	596	493
Y	82	121	115	107	107
SR	320	34	250	55	59
LA	21	39	30	32	24
CE	40	76	65	69	48
RB	1	2	1	2	1
BA	29	42	33	47	45
ZN	1	0	0	0	0
CU	1	2	11	0	5
NI	0	2	1	2	0
CR	9	10	5	4	6

TABLE III.2.2A GROUP B BASALTS WHOLE ROCK ANALYSES

	P67	P85	P95	P119	P120	P121	P123	P124	P126	P161	P167	P168
WEIGHT %												
SIO2	51.81	44.13	55.23	54.27	44.07	45.23	49.34	49.12	46.77	45.73	51.82	49.58
AL2O3	12.24	10.63	11.35	11.13	9.67	11.28	14.77	15.13	11.12	14.17	17.12	14.72
FE2O3	13.81	13.99	9.78	9.73	11.46	12.42	12.45	12.19	13.18	13.71	11.48	13.23
MGO	4.76	6.01	5.27	4.59	7.01	7.74	5.21	8.24	2.66	10.35	10.11	7.91
CAO	12.72	17.91	16.50	18.56	21.93	18.27	12.33	9.46	21.67	11.03	3.08	7.44
NA2O	2.64	4.35	0.26	0.05	3.48	2.74	3.96	4.20	2.71	2.85	3.86	2.86
K2O	0.00	0.24	0.00	0.00	1.11	1.00	0.00	0.05	0.00	0.68	0.22	1.70
TIO2	1.73	2.23	1.23	1.30	0.88	0.98	1.43	1.13	1.34	0.97	1.53	1.90
MNO	0.10	0.31	0.17	0.17	0.19	0.17	0.12	0.18	0.26	0.21	0.34	0.19
S	0.01	0.02	0.02	0.02	0.02	0.01	0.01	0.01	0.02	0.09	0.01	0.01
P2O5	0.18	0.19	0.20	0.18	0.18	0.16	0.37	0.29	0.25	0.21	0.43	0.46
PPM												
NB	8	9	12	12	9	10	25	14	14	9	14	24
ZR	117	120	83	84	33	60	127	99	83	73	216	150
Y	39	45	29	27	17	23	39	33	28	29	62	48
SR	19	98	37	21	146	230	56	64	48	176	137	276
LA	9	13	15	14	16	16	57	24	24	18	12	37
CE	19	32	31	35	29	28	99	42	51	32	27	64
RB	3	5	1	2	20	23	2	3	2	6	4	18
BA	42	70	43	49	196	174	70	68	50	860	93	658
ZN	175	95	49	43	32	47	99	53	58	75	161	93
CU	8	89	78	24	20	79	8	86	44	88	1	47
NI	15	4	37	35	75	60	0.0	27	28	25	8	25
CR	65	20	110	26	250	113	15	63	15	31	45	60

TABLE III.2.2A GROUP B BASALTS WHOLE ROCK ANALYSES - CONT'D

	P182B	P185A	P188	P192B	P193	P209	P211B	P219
WEIGHT %								
SIO2	47.59	48.77	47.25	46.71	54.33	54.86	42.02	52.89
AL2O3	12.29	16.49	17.48	15.45	15.58	12.04	17.04	15.11
FE2O3	11.55	14.56	10.51	12.84	11.19	10.03	15.19	12.25
MGO	9.00	7.93	10.11	5.63	7.50	9.55	14.04	9.08
CAO	15.50	5.79	8.97	12.79	4.64	8.99	6.00	5.06
NA2O	1.77	3.18	2.12	2.64	4.37	2.82	2.76	3.72
K2O	0.78	0.38	2.11	1.33	0.00	0.00	0.00	0.02
TIO2	1.06	1.80	1.01	2.07	1.68	1.31	2.19	1.37
MNO	0.26	0.38	0.21	0.19	0.22	0.18	0.34	0.18
S	0.04	0.07	0.01	0.01	0.01	0.07	0.10	0.01
P2O5	0.17	0.66	0.22	0.32	0.48	0.14	0.25	0.30
PPM								
NB	8	31	5	11	15	7	12	12
ZR	65	163	101	150	199	80	139	201
Y	25	72	27	42	55	30	52	60
SR	82	308	127	97	297	62	117	104
LA	19	49	14	9	12	12	9	14
CE	32	79	30	33	31	16	28	31
RB	15	7	28	13	1	3	2	2
BA	378	221	607	142	34	59	194	76
ZN	44	182	68	95	100	171	570	85
CU	924	30	42	24	0	23	119	0
NI	65	1	99	3	0	29	27	46
CR	43	28	204	26	14	75	85	124

TABLE III.2.2B GROUP B ANDESITES WHOLE ROCK ANALYSES

	P64	P69	P88	P109	P112	P116	P171	P184	P22	P222	P225	P233
WEIGHT %												
SIO2	52.06	66.24	65.35	47.70	51.53	52.13	52.64	65.83	54.27	54.53	60.81	57.58
AL2O3	12.44	12.99	13.30	15.80	17.35	15.37	16.50	13.24	14.86	16.49	14.84	15.58
FE2O3	12.98	7.46	7.29	16.37	12.62	13.57	12.87	6.63	10.91	10.54	9.41	9.68
MGO	3.09	1.50	2.18	5.48	9.23	6.36	7.96	1.94	9.03	4.85	6.17	7.28
CAO	13.76	3.73	3.86	8.19	2.99	4.93	4.05	4.21	5.78	5.67	3.05	3.26
NA2O	3.19	6.18	5.93	3.03	2.40	3.30	3.49	5.96	2.81	5.55	3.82	4.46
K2O	0.00	0.01	0.06	0.37	1.38	1.51	0.05	0.02	0.00	0.00	0.04	0.00
TIO2	1.81	1.44	1.60	2.46	1.66	1.99	1.59	1.56	1.57	1.70	1.20	1.52
MNO	0.17	0.06	0.07	0.22	0.40	0.21	0.23	0.12	0.26	0.13	0.15	0.15
S	0.01	0.00	0.00	0.01	0.02	0.01	0.01	0.01	0.00	0.00	0.00	0.00
P2O5	0.49	0.39	0.34	0.35	0.43	0.60	0.62	0.48	0.52	0.53	0.49	0.50
PPM												
NB	16	19	16	16	18	38	20	21	23	23	14	19
ZR	234	279	210	216	286	218	294	324	363	380	227	264
Y	67	64	65	63	77	69	70	86	76	88	55	65
SR	29	52	118	47	101	333	217	71	297	450	131	167
LA	17	16	16	13	22	55	23	20	15	19	11	21
CE	41	44	36	34	46	98	44	54	43	43	35	39
RB	2	2	3	7	15	15	3	1	1	1	2	1
BA	29	59	58	102	150	1063	52	44	46	27	37	39
ZN	77	99	97	141	615	95	92	85	435	39	27	71
CU	16	10	4	61	52	10	0	10	127	354	225	822
NI	0	0	0	16	10	2	0	0	0	4	0	0
CR	10	13	6	46	34	20	14	3	10	18	12	13

TABLE III.2.2C GROUP B DACITES WHOLE ROCK ANALYSES

	P163	P19	P203
WEIGHT %			
SIO2	57.09	59.66	59.02
AL203	17.29	17.17	15.79
FE203	10.78	10.80	10.34
MGO	6.73	5.33	3.60
CAO	1.52	0.79	3.96
NA20	5.13	4.66	5.58
K20	0.03	0.00	0.07
TIO2	0.93	1.03	1.14
MNO	0.21	0.16	0.20
S	0.00	0.01	0.01
P205	0.28	0.36	0.31
PPM			
NB	25	26	28
ZR	462	446	484
Y	77	78	104
SR	111	32	168
LA	28	18	28
CE	58	39	67
RB	1	2	2
BA	61	58	138
ZN	175	109	123
CU	0	2	17
NI	0	0	4
CR	11	11	11

TABLE III.2.3A GROUP C BASALTS WHOLE ROCK ANALYSES

	P135	P155B	P156	P158	P173A	P173B	P189
WEIGHT %							
SIO2	52.62	47.42	53.02	48.82	64.64	68.35	52.86
AL2O3	15.77	18.35	15.23	18.06	18.73	22.42	17.81
FE2O3	10.94	15.04	11.24	14.49	4.75	0.77	11.49
MGO	13.12	11.45	10.43	13.03	1.73	0.67	7.88
CAO	2.63	0.53	0.48	0.46	0.25	0.10	0.53
NA2O	2.61	2.25	3.02	1.11	3.29	1.99	1.78
K2O	0.03	0.07	0.00	0.30	2.92	4.71	1.33
TIO2	1.70	2.48	2.09	1.70	0.48	0.82	2.06
MNO	0.23	1.13	0.23	0.41	0.05	0.01	0.70
S	0.15	1.01	4.01	1.33	3.04	0.12	3.30
P2O5	0.21	0.27	0.25	0.28	0.13	0.04	0.27
PPM							
NB	11	10	12	10	5	5	10
ZR	147	152	159	160	94	113	146
Y	45	34	34	48	25	13	52
SR	170	21	23	16	129	79	25
LA	11	7	15	9	11	4	9
CE	26	21	36	29	33	13	17
RB	2	2	2	6	64	118	9
BA	138	52	39	81	323	627	343
ZN	801	4983	183	289	96	22	5400
CU	45	611	6	1043	20	2	572
NI	22	13	2	8	0	0	14
CR	55	53	29	62	9	13	48

TABLE III.2.3B GROUP C ANDESITES WHOLE ROCK ANALYSES

	P74	P108	P115B	P136	P149	P155A	P185B	P194	P211A	P215	P244	P263A	P269
WEIGHT %													
SIO2	60.37	52.16	55.40	68.64	51.81	63.79	52.52	56.02	50.07	57.89	55.26	56.97	54.76
AL2O3	18.98	16.63	17.90	16.18	19.77	16.21	18.64	15.89	18.95	15.16	16.92	15.69	16.92
FE2O3	6.95	13.64	9.45	4.29	8.25	6.24	9.52	10.96	11.80	7.81	9.47	7.62	10.22
MGO	3.16	8.89	11.00	4.07	14.64	5.47	11.25	7.18	10.61	4.69	10.38	8.51	7.94
CAO	0.80	2.09	0.69	0.33	0.28	0.40	1.61	2.97	2.38	6.14	1.40	1.59	2.63
NA2O	6.88	2.36	2.40	0.10	0.07	4.18	3.26	4.36	4.27	4.24	3.60	4.69	4.40
K2O	0.00	0.32	0.33	3.21	1.32	0.71	0.16	0.02	0.02	0.00	0.00	0.00	0.00
TIO2	1.10	1.68	1.63	0.86	1.80	1.03	1.62	1.93	1.13	1.88	1.24	1.69	1.52
MNO	0.30	0.68	0.21	0.09	0.18	0.32	0.31	0.20	0.21	0.33	0.19	0.17	0.46
S	2.19	1.14	0.92	2.00	1.51	1.40	0.58	0.01	0.27	1.56	1.09	2.61	0.67
P2O5	0.26	0.40	0.07	0.22	0.36	0.25	0.52	0.46	0.30	0.31	0.46	0.45	0.48
PPM													
NB	22	15	18	23	17	21	22	15	25	21	22	18	18
ZR	365	234	297	375	273	388	381	226	411	343	349	292	266
Y	69	62	38	65	78	51	94	66	109	81	76	61	70
SR	52	44	103	6	7	36	64	116	176	273	32	28	98
LA	4	20	15	33	19	23	17	17	34	19	18	12	18
CE	28	35	25	68	40	46	45	32	58	44	47	37	44
RB	1	5	7	34	15	9	4	2	1	1	1	2	2
BA	36	224	132	1327	672	793	76	45	159	40	36	35	37
ZN	269	2102	327	263	253	328	367	47	2728	372	88	94	214
CU	624	251	300	9	18	6	0	1338	49	571	1	7	56
NI	0	3	0	0	2	0	0	17	16	1	0	0	2
CR	12	34	29	9	82	15	18	26	0	29	9	11	24

TABLE III.2.3C GROUP C DACITES WHOLE ROCK ANALYSES

	P113	P143	P151	P169	P247	P249
WEIGHT %						
SIO2	71.66	50.25	67.09	66.35	62.41	62.06
AL203	14.08	20.43	15.34	15.24	15.89	17.31
FE203	4.42	8.66	6.74	6.45	6.84	5.66
MGO	2.06	9.67	2.47	4.86	4.45	7.30
CAO	0.25	1.09	1.01	0.40	1.76	0.35
NA2O	5.92	2.08	5.39	5.02	5.66	4.19
K2O	0.15	1.87	0.40	0.04	0.04	0.12
TIO2	0.69	2.00	0.76	0.88	0.98	1.12
MNO	0.08	0.33	0.10	0.16	0.26	0.15
S	0.52	2.86	0.46	0.39	1.37	1.42
P2O5	0.16	0.76	0.25	0.19	0.35	0.30
PPM						
NB	29	26	25	29	26	24
ZR	512	398	435	568	472	418
Y	80	98	90	88	83	99
SR	56	42	67	74	98	31
LA	26	40	42	17	24	23
CE	51	78	68	34	57	59
RB	3	20	7	2	2	3
BA	52	444	100	58	44	40
ZN	31	388	160	102	140	170
CU	5	8	125	228	0	4
NI	0	0	0	1	0	4
CR	6	47	3	11	5	14

TABLE III.2.4A FE-MN-OXIDE RICH CHERTS WHOLE ROCK ANALYSES

	P92	P145	P235	P236
WEIGHT %				
SIO2	87.01	43.47	28.12	28.98
AL2O3	0.27	1.50	2.41	1.43
FE2O3	12.38	49.63	30.34	27.92
MGO	0.21	0.78	1.62	0.79
CAO	0.03	0.40	14.46	27.23
NA2O	0.00	0.00	0.00	0.00
K2O	0.00	0.19	0.03	0.00
TIO2	0.03	3.49	0.15	0.11
MNO	0.03	0.01	22.58	13.39
S	0.01	0.47	0.02	0.01
P2O5	0.03	0.06	0.27	0.13
PPM				
NB	2	23	5	4
ZR	2	202	44	33
Y	6	21	85	84
SR	3	36	33	43
LA	6	45	170	116
CE	3	15	25	20
RB	1	6	5	4
BA	29	6386	238	27
ZN	0	199	327	73
CU	62	289	11	14
NI	0	0	693	429
CR	130	450	480	300

TABLE III.3.1A GROUP A BASALTS NORMATIVE MINERALOGY

	P66	P93	P118	P140	P157	P183	P204	P210	P213	P214	P234	P252
CORUNDUM	0.0	0.0	0.0	0.0	0.0	0.0	0.0	0.0	0.0	0.0	0.0	0.0
ORTHOCLASE	1.0	0.4	3.6	3.0	0.6	0.0	0.5	0.0	2.0	5.0	0.3	0.0
ALBITE	15.4	28.8	17.6	10.9	30.8	34.2	28.1	21.9	16.3	13.1	42.8	34.4
ANORTHITE	20.3	16.8	23.7	30.1	26.3	17.9	27.2	31.9	22.4	22.2	15.5	22.6
NEPHELINE	6.8	5.2	5.2	3.7	0.0	0.0	0.0	0.0	6.1	5.1	0.0	1.3
DIOPSIDE	39.8	31.9	19.9	17.8	5.8	18.9	6.5	0.0	25.9	35.6	19.5	15.0
HYPERSTHENE	0.0	0.0	0.0	0.0	20.1	14.0	8.5	12.3	0.0	0.0	5.8	0.0
OLIVINE	10.0	9.3	22.2	27.4	7.2	7.0	20.7	25.0	19.5	14.1	8.7	20.0
MAGNETITE	4.0	3.7	4.2	4.0	4.3	4.3	4.4	4.6	4.0	3.1	3.4	3.8
ILMENITE	2.4	3.5	3.1	2.6	4.0	3.3	3.6	3.7	3.3	1.5	3.4	2.4
APATITE	0.3	0.5	0.4	0.5	0.9	0.4	0.5	0.5	0.5	0.2	0.6	0.5
PYRITE	0.0	0.0	0.1	0.1	0.0	0.0	0.1	0.1	0.0	0.0	0.0	0.0
DIFF. INDEX	23.2	54.4	26.5	17.6	31.4	34.2	28.6	21.9	24.4	23.2	43.0	35.7
NA/(NA+K)	0.97	0.99	0.89	0.86	0.98	1.00	0.98	1.00	0.94	0.83	0.99	1.00
(NA+K)/AL	0.43	0.55	0.41	0.27	0.39	0.50	0.36	0.27	0.41	0.39	0.60	0.46
F3/(F2+F3)	0.21	0.21	0.21	0.21	0.21	0.21	0.21	0.21	0.21	0.21	0.21	0.21

TABLE III.3.1A GROUP A BASALTS NORMATIVE MINERALOGY - CONT'D

	P253	P271	P276	P280	P282	P286	P287
ORTHOCLASE	0.0	0.8	0.4	0.5	1.7	0.0	0.4
ALBITE	35.6	29.2	39.0	29.2	22.8	31.1	36.6
ANORTHITE	20.3	21.3	16.0	21.1	23.9	22.7	17.3
NEPHELINE	0.0	0.0	0.0	0.0	0.0	0.9	0.0
DIOPSIDE	14.2	17.9	19.6	20.3	20.0	18.6	14.0
HYPERSTHENE	12.5	5.0	11.6	14.8	9.8	0.0	10.5
OLIVINE	9.2	17.0	5.9	6.4	15.0	19.7	11.3
MAGNETITE	4.1	4.4	3.8	4.1	4.0	4.0	3.8
ILMENITE	3.5	3.5	3.0	2.9	2.6	2.4	3.5
APATITE	0.6	0.9	0.7	0.7	0.3	0.5	0.7
PYRITE	0.0	0.0	0.0	0.0	0.1	0.0	0.0
DIFF. INDEX	35.6	30.0	39.4	29.8	24.5	32.0	36.9
NA/(NA+K)	1.00	0.97	0.99	0.98	0.94	1.00	0.99
(NA+K)/AL	0.48	0.43	0.57	0.43	0.35	0.43	0.50
F3/(F2+F3)	0.21	0.21	0.21	0.21	0.21	0.21	0.21

TABLE III.3.1B GROUP A ANDESITES NORMATIVE MINERALOGY

	P73	P78	P80	P82	P101	P104	P117	P133	P134	P137	P142	P154
QUARTZ	10.6	10.5	3.5	13.7	5.4	2.4	5.5	12.4	9.8	12.1	6.9	5.2
CORUNDUM	4.8	0.0	0.0	2.9	0.0	0.0	3.2	2.8	9.9	4.4	11.9	0.0
ORTHOCLASE	0.0	0.0	1.0	2.7	2.1	0.8	0.8	0.2	0.0	0.2	0.1	0.7
ALBITE	43.3	40.8	53.2	46.3	41.6	42.5	41.0	52.2	25.7	34.1	29.2	35.1
ANORTHITE	9.5	14.4	16.4	9.3	18.6	18.9	15.0	8.7	6.5	13.9	3.6	21.7
DIOPSIDE	0.0	20.5	0.6	0.0	5.6	4.8	0.0	0.0	0.0	0.0	0.0	4.5
HYPERSTHENE	23.7	6.1	17.9	17.6	19.3	23.0	28.3	18.0	38.8	26.6	40.1	25.7
MAGNETITE	3.4	3.1	2.7	2.7	3.4	3.8	3.4	2.9	4.1	3.9	3.9	3.4
ILMENITE	3.4	3.6	3.6	3.5	2.8	2.9	1.8	2.1	3.5	3.2	3.3	2.9
APATITE	1.2	0.9	1.2	1.2	1.1	0.9	0.8	0.8	1.7	1.4	0.9	0.9
PYRITE	0.1	0.0	0.0	0.0	0.0	0.0	0.1	0.0	0.0	0.0	0.0	0.0
DIFF. INDEX	53.9	51.3	57.6	62.8	49.2	45.7	47.4	64.7	35.5	46.5	36.3	40.9
NA/(NA+K)	1.00	1.00	0.98	0.95	0.95	0.98	0.98	1.00	1.00	0.99	1.00	0.98
(NA+K)/AL	0.50	0.60	0.64	0.60	0.56	0.55	0.48	0.63	0.29	0.41	0.30	0.47
F3/(F2+F3)	0.21	0.21	0.21	0.21	0.21	0.21	0.21	0.21	0.21	0.21	0.21	0.21

TABLE III.3.1B GROUP A ANDESITES NORMATIVE MINERALOGY - CONT'D

	P159	P170B	P181	P191	P195	P202	P205	P206	P224	P226	P238	P243
QUARTZ	10.8	7.4	0.7	12.9	4.7	2.5	13.8	1.8	11.1	4.5	0.0	0.8
CORUNDUM	11.8	7.7	0.0	8.4	2.1	2.1	0.0	0.0	2.2	3.7	0.0	0.9
ORTHOCLASE	0.0	2.7	4.2	1.3	0.1	0.2	0.6	1.7	0.1	3.8	0.4	3.3
ALBITE	25.6	29.0	32.2	41.2	43.3	34.3	46.3	44.0	39.2	36.4	47.0	34.1
ANORTHITE	3.8	10.1	23.6	3.7	16.0	18.6	14.7	18.5	13.1	14.2	13.5	20.5
DIOPSIDE	0.0	0.0	3.4	0.0	0.0	0.0	4.2	1.7	0.0	0.0	12.3	0.0
HYPERSTHENE	40.5	34.3	28.7	25.0	26.9	33.8	14.1	24.7	26.2	29.2	11.3	32.6
OLIVINE	0.0	0.0	0.0	0.0	0.0	0.0	0.0	0.0	0.0	0.0	8.3	0.0
MAGNETITE	3.4	4.2	3.7	3.1	3.1	3.9	2.7	3.5	3.7	3.7	3.8	3.9
ILMENITE	3.1	3.5	2.6	3.2	2.8	3.7	2.8	3.2	3.3	3.1	2.8	2.7
APATITE	0.9	1.0	0.8	1.3	1.1	1.0	0.8	1.0	1.1	1.4	0.5	1.0
PYRITE	0.1	0.0	0.1	0.0	0.0	0.0	0.0	0.0	0.0	0.0	0.0	0.2
DIFF. INDEX	36.4	39.2	37.1	55.4	48.1	36.9	60.7	47.5	50.3	44.6	47.4	38.2
NA/(NA+K)	1.00	0.92	0.89	0.97	1.00	1.00	0.99	0.96	1.00	0.91	0.99	0.92
(NA+K)/AL	0.27	0.35	0.45	0.46	0.52	0.43	0.63	0.57	0.52	0.46	0.65	0.46
F3/(F2+F3)	0.21	0.21	0.21	0.21	0.21	0.21	0.21	0.21	0.21	0.21	0.21	0.21

TABLE III.3.1B GROUP A ANDESITES NORMATIVE MINERALOGY - CONT'D

	P245	P248	P250	P251	P256	P257	P263B	P289
QUARTZ	3.4	0.0	10.3	4.2	0.0	1.6	5.2	3.7
CORUNDUM	0.9	0.0	3.5	5.2	0.0	4.0	8.6	0.7
ORTHOCLASE	1.2	0.1	0.0	0.0	0.0	0.0	0.1	0.0
ALBITE	38.5	44.1	36.8	34.2	48.9	31.1	31.6	44.8
ANORTHITE	20.1	16.3	13.3	11.2	14.3	18.1	7.6	16.1
DIOPSIDE	0.0	6.8	0.0	0.0	9.7	0.0	0.0	0.0
HYPERSTHENE	29.7	20.4	28.2	36.2	9.8	37.2	38.9	27.5
OLIVINE	0.0	4.8	0.0	0.0	8.9	0.0	0.0	0.0
MAGNETITE	3.4	3.7	3.3	3.8	3.8	4.0	3.9	3.5
ILMENITE	2.2	2.9	3.1	4.0	3.6	3.0	2.9	2.7
APATITE	0.8	1.0	1.5	1.1	1.2	1.0	0.9	1.1
PYRITE	0.0	0.0	0.0	0.0	0.0	0.0	0.3	0.0
DIFF. INDEX	43.0	44.2	47.1	38.3	46.9	32.7	37.0	48.5
NA/(NA+K)	0.97	1.00	1.00	1.00	1.00	1.00	1.00	1.00
(NA+K)/AL	0.48	0.59	0.46	0.42	0.64	0.36	0.35	0.57
F3/(F2+F3)	0.21	0.21	0.21	0.21	0.21	0.21	0.21	0.21

TABLE III.3.1C GROUP A DACITES NORMATIVE MINERALOGY

	P65	P71	P144	P218	P223
QUARTZ	25.9	16.1	19.3	18.2	33.1
CORUNDUM	0.0	1.4	4.4	2.2	0.0
ORTHOCLASE	4.9	0.4	1.0	0.2	0.0
ALBITE	46.5	62.5	50.9	50.2	46.2
ANORTHITE	8.7	4.9	5.4	8.7	8.2
DIOPSIDE	6.8	0.0	0.0	0.0	4.5
HYPERSTHENE	4.1	10.9	14.6	15.7	5.6
MAGNETITE	1.8	2.2	2.6	2.7	1.7
ILMENITE	1.0	1.3	1.4	1.4	0.6
APATITE	0.2	0.4	0.4	0.7	0.1
PYRITE	0.0	0.0	0.0	0.0	0.0
DIFF. INDEX	77.3	78.9	71.2	68.6	79.3
NA/(NA+K)	0.91	0.99	0.98	1.00	1.00
(NA+K)/AL	0.76	0.79	0.61	0.64	0.75
F3/(F2+F3)	0.21	0.21	0.21	0.21	0.21

TABLE III.3.1D GROUP A GABBROS NORMATIVE MINERALOGY

	P239	P246	P255	P258	P272	P277	P279B
ORTHOCLASE	4.0	4.1	3.8	10.9	4.3	2.3	7.1
ALBITE	26.2	13.3	27.4	28.5	25.9	32.2	12.9
ANORTHITE	29.5	29.8	27.7	31.4	26.2	19.4	34.9
DIOPSIDE	9.8	14.6	10.5	8.0	8.8	19.4	14.2
HYPERSTHENE	5.6	15.9	11.0	1.7	22.2	2.0	8.4
OLIVINE	19.7	17.8	14.6	15.3	3.8	14.1	19.1
MAGNETITE	3.2	3.1	2.9	2.6	4.0	4.7	2.5
ILMENITE	1.6	1.2	1.6	1.4	3.8	5.1	0.8
APATITE	0.3	0.3	0.4	0.3	0.9	0.7	0.1
PYRITE	0.0	0.0	0.0	0.0	0.2	0.0	0.0
DIFF. INDEX	30.2	17.4	31.2	39.4	30.2	34.5	20.0
NA/(NA+K)	0.87	0.78	0.89	0.74	0.86	0.94	0.66
(NA+K)/AL	0.35	0.23	0.37	0.40	0.38	0.48	0.23
F3/(F2+F3)	0.21	0.21	0.21	0.21	0.21	0.21	0.21

TABLE III.3.1E GROUP A PLAGIOGRANITES NORMATIVE MINERALOGY

	P254	P264A	P264B	P270	P274
QUARTZ	3.4	5.5	6.0	19.9	16.5
CORUNDUM	0.0	4.5	0.0	1.5	1.2
ORTHOCLASE	0.1	0.0	0.0	0.1	0.3
ALBITE	67.7	64.5	62.9	65.5	68.3
ANORTHITE	6.0	2.4	11.7	2.5	2.6
DIOPSIDE	13.8	0.0	0.9	0.0	0.0
HYPERSTHENE	4.6	17.3	13.7	7.9	8.2
MAGNETITE	2.2	3.3	2.8	1.7	1.8
ILMENITE	1.4	1.4	1.4	0.7	0.9
APATITE	0.8	1.1	0.6	0.2	0.3
PYRITE	0.0	0.0	0.0	0.0	0.0
DIFF. INDEX	71.2	70.0	68.9	85.4	85.0
NA/(NA+K)	1.00	1.00	1.00	1.00	1.00
(NA+K)/AL	0.86	0.70	0.74	0.84	0.86
F3/(F2+F3)	0.21	0.21	0.21	0.21	0.21

APPENDIX IV

ELECTRON PROBE ANALYSES

IV.1. Operating conditions

Mineral analyses were carried out using a Cambridge Instrument Company "Geoscan-Mark II" electron microprobe analyser at the University of Durham. The Geoscan was operated under high vacuum (0.01 mm Hg) with an acceleration voltage of 15 kV for silicate minerals, 20 kV for sulphides and a specimen current of 40 nanoamps for silicates, 20 nanoamps for sulphides.

Samples were prepared as polished mounts and polished thin sections and were simultaneously carbon-coated with the standards to ensure uniform carbon-coating. Both standards and samples were kept in a dessicator between analysing periods to prevent deterioration of the coating.

The electron beam was normally kept focussed to produce a spot analysis of diameter 2-5 microns. A slightly defocussed beam was used for plagioclase and water bearing silicate mineral analyses and a defocussed beam, several microns in diameter, for the chalcopyrite-idaite intergrowth to achieve representative combined compositions.

Secondary x-rays were analysed using a wavelength dispersive system with two single crystal spectrometers and three analysing crystals, L.I.F., P.E.T., K.A.P., which allowed simultaneous analyses of two elements. The optimum conditions for the analysed elements are given in Table IV.1. In general, 4 - 6 ten second cound accumulations were obtained and averaged for each peak and background positions and for each element. The background readings for each mineral type were used throughout each analytical period. Slits were used for Co analyses in sulphides in order to avoid interference of Fe K_{β}.

Data handling was by an on-line Varian 620L/100 computer using the programmes TIM3 and the modified version TIM4, both written by Dr.A.Peckett

TABLE IV.1

Optimum analysing conditions and standards used for electron microprobe analyses

Atomic Number	Element	Line	Analysing Crystal	Counter	Peak	Background	Standard
11	Na	$K\alpha_1$	K.A.P.	Flow	53° 15'	$\bar{+}2^\circ$	Jadeite
12	Mg	"	"	"	43° 43'	"	MgO
13	Al	"	"	"	36° 35'	"	Al_2O_3
14	Si	"	P.E.T.	"	109° 07'	"	Wollastonite
16	S	"	"	"	75° 50'	"	FeS_2
19	K	"	"	"	50° 37'	"	K-feldspar
20	Ca	"	LiF	"	113° 02'	"	Wollastonite
22	Ti	"	"	"	86° 11'	"	TiO_2
23	V	"	"	"	76° 49'	"	V_2O_5
24	Cr	"	"	"	69° 19'	"	Cr
25	Mn	"	"	"	62° 56'	"	Rhodonite
26	Fe	"	"	"	57° 23'	"	Fe,FeS_2
27	Co	"	"	"	52° 44'	"	Co
28	Ni	"	"	"	48° 30'	"	Ni
29	Cu	"	"	"	44° 52'	"	Cu
30	Zn	"	"	"	41° 36'	"	Zn
31	Ga	"	"	"	38° 41'	$\bar{+}\frac{1}{2}^\circ$	Ga_2O_3
32	Ge	"	"	"	36° 07'	$-1^\circ/+2^\circ$	Ge
33	As	$L\alpha_1$	K.A.P.	"	42° 43'	$-1^\circ/+2^\circ$	As
34	Se	"	"	"	39° 34'	$\bar{+}2^\circ$	CdSe
47	Ag	"	P.E.T.	"	59° 40'	"	Ag
48	Cd	"	"	"	53° 44'	$-1^\circ/+2^\circ$	CdSe
50	Sn	"	LiF	"	126° 41'	$\bar{+}2^\circ$	Sn
51	Sb	"	"	"	117° 30'	"	Sb
52	Te	"	"	"	109° 31'	"	Te
79	Au	"	"	"	31° 17'	"	Au
82	Pb	$M\alpha_1$	P.E.T.	"	74° 22'	-2°	PbS
83	Bi	$M_{\beta 1}$	"	"	68° 15'	"	Bi

of the Department, which perform all the necessary corrections for atomic number, mass absorption and fluorescence on peak and background data for standards and samples. The programmes estimate the water content and FeO and Fe_2O_3 contents of the appropriate analysed minerals.

The standard error for each element varies with concentration, but is approximated by :

wt% oxide/element	relative error
10 - 50	± 2%
1 - 10	± 5%
1	± 10%

Calculated detection limit for the elements are in the range 200-500 ppm.

IV.2. Silicate analyses

The results are set out in the following tables starting with "Table IV.2".

IV.3. Ore mineral analyses

The results are tabulated in the following tables starting with "Table IV.3".

TABLE IV.2.1A CLINOPYROXENE ANALYSES FROM BASALTS

	P66-1A	P66-1B	P66-1C	P66-1D	P66-1E	P66-2A	P66-2B	P66-2C	P75-1A	P75-2A	P76-1A	P76-1B
WEIGHT %												
SIO2	51.53	50.43	52.83	51.83	51.85	51.75	49.05	53.45	51.23	50.55	51.11	51.38
TIO2	0.77	1.02	0.41	0.46	0.50	0.51	1.62	0.46	0.74	1.01	0.77	0.57
AL203	2.82	3.60	2.54	3.12	3.16	2.17	5.72	2.23	3.69	4.72	3.64	3.40
FE203	0.00	0.00	0.00	0.00	0.00	0.00	0.00	0.00	0.00	0.00	0.00	0.00
FEO	8.45	8.88	4.93	5.09	5.21	6.44	8.83	6.96	6.04	6.98	7.16	6.51
MNO	0.21	0.20	0.14	0.15	0.14	0.17	0.21	0.22	0.14	0.14	0.14	0.13
MGO	15.04	14.73	17.50	16.89	17.27	17.18	14.14	17.03	16.26	16.19	15.76	15.48
CAO	21.35	21.42	22.17	22.10	21.96	21.12	20.32	20.06	21.00	19.13	20.31	21.36
NA20	0.25	0.34	0.19	0.18	0.18	0.22	0.29	0.25	0.28	0.26	0.24	0.28
K20	0.00	0.00	0.00	0.00	0.00	0.00	0.00	0.00	0.00	0.00	0.00	0.00
TOTAL	100.42	100.63	100.71	99.82	100.26	99.57	100.17	100.66	99.39	98.98	99.13	99.11
ATOMIC FORMULA - ON BASIS OF 6 OXYGENS												
SI	1.909	1.872	1.921	1.905	1.898	1.916	1.824	1.948	1.894	1.875	1.900	1.910
TI	0.021	0.029	0.011	0.013	0.013	0.014	0.045	0.013	0.021	0.028	0.021	0.016
AL	0.123	0.158	0.109	0.135	0.136	0.094	0.251	0.096	0.161	0.206	0.160	0.149
FE3+	0.000	0.000	0.000	0.000	0.000	0.000	0.000	0.000	0.000	0.000	0.000	0.000
FE2+	0.262	0.276	0.150	0.157	0.160	0.200	0.275	0.212	0.187	0.217	0.222	0.202
MN	0.007	0.006	0.004	0.004	0.004	0.006	0.007	0.007	0.004	0.004	0.004	0.004
MG	0.830	0.815	0.948	0.924	0.942	0.948	0.784	0.924	0.896	0.895	0.873	0.858
CA	0.847	0.852	0.864	0.870	0.861	0.838	0.810	0.783	0.832	0.760	0.809	0.850
NA	0.018	0.025	0.013	0.012	0.012	0.016	0.021	0.018	0.020	0.019	0.017	0.020
K	0.000	0.000	0.000	0.000	0.000	0.000	0.000	0.000	0.000	0.000	0.000	0.001
MOLECULAR PROPORTIONS												
WOLLAST.	43.12	43.97	43.91	44.16	43.80	42.92	40.51	39.40	42.17	37.55	40.59	43.14
ENSTAT.	43.25	41.86	48.43	47.76	48.06	47.16	44.06	49.29	47.86	50.29	47.35	46.01
FERROSIL.	13.63	14.17	7.66	8.09	8.14	9.92	15.43	11.31	9.97	12.17	12.06	10.85
MG-NUMBER	76.04	74.71	86.35	85.52	85.52	82.61	74.06	81.34	82.75	80.52	79.70	80.91

TABLE IV.2.1A CLINOPYROXENE ANALYSES FROM BASALTS - CONT'D

	P85-2A	P91-1B	P91-1C	P93-1A	P93-1B	P93-2A	P93-2B	P95-1A	P96-1A	P96-2A	P118-1A	P118-1B
WEIGHT %												
SIO2	50.24	51.61	51.81	52.40	50.63	49.70	50.18	50.80	52.68	50.37	50.08	50.25
TIO2	1.36	1.06	1.02	0.65	1.23	1.22	0.98	0.74	0.83	1.15	1.17	1.52
AL2O3	4.40	2.91	2.67	2.10	4.01	4.36	2.73	3.61	2.81	4.91	4.68	6.27
FE2O3	0.03	0.00	0.02	0.00	0.00	0.00	0.01	0.00	0.03	0.03	0.01	0.02
FEO	10.54	10.24	10.81	7.71	8.18	8.88	11.45	6.03	7.69	7.58	7.50	8.61
MNO	0.25	0.32	0.34	0.24	0.26	0.26	0.36	0.12	0.25	0.23	0.19	0.18
MGO	13.34	13.57	13.74	16.25	14.66	14.56	14.82	14.97	15.92	13.91	15.36	14.38
CAO	19.61	20.24	19.47	20.25	20.66	20.09	18.35	22.89	20.09	20.66	20.16	18.50
NA2O	0.48	0.44	0.44	0.28	0.29	0.40	0.21	0.16	0.28	0.31	0.29	0.34
K2O	0.02	0.00	0.01	0.00	0.00	0.00	0.01	0.00	0.02	0.02	0.00	0.01
TOTAL	100.27	100.39	100.32	99.88	99.91	99.48	99.10	99.33	100.61	99.16	99.46	100.07
ATOMIC FORMULA - ON BASIS OF 6 OXYGENS												
SI	1.875	1.922	1.931	1.937	1.881	1.861	1.899	1.890	1.930	1.878	1.861	1.852
TI	0.038	0.030	0.029	0.018	0.034	0.034	0.028	0.021	0.023	0.032	0.033	0.042
AL	0.194	0.128	0.117	0.092	0.176	0.193	0.122	0.154	0.121	0.216	0.205	0.273
FE3+	0.001	0.000	0.000	0.000	0.000	0.000	0.000	0.000	0.001	0.001	0.000	0.001
FE2+	0.329	0.319	0.337	0.238	0.254	0.278	0.362	0.188	0.236	0.236	0.233	0.265
MN	0.008	0.010	0.011	0.008	0.008	0.008	0.012	0.004	0.008	0.007	0.006	0.006
MG	0.742	0.753	0.763	0.895	0.812	0.813	0.836	0.830	0.869	0.773	0.851	0.790
CA	0.784	0.807	0.777	0.802	0.822	0.806	0.744	0.913	0.789	0.826	0.803	0.730
NA	0.035	0.032	0.032	0.020	0.021	0.029	0.015	0.012	0.020	0.022	0.021	0.024
K	0.001	0.000	0.000	0.000	0.000	0.000	0.000	0.000	0.001	0.001	0.000	0.001
MOLECULAR PROPORTIONS												
WOLLAST.	39.89	41.20	39.68	40.71	41.41	41.18	37.33	46.24	39.79	41.67	40.32	36.26
ENSTAT.	41.65	41.31	41.85	46.82	44.61	43.82	43.72	43.85	47.37	44.67	46.85	47.71
FERROSIL.	18.46	17.49	18.47	12.47	13.97	14.99	18.95	9.91	12.84	13.65	12.83	16.02
MG-NUMBER	69.29	70.26	69.38	78.97	76.15	74.51	69.76	81.56	78.67	76.59	78.50	74.86

TABLE IV.2.1A CLINOPYROXENE ANALYSES FROM BASALTS - CONT'D

	P118-1C	P118-2A	P121-1A	P121-2A	P123-1A	P123-2A	P124-1A	P124-1B	P124-2A	P132-1A	P140-1A	P140-1
WEIGHT %												
SIO2	53.12	50.14	50.04	50.60	50.69	52.14	52.21	49.92	50.78	50.80	52.77	50.05
TIO2	0.78	1.55	1.08	0.75	0.81	0.72	0.67	1.03	0.89	0.78	0.54	1.17
AL2O3	2.73	5.98	5.42	5.21	2.88	2.12	2.37	3.81	2.41	4.31	2.46	5.13
FE2O3	0.01	0.00	0.04	0.00	0.02	0.00	0.00	0.00	0.00	0.00	0.00	0.00
FEO	8.07	8.15	6.90	5.46	11.96	9.56	7.45	7.50	9.57	6.65	5.49	6.75
MNO	0.19	0.19	0.12	0.07	0.47	0.35	0.20	0.20	0.28	0.16	0.12	0.14
MGO	16.90	14.39	14.32	15.28	12.57	14.55	15.45	14.70	14.12	16.02	16.32	14.37
CAO	17.98	19.31	21.26	21.29	19.41	20.83	21.98	21.82	21.00	21.14	21.72	21.85
NA2O	0.22	0.27	0.30	0.21	0.35	0.27	0.20	0.31	0.32	0.14	0.15	0.26
K2O	0.01	0.00	0.02	0.00	0.01	0.00	0.00	0.00	0.00	0.00	0.00	0.00
TOTAL	100.02	99.98	99.50	98.87	99.16	100.54	100.52	99.29	99.37	100.01	99.57	99.72
ATOMIC FORMULA - ON BASIS OF 6 OXYGENS												
SI	1.945	1.851	1.858	1.874	1.925	1.935	1.925	1.870	1.913	1.873	1.941	1.856
TI	0.022	0.043	0.030	0.021	0.023	0.020	0.018	0.029	0.025	0.022	0.015	0.033
AL	0.118	0.260	0.237	0.228	0.129	0.093	0.103	0.168	0.107	0.188	0.107	0.224
FE3+	0.000	0.000	0.001	0.000	0.001	0.000	0.000	0.000	0.000	0.000	0.000	0.000
FE2+	0.247	0.252	0.214	0.169	0.380	0.297	0.230	0.235	0.302	0.205	0.169	0.209
MN	0.006	0.006	0.004	0.002	0.015	0.011	0.006	0.006	0.009	0.005	0.004	0.005
MG	0.923	0.792	0.792	0.843	0.711	0.305	0.849	0.821	0.793	0.880	0.894	0.794
CA	0.706	0.764	0.846	0.845	0.790	0.829	0.868	0.876	0.848	0.835	0.856	0.869
NA	0.016	0.019	0.022	0.015	0.026	0.019	0.014	0.023	0.023	0.010	0.011	0.018
K	0.000	0.000	0.001	0.000	0.001	0.000	0.000	0.000	0.000	0.000	0.000	0.000
MOLECULAR PROPORTIONS												
WOLLAST.	35.67	37.93	42.52	42.11	39.85	42.03	44.01	45.08	43.51	41.77	43.06	43.73
ENSTAT.	50.74	47.11	45.24	48.22	39.21	42.36	44.07	42.69	40.92	47.24	47.90	44.53
FERROSIL.	13.60	14.96	12.24	9.67	20.94	15.61	11.92	12.23	15.57	10.99	9.04	11.74
MG-NUMBER	78.86	75.90	78.71	83.29	65.19	73.07	78.70	77.73	72.44	81.12	84.12	79.14

TABLE IV.2.1A CLINOPYROXENE ANALYSES FROM BASALTS - CONT'D

	P161-1A	P161-1B	P161-1C	P182B-3D	P182B-3E	P182B-3F	P185A-1A	P185A-2A	P188-1B	P188-1C	P188-3C	P204-2
WEIGHT %												
SIO2	51.96	49.14	49.73	50.73	53.34	53.46	52.80	50.02	51.99	49.59	50.21	51.45
TIO2	0.52	1.25	1.04	0.96	0.47	0.46	0.77	1.45	0.60	1.06	1.09	1.04
AL2O3	2.06	3.83	3.90	4.55	2.45	2.16	2.22	4.88	2.42	5.51	4.50	3.07
FE2O3	0.00	0.00	0.00	0.00	0.00	0.00	0.00	0.00	0.03	0.01	0.51	0.00
FEO	7.38	11.47	9.47	6.10	6.02	4.61	9.31	9.53	3.34	7.50	8.19	9.48
MNO	0.16	0.31	0.25	0.11	0.15	0.05	0.26	0.24	0.25	0.08	0.24	0.27
MGO	16.00	12.32	13.64	15.63	17.08	17.01	15.20	13.40	16.00	15.21	14.16	14.84
CAO	21.61	20.46	21.12	20.93	19.89	21.31	19.33	19.83	19.24	20.28	20.01	20.02
NA2O	0.14	0.41	0.38	0.20	0.20	0.13	0.26	0.34	0.20	0.19	0.38	0.36
K2O	0.00	0.00	0.00	0.00	0.00	0.00	0.00	0.00	0.02	0.01	0.30	0.00
TOTAL	99.82	99.19	99.52	99.21	99.59	99.20	100.14	99.71	99.09	99.44	99.59	100.54
ATOMIC FORMULA - ON BASIS OF 6 OXYGENS												
SI	1.927	1.372	1.872	1.878	1.953	1.960	1.952	1.869	1.937	1.843	1.874	1.906
TI	0.014	0.036	0.029	0.027	0.013	0.013	0.021	0.041	0.017	0.030	0.031	0.029
AL	0.090	0.172	0.173	0.199	0.106	0.094	0.097	0.215	0.106	0.242	0.198	0.134
FE3+	0.000	0.000	0.000	0.000	0.000	0.000	0.000	0.000	0.001	0.000	0.014	0.000
FE2+	0.229	0.366	0.298	0.189	0.184	0.141	0.288	0.298	0.260	0.233	0.256	0.294
MN	0.005	0.010	0.008	0.003	0.005	0.002	0.008	0.008	0.008	0.003	0.008	0.009
MG	0.884	0.699	0.766	0.862	0.932	0.930	0.837	0.746	0.888	0.843	0.788	0.819
CA	0.859	0.835	0.852	0.830	0.780	0.837	0.766	0.794	0.768	0.807	0.800	0.795
NA	0.010	0.030	0.028	0.015	0.014	0.009	0.018	0.025	0.015	0.014	0.028	0.026
K	0.000	0.000	0.000	0.000	0.000	0.000	0.000	0.000	0.001	0.000	0.014	0.000
MOLECULAR PROPORTIONS												
WOLLAST.	43.49	42.94	43.91	41.35	39.53	42.55	38.97	39.82	38.33	40.03	41.13	40.41
ENSTAT.	44.89	37.48	40.37	48.10	50.49	49.86	45.42	43.01	47.67	46.98	44.45	43.86
FERROSIL.	11.62	19.58	15.72	10.54	9.98	7.59	15.61	17.16	13.95	12.99	14.43	15.73
MG-NUMBER	79.44	65.68	71.97	82.02	83.49	86.79	74.42	71.48	77.37	78.34	75.50	73.61

TABLE IV.2.1A CLINOPYROXENE ANALYSES FROM BASALTS - CONT'D

	P211B-2A	P214-1A	P286-1A	P286-1B	P286-1C	P286-1D	P286-2A	P286-2B	P286-2C
WEIGHT %									
SIO2	50.99	52.30	50.85	50.36	53.20	50.84	52.94	51.76	51.83
TIO2	0.86	0.48	0.72	1.14	0.53	1.06	0.32	0.55	0.48
AL2O3	3.60	3.12	3.11	3.24	2.01	2.95	2.23	4.08	4.05
FE2O3	0.01	0.02	0.00	0.00	0.00	0.00	0.00	0.00	0.00
FEO	7.52	5.22	8.40	10.24	6.95	9.81	4.72	5.24	4.79
MNO	0.19	0.17	0.17	0.27	0.19	0.26	0.14	0.16	0.12
MGO	15.05	16.23	14.87	13.42	16.18	13.93	17.45	16.73	16.60
CAO	21.19	21.87	21.04	20.71	20.94	20.69	21.14	20.89	21.78
NA2O	0.32	0.14	0.30	0.32	0.22	0.28	0.24	0.21	0.20
K2O	0.01	0.01	0.00	0.00	0.00	0.00	0.00	0.00	0.00
TOTAL	99.75	99.56	99.46	99.70	100.20	99.83	99.19	99.63	99.26
ATOMIC FORMULA - ON BASIS OF 6 OXYGENS									
SI	1.894	1.923	1.902	1.895	1.953	1.905	1.945	1.898	1.904
TI	0.024	0.013	0.020	0.032	0.015	0.030	0.004	0.015	0.013
AL	0.158	0.136	0.137	0.144	0.087	0.131	0.097	0.177	0.176
FE3+	0.000	0.001	0.000	0.000	0.000	0.000	0.000	0.000	0.000
FE2+	0.234	0.161	0.263	0.322	0.213	0.308	0.145	0.161	0.147
MN	0.006	0.005	0.005	0.009	0.006	0.008	0.005	0.005	0.004
MG	0.833	0.890	0.829	0.753	0.885	0.778	0.956	0.914	0.909
CA	0.843	0.862	0.843	0.835	0.823	0.831	0.832	0.821	0.834
NA	0.023	0.010	0.022	0.023	0.016	0.021	0.017	0.015	0.015
K	0.000	0.001	0.000	0.000	0.000	0.000	0.000	0.000	0.000
MOLECULAR PROPORTIONS									
WOLLAST.	42.99	43.08	43.07	42.48	41.59	42.12	42.13	41.00	41.63
ENSTAT.	44.52	48.22	43.23	40.27	47.07	41.48	50.25	50.18	50.23
FERROSIL.	12.49	8.70	13.70	17.24	11.34	16.39	7.62	8.82	8.14
MG-NUMBER	78.10	84.72	75.93	70.02	80.58	71.67	86.83	85.06	86.05

TABLE IV.2.1B CLINOPYROXENE ANALYSES FROM ANDESITES

	P80-1A	P104-2A	P206-1C	P206-1D	P206-2D	P206-2E	P243-1A	P243-1B	P243-2A	P243-2B	P245-1F	P245-3	P245-3D
WEIGHT %													
SIO2	50.92	51.47	50.62	52.45	51.73	51.93	49.87	51.61	51.68	51.09	50.10	50.18	50.22
TIO2	0.85	0.78	1.22	0.62	0.66	0.67	1.44	0.79	0.92	1.02	1.29	1.23	1.32
AL2O3	1.99	2.29	3.40	1.58	1.50	1.80	4.01	1.58	2.35	2.65	4.01	3.59	3.91
FE2O3	0.00	0.01	0.00	0.00	0.00	0.00	0.00	0.00	0.00	0.00	0.00	0.00	0.00
FEO	11.01	11.99	10.34	10.27	11.00	10.40	11.01	11.62	11.13	10.77	10.50	9.50	10.11
MNO	0.37	0.37	0.30	0.32	0.39	0.35	0.26	0.34	0.34	0.27	0.89	0.13	0.25
MGO	13.79	14.41	13.62	14.98	15.69	14.85	13.50	14.54	14.67	14.47	13.03	13.98	13.39
CAO	20.30	18.19	20.02	19.06	18.29	19.62	19.22	18.77	19.18	19.40	20.00	20.40	19.65
NA2O	0.36	0.36	0.38	0.26	0.30	0.37	0.47	0.22	0.30	0.25	0.32	0.42	0.42
K2O	0.00	0.01	0.00	0.00	0.00	0.00	0.00	0.00	0.00	0.00	0.00	0.00	0.00
TOTAL	99.59	99.89	99.91	99.54	99.56	100.01	99.79	99.48	100.57	99.91	100.12	99.43	99.27
ATOMIC FORMULA - ON BASIS OF 6 OXYGENS													
SI	1.924	1.932	1.897	1.961	1.941	1.940	1.875	1.945	1.924	1.913	1.880	1.885	1.890
TI	0.024	0.022	0.034	0.017	0.019	0.019	0.041	0.023	0.026	0.029	0.036	0.035	0.037
AL	0.089	0.102	0.150	0.070	0.067	0.080	0.178	0.070	0.103	0.117	0.177	0.159	0.174
FE3+	0.000	0.000	0.000	0.000	0.000	0.000	0.000	0.000	0.000	0.000	0.000	0.000	0.000
FE2+	0.348	0.376	0.324	0.321	0.345	0.325	0.346	0.366	0.346	0.337	0.329	0.299	0.318
MN	0.012	0.012	0.010	0.010	0.012	0.011	0.008	0.011	0.011	0.008	0.028	0.004	0.008
MG	0.776	0.806	0.761	0.835	0.878	0.827	0.756	0.816	0.814	0.807	0.729	0.783	0.751
CA	0.822	0.732	0.804	0.764	0.736	0.786	0.774	0.758	0.765	0.779	0.804	0.821	0.793
NA	0.027	0.027	0.028	0.019	0.022	0.027	0.034	0.016	0.022	0.018	0.023	0.031	0.031
K	0.000	0.000	0.000	0.000	0.000	0.000	0.000	0.000	0.000	0.000	0.000	0.000	0.000
MOLECULAR PROPORTIONS													
WOLLAST.	42.33	37.10	40.82	38.65	37.48	40.30	39.47	38.17	38.72	39.20	40.24	42.16	40.10
ENSTAT.	39.83	42.88	41.50	44.30	44.87	42.85	41.53	42.69	42.98	42.89	41.15	41.87	42.07
FERROSIL.	17.84	20.02	17.68	17.05	17.65	16.84	19.01	19.14	18.30	17.92	18.61	15.97	17.83
MG-NUMBER	69.06	68.16	70.13	72.21	71.77	71.78	68.60	69.04	70.14	70.53	68.86	72.39	70.23

TABLE IV.2.1C CLINOPYROXENE ANALYSES FROM GABBROS

	P239-1F	P239-2E	P239-3D	P255-3B	P258-1A	P258-2A	P258-2C	P258-3A	P272-1C	P272-2B	P277-1A	P277-2
WEIGHT %												
SIO2	51.94	52.10	52.68	51.97	51.59	53.14	53.11	51.84	52.78	50.87	50.37	51.18
TIO2	0.69	0.43	0.39	0.45	0.58	0.42	0.49	0.59	0.99	1.45	1.26	0.92
AL2O3	2.64	2.93	2.49	1.99	2.33	2.06	2.08	2.44	2.25	3.38	2.80	1.90
FE2O3	0.00	0.02	0.00	0.01	0.00	0.00	0.00	0.00	0.01	0.02	0.00	0.00
FEO	7.27	5.46	5.35	6.39	8.25	5.79	6.91	8.50	10.64	10.40	10.56	11.09
MNO	0.22	0.17	0.14	0.17	0.22	0.19	0.21	0.27	0.39	0.27	0.31	0.34
MGO	14.98	16.09	16.82	16.87	15.45	16.38	16.31	15.10	13.70	13.28	13.05	13.15
CAO	21.68	21.96	22.07	21.84	20.94	21.43	20.37	20.10	19.64	19.70	20.77	20.35
NA2O	0.23	0.27	0.21	0.18	0.24	0.14	0.29	0.25	0.33	0.41	0.34	0.29
K2O	0.00	0.01	0.00	0.00	0.00	0.00	0.00	0.00	0.01	0.01	0.00	0.00
TOTAL	99.67	99.46	100.15	99.88	99.61	99.53	99.76	99.09	100.73	99.77	99.46	99.24
ATOMIC FORMULA - ON BASIS OF 6 OXYGENS												
SI	1.928	1.923	1.929	1.921	1.923	1.956	1.955	1.938	1.954	1.906	1.904	1.940
TI	0.019	0.012	0.011	0.013	0.016	0.012	0.014	0.017	0.028	0.041	0.036	0.027
AL	0.116	0.128	0.108	0.087	0.102	0.089	0.090	0.108	0.098	0.149	0.125	0.084
FE3+	0.000	0.001	0.000	0.000	0.000	0.000	0.000	0.000	0.000	0.001	0.000	0.000
FE2+	0.226	0.169	0.164	0.198	0.257	0.178	0.213	0.266	0.330	0.326	0.334	0.352
MN	0.007	0.005	0.004	0.005	0.007	0.006	0.007	0.009	0.012	0.009	0.010	0.011
MG	0.829	0.885	0.918	0.929	0.858	0.898	0.895	0.841	0.756	0.741	0.735	0.743
CA	0.862	0.869	0.866	0.865	0.836	0.845	0.803	0.805	0.779	0.791	0.841	0.826
NA	0.017	0.019	0.015	0.013	0.017	0.010	0.021	0.018	0.023	0.030	0.025	0.022
K	0.000	0.001	0.000	0.000	0.000	0.000	0.000	0.000	0.000	0.001	0.000	0.000
MOLECULAR PROPORTIONS												
WOLLAST.	43.57	44.19	43.95	44.23	42.57	42.62	40.76	40.51	40.19	40.37	42.95	41.93
ENSTAT.	44.36	46.88	47.57	45.99	44.19	47.88	47.86	45.21	41.65	41.42	39.23	39.41
FERROSIL.	12.08	8.93	8.48	9.78	13.24	9.50	11.38	14.28	18.16	18.20	17.82	18.66
MG-NUMBER	78.60	84.00	84.86	82.46	76.94	83.45	80.79	76.00	69.64	69.47	68.77	67.87

TABLE IV.2.1C CLINOPYROXENE ANALYSES FROM GABBROS - CONT'D

	P277-2D	P279B-2B	P281-1C	P281-3A	P281-3B
WEIGHT %					
SIO2	51.67	51.60	52.17	52.65	52.45
TIO2	0.69	0.59	0.52	0.52	0.61
AL2O3	1.63	3.38	1.01	0.96	1.18
FE2O3	0.00	0.01	0.00	0.00	0.00
FEO	11.30	5.81	12.70	13.53	12.78
MNO	0.36	0.14	0.25	0.31	0.29
MGO	13.72	16.19	12.43	12.94	12.79
CAO	20.55	21.86	20.01	18.90	19.71
NA2O	0.33	0.26	0.34	0.44	0.51
K2O	0.00	0.01	0.00	0.00	0.00
TOTAL	100.26	99.87	99.44	100.25	100.32
ATOMIC FOLMULA - ON BASIS OF 6 OXYGENS					
SI	1.940	1.901	1.981	1.983	1.973
TI	0.020	0.017	0.015	0.015	0.017
AL	0.072	0.147	0.045	0.043	0.053
FE3+	0.000	0.000	0.000	0.000	0.000
FE2+	0.355	0.179	0.403	0.426	0.402
MN	0.012	0.005	0.008	0.010	0.009
MG	0.768	0.889	0.703	0.726	0.717
CA	0.827	0.863	0.814	0.763	0.794
NA	0.024	0.019	0.025	0.032	0.037
K	0.000	0.000	0.000	0.000	0.000
MOLECULAR PROPORTIONS					
WOLLAST.	42.44	43.98	41.83	39.34	41.15
ENSTAT.	39.37	46.62	36.96	38.23	37.71
FERROSIL.	18.20	9.40	21.20	22.43	21.14
MG-NUMBER	68.39	83.23	63.55	63.02	64.08

TABLE IV.2.2A ACTINOLITE (FIBROUS AMPHIBOLE) ANALYSES FROM POLUSAGI

	P239-1A2	P239-2A	P248-1B	P248-2A	P253-1A	P253-2A	P253-2B	P253-3D	P254-1D	P254-2A	P256-1A	P256-2A
WEIGHT %												
SIO2	51.81	51.65	48.69	49.04	48.61	50.98	50.51	49.18	50.82	52.36	50.57	51.69
TIO2	0.23	0.32	0.24	0.26	0.91	0.45	0.55	0.43	0.34	0.20	0.47	0.32
AL2O3	1.90	3.03	4.98	4.76	4.63	3.94	4.34	3.95	4.36	2.01	4.12	4.04
FE2O3	4.64	2.15	5.03	6.65	6.51	5.63	4.77	5.37	2.74	0.62	0.45	4.44
FEO	15.34	15.07	17.41	14.65	13.37	11.68	14.05	12.82	15.92	21.39	19.83	12.43
MNO	0.49	0.41	0.38	0.44	0.47	0.41	0.32	0.38	0.36	0.39	0.59	0.70
MGO	12.07	12.10	10.24	12.06	11.84	13.23	11.60	12.35	10.63	9.27	9.39	13.32
CAO	11.05	11.80	9.70	9.42	10.49	11.25	11.76	10.32	11.02	12.08	10.93	10.94
NA2O	0.47	0.55	0.38	0.40	0.52	0.61	0.51	0.57	0.74	0.31	0.38	0.61
K2O	0.11	0.13	0.08	0.09	0.02	0.06	0.07	0.05	0.07	0.06	0.00	0.02
H2O	2.04	2.03	2.00	2.03	2.02	2.07	2.05	2.00	2.02	2.02	1.99	2.08
TOTAL	100.14	99.25	99.12	99.81	99.40	100.30	100.51	97.40	99.02	100.71	98.73	100.59
ATOMIC FORMULA - ON BASIS OF 24 OXYGENS AND 2 HYDROGENS												
SI	7.631	7.624	7.311	7.252	7.207	7.399	7.384	7.386	7.541	7.790	7.611	7.468
TI	0.025	0.035	0.027	0.029	0.102	0.050	0.060	0.048	0.038	0.023	0.053	0.035
AL	0.330	0.528	0.882	0.831	0.810	0.674	0.747	0.700	0.763	0.352	0.732	0.688
FE3+	0.514	0.239	0.568	0.740	0.727	0.615	0.524	0.607	0.306	0.070	0.052	0.483
FE2+	1.889	1.861	2.186	1.812	1.658	1.417	1.717	1.611	1.976	2.661	2.496	1.502
MN	0.062	0.051	0.048	0.056	0.059	0.050	0.040	0.048	0.045	0.049	0.076	0.086
MG	2.650	2.662	2.291	2.657	2.617	2.862	2.527	2.765	2.350	2.055	2.107	2.869
CA	1.743	1.866	1.562	1.492	1.667	1.749	1.841	1.660	1.752	1.926	1.762	1.693
NA	0.133	0.157	0.120	0.115	0.150	0.173	0.146	0.166	0.214	0.089	0.111	0.172
K	0.021	0.025	0.016	0.017	0.004	0.012	0.013	0.009	0.014	0.011	0.001	0.004
H	2.000	2.000	2.000	2.000	2.000	2.000	2.000	2.000	2.000	2.000	2.000	2.000
STRUCTURAL FORMULA												
Z	8.000	8.000	8.000	8.000	8.000	8.000	8.000	8.000	8.000	8.000	8.000	8.000
Y	5.000	5.000	5.000	5.000	5.000	5.000	5.000	5.000	5.000	5.000	5.000	5.000
X	1.976	2.000	1.984	1.983	1.996	1.988	1.987	1.991	1.986	2.000	1.999	1.996
A	0.021	0.048	0.016	0.017	0.004	0.012	0.013	0.009	0.014	0.026	0.001	0.004
MG-NO.	58.37	58.86	51.17	59.46	61.22	66.88	59.53	63.18	54.32	43.57	45.78	65.64

TABLE IV.2.2A ACTINOLITE (FIBROUS AMPHIBOLE) ANALYSES FROM POLUSAGI - CONT'D

	P271-1C	P271-2A	P272-1B	P272-3A	P276-1D	P276-2D	P276-2E	P276-3B	P276-2F	P277-1B	P277-2B	P277-2C
WEIGHT %												
SIO2	50.41	50.26	50.56	51.51	50.25	52.14	51.72	51.98	51.30	50.69	51.22	51.71
TIO2	0.27	0.40	0.14	0.18	0.43	0.29	0.22	0.69	0.27	0.45	0.47	0.38
AL2O3	4.40	3.68	3.57	4.05	4.08	2.50	3.08	4.04	2.84	2.25	1.76	1.65
FE2O3	0.50	2.71	1.13	0.00	3.90	2.02	1.53	1.70	3.13	4.53	2.39	2.50
FEO	17.56	15.93	21.01	22.33	16.65	16.10	16.10	15.14	16.19	17.69	18.87	20.14
MNO	0.33	0.24	0.53	0.47	0.32	0.28	0.24	0.29	0.27	0.39	0.51	0.47
MGO	11.98	11.24	9.95	10.02	10.29	12.59	12.67	12.49	11.69	10.73	10.84	10.55
CAO	9.64	11.18	8.76	8.49	11.19	11.06	10.81	11.32	11.34	10.81	10.39	10.41
NA2O	0.19	0.35	0.44	0.28	0.55	0.29	0.23	0.45	0.32	0.36	0.30	0.26
K2O	0.04	0.10	0.05	0.04	0.07	0.05	0.05	0.09	0.06	0.10	0.11	0.07
H2O	1.99	2.00	1.98	2.00	2.02	2.03	2.03	2.06	2.02	2.01	1.99	2.01
TOTAL	97.31	98.09	98.11	99.35	99.74	99.35	98.67	100.26	99.45	100.01	98.85	100.16
ATOMIC FORMULA - ON BASIS OF 24 OXYGENS AND 2 HYDROGENS												
SI	7.581	7.538	7.671	7.702	7.463	7.685	7.659	7.557	7.599	7.558	7.709	7.716
TI	0.031	0.045	0.016	0.020	0.048	0.032	0.025	0.076	0.030	0.051	0.054	0.043
AL	0.781	0.651	0.639	0.713	0.715	0.435	0.538	0.693	0.496	0.396	0.313	0.290
FE3+	0.056	0.306	0.129	0.000	0.436	0.224	0.171	0.186	0.349	0.509	0.271	0.281
FE2+	2.209	1.998	2.665	2.792	2.069	1.984	1.994	1.841	2.006	2.205	2.375	2.513
MN	0.042	0.031	0.068	0.059	0.040	0.035	0.030	0.036	0.033	0.049	0.065	0.060
MG	2.684	2.513	2.249	2.232	2.277	2.765	2.795	2.706	2.582	2.384	2.431	2.345
CA	1.553	1.796	1.423	1.360	1.780	1.747	1.715	1.763	1.800	1.727	1.675	1.664
NA	0.054	0.103	0.131	0.081	0.159	0.083	0.065	0.127	0.092	0.103	0.088	0.074
K	0.008	0.019	0.010	0.009	0.013	0.010	0.009	0.016	0.012	0.019	0.020	0.014
H	2.000	2.000	2.000	1.996	2.000	2.000	2.000	2.000	2.000	2.000	2.000	2.000
STRUCTURAL FORMULA												
Z	8.000	8.000	8.000	8.000	8.000	8.000	8.000	8.000	8.000	8.000	8.000	8.000
Y	5.000	5.000	5.000	5.000	5.000	5.000	5.000	5.000	5.000	5.000	5.000	5.000
X	1.992	1.981	1.990	1.960	1.986	1.990	1.991	1.984	1.988	1.981	1.980	1.986
A	0.008	0.019	0.010	0.009	0.013	0.010	0.009	0.016	0.012	0.019	0.020	0.014
MG-NO.	54.86	55.70	45.77	44.43	52.40	58.22	58.37	59.52	56.28	51.95	50.58	48.27

TABLE IV.2.2A ACTINOLITE (FIBROUS AMPHIBOLE) ANALYSES FROM POLUSAGI - CONT'D

	P277-2E	P280-2A	P280-3B	P287-1A	P287-2A
WEIGHT %					
SIO2	49.29	50.07	52.11	48.28	48.81
TIO2	0.26	0.41	0.42	0.52	0.31
AL2O3	4.03	4.09	3.00	5.92	5.99
FE2O3	4.62	1.84	0.00	4.97	4.04
FEO	19.04	16.01	19.06	11.69	12.72
MNO	0.47	0.29	0.52	0.38	0.36
MGO	9.70	11.76	10.37	13.66	13.27
CAO	8.96	10.56	10.84	9.29	9.10
NA2O	0.59	0.29	0.34	0.37	0.47
K2O	0.08	0.06	0.05	0.04	0.03
H2O	1.99	1.99	2.00	2.01	2.01
TOTAL	99.01	97.37	98.72	97.12	97.10
ATOMIC FORMULA - ON BASIS OF 24 OXYGENS AND 2 HYDROGENS					
SI	7.443	7.534	7.785	7.201	7.281
TI	0.029	0.047	0.047	0.058	0.035
AL	0.718	0.726	0.528	1.041	1.054
FE3+	0.525	0.209	0.000	0.558	0.454
FE2+	2.404	2.015	2.382	1.458	1.587
MN	0.061	0.037	0.066	0.048	0.046
MG	2.184	2.636	2.309	3.036	2.950
CA	1.449	1.702	1.735	1.484	1.454
NA	0.172	0.084	0.100	0.108	0.135
K	0.015	0.011	0.009	0.008	0.005
H	2.000	2.000	1.995	2.000	2.000
STRUCTURAL FORMULA					
Z	8.000	8.000	8.000	8.000	8.000
Y	5.000	5.000	5.000	5.000	5.000
X	1.985	1.989	1.952	1.992	1.949
A	0.015	0.011	0.009	0.008	0.005
MG-NO.	47.59	56.68	49.23	67.55	65.02

TABLE IV.2.2B 'GREEN AMPHIBOLE' ANALYSES FROM POLUSAGI

	P239-1D	P239-3A	P239-3C	P246-1C	P246-2C	P255-2D	P258-1B	P258-2B	P273-1D	P273-3A	P279B-1B	P279B-2C
WEIGHT %												
SIO2	52.93	52.30	52.86	52.27	52.94	51.06	50.58	49.88	51.32	47.56	53.17	49.14
TIO2	0.57	0.68	0.37	0.89	0.70	0.77	0.86	0.86	0.77	0.23	0.06	0.56
AL2O3	2.35	3.17	2.52	3.02	2.84	2.71	3.52	3.66	5.44	7.42	2.70	6.59
FE2O3	5.52	5.58	4.21	6.06	6.10	8.42	8.02	9.39	4.58	11.93	4.73	4.96
FEO	8.84	8.16	10.95	5.26	5.19	8.69	10.47	10.90	9.88	3.97	7.71	7.41
MNO	0.34	0.28	0.44	0.20	0.20	0.32	0.41	0.41	0.28	0.30	0.22	0.22
MGO	15.68	15.42	14.14	17.28	17.64	14.94	12.97	12.40	14.06	14.44	17.32	15.67
CAO	11.17	11.27	11.06	11.55	11.52	9.40	10.01	8.96	10.72	10.24	10.81	12.30
NA2O	0.76	0.85	0.87	0.81	0.72	1.13	1.17	1.41	0.99	2.07	0.54	1.35
K2O	0.16	0.16	0.15	0.23	0.18	0.18	0.24	0.26	0.05	0.12	0.02	0.08
H2O	2.10	2.09	2.07	2.11	2.12	2.07	2.06	2.05	2.09	2.09	2.10	2.09
TOTAL	100.40	99.96	99.65	99.67	100.15	99.69	100.33	100.18	100.19	100.37	99.38	100.37
ATOMIC FORMULA - ON BASIS OF 24 OXYGENS AND 2 HYDROGENS												
SI	7.564	7.492	7.652	7.436	7.480	7.402	7.354	7.298	7.353	6.827	7.590	7.035
TI	0.061	0.073	0.041	0.095	0.074	0.084	0.094	0.094	0.083	0.025	0.006	0.060
AL	0.396	0.535	0.430	0.506	0.473	0.463	0.604	0.632	0.920	1.257	0.455	1.113
FE3+	0.594	0.602	0.459	0.649	0.649	0.919	0.878	1.034	0.494	1.288	0.508	0.535
FE2+	1.056	0.977	1.326	0.626	0.613	1.054	1.274	1.333	1.184	0.476	0.921	0.887
MN	0.041	0.034	0.053	0.024	0.024	0.040	0.050	0.050	0.034	0.037	0.026	0.026
MG	3.339	3.292	3.051	3.664	3.714	3.227	2.810	2.703	3.002	3.090	3.686	3.343
CA	1.710	1.729	1.715	1.760	1.744	1.460	1.559	1.404	1.646	1.576	1.653	1.886
NA	0.210	0.236	0.246	0.222	0.197	0.317	0.331	0.401	0.274	0.576	0.350	0.375
K	0.029	0.030	0.028	0.042	0.032	0.034	0.045	0.049	0.009	0.023	0.004	0.014
H	2.000	2.000	2.000	2.000	2.000	2.000	2.000	2.000	2.000	2.000	2.000	2.000
STRUCTURAL FORMULA												
Z	8.000	8.000	8.000	8.000	8.000	8.000	8.000	8.000	8.000	8.000	8.000	8.000
Y	5.000	5.000	5.000	4.999	5.000	5.000	5.000	5.000	5.000	5.000	5.000	5.000
X	1.970	1.970	1.972	1.983	1.968	1.965	1.955	1.951	1.989	2.000	1.995	2.000
A	0.029	0.030	0.028	0.042	0.032	0.034	0.045	0.049	0.009	0.174	0.004	0.275
MG-NO.	75.97	77.11	69.71	85.41	85.83	75.39	68.81	66.97	71.71	86.65	80.01	79.02

TABLE IV.2.2B 'GREEN AMPHIBOLE' ANALYSES FROM POLUSAGI - CONT'D

	P282-1A	P282-2B	P282-2C
WEIGHT %			
SIO2	47.47	50.94	49.19
TIO2	1.33	0.54	0.98
AL2O3	6.82	4.84	5.74
FE2O3	4.68	7.82	7.57
FEO	12.12	8.47	9.46
MNO	0.23	0.27	0.32
MGO	12.12	13.77	12.52
CAO	11.13	10.50	10.14
NA2O	1.81	1.31	1.61
K2O	0.16	0.08	0.09
H2O	2.04	2.09	2.06
TOTAL	99.91	100.63	99.69
ATOMIC FORMULA - ON BASIS OF 24 OXYGENS AND 2 HYDROGENS			
SI	6.978	7.301	7.166
TI	0.147	0.059	0.107
AL	1.182	0.817	0.987
FE3+	0.518	0.843	0.830
FE2+	1.490	1.015	1.152
MN	0.029	0.032	0.039
MG	2.656	2.941	2.719
CA	1.753	1.613	1.583
NA	0.515	0.364	0.455
K	0.031	0.015	0.017
H	2.000	2.000	2.000
STRUCTURAL FORMULA			
Z	8.000	8.000	8.000
Y	5.000	5.000	5.000
X	2.000	1.985	2.000
A	0.298	0.015	0.054
MG-NO.	64.06	74.34	70.23

TABLE IV.2.2C BROWN AMPHIBOLE (HORNBLENDE) ANALYSES FROM POLUSAGI

	P246-1A1	P246-1A2	P255-2E	P255-3A	P273-3B	P279B-1A	P279B-2A	P281-1A	P281-1B	P281-2A	P282-1B	P282-2A
WEIGHT %												
SIO2	43.98	44.35	43.46	44.18	45.48	42.86	42.81	47.25	47.26	47.41	44.80	44.51
TIO2	3.65	3.60	2.87	2.47	2.48	3.44	3.95	1.79	1.76	1.88	3.20	3.38
AL2O3	9.00	9.10	10.17	9.01	7.41	10.69	10.12	5.44	5.26	5.49	9.36	9.69
FE2O3	4.30	4.34	8.20	7.24	7.51	1.93	0.00	8.79	9.44	10.06	2.93	4.35
FEO	7.56	7.66	6.56	8.59	7.24	9.09	10.80	8.61	8.44	7.73	11.85	10.51
MNO	0.17	0.16	0.22	0.26	0.11	0.17	0.15	0.21	0.22	0.24	0.17	0.23
MGO	14.79	14.75	13.24	12.44	13.95	14.42	13.97	13.36	12.85	13.17	12.00	12.22
CAO	11.12	11.15	10.52	10.39	9.96	11.98	12.15	9.80	10.01	9.73	10.70	10.65
NA2O	2.81	2.77	2.59	2.46	2.76	2.65	2.59	2.74	1.85	2.23	2.64	2.51
K2O	0.35	0.38	0.20	0.21	0.51	0.61	0.49	0.20	0.24	0.24	0.24	0.28
H2O	2.05	2.07	2.06	2.03	2.05	2.05	2.02	2.05	2.04	2.06	2.04	2.05
TOTAL	99.78	100.34	100.07	99.29	99.45	99.89	99.07	100.25	99.37	100.26	99.94	100.39
ATOMIC FORMULA - ON BASIS OF 24 OXYGENS AND 2 HYDROGENS												
SI	6.419	6.435	6.336	6.523	0.000	6.278	6.341	0.000	6.959	6.912	6.588	6.505
TI	0.400	0.393	0.315	0.274	6.668	0.379	0.440	6.908	0.195	0.207	0.354	0.371
AL	1.549	1.557	1.748	1.570	0.273	1.847	1.768	0.197	0.914	0.944	1.624	1.670
FE3+	0.472	0.474	0.899	0.804	1.281	0.213	0.000	0.938	1.046	1.104	0.324	0.479
FE2+	0.923	0.930	0.800	1.061	0.829	1.114	1.338	0.967	1.039	0.943	1.458	1.285
MN	0.021	0.020	0.027	0.033	0.887	0.021	0.019	1.053	0.027	0.030	0.022	0.029
MG	3.216	3.190	2.875	2.736	0.014	3.148	3.084	0.026	2.820	2.861	2.430	2.661
CA	1.740	1.733	1.643	1.644	3.048	1.880	1.928	2.912	1.579	1.520	1.687	1.669
NA	0.796	0.780	0.731	0.705	1.564	0.753	0.743	1.535	0.529	0.631	0.752	0.711
K	0.066	0.070	0.038	0.039	0.785	0.114	0.092	0.778	0.044	0.045	0.044	0.052
H	2.000	2.000	2.000	2.000	0.095	2.000	1.999	0.038	2.000	2.000	2.000	2.000
STRUCTURAL FORMULA												
Z	8.000	8.000	8.000	8.000	2.000	8.000	8.000	2.000	8.000	8.000	8.000	8.000
Y	5.000	4.999	5.000	5.000	8.000	5.000	4.990	8.000	5.000	5.000	4.999	5.000
X	2.000	2.000	2.000	2.000	2.000	2.000	2.000	2.000	2.000	2.000	2.000	2.000
A	0.602	0.583	0.411	0.388	0.444	0.746	0.763	0.351	0.159	0.196	0.483	0.432
MG-NO.	77.69	77.43	78.24	72.06	77.46	73.87	69.74	73.45	73.08	75.21	64.34	67.44

TABLE IV.2.3A CHLORITE ANALYSES FROM BASALTS

	P50-1A	P50-2A	P50-2B	P76-3A	P91-1A	P93-3A	P93-3B	P93-3C	P93-3D	P93-1D	P118-1D	P123-1C
WEIGHT %												
SIO2	29.00	28.08	28.55	30.05	28.60	27.03	27.13	28.56	28.32	29.81	29.16	28.81
TIO2	0.00	0.01	0.00	0.00	0.02	0.00	0.00	0.00	0.00	0.00	0.00	0.06
AL2O3	16.52	16.78	16.83	17.45	16.81	17.90	17.88	16.19	16.35	14.75	15.73	15.78
FE2O3	0.00	0.00	0.00	0.00	0.00	0.00	0.00	0.00	0.00	0.00	0.00	0.00
FEO	23.13	23.26	22.66	15.53	27.82	25.06	24.71	24.84	24.80	24.11	23.42	25.55
MNO	0.51	0.42	0.38	0.53	0.59	0.56	0.58	0.58	0.47	0.46	0.24	0.42
MGO	17.53	17.39	17.31	22.48	13.69	16.15	15.84	16.11	16.02	17.27	17.98	15.49
CAO	0.27	0.32	0.31	0.19	0.32	0.10	0.08	0.43	0.34	0.41	0.17	0.52
NA2O	0.00	0.00	0.00	0.00	0.06	0.01	0.00	0.00	0.00	0.02	0.00	0.02
K2O	0.01	0.02	0.01	0.01	0.01	0.01	0.00	0.05	0.05	0.04	0.01	0.02
H2O	11.43	11.31	11.33	11.83	11.27	11.25	11.20	11.27	11.22	11.35	11.39	11.23
TOTAL	98.40	97.60	97.37	98.08	99.18	98.07	97.43	98.04	97.57	98.23	98.11	97.89
ATOMIC FORMULA - ON BASIS OF 36 OXYGENS AND 16 HYDROGENS												
SI	6.086	5.959	6.044	6.091	6.088	5.763	5.810	6.080	6.055	6.300	6.143	6.157
TI	0.000	0.002	0.000	0.000	0.004	0.000	0.000	0.000	0.000	0.000	0.000	0.010
AL VI	1.914	2.041	1.957	1.909	1.912	2.238	2.190	1.920	1.945	1.700	1.858	1.843
AL IV	2.175	2.159	2.244	2.263	2.308	2.262	2.327	2.144	2.177	1.976	2.051	2.133
FE3+	0.000	0.000	0.000	0.000	0.000	0.000	0.000	0.000	0.000	0.000	0.000	0.000
FE2+	4.060	4.127	4.011	2.634	4.953	4.467	4.426	4.422	4.435	4.262	4.126	4.567
MN	0.090	0.076	0.069	0.092	0.106	0.101	0.105	0.105	0.085	0.083	0.043	0.077
MG	5.484	5.498	5.461	6.792	4.342	5.132	5.055	5.111	5.103	3.438	5.643	4.933
CA	0.060	0.074	0.069	0.042	0.073	0.023	0.018	0.099	0.079	0.094	0.040	0.118
NA	0.000	0.002	0.000	0.000	0.024	0.003	0.000	0.000	0.000	0.009	0.000	0.008
K	0.002	0.005	0.003	0.002	0.003	0.001	0.000	0.014	0.014	0.010	0.002	0.007
H	16.000	16.000	16.000	16.000	16.000	16.000	16.000	16.000	16.000	16.000	16.000	16.000
STRUCTURAL FORMULA												
Z	8.000	8.000	8.000	8.000	8.000	8.000	8.000	8.000	8.000	8.000	8.000	8.000
Y	11.871	11.943	11.948	11.824	11.813	11.989	11.932	11.895	11.891	11.871	11.905	11.852
MG-NO.	57.46	57.12	57.65	72.06	46.71	53.46	53.32	53.61	53.50	56.06	57.76	51.93
TYPE	BLUISH	BLUISH	BLUISH	BROWN.	GREEN.	BLUISH	BLUISH	GREEN.	GREEN.	GREEN.	BLUISH	GREEN.
ZONE	A	A	A	A	A	A	A	A	A	A	A	A
MIN. ?	NO	NO	NO	NO	NO	NO	NO	NO	NO	NO	NO	NO

	P124-1D	P124-2C	P155B-1A	P161-1D	P161-1H	P168-1I	P168-2F	P183-1B	P183-1A	P185A-1B	P185A-2B	P189-2B
WEIGHT %												
SIO2	27.63	27.81	27.13	28.13	28.16	28.65	29.13	27.58	29.26	26.08	27.37	26.92
TIO2	0.00	0.01	0.02	0.01	0.00	0.00	0.00	0.03	0.00	0.01	0.00	0.07
AL2O3	17.35	17.56	18.96	15.82	16.36	15.78	15.27	17.41	13.57	18.06	17.12	21.12
FE2O3	0.00	0.00	0.00	0.00	0.00	0.00	0.00	0.00	0.00	0.34	0.00	0.00
FEO	25.93	25.73	25.21	27.56	27.08	26.39	26.06	25.05	25.77	29.33	29.18	22.32
MNO	0.36	0.36	2.06	0.37	0.34	0.42	0.42	0.34	0.19	0.83	0.00	2.05
MGO	15.20	15.29	13.66	14.55	14.72	15.48	15.91	15.97	17.15	12.36	13.33	15.19
CAO	0.32	0.38	0.07	0.18	0.19	0.21	0.27	0.21	0.14	0.21	0.12	0.06
NA2O	0.00	0.00	0.05	0.00	0.00	0.01	0.00	0.00	0.00	0.08	0.00	0.00
K2O	0.01	0.01	0.07	0.02	0.02	0.02	0.02	0.01	0.00	0.10	0.01	0.15
H2O	11.22	11.29	11.24	11.10	11.17	11.22	11.26	11.25	11.10	11.01	11.09	11.52
TOTAL	98.02	98.42	98.46	97.74	98.04	98.19	98.33	97.83	97.21	98.40	98.22	99.40
ATOMIC FORMULA - ON BASIS OF 36 OXYGENS AND 16 HYDROGENS												
SI	5.908	5.912	5.791	6.081	6.049	6.126	6.206	5.883	6.305	5.682	5.922	5.605
TI	0.000	0.001	0.003	0.001	0.000	0.000	0.000	0.004	0.000	0.001	0.000	0.011
AL VI	2.092	2.088	2.210	1.919	1.951	1.875	1.794	2.117	1.695	2.318	2.078	2.395
AL IV	2.283	2.314	2.565	2.116	2.194	2.105	2.042	2.263	1.754	2.322	2.289	2.789
FE3+	0.000	0.000	0.000	0.000	0.000	0.000	0.000	0.000	0.000	0.055	0.000	0.000
FE2+	4.636	4.574	4.501	4.984	4.865	4.717	4.644	4.469	4.643	5.344	5.279	3.886
MN	0.066	0.065	0.372	0.067	0.063	0.076	0.076	0.062	0.035	0.154	0.000	0.361
MG	4.845	4.844	4.344	4.688	4.712	4.933	5.051	5.077	5.507	4.015	4.298	4.712
CA	0.074	0.087	0.014	0.041	0.043	0.049	0.061	0.047	0.032	0.048	0.028	0.014
NA	0.000	0.000	0.020	0.000	0.000	0.005	0.000	0.000	0.000	0.034	0.000	0.000
K	0.002	0.002	0.018	0.006	0.006	0.005	0.004	0.002	0.000	0.028	0.003	0.039
H	16.000	16.000	16.000	16.000	16.000	16.000	16.000	16.000	16.000	16.000	16.000	16.000
STRUCTURAL FORMULA												
Z	8.000	8.000	8.000	8.000	8.000	8.000	8.000	8.000	8.000	8.000	8.000	8.000
Y	11.906	11.887	11.839	11.904	11.881	11.890	11.878	11.924	11.971	12.000	11.897	11.812
MG-NO.	51.10	51.43	49.11	48.47	49.20	51.12	52.10	53.18	54.25	42.90	44.88	54.80
TYPE	BLUISH	BLUISH	BLUISH	GREEN.	GREEN.	GREEN.	GREEN.	BLUISH	BLUISH	GREEN.	GREEN.	BROWN.
ZONE	A	A	B	A	A	A	A	A	A	A	A	A
MIN. ?	NO	NO	YES	NO	NO	NO	NO	NO	NO	YES	YES	YES

TABLE IV.2.3A CHLORITE ANALYSES FROM BASALTS - CONT'D

	P204-1A	P204-2A	P211B-1A	P212-1A	P212-2A	P213-4D	P252-1C	P252-2C	P276-2G	P286-1F	P286-2E
WEIGHT %											
SIO2	28.46	28.51	27.14	27.38	27.41	29.43	28.59	26.84	28.31	27.20	27.71
TIO2	0.04	0.02	0.04	0.02	0.03	0.00	0.03	0.01	0.00	0.06	0.02
AL2O3	16.22	17.00	17.01	16.57	16.70	17.00	17.07	18.61	17.96	16.92	16.90
FE2O3	0.00	0.00	0.00	0.00	0.00	0.00	0.00	0.00	0.00	0.00	0.00
FEO	26.36	27.16	25.04	26.32	27.39	17.47	25.07	25.94	23.41	26.08	26.44
MNO	0.34	0.34	0.66	1.13	1.23	0.43	0.34	0.43	0.34	0.30	0.44
MGO	15.44	14.38	15.73	14.48	13.80	21.46	16.10	14.64	17.56	15.72	14.87
CAO	0.32	0.42	0.13	0.14	0.09	0.21	0.50	0.16	0.38	0.12	0.56
NA2O	0.00	0.00	0.01	0.00	0.00	0.00	0.06	0.00	0.00	0.00	0.00
K2O	0.01	0.01	0.00	0.01	0.01	0.00	0.04	0.02	0.01	0.00	0.00
H2O	11.26	11.31	11.10	11.04	11.05	11.66	11.42	11.19	11.55	11.14	11.19
TOTAL	98.45	99.15	96.84	97.07	97.71	97.66	99.21	97.83	99.52	97.55	98.15
ATOMIC FORMULA - ON BASIS OF 36 OXYGENS AND 16 HYDROGENS											
SI	6.066	6.048	5.867	5.952	5.949	6.054	6.006	5.752	5.879	5.856	5.941
TI	0.006	0.003	0.006	0.003	0.005	0.000	0.004	0.001	0.000	0.010	0.004
AL VI	1.934	1.952	2.133	2.048	2.051	1.946	1.994	2.248	2.120	2.144	2.060
AL IV	2.144	2.299	2.204	2.200	2.228	2.178	2.237	2.455	2.278	2.151	2.214
FE3+	0.000	0.000	0.000	0.000	0.000	0.000	0.000	0.000	0.000	0.000	0.000
FE2+	4.699	4.818	4.527	4.786	4.971	3.006	4.405	4.649	4.065	4.697	4.740
MN	0.061	0.062	0.121	0.207	0.225	0.075	0.060	0.078	0.060	0.055	0.081
MG	4.905	4.545	5.068	4.692	4.463	6.578	5.040	4.675	5.433	5.046	4.750
CA	0.072	0.096	0.029	0.032	0.022	0.047	0.112	0.036	0.085	0.027	0.130
NA	0.000	0.000	0.004	0.000	0.000	0.000	0.023	0.000	0.000	0.000	0.000
K	0.003	0.003	0.000	0.003	0.003	0.000	0.011	0.005	0.002	0.001	0.001
H	16.000	16.000	16.000	16.000	16.000	16.000	15.999	16.000	16.000	16.000	16.000
STRUCTURAL FORMULA											
Z	8.000	8.000	8.000	8.000	8.000	8.000	8.000	8.000	8.000	8.000	8.000
Y	11.891	11.826	11.960	11.923	11.911	11.884	11.892	11.898	11.922	11.987	11.920
MG-NO.	51.07	48.54	52.82	49.51	47.31	68.63	53.36	50.14	57.21	51.79	50.05
TYPE	GREEN.	GREEN.	BLUISH	GREEN.	GREEN.	BROWN.	BLUISH	BLUISH	BLUISH	BLUISH	BLUISH
ZONE	A	A	A	A	A	A	B	B	B	B	B
MIN. ?	NO	NO	YES	YES	YES	YES	NO	NO	NO	NO	NO

TABLE IV.2.3B CHLORITE ANALYSES FROM ANDESITES

	P108-1A	P117-1A	P133-1A	P137-1A	P142-1A	P147-1AA	P147-2A	P171-1A	P181-1B	P202-2A	P206-2C	P224-1D
WEIGHT %												
SIO2	27.02	27.65	27.13	26.23	27.70	28.93	28.86	27.17	28.03	28.51	27.88	27.54
TIO2	0.09	0.01	0.00	0.01	0.00	0.04	0.04	0.00	0.04	0.00	0.02	0.04
AL2O3	18.09	17.03	17.44	18.49	18.38	19.73	19.44	18.47	16.80	16.85	16.25	18.38
FE2O3	0.00	0.00	0.00	0.00	0.00	0.00	0.00	0.00	0.00	0.00	0.00	0.00
FEO	27.17	25.86	26.88	30.27	22.44	16.29	17.14	25.29	26.50	22.47	26.69	22.83
MNO	1.45	0.40	1.15	0.75	0.46	0.32	0.39	0.54	0.45	0.41	0.43	0.33
MGO	12.99	15.43	13.62	11.72	17.67	20.80	20.40	15.56	14.31	17.72	15.21	17.51
CAO	0.07	0.34	0.26	0.14	0.11	0.13	0.11	0.14	0.23	0.15	0.33	0.08
NA2O	0.04	0.00	0.00	0.02	0.00	0.00	0.00	0.01	0.10	0.00	0.12	0.00
K2O	0.05	0.02	0.03	0.01	0.00	0.19	0.13	0.02	0.00	0.01	0.02	0.01
H2O	11.11	11.20	11.06	11.03	11.44	11.82	11.78	11.31	11.15	11.36	11.17	11.42
TOTAL	98.08	97.93	97.56	98.67	98.20	98.25	98.28	98.50	97.62	97.48	98.12	98.16
ATOMIC FORMULA - ON BASIS OF 36 OXYGENS AND 16 HYDROGENS												
SI	5.836	5.921	5.881	5.703	5.809	5.871	5.879	5.765	6.034	6.023	5.988	5.788
TI	0.014	0.001	0.000	0.001	0.000	0.006	0.006	0.000	0.007	0.001	0.003	0.007
AL VI	2.164	2.080	2.119	2.297	2.191	2.129	2.121	2.235	1.966	1.977	2.001	2.212
AL IV	2.445	2.221	2.341	2.445	2.354	2.594	2.550	2.253	2.300	2.220	2.114	2.344
FE3+	0.000	0.000	0.000	0.000	0.000	0.000	0.000	0.000	0.000	0.000	0.000	0.000
FE2+	4.909	4.632	4.874	5.505	3.936	2.765	2.920	4.488	4.770	3.970	4.794	4.012
MN	0.266	0.072	0.211	0.138	0.082	0.056	0.067	0.096	0.083	0.074	0.077	0.060
MG	4.181	4.923	4.400	3.798	5.523	6.290	6.195	4.919	4.591	5.579	4.869	5.485
CA	0.016	0.077	0.060	0.032	0.024	0.027	0.025	0.031	0.054	0.033	0.077	0.019
NA	0.019	0.000	0.000	0.007	0.000	0.000	0.000	0.002	0.042	0.000	0.051	0.000
K	0.013	0.004	0.009	0.004	0.000	0.050	0.034	0.005	0.000	0.003	0.006	0.003
H	16.000	15.999	16.000	16.000	16.000	16.000	16.000	16.000	16.000	16.000	16.000	16.000
STRUCTURAL FORMULA												
Z	8.000	8.000	8.000	8.000	8.000	8.000	8.000	8.000	8.000	8.000	8.000	8.000
Y	11.861	11.931	11.894	11.930	11.919	11.787	11.796	11.800	11.847	11.879	11.991	11.929
MG-NO.	45.99	51.53	47.44	40.83	58.38	69.46	67.97	52.29	49.05	58.42	50.39	57.76
TYPE	BLUISH	GREEN.	GREEN.	GREEN.	BLUISH	BROWN.	BROWN.	BLUISH	GREEN.	BLUISH	GREEN.	BLUISH
ZONE	A	A	A	A	A	A	A	B	A	B	A	B
MIN. ?	YES	NO	YES	YES	YES	YES	YES	NO	NO	NO	NO	NO

TABLE XVIII - CHLORITE ANALYSES FROM ANDESITES - CONT'D

	P224-2B	P226-2B	P243-1D	P243-2D	P244-1A	P245-1A	P245-3A	P248-1A	P257-1C	P257-2C	P257-3B	P263B-1A
WEIGHT %												
SIO2	27.80	28.03	27.42	28.01	28.50	28.79	28.25	26.56	28.79	26.89	26.37	26.08
TIO2	0.09	0.00	0.02	0.04	0.02	0.02	0.00	0.00	0.03	0.00	0.03	0.09
AL2O3	18.23	16.09	16.35	16.08	19.46	17.46	17.20	18.29	16.62	17.56	18.75	18.52
FE2O3	0.00	0.00	0.00	0.00	0.00	0.00	0.00	0.00	0.00	0.86	0.18	0.00
FEO	22.46	25.90	27.40	26.77	19.93	24.01	24.52	29.26	21.69	24.51	25.93	26.77
MNO	0.27	0.57	0.60	0.54	0.44	0.37	0.68	0.47	0.74	0.89	0.84	0.72
MGO	17.13	14.82	14.87	15.02	19.69	16.90	16.70	12.62	18.51	16.25	15.18	13.32
CAO	0.23	0.34	0.15	0.02	0.07	0.27	0.11	0.24	0.13	0.10	0.08	0.11
NA2O	0.01	0.00	0.00	0.03	0.00	0.00	0.00	0.00	0.00	0.02	0.00	0.00
K2O	0.00	0.02	0.00	0.00	0.01	0.01	0.01	0.02	0.02	0.00	0.01	0.01
H2O	11.37	11.06	11.10	11.12	11.82	11.51	11.40	11.09	11.44	11.26	11.25	10.97
TOTAL	97.59	96.84	97.92	97.64	99.94	99.34	98.88	98.54	97.97	98.35	98.62	96.59
ATOMIC FORMULA - ON BASIS OF 36 OXYGENS AND 16 HYDROGENS												
SI	5.862	6.077	5.927	6.042	5.786	5.999	5.946	5.746	6.037	5.729	5.624	5.703
TI	0.014	0.000	0.004	0.006	0.003	0.003	0.000	0.000	0.005	0.001	0.005	0.016
AL VI	2.138	1.923	2.073	1.958	2.214	2.001	2.054	2.254	1.963	2.271	2.376	2.297
AL IV	2.396	2.192	2.094	2.134	2.446	2.290	2.216	2.413	2.146	2.141	2.341	2.479
FE3+	0.000	0.000	0.000	0.000	0.000	0.000	0.000	0.000	0.000	0.139	0.029	0.000
FE2+	3.961	4.697	4.954	4.828	3.384	4.185	4.316	5.295	3.804	4.367	4.626	4.897
MN	0.049	0.105	0.109	0.099	0.076	0.066	0.122	0.086	0.131	0.161	0.152	0.134
MG	5.385	4.789	4.790	4.828	5.956	5.248	5.239	4.069	5.786	5.161	4.826	4.342
CA	0.052	0.079	0.036	0.004	0.015	0.060	0 025	0.055	0.030	0.023	0.018	0.025
NA	0.002	0.000	0.000	0.013	0.000	0.000	0.000	0.000	0.000	0.008	0.001	0.000
K	0.001	0.007	0.001	0.000	0.003	0.003	0.002	0.005	0.004	0.001	0.002	0.003
H	15.999	16.000	16.000	16.000	16.000	16.000	16.000	16.000	16.000	15.999	16.000	16.000
STRUCTURAL FORMULA												
Z	8.000	8.000	8.000	8.000	8.000	8.000	8.000	8.000	8.000	8.000	8.000	8.000
Y	11.859	11.869	11.987	11.913	11.883	11.854	11.920	11.923	11.906	12.000	12.000	11.895
MG-NO.	57.62	50.48	49.16	50.00	63.77	55.64	54.83	43.45	60.34	54.17	51.05	46.99
TYPE	BLUISH	GREEN.	GREEN.	GREEN.	BROWN.	BLUISH	BLUISH	GREEN.	BLUISH	BLUISH	BLUISH	BLUISH
ZONE	B	A	A	A	B	B	B	B	B	B	B	B
MIN. ?	NO	NO	NO	NO	YES	NO	NO	NO	YES	YES	YES	YES

TABLE IV.2.3C CHLORITE ANALYSES FROM DACITES

	P163-1A	P203-1A	P247-1A
WEIGHT %			
SIO2	27.56	26.96	28.09
TIO2	0.01	0.00	0.06
AL2O3	17.77	17.61	18.12
FE2O3	0.00	0.00	0.00
FEO	24.85	31.15	21.11
MNO	0.65	0.84	1.17
MGO	14.85	10.97	17.37
CAO	0.13	0.30	0.09
NA2O	0.00	0.04	0.02
K2O	0.02	0.04	0.00
H2O	11.16	11.02	11.39
TOTAL	97.01	98.92	97.42
ATOMIC FORMULA - ON BASIS OF 36 OXYGENS AND 16 HYDROGENS			
SI	5.927	5.871	5.914
TI	0.002	0.000	0.009
AL VI	2.073	2.129	2.086
AL IV	2.435	2.394	2.415
FE3+	0.000	0.000	0.000
FE2+	4.469	5.674	3.717
MN	0.118	0.155	0.209
MG	4.760	3.562	5.451
CA	0.030	0.069	0.020
NA	0.002	0.017	0.010
K	0.006	0.010	0.001
H	16.000	16.000	16.000
STRUCTURAL FORMULA			
Z	8.000	8.000	8.000
Y	11.821	11.881	11.832
MG-NO.	51.58	38.57	59.45
TYPE	BLUISH	GREEN.	BLUISH
ZONE	B	A	B
MIN. ?	NO	YES	YES

TABLE IV.2.3b - CHLORITE ANALYSES FROM GABBROS

	P239-1B	P239-3E	P246-3B	P258-1C	P258-2D	P258-3B
WEIGHT %						
SIO2	29.01	29.11	30.20	29.53	30.20	29.59
TIO2	0.00	0.00	0.00	0.01	0.01	0.01
AL2O3	16.79	16.97	15.90	15.44	14.07	15.44
FE2O3	0.00	0.00	0.00	0.00	0.00	0.00
FEO	19.99	18.34	15.42	20.37	19.81	19.85
MNO	0.29	0.28	0.14	0.46	0.31	0.48
MGO	20.39	20.68	23.75	19.95	20.96	20.19
CAO	0.16	0.25	0.17	0.23	0.13	0.21
NA2O	0.02	0.03	0.00	0.03	0.01	0.00
K2O	0.02	0.02	0.01	0.00	0.00	0.00
H2O	11.59	11.56	11.75	11.47	11.44	11.47
TOTAL	98.25	97.24	97.34	97.48	96.94	97.24
ATOMIC FORMULA - ON BASIS OF 36 OXYGENS AND 16 HYDROGENS						
SI	6.005	6.040	6.167	6.178	6.333	6.191
TI	0.000	0.000	0.000	0.001	0.002	0.002
AL VI	1.995	1.960	1.833	1.822	1.667	1.809
AL IV	2.104	2.193	1.995	1.989	1.812	2.000
FE3+	0.000	0.000	0.000	0.000	0.000	0.000
FE2+	3.461	3.183	2.634	3.566	3.475	3.473
MN	0.051	0.049	0.025	0.082	0.056	0.086
MG	6.289	6.395	7.228	6.221	6.550	6.295
CA	0.035	0.056	0.037	0.052	0.029	0.047
NA	0.008	0.011	0.000	0.011	0.004	0.000
K	0.004	0.005	0.003	0.001	0.000	0.001
H	16.000	16.000	16.000	16.000	16.000	16.000
STRUCTURAL FORMULA						
Z	8.000	8.000	8.000	8.000	8.000	8.000
Y	11.952	11.892	11.921	11.922	11.928	11.903
MG-NO.	64.50	66.77	73.29	63.57	65.34	64.45
TYPE	BROWN.	BROWN.	BROWN.	BROWN.	BROWN.	BROWN.
ZONE	B	B	B	B	B	B
MIN. ?	NO	NO	NO	NO	NO	NO

	P240-2C	P240-3C	P264A-3A	P264A-3B	P264A-4B	P264A-4C	P270-1A	P274-1A
WEIGHT %								
SIO2	27.19	27.45	25.61	25.35	26.49	26.35	26.52	25.71
TIO2	0.02	0.06	0.03	0.14	0.02	0.03	0.00	0.04
AL2O3	17.69	17.93	20.11	19.61	17.74	17.70	16.84	17.68
FE2O3	0.00	0.00	0.00	0.00	0.00	0.00	0.00	0.00
FEO	24.25	24.47	27.46	30.48	28.44	30.05	30.72	32.52
MNO	0.60	0.59	0.19	0.29	0.28	0.33	0.34	0.53
MGO	16.16	15.11	12.59	10.30	12.52	11.18	10.49	9.30
CAO	0.16	0.36	0.12	0.23	0.15	0.16	0.33	0.07
NA2O	0.00	0.16	0.00	0.00	0.00	0.01	0.00	0.00
K2O	0.01	0.03	0.01	0.05	0.01	0.02	0.07	0.01
H2O	11.20	11.21	11.04	10.88	10.90	10.82	10.70	10.65
TOTAL	97.29	97.39	97.15	97.32	96.56	96.65	96.02	96.52
ATOMIC FORMULA - ON BASIS OF 36 OXYGENS AND 16 HYDROGENS								
SI	5.822	5.877	5.564	5.591	5.830	5.840	5.948	5.790
TI	0.003	0.010	0.004	0.024	0.003	0.005	0.000	0.007
AL VI	2.178	2.123	2.436	2.409	2.170	2.160	2.052	2.210
AL IV	2.290	2.406	2.717	2.692	2.434	2.466	2.403	2.484
FE3+	0.000	0.000	0.000	0.000	0.000	0.000	0.000	0.000
FE2+	4.343	4.382	4.990	5.621	5.234	5.572	5.763	6.124
MN	0.109	0.108	0.035	0.053	0.053	0.062	0.065	0.102
MG	5.159	4.823	4.079	3.386	4.107	3.692	3.506	3.120
CA	0.038	0.083	0.029	0.053	0.035	0.038	0.078	0.017
NA	0.000	0.068	0.000	0.000	0.000	0.006	0.000	0.000
K	0.002	0.009	0.004	0.014	0.004	0.005	0.020	0.004
H	16.000	16.000	16.000	16.000	15.999	16.000	16.000	16.000
STRUCTURAL FORMULA								
Z	8.000	8.000	8.000	8.000	8.000	8.000	8.000	8.000
Y	11.942	11.888	11.857	11.843	11.868	11.847	11.834	11.858
MG-NO.	54.29	52.39	44.98	37.59	43.97	39.86	37.83	33.75
TYPE	BLUISH	BLUISH	GREEN.	GREEN.	GREEN.	GREEN.	GREEN.	GREEN.
ZONE	B	B	B	B	B	B	B	B
MIN. ?	NO	NO	NO	NO	NO	NO	NO	NO

TABLE IV.2.4A PLAGIOCLASE ANALYSES FROM BASALTS

	P66-2D	P93-1C	P93-2C	P93-2D	P123-1B	P123-2B	P124-1C	P124-2B	P140-1C	P140-1D	P161-1I	P185A-1
WEIGHT %												
SIO2	68.16	67.84	68.16	67.22	69.16	68.51	69.68	69.77	68.34	68.15	68.80	68.46
TIO2	0.00	0.00	0.00	0.00	0.00	0.00	0.00	0.00	0.00	0.00	0.00	0.00
AL2O3	19.69	19.81	19.64	19.98	19.02	19.23	19.21	19.08	19.37	19.77	19.76	20.40
FEO	0.09	0.10	0.23	0.36	0.11	0.18	0.12	0.18	0.11	0.13	0.11	0.12
MNO	0.00	0.01	0.04	0.02	0.02	0.04	0.04	0.04	0.01	0.05	0.00	0.00
MGO	0.03	0.03	0.05	0.15	0.02	0.02	0.00	0.05	0.05	0.04	0.04	0.08
CAO	0.62	0.31	0.44	0.23	0.21	0.21	0.15	0.20	0.30	0.64	0.51	0.85
NA2O	11.83	11.76	11.82	11.33	11.27	12.02	11.36	11.41	10.91	11.25	11.50	10.33
K2O	0.08	0.11	0.10	0.10	0.06	0.08	0.09	0.12	0.09	0.12	0.16	0.12
TOTAL	100.51	99.96	100.48	99.39	99.86	100.29	100.65	100.84	99.17	100.15	100.90	100.35
ATOMIC FORMULA - ON BASIS OF 8 OXYGENS												
SI	2.972	2.971	2.974	2.961	3.019	2.992	3.018	3.019	3.003	2.977	2.983	2.973
TI	0.000	0.000	0.000	0.000	0.000	0.000	0.000	0.000	0.000	0.000	0.000	0.000
AL	1.013	1.023	1.010	1.038	0.979	0.990	0.981	0.974	1.004	1.019	1.010	1.045
FE	0.003	0.004	0.009	0.013	0.004	0.007	0.004	0.007	0.004	0.005	0.005	0.005
MN	0.000	0.000	0.002	0.001	0.001	0.001	0.001	0.002	0.000	0.002	0.000	0.000
MG	0.002	0.002	0.003	0.010	0.001	0.002	0.000	0.003	0.003	0.003	0.002	0.005
CA	0.029	0.014	0.021	0.011	0.010	0.010	0.007	0.009	0.014	0.030	0.024	0.039
NA	1.000	0.999	1.000	0.968	0.954	1.018	0.954	0.957	0.930	0.953	0.967	0.876
K	0.005	0.006	0.006	0.006	0.003	0.004	0.005	0.007	0.005	0.007	0.009	0.006
MOLECULAR PROPORTIONS												
AN	2.82	1.40	1.99	1.11	0.99	0.96	0.74	0.94	1.47	3.03	2.38	4.30
AB	96.73	97.98	97.47	98.33	98.65	98.61	98.76	98.39	97.98	96.30	96.72	95.00
OR	0.45	0.62	0.53	0.56	0.35	0.43	0.50	0.67	0.55	0.66	0.90	0.70
DESCRIPTION												
ZONE	A	A	A	A	A	A	A	A	A	A	A	A
MIN. ?	YES	YES	YES	YES	NO	NO	NO	NO	YES	YES	NO	YES

TABLE IV.2.4A PLAGIOCLASE ANALYSES FROM BASALTS - CONT'D

	P188-1A	P188-2A	P252-1D	P252-2D	P253-2C	P253-3F	P276-2C	P286-1E	P286-2D
WEIGHT %									
SIO2	69.01	68.16	67.58	68.62	69.99	68.94	68.35	67.78	68.90
TIO2	0.00	0.00	0.00	0.00	0.01	0.00	0.00	0.00	0.00
AL203	20.03	19.68	19.59	19.70	19.28	19.25	19.58	18.79	19.76
FEO	0.10	0.33	0.06	0.01	0.11	0.13	0.06	0.84	0.09
MNO	0.03	0.00	0.00	0.00	0.04	0.03	0.04	0.02	0.02
MGO	0.03	0.13	0.00	0.00	0.04	0.02	0.02	0.59	0.01
CAO	0.94	0.75	0.11	0.21	0.12	0.09	0.72	0.71	0.33
NA2O	10.30	10.54	11.88	11.39	11.23	11.87	10.96	11.15	11.44
K2O	0.43	0.51	0.02	0.04	0.06	0.08	0.22	0.09	0.07
TOTAL	100.88	100.11	99.24	99.97	100.89	100.41	99.95	99.97	100.63
ATOMIC FORMULA - ON BASIS OF 8 OXYGENS									
SI	2.986	2.980	2.978	2.993	3.021	3.001	2.988	2.979	2.990
TI	0.000	0.000	0.000	0.000	0.000	0.000	0.000	0.000	0.000
AL	1.022	1.015	1.018	1.013	0.982	0.989	1.009	0.974	1.011
FE	0.004	0.012	0.002	0.001	0.004	0.005	0.002	0.031	0.003
MN	0.001	0.000	0.000	0.000	0.002	0.001	0.001	0.001	0.001
MG	0.002	0.009	0.000	0.000	0.003	0.001	0.001	0.039	0.001
CA	0.044	0.035	0.005	0.010	0.006	0.004	0.034	0.033	0.015
NA	0.864	0.894	1.015	0.963	0.940	1.002	0.930	0.950	0.962
K	0.024	0.028	0.001	0.002	0.003	0.005	0.012	0.005	0.004
MOLECULAR PROPORTIONS									
AN	4.70	3.69	0.53	1.03	0.60	0.40	3.46	3.38	1.57
AB	92.74	93.37	99.37	98.73	99.07	99.16	95.29	96.13	98.06
OR	2.56	2.94	0.11	0.24	0.33	0.44	1.25	0.49	0.37
DESCRIPTION									
ZONE	A	A	B	B	B	B	B	B	B
MIN. ?	YES	YES	NO	NO	NO	NO	NO	NO	NO

TABLE IV.2.4B PLAGIOCLASE ANALYSES FROM ANDESITES

	P82-1A	P82-3A	P104-1B	P104-1C	P104-1D	P112-1A	P141-1B	P142-1B	P171-2A	P171-2B	P171-3A	P205-1A
WEIGHT %												
SIO2	67.85	67.55	68.14	68.25	68.54	67.54	68.11	68.10	68.89	68.81	68.61	69.33
TIO2	0.05	0.00	0.00	0.00	0.00	0.01	0.00	0.00	0.02	0.00	0.02	0.00
AL2O3	19.39	20.45	19.25	19.40	19.25	19.86	19.76	18.70	19.53	19.49	19.28	19.16
FEO	0.25	0.09	0.07	0.07	0.06	0.09	0.40	0.37	0.18	0.14	0.23	0.08
MNO	0.05	0.00	0.05	0.02	0.02	0.00	0.04	0.00	0.02	0.00	0.00	0.04
MGO	0.02	0.00	0.01	0.01	0.00	0.02	0.11	0.06	0.05	0.01	0.06	0.02
CAO	0.59	0.35	0.20	0.24	0.17	0.31	0.36	0.08	0.14	0.16	0.22	0.10
NA2O	11.42	11.74	11.82	11.98	11.81	11.78	11.01	11.70	11.72	11.94	11.61	11.46
K2O	0.15	0.09	0.07	0.11	0.10	0.07	0.09	0.05	0.07	0.06	0.06	0.08
TOTAL	99.78	100.27	99.60	100.09	99.96	99.68	99.88	99.05	100.62	100.61	100.09	100.27
ATOMIC FORMULA - ON BASIS OF 8 OXYGENS												
SI	2.980	2.950	2.992	2.986	2.998	2.967	2.980	3.008	2.993	2.992	2.997	3.015
TI	0.002	0.000	0.000	0.000	0.000	0.000	0.000	0.000	0.001	0.000	0.001	0.000
AL	1.004	1.053	0.997	1.001	0.993	1.029	1.020	0.974	1.000	0.999	0.993	0.983
FE	0.009	0.003	0.003	0.003	0.002	0.003	0.015	0.014	0.007	0.005	0.009	0.003
MN	0.002	0.000	0.002	0.001	0.001	0.000	0.002	0.000	0.001	0.000	0.000	0.001
MG	0.002	0.000	0.001	0.000	0.000	0.002	0.007	0.004	0.004	0.001	0.004	0.001
CA	0.028	0.016	0.010	0.012	0.008	0.015	0.017	0.004	0.007	0.007	0.010	0.005
NA	0.973	0.994	1.007	1.017	1.002	1.003	0.934	1.002	0.987	1.007	0.983	0.967
K	0.008	0.005	0.004	0.006	0.006	0.004	0.005	0.003	0.004	0.003	0.004	0.005
MOLECULAR PROPORTIONS												
AN	2.74	1.60	0.93	1.11	0.78	1.43	1.78	0.38	0.67	0.71	1.03	0.49
AB	96.42	97.91	98.68	98.29	98.65	98.17	97.67	99.35	98.96	98.95	98.61	99.05
OR	0.83	0.49	0.39	0.60	0.57	0.41	0.55	0.28	0.37	0.34	0.36	0.46
DESCRIPTION												
ZONE	A	A	A	A	A	B	A	A	B	B	B	A
MIN. ?	YES	YES	NO	NO	NO	NO	NO	NO	NO	NO	NO	NO

TABLE IV.2.4B PLAGIOCLASE ANALYSES FROM ANDESITES - CONT'D

	P205-1B	P205-2A	P205-2B	P206-1A	P206-1B	P206-2A	P206-2B	P216-1A	P224-1A	P224-2A	P226-1A	P226-1B
WEIGHT %												
SIO2	68.55	68.49	68.74	67.82	68.02	68.04	68.79	68.04	67.44	68.48	67.24	67.52
TIO2	0.00	0.00	0.00	0.00	0.00	0.00	0.01	0.00	0.02	0.00	0.00	0.00
AL2O3	19.51	19.20	19.28	19.27	19.32	19.63	19.28	18.67	19.57	19.69	20.08	20.03
FEO	0.13	0.13	0.23	0.04	0.17	0.07	0.04	0.53	0.24	0.12	0.08	0.07
MNO	0.02	0.01	0.01	0.02	0.03	0.02	0.03	0.03	0.02	0.05	0.01	0.00
MGO	0.02	0.03	0.00	0.03	0.00	0.00	0.00	0.14	0.06	0.05	0.03	0.00
CAO	0.17	0.00	0.02	0.31	0.37	0.22	0.20	0.41	0.35	0.17	1.08	0.96
NA2O	11.66	11.89	11.87	11.80	12.00	11.87	11.62	11.40	12.28	10.74	11.34	11.23
K2O	0.07	0.08	0.08	0.11	0.10	0.07	0.06	0.12	0.05	0.16	0.13	0.18
TOTAL	100.14	99.83	100.24	99.39	100.02	99.92	100.03	99.33	100.04	99.47	100.00	100.00
ATOMIC FORMULA - ON BASIS OF 8 OXYGENS												
SI	2.992	2.999	2.999	2.987	2.982	2.980	3.003	3.002	2.962	2.998	2.950	2.959
TI	0.000	0.000	0.000	0.000	0.000	0.000	0.000	0.000	0.001	0.000	0.000	0.000
AL	1.004	0.992	0.992	1.001	0.999	1.014	0.992	0.972	1.014	1.017	1.039	1.035
FE	0.005	0.005	0.008	0.002	0.006	0.002	0.002	0.020	0.009	0.004	0.003	0.003
MN	0.001	0.000	0.001	0.001	0.001	0.001	0.001	0.001	0.001	0.002	0.001	0.000
MG	0.002	0.002	0.000	0.002	0.000	0.000	0.000	0.009	0.004	0.003	0.002	0.000
CA	0.008	0.000	0.001	0.014	0.018	0.010	0.009	0.019	0.017	0.008	0.051	0.045
NA	0.987	1.010	1.004	1.007	1.020	1.008	0.984	0.975	1.046	0.912	0.965	0.954
K	0.004	0.004	0.005	0.006	0.005	0.004	0.004	0.007	0.003	0.009	0.007	0.010
MOLECULAR PROPORTIONS												
AN	0.79	0.01	0.11	1.41	1.67	1.00	0.94	1.91	1.56	0.84	4.97	4.49
AB	98.82	99.56	99.44	98.02	97.81	98.60	98.70	97.42	98.19	98.20	94.31	94.51
OR	0.39	0.43	0.46	0.58	0.52	0.40	0.36	0.66	0.25	0.96	0.72	1.01
DESCRIPTION												
ZONE	A	A	A	A	A	A	A	B	B	B	A	A
MIN. ?	NO	NO	NO	NO	NO	NO	NO	NO	NO	NO	NO	NO

TABLE IV.2.4B PLAGIOCLASE ANALYSES FROM ANDESITES - CONT'D

	P226-2A	P243-1C	P243-2C	P245-1B	P245-1C	P245-1D	P245-1E	P245-2A	P245-2B	P245-2C	P245-3E	P245-3F
WEIGHT %												
SIO2	67.42	68.26	67.76	69.78	68.51	68.96	69.37	68.06	67.90	67.73	68.88	68.83
TIO2	0.00	0.00	0.45	0.04	0.00	0.00	0.00	0.00	0.02	0.00	0.00	0.02
AL2O3	20.43	19.50	19.02	18.96	19.42	19.32	19.64	19.58	19.49	19.49	19.19	19.46
FEO	0.09	0.46	0.64	0.01	0.09	0.00	0.03	0.06	0.08	0.14	0.20	0.07
MNO	0.00	0.02	0.04	0.00	0.00	0.00	0.00	0.00	0.03	0.02	0.02	0.04
MGO	0.02	0.18	0.14	0.00	0.06	0.00	0.00	0.01	0.03	0.05	0.05	0.13
CAO	1.19	0.56	0.76	0.14	0.19	0.10	0.15	0.38	0.28	0.40	0.39	1.20
NA2O	11.28	10.87	11.22	11.43	10.99	11.26	11.28	11.80	11.76	11.83	11.00	10.55
K2O	0.10	0.20	0.17	0.08	0.76	0.08	0.12	0.10	0.15	0.15	0.57	0.08
TOTAL	100.53	100.05	100.20	100.44	100.02	99.73	100.59	100.00	99.73	99.81	100.31	100.38
ATOMIC FORMULA - ON BASIS OF 8 OXYGENS												
SI	2.941	2.985	2.972	3.026	2.997	3.012	3.005	2.980	2.981	2.975	3.004	2.993
TI	0.000	0.000	0.015	0.001	0.000	0.000	0.000	0.000	0.001	0.000	0.000	0.001
AL	1.051	1.006	0.984	0.970	1.002	0.995	1.004	1.011	1.009	1.010	0.987	0.998
FE	0.003	0.017	0.024	0.000	0.003	0.000	0.001	0.002	0.003	0.005	0.008	0.003
MN	0.000	0.001	0.002	0.000	0.000	0.000	0.000	0.000	0.001	0.001	0.001	0.002
MG	0.001	0.012	0.009	0.000	0.004	0.000	0.000	0.001	0.002	0.003	0.003	0.009
CA	0.056	0.026	0.036	0.007	0.009	0.005	0.007	0.018	0.013	0.019	0.018	0.056
NA	0.955	0.922	0.954	0.961	0.932	0.954	0.947	1.002	1.001	1.007	0.931	0.890
K	0.005	0.011	0.009	0.004	0.042	0.005	0.007	0.006	0.008	0.008	0.032	0.004
MOLECULAR PROPORTIONS												
AN	5.46	2.75	3.57	0.69	0.93	0.51	0.74	1.75	1.27	1.83	1.85	5.90
AB	94.01	96.11	95.50	98.87	94.76	99.01	98.55	97.70	97.91	97.36	94.90	93.64
OR	0.53	1.15	0.93	0.44	4.32	0.48	0.71	0.56	0.81	0.81	3.25	0.47
DESCRIPTION												
ZONE	A	A	A	B	B	B	B	B	B	B	B	B
MIN. ?	NO	YES	YES	NO	NO	NO	NO	NO	NO	NO	NO	NO

TABLE IV.2.4B PLAGIOCLASE ANALYSES FROM ANDESITES - CONT'D

	P245-3G	P248-1C	P257-2A	P289-1C	P289-2B
WEIGHT %					
SIO2	68.80	69.70	68.08	68.33	68.16
TIO2	0.11	0.00	0.01	0.00	0.00
AL2O3	19.12	19.16	19.41	19.29	19.32
FEO	0.08	0.08	0.33	0.05	0.05
MNO	0.06	0.48	0.00	0.02	0.03
MGO	0.04	0.04	0.05	0.00	0.00
CAO	0.43	0.20	0.07	0.18	0.22
NA2O	10.87	10.75	11.47	11.57	11.66
K2O	0.24	0.08	0.06	0.06	0.06
TOTAL	99.76	100.49	99.47	99.51	99.51
ATOMIC FORMULA - ON BASIS OF 8 OXYGENS					
SI	3.009	3.022	2.991	2.999	2.994
TI	0.004	0.000	0.000	0.000	0.000
AL	0.986	0.980	1.006	0.998	1.001
FE	0.003	0.003	0.012	0.002	0.002
MN	0.002	0.018	0.000	0.001	0.001
MG	0.003	0.003	0.003	0.000	0.000
CA	0.020	0.009	0.003	0.009	0.010
NA	0.922	0.904	0.977	0.985	0.993
K	0.013	0.005	0.003	0.003	0.003
MOLECULAR PROPORTIONS					
AN	2.13	1.00	0.35	0.86	1.01
AB	96.49	98.51	99.33	98.79	98.68
OR	1.37	0.49	0.32	0.35	0.32
DESCRIPTION					
ZONE	B	B	B	B	B
MIN. ?	NO	NO	NO	NO	NO

TABLE IV.2.4C PLAGIOCLASE ANALYSES FROM DACITES

	P143-1A	P203-1B	P218-3B	P247-2A
WEIGHT %				
SIO2	69.48	67.97	68.55	68.70
TIO2	0.02	0.01	0.01	0.00
AL2O3	19.34	20.62	19.42	19.08
FEO	0.10	0.32	0.03	0.02
MNO	0.03	0.02	0.02	0.00
MGO	0.06	0.08	0.00	0.02
CAO	0.32	0.89	0.12	0.22
NA2O	11.31	11.40	12.22	11.31
K2O	0.07	0.18	0.14	0.10
TOTAL	100.73	101.50	100.50	99.45
ATOMIC FORMULA - ON BASIS OF 8 OXYGENS				
SI	3.009	2.940	2.987	3.012
TI	0.001	0.000	0.000	0.000
AL	0.988	1.052	0.998	0.987
FE	0.004	0.012	0.001	0.001
MN	0.001	0.001	0.001	0.000
MG	0.004	0.005	0.000	0.002
CA	0.015	0.041	0.006	0.010
NA	0.949	0.956	1.032	0.962
K	0.004	0.010	0.008	0.006
MOLECULAR PROPORTIONS				
AN	1.55	4.11	0.55	1.05
AB	98.05	94.90	98.71	98.38
OR	0.40	0.99	0.73	0.57
DESCRIPTION				
ZONE	A	A	B	B
MIN. ?	NO	YES	NO	NO

TABLE IV.2.4D PLAGIOCLASE ANALYSES FROM GABBROS

	P246-2B	P246-3A1	P246-3A2	P246-3A3	P258-2E	P258-3E	P277-2F
WEIGHT %							
SIO2	58.48	60.70	58.78	67.95	65.71	65.39	68.07
TIO2	0.04	0.04	0.03	0.00	0.00	0.00	0.00
AL2O3	25.82	24.13	25.77	19.28	21.60	21.71	19.73
FEO	0.44	0.41	0.41	0.23	0.25	0.32	0.16
MNO	0.03	0.00	0.03	0.00	0.00	0.01	0.04
MGO	0.13	0.11	0.09	0.25	0.01	0.00	0.03
CAO	8.57	7.35	8.54	0.54	3.21	3.30	0.67
NA2O	6.34	7.72	7.09	11.18	8.81	8.48	11.46
K2O	0.27	0.34	0.26	0.13	0.24	0.18	0.08
TOTAL	100.13	100.80	100.99	99.56	99.83	99.40	100.24
ATOMIC FORMULA - ON BASIS OF 8 OXYGENS							
SI	2.617	2.694	2.614	2.986	2.888	2.885	2.974
TI	0.002	0.002	0.001	0.000	0.000	0.000	0.000
AL	1.362	1.263	1.352	0.999	1.120	1.130	1.017
FE	0.017	0.015	0.015	0.009	0.009	0.012	0.006
MN	0.001	0.000	0.001	0.000	0.000	0.000	0.002
MG	0.009	0.007	0.006	0.016	0.001	0.000	0.002
CA	0.411	0.349	0.407	0.025	0.151	0.156	0.031
NA	0.551	0.664	0.611	0.953	0.751	0.725	0.971
K	0.015	0.019	0.015	0.007	0.013	0.010	0.004
MOLECULAR PROPORTIONS							
AN	42.07	33.82	39.41	2.58	16.51	17.51	3.11
AB	56.37	64.30	59.15	96.70	82.04	81.34	96.46
OR	1.56	1.88	1.44	0.72	1.45	1.15	0.43
DESCRIPTION							
ZONE	B	B	B	B	B	B	B
MIN. ?	NO	NO	NO	NO	NO	NO	NO

TABLE IV.2.4E PLAGIOCLASE ANALYSES FROM PLAGIOGRANITES

	P240-1A	P240-2A	P240-2B	P240-3A	P254-1A	P264A-1A	P264A-2A	P264A-3C	P264A-3D	P264A-4A	P270-1B	P274-3A
WEIGHT %												
SIO2	68.40	68.99	68.97	69.23	68.74	69.17	68.67	67.79	68.88	69.23	68.40	69.49
TIO2	0.00	0.01	0.00	0.00	0.00	0.00	0.00	0.02	0.00	0.00	0.00	0.00
AL2O3	19.30	19.32	19.11	19.63	19.08	19.51	19.27	19.32	19.15	19.72	19.39	19.41
FEO	0.02	0.03	0.04	0.01	0.00	0.01	0.03	0.05	0.04	0.00	0.00	0.00
MNO	0.00	0.01	0.03	0.01	0.02	0.02	0.01	0.01	0.03	0.00	0.00	0.00
MGO	0.02	0.00	0.02	0.00	0.00	0.00	0.03	0.00	0.02	0.00	0.00	0.00
CAO	0.08	0.11	0.12	0.12	0.07	0.09	0.13	0.08	0.08	0.08	0.05	0.06
NA2O	12.00	11.99	11.83	11.80	10.71	11.97	11.77	12.00	11.57	11.93	11.68	11.56
K2O	0.06	0.05	0.05	0.06	0.08	0.03	0.04	0.04	0.03	0.01	0.05	0.04
TOTAL	99.88	100.52	100.17	100.85	98.70	100.81	99.94	99.31	99.80	100.98	99.56	100.56
ATOMIC FORMULA - ON BASIS OF 8 OXYGENS												
SI	2.994	3.000	3.007	2.997	3.026	2.998	3.001	2.987	3.011	2.994	2.998	3.011
TI	0.000	0.000	0.000	0.000	0.000	0.000	0.000	0.001	0.000	0.000	0.000	0.000
AL	0.997	0.991	0.983	1.002	0.990	0.997	0.993	1.004	0.987	1.006	1.002	0.992
FE	0.001	0.001	0.002	0.000	0.000	0.001	0.001	0.002	0.002	0.000	0.000	0.000
MN	0.000	0.000	0.001	0.000	0.001	0.001	0.000	0.001	0.001	0.000	0.000	0.000
MG	0.001	0.000	0.001	0.000	0.000	0.000	0.002	0.000	0.001	0.000	0.000	0.000
CA	0.004	0.005	0.005	0.005	0.003	0.004	0.006	0.004	0.004	0.004	0.002	0.003
NA	1.019	1.011	1.001	0.991	0.914	1.006	0.997	1.026	0.980	1.001	0.993	0.972
K	0.004	0.003	0.003	0.003	0.005	0.002	0.002	0.002	0.002	0.001	0.003	0.002
MOLECULAR PROPORTIONS												
AN	0.36	0.49	0.54	0.53	0.37	0.40	0.59	0.37	0.39	0.35	0.21	0.29
AB	99.29	99.24	99.20	99.14	99.14	99.44	99.19	99.41	99.42	99.60	99.53	99.46
OR	0.35	0.27	0.26	0.33	0.49	0.16	0.22	0.22	0.18	0.05	0.26	0.25
DESCRIPTION												
ZONE	B	B	B	B	B	B	B	B	B	B	B	B
MIN. ?	NO	NO	NO	NO	NO	NO	NO	NO	NO	NO	NO	NO

TABLE IV.2.5A EPIDOTE ANALYSES FROM BASALTS

	P193-1A	P210-1B	P211B-1A	P211B-2A	P252-1E	P276-1B	P276-2B	P287-1B
WEIGHT %								
SIO2	37.52	38.27	37.41	37.91	37.56	38.43	39.13	39.56
TIO2	0.08	0.04	0.02	0.01	0.20	0.14	0.46	0.11
AL2O3	22.46	23.94	18.74	19.80	23.13	22.10	24.41	22.40
FE2O3	13.16	11.83	16.46	14.63	12.84	12.49	8.07	10.64
FEO	0.62	1.38	2.10	2.38	0.00	0.91	2.26	2.18
MNO	0.28	0.29	0.00	0.11	0.18	0.12	0.08	0.13
MGO	0.04	0.00	0.01	0.02	0.11	0.47	ND	0.41
CAO	22.55	22.62	21.89	21.95	23.69	22.74	22.39	22.33
NA2O	0.05	0.00	0.00	0.00	0.02	0.03	0.04	0.13
K2O	0.01	0.01	0.02	0.01	0.01	0.00	0.00	0.02
H2O	1.86	1.89	1.82	1.84	1.88	1.87	1.89	1.89
TOTAL	98.63	100.27	98.48	98.66	99.63	99.29	99.23	99.80
ATOMIC FORMULA - ON BASIS OF 13 OXYGENS AND 1 HYROGEN								
SI	3.030	3.029	3.080	3.097	2.999	3.075	3.096	3.139
TI	0.005	0.002	0.001	0.000	0.012	0.008	0.028	0.006
AL	2.140	2.234	1.820	1.908	2.177	2.086	2.278	2.097
FE3+	0.800	0.704	1.020	0.900	0.771	0.752	0.480	0.635
FE2+	0.042	0.091	0.145	0.163	0.000	0.061	0.149	0.145
MN	0.019	0.019	0.000	0.008	0.012	0.008	0.005	0.009
MG	0.005	0.000	0.001	0.003	0.014	0.057	0.059	0.049
CA	1.951	1.918	1.931	1.922	2.026	1.950	1.898	1.899
NA	0.008	0.000	0.000	0.000	0.003	0.004	0.006	0.020
K	0.001	0.001	0.002	0.001	0.001	0.000	0.000	0.002
PS %	27.21	23.97	35.91	32.04	26.16	26.50	17.41	23.25
ZONE	B	A	A	A	B	B	B	B
MIN. ?	NO	YES	YES	YES	NO	NO	NO	NO

TABLE IV.2.5B EPIDOTE ANALYSES FROM ANDESITES

	P80-1B	P133-1B	P170B-1A	P171-1B	P171-3C	P184-1B	P202-1A	P215-1A	P216-1B	P220-1A	P224-1B	P224-1C
WEIGHT %												
SIO2	37.86	37.56	37.37	37.70	37.63	38.46	37.62	37.10	38.72	38.12	36.97	37.16
TIO2	0.09	0.43	0.25	0.17	0.23	0.11	0.23	0.10	0.11	0.26	0.35	0.01
AL203	18.23	20.16	23.43	21.82	21.56	22.25	22.17	21.74	21.42	21.75	22.02	22.86
FE203	16.47	16.76	12.60	15.21	15.21	12.03	12.71	15.17	12.29	12.66	14.95	13.88
FEO	0.00	0.00	0.00	0.00	0.00	1.65	1.53	0.93	2.61	1.87	0.00	0.00
MNO	0.25	0.30	0.89	0.56	0.51	0.19	0.17	0.60	0.96	0.28	0.15	0.03
MGO	1.71	0.09	0.24	0.12	0.39	0.04	0.08	0.34	0.02	0.07	0.04	0.00
CAO	22.68	23.21	22.44	23.03	22.35	22.35	22.11	21.40	21.48	22.23	23.54	23.72
NA2O	0.01	0.05	0.03	0.03	0.10	0.12	0.05	0.01	0.08	0.04	0.01	0.00
K2O	0.02	0.00	0.03	0.00	0.01	0.02	0.01	0.01	0.01	0.01	0.00	0.00
H2O	1.85	1.87	1.87	1.88	1.87	1.87	1.85	1.86	1.87	1.86	1.87	1.87
TOTAL	99.18	100.42	99.14	100.53	99.87	99.09	98.52	99.26	99.57	99.14	99.91	99.53
ATOMIC FORMULA - ON BASIS OF 13 OXYGENS AND 1 HYROGEN												
SI	3.077	3.016	2.995	3.006	3.016	3.087	3.045	2.998	3.113	3.071	2.967	2.979
TI	0.006	0.026	0.015	0.010	0.014	0.007	0.014	0.006	0.007	0.016	0.021	0.001
AL	1.747	1.909	2.214	2.052	2.038	2.106	2.116	2.072	2.031	2.067	2.084	2.162
FE3+	1.007	1.013	0.760	0.913	0.918	0.727	0.774	0.922	0.743	0.768	0.903	0.837
FE2+	0.000	0.000	0.000	0.000	0.000	0.111	0.104	0.063	0.176	0.126	0.000	0.000
MN	0.017	0.021	0.061	0.038	0.035	0.013	0.011	0.041	0.065	0.019	0.010	0.002
MG	0.208	0.010	0.028	0.014	0.047	0.005	0.010	0.041	0.002	0.008	0.005	0.000
CA	1.975	1.997	1.927	1.967	1.919	1.923	1.917	1.853	1.850	1.919	2.025	2.038
NA	0.001	0.008	0.005	0.005	0.016	0.019	0.008	0.002	0.012	0.006	0.002	0.000
K	0.002	0.000	0.003	0.000	0.001	0.002	0.001	0.002	0.001	0.001	0.000	0.000
PS %	36.57	34.67	25.55	30.79	31.05	25.65	26.78	30.80	26.79	27.08	30.24	27.92
ZONE	A	A	A	B	B	A	B	B	B	B	B	B
MIN. ?	NO	YES	YES	NO	NO	NO	NO	NO	YES	NO	NO	NO

TABLE IV.2.5C EPIDOTE ANALYSES FROM ANDESITES (1-6) AND DACITES (7-12)

	P248-1D	P256-1B	P257-1A	P257-1B	P257-2B	P257-3A	P211A-1A	P211A-2A	P218-2A	P218-1B	P218-2A	P218-3A
WEIGHT %												
SIO2	39.09	37.97	37.16	37.74	37.67	37.82	37.35	37.70	37.01	37.22	37.06	38.06
TIO2	0.13	0.04	0.22	0.06	0.00	0.03	0.06	0.02	0.14	0.20	0.14	0.08
AL2O3	22.49	20.54	20.58	22.19	22.30	22.52	19.73	20.17	21.54	22.01	21.58	24.22
FE2O3	12.23	15.85	16.66	14.59	14.34	13.23	16.19	15.71	14.48	14.72	15.89	13.87
FEO	0.58	0.17	0.00	0.05	0.46	0.32	1.91	1.63	0.29	0.00	0.19	0.47
MNO	0.19	0.06	0.27	0.54	0.24	0.26	0.20	0.36	0.56	0.44	0.56	0.18
MGO	0.03	0.09	0.13	0.09	0.10	0.08	0.03	0.00	0.11	0.06	0.11	0.07
CAO	23.85	23.19	22.82	22.74	22.58	22.67	21.65	22.07	22.34	22.88	22.34	23.01
NA2O	0.06	0.09	0.03	0.07	0.06	0.12	0.03	0.01	0.00	0.01	0.00	0.00
K2O	0.01	0.02	0.01	0.00	0.01	0.01	0.01	0.01	0.00	0.00	0.00	0.00
H2O	1.90	1.87	1.86	1.88	1.87	1.87	1.84	1.85	1.84	1.86	1.86	1.92
TOTAL	100.57	99.88	99.74	99.95	99.62	98.93	99.01	99.52	98.30	99.41	99.73	101.89
ATOMIC FORMULA - ON BASIS OF 13 OXYGENS AND 1 HYROGEN												
SI	3.087	3.052	3.001	3.017	3.019	3.040	3.051	3.057	3.014	2.996	2.985	2.972
TI	0.008	0.003	0.013	0.004	0.000	0.002	0.004	0.001	0.008	0.012	0.008	0.005
AL	2.095	1.947	1.960	2.092	2.108	2.135	1.901	1.929	2.069	2.089	2.051	2.231
FE3+	0.727	0.959	1.013	0.878	0.865	0.801	0.995	0.959	0.887	0.892	0.963	0.815
FE2+	0.039	0.011	0.000	0.003	0.031	0.022	0.131	0.110	0.020	0.000	0.013	0.031
MN	0.013	0.004	0.019	0.036	0.017	0.018	0.014	0.025	0.039	0.030	0.038	0.012
MG	0.004	0.011	0.016	0.011	0.011	0.010	0.004	0.000	0.013	0.007	0.013	0.008
CA	2.018	1.998	1.975	1.948	1.939	1.953	1.895	1.917	1.950	1.974	1.928	1.926
NA	0.010	0.014	0.004	0.011	0.010	0.019	0.004	0.001	0.000	0.002	0.000	0.000
K	0.001	0.002	0.001	0.000	0.001	0.001	0.001	0.001	0.000	0.000	0.000	0.000
PS %	25.76	32.99	34.06	29.56	29.10	27.27	34.36	33.20	30.01	29.91	31.96	26.76
ZONE	B	B	B	B	B	B	A	A	B	B	B	B
MIN. ?	NO	NO	YES	YES	YES	YES	YES	YES	NO	NO	NO	NO

TABLE IV.2.5D EPIDOTE ANALYSES FROM GABBROS (1-2) AND PLAGIOGRANITES (3-8)

	P239-1E	P272-1A	P240-1B	P240-1C	P240-3B	P254-1C	P274-2A	P254-2B
WEIGHT %								
SIO2	37.92	37.84	37.12	36.88	37.44	38.63	37.25	38.49
TIO2	0.00	0.06	0.02	0.13	0.07	0.01	0.14	0.24
AL2O3	22.65	21.50	21.33	20.32	23.83	20.25	22.31	20.19
FE2O3	14.07	15.12	15.42	16.47	11.83	14.32	14.88	13.57
FEO	0.00	1.48	0.00	0.00	0.00	1.96	0.00	2.37
MNO	0.15	0.09	0.16	0.03	0.54	0.10	0.11	0.08
MGO	0.60	0.10	0.08	0.00	0.11	0.04	0.00	0.14
CAO	22.84	22.20	22.82	23.08	22.63	22.31	23.03	22.19
NA2O	0.03	0.03	0.08	0.05	0.14	0.13	0.04	0.06
K2O	0.01	0.01	0.03	0.01	0.03	0.02	0.00	0.01
H2O	1.89	1.87	1.85	1.84	1.87	1.86	1.87	1.85
TOTAL	100.15	100.31	98.92	98.81	98.49	99.63	99.64	99.21
ATOMIC FORMULA - ON BASIS OF 13 OXYGENS AND 1 HYROGEN								
SI	3.013	3.029	3.009	3.007	3.001	3.113	2.989	3.114
TI	0.000	0.004	0.001	0.008	0.004	0.001	0.009	0.015
AL	2.122	2.029	2.039	1.954	2.259	1.925	2.111	1.927
FE3+	0.841	0.911	0.941	1.011	0.716	0.869	0.898	0.827
FE2+	0.000	0.099	0.000	0.000	0.000	0.132	0.000	0.151
MN	0.010	0.006	0.011	0.002	0.037	0.007	0.008	0.006
MG	0.071	0.012	0.009	0.000	0.013	0.005	0.001	0.017
CA	1.945	1.904	1.982	2.016	1.949	1.927	1.980	1.924
NA	0.004	0.004	0.013	0.007	0.022	0.020	0.006	0.009
K	0.001	0.002	0.003	0.001	0.003	0.002	0.000	0.002
PS %	28.39	30.98	31.57	34.10	24.06	31.10	29.84	30.06
ZONE	B	B	B	B	B	B	B	B
MIN. ?	NO	NO	NO	NO	NO	NO	NO	NO

TABLE IV.2.6A PREHNITE ANALYSES FROM BASALTS

	P118-2C	P118-2D	P161-1G	P182B-3A	P182B-3B	P182B-3C	P213-1A	P213-1B	P213-2A	P213-2B	P252-2E	P271-1A
WEIGHT %												
SIO2	42.64	42.81	42.94	42.37	42.97	42.82	42.26	42.99	42.70	42.52	42.80	43.17
TIO2	0.07	0.01	0.01	0.00	0.00	0.00	0.07	0.09	0.13	0.04	0.05	0.00
AL2O3	21.16	21.52	20.95	21.35	21.16	20.22	19.14	20.63	18.48	18.97	21.20	22.47
FE2O3	4.00	3.73	2.80	3.80	2.36	2.76	6.33	2.50	6.99	5.03	4.11	0.00
FEO	0.00	0.00	0.00	0.00	0.96	1.36	0.26	1.93	0.76	1.59	0.00	2.00
MNO	0.00	0.00	0.02	0.12	0.17	0.17	0.08	0.29	0.01	0.01	0.04	0.06
MGO	0.40	0.34	0.27	0.12	0.00	0.00	0.05	0.08	0.04	0.04	0.50	0.31
CAO	26.32	27.40	26.53	26.35	25.96	26.17	25.90	25.37	25.94	25.22	26.63	24.85
NA2O	0.13	0.07	0.05	0.03	0.04	0.04	0.06	0.05	0.06	0.03	0.12	0.00
K2O	0.00	0.00	0.00	0.00	0.00	0.00	0.00	0.00	0.00	0.00	0.00	0.01
H2O	4.27	4.31	4.22	4.24	4.22	4.20	4.19	4.21	4.21	4.16	4.30	4.21
TOTAL	98.99	100.20	98.71	98.37	87.83	97.72	98.33	98.13	99.32	97.62	99.74	97.06
ATOMIC FORMULA - ON BASIS OF 24 OXYGENS AND 4 HYDROGENS												
SI	6.003	5.965	6.093	6.001	6.106	6.122	6.048	6.116	6.072	6.125	5.986	6.133
TI	0.007	0.002	0.001	0.000	0.000	0.000	0.008	0.009	0.014	0.004	0.005	0.000
AL	3.512	3.536	3.504	3.564	3.545	3.407	3.229	3.461	3.098	3.222	3.496	3.764
FE3+	0.424	0.391	0.298	0.405	0.252	0.297	0.681	0.267	0.748	0.545	0.432	0.000
FE2+	0.000	0.000	0.000	0.000	0.114	0.163	0.031	0.230	0.090	0.192	0.000	0.237
MN	0.000	0.000	0.003	0.014	0.020	0.020	0.010	0.034	0.001	0.001	0.005	0.007
MG	0.085	0.070	0.058	0.024	0.000	0.000	0.010	0.016	0.008	0.009	0.103	0.065
CA	3.970	4.091	4.034	3.998	3.952	4.008	3.971	3.868	3.953	3.893	3.991	3.779
NA	0.035	0.020	0.013	0.008	0.010	0.011	0.002	0.012	0.016	0.009	0.033	0.000
K	0.000	0.000	0.000	0.000	0.000	0.000	0.000	0.000	0.000	0.000	0.001	0.002
H	4.010	4.012	4.002	4.005	4.000	4.008	4.001	4.004	4.000	4.000	4.015	3.997

TABLE IV.2.6B PREHNITE ANALYSES FROM GABBROS

	P239-1A1	P239-1C	P239-2B	P239-3B	P246-2A	P258-3C	P258-3D	P273-2A
WEIGHT %								
SIO2	43.31	43.27	43.54	43.62	43.50	43.17	42.66	42.92
TIO2	0.08	0.02	0.00	0.00	0.01	0.02	0.04	0.04
AL2O3	21.30	20.40	19.28	21.90	23.16	22.62	20.08	24.03
FE2O3	4.14	6.14	6.11	3.50	1.11	1.08	4.44	0.30
FEO	0.04	0.00	0.52	0.00	0.00	1.17	0.85	0.00
MNO	0.09	0.05	0.01	0.02	0.00	0.05	0.08	0.02
MGO	0.29	0.78	0.12	0.39	0.16	0.42	0.08	0.11
CAO	26.37	26.06	26.43	26.76	26.78	25.25	25.35	26.26
NA2O	0.05	0.05	0.07	0.04	0.09	0.04	0.16	0.11
K2O	0.01	0.01	0.01	0.01	0.02	0.00	0.00	0.03
H2O	4.30	4.33	4.28	4.34	4.32	4.26	4.20	4.27
TOTAL	99.80	101.10	100.38	100.59	99.13	98.14	97.94	98.10
ATOMIC FORMULA - ON BASIS OF 24 OXYGENS AND 4 HYDROGENS								
SI	6.034	5.995	6.097	6.026	6.047	6.071	6.089	6.018
TI	0.008	0.002	0.000	0.000	0.001	0.002	0.005	0.004
AL	3.499	3.333	3.184	3.567	3.795	3.751	3.379	3.971
FE3+	0.434	0.640	0.644	0.364	0.116	0.114	0.477	0.003
FE2+	0.004	0.000	0.000	0.000	0.000	0.137	0.102	0.000
MN	0.010	0.006	0.002	0.002	0.000	0.006	0.010	0.003
MG	0.059	0.161	0.026	0.080	0.034	0.101	0.017	0.023
CA	3.936	3.869	3.966	3.961	3.989	3.805	3.877	3.945
NA	0.013	0.013	0.020	0.012	0.024	0.011	0.044	0.030
K	0.003	0.001	0.002	0.002	0.003	0.000	0.000	0.006
H	4.000	4.006	4.000	4.004	4.002	4.000	4.000	4.009

TABLE IV.2.7 PUMPELLYITE ANALYSES FROM BASALTS

	P76-2A	P76-2B	P76-3B	P76-3C	P213-3A	P213-4A	P213-4B	P213-4C	P271-1B
WEIGTX									
SIO2	38.08	37.78	38.10	38.22	38.19	37.12	35.98	36.32	37.86
TIO2	0.02	0.03	0.03	0.03	0.06	0.04	0.01	0.03	0.03
AL203	22.21	21.98	19.87	22.12	22.70	19.88	19.01	19.38	22.56
FE203	3.81	5.16	8.13	4.28	2.87	8.44	9.37	8.99	3.22
FEO	5.94	4.87	4.59	4.99	9.37	3.43	2.65	2.91	9.03
MNO	0.14	0.23	0.20	0.18	0.51	0.13	0.10	0.08	0.20
MGO	2.16	2.15	2.16	2.29	0.09	2.28	2.33	2.61	0.42
CAO	21.69	22.39	21.56	22.52	22.03	22.57	22.38	22.08	21.37
NA20	0.06	0.04	0.42	0.07	0.01	0.12	0.08	0.08	0.11
K20	0.01	0.00	0.01	0.00	0.00	0.07	0.00	0.00	0.02
H20	6.47	6.50	6.47	6.53	6.50	6.37	6.25	6.30	6.45
TOTAL	100.58	101.13	101.52	101.23	102.33	100.75	98.11	98.79	101.25
ATOMIC FORMULA - ON BASIS OF 28 OXYGENS AND 7 HYDROGENS									
SI	6.163	6.098	6.169	6.137	6.161	6.077	6.039	6.043	6.157
TI	0.003	0.004	0.004	0.004	0.007	0.005	0.001	0.004	0.004
AL	4.237	4.182	3.794	4.188	4.317	3.837	3.763	3.803	4.325
FE3+	0.464	0.627	0.991	0.537	0.348	1.040	1.184	1.126	0.394
FE2+	0.805	0.657	0.621	0.671	1.264	0.469	0.371	0.405	1.228
MN	0.019	0.031	0.027	0.025	0.070	0.018	0.014	0.011	0.028
MG	0.522	0.516	0.520	0.548	0.021	0.556	0.583	0.647	0.101
CA	3.762	3.873	3.740	3.874	3.808	3.958	4.018	3.936	3.725
NA	0.019	0.013	0.130	0.023	0.003	0.039	0.026	0.024	0.035
K	0.002	0.000	0.002	0.000	0.001	0.002	0.000	0.000	0.004
H	6.988	7.000	7.000	7.003	7.000	7.000	7.000	7.000	7.000
STRUCTURAL FORMULA									
Z	6.163	6.098	6.169	6.137	6.161	6.077	6.039	6.043	6.157
Y	4.000	4.000	4.000	4.000	4.000	4.000	4.000	4.000	4.000
X	2.000	2.000	1.957	1.973	2.000	1.925	1.916	1.996	2.000
W	3.833	3.903	3.872	3.897	3.849	3.999	4.044	3.960	3.844

TABLE IV.3.1 PYRITE ANALYSES FROM POLUSAGI

	P72C-1	P72C-2	P72C-3	P72C-4	P132-1B	P132-7B	P150-1	P150-2	P150-3	P150-4	P208E-1	P208E-2
WEIGHT %												
FE	46.12	46.34	45.74	46.31	45.83	45.96	46.93	47.24	47.56	47.13	46.69	46.31
S	52.57	52.75	53.84	52.54	52.99	52.60	52.81	52.93	52.91	52.78	52.45	52.97
CO	0.10	0.11	0.13	0.11	0.13	0.13	0.13	0.11	0.13	0.11	0.10	0.09
NI	0.01	0.00	0.00	0.00	0.00	0.00	0.00	0.00	0.00	0.00	0.00	0.00
MN	0.00	0.00	0.01	0.00	0.00	0.00	0.10	0.00	0.04	0.00	0.00	0.00
CU	0.08	0.07	0.00	0.09	0.34	0.34	0.05	0.04	0.07	0.05	0.05	0.10
ZN	0.01	0.00	0.00	0.01	0.02	0.02	0.02	0.03	0.00	0.07	0.04	0.09
SE	0.16	0.02	0.26	0.00	0.38	0.37	0.00	0.14	0.29	0.19	0.00	0.03
TOTAL	99.05	99.29	99.98	99.06	99.69	99.42	100.04	100.49	101.00	100.33	99.33	99.59

	P208E-3	P208E-4	P208E-5	P209-1	P209-2	P209-3	P209-4	P209-5	0210A-1A	P210A-1B	P210A-2A	P210A-2B
WEIGHT %												
FE	47.16	46.33	46.23	47.32	46.40	46.21	46.60	46.83	47.31	46.85	46.89	47.04
S	52.68	52.86	52.82	52.71	52.78	52.68	52.40	52.78	52.87	52.57	52.84	52.93
CO	0.11	0.11	0.13	0.13	0.12	0.10	0.15	0.19	0.12	0.13	0.14	0.13
NI	0.02	0.00	0.01	0.00	0.00	0.00	0.01	0.00	0.01	0.00	0.03	0.00
MN	0.02	0.01	0.04	0.02	0.04	0.07	0.00	0.00	0.00	0.00	0.00	0.00
CU	0.02	0.16	0.39	0.06	0.02	0.04	0.06	0.01	0.15	0.03	0.10	0.00
ZN	0.00	0.06	0.06	0.00	0.00	0.12	0.00	0.00	0.28	0.43	0.07	0.01
SE	0.09	0.00	0.13	0.18	0.07	0.07	0.12	0.00	0.00	0.00	0.12	0.00
TOTAL	100.10	99.53	99.81	100.42	99.43	99.29	99.34	99.81	100.74	100.01	100.19	100.11

TABLE IV.3.1 PYRITE ANALYSES FROM POLUSAGI - CONT'D

	P210A-3A	P210A-4A	P210A-4B	0211-1	P211-2	P211-3	P211-4	P211A-1	P211A-2	P211B-1	P211B-2	P211B-3
WEIGHT %												
FE	46.48	46.81	47.00	46.60	47.94	46.69	46.43	47.00	47.06	46.86	47.16	47.27
S	52.38	52.88	52.77	52.99	51.14	52.48	52.61	52.27	52.43	52.82	52.77	52.22
CO	0.11	0.13	0.12	0.13	0.13	0.15	0.14	0.13	0.13	0.11	0.09	0.16
NI	0.02	0.02	0.00	0.01	0.00	0.00	0.00	0.01	0.01	0.03	0.00	0.01
MN	0.00	0.00	0.17	0.05	0.03	0.06	0.03	0.01	0.01	0.00	0.00	0.00
CU	0.01	0.00	0.04	0.07	0.07	0.08	0.37	0.06	0.14	0.25	0.22	0.06
ZN	0.03	0.03	0.00	0.06	0.04	0.03	0.05	0.00	0.36	0.00	0.04	0.02
SE	0.13	0.10	0.00	0.00	0.05	0.32	0.11	0.18	0.00	0.00	0.04	0.28
TOTAL	99.16	99.97	100.10	99.91	99.40	99.81	99.74	99.66	100.14	100.07	100.32	100.02

	P211B-4	P211B-5	P211B-6	P211B-7	P211B-8	P211B-9	P211B-1	P212-3A	P212-3B	P212-3C	P212-3D	P212-4A
WEIGHT %												
FE	46.98	46.12	46.30	42.86	46.79	46.45	43.82	47.20	46.33	47.04	46.49	47.25
S	52.52	52.76	52.82	50.20	52.90	52.86	51.30	52.51	52.53	52.76	52.84	52.96
CO	0.10	0.12	0.11	0.12	0.13	0.15	0.12	0.06	0.13	0.12	0.11	0.12
NI	0.00	0.01	0.00	0.01	0.00	0.00	0.01	0.00	0.01	0.00	0.03	0.00
MN	0.01	0.01	0.00	0.25	0.01	0.00	0.29	0.00	0.13	0.00	0.00	0.00
CU	0.16	0.19	0.13	0.44	0.07	0.21	0.24	0.06	0.58	0.11	0.19	0.07
ZN	0.00	0.03	0.05	5.25	0.05	0.00	3.58	0.00	0.24	0.00	0.04	0.00
SE	0.06	0.14	0.01	0.00	0.09	0.24	0.10	0.00	0.00	0.00	0.10	0.00
TOTAL	99.83	99.38	99.42	99.13	100.04	99.91	99.46	99.83	99.95	100.03	99.80	100.40

TABLE IV.3.1 PYRITE ANALYSES FROM POLUSAGI - CONT'D

WEIGHT %	P212-4B	P212-5A	P212-6A	P213B-1	P213B-2	P213B-3	P268B-1	P268B-2	P268B-3	P268B-4	P268B-5	P268B-6
FE	47.14	46.40	46.40	47.33	46.54	46.52	46.52	46.17	46.53	46.15	46.00	46.52
S	53.00	52.67	53.10	52.86	52.92	52.72	52.64	52.91	52.85	53.13	52.70	53.15
CO	0.11	0.16	0.12	0.11	0.12	0.13	0.13	0.12	0.12	0.09	0.10	0.10
NI	0.00	0.09	0.05	0.00	0.00	0.00	0.00	0.00	0.00	0.00	0.00	0.00
MN	0.00	0.02	0.00	0.00	0.00	0.00	0.00	0.05	0.00	0.01	0.13	0.00
CU	0.02	0.13	0.00	0.00	0.01	0.03	0.01	0.03	0.00	0.00	0.00	0.01
ZN	0.00	0.59	0.00	0.00	0.04	0.07	0.04	0.23	0.02	0.00	0.69	0.06
SE	0.33	0.00	0.00	0.00	0.08	0.00	0.00	0.00	0.00	0.00	0.00	0.01
TOTAL	100.60	100.06	99.67	100.30	99.71	99.47	99.34	99.51	99.52	99.38	99.62	99.85

WEIGHT %	P268B-7	P268!-8	P268B-9	P268B-1	P268B-11	P268B-12	P268B-13
FE	46.36	46.65	46.46	46.85	46.91	46.35	47.45
S	52.97	53.06	53.22	53.13	53.07	53.73	52.76
CO	0.15	0.11	0.16	0.10	0.15	0.14	0.14
NI	0.00	0.00	0.00	0.00	0.00	0.00	0.00
MN	0.00	0.00	0.01	0.02	0.00	0.00	0.00
CU	0.39	0.02	0.01	0.00	0.03	0.00	0.00
ZN	0.00	0.09	0.04	0.00	0.00	0.00	0.00
SE	0.00	0.00	0.00	0.00	0.00	0.00	0.00
TOTAL	99.86	99.93	99.91	100.10	100.16	99.22	100.36

TABLE IV.3.2 CHALCOPYRITE ANALYSES FROM POLUSAGI

	P72-2B	P72-4A	P72-4D	P72B-1E	P72D-1C	P72D-2B	P72D-3C	P132-1B	P132-2B	P132-3B	P132-7C	P208C-1B
WEIGHT %												
FE	31.96	31.22	30.86	30.24	30.21	30.01	29.79	30.09	30.11	29.94	30.83	29.91
CU	33.52	33.92	33.97	33.68	33.94	33.61	33.85	34.75	34.50	34.57	34.03	33.85
S	33.67	34.20	34.13	34.19	34.35	34.27	34.39	34.01	34.35	34.18	33.53	34.32
CO	0.04	0.08	0.11	0.06	0.03	0.00	0.00	0.06	0.05	0.03	0.00	0.07
NI	0.00	0.00	0.00	0.00	0.00	0.00	0.00	0.00	0.00	0.00	0.00	0.01
MN	0.02	0.01	0.00	0.03	0.00	0.02	0.00	0.00	0.00	0.01	0.01	0.00
ZN	0.02	0.00	0.00	0.57	0.54	1.56	1.33	0.54	0.02	0.55	0.51	2.11
SE	0.00	0.00	0.00	0.00	0.00	0.00	0.00	0.00	0.00	0.00	0.13	0.01
TOTAL	99.23	99.43	99.07	98.77	99.07	99.47	99.36	99.45	99.03	99.28	99.04	100.29

	P208C-2B	P208C-3C	P212-1A	P212-2C	P212A-1C
WEIGHT %					
FE	29.67	30.27	30.91	30.32	29.97
CU	34.29	34.62	34.17	34.09	33.83
S	33.82	34.08	33.92	34.62	34.38
CO	0.04	0.06	0.00	0.12	0.04
NI	0.00	0.01	0.03	0.01	0.00
MN	0.00	0.00	0.01	0.04	0.02
ZN	0.45	0.36	1.65	1.38	1.11
SE	0.00	0.00	0.00	0.00	0.02
TOTAL	98.27	99.40	100.70	100.58	99.37

TABLE IV.3.3A SPHALERITE ANALYSES FROM POLUSAGI

	P72A-2A	P72A-2B	P27A-2C	P72A-2D	P72A-3A	P72A-3B	P72A-3C	P72A-3D	P72B-1C	P72B-1D	P72B-4B	P72B-4C
WEIGHT %												
ZN	66.64	67.01	65.57	64.73	64.69	66.03	64.82	64.00	67.05	67.02	65.63	66.93
S	32.21	32.50	32.12	32.04	32.45	32.05	31.89	32.00	32.30	32.41	32.36	32.22
FE	0.27	0.27	1.09	1.28	1.94	1.04	1.17	1.88	0.14	0.47	1.16	0.50
MN	0.03	0.04	0.02	0.02	0.00	0.00	0.00	0.00	0.02	0.00	0.02	0.00
CU	0.08	0.01	0.92	0.77	0.02	0.16	1.06	1.44	0.02	0.31	0.01	0.17
SE	0.02	0.00	0.00	0.01	0.11	0.08	0.02	0.08	0.04	0.07	0.14	0.04
AG	0.00	0.00	0.00	0.00	0.00	0.00	0.00	0.00	0.00	0.00	0.00	0.00
CD	0.21	0.19	0.25	0.34	0.19	0.19	0.18	0.15	0.25	0.25	0.25	0.27
TOTAL	99.46	100.02	99.97	99.19	99.40	99.55	99.14	99.55	99.82	100.53	99.57	100.13

	P72D-1A	P72D-2C	P72D-3A	P132-3C	P208C-1C	P208C-2A	P208C-3B	P208D-1A	P208D-2B	P210A-5B	P210A-5C	P211AB-4
WEIGHT %												
ZN	63.55	64.51	65.70	64.02	66.16	65.11	65.92	66.25	66.21	66.41	66.61	66.25
S	32.58	32.41	32.58	32.66	32.59	32.63	32.40	32.29	32.30	32.32	32.52	32.56
FE	1.90	1.42	0.42	1.24	0.93	1.32	0.99	0.21	0.25	0.32	0.46	0.39
MN	0.03	0.02	0.01	0.05	0.04	0.00	0.00	0.00	0.00	0.04	0.08	0.00
CU	1.31	0.78	0.24	1.00	0.54	0.93	0.58	0.08	0.19	0.00	0.00	0.12
SE	0.00	0.02	0.11	0.07	0.01	0.06	0.07	0.05	0.11	0.03	0.03	0.01
AG	0.01	0.02	0.00	0.01	0.04	0.01	0.02	0.02	0.00	0.00	0.00	0.00
CD	0.12	0.18	0.13	0.36	0.36	0.11	0.12	0.17	0.14	0.15	0.16	0.18
TOTAL	99.50	99.36	99.19	99.41	100.67	100.17	100.10	99.07	99.20	99.27	99.86	99.52

TABLE IV.3.3A SPHALERITE ANALYSES FROM POLUSAGI - CONT'D

	P212-1B	P212-2B	P212A-1B	P212A-2B	P213[illegible]2A
WEIGHT %					
ZN	65.70	66.49	66.17	66.45	67.33
S	32.80	32.84	32.35	32.56	32.45
FE	0.06	0.36	0.63	0.05	0.35
MN	0.00	0.02	0.01	0.04	0.02
CU	0.19	0.09	0.12	0.15	0.04
SE	0.05	0.06	0.01	0.00	0.09
AG	0.00	0.00	0.00	0.00	0.00
CD	0.15	0.14	0.18	0.16	0.16
TOTAL	98.95	100.00	99.47	99.41	100.45

TABLE IV.3.3B SPHALERITE ANALYSES FROM CANAKCI

	E1-6A-1C	E1-6B-1A	E1-7-1D	E1-7-1E	E3A-3-2A	E3A-3-2B	E4-4-2D	E5-3-1A	E5-A-1A	E5-A-2B	E5-B-2D
WEIGHT %											
ZN	66.29	66.37	66.75	66.88	65.24	64.71	66.69	65.90	66.42	66.17	65.55
S	32.43	32.28	32.53	32.68	32.04	31.95	32.62	32.58	32.75	32.62	32.83
FE	0.13	0.22	0.03	0.04	0.99	0.74	0.15	0.60	0.64	0.54	0.91
MN	0.03	0.00	0.00	0.00	0.12	0.09	0.00	0.00	0.00	0.00	0.02
CU	0.43	0.33	0.00	0.08	1.19	0.34	0.14	0.08	0.04	0.32	0.17
SE	0.02	0.10	0.03	0.00	0.06	0.00	0.06	0.06	0.05	0.03	0.04
AG	0.00	0.00	0.00	0.00	0.00	0.00	0.00	0.00	0.00	0.00	0.00
CD	0.92	0.91	0.77	0.94	0.76	0.69	1.18	0.32	0.30	0.30	0.26
TOTAL	100.25	100.21	100.11	100.62	100.40	98.52	100.84	99.54	100.20	99.98	99.78

TABLE IV.3.4A GALENA ANALYSES FROM POLUSAGI

	P72-2A	P72-4B	P72-4C	P72B-1B	P72B-1F	P72B-4A	P72B-4D	P72D-1B	P72D-2A	P72D-3B	P132-1A	P132-2A	P132-3A
WEIGHT %													
PB	85.53	85.92	85.64	86.33	86.40	86.42	86.33	86.68	86.91	85.87	86.52	85.27	85.20
S	13.23	13.56	13.23	13.34	13.34	12.53	13.11	13.62	13.60	13.45	12.71	12.83	12.77
MN	0.00	0.00	0.03	0.00	0.00	0.03	0.04	0.01	0.00	0.00	0.00	0.01	0.00
AS	0.00	0.00	0.00	0.00	0.00	0.00	0.00	0.00	0.00	0.00	0.00	0.00	0.00
SE	0.38	0.34	0.41	0.07	0.09	0.02	0.17	0.00	0.00	0.00	1.29	1.21	1.64
AG	0.00	0.00	0.02	0.00	0.00	0.00	0.00	0.32	0.05	0.21	0.08	0.07	0.00
CD	0.11	0.08	0.09	0.09	0.14	0.04	0.06	0.14	0.12	0.15	0.08	0.11	0.14
SB	0.00	0.00	0.00	0.00	0.00	0.01	0.01	0.02	0.01	0.04	0.04	0.00	0.00
TE	0.03	0.04	0.08	0.02	0.05	0.00	0.08	0.11	0.01	0.03	0.10	0.00	0.08
BI	0.00	0.00	0.00	0.01	0.00	0.00	0.04	0.00	0.00	0.00	0.06	0.04	0.06
TOTAL	99.28	99.94	99.50	99.86	100.02	99.05	99.84	100.90	100.70	99.75	100.88	99.54	99.89

	P208C-1A	P208C-2C	P208C-1A	P208D-1B	P208D-2A	P210A-5A	P210A-5D	P210AB-4A	P212-1C	P212-2A	P212A-1A	P212A-2A	P213-2B
WEIGHT %													
PB	86.56	86.45	86.94	86.57	86.23	85.88	86.55	86.38	86.61	86.74	85.51	86.65	84.25
S	13.40	13.24	13.30	13.24	13.51	13.45	13.40	13.42	13.42	13.34	13.28	13.48	13.41
MN	0.01	0.00	0.01	0.02	0.00	0.00	0.05	0.00	0.01	0.01	0.00	0.01	0.00
AS	0.00	0.00	0.04	0.00	0.02	0.04	0.06	0.04	0.00	0.00	0.00	0.00	0.02
SE	0.01	0.07	0.01	0.00	0.00	0.04	0.08	0.21	0.00	0.00	0.00	0.00	0.00
AG	0.00	0.00	0.00	0.13	0.10	0.03	0.05	0.03	0.03	0.04	0.01	0.06	0.02
CD	0.08	0.11	0.12	0.16	0.11	0.18	0.18	0.14	0.12	0.14	0.13	0.18	0.08
SB	0.02	0.00	0.00	0.02	0.00	0.00	0.00	0.00	0.06	0.00	0.03	0.00	0.02
TE	0.06	0.11	0.16	0.07	0.10	0.00	0.07	0.00	0.02	0.05	0.10	0.04	0.03
BI	0.05	0.13	0.05	0.14	0.08	0.00	0.00	0.02	0.01	0.02	0.00	0.00	0.04
TOTAL	100.19	100.11	100.63	100.35	100.15	99.62	100.44	100.24	100.28	100.35	99.05	100.43	99.87

TABLE IV.3.4B GALENA ANALYSES FROM CANAKCI

	E1-6A-1B	E1-6B-1B	E1-7-1C	E1-7-1F	E4-4-2C	E5-3-1B	E5B-2C	E5A-2A	E5A-1B
WEIGHT %									
PB	86.67	85.77	86.62	86.63	85.89	86.22	86.45	86.10	86.06
S	13.19	13.13	13.08	13.11	13.11	13.43	13.42	13.40	13.22
MN	0.00	0.00	0.01	0.00	0.00	0.01	0.00	0.00	0.00
AS	0.05	0.00	0.00	0.05	0.00	0.02	0.04	0.02	0.01
SE	0.41	0.52	0.76	0.17	0.87	0.24	0.00	0.01	0.11
AG	0.04	0.05	0.03	0.07	0.04	0.01	0.05	0.03	0.03
CD	0.16	0.15	0.13	0.14	0.13	0.16	0.15	0.13	0.12
SB	0.00	0.01	0.01	0.07	0.01	0.04	0.00	0.03	0.00
TE	0.03	0.01	0.01	0.00	0.07	0.04	0.09	0.05	0.06
BI	0.00	0.02	0.00	0.00	0.04	0.01	0.03	0.01	0.02
TOTAL	100.56	99.66	100.66	100.23	100.16	100.17	100.23	99.77	99.64

TABLE IV.3.5 BORNITE ANALYSES FROM CANAKCI

	E1-6-4	E1-6-5	E1-6-7	E1-6-8
WEIGHT %				
FE	11.39	11.74	12.58	11.26
CU	62.08	62.49	60.39	63.09
S	25.17	25.15	25.20	24.14
ZN	0.13	0.00	0.10	0.00
AG	0.05	0.01	0.00	0.04
TOTAL	98.87	99.38	98.28	98.54

TABLE IV.3.6 HAWSONITE ANALYSES FROM CANAKCI

	E1-6-1	E1-6-1A	E1-6A-2A	E1-61A-2A	E1-61A-2B	E1-61A-2C	E1-61A-2D	E1-61B-1A	E1-61B-2A	E1-61B-3A
WEIGHT %										
FE	12.62	14.05	14.04	12.88	13.17	12.83	11.23	14.05	13.94	12.19
S	28.37	28.63	28.66	28.43	28.61	28.87	28.89	27.83	28.38	28.64
CU	41.18	41.88	42.06	44.93	44.25	44.30	45.00	42.90	43.07	43.14
ZN	1.41	0.05	0.11	0.04	0.05	0.00	0.09	0.14	0.11	0.08
AG	0.02	0.00	0.00	0.06	0.06	0.06	0.05	0.00	0.00	0.00
SN	15.32	14.71	14.92	13.59	14.17	13.90	14.57	14.87	14.87	16.26
TOTAL	98.91	99.33	99.79	99.93	100.31	99.97	99.83	99.79	100.37	100.31
ATOMIC FORMULA - ON BASIS OF 17 ATOMS										
FE	2.012	2.218	2.209	2.021	2.06	2.008	1.767	2.225	2.188	1.924
S	7.878	7.871	7.855	7.771	7.799	7.869	7.917	7.678	7.759	7.873
CU	5.769	5.811	5.817	6.195	6.086	6.094	6.221	5.971	5.94	5.984
ZN	0.192	0.007	0.014	0.005	0.007	0.001	0.012	0.019	0.015	0.011
AG	0.002	0.000	0.000	0.005	0.005	0.005	0.004	0.000	0.000	0.000
SN	1.149	1.093	1.105	1.003	1.043	1.024	1.078	1.108	1.098	1.207

TABLE IV.3.7 HEXASTANNITE ANALYSES FROM CANAKCI

	E1-61B-4A	E1-61B-4B
WEIGHT %		
FE	9.23	9.16
S	28.76	28.88
CU	38.90	39.32
ZN	5.03	5.15
AG	0.05	0.02
SN	18.30	18.48
TOTAL	100.27	101.01
ATOMIC FORMULA - ON BASIS OF 25 ATOMS		
FE	2.168	2.137
S	11.765	11.740
CU	8.029	8.065
ZN	1.009	1.026
AG	0.006	0.003
SN	2.023	2.029

TABLE IV.3.8 COLUSITE ANALYSES FROM CANAKCI

	E1-62-1A	E1-63-1A	E1-63-1B	E1-63-1C	E1-7-3A	E2-3-2A	E4-1-1A	E4-1-1B	E4-1-1C	E4-1-1D	E4-4-3A	E4-4-4A
WEIGHT %												
FE	1.22	3.92	5.19	5.19	0.71	2.07	1.42	1.38	1.13	1.02	0.17	2.69
S	30.94	30.76	29.70	29.71	31.35	31.15	31.26	31.28	31.13	31.27	31.20	31.46
V	2.79	2.11	2.00	1.98	3.20	3.14	3.17	3.34	3.24	3.29	3.17	3.20
CU	50.44	50.68	52.88	52.89	50.97	49.80	50.23	50.21	50.21	50.60	49.65	49.81
ZN	0.05	0.16	0.08	0.08	0.29	0.00	0.00	0.00	0.02	0.00	3.03	0.00
GA	0.03	0.05	0.04	0.04	0.12	0.00	0.02	0.00	0.00	0.03	0.06	0.02
GE	3.00	1.96	2.31	2.30	2.94	3.60	3.37	3.26	3.29	3.34	3.81	4.01
AS	8.67	7.59	7.92	7.92	8.44	8.74	8.98	9.18	8.89	9.03	8.30	8.41
AG	0.02	0.04	0.04	0.02	0.09	0.01	0.01	0.02	0.01	0.00	0.01	0.00
SN	1.06	1.96	1.22	1.23	1.39	0.67	0.89	0.86	1.16	0.99	0.26	0.46
TOTAL	98.22	99.24	101.39	101.34	99.49	99.18	99.35	99.54	99.08	99.57	99.65	100.08
ATOMIC FORMULA - ON BASIS OF 4 SULPHUR												
FE	0.091	0.293	0.401	0.401	0.052	0.153	0.105	0.101	0.083	0.075	0.013	0.197
S	4.000	4.000	4.000	4.000	4.000	4.000	4.000	4.000	4.000	4.000	4.000	4.000
V	0.227	0.173	0.170	0.168	0.257	0.254	0.255	0.269	0.262	0.264	0.256	0.256
CU	3.291	3.325	3.593	3.593	3.281	3.227	3.242	3.239	3.254	3.266	3.212	3.196
ZN	0.003	0.010	0.005	0.005	0.018	0.000	0.000	0.000	0.001	0.000	0.191	0.000
GA	0.002	0.003	0.002	0.002	0.007	0.000	0.001	0.000	0.000	0.002	0.003	0.001
GE	0.172	0.113	0.138	0.137	0.165	0.204	0.190	0.184	0.189	0.189	0.216	0.226
AS	0.480	0.422	0.456	0.456	0.461	0.480	0.492	0.503	0.489	0.494	0.455	0.458
AG	0.001	0.002	0.002	0.001	0.003	0.000	0.000	0.001	0.000	0.000	0.000	0.000
SN	0.037	0.069	0.044	0.045	0.048	0.023	0.031	0.030	0.040	0.034	0.009	0.016

TABLE IV.3.8 COLUSITE ANALYSES FROM CANAKCI - CONT'D

	E5-A-3A	E5-A-4A	E5-3-4A	E5-3-5A	E5-3-5B
WEIGHT %					
FE	2.45	2.91	2.81	1.32	1.44
S	31.42	31.27	31.43	31.24	31.13
V	3.10	3.22	3.25	3.22	3.26
CU	49.81	48.96	50.05	50.47	51.42
ZN	0.00	0.00	0.00	0.00	0.00
GA	0.00	0.09	0.06	0.00	0.00
GE	3.15	2.63	2.99	3.83	3.76
AS	8.92	9.30	9.05	8.85	8.36
AG	0.02	0.02	0.00	0.00	0.00
SN	0.82	1.37	0.29	0.22	0.20
TOTAL	99.690	99.770	99.940	99.160	99.580
ATOMIC FORMULA - ON BASIS OF 4 SULPHUR					
FE	0.179	0.214	0.206	0.097	0.106
S	4.000	4.000	4.000	4.000	4.000
V	0.248	0.260	0.260	0.260	0.264
CU	3.199	3.160	3.214	3.260	3.334
ZN	0.000	0.000	0.000	0.000	0.000
GA	0.000	0.005	0.003	0.000	0.000
GE	0.177	0.148	0.168	0.217	0.214
AS	0.486	0.509	0.493	0.485	0.460
AG	0.001	0.001	0.000	0.000	0.000
SN	0.028	0.047	0.010	0.008	0.007

TABLE IV.3.9A FAHLORE ANALYSES FROM POLUSAGI

	P72-1A	P72-3A	P72A-1A	P72B-2A	P72B-2B	P72B-2C	P72B-2D	P72B-2E	P72B-2F	P72B-2G	P72B-2H	P72B-3A
WEIGHT %												
FE	1.61	1.48	2.46	0.57	0.25	0.22	0.46	0.52	0.86	1.12	0.22	0.07
S	27.16	27.03	26.90	26.37	26.26	26.38	26.50	26.51	26.54	26.78	26.62	26.24
CU	42.32	42.14	41.26	41.81	41.22	41.85	41.38	41.06	41.31	41.29	41.45	40.84
ZN	8.28	8.35	8.37	9.04	10.66	9.09	9.12	9.72	8.60	8.42	8.93	10.07
AS	17.18	18.26	16.05	13.83	12.87	13.76	13.89	13.87	13.40	13.61	13.65	10.75
AG	0.06	0.19	0.04	0.03	0.03	0.05	0.03	0.03	0.02	0.03	0.02	0.04
SB	4.38	2.55	5.86	9.27	9.94	10.01	9.50	9.66	10.01	9.65	9.65	13.53
TE	0.00	0.00	0.00	0.01	0.01	0.00	0.00	0.00	0.00	0.00	0.06	0.02
BI	0.00	0.00	0.00	0.00	0.00	0.00	0.00	0.00	0.00	0.00	0.00	0.00
TOTAL	100.99	100.00	100.95	100.94	101.25	101.35	100.87	101.36	100.76	100.89	100.60	101.56
ATOMIC FORMULA - ON BASIS OF TOTAL METALLIC ATOMS=16												
FE	0.423	0.392	0.650	0.152	0.067	0.058	0.123	0.138	0.233	0.302	0.061	0.018
S	12.465	12.446	12.384	12.327	12.248	12.328	12.443	12.379	12.515	12.613	12.592	12.437
CU	9.800	9.989	9.582	9.862	9.700	9.869	9.806	9.674	9.827	9.811	9.892	9.765
ZN	1.864	1.885	1.890	2.073	2.439	2.084	2.101	2.226	1.989	1.945	2.071	2.341
AS	3.376	3.598	3.161	2.766	2.569	2.752	2.792	2.771	2.704	2.742	2.763	2.179
AG	0.008	0.026	0.006	0.004	0.005	0.006	0.005	0.004	0.004	0.004	0.003	0.006
SB	0.529	0.309	0.711	1.141	1.220	1.231	1.174	1.187	1.243	1.197	1.203	1.689
TE	0.000	0.000	0.000	0.002	0.001	0.000	0.000	0.000	0.000	0.000	0.007	0.003
BI	0.000	0.000	0.000	0.000	0.000	0.000	0.000	0.000	0.000	0.000	0.000	0.000

TABLE IV.3.9A FAHLORE ANALYSES FROM POLUSAGI - CONT'D

	P72D-5A	P132-5A	P132-6A	P132-7A	P132-8A	P132-9A	P132A-1A	P132B-1A	P132B-2A	P208C-4A	P208C-4B	P208C-4C
WEIGHT %												
FE	2.45	1.29	1.66	0.29	1.57	0.92	0.95	1.47	1.36	1.33	1.38	1.55
S	25.56	27.16	27.81	27.40	27.35	27.73	27.81	26.98	27.00	27.20	27.34	27.09
CU	39.40	43.18	41.45	43.04	42.28	43.09	44.21	41.78	42.66	41.59	39.51	40.33
ZN	8.90	7.67	7.88	7.95	7.79	6.28	8.14	8.15	8.04	8.25	9.18	8.63
AS	8.01	18.53	18.10	18.07	17.11	17.34	18.21	18.50	19.28	15.45	15.65	15.49
AG	0.06	0.02	0.01	0.00	0.02	0.04	0.01	0.00	0.01	0.04	0.02	0.04
SB	16.97	3.04	2.57	2.96	3.34	3.74	1.01	2.42	2.37	7.07	6.19	7.30
TE	0.07	0.05	0.09	0.09	0.00	0.00	0.00	0.03	0.06	0.03	0.07	0.02
BI	0.00	0.08	0.05	0.00	0.00	0.00	0.14	0.00	0.12	0.00	0.00	0.00
TOTAL	101.42	101.02	99.62	99.80	99.45	99.15	100.48	99.32	100.89	100.96	99.34	100.45
ATOMIC FORMULA - ON BASIS OF TOTAL METALLIC ATOMS=16												
FE	0.670	0.338	0.447	0.077	0.420	0.251	0.251	0.391	0.356	0.357	0.377	0.420
S	12.179	12.397	13.016	12.775	12.770	13.132	12.739	12.521	12.289	12.690	13.025	12.734
CU	9.471	9.946	9.788	10.126	9.961	10.295	10.218	9.783	9.795	9.793	9.497	9.564
ZN	2.080	1.718	1.808	1.818	1.784	1.458	1.828	1.854	1.794	1.889	2.146	1.989
AS	1.633	3.619	3.624	3.605	3.419	3.515	3.571	3.673	3.754	3.085	3.192	3.115
AG	0.009	0.003	0.002	0.000	0.003	0.006	0.001	0.000	0.001	0.006	0.003	0.005
SB	2.129	0.366	0.317	0.364	0.411	0.466	0.122	0.296	0.283	0.868	0.776	0.904
TE	0.008	0.006	0.011	0.011	0.000	0.000	0.000	0.004	0.007	0.003	0.009	0.003
BI	0.000	0.006	0.004	0.000	0.000	0.000	0.010	0.000	0.008	0.000	0.000	0.000

TABLE IV.3.9A FAHLORE ANALYSES FROM POLUSAGI - CONT'D

	P208C-4D	P208C-4E	P208C-4F	P208C-5A	P208C-5B	P208C-6A	P208D-3A	P208D-4A	P211AB-1A	P211AB-1B	P211AB-1C	P211AB-1
WEIGHT %												
FE	1.58	1.53	1.67	2.05	2.17	1.39	2.12	2.24	4.47	3.28	3.33	5.91
S	27.19	27.21	26.99	26.90	27.04	26.17	27.53	27.43	27.23	27.06	27.34	28.07
CU	39.98	40.31	40.39	40.28	41.81	41.68	40.25	41.19	41.88	42.09	41.78	39.89
ZN	9.20	8.56	8.81	7.72	8.10	8.45	7.85	7.76	5.59	5.39	5.17	4.75
AS	15.41	15.31	14.90	15.39	15.49	15.19	17.46	17.45	11.19	15.77	16.71	13.18
AG	0.04	0.04	0.03	0.07	0.07	0.01	0.03	0.01	0.09	0.04	0.06	0.04
SB	7.18	7.89	7.76	7.03	6.64	7.47	3.91	3.93	9.68	6.01	5.60	8.77
TE	0.02	0.12	0.04	0.00	0.05	0.08	0.00	0.03	0.00	0.04	0.00	0.04
BI	0.00	0.00	0.00	0.00	0.00	0.00	0.20	0.69	0.00	0.00	0.00	0.00
TOTAL	100.61	100.96	100.60	99.45	101.37	100.43	99.35	100.74	100.12	99.70	100.00	100.63
ATOMIC FORMULA - ON BASIS OF TOTAL METALLIC ATOMS=16												
FE	0.426	0.412	0.450	0.557	0.573	0.371	0.575	0.595	1.214	0.883	0.895	1.605
S	12.762	12.773	12.666	12.757	12.458	12.153	12.985	12.725	12.889	12.691	12.803	13.282
CU	9.466	9.547	9.563	9.636	9.720	9.765	9.579	9.640	10.002	9.959	9.871	9.523
ZN	2.118	1.970	2.027	1.796	1.831	1.923	1.816	1.766	1.298	1.241	1.187	1.102
AS	3.095	3.075	2.992	3.122	3.054	3.019	3.525	3.465	2.267	3.165	3.349	2.668
AG	0.006	0.005	0.004	0.010	0.010	0.001	0.005	0.002	0.012	0.005	0.008	0.005
SB	0.887	0.976	0.959	0.878	0.806	0.913	0.486	0.481	1.206	0.743	0.690	1.093
TE	0.003	0.015	0.005	0.000	0.006	0.009	0.000	0.003	0.000	0.005	0.000	0.005
BI	0.000	0.000	0.000	0.000	0.000	0.000	0.015	0.049	0.000	0.000	0.000	0.000

TABLE IV.3.9A FAHLORE ANALYSES FROM POLUSAGI - CONT'D

	P211AB-2A	P211AB-2B	P211AB-3A	P211AB-3B
WEIGHT %				
FE	2.6	2.75	2.87	3.03
S	27.23	27.27	26.72	26.80
CU	41.18	41.25	41.10	41.37
ZN	7.83	7.68	6.27	5.66
AS	14.00	14.33	13.17	13.31
AG	0.12	0.11	0.04	0.07
SB	7.86	7.97	10.71	10.53
TE	0.06	0.07	0.00	0.02
BI	0.00	0.00	0.00	0.00
TOTAL	100.84	101.45	100.89	100.80
ATOMIC FORMULA - ON BASIS OF TOTAL METALLIC ATOMS=16				
FE	0.697	0.734	0.778	0.821
S	12.735	12.671	12.598	12.656
CU	9.717	9.668	9.779	9.857
ZN	1.796	1.750	1.451	1.311
AS	2.802	2.849	2.657	2.689
AG	0.017	0.015	0.006	0.009
SB	0.963	0.975	1.330	1.310
TE	0.007	0.009	0.000	0.003
BI	0.000	0.000	0.000	0.000

TABLE IV.3.9B FAHLORE ANALYSES FROM CANAKCI

	E1-1-1A	E1-1-1B	E1-1-1C	E1-6	E1-6A-1A	E1-6B-1C	E1-6B-1D	E1-6B-1E	E1-7-1A	E1-7-1B	E1-7-2A	E2-3-1A	E2-4-1A
WEIGHT %													
FE	0.81	1.08	1.02	0.15	0.27	0.15	0.10	0.17	0.08	0.10	0.20	1.13	1.29
S	27.18	27.31	27.56	26.87	27.50	27.45	27.53	27.37	27.52	27.83	26.33	27.56	27.31
CU	43.81	43.39	43.99	43.07	43.65	42.91	42.13	42.57	43.02	42.85	44.31	43.12	43.04
ZN	7.89	7.83	7.84	7.76	7.86	8.25	8.73	8.29	8.19	8.11	7.97	7.68	6.98
AS	19.71	19.34	19.64	19.46	19.59	19.00	19.19	19.20	19.38	19.19	19.01	19.08	18.62
AG	0.07	0.08	0.08	0.02	0.02	0.05	0.05	0.03	0.04	0.03	0.03	0.03	0.06
SB	0.40	0.32	0.42	0.59	0.41	0.61	0.56	0.59	0.46	0.64	0.55	0.69	0.05
TE	0.94	0.79	0.82	0.99	0.96	0.95	0.94	0.90	0.97	1.01	0.98	1.01	1.85
BI	0.20	0.21	0.18	0.21	0.11	0.14	0.15	0.09	0.18	0.18	0.24	0.35	0.20
TOTAL	100.99	100.35	101.54	99.12	100.37	99.50	99.38	99.22	99.84	99.95	99.61	100.63	99.39
ATOMIC FORMULA - ON BASIS OF TOTAL METALLIC ATOMS=16													
FE	0.211	0.283	0.265	0.040	0.072	0.039	0.027	0.046	0.022	0.027	0.052	0.297	0.346
S	12.332	12.494	12.456	12.501	12.650	12.787	12.866	12.781	12.777	12.972	12.041	12.658	12.711
CU	10.029	10.018	10.032	10.109	10.128	10.086	9.936	10.030	10.077	10.078	10.224	9.994	10.108
ZN	1.755	1.757	1.738	1.770	1.773	1.865	2.002	1.898	1.865	1.854	1.758	1.731	1.593
AS	3.827	3.787	3.800	3.875	3.855	3.788	3.838	3.836	3.849	3.828	3.720	3.750	3.708
AG	0.010	0.011	0.010	0.003	0.003	0.007	0.006	0.005	0.006	0.004	0.004	0.004	0.008
SB	0.047	0.038	0.049	0.073	0.049	0.075	0.069	0.072	0.056	0.078	0.066	0.083	0.007
TE	0.107	0.091	0.093	0.116	0.112	0.111	0.111	0.106	0.113	0.118	0.113	0.116	0.216
BI	0.014	0.015	0.013	0.015	0.008	0.010	0.011	0.006	0.013	0.013	0.017	0.025	0.015

TABLE IV.3.9B FAHLORE ANALYSES FROM CANAKCI - CONT'D

	E2-4-1B	E3-1A	E3-A3-1	E4-4-1A	E4-4-2A	E4-4-2B	E5-A-1C	E5-A-2C	E5-B-1A	E5-3-1C	E5-3-1D	E5B-2A	E5B-2B
WEIGHT %													
FE	0.95	0.38	2.57	0.10	0.27	0.35	0.48	0.83	0.22	0.30	0.22	0.11	0.15
S	27.75	27.48	26.67	27.44	27.50	27.57	27.80	27.59	27.45	27.58	27.13	27.68	27.80
CU	43.84	44.32	41.49	44.16	43.08	42.51	43.03	42.67	44.20	43.69	42.90	43.17	44.69
ZN	7.04	7.91	7.14	8.24	8.24	7.89	9.18	8.38	8.71	8.51	8.65	8.65	8.38
AS	18.55	18.98	15.94	17.92	18.70	18.49	18.36	18.85	18.87	19.27	18.66	18.55	18.08
AG	0.05	0.03	0.02	0.02	0.05	0.02	0.03	0.01	0.00	0.02	0.03	0.04	0.06
SB	0.43	0.44	3.47	1.05	1.14	1.19	1.44	1.63	1.49	1.80	1.59	1.58	1.47
TE	1.60	0.92	1.48	1.42	1.18	1.33	0.22	0.23	0.30	0.14	0.14	0.31	0.22
BI	0.23	0.38	1.05	0.14	0.44	0.41	0.16	0.14	0.13	0.20	0.15	0.13	0.10
TOTAL	100.43	100.83	99.82	100.49	100.59	99.76	100.69	100.32	101.36	101.52	99.48	100.23	100.94
ATOMIC FORMULA - ON BASIS OF TOTAL METALLIC ATOMS=16													
FE	0.253	0.099	0.690	0.027	0.071	0.095	0.126	0.219	0.057	0.080	0.060	0.029	0.038
S	12.827	12.563	12.482	12.651	12.712	12.919	12.779	12.726	12.456	12.541	12.589	12.821	12.728
CU	10.223	10.224	9.798	10.271	10.048	10.050	9.980	9.930	10.120	10.024	10.042	10.088	10.322
ZN	1.596	1.775	1.638	1.864	1.868	1.812	2.069	1.896	1.938	1.899	1.969	1.964	1.882
AS	3.668	3.713	3.192	3.535	3.699	3.707	3.611	3.720	3.665	3.750	3.704	3.676	3.542
AG	0.007	0.004	0.003	0.003	0.006	0.003	0.005	0.002	0.000	0.003	0.004	0.005	0.008
SB	0.053	0.053	0.427	0.128	0.139	0.147	0.174	0.197	0.178	0.216	0.195	0.193	0.177
TE	0.186	0.106	0.174	0.164	0.137	0.157	0.025	0.027	0.034	0.016	0.016	0.037	0.025
BI	0.016	0.027	0.075	0.010	0.031	0.030	0.011	0.010	0.009	0.014	0.011	0.010	0.007

TABLE IV.3.10 MAGNETITE ANALYSES FROM POLUSAGI

	P212-2A	P212-2B
WEIGHT %		
FE2O3	66.04	65.740
FEO	29.37	29.460
SO3	3.25	3.330
ZNO	0.56	0.320
TOTAL	99.22	100.130

TABLE IV.3.11 CHROMITE ANALYSES FROM CANAKCI

	CR-1A	CR-1B	CR-2A	CR-2B	CR-3A	CR-3B	CR-4A	CR-4B
WEIGHT %								
SIO2	0.05	0.35	0.06	0.04	0.08	0.56	0.14	0.07
TIO2	0.16	0.10	0.12	0.13	0.12	0.11	0.15	0.15
AL2O3	10.94	10.59	10.99	11.18	11.00	10.26	10.57	11.04
CR2O3	59.55	58.25	58.76	59.73	59.95	58.77	58.65	59.68
FE2O3	3.68	3.60	2.69	2.81	2.69	3.57	3.28	3.13
FEO	11.90	12.53	12.72	12.46	12.70	12.09	12.26	12.26
MNO	0.87	0.76	0.54	0.72	0.89	0.65	0.83	1.06
MGO	14.06	13.62	13.32	13.69	13.48	14.18	13.52	13.68
V2O3	0.07	0.13	0.07	0.05	0.05	0.00	0.10	0.06
NIO	0.13	0.13	0.12	0.16	0.13	0.13	0.09	0.14
TOTAL	101.41	100.05	99.40	100.96	101.08	100.32	99.60	101.28
ATOMIC FORMULA - ON BASIS OF 4 OXYGENS								
SI	0.002	0.011	0.002	0.001	0.003	0.018	0.004	0.002
TI	0.004	0.002	0.003	0.003	0.003	0.003	0.004	0.004
AL	0.409	0.402	0.420	0.420	0.413	0.387	0.403	0.414
CR	1.491	1.481	1.503	1.503	1.510	1.486	1.499	1.499
FE3+	0.088	0.087	0.066	0.067	0.064	0.086	0.080	0.075
FE2+	0.315	0.337	0.344	0.332	0.338	0.324	0.331	0.326
MN	0.023	0.021	0.015	0.019	0.024	0.018	0.023	0.028
MG	0.664	0.653	0.643	0.649	0.640	0.676	0.651	0.648
V	0.002	0.003	0.002	0.001	0.001	0.000	0.002	0.002
NI	0.003	0.003	0.003	0.004	0.003	0.003	0.002	0.004

TABLE IV.3.12 GOLD ANALYSES FROM CANAKCI

	E2-4-2B	E2-4-2C	E2-4-2D
WEIGHT %			
FE	0.67	0.77	0.67
S	16.65	16.41	16.53
CU	23.70	23.95	23.63
ZN	3.56	3.64	3.44
AG	6.12	5.93	5.94
AU	51.85	51.25	51.17
PT	0.00	0.00	0.00
BI	0.14	0.14	0.14
TOTAL	102.68	102.10	101.51

TABLE IV.3.13A IDAITE-CHALCOPYRITE INTERGROWTH FROM POLUSAGI

	P72B-6A1	P72B-6A2	P72B-6A3
WEIGHT %			
FE	16.02	15.97	15.91
CU	50.47	49.87	49.82
S	33.22	33.01	33.17
TOTAL	99.71	98.86	98.90

TABLE IV.3.13B IDAITE-CHALCOPYRITE INTERGROWTH ANALYSES FROM CANAKCI

	E3-2A	E3-2B	E3-2C	E3-2D	E3-2E	E3-2F	E3-2G	E3-2	E3-3A	E3-3B	E3-3C	E3-3D
WEIGHT %												
FE	15.32	15.70	15.46	15.71	15.62	15.51	15.74	15.44	16.14	15.61	15.43	15.51
CU	50.12	49.63	49.90	50.17	50.29	49.53	50.19	50.30	49.86	49.93	49.86	49.78
S	33.53	33.87	33.70	33.94	33.93	33.76	33.80	33.79	34.03	33.91	34.03	34.19

	E3-3E	E3-3F	E3-3G	E3-3H	E3-3I	E3-4A	E3-4B	E3-4C	E3-5A
WEIGHT %									
FE	15.51	15.69	15.83	15.66	15.71	15.95	15.94	15.67	15.67
CU	49.89	50.01	50.28	50.38	50.54	50.03	50.01	50.33	49.82
S	34.02	33.69	33.58	33.84	33.81	33.44	33.26	33.70	34.24
TOTAL	99.42	99.39	99.69	99.88	100.06	99.42	99.21	99.70	99.73

Strike and dip
Fault
Thrust
Landslide
Stream
Drill-hole location
① Massive sulphide location
Sulphide mineralisation and limonitic zone
Pillow-lava

U. Cretaceous-Eocene
Fe-Mn rich siliceous sediment
Volcanics
Agglomerate
Red-schist
Calc-schist
Fossiliferous white limestone
Gabbro
Plagiogranite

Palaeozoic
Mica-schist

MAP 1

GEOLOGICAL MAP OF THE POLUŞAĞI AREA

0 0.5 1.0 1.5 Km

N

M. Özçelik 1979

ZER T.
1840m

SÜTİME T.
1850m

SİFTAL T.
1745m

HASENAK T.
1575m

TOSPAH T.
1771m

MEGALİSÖR T.
1725m

PİRİK T.

CUTICALLİ T.
1845m

ÇATIOLE T.
1627m

BEYAZTAŞ T.
1680m

DARIŞK T.
1809m

KIYMIŞZİYARETİ T.
1789m

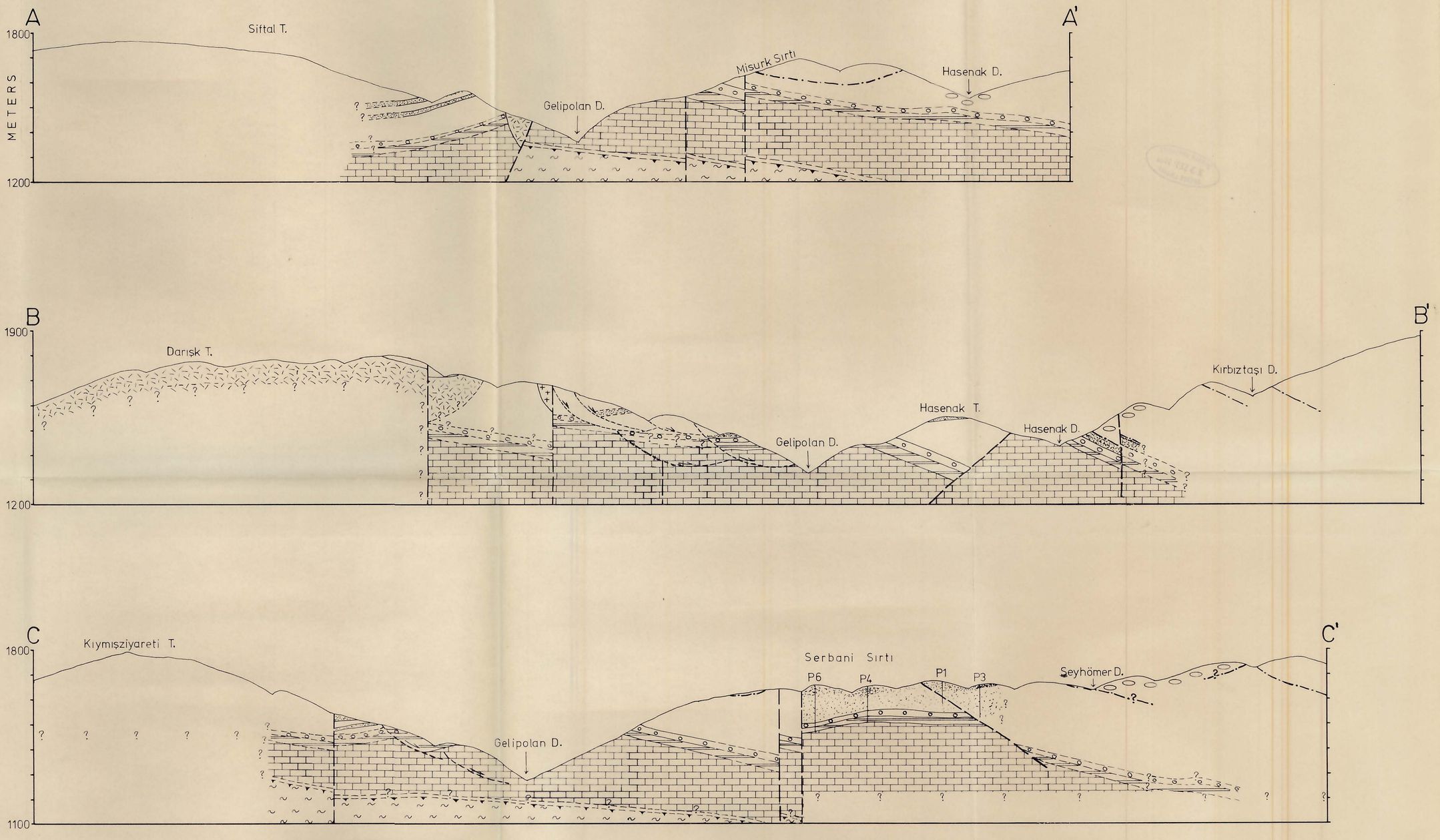
Günlk D.
Berik D.
Siftal D.
Misurk Sırtı
Hasenak D.
Kirbizası D.
Seyhömer D.
Serbani D.
Serbani Sırtı
Pirik D.
Garikuze Sırtı
GELİPOLAN DERESİ
Madan D.
Havsu D.
Gorden D.

0 0.5 1.0 1.5 Km

N

MAP 3
SAMPLE LOCATION MAP OF THE POLUŞAĞI AREA

M. Özçelik 1979



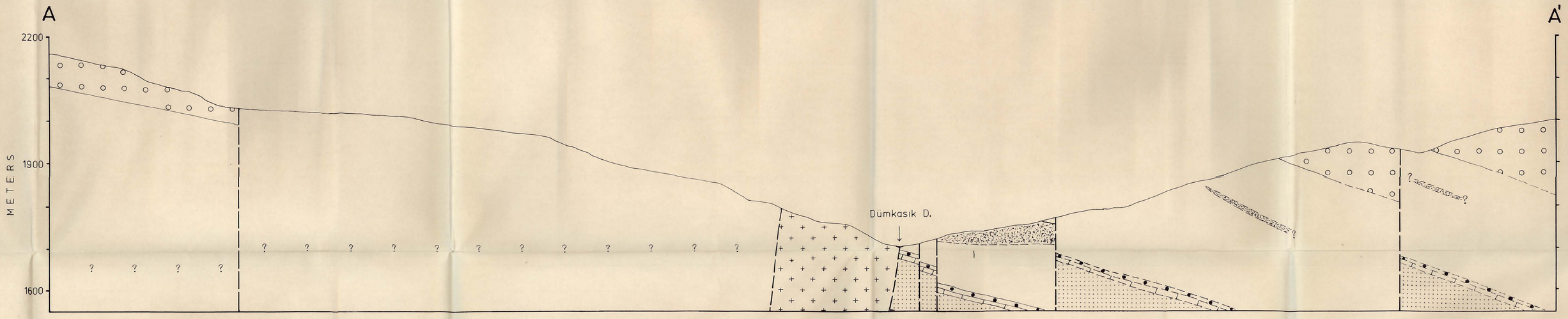
CROSS-SECTIONS: 1 , THE POLUŞAĞI AREA

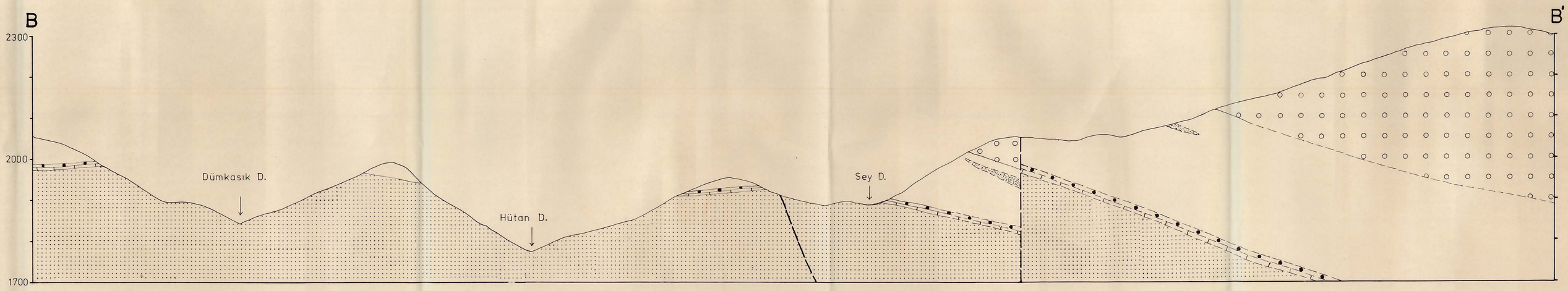
Landslide

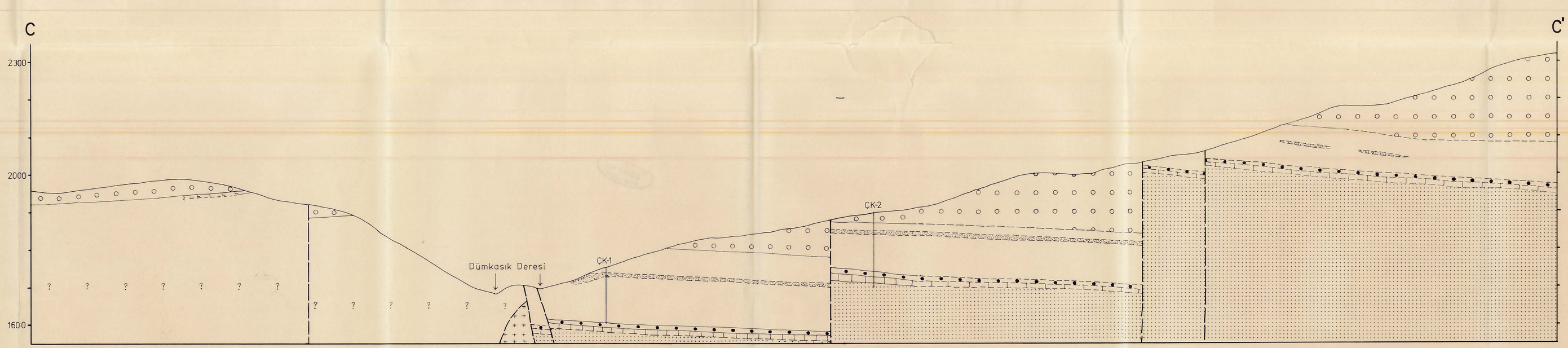
LEGEND AS FOR MAP 1

CROSS-SECTIONS : 2

THE ÇANAKÇI AREA, LEGEND AS FOR MAP 2







MAP-2

GEOLOGICAL MAP OF THE ÇANAKÇI AREA

- Agglomerate
- Calc-schist + red-schist
- Fossiliferous white limestone
- Red limestone
- Breccia-conglomerate

} U. Cretaceous-Eocene

- Quartzite
- Mica-schist

} Palaeozoic

- Serpentinite
- Sulphide mineralisation
- ① Ore-body location
- Drill-hole location
- Fault
- Strike and dip
- Stream

0 250 500 750

Meters

N

M. Özçelik 1978

A

A'

B

B'

C

C'

ÇK-1

ÇK-2

① ②

Marz Deresi

Sey Deresi

Dümkasık Deresi

Hütan Deresi

Herik Deresi